

**Isolation and Structural Elucidation of Novel Anti-Infective  
Naphthylisoquinoline Alkaloids from *Ancistrocladus ealaensis*, and  
Phytochemical Analysis of Two Congolese Medicinal Plants**

**Isolierung und Strukturaufklärung von neuen anti-infektiven  
Naphthylisochinolin-Alkaloiden aus *Ancistrocladus ealaensis* und  
phytochemische Analyse von zwei kongolesischen Heilpflanzen**



Doctoral thesis for a doctoral degree  
at the Graduate School of Life Sciences,  
Julius-Maximilians-Universität Würzburg,  
Section: Infection and Immunity

submitted by

Dieudonné Tshitenge Tshitenge

from

Kananga, Democratic Republic of the Congo

Würzburg 2017

Reverse page

Submitted on: .....

Office stamp

Members of the *Promotionskomitee*:

Chairperson: Prof. Dr. Utz Fischer

Primary Supervisor: Prof. Dr. Dr. h.c. mult. Gerhard Bringmann

Supervisor (Second): Prof. Dr. Ulrike Holzgrabe

Supervisor (Third): P.D. Dr. Heike Bruhn

Supervisor (Fourth): Prof. Dr. Karine Ndjoko-Ioset

Date of Public Defence: .....

Date of Receipt of Certificates: .....



Die vorliegende Arbeit wurde in der Zeit von April 2013 bis Juni 2017 am  
Institut für Organische Chemie der Universität Würzburg angefertigt.

Herrn Prof. Dr. Dr. h.c. mult. G. Bringmann danke ich für  
die hervorragende Unterstützung bei der Durchführung der Arbeiten, die  
freundliche Atmosphäre und die exzellenten Arbeitsbedingungen.

Teile der im Rahmen dieser Arbeit erzielten Ergebnisse waren bereits Gegenstand von  
Publikationen<sup>[163, 214, 259]</sup> sowie von Posterpräsentationen und Vorträgen.





**Dedicated to my family**

**and to everyone who made these wonderful years in Würzburg enjoyable and memorable**

**also to all the million Congolese people victims of the human cruelty**



# Contents

Abbreviations.....	V
Introduction.....	1
I. Specific Background.....	5
I.1. Introduction to Naphthylisoquinoline Alkaloids.....	6
I.2. Introduction to 2,3-Dihydrobenzo[ $\beta$ ]furan Neolignans and <i>Gardenia ternifolia</i> .....	18
II. Results and Discussions .....	21
II.0. <i>Ancistrocladus ealaensis</i> , a Rich Source of Naphthylisoquinoline Alkaloids.....	22
II.1. Ealapasamines, the First Fully Characterized 'Mixed' Heterodimers.....	25
II.2. <i>A. ealaensis</i> as a Rich Source of Dimeric Naphthylisoquinolines Related to Mbandakamine A and Michellamine F.....	40
II.3. Cyclombandakamines, a Unique Series of Novel Dimeric Alkaloids .....	55
II.4. Ealamines A-H, Enthralling Naphthylisoquinoline Alkaloids with Promising Bioactivities from <i>A. ealaensis</i> .....	79
II.5. Synthesis of Ealajoziminone A and Ealajoziminone B.....	101
II.6. Ealaines A-D, Naphthalene-Devoid Alkaloids .....	112
II.7. Further New and Known Monomeric Alkaloids from <i>A. ealaensis</i> .....	117
II.8. Chemo-Taxonomic Position of <i>A. ealaensis</i> within the African Species.....	126
II.9. Gardenifolins A-H, Scalemic Neolignans from <i>Gardenia ternifolia</i> : Chiral Resolution of Eight Stereoisomers, Configurational Assignment, and Antiproliferative Activities.....	131
II.10. Phytochemical and Qualitative Analysis of KILMA and N'Sansiphos.....	147
II.10.1. Introduction to Congolese Herbal Medicinal Products.....	147
II.10.2. Rational Quality Assessment Procedure for Less-Investigated Herbal Drug: Case of SIROP KILMA <sup>®</sup> .....	149
II.10.3. Quality Analysis of Three Batches of N'Sansiphos <sup>®</sup> .....	152
III. Summary/Zusammenfassung .....	154
III.1. Summary.....	154
III.2. Zusammenfassung.....	162
IV. Experimental Section.....	172
IV.1. General Experimental Aspects .....	173
IV.2. Ealapasamines, the First Fully Characterized 'Mixed' Heterodimers Naphthylisoquinoline Alkaloids from <i>A. ealaensis</i> .....	178
IV.2.1. Extractions, Isolation, and HPLC conditions.....	178
IV.2.1.3. Isolated ealapasamines.....	179

---

Ealapasamine A ( <b>42</b> ).....	179
Ealapasamine B ( <b>43</b> ).....	182
Ealapasamine C ( <b>44</b> ).....	185
IV.3. <i>A. ealaensis</i> as a Reliable Source of Dimeric Naphthylisoquinolines Related to Mbandakamine A and Michellamine F.....	189
IV.3.1. Extractions, Isolation, and HPLC conditions.....	189
1- <i>epi</i> -Mbandakamine A ( <b>47</b> ).....	1900
Mbandakamine C ( <b>48</b> ).....	193
Mbandakamine D ( <b>49</b> ).....	194
Michellamine F <sub>2</sub> ( <b>50</b> ).....	196
IV.4. Cyclombandakamines, a Thrilling Series of Novel Dimeric Alkaloids.....	198
IV.4.1. Extractions, Isolation, and HPLC conditions.....	198
Cyclombandakamine A ( <b>51</b> ).....	200
1- <i>epi</i> -Cyclombandakamine A ( <b>52</b> ).....	204
Cyclombandakamine A <sub>3</sub> ( <b>53</b> ).....	206
Cyclombandakamine A <sub>4</sub> ( <b>54</b> ).....	208
Cyclombandakamine A <sub>5</sub> ( <b>55</b> ).....	210
Cyclombandakamine A <sub>6</sub> ( <b>56</b> ).....	212
Cyclombandakamine A <sub>7</sub> ( <b>57</b> ).....	214
IV.5. Ealamines A-H, Enthralling Naphthylisoquinoline Alkaloids with Promising Bioactivities from <i>A. ealaensis</i> .....	216
IV.5.1. Extractions, Isolation, and HPLC conditions.....	216
Ealamine A ( <i>P</i> - <b>62</b> ).....	218
Ealamine B ( <i>M</i> - <b>62</b> ).....	220
Ealamine C ( <b>63</b> ).....	221
Ealamine D ( <b>64</b> ).....	222
Ealamine E ( <b>65</b> ).....	223
Ealamine F ( <b>66</b> ).....	224
Ealamine G ( <b>67</b> ).....	225
Ealamine H ( <b>68</b> ).....	226
IV.6. Synthesis of Ealajoziminone A and Ealajoziminone B.....	227
IV.6.1. Isolation and HPLC conditions.....	227
Ealajoziminone A ( <b>70</b> ).....	227
Ealajoziminone B ( <b>71</b> ).....	229

---

IV.7. Ealaines A-D, Naphthalene-Devoid Alkaloids.....	231
IV.7.1. Extractions, Isolation, and HPLC conditions.....	231
Ealaine A ( <b>72</b> ).....	231
Ealaine B ( <b>73</b> ).....	232
Ealaine C ( <b>74</b> ).....	233
Ealaine D ( <b>75</b> ).....	234
IV.8. Further New Monomeric Alkaloids from <i>A. ealaensis</i> .....	235
IV.8.1. Extractions, Isolation, and HPLC conditions.....	235
1- <i>epi</i> -Korupensamine A ( <b>76</b> ).....	235
Ancistroealaine C ( <b>77</b> ).....	237
5- <i>epi</i> -Ancistroealaine B ( <b>79</b> ).....	238
Ancistroealaine D ( <b>81</b> ).....	239
IV.9. Gardenifolins A-H, Scalemic Neolignans from <i>Gardenia ternifolia</i> .....	240
IV.9.1. Extractions, Isolation, and HPLC conditions.....	240
Gardenifolin A ( <b>83a</b> ).....	242
Gardenifolin B ( <b>83b</b> ).....	243
Gardenifolin C ( <b>83c</b> ).....	244
Gardenifolin D ( <b>83d</b> ).....	245
Gardenifolin E ( <b>84a</b> ).....	246
Gardenifolin F ( <b>84b</b> ).....	247
Gardenifolin G ( <b>84c</b> ).....	248
Gardenifolin H ( <b>84d</b> ).....	249
IV.10. Quality Analysis of Three Batches of N'Sansiphos.....	250
V. Literature.....	252
VI. Acknowledgements.....	280
VII. Publications, Posters, Oral Presentations, and Workshops.....	283
VIII. Resume.....	286
Affidavit.....	287



---

## Abbreviations

<b>2,3-DBF</b>	2,3-dihydro[b]benzofuran (a type of neolignans)
<b>CD<sub>3</sub>OD</b>	Deuterated methanol for NMR measurement
<b>CDCl<sub>3</sub></b>	Deuterated chloroform for NMR measurement
<b>CD<sub>3</sub>COCD<sub>3</sub></b>	Deuterated acetone for NMR measurement
<b>CH<sub>2</sub>Cl<sub>2</sub></b>	Dichloromethane
<b>COSY</b>	Correlation Spectroscopy
<b>DFT</b>	Density Functional Theory
<b>ECD</b>	Electronic Circular Dichroism
<b>HPLC-DAD</b>	High Performance Liquid Chromatography - Diode Array Detector
<b>H<sub>2</sub>O</b>	Water (ultrapure quality for chromatography)
<b>HMBC</b>	Heteronuclear Multiple Bond Correlation
<b>HSQC</b>	Heteronuclear Single Quantum Correlation
<b>HRESIMS</b>	High Resolution Electrospray Ionization Mass Spectrometry
<b>HOMO</b>	Highest Occupied Molecular Orbital
<b>LC-MS</b>	Liquid Chromatography coupled to a Mass Spectrometer
<b>LUMO</b>	Lowest Unoccupied Molecular Orbital
<b>MeOH</b>	Methanol
<b>NIQ</b>	Naphthylisoquinoline (a type of alkaloids)
<b>NMR</b>	Nuclear Magnetic Resonance
<b>NOESY</b>	Nuclear Overhauser Effect Spectroscopy
<b>ROESY</b>	Rotating Frame Nuclear Overhauser Effect Spectroscopy
<b>SI</b>	Selectivity Index
<b>TOCSY</b>	Total Correlation Spectroscopy







## Introduction

For many centuries, natural resources have constituted a sustainable and reliable source of important bioactive materials for humans.<sup>[1]</sup> These products result from their producers metabolism.<sup>[2]</sup> The biochemical processes for the catabolism and the anabolism of carbohydrates, fatty acids, proteins, and nucleic acids are common in most organisms.<sup>[2]</sup> These compounds, known also as primary metabolites, are ubiquitous and vital for all living matters.<sup>[3]</sup> Apart from them, there is an additional part of the metabolism with a much more limited distribution in terms of resulting products which is, thus, characteristic to a single or a group of individuals.<sup>[3-4]</sup> These specific substances, also called secondary metabolites, represent the fingerprint of each species, and are even used as markers in the phylogeny and taxonomy of plants.<sup>[4]</sup> Despite the broad structural diversity and complexity, their biosynthesis is derived from intermediates of the primary metabolism, mainly acetyl-CoA, shikimic acid, mevalonic acid, and methylerythritol phosphate, which represent key substances in their specific biosynthetic routes.<sup>[2]</sup> However, proteins, alkaloids, peptides, and many antibiotics are derived from some amino acids, while most aromatic amino acids are formed by the shikimate pathway.<sup>[2]</sup> *L*-Ornithine and *L*-lysine, which are important in the synthesis of some alkaloids, have their origin from the Krebs cycle.<sup>[2]</sup>

The functions of secondary metabolites have not yet been unambiguously established for every organism, but many studies have proven that they are mostly involved in the defense for the survival of their producers.<sup>[5]</sup> Plants are known as the major providers of these natural products.<sup>[6]</sup> In some plant species, these multi-functional substances have been used to interact profitably with their immediate environment, for example as insect attractants in flowers (for pollination) by producing anthocyanins or terpenes, which can be, at the same time, insecticidal or antimicrobial.<sup>[1]</sup> Evolutionary reports have indicated that metabolites like alkaloids, glucosinolates, terpenes, saponins, tannins, antraquinones, cyanogenetic glycosides, and polyacetylenes are allelochemicals, adaptively formed to protect the plants against fungi, viruses, bacteria, other parasites, and herbivores.<sup>[5, 7]</sup> Therefore, the need for survival in a hostile and perpetually evolutionary environment has triggered the occurrence of different types of natural products in these organisms.

Most interestingly, these specific plant-derived metabolites display a broad range and degree of biological activities that can be beneficial in human medicine.<sup>[8-11]</sup> Indeed, many drugs currently available on the pharmaceutical market are of plant origin.<sup>[12-13]</sup>

From a chemical point of view, nature can be a source of fascinating and structurally intriguing compounds, *e.g.*, with high numbers of chiral elements, sterically hindered biaryl axes, and macrocyclic scaffolds.<sup>[11, 14-16]</sup> The group of alkaloids should be emphasized, showing fascinating structural complexities and prominent activities, which have captivated research in the field of natural product chemistry for many years.<sup>[14, 17-19]</sup> Together with the diterpenoids, the class of alkaloids has been reported among the main sources of promising novel anti-infective agents, like against *P. falciparum* in the case of compounds **1-3**.<sup>[8, 20-22]</sup>

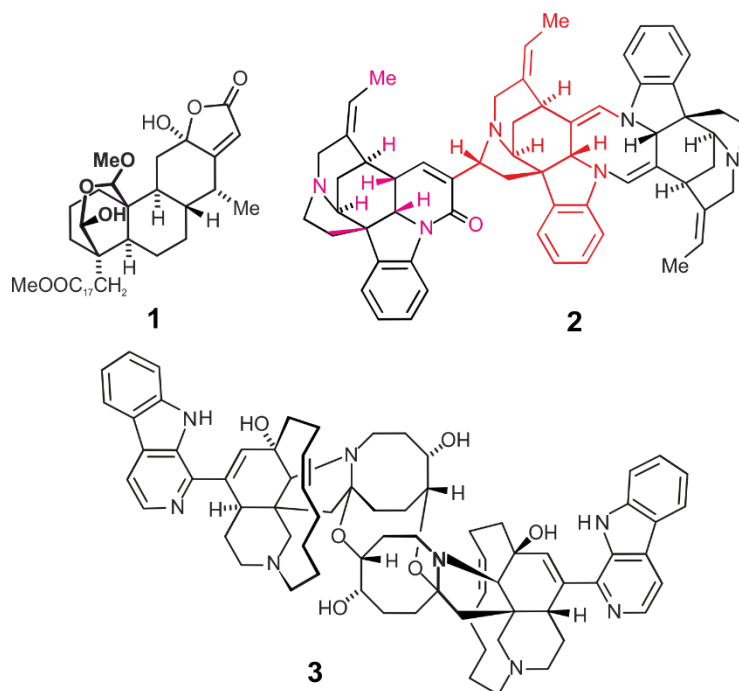


Figure 1. Naturally occurring metabolites with promising antiplasmodial activities: caesalsappanin H (**1**), strychnohexamine (**2**), and neo-kauliamine (**3**) with  $IC_{50}$  values against *Plasmodium falciparum* of 0.52, 1.0, and 0.006  $\mu$ M, respectively.<sup>[14, 21-22]</sup>

The structural diversity and complexity of different classes of plant-derived natural products have triggered, for a long time, numerous scientific research activities,<sup>[1, 14, 16, 23-26]</sup> which have led to revolutionary discoveries that have significantly increased life expectancy on earth by treating various severe diseases.<sup>[9, 24]</sup> The history of quinine (**4**) and artemisinin (**6**) and their medical use represent good examples to be named.<sup>[24, 27-29]</sup> The recent 2015 Physiology or Medicine Nobel Prize for the discovery of the antimalarial artemisinin<sup>[30]</sup> attests the appreciation of the community in the fight against infections.

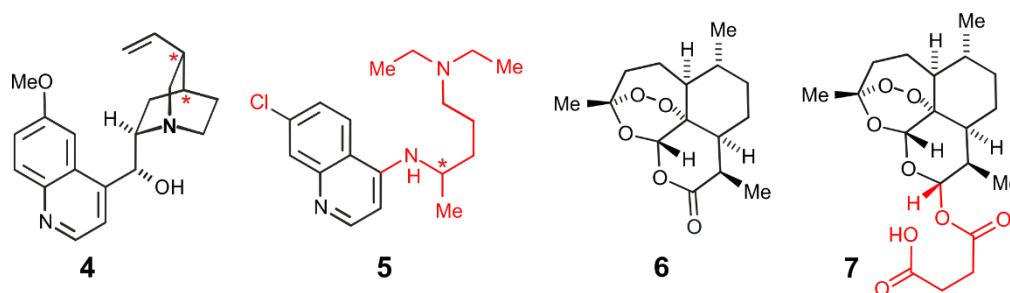


Figure 2. Quinine (**4**) and artemisinin (**6**), two naturally occurring antimalarial drugs, with two of their synthetic analogues chloroquine (**5**) and artesunate (**7**).

Among the alkaloids, the group of naphthylisoquinolines is consisted of very promising anti-infective agents. This singular class of metabolites has been in the focus of outstanding scientific interests due to their unique biosynthetic origin, their structural diversity, and the variety of their biological activities.<sup>[31-35]</sup>

Most of the plant metabolites are found in complex mixtures. It remains a highly challenging task to access pure material by systematic isolation, and even more challenging to assign the full absolute structures. After the isolation and structural identification, the substance must fit in the right biotesting model system – with an acceptable selectivity index – to have a value. These features will be decisive for the future of a new candidate throughout the drug discovery process. To make sure that the isolated compound is active, a bio-guided fractionation procedure is mostly recommended.<sup>[36-37]</sup>

Despite the discovery of many bioactive natural products, pathogens of infectious diseases are still affecting several millions of people every year in our modern world, due to the phenomenon of multi-drug resistance and strain mutations.<sup>[38-40]</sup> Named in the top five of the most lethal diseases in human history, malaria has remained a major life-threatening infection with 212 million cases and half a million deaths recorded in 2015.<sup>[39, 41-42]</sup> Moreover, many other diseases remain severe menaces to mankind, in particular, leishmaniosis, various resistant bacterial and fungal infections.<sup>[43-44]</sup> This alarming situation makes the search for new drug candidates a rewarding and urgent task for our humanity.

The studies reported in this thesis were done in the frame of the research network SFB 630, 'Agents against Infectious Diseases'. This search for discovery of novel drug candidates was conducted on the less-investigated Central African liana *Ancistrocladus ealaensis* J. Léonard (Ancistrocladaceae), and some Congolese herbal medicines and their medicinal plants. Moreover, the choice of the tropical liana was highly valuable from a botanical perspective

because very recently, numerous new *Ancistrocladus* species were detected in the Northwestern region of the Democratic Republic of the Congo,<sup>[45]</sup> many of them were related to the well-known<sup>[46]</sup> plant *A. ealaensis*. Since very few secondary metabolites are known from this plant species, it was necessary to establish a representative metabolic profile of this well-identified liana for a better discrimination.

Herein described are the isolation, structural elucidation, and biological evaluation of highly thrilling monomeric and dimeric new naphthylisoquinoline alkaloids from *A. ealaensis*. The separation, chiral resolution, and characterization of a series of stereoisomeric 2,3-dihydrobenzofuran neolignans are also reported. The analytical and phytochemical analysis on two Congolese antimalarial herbal drugs is part of the last chapter of the results. In this last case, major concerns on widely used Congolese herbal drugs are discussed.

The thesis is organized in three main parts: specific background, results and discussions, and experimental details. The results are organized in ten chapters preceded by a concise overview of the achievements described. The experimental part provides all the detailed aspects related to the reported results.

The general aim of this work was the contribution to fight human illnesses, with a focus on infectious diseases.

The specific goals assigned to this work were:

- 1) Isolation, structural characterization, and biological evaluation of new secondary metabolites occurring in *Ancistrocladus ealaensis*
- 2) Establishment of the chemotaxonomic position of *A. ealaensis* within the Central African related species
- 3) Isolation, structural characterization, and biological evaluation of secondary metabolites occurring in *Gardenia ternifolia*, used in a Congolese phytomedicine, KILMA
- 4) Quality evaluations of the phytomedicines KILMA and N'Sansiphos
- 5) Semi-synthesis of selected promising compounds

**I. Specific Background**

## I.1. Introduction to Naphthylisoquinoline Alkaloids

Alkaloids belong to the most bioactive natural products.<sup>[8, 37]</sup> Numerous representatives carrying various structural scaffolds have been known mostly from plants, and to a small extent, also from microorganisms and animals.<sup>[2, 10]</sup> These secondary metabolites are low-molecular weight nitrogen-containing compounds, and are often classified based on the constitutional feature: *e.g.* indole, isoquinoline, quinoline, quinazoline, piperidine, pyrrolidine, and tropane.<sup>[2]</sup> The nitrogen often derives from amino acid precursors, or is acquired by reductive amination reactions.<sup>[2, 47-49]</sup>

Some types of alkaloids have a broad distribution in the plant kingdom, and, interestingly, some have a more restricted occurrence like the class of naphthylisoquinolines.<sup>[50]</sup> This chapter will focus on this class of compounds, the peculiarities of which deserve particular attention. Naphthylisoquinoline alkaloids (NIQs) are known to occur exclusively in the two palaeotropical plant families of Ancistrocladaceae and Dioncophyllaceae (Caryophyllales).<sup>[50]</sup> The geographic distribution of these lianas is mainly restricted to Southwest and Central African regions, but also to Southeast Asia, with outliers in East Africa, Sri Lanka, and India.<sup>[45-46, 51-52]</sup> Plant species belonging to the Ancistrocladaceae family are easily recognizable by their distinctive hooked twigs, while those from the Dioncophyllaceae family possess crowned leaves (Figure 3).<sup>[53-54]</sup> The word '*Ancistrocladus*' derives from the Greek *ankistro* (= hook) and *klados* (= shoot), thus carrying the main trait of this genus of ca. 30 species known and about 20 are firmly described so far.<sup>[53, 55]</sup>



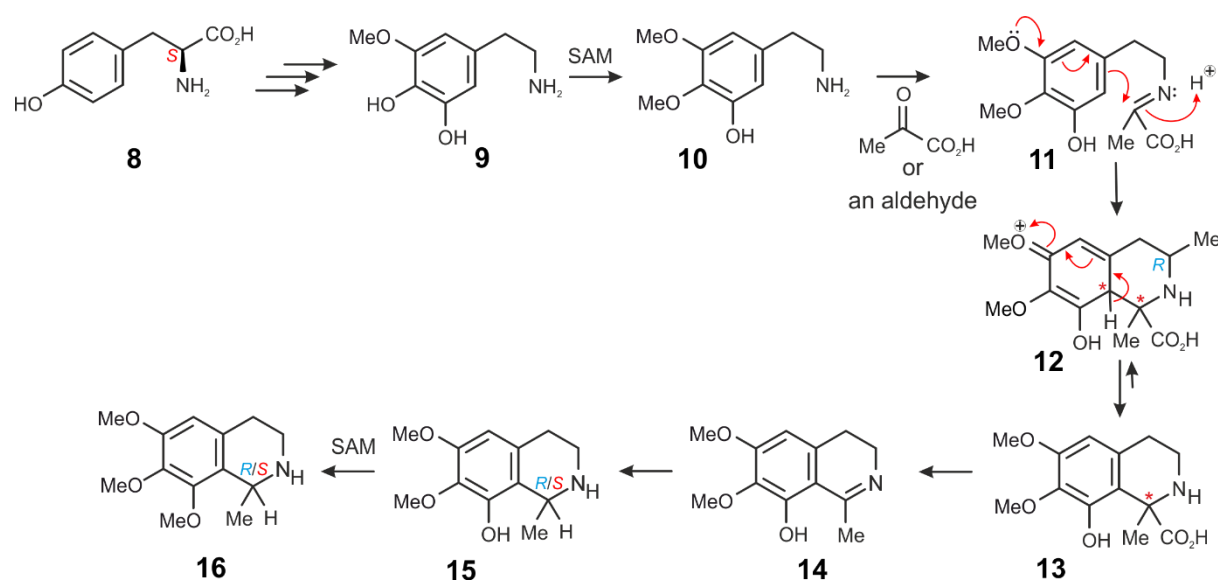
Figure 3. Typical hooked twigs of an Ancistrocladaceae liana (left) and hooked-leaf material of a Dioncophyllaceae species (right). (Pictures taken from the research group Bringmann)

The main group of secondary metabolites synthesized in these tropical lianas belongs to the class of naphthylisoquinoline alkaloids, which represent a unique class of compounds in several



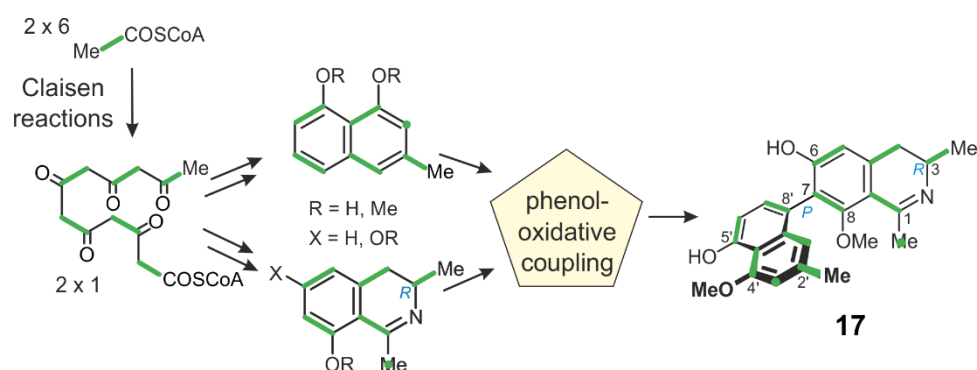
aspects.<sup>[50]</sup> Over the last decades, this type of natural products has increasingly attracted scientific attention.<sup>[34, 56-61]</sup>

The uniqueness of naphthylisoquinolines is due to their extraordinary biosynthetic origin. All other tetrahydroisoquinoline alkaloids, like morphine, are known to be produced from aromatic amino acids such as (*L*)-tyrosine (**8**) formed *via* a Pictet-Spengler condensation of a 2-arylethylamine derivative (*e.g.* dopamine) with an  $\alpha$ -keto acid or an aldehyde (Scheme 1).<sup>[2, 62-63]</sup>



Scheme 1. Biosynthetic pathway to simple tetrahydroisoquinoline alkaloids.<sup>[2, 62]</sup>

Our research group has shown, however, that the entire carbon skeleton of naphthylisoquinoline alkaloids, is synthesized from acetate-polymalonate precursors.<sup>[63-66]</sup> Their untypical biosynthesis proceeds *via* a common  $\beta$ -pentaketo ester intermediate through Claisen reactions of single acetates, which by aldol condensations and aromatization, and reductive amination for the isoquinoline (*e.g.* by transamination), ultimately leads to the alkaloids by phenol-oxidative coupling reactions (Scheme 2).<sup>[63, 65]</sup>



Scheme 2. Biosynthetic route to naphthylisoquinoline alkaloids, based on the data reported for dioncophylline A,<sup>[63]</sup> adapted to the case of yaoundamine A (**17**).

Before the class of naphthylisoquinolines, only the group of alkaloids occurring in *Conium maculatum*, *i.e.* coniine,  $\gamma$ -coniceine, and *N*-methylconiine featuring simple piperidine rings, had been known to derive from acetate units.<sup>[67-69]</sup> However, the naphthylisoquinoline alkaloids remain the very first tetrahydroisoquinolines of polyketidic origin, and their biosynthetic pathway is a general principle within the Ancistrocladaceae and Dioncophyllaceae plant families.<sup>[64-65]</sup>

Apart from the biosynthesis, further singularities of these compounds are their thrilling stereochemical peculiarities and structural diversity. The monomers are basically built up from a naphthalene part, which can be *C,C*- or *N,C*-linked to an isoquinoline moiety by a biaryl axis.<sup>[60, 70]</sup> The linkage between the two building blocks is often sterically hindered, forming an additional element of chirality, which leads to the phenomenon of atropisomerism.<sup>[71]</sup> It concerns stereoisomers consisting of at least one rotationally hindered single bond for which the rotational barrier is high enough to enable their isolation.<sup>[50, 71-72]</sup> Atropisomers, from the Greek *a* 'not' and *tropos* 'turn', are often categorized based on the hybridization of the linked atoms into the  $sp^2$ - $sp^2$ ,  $sp^2$ - $sp^3$ , and  $sp^3$ - $sp^3$  types,<sup>[50, 73]</sup> and most of the axially chiral natural products fit into the first group.<sup>[73]</sup> They can likewise be classified in the two groups of bridged and non-bridged biaryls.<sup>[74]</sup> Among the bridged natural products are, for example, those formed by a hindered rotation inside of a macrocycle<sup>[75-78]</sup> and those made of a configurationally stable macrocycle.<sup>[79]</sup> Numerous atropisomeric conformers are of high interest in drug discovery and chemical synthesis.<sup>[72, 80-82]</sup>

The main structural attribute of naphthylisoquinoline is their unprecedented structural and stereochemical divergence.<sup>[31, 34, 50, 57]</sup> With four coupling positions in the naphthalene and three in the isoquinoline moieties, in principle twelve *C,C*- or *N,C*-axial linkages are possible to form

different types of classical monomeric naphthylisoquinolines, as exemplified by **17-25** depicted in Figure 4. These biaryls always display at least one element of chirality, often two stereogenic centers and one chiral axis, enhancing the structural variations within the class.<sup>[83-84]</sup> NIQs can be therefore be differentiated based on the linkage type. From early observations, the presence of an oxygen function at C-6 combined with an *S*-configuration at C-3 was found to be characteristic for metabolites from Ancistrocladaceae species and was thus defined as a typical Ancistrocladaceae fingerprint.<sup>[50]</sup> The compounds from Dioncophyllaceae species, by contrast, showed no oxygen function at C-6 and a *3R*-configuration, they were thus named Dioncophyllaceae-type NIQs.<sup>[50]</sup> In some species, furthermore, so-called Ancistrocladaceae/Dioncophyllaceae hybrid-type alkaloids have been found, with RO-6 and *3R*,<sup>[50]</sup> and the inverse type featuring no oxygen function at C-6, but with a *3S*-configured isoquinoline portion.<sup>[50]</sup> Hence, all these aspects can be used to categorize the occurring group of metabolites.

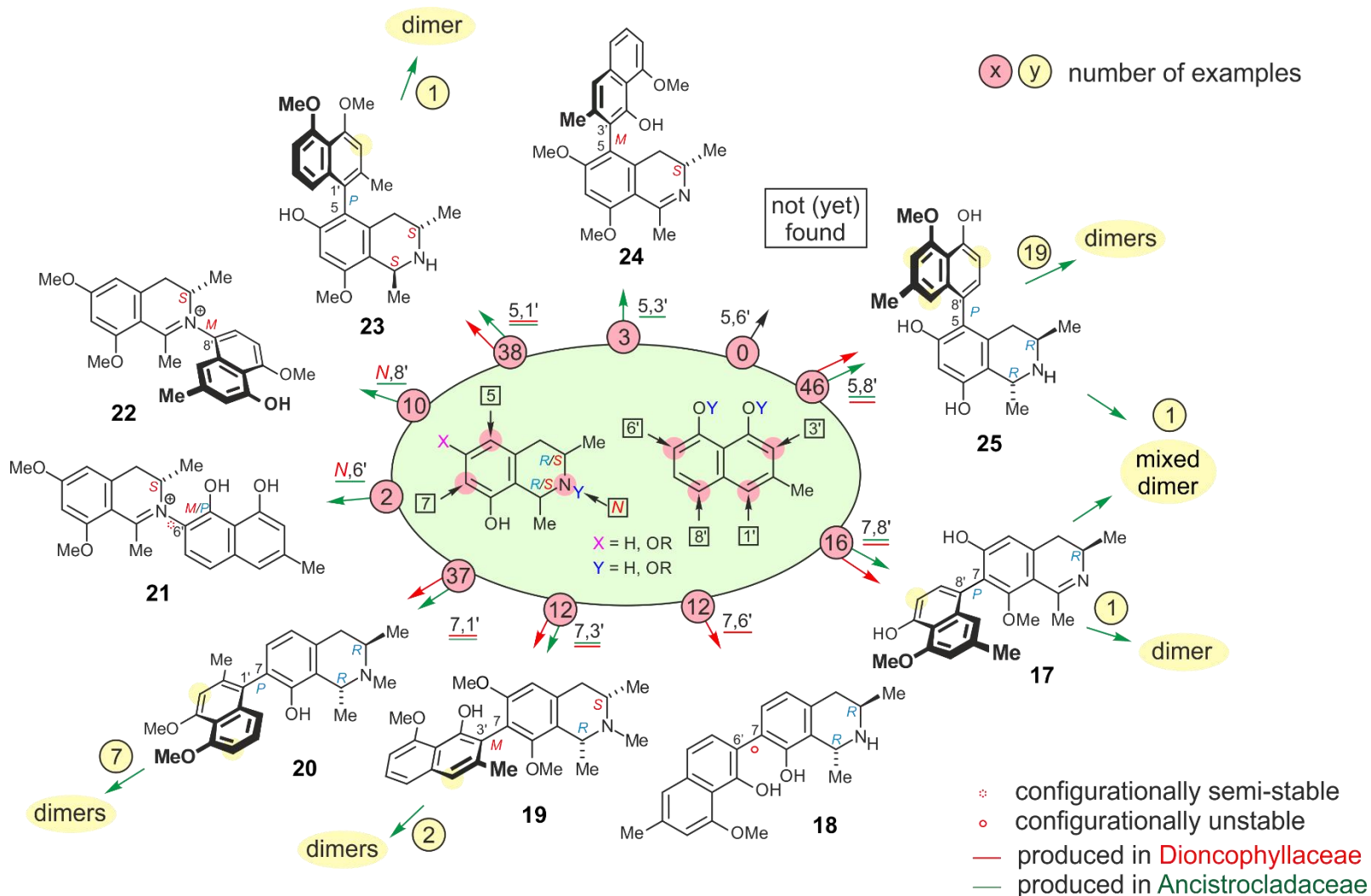


Figure 4. Naphthylisoquinoline alkaloids, structural diversity<sup>[85]</sup> and coupling possibilities: yaoundamine A (**17**), dioncophyllinol B (**18**), ancistrotectorine (**19**), *N*-methyldioncophylline A (**20**), ancistrocladinium B (**21**), 4'-*O*-demethyl-ancistrocladinium A (**22**), ancistrocladine (**23**), ancistrotanzanine A (**24**), and korupensamine A (**25**). Notice that some numbers are based on yet unpublished results.

Beyond the exceptional chemical variety, naphthylisoquinoline alkaloids are of high interest because of their significant anti-infective activities against diverse pathogens responsible for tropical diseases.<sup>[66, 83]</sup> More than a coincidence, these lianas occur in regions endemic to most of these infectious illnesses, hinting at an accommodation to the environment of the species.<sup>[46, 53, 86-88]</sup> Reports on the use of these plants in traditional medicine in Asia and Africa,<sup>[89-91]</sup> are clear indications of the high medicinal value of their active ingredients. From the knowledge gathered so far, and depending on the coupling type, the degree of steric hindrance at the biaryl axis, and the number of chiral elements, these alkaloids show a broad variety of biological activities against several parasites, *i.e.* *Plasmodium falciparum*, *Leishmania donovani*, and *Trypanosoma brucei*.<sup>[34, 83, 92-95]</sup> The cases of ancistrocladinium A (**26**),<sup>[92, 96]</sup> dioncophylline C (**27**),<sup>[93]</sup> dioncophylline A (**28**),<sup>[97]</sup> and ancistrolikokine B (**29**)<sup>[98]</sup> illustrate quite well this statement (Figure 5).

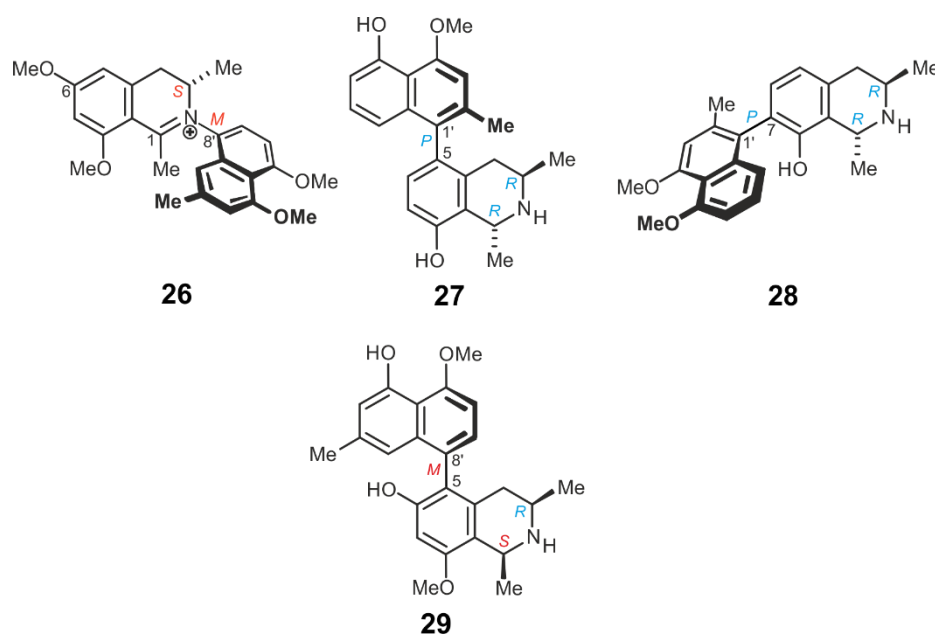


Figure 5. Selected monomeric naphthylisoquinoline alkaloids, with their respective half-maximal inhibitory concentrations ( $IC_{50}$ ) and selectivity indices (SI): ancistrocladinium (**26**) against *Leishmania major* ( $IC_{50}$  5.8  $\mu$ M, SI 7), dioncophylline C (**27**) against *Plasmodium falciparum* ( $IC_{50}$  10 nM), dioncophylline A (**28**) against *P. falciparum* ( $IC_{50}$  3.8  $\mu$ M), ancistrolikokine B (**29**) against *Trypanosoma brucei* ( $IC_{50}$  1.9  $\mu$ M, SI 43).

Most interesting is the ability of some plants species to synthesize dimeric NIQs from the monomeric units by further phenol-oxidative coupling reactions, thus enhancing the molecular complexity considerably.<sup>[99-101]</sup> The two classical monomers still have coupling positions to form an additional biaryl linkage. This new bridge is often a C,C-bond built up between the

two electron-rich naphthalene rings, leading to a complex molecular architecture consisted of three consecutive biaryl axes. The central one can be configurationally stable (or semi-stable), and thus constitute also an element of chirality.<sup>[101]</sup> When the coupled monomers are identical, like in the cases of ancistrogriffithine A (**30**)<sup>[102]</sup> and jozimine A<sub>2</sub> (**31**),<sup>[32]</sup> they are C<sub>2</sub>-symmetric. If different monomeric units are combined, *e.g.* like in michellamine F (**32**)<sup>[100]</sup> and mbandakamine A (**33**),<sup>[103]</sup> the dimers are unsymmetric. The dimers can be sub-classified based on the degree of steric hindrance at the central axis, which can be in general stable or unstable as depicted in Figure 6. Additionally, the challenges for the chromatographic resolution and structural assignment are enhanced by the occurrence of these dimeric naphthylisoquinoline alkaloids in the plant species. This fact also explains the limited number of known dimers before this work, *viz.* ca. 20 known only.

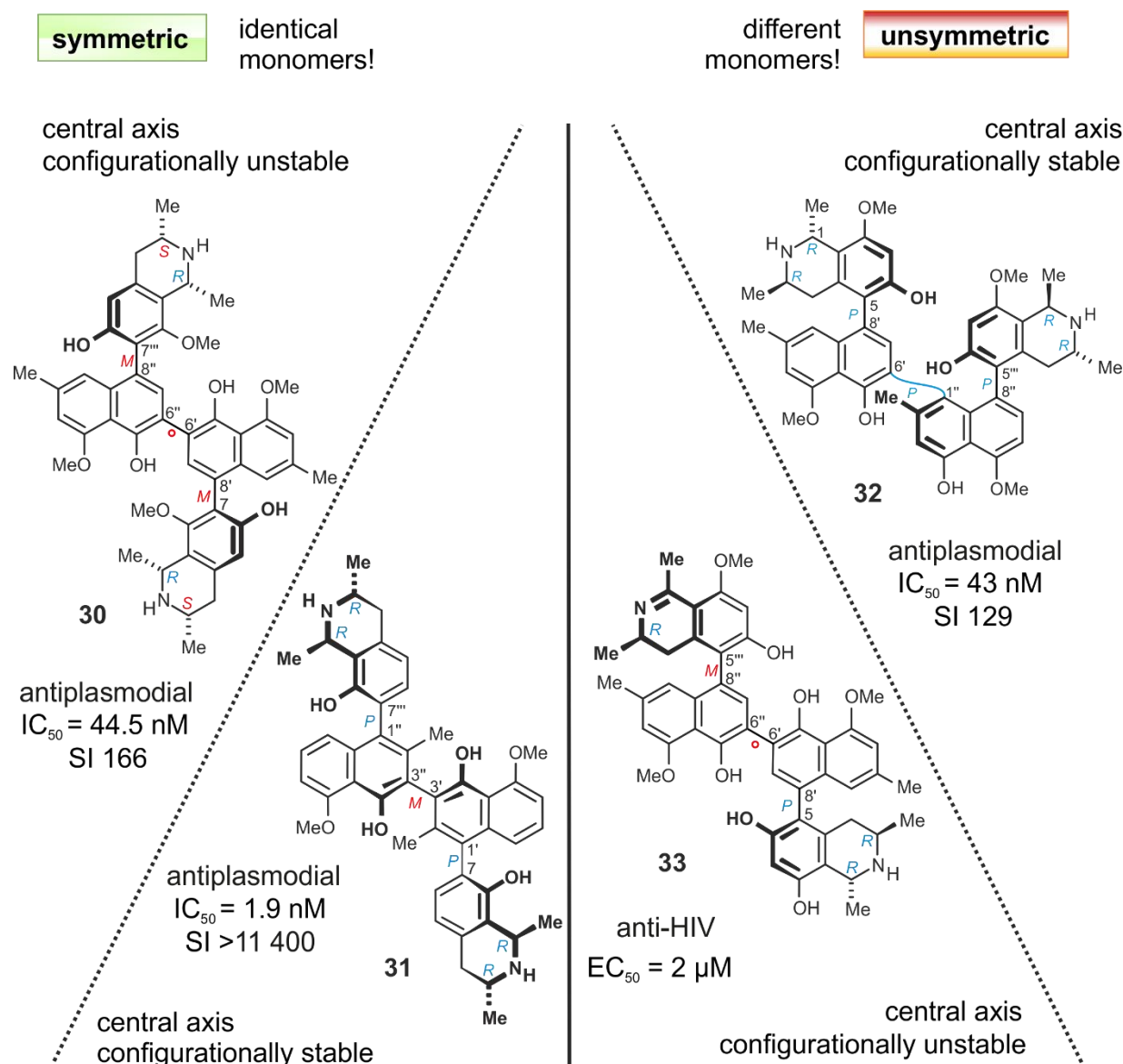


Figure 6. Classification of dimeric naphthylisoquinoline alkaloids, exemplified by ancistrogriffithine A (**30**), jozimine A<sub>2</sub> (**31**), mbandakamine A (**32**), and michellamine F (**33**). Notice also that the central axes can be semi-stable, thus, leading to the interconversion of both atropo-diastereomers.

Moreover, dimeric alkaloids have shown pronounced biological activities against a variety of pathogens responsible for tropical diseases and HIV responsible for AIDS.<sup>[103-104]</sup> The first known dimeric naphthylisoquinolines were the michellamines A-F from the Cameroonian species *A. korupensis*,<sup>[105-106]</sup> among which the most active michellamines B and F exhibited pronounced anti-HIV activities with half-maximal effective concentrations ( $EC_{50}$ ) of  $6 \text{ }\mu\text{M}$  and  $2 \text{ }\mu\text{M}$ , respectively.<sup>[100]</sup> The mixed dimer korundamine A was detected in this liana and has remained not fully assigned.<sup>[107]</sup> The first dimer from an Asian species, ancistrogriffithine A (**30**), was reported in *A. griffithii* and showed 7,8'-coupled building blocks linked by a 6',6''-central axis typical to michellamines.<sup>[102]</sup> In the Asian species *A. tectorius* a series of the five

shuangancistropectorines A-E was discovered, which displayed for the first time three axially chiral central axes, and very good antiplasmodial profiles (NF54) with  $IC_{50} = 52$  nM for shuangancistropectorine A.<sup>[101]</sup> Jozimine A<sub>2</sub> (**31**) was discovered from a hitherto undescribed Congolese *Ancistrocladus* species, which is the first dimer of a Dioncophyllaceae-type monomer and has meanwhile become the most active and selective naphthylisoquinoline against the strain NF54 of *P. falciparum* ( $IC_{50} = 1.9$  nM).<sup>[32]</sup> Remarkably, its monomeric portion, dioncophylline A,<sup>[108]</sup> was found to show only moderate antiplasmodial activity with an  $IC_{50}$  value of 3.8  $\mu$ M, further demonstrating the attractiveness of dimeric alkaloids as potential drug candidates.<sup>[34]</sup>

To be mentioned are the findings of further michellamines and the novel unsymmetric mbandakamines A and B dimers in *A. congolensis* and a probably new Congolese *Ancistrocladus* species, respectively.<sup>[103-104]</sup>

This overview provided strong hints that the Congolese *Ancistrocladus* species constitute an unexplored reservoir of dimeric alkaloids with useful bioactivities. To start a series of thorough metabolites screening in these less-investigated lianas, it was mandatory to learn more about the synthetic potential of the well-described<sup>[46]</sup> *A. ealaensis*.

*Ancistrocladus ealaensis* J. Léonard is a widespread Central African liana mainly occurring in the northwestern part of the Democratic Republic of the Congo.<sup>[45-46, 51]</sup> Foucher *et al.* had reported the isolation of five compounds with constitutions corresponding to 5,1'- and 7,1'-linked monomeric naphthylisoquinoline alkaloids from the stem and root barks of '*A. ealaensis*', namely ancistrine, ancistine, ancistrocladonine, ancistroealaensine, and the 'known' ancistrocladeine (constitutions not shown herein due to their unreliability).<sup>[109-111]</sup> The lack of any stereochemical and even spectroscopical consideration in the structural assignments of the isolated materials can be seen at first glimpse in the two papers. Apart from the unreliable chemical assignments, the authors had not addressed the absolute configurations at the stereogenic centers, even not a single allusion to the axial chirality present in the molecules described. Therefore, no credit can be given to such reports, which had overlooked crucial aspects while describing five compounds in this 'liana'. For this reasons, their reports were disregarded when our group started the reliable reinvestigation on *A. ealaensis*<sup>[98]</sup> in 2000.

The preliminary phytochemical studies led to the discovery of two 5,8'-coupled monomeric alkaloids, namely ancistroealaines A (**34**) and B (**35**) from root and stem barks, together with some related naphthoic acid derivatives as shown in Figure 7.<sup>[98]</sup> In contrast to the good



antileishmanial activity exhibited by **34**, both monomers displayed very poor antiplasmodial profiles. Therefore, *A. ealaensis* did not attract further phytochemical interests.

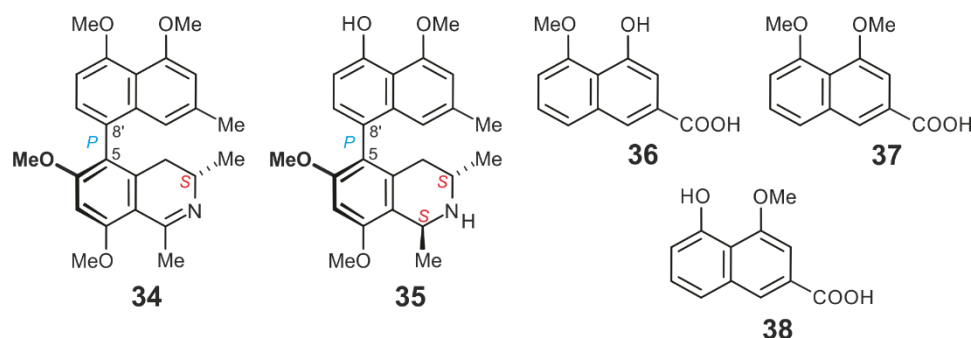


Figure 7. Structures of natural compounds reliably reported so far from *A. ealaensis*, namely ancistroealaine A (**34**), ancistroealaine B (**35**), eleutherolic acid (**36**), ancistronaphthoic acid A (**37**) and ancistronaphthoic acid B (**38**).<sup>[98]</sup>

Renewed interest has, however, arisen from the isolation of the structurally unique mbandakamines A and B,<sup>[45, 103]</sup> from a phylogenetically related and probably new *Ancistrocladus* species, triggering the necessity for further phytochemical investigations on *A. ealaensis*, to search for possible dimers.<sup>[45]</sup> This screening did not only aim at a discrimination of the plant species, but also to understand the chemotaxonomic position of *A. ealaensis* within the Central African related lianas.

In the course of these investigations, it turned out that this tropical liana was a rich source of unique structurally intriguing monomeric and dimeric alkaloids. By means of diverse mild extraction and isolation strategies, an unpredictable plethora of diverse metabolites was discovered. To reach this result, the full stereochemical assignment of naphthylisoquinoline alkaloids involved a combination of mass spectrometry, 1D and 2D NMR, electronic circular dichroism, quantum-chemical calculations, and ruthenium(VIII)-mediated oxidative degradation.<sup>[50, 112-113]</sup>

By means of the NMR technique,<sup>[114-115]</sup> the constitution and the relative configuration of naphthylisoquinoline alkaloids can be reliably addressed. In the case of overlapping signals, the thorough analysis of all the two-dimensional experiments (2D NMR) often enables the discrimination of overlying or merged signals. In the elucidation of the constitution, the <sup>13</sup>C NMR spectrum is less prone to drastic changes, so that significant shifts of signals reliably indicate a drastic modification of the carbon skeleton. Based on our experience and the published data, we have defined average values of chemical shifts for each position on the two basic building blocks observed for Ancistrocladaceae- (6-OR, 3*S*) and hybrid-type (6-OR, 3*R*)

alkaloids,<sup>[50]</sup> as depicted in Figure 8. The awareness of these values can enable a rapid guess of the relative configuration in tetrahydroisoquinoline units. In *N*-protonated (*N*-H) monomeric NIQs, a significant upfield shift of the signal corresponding to C-3 (on the <sup>13</sup>C spectrum) from ca. 44 to ca. 51 ppm is a strong hint at a 1,3-*cis*-relative configuration. The diaxial orientation of the protons at positions 1 and 3 can also be monitored by NOESY for confirmation. In *N*-methylated (*N*-Me) *cis*-configured tetrahydroisoquinolines, both the C-1 and C-3 are shifted downfield from ca. 56 and 47 to ca. 61 and 60 ppm, respectively. All drastic changes of these defined values, in particular for <sup>13</sup>C NMR, would be the first hint at a major modification in the core structure.

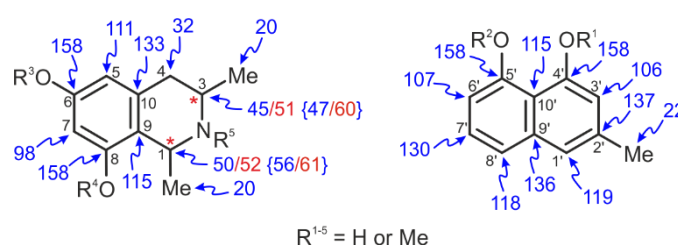


Figure 8. Average <sup>13</sup>C-chemical shifts of all the positions on the two building blocks of naphthylisoquinoline alkaloids (Ancistrocladaceae and hybrid types). The characteristic average values for 1,3-*cis*-configured tetrahydroisoquinolines in red, and in blue for *trans*. Shift values for *N*-methylated tetrahydroisoquinolines *trans* (in blue) / *cis* (in red) in curly brackets.

Besides the relative configuration, which is established by NOESY or ROESY experiments, the assignment of the absolute configuration is quite laborious due to the presence of stereocenters and biaryl axes. It requires information from NOE or ROE for the relative assignments, from electronic circular dichroism (ECD) spectra for the chiral axial configuration, and from the results of the ruthenium(VIII)-mediated oxidative degradation<sup>[113]</sup> for the stereogenic centers. The ECD spectra can be compared to those of related compounds of known absolute configuration, usually of the same coupling type and differing by the methoxy-hydroxy pattern.<sup>[112, 116]</sup> In the case of a novel structure, conformational analysis and quantum-chemical calculations to predict the experimental ECD spectrum are carried out.<sup>[103, 117]</sup> So far, DFT-based quantum-chemical calculations are used for this purpose, because of the attractive combination of computational robustness, accuracy and low computational costs.<sup>[118-119]</sup>

An additional structural proof can be provided by performing an X-ray analysis of single crystals of the natural product.<sup>[97]</sup> This can be also achieved by chemical derivatization of the compound, aiming at the introduction of a heavy atom in the constitution to enable the

---

assignment of the absolute configuration. In the case of affordable single crystals of the natural alkaloid,<sup>[32, 97]</sup> at least its constitution can be confirmed by X-ray. Details on the techniques can be found in the literature,<sup>[120-123]</sup> and their pertinent aspects will be addressed together within the results and discussions section.

## I.2. Introduction to 2,3-Dihydrobenzo[ $\beta$ ]furan Neolignans and *Gardenia ternifolia*

Lignans and neolignans represent groups of widely distributed plant secondary metabolites, showing a broad structural diversity.<sup>[124]</sup> Biosynthetically, they arise from the shikimic acid pathway, formed by dimerization of two phenylpropenoid units.<sup>[124-125]</sup> Many representatives from this class of natural products showed promising biological properties.<sup>[126-127]</sup> In particular, in the sub-group of 2,3-dihydro[ $\beta$ ]benzofuran neolignans (2,3-DBFs), metabolites exhibiting antiviral,<sup>[128]</sup> antiparasitic,<sup>[129-130]</sup> antioxidant,<sup>[131-133]</sup> cytotoxic,<sup>[128, 133-135]</sup> PGI<sub>2</sub> release inducer,<sup>[136]</sup> or antiplatelet<sup>[137]</sup> activities were identified, showing the importance of these widely distributed metabolites in the plant kingdom. Exemplarily depicted in Figure 9 are three naturally occurring 2,3-DBFs with related structures.<sup>[129, 138]</sup>

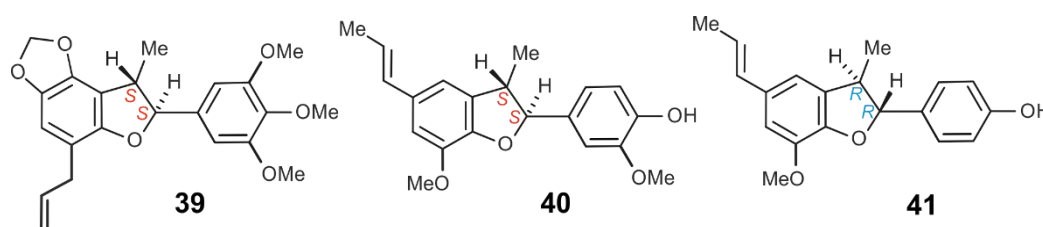


Figure 9. Selected naturally occurring 2,3-dihydrobenzofuran neolignans: the antiplasmodial (IC<sub>50</sub> 0.45  $\mu$ M) ococymosin (**39**),<sup>[129]</sup> the neuroprotective (+)-licarin A (**40**) and (2*R*,3*R*)-2,3-dihydro-2-(4-hydroxyphenyl)-7-methoxy-3-methyl-5-(*E*)-propenylbenzofuran (**41**).<sup>[138]</sup>

Despite the occurrence of a plethora of known 2,3-dihydro[ $\beta$ ]benzofuran neolignans,<sup>[124, 126, 129]</sup> the unambiguous determination of the absolute configuration of 2,3-DBFs has remained an exciting task.<sup>[138-140]</sup> Several cases of misleading assignments and structural revisions have been known from literature,<sup>[138, 140-141]</sup> and some natural products have even remained without a reliable attribution of the absolute stereostructures.<sup>[136, 142-143]</sup> For the determination of the full three-dimensional structures of these neolignans, several techniques have been used, namely NMR spectroscopy, X-ray crystallography, electronic circular dichroism (ECD) spectroscopy, optical rotatory dispersion (ORD), interpretation of proven chiroptical rules, and quantum-chemical ECD calculations.<sup>[141-147]</sup>

The determination of the relative configuration in the furan ring is usually assigned by NOESY experiments.<sup>[145]</sup> In case of ambiguous interactions within this tight furan ring, the relative configuration is firmly established by NOE difference (NOEDIFF) experiments.<sup>[142]</sup> These NOEDIFF experiments, also known as mono-dimensional NOE experiments (1D-NOE)

proceed by targeted irradiations of proton signals in order to enhance selectively the signals corresponding to the protons in their spatial proximity.<sup>[148-149]</sup> Only the proton signals in the vicinity of the one irradiated are enhanced, and, thus, to be seen on the NOEDIFF spectrum.<sup>[148-149]</sup> In the case of 2,3-DBFs, if the irradiation of H-7 does not induce the enhancement of H-8, their relative *trans*-orientation can be deduced. Most naturally occurring 2,3-DBFs displayed the *trans*-relative configuration in the furan ring, which is thermodynamically most stable.<sup>[140, 150-151]</sup> The natural occurrence of *cis*-configured 2,3-DBFs had been scarcely reported in the literature, and to the best of our knowledge only once reliably.<sup>[152]</sup> Besides, the coupling constant of H-7 and H-8 was incorrectly used to elucidate the relative configuration of such compounds.<sup>[153]</sup> This inappropriated practice may lead to wrong assignments.<sup>[143]</sup>

For the attribution of the absolute configurations of 2,3-DBFs, the 'absolute' conformation of the fused dihydrofuran ring has to be deduced from the sign of the  $^1L_b$  band of the ECD spectrum corresponding to its helicity.<sup>[141-142, 152, 154]</sup> This helicity describes the chirality of the furan heterocycle, as depicted in Figure 10, which adopts an envelope-like half-chair conformation, with a defined dihedral angle of the bonds a *versus* c.<sup>[141, 154]</sup> The aryl substituent at C-7 is decisive for the respective conformation of the dihydrofuran portion, since it tends to adopt an equatorial orientation, regardless of the configuration at C-8, where usually a 'slender' substituent can be in axial or equatorial position. Consequently, *S*-configuration at C-7 leads to a so-called *P*-helicity, as shown in Figure 10, while *7R* implies *M*-helicity. The chiroptical rule established by Snatzke *et al.*<sup>[155-157]</sup> permits the deduction of this helicity – and thus the absolute configuration at C-7 – from the sign of the Cotton effect within the  $^1L_b$  band (around 270–300 nm) of the ECD spectrum.<sup>[141, 154]</sup> It is also known<sup>[141, 154]</sup> that the substitution at C-6' of the benzene ring by an achiral group having a large spectroscopic moment such as hydroxy, alkoxy, or alkenyl residues, results in an inversion of the sign of the Cotton effect in the  $^1L_b$  band, even though the absolute configuration and conformation of the furan ring remains unchanged. Therefore, the presence of a methoxy group at C-6' implies the application of the reversed helicity rule<sup>[141, 154]</sup>. According to this modified chiroptical rule, *P*-helicity of the dihydrofuran ring should lead to a positive sign of the  $^1L_b$  band in the ECD spectrum (Figure 10) and, *vice versa*, *M*-helicity should result in a negative Cotton effect.<sup>[141, 154]</sup>

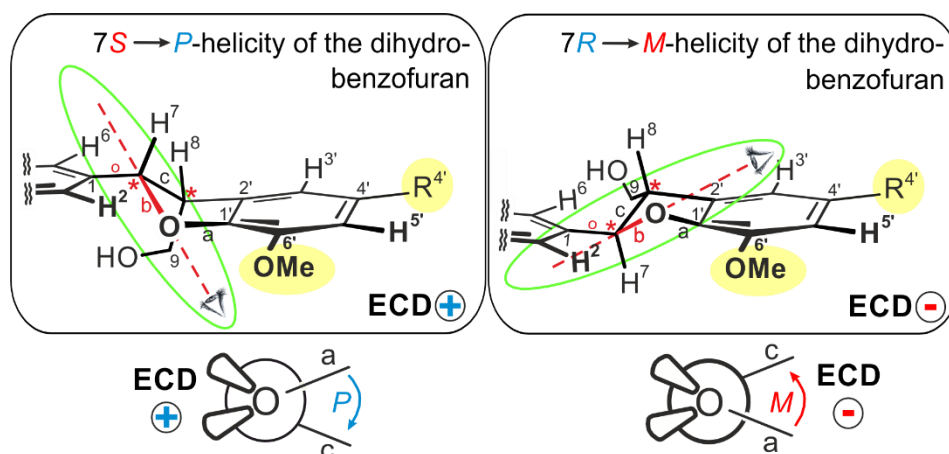


Figure 10. Assignment of the dihydrofuran ring helicity based on the reversed helicity rule and the ECD sign of the Cotton effect at the  $^1L_b$  band for substituted 2,3-dihydrobenzo[ $\beta$ ]furans.

The preliminary investigations on authorized Congolese herbal products<sup>[158]</sup> led to the screening of constitutive plants. One of them, the African evergreen shrub species *Gardenia ternifolia* Schumach. & Thonn. (Rubiaceae) was well known in traditional medicine for its virtues against infectious diseases.<sup>[159]</sup> Despite its wide use and long-time description, the species had remained phytochemically less investigated.<sup>[160]</sup> Most scientific reports concerning *G. ternifolia* dealt with biological evaluations of crude extracts without isolation of the active ingredients.<sup>[160-161]</sup> Therefore, virtually nothing had been reported on its chemical constituents. Since most available medical drugs are structurally chiral, a strong emphasis is put on stereochemical aspects, all over this thesis.

## **II. Results and Discussions**

## II.0. A. ealaensis, a Rich Source of Naphthylisoquinoline Alkaloids

During the last decades, a plethora of alkaloids, ca. 180 representatives, has been discovered in many *Ancistrocladus* species. However, *Ancistrocladus ealaensis*, which is a quite well-described species and largely distributed in Central Africa, has remained less investigated.<sup>[98]</sup> The discovery of mbandakamines A and B,<sup>[103]</sup> from a probably new *Ancistrocladus* taxon, phylogenetically related to *A. ealaensis*,<sup>[45]</sup> raised the necessity to re-investigate this tropical liana.

Extracts produced from several parts of *A. ealaensis* were systematically screened by LC-DAD and LC-MS<sup>[162]</sup> (Figure 11). Most interestingly, biological assays of these extracts indicated that the twigs and the leaves extracts were quite promising in terms of active metabolites (Table 1). Indeed, the crude extract of the twigs was found to be active against *Trypanosoma brucei rhodesiense*, *Trypanosoma cruzi*, and *Leishmania donovani* with IC<sub>50</sub> values of 0.59, 0.32, and 0.42  $\mu\text{g mL}^{-1}$ , respectively. The crude leaf extract, by contrast, exhibited high and specific antiplasmodial activity with IC<sub>50</sub> = 0.52  $\mu\text{g mL}^{-1}$ , with the highest selectivity index (SI: 113) in the series. Based on these results, the biologically promising extracts of leaves and twigs were systematically analyzed by LC-MS-DAD guided screening to reveal the presence of further constituents, in particular, those with MS and UV profiles typical of monomeric and dimeric naphthylisoquinoline alkaloids.



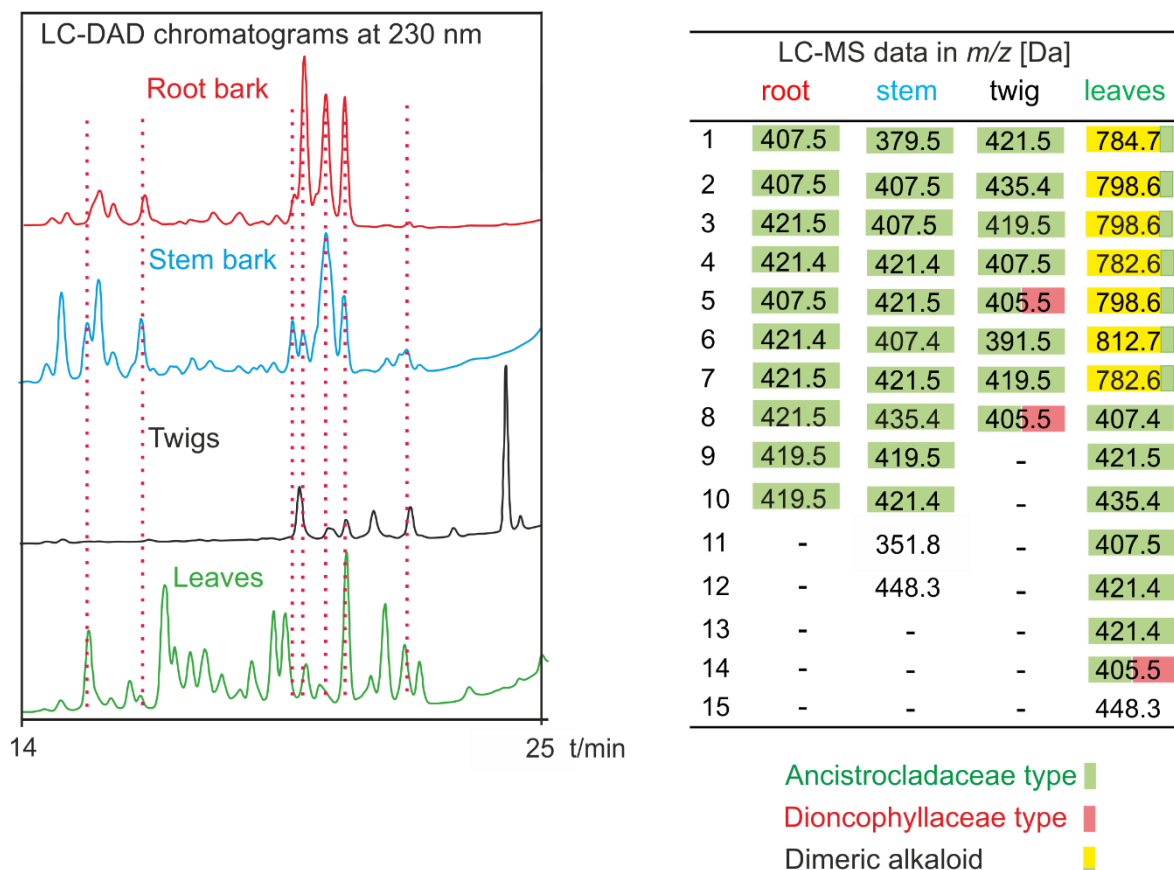


Figure 11. LC-DAD chromatograms at the wavelength of 230 nm and LC-MS data of the analyzed plant materials of *A. ealaensis*.

Table 1. Biological evaluation of the methanolic extracts of plant material of *A. ealaensis* against *Trypanosoma brucei rhodesiense*, *T. cruzi*, *Leishmania donovani*, *Plasmodium falciparum* (strain: NF54).<sup>[162]</sup> Also the cytotoxicities against rat skeletal myoblasts, L6 cells, ( $IC_{50}$  in  $\mu M$ ).<sup>[162]</sup>

Samples	<i>T. bruc. rhod.</i> $IC_{50}$ [ $\mu g mL^{-1}$ ]	<i>T. cruzi</i> $IC_{50}$ [ $\mu g mL^{-1}$ ]	<i>L. don.</i> $IC_{50}$ [ $\mu g mL^{-1}$ ]	<i>P. falc.</i> $IC_{50}$ [ $\mu g mL^{-1}$ ]	Cytotox. L6 $IC_{50}$ [ $\mu g mL^{-1}$ ]	Selectivity index ( $L6_{50}/IC_{50}$ )
Reference	0.003 <sup>[1]</sup>	0.528 <sup>[2]</sup>	0.079 <sup>[3]</sup>	0.002 <sup>[4]</sup>	0.007 <sup>[5]</sup>	-
Stem bark	16.85	59.05	30.65	3.98	60.1	15
Leaves	15.42	49.10	23.15	0.52	58.7	113
Root bark	14.75	42.10	30.30	3.02	55.2	18
Twigs	0.59	0.32	0.42	2.43	38.2	16

[1] Melarsoprol. [2] Benznidazole. [3] Miltefosine. [4] Chloroquine. [5] Podophyllotoxin.

The approach developed during these studies, based on an MS-UV metabolite targeting (Figure 12) and spectroscopic elucidation of purified material, permitted the isolation and full characterization of unknown metabolites, namely four new naphthalene-devoid isoquinoline alkaloids, as well as 13 new monomeric and 14 new dimeric naphthylisoquinoline alkaloids.

From these investigations, many quateraryls of the type naphthylisoquinoline in this liana were discovered. Remarkably, one dimer turned out to be the as yet most active naphthylisoquinoline against the chloroquine/pyrimethamine-resistant strain K1 of *P. falciparum*. A whole series of seven novel cage-like dimeric alkaloids was also discovered, featuring an unprecedented scaffold and the probable biosynthesis proven by a biomimetic synthesis. Along with these new compounds, eight known monomers and one recently reported dimer were isolated. The herein reported results make this initially neglected plant species the best investigated source of interesting and structurally diverse natural products of the type naphthylisoquinoline alkaloids. This achievement enabled also a better understanding of the chemo-taxonomical position of *A. ealaensis* within the other species found in the Congo Basin.

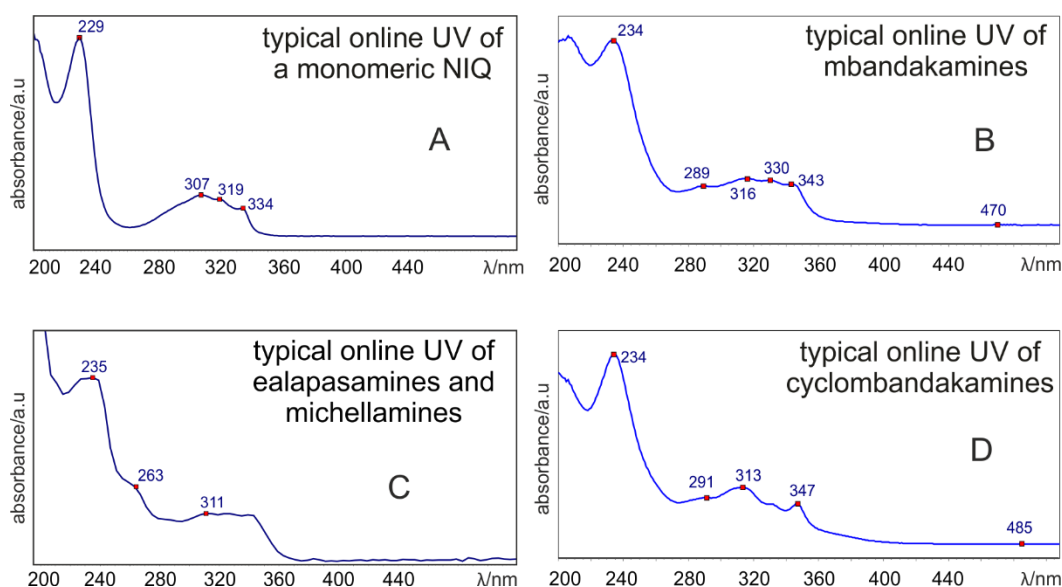


Figure 12. Typical online UV spectra of monomeric naphthylisoquinolines (A), the dimeric mbandakamines (B), ealapasamines (C), michellamines (C), and cyclombandakamines (D).

## II.1. Ealapasamines, the First Fully Characterized 'Mixed' Heterodimers

LC-MS and LC-DAD guided analysis of an enriched alkaloidal leaf fraction of *A. ealaensis* revealed the presence of further constituents, with MS profiles typical of dimeric naphthylisoquinoline alkaloids. For the isolation of these compounds, ground air-dried leaves were macerated with MeOH, and the resulting extract was partitioned between water and dichloromethane to abstract the metabolites of interest, according to the protocol described in the experimental section. This procedure involved for the first time an efficient fractionation by preparative liquid chromatography using RP<sub>18</sub> material. In two repeats, advanced fractions have been obtained for preparative-HPLC isolation, which provided, in this case, the three new dimers. Their typical UV spectrum corresponded to Figure 12C, and the HPLC chromatogram is depicted in Figure 13. The high degree of coelution in the advanced fraction A can be seen by the acquisition of the chromatograms at different wavelengths in this illustration.

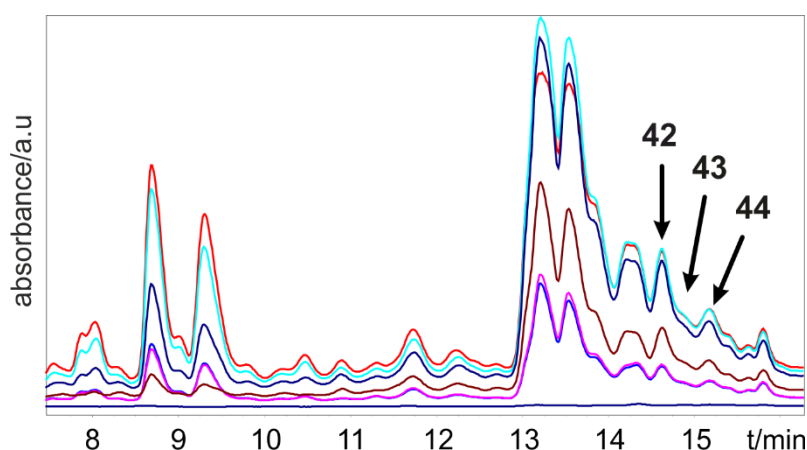


Figure 13. Chromatograms of an advanced fraction of leaf extract (fraction A) – recorded at several wavelengths – containing the three dimeric naphthylisoquinoline alkaloids ealapasamines A (**42**), B (**43**), and C (**44**).

Herein is described the isolation and structural elucidation of three unusual heterodimers, named ealapasamine A (**42**), ealapasamine B (**43**), and ealapasamine C (**44**), naturally occurring in *A. ealaensis* (Figure 14). These 'mixed', constitutionally unsymmetric quateraryls are the first stereochemically fully characterized products of 5,8'- and 7,8'-coupled naphthylisoquinoline monomers linked *via* C-6' of their naphthalene moieties. This is the highest degree of coupling unsymmetry known so far within this class of alkaloids. The compounds exhibited excellent and specific antiplasmodial activities, in the low nanomolar

range, on *P. falciparum*. An oxidized product of the natural product **44** was also generated and named ealapasamine C<sub>2</sub> (**45**).

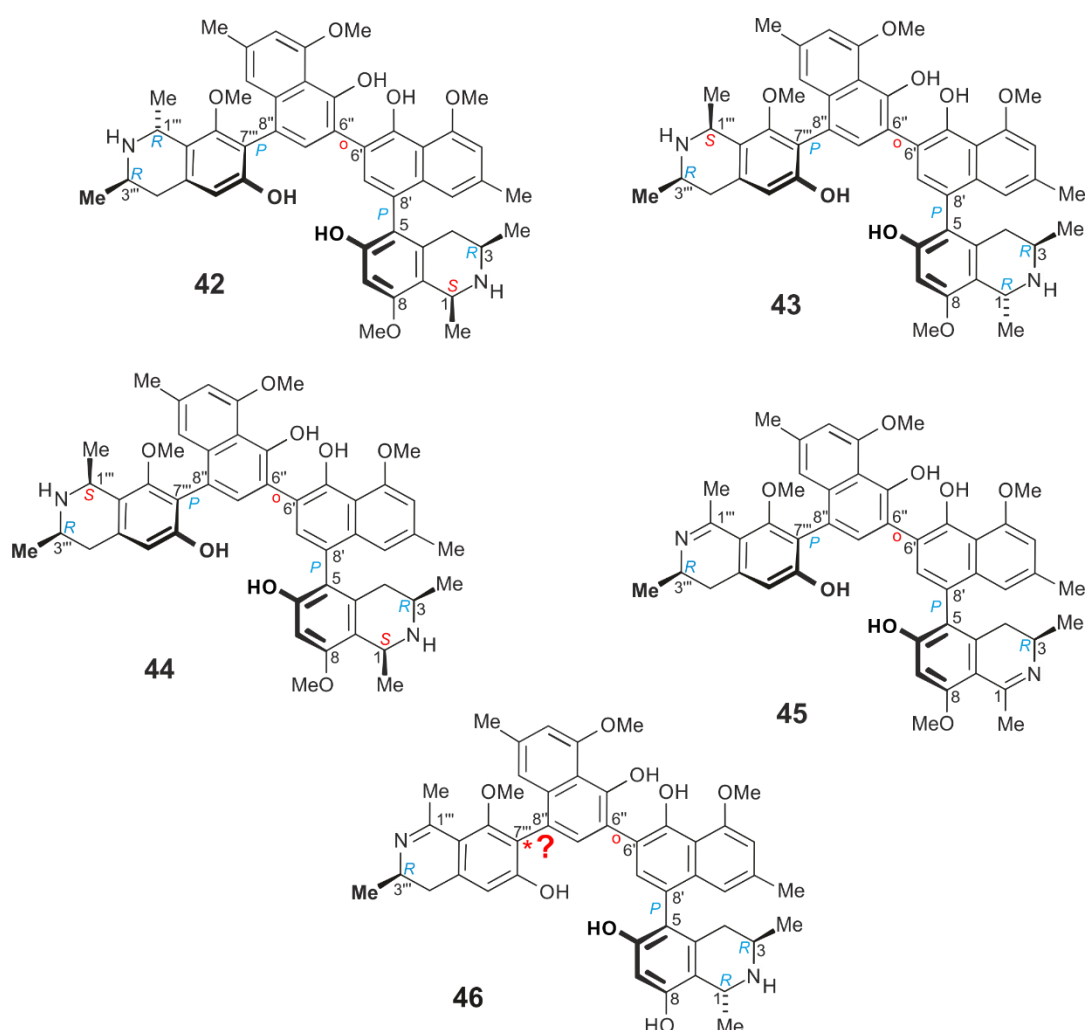


Figure 14. Ealapasamines A-C (**42-44**), unusual mixed heterodimeric naphthylisoquinoline alkaloids from *A. ealaensis*, and the related korundamine A (**46**)<sup>[107]</sup> previously isolated from *A. korupensis*. The unnatural ealapasamine C<sub>2</sub> (**45**), obtained analytically by air oxidation of **44**.

The main results described in this chapter were published in *Scientific Reports* and the text herein adapted from the manuscript upon permission.<sup>[163]</sup>

## Structural elucidation and discussion

The first dimer was obtained as a colorless solid. By HRESIMS, the molecular formula was determined to be  $C_{48}H_{52}N_2O_8$  from an  $m/z$  fragment at 785.37804  $[M+H]^+$  (calcd for  $C_{48}H_{53}N_2O_8$ , 785.38019). The formula suggested either the presence of the known dimers, mbandakamines A and B<sup>[103]</sup> or ancistrogriffithine A,<sup>[102]</sup> or a new metabolite. The  $^1H$  NMR spectrum showed a full set of signals, hinting at the presence of an unsymmetric dimer. DEPT-135, HSQC, HMBC, and COSY data indicated the presence of 24 protonated carbon atoms, among them eight aromatic methine groups belonging to six spin systems at  $\delta_C = 135.2$  (C-7''), 134.7 (C-7'), 119.8 (C-1''), 119.1 (C-1'), 111.2 (C-5'''), 108.0 (C-3'), 107.9 (C-3''), 99.3 ppm (C-7), two methylene functions  $\delta_C = 34.5$  ppm (C-4'''), 33.1 (C-4), and four aromatic *O*-methyl groups  $\delta_C$  60.9 (C-8'''), 57.0 (C-4'), 57.0 (C-4''), 55.9 ppm (on C-8). The unsymmetric structure, as also confirmed by the presence of 48 signals in the  $^{13}C$  NMR spectrum, excluded the known  $C_2$ -symmetric dimer ancistrogriffithine A, which has the same molecular formula. The only other dimers having the same molecular formula, mbandakamines A and B, showed substantially different NMR spectra as compared to the alkaloid now isolated from *A. ealaensis*, i.e., the lack of *ortho*-coupled aromatic doublets in the  $^1H$  NMR spectrum evidenced the occurrence of a new metabolite.

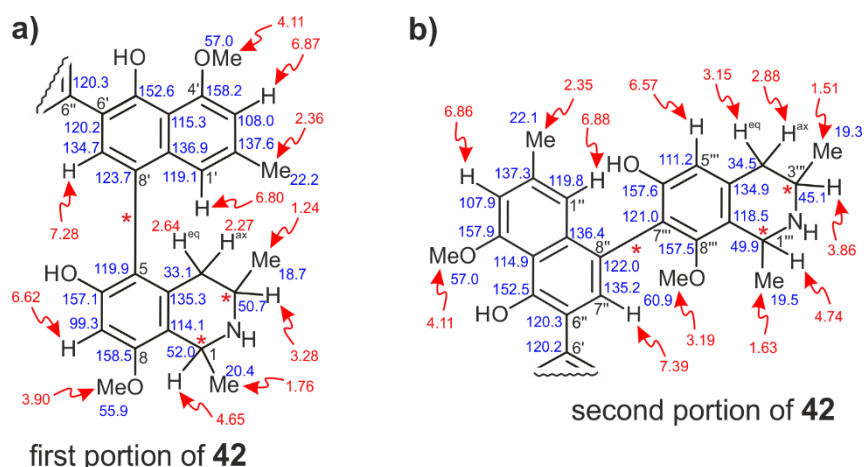


Figure 15. (a) The southeastern and (b) the northwestern molecular portions of ealapasamine A (**42**),  $^1H$  and  $^{13}C$  NMR chemical shifts in red and blue, respectively.

The 'southeastern' half of the new dimer displayed a total of four aromatic protons in the  $^1H$  NMR spectrum (Figure 15a). This portion furthermore showed the presence of one aromatic singlet, H-7' ( $\delta_H = 7.28$  ppm), two aromatic protons with a *meta*-coupling pattern, H-1' ( $\delta_H =$

6.80, d,  $J = 1.18$  Hz) and H-3' ( $\delta_{\text{H}} = 6.87$ , d,  $J = 1.22$  Hz), one aromatic methyl group, 2'-CH<sub>3</sub> ( $\delta_{\text{H,C}} = 2.36$ , 22.2), one methoxy function, 4'-OCH<sub>3</sub> ( $\delta_{\text{H,C}} = 4.11$ , 57.0), and one isolated proton, H-7' ( $\delta_{\text{H}} = 6.80$ , d,  $J = 1.18$  Hz). HMBC correlations were monitored from H-1' and H-3' to 2'-CH<sub>3</sub> (Figure 16a), from H-3' and 4'-OCH<sub>3</sub> to C-4' ( $\delta_{\text{C}} = 158.2$ ), and from H-7' to C-5' (C-OH,  $\delta_{\text{C}} = 152.6$ ), to C-9' ( $\delta_{\text{C}} = 136.9$ ), to C-5 ( $\delta_{\text{C}} = 119.9$ ), and to C-6'' ( $\delta_{\text{C}} = 120.3$ ). ROESY interactions of H-3' with both, 2'-CH<sub>3</sub> and 4'-OCH<sub>3</sub> confirmed the presence of a 6',8'-bisubstituted naphthalene subunit, which assignment agreed with the HMBC, HSQC, COSY, and DEPT-135 data (see experimental part). Moreover, a substituted tetrahydroisoquinoline subportion was assigned according to a shielded aromatic proton at  $\delta_{\text{H}} = 6.62$  (H-7), one aromatic methoxy group at  $\delta_{\text{H}} = 3.90$  (8-OCH<sub>3</sub>), two diastereotopic protons, 4-H<sub>eq</sub> ( $\delta_{\text{H}} = 2.64$ , dd,  $J = 3.35$ , 17.78 Hz) and 4-H<sub>ax</sub> ( $\delta_{\text{H}} = 2.27$ , dd,  $J = 12.14$ , 17.37 Hz), two methyl groups, 1-CH<sub>3</sub> ( $\delta_{\text{H}} = 1.76$ , d,  $J = 6.70$  Hz) and 3-CH<sub>3</sub> ( $\delta_{\text{H}} = 1.24$ , d,  $J = 6.52$  Hz), one quartet, H-1 ( $\delta_{\text{H}} = 4.65$ , q,  $J = 6.63$  Hz), and one multiplet, H-3 ( $\delta_{\text{H}} = 3.28$ , m). The position of H-7 was confirmed by its HMBC cross peaks with C-6 (C-OH,  $\delta_{\text{C}} = 157.2$ ), C-8 (C-OCH<sub>3</sub>,  $\delta_{\text{C}} = 158.0$ ), C-9 ( $\delta_{\text{C}} = 114.1$ ), and C-1 ( $\delta_{\text{C}} = 52.0$ ). HMBC correlations from H-7, H-7', and 4-H<sub>eq</sub> to C-5 ( $\delta_{\text{C}} = 119.9$ ) proved that the two subunits of this monomeric half were 5,8'-coupled and, thus, linked *via* a rotationally hindered biaryl axis.

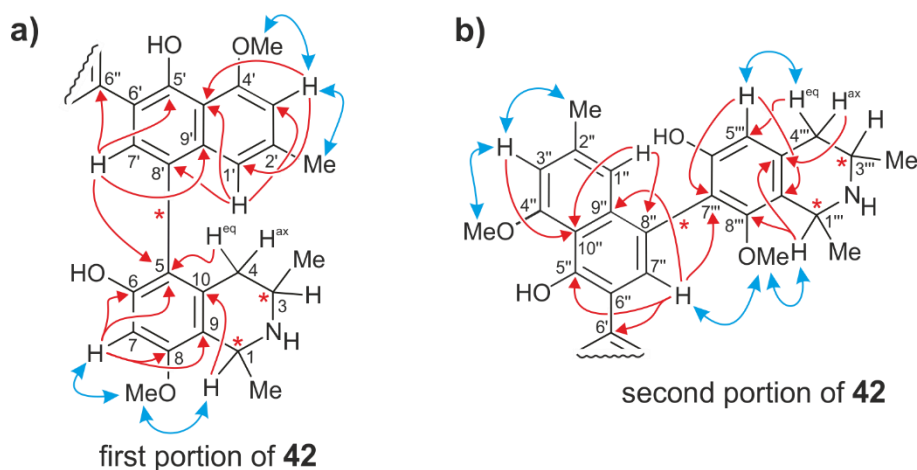


Figure 16. HMBC (red arrows) and ROESY (black arrows) interactions indicative of the constitutions of the southeastern (a) and the northwestern (b) moieties of **42**.

The position of the methoxy substituent at C-8 was corroborated by its ROE correlations with H-7 and H-1 (Figure 17a). The ROESY interactions between H-1 and H-3 supported the relative *cis*-configuration at the two stereogenic centers in the isoquinoline moiety. The shielded chemical shift of C-3 ( $\delta_{\text{C}} = 50.7$ ) was also in agreement with this assignment. The

ROESY correlations between 8-OCH<sub>3</sub> and H-1, 1-CH<sub>3</sub>, and H-7, and between 4'-OCH<sub>3</sub> and H-3', agreed with the proposed constitution for the southeastern half as depicted in Figures 15 and 17a. The absolute configurations at the chiral centers C-3 and C-3''' were determined to be *R* by ruthenium-mediated oxidative degradation,<sup>[113]</sup> providing (*R*)-3-aminobutyric acid. Due to the above-established relative *cis*-configuration at C-1 *versus* C-3, the absolute configuration at C-1 was deduced to be *S*. Based on the ROESY interactions from H-1' to 4-H<sub>ax</sub> and 1-CH<sub>3</sub>, and from 4-H<sub>eq</sub> to H-7', the axial configuration in this southeastern portion was assigned as *P* (Figure 17a).

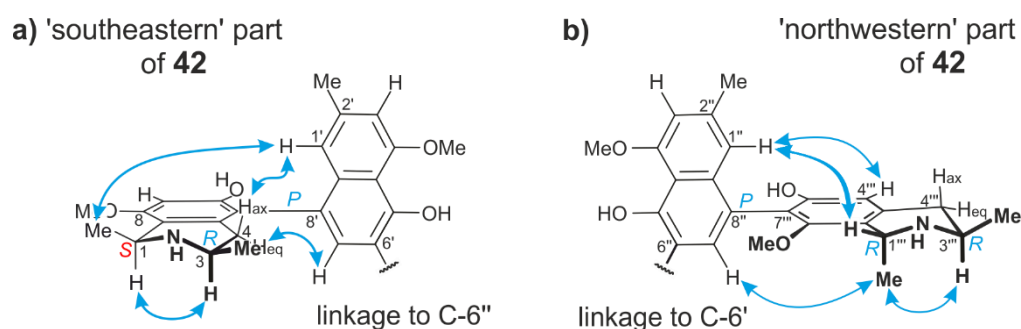


Figure 17. ROESY interactions defining the relative configurations at the stereogenic centers and axes within the monomeric halves of **42**: (a) for the 5,8'-coupled part, and (b) for the 7,8'-linked portion.

The NMR data corresponding to the second molecular half displayed one isolated singlet at  $\delta_{\text{H}}$  7.39 (s, H-7'',  $\delta_{\text{C}}$  = 135.2 ppm), two doublets with a *meta*-coupling pattern at  $\delta_{\text{H}}$  6.88 (d,  $J$  = 1.18 Hz, H-1'',  $\delta_{\text{C}}$  119.8) and 6.86 (d,  $J$  = 1.16 Hz, H-3'',  $\delta_{\text{C}}$  = 107.9), one methoxy group at  $\delta_{\text{H}}$  4.11 (s, 4''-OCH<sub>3</sub>,  $\delta_{\text{C}}$  = 57.0), a methyl group at  $\delta_{\text{H}}$  2.35 (s, 2''-CH<sub>3</sub>,  $\delta_{\text{C}}$  = 22.1), reminiscent of the naphthalene subunit in the southeastern portion. These assignments agreed with the HSQC and HMBC correlations (Figures 15b and 16b). 1D and 2D NMR data revealed further aromatic and heterocyclic spin systems, namely an aromatic singlet at  $\delta_{\text{H}}$  6.57 (s, H-5''',  $\delta_{\text{C}}$  = 111.2), a quartet at 4.74 (q,  $J$  = 6.77 Hz, H-1''',  $\delta_{\text{C}}$  = 49.9), a multiplet at  $\delta_{\text{H}}$  = 3.86 (m, H-3''',  $\delta_{\text{C}}$  = 45.1), two doublets of doublets for the diastereotopic protons at C-4''' at  $\delta_{\text{H}}$  3.15 (dd,  $J$  = 4.81, 17.58 Hz, 4'''-H<sub>eq</sub>,  $\delta_{\text{C}}$  = 34.5) and 2.88 (dd,  $J$  = 11.72, 17.78 Hz, 4'''-H<sub>ax</sub>,  $\delta_{\text{C}}$  = 34.5), one high-field shifted methoxy group at  $\delta_{\text{H}}$  3.19 (s, 8'''-OCH<sub>3</sub>,  $\delta_{\text{C}}$  = 61.0), two methyl groups at  $\delta_{\text{H}}$  1.63 (d,  $J$  = 6.90 Hz, 1'''-CH<sub>3</sub>,  $\delta_{\text{C}}$  = 19.5) and 1.51 (d,  $J$  = 6.87 Hz, 3'''-CH<sub>3</sub>,  $\delta_{\text{C}}$  = 19.3). The HMBC interactions from H-5''' to C-4''', to C-7''' ( $\delta_{\text{C}}$  = 121.0), and to C-6''' (C-OH,  $\delta_{\text{C}}$  = 157.6), and from H-1''' to C-8''' ( $\delta_{\text{C}}$  = 157.5) suggested the presence of a tetrahydroisoquinoline subunit with no substituent at C-5'''. Moreover, the HMBC interactions from H-5''' and H-7'' to C-7''',

and from H-7'' to C-9'' ( $\delta_C = 136.4$ ) and C-5'' ( $\delta_C = 152.5$ ) revealed that the naphthalene and isoquinoline subunits of this northwestern portion were connected *via* a 7''',8''-biaryl axis (Figure 16b). In the ROESY spectrum, the cross peaks between H-3''' and the protons of 1'''-CH<sub>3</sub> established the relative configuration of the stereocenters at C-1''' and C-3''' to be *trans* (Figure 17b), in contrast to the observed *cis*-configured subunit in the southeastern molecular portion. The oxidative degradation procedure again delivered only (*R*)-3-aminobutyric acid, thus the absolute configurations at C-3''' and C-1''' were attributed to be *R*.

Monomeric naphthylisoquinolines with a 7,8'-linkage are most challenging to be structurally assigned by NOEs and/or ECD, in particular when being part of a dimer.<sup>[102, 164]</sup> The stereogenic center at C-1''', with its spin systems H (above the isoquinoline plane) and CH<sub>3</sub> (below), was spatially quite close to the axis, which permitted long-range ROE interactions across the axis over to the naphthalene part. Thus, ROESY correlations between H-7'' and the axial 1'''-CH<sub>3</sub> (both below), and H-1'' with the equatorial H-1''' (both above) unambiguously established the axis in the 7''',8''-coupled portion of the dimer to be *P*-configured.

Since the molecular moieties of this new 'mixed' dimer and, thus, unsymmetric quateraryl, were coupled *via* C-6' of both naphthalene portions, *i.e.*, in the least-hindered positions, the central biaryl axis constituted not an additional element of chirality, but could rotate freely.

The new dimer thus had the full absolute stereostructure **42**, as shown in Figure 14. Based on its occurrence in *A. ealaensis*, and from the local language 'Lingala' word *pasa*, which means twins, the new dimer **42** was henceforth named ealapasamine A (see Figure 14).

Prior to this work, only one single alkaloid with a related molecular scaffold had been known, korundamine A (**46**) from the Cameroonian species *A. korupensis*.<sup>[107]</sup> This dimer likewise consists of a 5,8'- and a 7,8'-coupled monomer, but its structural elucidation had remained incomplete. The assignment of the relative (and, thus, absolute) axial configuration of the 7,8'-linked molecular half had failed because neither decisive ROE relationships were monitored in its dihydroisoquinoline part (Figure 18),<sup>[107]</sup> nor had the ECD spectrum of the compound been reported, leaving no chance for a later assignment of the full absolute configuration of **46**. Compared to the michellamine-type dimers, possessing a freely rotating 6',6''-linked central axis, compound **46** had shown a rather moderate antiplasmodial profile *in vitro* against *P. falciparum* with an IC<sub>50</sub> of 1.4  $\mu$ M. Ealapasamine A (**42**) is, thus, the very first stereochemically fully elucidated mixed heterodimer with two differently coupled naphthylisoquinoline portions



that has been completely assigned. This assignment was facilitated by the presence of an additional stereocenter at C-1''', as compared to **46**, with its 'flat' imino function at C-1'''.

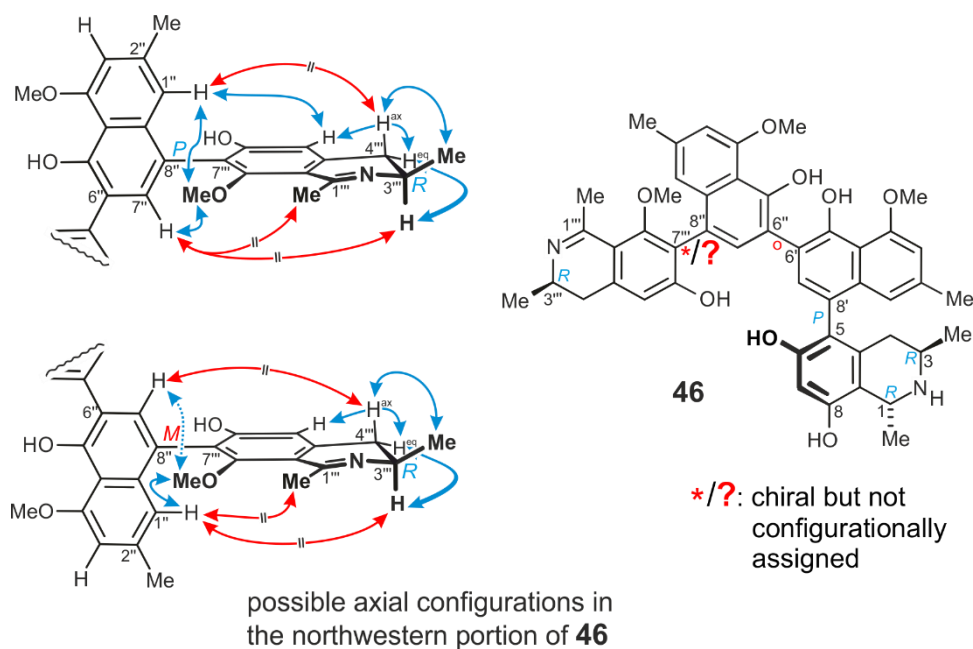


Figure 18. Lack of decisive ROEs for the axial configuration in the second half of korundamine A (**46**), isolated from *A. korupensis*,<sup>[107]</sup> leading to a to date undefined stereostructure. In red: non-observable ROESY interactions due to too long distance (> 4.8 Å).

From another dimer-enriched fraction of the leaves of *A. ealaensis*, a closely related second compound was isolated, albeit in very small quantities only. This compound showed also a protonated fragment in HRESIMS at  $m/z$  785.38042, calculated for  $[M+H]^+$  C<sub>48</sub>H<sub>53</sub>N<sub>2</sub>O<sub>8</sub> as in the case of ealapasamine A (**42**). Compound **43** displayed the same online UV spectrum and the same constitution by NMR as depicted in Figure 19, though it showed a slower elution by HPLC on an RP<sub>18</sub> column, thus, it was likewise assumed to be a new compound.

A point of difference to **42** was already detectable from the <sup>1</sup>H and <sup>13</sup>C spectra by superimposition: the probably new dimer presented a slightly deshielded chemical shift value of H-1 ( $\delta_H = 4.78$  ppm) and the shielded signal of C-3 ( $\delta_C = 45.1$  ppm) as compared to ealapasamine A, suggesting recognizably a *trans*-relative configuration in its first (southeastern) portion. Moreover, the chemical shifts of H-1''' ( $\delta_H = 4.69$  ppm) and C-3 ( $\delta_C = 51.3$  ppm) indicated a *cis*-configured tetrahydroisoquinoline in the second (northwestern) portion of **43** (see Figure 19a,b).

Remarkably, the relative configuration at C-1''' versus C-3''' in this half (Figure 19d) was confirmed to be *cis* from a ROESY correlation between H-1''' ( $\delta_{\text{H}} = 4.69$ ) and H-3''' ( $\delta_{\text{H}} = 3.47$ ), while a ROESY interaction between 1-CH<sub>3</sub> ( $\delta_{\text{H}} = 1.61$ ) and H-3 ( $\delta_{\text{H}} = 3.70$ ) revealed a relative *trans*-configuration at C-1 and C-3 in the isoquinoline portion of the southeastern half of the molecule (Figure 19c). In contrast to compound **42**, this dimer showed a slightly deshielded H-1 ( $\delta_{\text{H}} = 4.78$ ) and a shielded C-3 ( $\delta_{\text{C}} = 45.1$ ), and the chemical shifts of H-1''' and C-3''' ( $\delta_{\text{C}} = 51.3$ ), thus corroborating the assignment of the relative configurations in the two tetrahydroisoquinoline portions (see Figure 19b). The oxidative degradation<sup>[113]</sup> delivered aminobutyric acid as its *R*-enantiomer only, which implied the absolute configurations of the molecular halves of the compound to be *1R,3R* in the 5,8'-coupled monomer, and *1S,3R* in the 7,8'-linked half. Similar to **42**, the ROESY correlations between H-1' and 4-H<sub>ax</sub> in the southeastern moiety (Figure 19c), and between 1'''-CH<sub>3</sub> and H-1'' for the portion (Figure 19d) attributed a *P*-configuration to the two outer biaryl axes. Hence, this new dimer had the full absolute structure **43** (see Figure 14). Like for **42**, the central axis was configurationally unstable in this case, too, and, thus, not an element of chirality. The dimer **43** was named ealapasamine B.

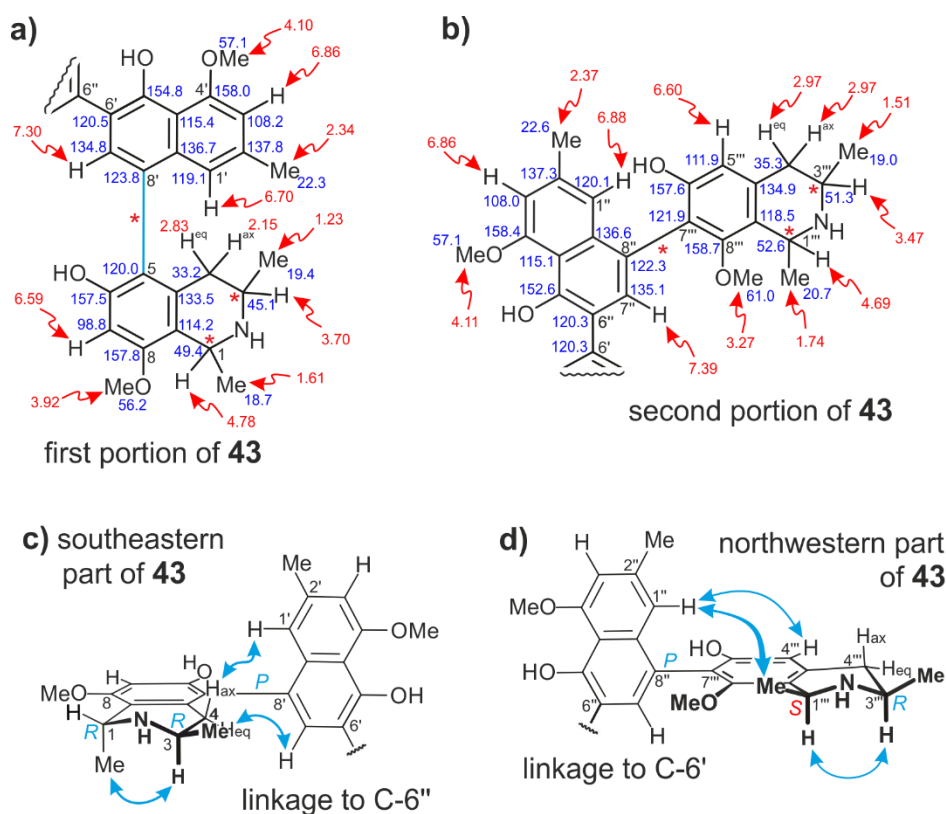


Figure 19. Chemical shifts in the southeastern (a) and the northwestern (b) portions of ealapasamine B (**43**). ROESY interactions indicative of the relative configurations at the stereogenic centers and axes within the southeastern (c) and the northwestern (d) molecular halves of ealapasamine B (**43**).

Along with ealapasamine B, a third compound was isolated, again with a molecular formula identical to those of **42** and **43**. Despite some different NMR shifts, its constitution was the same as that of **42** and **43**, displaying slightly shielded quartets at H-1 ( $\delta_{\text{H}} = 4.65$ ) and H-1''' ( $\delta_{\text{H}} = 4.68$ ), and deshielded signals of C-3 ( $\delta_{\text{C}} = 50.9$ ) and C-3''' ( $\delta_{\text{C}} = 51.3$ ) as depicted in Figure 20a,b. This hinted at relative 1,3-*cis*-configurations in both tetrahydroisoquinoline subunits, which was further confirmed by ROESY measurements (Figure 20c,d). Oxidative degradation determined the absolute configuration at both C-3 and C-3''' to be *R*, which, in combination with the relative *cis*-configurations of the two isoquinoline portions, established the stereocenters at C-1 and C-1''' to be *S*-configured. Long-range ROESY cross-peaks from H-7' with 4-H<sub>eq</sub>, and from H-1' with 1'''-CH<sub>3</sub> (see Figure 20c,d) assigned the two outer biaryl axes to be again *P*-configured. The uniqueness of this compound does only consist in its differently coupled consecutive biaryl axes, but also in the fact that it is the first unsymmetric NIQ dimer possessing two relative *cis*-configured isoquinoline moieties. It is a cross-coupling product of the 1,3-*cis*-configured portions in **42** and **43**. The new alkaloid had, thus, the structure **44** and was henceforth named ealapasamine C.

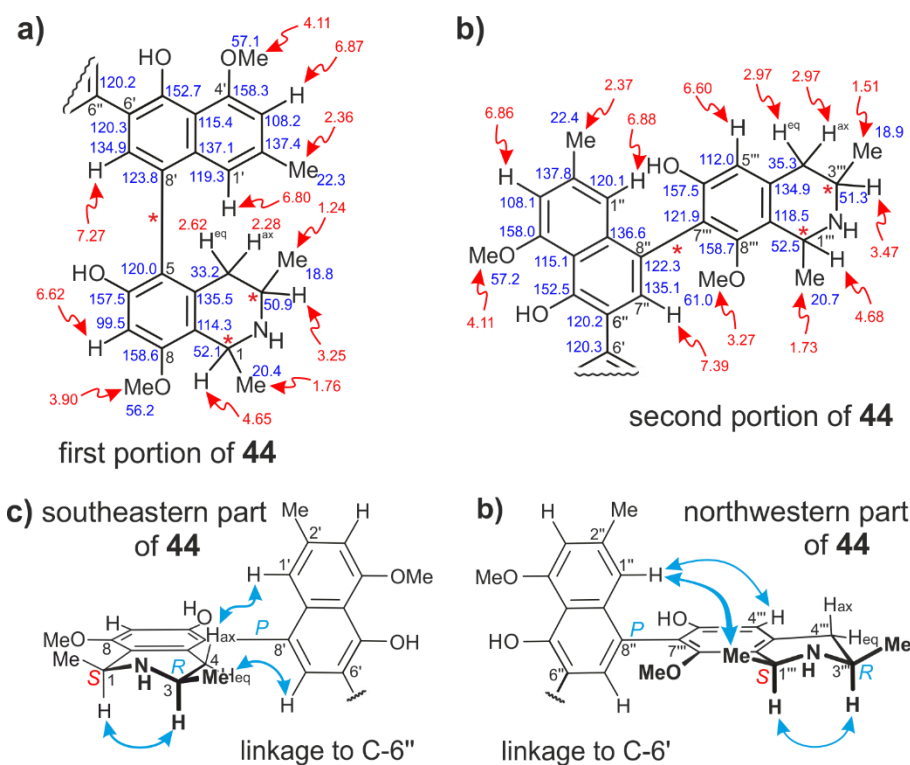


Figure 20. Chemical shifts in the southeastern (a) and the northwestern (b) moieties of ealapasamine C (44). (c) and (d) ROESY interactions decisive for the absolute configuration of ealapasamine C (44).

A small number of natural dimeric NIQs combining an *N*-protonated (*N*-H) tetrahydroisoquinoline moiety with a *cis*-relative configuration is documented.<sup>[101-102, 104]</sup> This is a strong indication of the mild extraction and workup procedures developed in the frame of this work, since such fragments are known to be prone to oxidation.<sup>[165]</sup> This was experimentally proven by the air oxidation of both *cis*-configured tetrahydroisoquinoline subunits of 44 into the corresponding dihydroisoquinoline forms. From a diluted solution of 44, left at room temperature for six weeks on the bench, in HRESIMS a fragment at  $m/z$  781.3470  $[M+H]^+$  was detected, corresponding to a molecular formula of  $C_{48}H_{48}N_2O_8$ , evidencing the loss of four protons and an increase of two units for the insaturation rate as compared to 44. The unnatural compound was, thus, identified and named ealapasamine C<sub>2</sub> (45) as depicted in Figure 14.

Moreover, the overall ECD spectra of these heterodimers was dominated by the strong Cotton effect of the 5,8'-coupled moieties,<sup>[166-167]</sup> while the 7,8'-coupled part showed a weak CD effect (Figure 21a).<sup>[164, 168]</sup> These dimers consisted of a freely rotating, thus, configurationally unstable central axis, which leads to a large array of structural flexibility. This conformational diversity and the different CD effect behavior of the two molecular halves constituted a major

drawback for in-depth quantum-chemical calculations. Indeed, the structure of ealapasamine dimers represents one of the rare cases where even most time demanding exciton chirality methods cannot reliably contribute to the full absolute configuration assignment.<sup>[119, 169-170]</sup>

The ECD spectra of **42-44** were all dominated by the chiroptical contributions of the outer axes because their spectra were most similar to each other (Figure 21).<sup>[168]</sup>

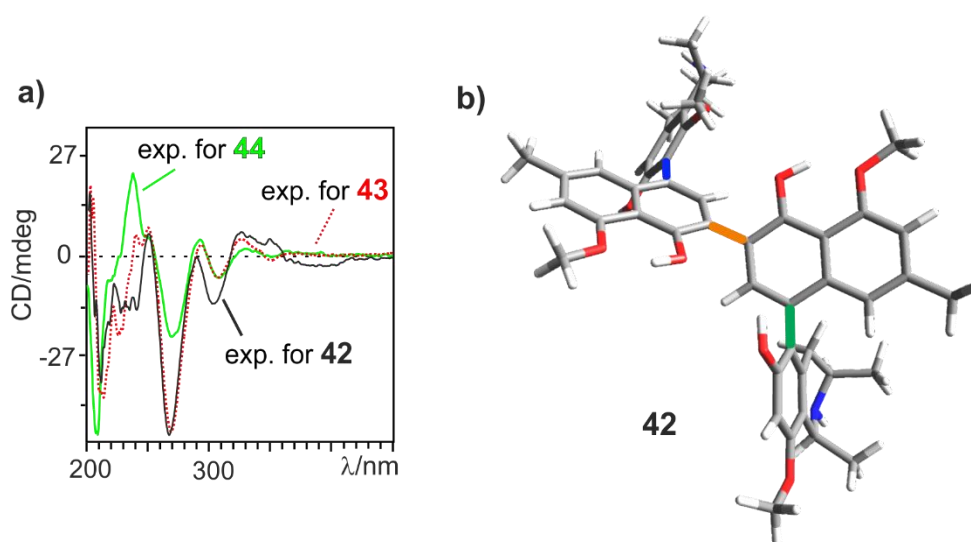


Figure 21. (a) ECD spectra of ealapasamines A-C (**42-44**) recorded in MeOH. (b) DFT-optimized conformer of **42** at the B3LYP-D3/def2-SVP level.

The geometrical optimizations of **42-44** were performed by density functional (DFT) quantum-chemical calculations.<sup>[171]</sup> These theoretical investigations were carried out using several methods and basis sets to identify most stable conformers. The best results were obtained by DFT calculations at the B3LYP-D3/def2-SVP. The HOMO-LUMO energy gaps ( $\Delta_{HL}$ ) were deduced, indicating their stability levels. The energetic gap of the calculated conformer of **42a** was 90.84 kcal mol<sup>-1</sup>, while 63.65 kcal mol<sup>-1</sup> was found for the conformer **42b**, proving that **42a** was indeed the most stable geometry as depicted in Figure 22.

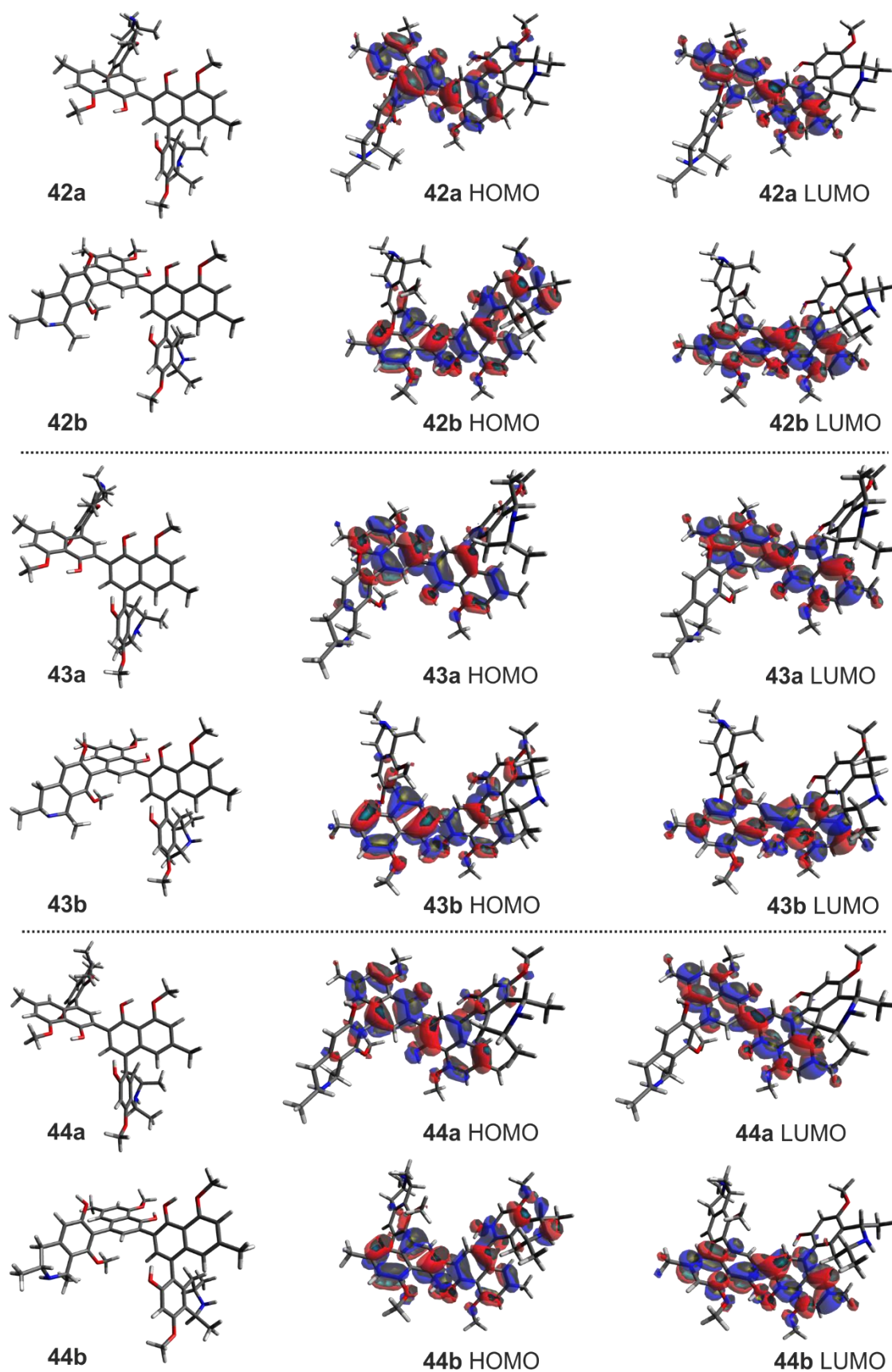


Figure 22. DFT-structural optimization of two conformers of compounds **42-44** (**42-44a** and **42-44b**), and their HOMO and LUMO molecular orbitals. The most favorable conformers **42-44a** found with the highest HOMO-LUMO gaps by DFT calculations with B3LYP-D3/def2-SVP.

## Biological evaluation of the new compounds and general discussion

Ealapasamines A-C (**42-44**) exhibited excellent antiplasmodial activities *in vitro* against the chloroquine-sensitive (NF54) and chloroquine-/pyrimethamine-resistant (K1) strains of *P. falciparum*, the malaria parasite (Table 2), with IC<sub>50</sub> values of 418 (NF54) and 452 nM (K1) for **42**, 210 (NF54) and 138 nM (K1) for **43**, and 34 (NF<sub>54</sub>) and 6 nM (K1) for **44**. Remarkably, ealapasamine C (**44**) was ten times more active against both strains of *P. falciparum* than the other alkaloids, even more active than the reported mbandakamines, with excellent cytotoxicity profiles on the L6 cell line (6.0 μM). Remarkable was the excellent and highly selective antiplasmodial potential of ealapasamine C against the resistant strain K1, with an IC<sub>50</sub> value of 6 nM and a high selectivity index (SI) of nearly 1000 (see Table 2). Compound **44** was, thus, not only the most active unsymmetric dimer against NF54 and K1, but also the as yet most potent and selective naphthylisoquinoline alkaloid against the resistant strain K1, even better than jozimine A<sub>2</sub> (K1: IC<sub>50</sub> 16 nM, SI 53.5). From the values shown in Table 2, the K1/NF54 degree of resistance (D.R.) to *P. falciparum* can be calculated.<sup>[172-173]</sup> The dimers **42**, **43**, and **44** displayed very low resistance profiles of 1.08, 0.65 and 0.20, respectively. In other words, the standard drug chloroquine, which displayed a D.R. ratio of 61.62 was 308 times more resistant than **44** on to *P. falciparum*. With this profile, ealapasamine C (**44**) is, thus, the as yet most active naphthylisoquinoline against the resistant strain K1.

Moreover, these compounds were tested against *Trypanosoma b. rhodesiense* and *Leishmania donovani*, and, by contrast to *P. falciparum*, virtually no activities were determined, which demonstrates the high specificity of the antiplasmodial activities of **42-44**, making advanced biological evaluations on **44**, as the most active dimer, a rewarding task.

Table 2. Biological evaluations of **42-44** against *Plasmodium falciparum* (strains: NF54 and K1), *Trypanosoma brucei rhodesiense*, *T. cruzi*, and *Leishmania donovani*, as well as the cytotoxicities against rat skeletal myoblasts (L6 cells) (IC<sub>50</sub> in μM). For comparison, the antiplasmodial profile of jozimine A<sub>2</sub> (**31**) is shown.

Compounds	<i>T. b. rhod.</i>	<i>T. cruzi</i>	<i>L. donovani</i> ax. am.	<i>P. falciparum</i> NF54/K1	Cytotox. L6	Selectivity index to NF54/K1
Standard	0.007 <sup>[1]</sup>	3.56 <sup>[2]</sup>	0.43 <sup>[3]</sup>	0.008 <sup>[4]</sup> : NF54 0.364 <sup>[4]</sup> : K1	0.041 <sup>[5]</sup>	n.d.
<b>42</b>	16.33	74.04	>100	0.418 0.452	61.29	147 136
<b>43</b>	5.45	-	>10	0.210 0.138	>12.73	>61 >93
<b>44</b>	1.87	-	>10	0.034 (NF54) <b>0.006</b> (K1)	5.98	174 <b>997</b>
<b>31</b> <sup>[15b]</sup>	-	-	-	0.001 0.016	-	11400 -

[1] Melarsoprol. [2] Benznidazole. [3] Miltefosine. [4] Chloroquine. [5] Podophyllotoxin. All values in μM. n.d.: not determined. Selectivity index determined for *P. falciparum*.

For a better appreciation of the outstanding antiplasmodial profile of ealapasamine C (**44**), it shall be considered that most of the dimers with a 6',6''-coupling type at the central axis, like *e.g.*, the michellamines, are virtually inactive against the malaria pathogen.<sup>[104, 107]</sup> Ealapasamine C is even more than two times better than the known dimer jozimine A<sub>2</sub>,<sup>[32]</sup> with its inhibition concentration of 6 nM (see Table 2). The IC<sub>50</sub> value of **44** – compared to those of **42** and **43** – demonstrates how minor stereochemical changes in a molecule can lead to drastically different degrees of bioactivities.

Preliminary biological investigations on **42** revealed an extremely high anticancer potential (IC<sub>50</sub> 0.89 μM) on the T-lymphoblastic leukemia cell line CCRF-CEM. This excellent cytotoxic activity of **42** is indicative of its specificity towards normal human cells. Additional evaluations of the complete series may be highly informative.

The ealapasamines are structurally unique in many respects: among the small subfamily of dimeric naphthylisoquinoline alkaloids (presently ca. 20 compounds), they are the only fully elucidated mixed heterodimers with different coupling types at the three biaryl axes (5,8'-, 6',6''-, and 7''',8''-coupling). Besides the unprecedented occurrence of such unsymmetric dimers in *A. ealaensis* (and previously, but not fully assigned, in *A. korupensis*<sup>[107]</sup>), these alkaloids display remarkable antiplasmodial activities. For this reason, ealapasamine C (**44**) is currently



under biological investigations on the gametocytes form of the malaria pathogen. The formation and presence of gametocytes are essential for the propagation of this infectious disease.<sup>[174-176]</sup> They are produced in the vascular stage of the disease in human and are the only form that will develop in the female *Anopheles* to maintain the disease life cycle.<sup>[174]</sup> Tackling this form of the parasite is considered as one of the most efficient ways to interrupt the cycle and, thus, the malaria infection.<sup>[174-177]</sup> This work is done in cooperation with partners located at the University of Pretoria, in South Africa.

## II.2. *A. ealaensis* as a Rich Source of Dimeric Naphthylisoquinolines Related to Mbandakamine A and Michellamine F

Following the discovery of the series of heterodimeric NIQs in *A. ealaensis*, further LC-MS-guided investigations were undertaken in order to explore in depth the synthetic potential of this tropical liana. Oriented by unusual online-UV spectra, while performing HPLC-DAD screening in the plant extract, the successful detection and chromatographic resolution of five promising peaks were achieved at a semi-preparative scale (Figure 23). They were obtained from several sub-fractions and displayed two types of UV spectra. The structural elucidation revealed the natural occurrence of mbandakamine- and michellamine-type dimers. Considering the numerous closely related species in the Congo Basin, this discovery makes the well-described species *A. ealaensis* a reliable source of mbandakamine-like dimers, like *A. korupensis* and *A. congolensis* are for the michellamines. Since the unambiguous identification of a plant species is one of the fundamental prerequisites in phytochemical research, this report is important for the availability of these compounds. A systematic fractionation of a hardly resolvable fraction of methanolic leaves extract of *A. ealaensis* led to the isolation and spectroscopic characterization of compounds **32**, **47-50** (Figure 24). From five purified peaks, four turned out to be new dimeric naphthylisoquinolines.

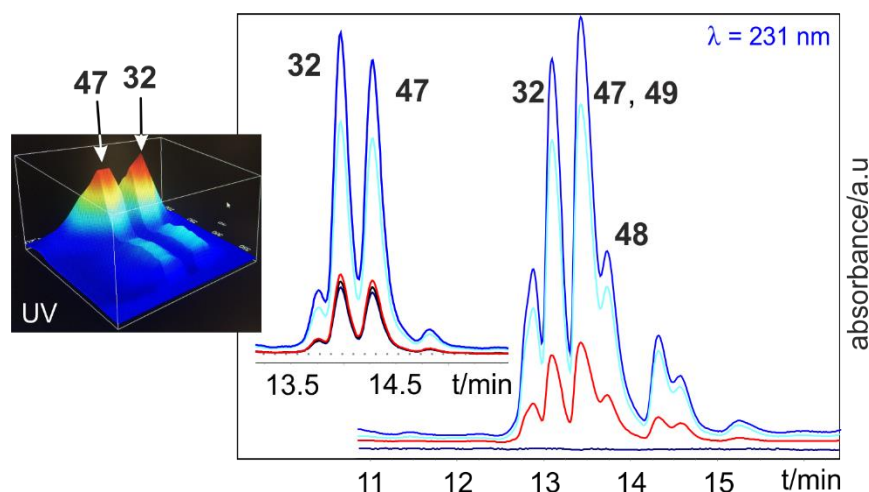


Figure 23. Chromatograms of advanced subfractions of leaf extract – recorded at several wavelengths – displaying four peaks corresponding to the dimeric alkaloids mbandakamine A (**32**), 1-*epi*-mbandakamine A (**47**), mbandakamine C (**48**) and mbandakamine D (**49**).

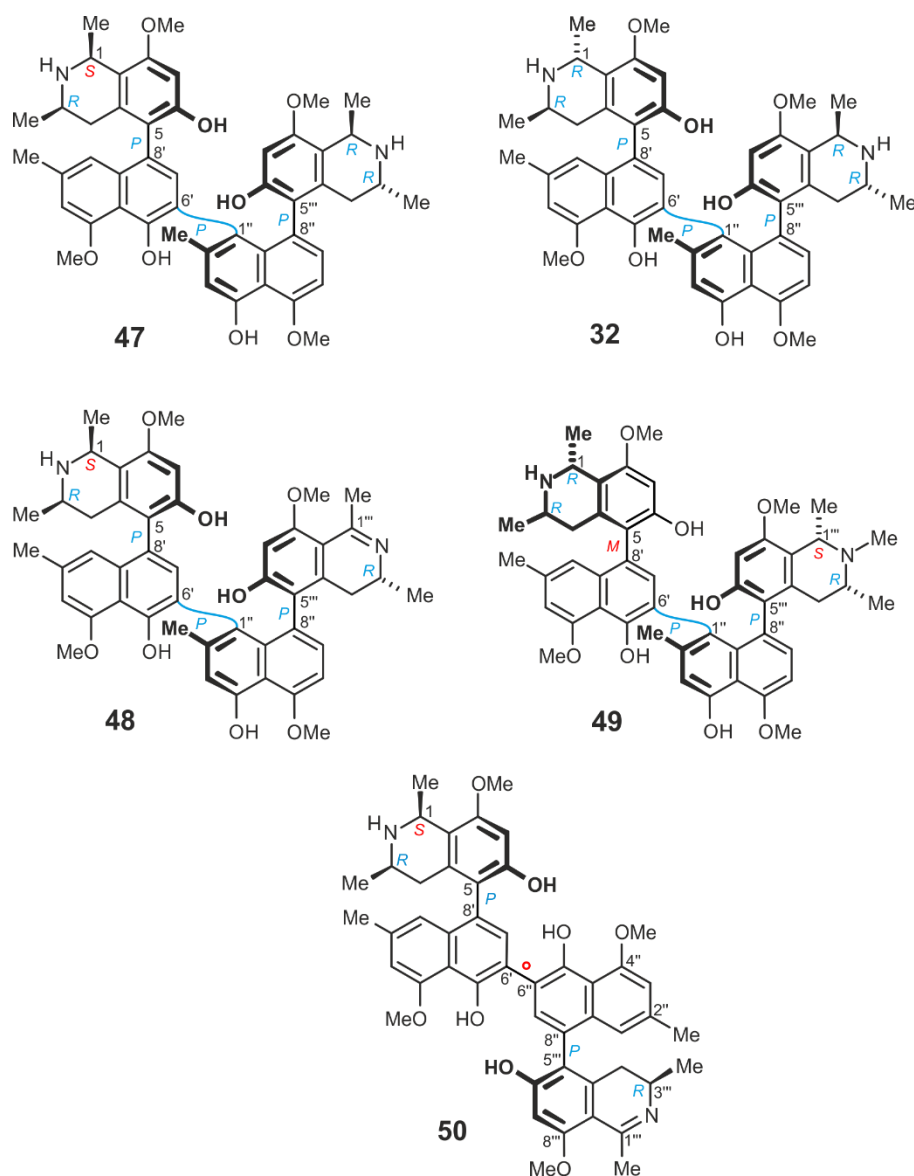


Figure 24. 1-*epi*-Mbandakamine A (**47**), mbandakamine C (**48**), mbandakamine D (**49**), and michellamine F<sub>2</sub> (**50**), representing four new dimeric naphthylisoquinolines, and the known mbandakamine A (**32**),<sup>[103]</sup> all isolated from *A. ealaensis*.

### Structural elucidation and discussion

The first characterized metabolite was Me obtained as a white powder. It showed a molecular formula of C<sub>48</sub>H<sub>52</sub>N<sub>2</sub>O<sub>8</sub>, like for the ealapasamines A-C, as deduced by HRESIMS. A comprehensive analysis of the NMR data of the pure substance led to the detection of an unsymmetric NIQ formed of two different molecular halves, as confirmed by 48 signals in the <sup>13</sup>C spectrum.

From the full-set assignments, the constitution of the first molecular half of **47** was reminiscent of a typical 5,8'-coupled part, as observed in **42**, too. Four out of eight aromatic protons were attributed to this half in the  $^1\text{H}$  NMR spectrum. The same spectrum displayed two aromatic singlets H-7' ( $\delta_{\text{H}} = 6.44$  ppm) and H-7 ( $\delta_{\text{H}} = 6.48$  ppm), two aromatic protons with a *meta*-coupling pattern H-1' ( $\delta_{\text{H}} = 6.74$  ppm, d,  $J = 1.0$  Hz) and H-3' ( $\delta_{\text{H}} = 6.75$  ppm, ps), one aromatic methyl 2'-CH<sub>3</sub> ( $\delta_{\text{H,C}} = 2.37, 22.3$  ppm), two methoxy 4'-OCH<sub>3</sub> ( $\delta_{\text{H,C}} = 4.09, 57.0$  ppm) and 8-OCH<sub>3</sub> ( $\delta_{\text{H}} = 3.83, 56.0$  ppm), two methyls 1-CH<sub>3</sub> ( $\delta_{\text{H}} = 1.76$  ppm, d,  $J = 6.56$  Hz) and 3-CH<sub>3</sub> ( $\delta_{\text{H}} = 1.50$  ppm, d,  $J = 6.51$  Hz), two diastereotopic protons 4-H<sub>eq</sub> ( $\delta_{\text{H}} = 3.68$  ppm, dd,  $J = 3.13, 17.06$  Hz) and 4-H<sub>ax</sub> ( $\delta_{\text{H}} = 2.55$  ppm, dd,  $J = 11.66, 16.85$  Hz), one quartet H-1 ( $\delta_{\text{H}} = 4.65$  ppm, q,  $J = 6.66$  Hz), and one multiplet H-3 ( $\delta_{\text{H}} = 3.27$  ppm, m). As for the ealapasamines A-C, these assignments were deduced from the DEPT-135, HMBC, HSQC, COSY, ROESY data. The position of H-7 was confirmed by its HMBC cross peaks with C-6 (C-OH,  $\delta_{\text{C}} = 157.5$  ppm), C-8 (C-OCH<sub>3</sub>,  $\delta_{\text{C}} = 158.1$  ppm) and C-1 ( $\delta_{\text{C}} = 52.1$  ppm). HMBC correlations from H-7, H-7', and 4-H<sub>eq</sub> to C-5 ( $\delta_{\text{C}} = 120.8$  ppm) implied that the two subunits of this monomeric first (northwestern) half were 5,8'-coupled, resulting in a sterically hindered biaryl axis (Figure 25a).

The ROESY interactions between H-1 and H-3 supported the relative *cis*-configuration at these stereogenic centers. The chemical shifts of C-3 ( $\delta_{\text{C}} = 52.7$  ppm) and H-1 corroborated this assignment.

From the ruthenium(VIII)-mediated oxidative degradation, the absolute configurations at C-3 and C-3''' positions were found to be *R*. The ROESY correlations between H-7' and 4-H<sub>eq</sub>, and from H-1' to 4-H<sub>ax</sub>, combined with the configuration at C-3, the absolute configuration was deduced as *P* at the biaryl axis in this part, like in ealapasamine A (**42**). The first, northwestern portion of **47** was, thus, identical to the southeastern part of **42**.

The drastic difference between **47** and **42** was observed in the second molecular half, which showed in  $^1\text{H}$  NMR a pair of *ortho*-coupled aromatic doublets H-6'' ( $\delta_{\text{H}} = 6.99$  ppm, d,  $J = 7.97$  Hz,  $\delta_{\text{C}} = 104.7$  ppm) and H-7'' ( $\delta_{\text{H}} = 7.05$  ppm, d,  $J = 7.90$  Hz,  $\delta_{\text{C}} = 132.4$  ppm), no *meta*-coupled doublets next to the shielded 2''-CH<sub>3</sub> ( $\delta_{\text{H}} = 1.91$  ppm, s,  $\delta_{\text{C}} = 21.5$  ppm), but only a singlet at H-3'' ( $\delta_{\text{H}} = 6.79$  ppm, s,  $\delta_{\text{C}} = 114.6$  ppm), thus, leaving C-1'' and C-8'' as coupling possibilities in the naphthalene subunit. HMBC interactions from H-7'', 4'''-H<sub>eq</sub> ( $\delta_{\text{H}} = 1.95$  ppm, dd,  $J = 4.21, 17.48$  Hz) and H-7''' ( $\delta_{\text{H}} = 5.32$  ppm, s,  $\delta_{\text{C}} = 97.0$  ppm) to C-5''' ( $\delta_{\text{C}} = 122.8$  ppm) confirmed the presence of a 5''',8''-linked naphthylisoquinoline residue (Figure 25b).

In contrast to the first half, the relative configuration in the tetrahydroisoquinoline part was found to be *trans*-configured by ROESY experiments. Considering the *3R*-configuration determined by oxidative degradation experiments and the observed ROEs in this half, the absolute axial configuration was likewise determined to be *P*.

The constitution of this dimer was found to be identical to the one of mbandakamine A, because the two molecular portions were connected *via* a chiral 6',1''-central biaryl axis. ROESY interactions across this central axis were found to be identical to the known dimer mbandakamine A,<sup>[103]</sup> e.g. the correlations between H-7''' / H-1' and 4-H<sub>ax</sub>, CH<sub>3</sub>O-8''' and H-3', and from H-1''' to CH<sub>3</sub>O-4' were likewise observed (Figure 25c). Therefore, the ECD spectrum of mbandakamine A was used as a reference to assign the absolute configuration at the central axis, in addition to the results of the ROE correlations. Based on the identical ECD spectra, the rotationally stable central axis of compound **47** was assigned to be *P*-configured, as for mbandakamine A. This new unsymmetric dimer combined the highest sterically hindered central axis, due to the *peri-peri* linkage in one of the naphthalene parts, so far limited to mbandakamines A and B, among the naturally occurring NIQs.<sup>[103]</sup> Hence, this new dimer **47** differed to the known mbandakamine A by the relative *cis*-configuration and the absolute configuration at C-1. Consequently, compound **47** was named 1-*epi*-mbandakamine A.

As discussed in the case of the ealapasamines, the configurationally unstable central axis and the weak CD effect resulting from the 7,8'-coupled moieties strongly hampered their computational investigations by DFT-based quantum-chemical calculations of the ECD spectra. In the case of the mbandakamines, it has been demonstrated that a configurational switch at the central axis, leads to opposite ECD spectra,<sup>[103]</sup> thus, proving the dominance of the spatial arrangement around the central junction. Therefore, in this case, the two outer axes and the stereogenic centers have marginal contributions to the overall ECD curve. Consequently, the axial configuration of the central axis of mbandakamine-type dimers can be reliably established by their comparison.

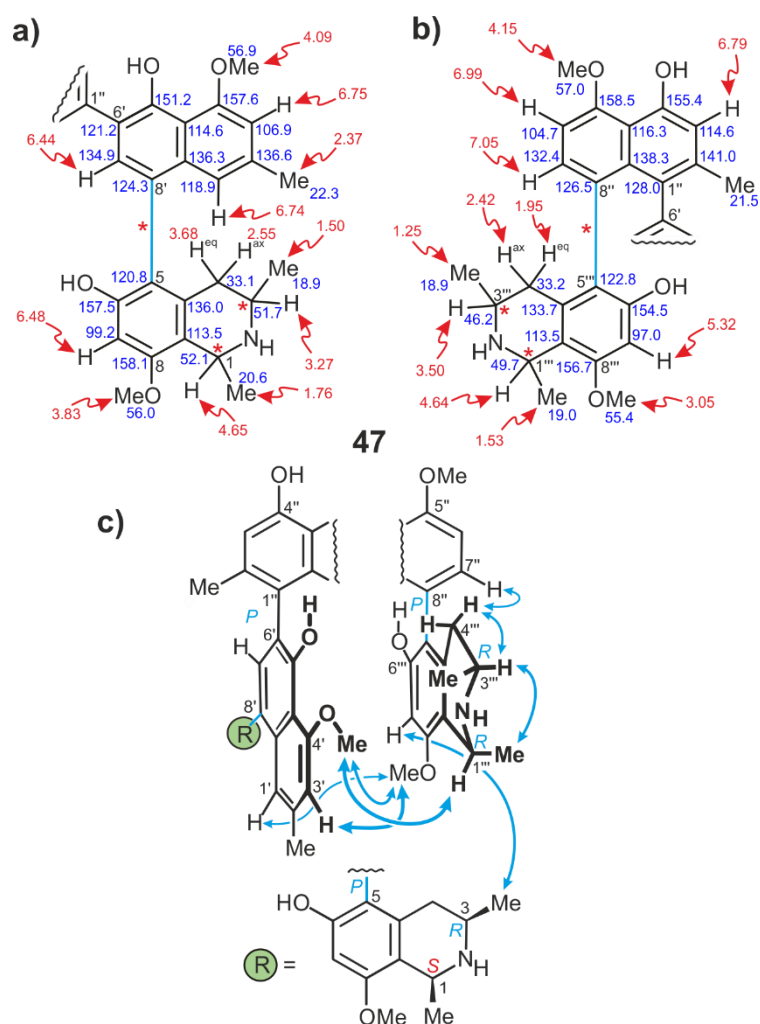


Figure 25. The chemical shifts (in ppm) in (a) the northwestern and (b) the southeastern portions of 1-*epi*-mbandakamine A (**47**). (c) The ROEs interactions across the central axis in **47**.

The spectral analysis of compound **32** led to the same constitution as for 1-*epi*-mbandakamine A. The oxidative degradation indicated the same *R*-configurations at C-3 and C-3<sup>'''</sup>. The ECD spectrum was also identical to the known mbandakamine A (see Figure 26), excluding the presence of the atropo-diastereomer, mbandakamine B, which is *M*-configured and has an opposite curve. From the ROESY spectrum, not a single difference was compared to the published data for mbandakamine A.<sup>[103]</sup> In-depth analysis of all the spectroscopic data unequivocally led to the identification of compound **32** as the known dimer mbandakamine A, in agreement with the published data.<sup>[103]</sup> An additional confirmation was provided by co-elution experiments on HPLC with an authentic reference sample available in the group.

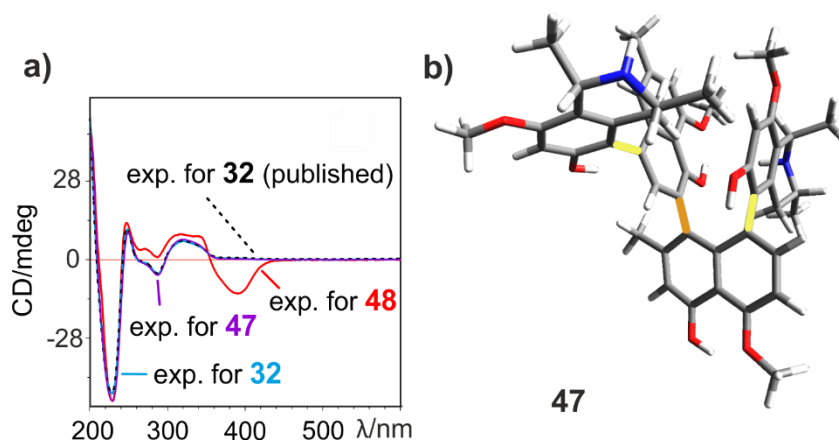


Figure 26. (a) Comparison of the ECD spectra of 1-*epi*-mbandakamine A (**47**), mbandakamine C (**48**), the isolated mbandakamine A (**32**), and an authentic spectrum of mbandakamine A. (b) DFT-optimized structure of **47** at the B3LYP-D3/def2-TZVP level.

Another peak purified, corresponding to compound **48**, eluted on Symmetry<sup>®</sup> column before the ealapasamines A-C and was obtained as a yellowish powder. The molecular formula deduced from HRESIMS was C<sub>48</sub>H<sub>50</sub>N<sub>2</sub>O<sub>8</sub> and, thus, different from **47** by two mass units, hinting at an oxidation by loss of two protons or at a new molecular skeleton.

In the proton spectrum, many similarities to 1-*epi*-mbandakamine A were detected, *e.g.* the one pair of aromatic protons with *meta*-coupling pattern H-1' ( $\delta_{\text{H}} = 6.77$  ppm, d,  $J = 1.07$  Hz,  $\delta_{\text{C}} = 119.3$  ppm) and H-3' ( $\delta_{\text{H}} = 6.82$  ppm, ps,  $\delta_{\text{C}} = 107.7$  ppm), two *ortho*-coupled aromatic doublets H-6'' ( $\delta_{\text{H}} = 7.02$  ppm, d,  $J = 8.06$  Hz,  $\delta_{\text{C}} = 104.7$  ppm) and H-7'' ( $\delta_{\text{H}} = 7.07$  ppm, d,  $J = 7.93$  Hz,  $\delta_{\text{C}} = 132.3$  ppm), and two isolated aromatic singlets H-7 ( $\delta_{\text{H}} = 6.48$  ppm, s,  $\delta_{\text{C}} = 99.3$  ppm) and H-7''' ( $\delta_{\text{H}} = 5.32$  ppm, s,  $\delta_{\text{C}} = 96.2$  ppm) interacting each in HMBC with two oxygenated carbons. Extensive analysis of the spectroscopic data corresponding to the first molecular half indicated the presence of a 5,8'-coupled tetrahydroisoquinoline moiety, identical to the one in 1-*epi*-mbandakamine A (**47**). The 1,3-diaxial arrangement of H-1 ( $\delta_{\text{H}} = 4.68$  ppm, *q*,  $J = 6.38$  Hz,  $\delta_{\text{C}} = 52.1$  ppm) and H-3 ( $\delta_{\text{H}} = 3.35$  ppm, *m*,  $\delta_{\text{C}} = 51.6$  ppm) was already detectable by the typical unshielded shift of C-3 in contrast to that of C-3''' ( $\delta_{\text{C}} = 46.2$  ppm), which inferred to a 1,3-*cis*-configuration, as in 1-*epi*-mbandakamine A (**47**).

However, the difference to **47** was the lack of a proton signal attached to C-1''' ( $\delta_{\text{C}} = 175.8$  ppm) and the presence of three aliphatic methyl doublets (usually  $J \approx 6.50$  Hz) in the high-field region, indicating a dihydroisoquinoline in the second southeastern molecular portion (Figure 27a,b). The presence of an oxidized isoquinoline residue was also evidenced by HMBC

correlations from 1'''-CH<sub>3</sub> ( $\delta_{\text{H}} = 2.65$  ppm, s,  $\delta_{\text{C}} = 24.8$  ppm) and H-7''' to the typically unshielded C-1''', and the ROESY interactions from H-7''' and 1'''-CH<sub>3</sub> to 8'''-OCH<sub>3</sub> ( $\delta_{\text{H}} = 3.28$  ppm, s,  $\delta_{\text{C}} = 56.2$  ppm).

Oxidative degradation experiments determined the absolute *R*-configurations at C-3 and C-3'''. Hence, the axial configurations in the two outer axes were evidenced to be *P* (Figure 27).

The absolute configuration at the central axis of **48** was deduced from its ROESY interactions (Figure 27c,d) and the ECD spectrum compared to those of the related **47** and **32** (see Figure 26a), and it was found to be *P*.

Thence, the unsymmetric alkaloid **48** was named mbandakamine C. It was the first mbandakamine-type dimer possessing largely different portions, *viz.* one possessing a relative *cis*-configuration, while the other one displayed a dihydroisoquinoline subunit.



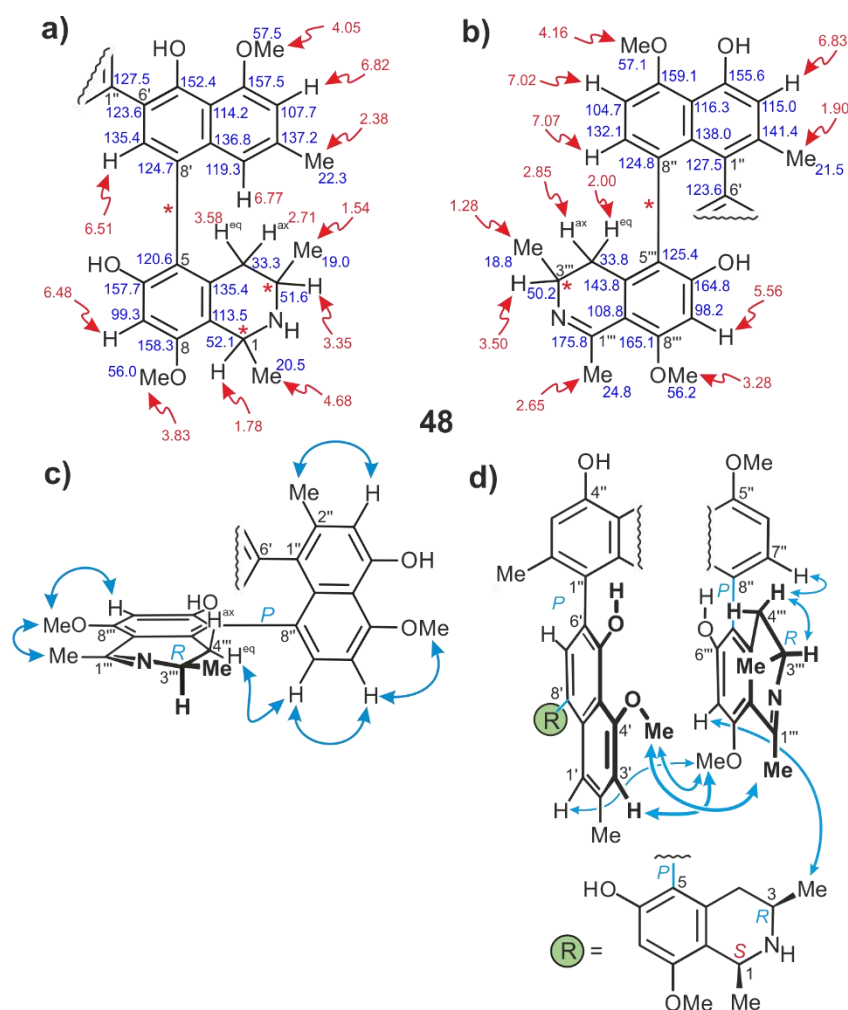


Figure 27. The chemical shifts (in ppm) in (a) the northwestern and (b) the southeastern portions of mbandakamine C (**48**). (c) Decisive ROEs in the southeastern moiety of **48**. (d) Selected ROESY interactions across the central axis of **48**.

Another alkaloid was discovered in an isolated fraction containing 1-*epi*-mbandakamine A, albeit in trace amount. In HRESIMS, it displayed a fragment  $[\text{M}+\text{H}]^+$  at  $m/z$  799.39125 calculated for a molecular formula of  $\text{C}_{49}\text{H}_{55}\text{N}_2\text{O}_8$ . If the compound was of the type mbandakamine or ealapasamine, its formula suggested an additional methyl group either at one of the four free hydroxy functions or the two nitrogen atoms. The  $^{13}\text{C}$  and the  $^1\text{H}$  spectra hinted at an unsymmetric dimer of the type mbandakamine. Extensive analysis of the 1D and 2D NMR data of the compound corroborated this constitution by assigning two different molecular halves (Figure 28).

The NMR analysis of the first (northwestern) half revealed the presence of a 5,8'-coupled naphthylisoquinoline alkaloid, with a constitution reminiscent of the related one in 1-*epi*-

mbandakamine A (**47**), e.g. four aromatic protons, namely two singlets H-7 ( $\delta_{\text{H}} = 6.69$  ppm, s,  $\delta_{\text{C}} = 97.9$  ppm) and H-7' ( $\delta_{\text{H}} = 6.82$ , s,  $\delta_{\text{C}} = 132.2$ ), and two protons in *meta*-coupling pattern H-1' ( $\delta_{\text{H}} = 6.55$ , ps,  $\delta_{\text{C}} = 118.7$ ) and H-3' ( $\delta_{\text{H}} = 6.82$ , ps,  $\delta_{\text{C}} = 108.0$ ). Additionally, two diastereotopic protons 4-H<sub>eq</sub> ( $\delta_{\text{H}} = 2.89$ , dd,  $J = 4.93, 17.68$  Hz,  $\delta_{\text{C}} = 33.1$ ) and 4-H<sub>ax</sub> ( $\delta_{\text{H}} = 1.76$ , dd,  $J = 11.5, 18.1$  Hz,  $\delta_{\text{C}} = 33.1$ ), a methyl at C-1 and C-3, a quartet H-1 ( $\delta_{\text{H}} = 4.72$ , q,  $J = 6.96$  Hz,  $\delta_{\text{C}} = 48.9$ ) and a multiplet H-3 ( $\delta_{\text{H}} = 3.66$ , m,  $\delta_{\text{C}} = 44.6$ ). For this molecular portion, the typical chemical shift of C-3 hinted at a 1,3-*trans* relative configuration, also confirmed by the ROESY interactions between CH<sub>3</sub>-1 ( $\delta_{\text{H}} = 1.57$ , d,  $J = 6.72$  Hz,  $\delta_{\text{C}} = 18.4$ ) and H-3.

Surprisingly, the ROESY correlations between H-7' and 4-H<sub>ax</sub>, and from H-1' to 4-H<sub>eq</sub> indicated that the relative axial configuration should be *PSS* or *MRR*. As mentioned above, the absolute configurations at C-1 and C-3 were determined by oxidative degradation experiments, which delivered *R*-configured aminobutyric acid and *N*-methyl-aminobutyric acid. Thus, the first portion of this dimer was assigned to be *1R3R*, and its biaryl axis was for the first time *M*-oriented.

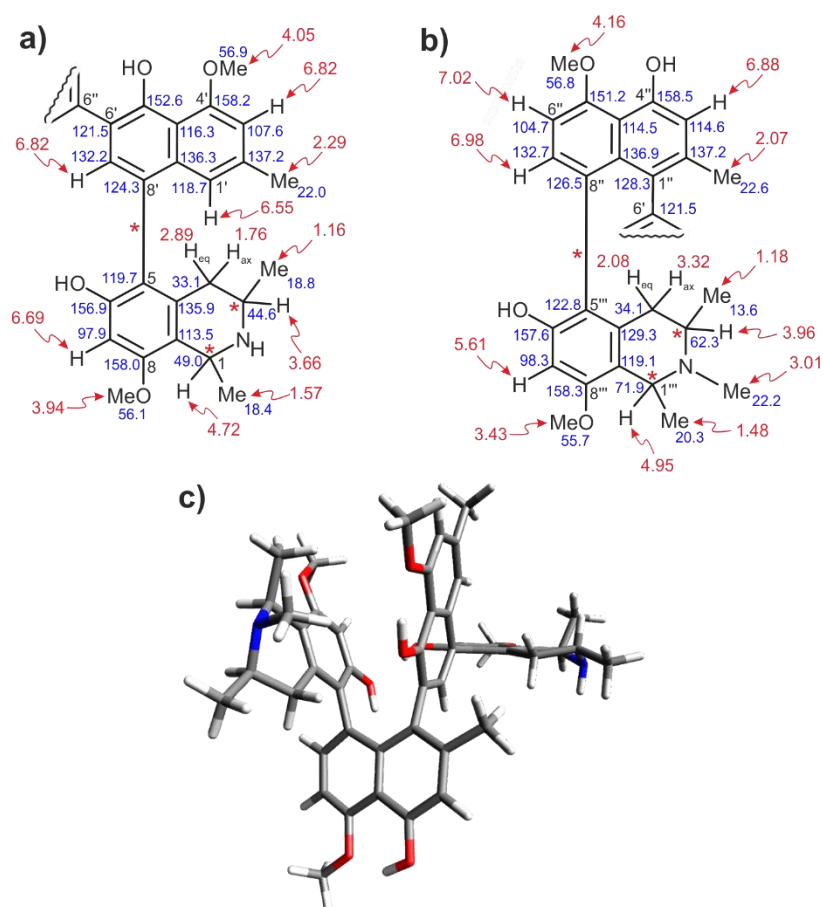


Figure 28. (a) and (b) Chemical shifts assigned to the two molecular halves of the dimer mbandakamine D (**49**). (c) DFT-optimized structure of **49** calculated at the B3LYP-D3/def2-TZVP level.

The southeastern portion was also found interestingly exotic, based on its constitution, which was different from all compounds so far described in this thesis. The elucidation of this half showed a 5,8'-coupled NIQ unit, like in **47**. However, the difference was due to an additional *N*-methyl group in the tetrahydroisoquinoline. These assignments were evidenced by the presence of a new methyl singlet at 3.01 ppm, and by ROESY interactions to H-1''', CH<sub>3</sub>-1''' and H-3'''. Furthermore, in this sub-portion a quartet H-1''' ( $\delta_{\text{H}} = 4.95$  ppm, q,  $J = 6.55$  Hz,  $\delta_{\text{C}} = 71.9$  ppm) and a multiplet H-3''' ( $\delta_{\text{H}} = 3.96$ , m,  $\delta_{\text{C}} = 62.3$ ) were detected, suggesting from their chemical shifts a relative *cis*-configuration, as discussed above. This configuration was corroborated with the observed ROEs between H-1''' and H-3''', confirming the diaxial orientation of both protons.

Based on the relative *cis*-configuration at C-1''' vs C-3''' and the ROESY correlation between H-7'' and 4'''-H<sub>eq</sub>, the absolute configuration should be *PRS* or *MSR*. The results of the oxidative degradation had revealed the presence of an *R*-configured *N*-methyl aminobutyric acid, which indicated that the configuration at C-3''' was *R*. Thence, the full assignment for the southeastern half was elucidated as *P* at the axis, *S*- and *R*-configured at C-1''' and C-3''', respectively.

Like performed for the other mbandakamine-like dimers, the configuration at the chiral central biaryl axis was established by ROESY and ECD experiments. These investigations revealed that the new dimer was *P*-configured at the central axis, due to the strong negative couplet seen at 235 nm on the ECD and the typical ROEs. Based on similar known dimers,<sup>[103]</sup> the new unsymmetric compound **49** was named mbandakamine D.

Along with mbandakamine A (**32**), another trace compound was detected. The molecular formula was deduced to be C<sub>48</sub>H<sub>50</sub>N<sub>2</sub>O<sub>8</sub>, as for mbandakamine C (**48**), and 48 signals were observed in the <sup>13</sup>C NMR spectrum, suggesting a further unsymmetric quateraryl. The full set NMR data analysis revealed many similarities to mbandakamine C, but some differences were noticed. In contrast to **48**, the dimer displayed two pairs of *meta*-coupled doublets H-1' ( $\delta_{\text{H}} = 6.67$  ppm, d,  $J = 0.8$  Hz,  $\delta_{\text{C}} = 119.5$  ppm) and H-3' ( $\delta_{\text{H}} = 6.82$ , d,  $J = 1.11$  Hz,  $\delta_{\text{C}} = 107.6$ ), and H-1'' ( $\delta_{\text{H}} = 6.85$ , d,  $J = 0.8$  Hz,  $\delta_{\text{C}} = 114.8$ ) and H-3'' ( $\delta_{\text{H}} = 7.01$ , br s,  $\delta_{\text{C}} = 104.8$ ), and no *ortho*-coupled doublets hinting at another type of heterodimer (Figure 29a,b).

The northwestern portion was found to be identical to the corresponding one in mbandakamine C (**48**) with respect to the constitution, the relative configuration, and the oxidative degradation.

This first portion, likewise featured a *cis*-oriented tetrahydroisoquinoline subunit and the ROESY interactions remained the same. The biaryl axis was therefore also *P*-configured.

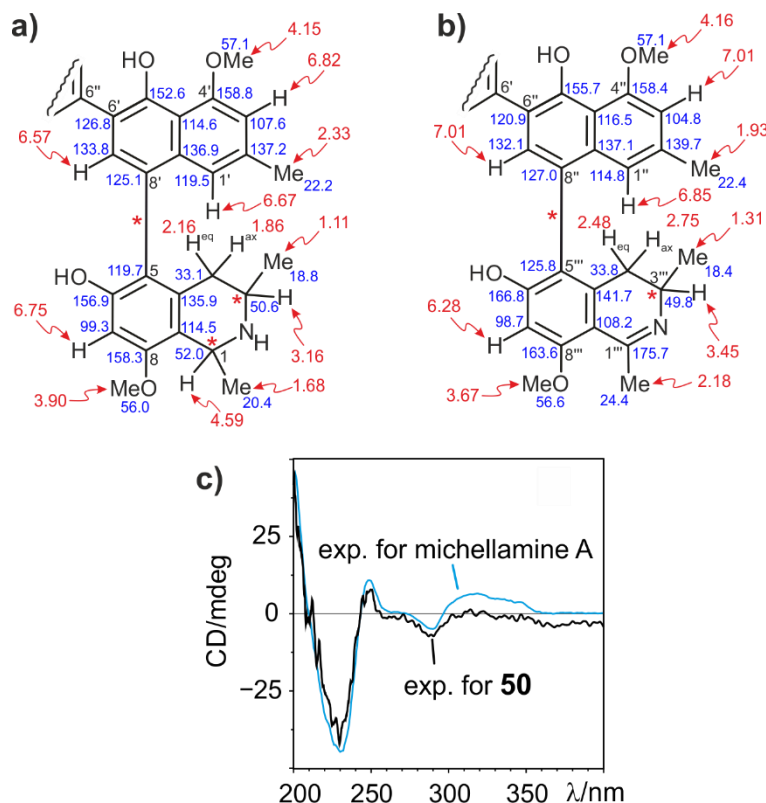


Figure 29. The chemical shifts (in ppm) in the first (a) and the second (b) moieties of michellamine F<sub>2</sub> (**50**). (c) Comparison of the ECD spectrum of **50** with the one of michellamine A.

The southeastern part of compound **50** differed from **48** by the coupling position of the central axis, localized in this case at C-6" ( $\delta_{\text{C}} = 123.3$ ) instead of C-1". Established as for of mbandakamine C, the relative and absolute configurations were found to be identical, *viz.* *P*-configured.

In conclusion, the central axis was configurationally unstable, formed between two 5,8'-coupled monomers by a linkage at C-6' ( $\delta_{\text{C}} = 126.8$ ) and C-6", characteristic for michellamine dimers.<sup>[104]</sup> In contrast to the central axis in the ealapasamines, in this case, the two molecular halves had more or less comparable chromophoric systems due to the common 5,8'-linkage at the outer biaryl axes. This enabled the interpretation of the ECD spectrum, due to the fact that both halves had nearly competitive CD effects, even though the chromophoric system of the second half was enlarged by the  $\pi$  electrons of the imino function. The ECD spectrum of compound **50** (Figure 29c) was like the one of michellamine A,<sup>[100, 166]</sup> indicating the same

configurational combination of *5P,8''P*. Thus, the full structure of compound **50** corresponded to 1-*epi*-8-*O*-methyl-8''-*epi*-michellamine F<sup>[100]</sup> and was named michellamine F<sub>2</sub>.

Michellamine F (**33**) is the most active such dimer against HIV-1 (viral strain RF) with an EC<sub>50</sub> of 2 μM,<sup>[100]</sup> suggesting that the new dimer **50** could exhibit a similar antiviral potential. However, no biological evaluation was performed on the new dimer **50**.

### Computational studies on the isolated dimers

Preliminary DFT-based structural optimizations and quantum-chemical calculations of the frontier molecular orbitals were performed with B3LYP-D3/def2-SVP and B3LYP-D3/def2-TZVP methods, in a similar manner as described for the ealapasamines A-C (**42-44**), in order to gain more theoretical knowledge on the thrilling mbandakamines. In this case, not only stable geometric arrangements were determined but also the minimum structures. Moreover, the single point-energies and estimations of the HOMO-LUMO gaps ( $\Delta_{HL}$ ) of the conformers were determined and analyzed to study the stability of these compounds. It has been documented that the stability and the preferred conformations of naphthylisoquinoline alkaloids largely depend on the type of intramolecular hydrogen bonds, the presence of other bonding interactions, and the mutual orientations of the constitutive building blocks.<sup>[57]</sup> Therefore, it was worthwhile to locate the electronic density distribution within these highly sterically hindered dimers. Such studies could enable a better understanding of the molecular stability and reactivity of mbandakamine-like alkaloids.

Analysis of the frontier molecular orbitals in the minimum structure of **47** exemplarily indicated an unusual electronic distribution (Figure 30). The estimated lowest unoccupied molecular orbital (LUMO) was predominantly located in the naphthalene part of the second moiety (B), while the highest occupied molecular orbital (HOMO) was located at its isoquinoline part (C) and the facing naphthalene belonging to the first moiety (A). The naphthalene A and the tetrahydroisoquinoline C seemed to be the most nucleophile while the naphthalene B was the most electrophile. These observations were not in agreement with a recent report made on monomeric NIQs, which indicated that both the HOMO and the LUMO are usually localized in the naphthalene, thus, no HOMO in the isoquinoline.<sup>[57]</sup> Our preliminary results suggested that A and C may react as Lewis bases and B as Lewis acid – triggered by the unfavorable *peri-peri* coupling in B – all driven by the search for more

stability. This indicated that the naphthalene B is the turning point of the reactivity of mbandakamine-like dimers.

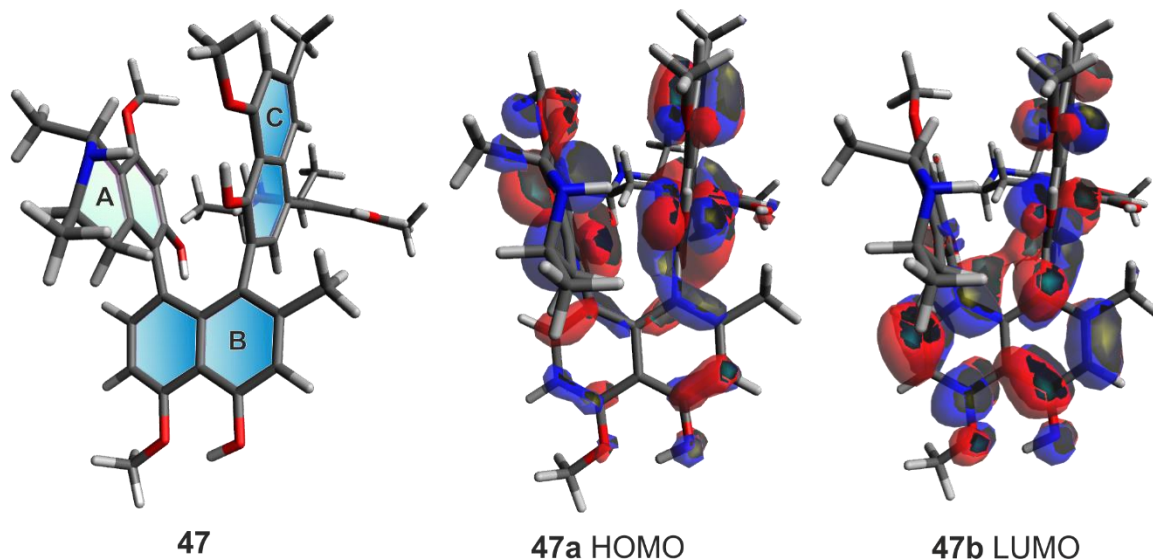


Figure 30. Minimum structure of 1-*epi*-mbandakamine A (**47**) and its DFT-calculated HOMO and LUMO molecular orbitals. The estimated HOMO-LUMO energetic gap was 94.0409 kcal mol<sup>-1</sup>, as determined by DFT calculations with B3LYP-D3/def2-TZVP.

### Biological-evaluation results and general discussion

Excellent *in vitro* activities were monitored for compounds **32**, **47**, and **48** on both chloroquine sensitive (NF54) and resistant (K1, resistant also to pyrimethamine) strains of *P. falciparum*. 1-*epi*-Mbandakamine A (**47**), mbandakamine C (**48**), and mbandakamine A (**32**) showed IC<sub>50</sub> values of 0.047 (NF54) and 0.064 μM (K1), 0.337 (NF54) and 0.126 μM (K1), and 0.060 μM (NF54), respectively (Table 3). Among these mbandakamines, **47** exhibited the best *in vitro* profile against the NF54 strain of *P. falciparum* with a selectivity index (SI) of 337, even better than its epimer **32**. The new dimer **48** displayed a reduced but still good activity on NF54. Intriguingly, **48** exhibited a better antimalarial potential on the resistant strain K1, with a marginal degree of resistance (D.R.) of 0.38. Based on the cases of ealapasamine C (**42**) and **47** (compared to **32**), it seems like a 1,3-*cis*-relative configuration is a feature in favor of the antiplasmodial activity for this type of alkaloids. This activity was reduced with the degree of methylation and reduction of the basicity of the isoquinoline nitrogen. Considering the high and quasi-exclusive prevalence of resistant strains of *P. falciparum* in regions endemic to

malaria,<sup>[40]</sup> like in Sub-Saharan countries, finding compounds with high inhibition potential and low D.R. against devastating pathogens is a priority in the drug discovery process.

Michellamine F<sub>2</sub> (**50**) was not tested for antiprotozoal activity, because of the well-known virtually inactive profile of related dimers.<sup>[104, 107]</sup> However, considering its structural closeness to michellamine F (**33**), compound **50** should also exhibit HIV-1 activity.

Table 3. Biological activities of **32**, **47**, **48** against *P. falciparum* (strains: NF54 and K1), *T. brucei rhodesiense*, *T. cruzi*, and *L. donovani*, as well as the cytotoxicities against rat skeletal myoblasts (L6 cells) (IC<sub>50</sub> in μM).

Compounds	<i>T. brucei rhod.</i>	<i>T. cruzi</i>	<i>L. donovani</i> ax. am.	<i>P. falciparum</i> NF54/K1	Cytotox. L6	Selectivity index to NF54/K1
Standard	0.007 <sup>[1]</sup>	3.56 <sup>[2]</sup>	0.43 <sup>[3]</sup>	0.008 <sup>[4]</sup> (NF54) /0.364 <sup>[4]</sup> (K1)	0.041 <sup>[5]</sup>	n.d.
<b>47</b>	1.8	41.8	>100	0.047/ 0.064	15.93	337/ 249
<b>32</b>	1.8	16.8	>100	0.060 <sup>[0.043]</sup> / -	16.56	277/ -
<b>48</b>	4.1	-	>10	0.337/ 0.126	8.87	26/ 70.4

[1] Melarsoprol. [2] Benznidazole. [3] Miltefosine. [4] Chloroquine. [5] Podophyllotoxin. All values in μM. [0.043] published IC<sub>50</sub> value of **32** on the NF54 strain.<sup>[103]</sup> n.d.: not determined. Selectivity index determined for *P. falciparum*.

The isolated dimers were also investigated for their antiproliferative potential against the human T-lymphoblastic leukemia cells CCRF-CEM strain and its multi-drug resistant form CEM/ADR5000, and against the cervical HeLa cells. The observed IC<sub>50</sub> values for **32**, **47**, and **48** were 7.403 μM (for CCRF-CEM) and 23.877 μM (for CEM/ADR5000), 1.498 μM (CCRF-CEM) and 27.706 μM (CEM/ADR5000), and 2.955 μM (CCRF-CEM) and 19.029 μM (CEM/ADR5000), respectively (Figure 31). Therefore, the degrees of resistance (D.R.)<sup>[173]</sup> can now be deduced as 3.23, 18.50, and 6.44 for dimers **32**, **47**, and **48**, respectively. In view of the extremely high D.R. value of the reference compound, doxorubicin, with 1768.82, the isolated dimers represent very promising anticancer drug candidates. Due to the restricted isolated quantity, compound **50** was tested against CCRF-CEM strain only and showed an IC<sub>50</sub> value of 18.803 μM.

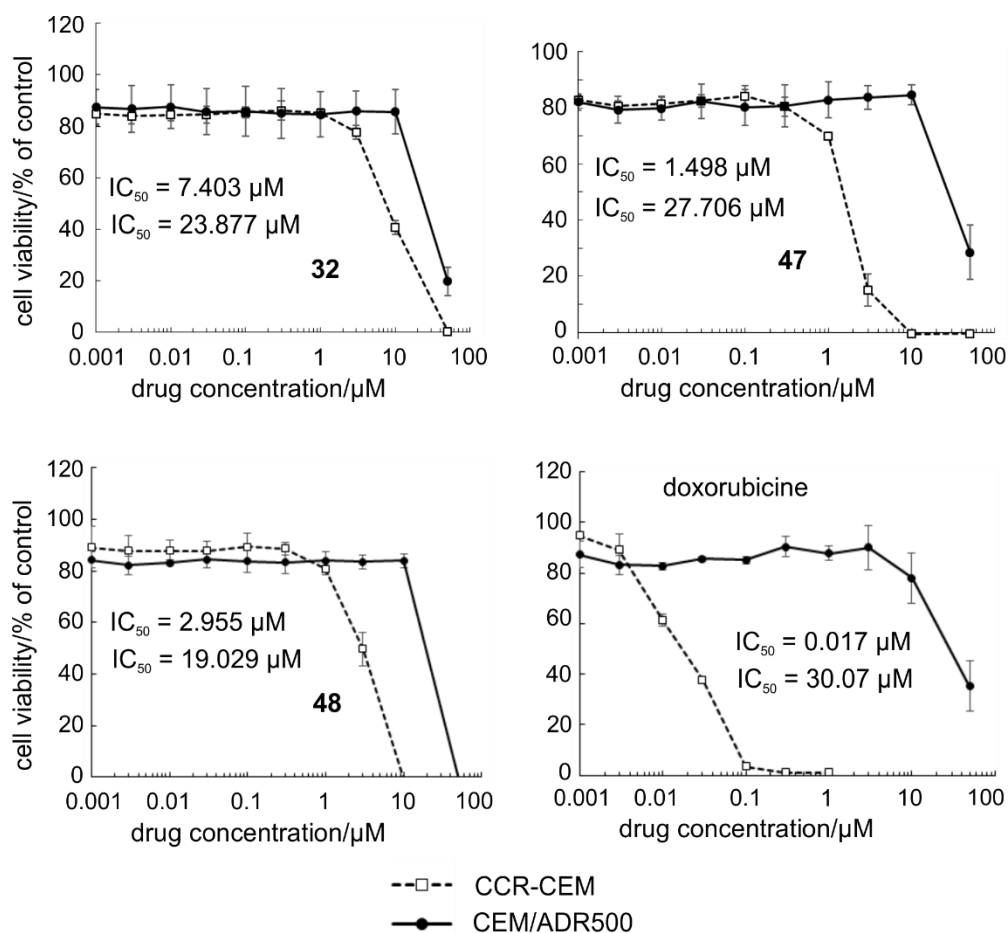


Figure 31. Antiproliferative effects of **32**, **47**, and **48** on the human T-lymphoblastic leukemia cells CCRF-CEM and the multi-drug resistant strain CEM/ADR5000. The profile of doxorubicin is shown as a reference.

The structural diversity shown by the dimers mentioned so far is already exclusive for one liana. The discovery of so many promising compounds with the relative *cis*-configuration in the tetrahydroisoquinoline subunit is quite unique considering that they are known to be unstable and may be oxidized during workup to dihydroisoquinolines.<sup>[165]</sup> This indicates the mildness of the used extraction and fractionation procedures.

From a phytochemical point of view, *A. ealaensis* is a remarkable liana capable of synthesizing dimers with extreme structural complexity, *viz.* mbandakamine-type, michellamine-type, and ealapasamine-type displaying promising bioactivities. Thus, this plant seems to be a rich source of dimeric alkaloids, hence justifying further phytochemical screening.



### II.3. Cyclombandakamines, a Unique Series of Novel Dimeric Alkaloids

Further in-depth phytochemical investigations of the leaf plant material of *A. ealaensis* led to the detection and characterization of a series of novel dimeric compounds showing an uncommon UV spectrum. Their chromatographic resolution was technically the most demanding as compared to the purification of the other quateraryls. Reproducible LC-DAD-MS-monitored fractionation and isolation procedures successfully enabled access to these uncommon alkaloids.

The structural elucidation revealed that the series of compounds shared an unprecedented structural array consisting of a twisted dihydrofuran-cyclohexenone-isochromene (pyrene) system. This condensed cage-like polycyclic 'backbone' drastically reduced the degree of freedom in the molecule and stabilized the dimeric structure. The full structural elucidation of seven representatives (Figure 32) is described in this chapter, including their biosynthetic origin, biomimetic synthesis, and bioactivities.

Nearly one year before this discovery, a compound of this class had been found for the first time. This alkaloid, which was later named cyclombandakamine A<sub>1</sub> (**58**),<sup>[178]</sup> was isolated from a chloroform fraction of a not fully described *Ancistrocladus* species. From the same source, mbandakamine A<sup>[103]</sup> had been discovered in 2012. All efforts for the re-isolation from the same plant material had remained in vain, so that the natural occurrence of this compound was questioned. Moreover, the compound had never been found again, even in new plant collections.

The search for chromatographic peaks with unusual UV spectra, aiming at an exhaustive exploration of the metabolic profile of *A. ealaensis*, now led to the characterization of seven such novel dimers in several enriched fractions.<sup>[179]</sup> This discovery proved for the first time, on the one hand, that the compounds can be isolated under mild extraction conditions, without acidic treatment of the extract, and on the other hand that *A. ealaensis* was the richest and reliable source of these novel quateraryls.<sup>[179]</sup> A reproducible phytochemical procedure was established for the reliable access to this novel class of metabolites, for the first time within this work.

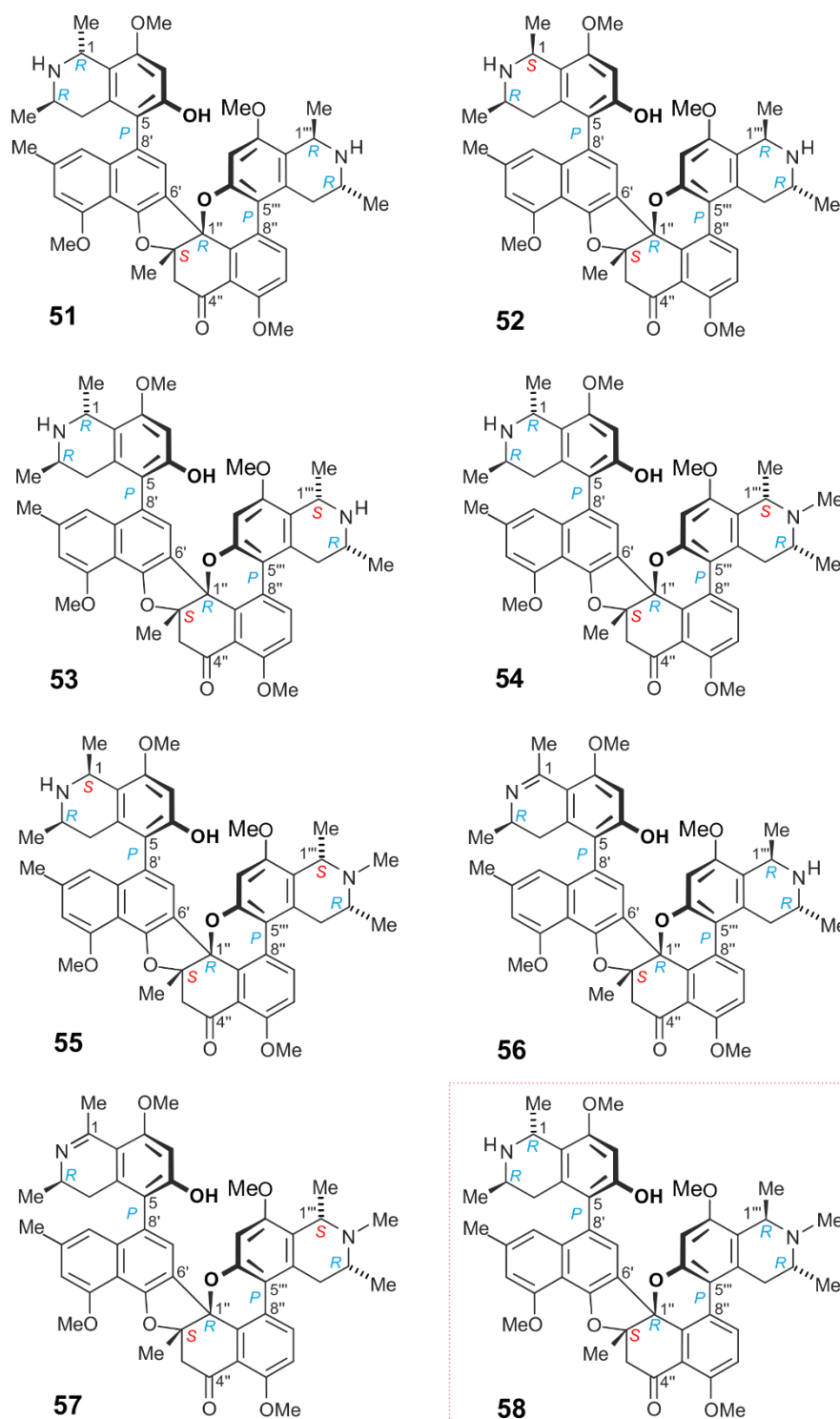


Figure 32. Cyclombandakamine A (**51**), 1-*epi*-cyclombandakamine A (**52**), and cyclombandakamines A<sub>3</sub>- A<sub>7</sub> (**53-57**), a series of alkaloids discovered in *A. ealaensis*. Cyclombandakamine A<sub>1</sub> (**58**),<sup>[178]</sup> isolated from a not-yet-described *Ancistrocladus* species.

## Structural elucidation and discussion

Further analysis of the dimeric enriched fractions led to the detection of several barely resolvable peaks jointly displaying an uncommon online-UV spectrum. The LC-MS profiles of these metabolites were typical to dihydroisoquinoline derivatives, and from the masses, they could correspond to mbandakamine-type dimers. As mentioned afore, the UV spectrum of the new mbandakamine C, which consisted of a dihydroisoquinoline portion, was very similar to the one of the related alkaloids. The combination of the MS and UV profiles suggested the presence of an unknown group of metabolites featuring different degrees of oxidation.

Depending on the chromatographic peak resolution, several combinations of HPLC columns were necessary to successfully purify these alkaloids, namely Symmetry<sup>®</sup> RP<sub>18</sub>, Chromolith<sup>®</sup> RP<sub>18</sub>, and Discovery<sup>®</sup> HS F5 bonded fluoro (pentafluorophenyl). The latter HPLC column (HS F5) offers separation processes that are different to those obtained by C<sub>18</sub> material, and it was used for the first time to resolve this class of alkaloids. High-speed silica-bonded pentafluorophenyl columns have the advantage to exhibit both, normal and reversed-phase behavior and proceed by hydrophobic and ion-exchange mechanisms to improve the selectivity of hardly resolvable basic compounds.<sup>[180]</sup>

From a sub-fraction, which was resolvable only by the silica-based HS F5 column, compound **51** was obtained in a pure form. By HRESIMS the compound exhibited a protonated molecular fragment at  $m/z$  783.36451, calculated for 783.36399 [M+H]<sup>+</sup>, leading to a molecular formula of C<sub>48</sub>H<sub>50</sub>N<sub>2</sub>O<sub>8</sub> with a degree of unsaturation of 25. The molecular formula was identical to that of the new mbandakamine C (**48**), but the UV, the ECD, and the NMR data were unambiguously different, hinting at an unknown type of dimer (see chromatogram and spectra depicted in Figure 33). The presence of 48 signals in the <sup>13</sup>C NMR spectrum indicated that the compound was unsymmetric. In contrast to all known heterodimers, including those so far described in this thesis, seven aromatic protons were detected instead of eight, which was unprecedented. Its demanding full structure was elucidated by means of extensive 1D and 2D NMR experiments, ruthenium-mediated oxidative degradation combined with GC-MS analysis, and ECD spectra measurements and DFT-based quantum-chemical calculations.

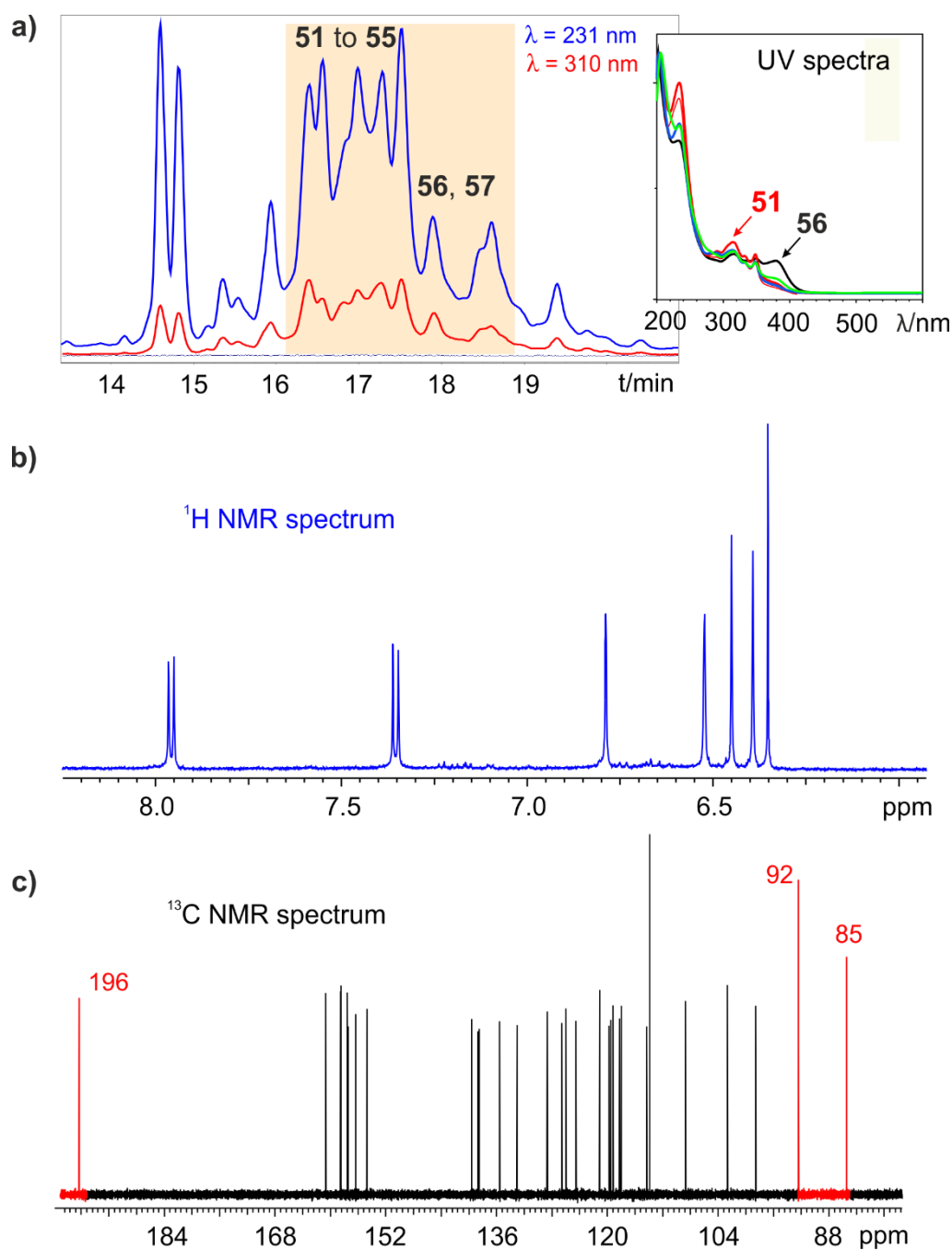


Figure 33. (a) An HPLC chromatogram of a representative fraction containing unresolved cyclombandakamines **51-57** (in the highlighted region), recorded at 231 nm (in blue) and 310 nm (in red). Distinctive offline UV spectra of isolated peaks, showing their identical feature. (b) The typical aromatic region of the  $^1\text{H}$  NMR spectrum, displaying seven proton signals only. (c) The characteristic upfield region of the  $^{13}\text{C}$  NMR spectrum, exhibiting uncommon signals at 196, 92 and 85 ppm.

The first northwestern portion of the molecule elucidated showed interestingly four aromatic protons, as in the case of **47**, two methoxy functions and seven further signals in the  $^1\text{H}$  NMR spectra. Data analysis revealed the presence of a tetrahydroisoquinoline subunit. This

isoquinoline possessed one aromatic singlet at H-7 ( $\delta_{H,C}$  6.39, 98.6 ppm) interacting in HMBC with two  $\alpha$ -oxygenated carbons C-6 and C-8). The presence of an *O*-methyl group was evidenced at C-8 by ROESY interactions from H-7 and H-1 ( $\delta_{H,C}$  4.68, 49.7) to CH<sub>3</sub>O-8 ( $\delta_H$  3.85), leaving the unprotonated position 5 ( $\delta_C$  119.7) as a coupling point. The typical two methyl doublets at C-1 and C-3 of NIQs, the two doublets of doublets at C-4, and the multiplet at C-3 ( $\delta_{H,C}$  3.52, 44.9) were detected as part of this portion. Its relative configuration was assigned to be *trans* by ROESY experiments.

Attached to this moiety, a two fold oxygenated naphthalene unit possessing one pair of *meta*-coupled signals at C-1' ( $\delta_{H,C}$  6.52, 118.0) and C-3' ( $\delta_{H,C}$  6.79, 108.7), one aromatic singlet H-7' ( $\delta_{H,C}$  6.35, 126.0), a methoxy at C-4' and a methyl at C-2' was identified. The presence of a singlet at C-7' suggested that C-6' and C-8' were substituted. This assumption was corroborated by two HMBC interactions with carbon atoms belonging to other spin systems. The HMBC cross peak between H-7' and C-5 indicated a 5,8' linkage to the tetrahydroisoquinoline unit (Figure 34a,b). Additionally, H-7' showed ROEs with 4-H<sub>eq</sub> ( $\delta_H$  2.35 ppm) while H-1' exhibited cross peaks in both dimensions with 4-H<sub>ax</sub> ( $\delta_H$  1.94 ppm), confirming further the coupling of the two subunits and, thus, establishing the relative configuration in this 5,8'-coupled moiety, *viz.* 5*P*,1*R*,3*R* or 5*M*,1*S*,3*S*.

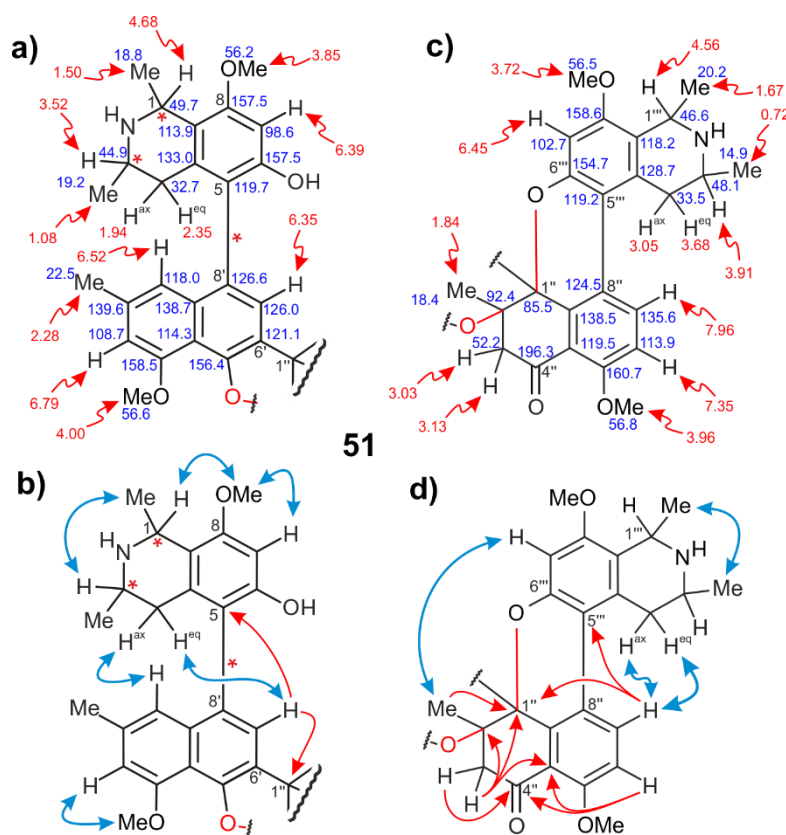


Figure 34. Chemical shifts (in ppm) of (a) the northwestern and (c) the southeastern halves of **51**. Selected ROESY (double blue arrows) and HMBC (single red arrows) interactions in (b) the first and in (d) the second half of cyclombandakamine A (**51**) are shown below.

The absolute configurations at C-3 and C-3''' were established by oxidative degradation. The experiment exclusively delivered the *R*-configured aminobutyric acid enantiomer, indicating an *R*-configuration at C-3 and C-3'''. Considering the relative orientation at the stereogenic centers, the absolute configuration in the first molecular half was deduced to be *5P,1R,3R*. Presenting a further substitution at C-6', as suggested by HMBC correlation of H-7' with C-1'' (see Figure 34b), the constitution of this northwestern portion was almost identical to that of the first half in mbandakamine A, but the chemical shift of C-7' indicated a major structural difference.

The HMBC correlation from H-7' to an uncommon signal at a resonance of 85.5 ppm – located in another molecular portion – triggered the necessity to elucidate its direct chemical environment. Besides H-7', three methyl protons with resonances of  $\delta_{\text{H,C}}$  1.84 and 18.4 ppm (CH<sub>3</sub>-2''), two doublets belonging to diastereotopic protons at the resonances of 3.13 (3''-H<sub>ax</sub>) and 3.03 ppm (3''-H<sub>eq</sub>) shown by HMBC  $^3J_{\text{C,H}}$  cross peaks with the same quaternary carbon at 85.5 ppm, which was numbered as C-1''. One binding site of C-1'' remained undefined, but the

low-field chemical shift suggested a linkage to an electron-withdrawing group, like a heteroatom. The presence of two further diastereotopic protons in this dimeric moiety, displaying geminal coupling constants of ca. 15 Hz attached to C-3" ( $\delta_C$  52.2 ppm), was unprecedented, and suggested the existence of a quaternary and asymmetric carbon atom next to C-3". The methyl group, attached to an aliphatic carbon C-2" ( $\delta_C$  92.4 ppm), showed exclusive HMBC interactions to C-1", C-2", and C-3". This indicated, on the one hand, the location of the methyl group between C-1" and C-3" and, on the other hand, the lack of a proton at C-2", which therefore should be the additional quaternary carbon atom in this spin system. One coordinate of C-2" remained yet unclear, and could be well defined only at a later stage of the elucidation.

HMBC correlations were observed from 3'-H<sub>eq</sub> and 3'-H<sub>ax</sub> to a signal at the low-field resonance of  $\delta_C$  196.3 ppm, corresponding to a carbonyl function at C-4". An aromatic doublet in the  $^1\text{H}$  spectrum displayed a  $^4J_{\text{C,H-HMBC}}$  interaction to C-4", hinting at the connection to another molecular fragment. This aromatic proton, occurring as a doublet ( $J = 9.0$  Hz) at a resonance of 7.35 ppm, was *ortho*-coupled to another one, but more deshielded, at 7.96 ppm. The ROESY interaction between a methoxy group (CH<sub>3</sub>O-5",  $\delta_{\text{H,C}}$  3.96, 56.8) and the proton H-6" ( $\delta_{\text{H,C}}$  7.35, 113.9), and the HMBC correlation from H-7" ( $\delta_{\text{H,C}}$  7.96, 135.6) to C-5" ( $\delta_C$  160.7 ppm) clarified the assignment in the aromatic system (Figure 34c,d).

Moreover, HMBC correlations from H-6" and 3"-H<sub>eq</sub> to a quaternary carbon at the resonance of 119.5 ppm (C-10"), from H-7" to C-9 ( $\delta_C$  138.5 ppm), and the  $^4J_{\text{C,H-HMBC}}$  cross peak observed from H-7" to C-1" unambiguously suggested the presence of a tetralone instead of a classical naphthalene moiety. In *Ancistrocladus* species, such acetogenic tetralone portions had been known to occur, *viz.* *cis*-isoshinanolone (**60**),<sup>[64, 181-184]</sup> but had never been found as part of a monomeric or dimeric naphthylisoquinoline alkaloid.<sup>[34]</sup>

The present dimer consisted of a *cis*-isoshinanolone-like portion, which showed a pair of *ortho*-coupled aromatic protons at H-6" and H-7", leaving C-8" ( $\delta_C$  124.5 ppm) as a connecting point to another spin system. In the HMBC spectrum, an additional cross peak observed from H-7" to a quaternary carbon at the resonance of  $\delta_C$  119.2 ppm (C-5''') suggested the existence of a further linkage to the tetralone. One aromatic singlet at H-7''' ( $\delta_{\text{H,C}}$  6.45, 102.7 ppm) was identified to be also in an HMBC relationship with C-5''', C-6''' ( $\delta_C$  154.7 ppm), C-8''' ( $\delta_C$  124.5 ppm), C-9''' ( $\delta_C$  118.2 ppm) and C-1''' ( $\delta_C$  46.6 ppm) reminiscent of a classical 1,3-dimethyl-tetrahydroisoquinoline subunit as in the northwestern part of the dimer (Figure 34d). The

characteristic quartet at C-1''', the multiplet at C-3''', and the two diastereotopic doublets of doublets at C-4''' typical of a tetrahydroisoquinoline were observed and assigned accordingly. The relative *trans*-configuration in this moiety was established by ROESY analysis. The oxidative degradation experiments revealed that all C-3 related position were *R*-configured, thus, leading to the elucidation of a 1'''*R*,3'''*R*-tetrahydroisoquinoline, which was 5'''-coupled to a 5''-methoxy-2''-methyl tetralone unit, in this second portion (see Figure 34c,d).

At this stage of the elucidation, all signals detected in the  $^{13}\text{C}$  and  $^1\text{H}$  NMR were assigned and all the ten heteroatoms suggested by the molecular formula positioned. Still, the calculated degree of unsaturation related to  $\text{C}_{48}\text{H}_{50}\text{N}_2\text{O}_8$  was not yet reached, but added up to 23 instead of 25. This discrepancy of two units could only be explained by the formation of two additional heterocyclic rings. As mentioned before, the resonance of the quaternary and  $\text{sp}^3$  C-1'' suggested a connection to a heteroatom, and in this case, only an oxygen function attached to C-6''' could explain its deshielded chemical shift at 85.5 ppm. This assumption was proven by the observed ROESY interactions from H-7'' to the two diastereotopic protons at C-4''', proposing a quasi-coplanar orientation of the tetrahydroisoquinoline towards the substituted tetralone, consecutive to the formation of a new pyran ring between the oxygen function at C-6''' and C-1'' (see Figure 34d).

The fourth bond of the quaternary C-2'' – in the tetralone unit – had also remained undefined. The extremely low-field shifted signal of C-2'', at a resonance of  $\delta_{\text{C}}$  92.4 ppm, hinted at a linkage to a neighboring oxygen function, which in this case could only be the one at C-5', which would be in accordance with the chemical shift of C-2''. The ROESY correlations observed between  $\text{CH}_3\text{O}-4'$  and  $\text{CH}_3-2''$  supported the formation of this five-membered dihydrobenzofuran ring attached to the tetralone, which would further stabilize the linkage of the northwestern half to the tetralone.

The full constitution of the new dimer was elucidated after all experimental data had been evaluated and had been found to form a consistent interpretation of the measured NMR signals (Figure 34). This novel dimer displayed two oxygen-bridged heterocyclic rings, both unprecedentedly twisted to a tetralone unit.

The assignment of the absolute configuration in the northwestern portion was achieved in a straightforward manner, like in the previous cases. However, the task for the second, southeastern one turned out to be challenging because of the two additional stereogenic centers present in the cyclohexenone ring, for which the degradation procedure could not directly



determine the spatial orientation. However, the steric constraints imposed by the cage-like twisted rings enabled the discrimination between the possible stereoisomers.

To achieve this goal, the absolute configuration at the biaryl axis between C-5''' and C-8'' was investigated. As mentioned above, the formation of the pyran ring forced the usually orthogonal-isoquinoline to become quasi-coplanar to the tetralone with an angle of 28.5°. This unprecedented orientation of the two subunits brought the axial and equatorial diastereotopic protons at C-4''' in the vicinity of H-7''. However, a stronger ROESY interaction of H-7'' to 4'''-H<sub>eq</sub> indicated an axial *P*-configuration in this molecular half. A *P*-configured biaryl axis additionally implied that the oxygen bridge to C-1'' must have been formed from above the plane, and thus inevitably suggesting the absolute configuration at C-1'' to be *R*. Within these atomic arrangements, C-1'' would have been *S* if the axis was *M*, which would not have explained the observed ROESY interactions between H-7'' and 4'''-H<sub>eq</sub>, those from H-7 and H-7' to 4'''-H<sub>ax</sub>, and from CH<sub>3</sub>-3''' to H-7 and H-7''. Hence, this all strongly indicated an *R*-configuration at C-1''. The later series of ROESY interactions were found plausible for both cases, the absolute configuration at C-2'' being either *R* or *S* (Figure 35a-d).

The analysis of the minimum structures presenting both scenarios indicated that in the case of an *R*-configuration at C-2'' (Figure 35a), the methyl CH<sub>3</sub>-2'' should be underneath the tetralone plane, and thus, on the opposite side of the new bridge at C-1'', and should show long-range ROESY interactions to 4-H<sub>eq</sub> – given the calculated distance of 3.269 Å – but no interaction possible to CH<sub>3</sub>O-4'. Additionally, these investigations predicted a decisive ROESY interaction between CH<sub>3</sub>-2'' and H-7''', which was found to be corroborative for the relative *trans*-configuration in the tetralone, *viz.* 1''*R*,2''*S* or 1''*S*,2''*R*. Knowing the spatial arrangement of C-1'' (*R*), only the diastereomer 1''*R*,2''*S* was plausible for the cyclohexenone unit. Moreover, the analysis of optimized structures featuring the relative *cis*-configuration, *i.e.* 1''*R*,2''*R* or 1''*S*,2''*S*, indicated that CH<sub>3</sub>-2'' and H-7''' showed opposite spatial orientations and should never exhibit a cross peak by ROESY. Thus, the absolute configuration at C-2'' was confirmed to be *S* (Figure 35d).

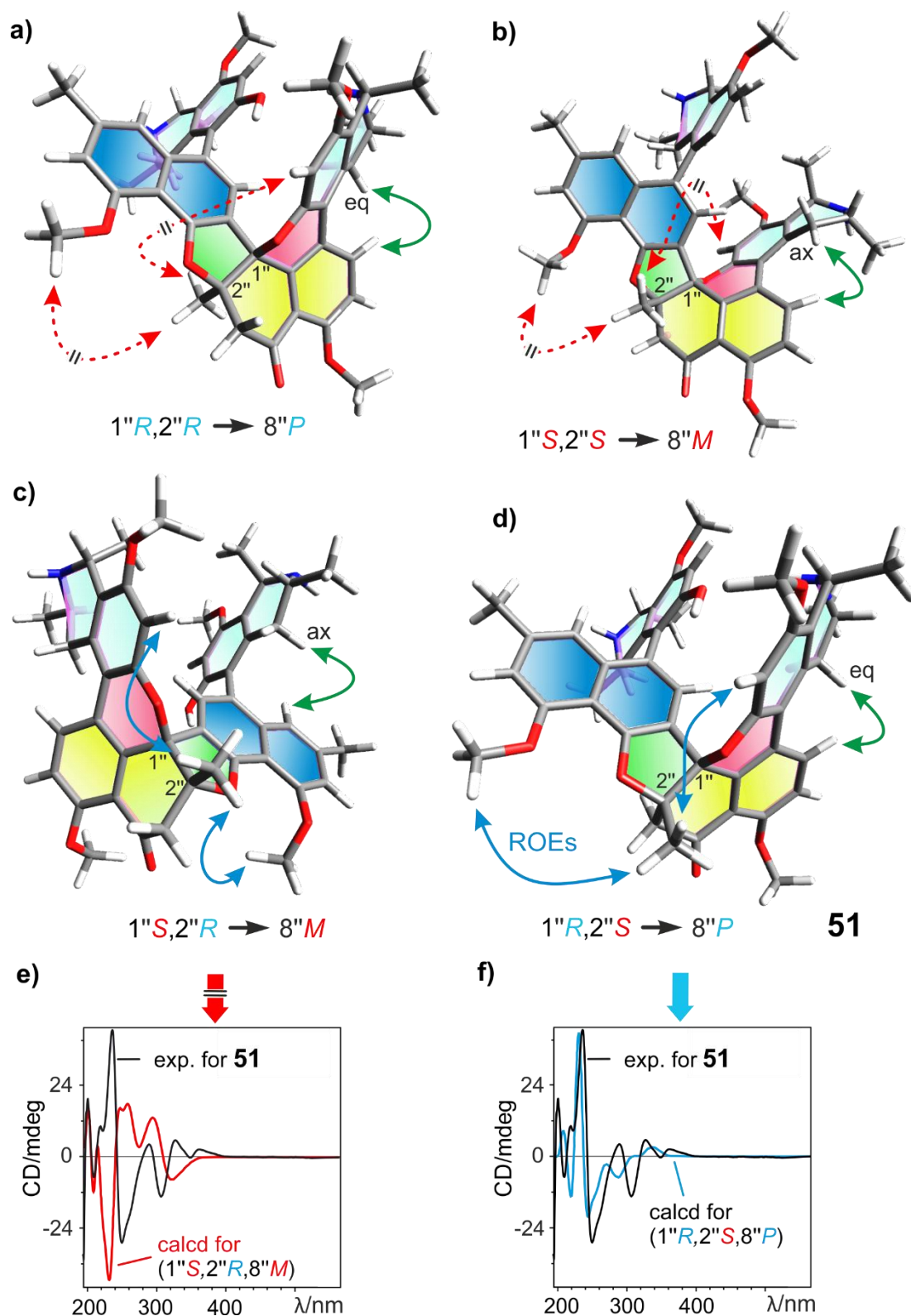


Figure 35. (a),(b),(c) and (d) Minimum structures (at the DFT-B3LYP-D3/def2-TZVP level) of the four most possible stereoisomers of cyclombandakamine A (**51**) with expected crucial ROEs for the relative configuration. The ROESY interactions in blue are indicative of the *trans*- or *cis*-orientation in the cyclohexanone while those in red are not expected to be observed. The green double arrows suggest the strongest ROEs between H-7'' and one of the diastereotopic protons at C-4'', relevant for the axial

configuration. (e) and (f) The experimental ECD spectrum of **51** compared to the calculated curves of the two most plausible *trans*-diastereomers ( $1''S,2''R$  and  $1''R,2''S$ ) in the tetralone subunit,<sup>[178]</sup> confirming that the isolated structure of **51** is shown at (d). The ECD spectra were calculated at the TDCAM-B3LYP/def2-TZVP level.<sup>[178]</sup>

Based on the aforementioned assignment, the full stereochemical features of the dimer **51** could only be  $5P,1R,3R,1''R,2''S,8''P,1'''R,3'''R$ . Additionally, the structural attributions agreed with the observed ROESY interactions across the two molecular halves, in particular, those between H-7 and H-1''', H-7' and H-1'', H-3 and 4'''-H<sub>ax</sub>, and from CH<sub>3</sub>-3''' to CH<sub>3</sub>O-8.

A supplementary proof of these assignments was provided by time-dependent density functional theory (TDDFT) quantum-chemical calculations of the ECD spectra performed with TDCAM-B3LYP/def2-TZVP (Figure 35e,f),<sup>[178-179]</sup> by Dr. T. Bruhn. The compound had the advantage to possess a cage-like rigid polycyclic ring system made of a dihydrobenzofuran-tetralone-isochromene chromophore. Therefore, the conformational analysis of the two relevant diastereomers consisted of a *cis*- and a *trans*-configured cyclohexenone, namely for  $1''R,2''S,8''P$  and  $1''S,2''R,8''M$ . As anticipated, the experimental and the calculated ECD spectra for the *trans* diastereomer of **51** in the cyclohexenone ( $1''R,2''S,8''P$ ) showed good agreement, while the *cis* diastereomer ( $1''S,2''R,8''M$ ) displayed a more or less opposite ECD curve, firmly validating the assignment obtained above. Because of its structural array, related to the known co-occurring mbandakamine A, the novel alkaloid was named cyclombandakamine A (**51**).

To learn more about this thrilling type of naphthylisoquinoline, it was worthy to invest efforts in the HPLC resolution of other chromatographic peaks displaying the similar online UV and MS features. Another substance, showing the same UV spectrum as cyclombandakamine A (**51**), was purified from a later RP<sub>18</sub> fraction using the same HS F5 prep-HPLC column. The isolated compound was found to possess the same molecular formula as **51**, *i.e.* C<sub>48</sub>H<sub>50</sub>N<sub>2</sub>O<sub>8</sub>, as deduced from HRESIMS. A meticulous structural data analysis, as for the elucidation of **51**, led to an identical constitution as that of cyclombandakamine A, hinting at a new dimer as well. The first glimpse on the <sup>1</sup>H and the <sup>13</sup>C NMR spectra revealed the typical seven aromatic protons, including the two *ortho*-coupled doublets, the two unusual diastereotopic protons at C-3'', the untypical signals at  $\delta_C$  196.3, 92.4, and 85.4 ppm, and the uncommon third methylene group in the DEPT-135 at the resonance of 52.2 ppm (C-3''), all strongly suggesting a cyclombandakamine A analog.

The main structural difference to **51** was found in the tetrahydroisoquinoline unit of the northwestern portion, which showed a relative *cis*-configuration instead of *trans*, as evidenced by the ROEs between H-1 ( $\delta_{H,C}$  4.52, 52.0 ppm) and H-3 ( $\delta_{H,C}$  3.09, 50.6 ppm) and their respective  $^1\text{H}$  and  $^{13}\text{C}$  resonances. Based on all the detected correlations, the absolute configuration in this first half could be either *5P,1S,3R* or *5M,1R,3S*. To figure this out, oxidative degradation experiments were performed and revealed, as in the case of **51**, that all C-3 positions in the tetrahydroisoquinolines were *R*-configured. Thus, this first half was *5P,1S,3R*.

Analysis of the full NMR data set, and in particular of the ROESY spectrum, indicated no further differences to cyclombandakamine A (**51**). Even their ECD spectra were identical, suggesting the same chromophoric orientation. Based on its structure corresponding to a 1-epimer of **51**, the new alkaloid was named 1-*epi*-cyclombandakamine A (**52**).

Interestingly, the earlier-described 1-*epi*-mbandakamine A (**47**) corresponds to the open-chain form of the cyclic alkaloid **52**, thus to its potential precursor.

Semi-preparative resolution on Chromolith<sup>®</sup> column enabled the purification of a trace alkaloid displaying the same UV spectrum as that of **51**. Although in a small amount, the full set spectroscopic data of the compound was recorded and analyzed. The compound did not only exhibit the same molecular formula by HRESIMS, but also the identical constitution as **51** and **52**.

Structural elucidation indicated that the first half (the northwestern one) was stereochemically identical to the one described for cyclombandakamine A and the chemical shifts remained overall intact (as depicted in Figure 34a,b). The second molecular portion was also similar to the one found in **51**, but in the tetrahydroisoquinoline unit, the ROESY interactions between H-1''' ( $\delta_{H,C}$  4.49, 52.9 ppm) and H-3''' ( $\delta_{H,C}$  3.81, 50.2 ppm) evidenced their diaxial orientations. The relative *cis*-configuration could again be characterized by the chemical shifts, as in the previous cases. Besides, all other interactions within this southeastern moiety remained identical to those observed in **51** (see Figure 34d). The configuration at all C-3 positions and the ECD spectrum were the same as for **51**, suggesting that the only difference to cyclombandakamine A was the absolute configuration at C-1''', *i.e.* *S*-configured. This structural change was validated by the new ROESY cross peak between CH<sub>3</sub>-1''' ( $\delta_{H,C}$  1.63, 20.4 ppm) and H-7 ( $\delta_{H,C}$  6.39, 98.6 ppm), while no ROEs were monitored between H-7 and H-1'''.

Therefore, the full stereostructure of the new alkaloid was  $5P,1R,3R,1''R,2''S,8''P,1'''S,3'''R$ , and it was named cyclombandakamine A<sub>3</sub> (**53**), but it could also be addressed as 1'''-epi-cyclombandakamine A.

In the same fraction as cyclombandakamine A<sub>3</sub> (**53**), the main chromatographic peak was isolated and purified, presenting the same uncommon online UV spectrum but eluting more slowly on Chromolith® HPLC column. High-resolution ESI-MS analysis led to the molecular formula of C<sub>49</sub>H<sub>52</sub>N<sub>2</sub>O<sub>8</sub>, signifying an increase of 14 units, and suggesting an additional methyl group compared to that of **51**. The degree of unsaturation remained the same. Extensive structural data analysis was conducted and led to the presence of a derivative of cyclombandakamine A, and all the yet typical signals were present in the NMR spectra (Figure 36).

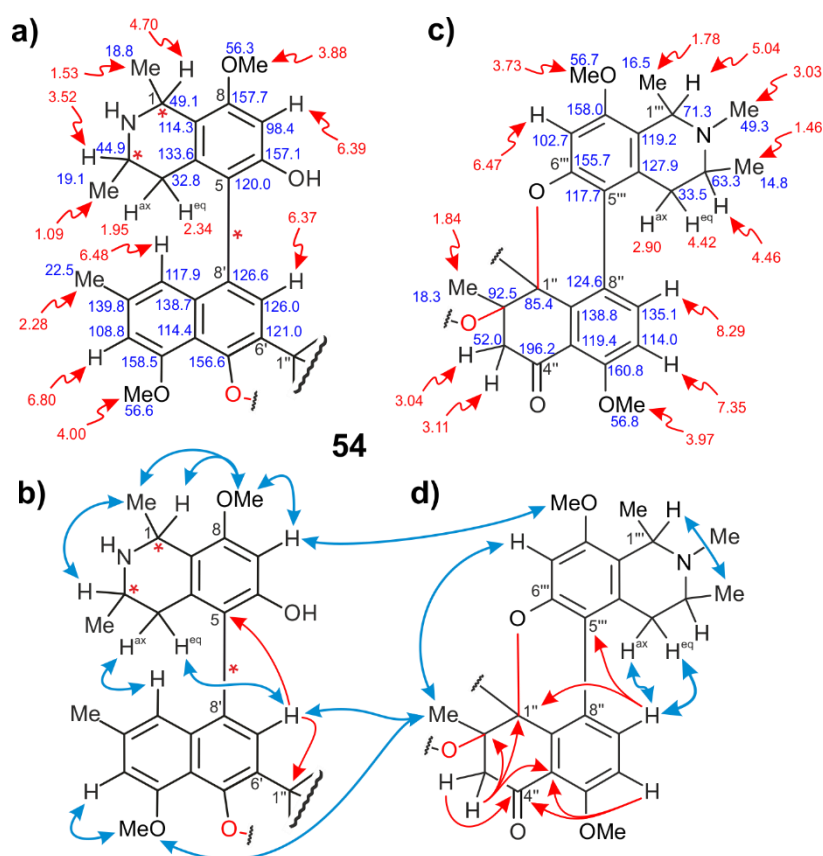


Figure 36. Chemical shift values in ppm of (a) the northwestern and (c) the southeastern halves of cyclombandakamine A<sub>4</sub> (**54**). Selected ROESY (double blue arrows) and HMBC (single red arrows) interactions in (b) the first and in (d) the second half of **54**.

The northwestern molecular portion of this alkaloid was found to be identical to the corresponding half of **51**, and no constitutional modification was noticed (see Figure 36a,b).

With identical results from the oxidative degradation experiments, the configuration in this part of the dimer was, thus, *5P,1R,3R*.

A similar constitution to the second, southeastern part of cyclombandakamine A (**51**) was also assigned in this case to the portion, but the structural elucidation revealed the additional presence of an *N*-methylated tetrahydroisoquinoline subunit. This was evidenced by a singlet at a resonance of 3.03 ppm, corresponding to a methyl group on the nitrogen (MeN-2'''), which was also proven by HSQC ( $\delta_C$  49.3 ppm). The *N*-methyl group seemed to be not the only difference to **51**. Since, the  $^1\text{H}$ - and  $^{13}\text{C}$  NMR shifts at C-1''' ( $\delta_{\text{H,C}}$  5.04, 71.3 ppm) and C-3''' ( $\delta_{\text{H,C}}$  4.46, 63.3 ppm) were extremely deshielded, like never observed before within this class of alkaloids, except in the case of **49**. The ROESY interactions from the low-field shifted quartet of H-1''' to the unusual multiplet H-3''' indicated a relative *cis*-configuration in this *N*-methylated tetrahydroisoquinoline moiety. As mentioned above, the formation of *R*-aminobutyric acid in the degradation experiment indicated the configuration at C-3'''. Additionally, the *R*-enantiomer of the *N*-methyl aminobutyric acid was detected and assigned to this second moiety. Knowing the *R*-configuration at C-3''', the one at C-1''' was deduced to be *S* based on the relative *cis*-configuration. The discriminating stronger ROESY interaction from H-7'' ( $\delta_{\text{H,C}}$  8.29, 135.1 ppm) to the deshielded 4'''-H<sub>eq</sub> ( $\delta_{\text{H,C}}$  4.43, 33.5 ppm) rather than to 4'''-H<sub>ax</sub> ( $\delta_{\text{H,C}}$  2.91, 33.5 ppm) indicated the 8''*P*,1''*R* orientation of the molecular half. The ROESY interaction between CH<sub>3</sub>-2'' ( $\delta_{\text{H,C}}$  1.84, 18.3 ppm) and H-7''' ( $\delta_{\text{H,C}}$  6.47, 102.7 ppm), like in the previous cases, suggested the *trans*-arrangement in the cyclohexenone, and thus, the 8''*P*,1''*R*,2''*S*,1'''*S*,3'''*R* configuration in this *N*-methylated *cis*-configured second molecular half (see Figure 36c,d). The ECD spectrum was found to be identical to the one of cyclombandakamine A, confirming the full absolute stereostructure to be *5P,1R,3R,1''R,2''S,8''P,1'''S,3'''R*. These new structural changes were in line with the observed ROESY interactions across the molecular halves, namely between MeN-2''' and H-7'' ( $\delta_{\text{H,C}}$  6.39, 98.4 ppm), and those from CH<sub>3</sub>O-8'' ( $\delta_{\text{H,C}}$  3.88, 56.3 ppm) to MeN-2'''. The new alkaloid was named cyclombandakamine A<sub>4</sub> (**54**).

The purification of another peak first obtained on a Symmetry<sup>®</sup> HPLC column led to the isolation of 1-*epi*-cyclombandakamine A (**52**) and an additional peak, displaying a similar UV spectrum. The high-resolution mass of the unknown compound corresponded to a molecular formula of C<sub>49</sub>H<sub>52</sub>N<sub>2</sub>O<sub>8</sub>, as obtained for **54**, suggesting the presence of another methylated form of cyclombandakamine A. The analysis of its structural data confirmed the presence of a further derivative of **51** but displaying the exact constitution as that of **54** (Figure 37).

From the full elucidation, the compound was found to be an epimer to **54**, and the main difference was found in the northwestern half, which turned out to be 1,3-*cis*-configured. This was evidenced by the ROESY interactions from H-1 ( $\delta_{H,C}$  4.53, 52.0 ppm) to H-3 ( $\delta_{H,C}$  3.09, 50.6 ppm), their remarkable chemical shifts, and the 3*R*,3''*R*-configurations deduced from oxidative degradation (see Figure 37a,b). As in the case of **54**, the degradation results revealed the presence of *R*-enantiomer of *N*-methyl aminobutyric acid attributable to the southeastern portion.

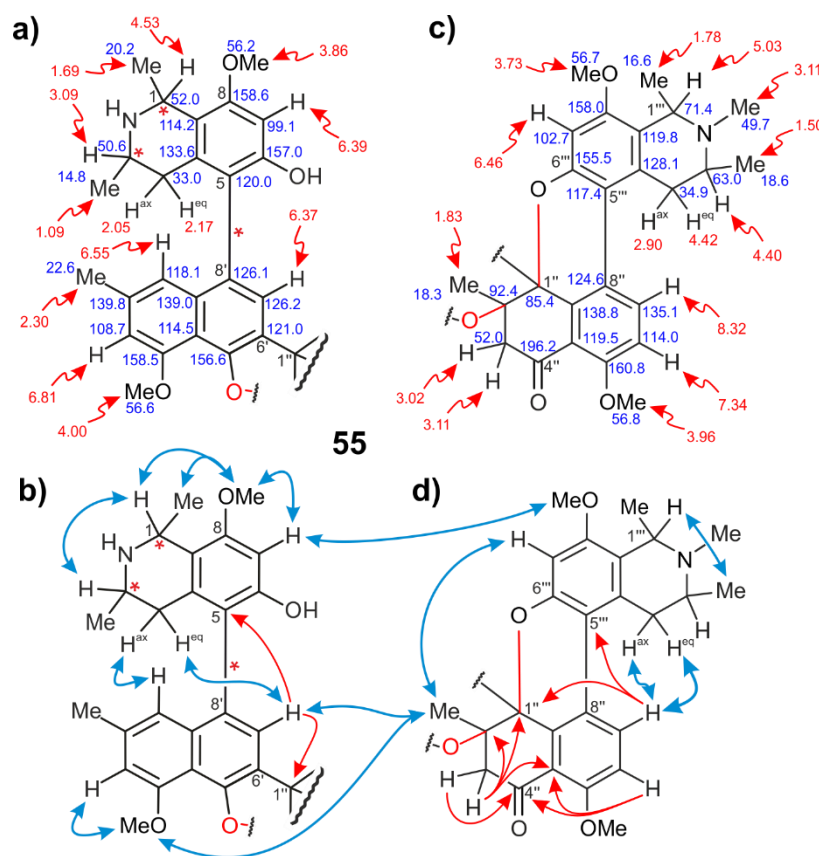


Figure 37. Chemical shifts (in ppm) of (a) the northwestern and (c) the southeastern halves of **55**. Selected ROESY (double blue arrows) and HMBC (single red arrows) interactions in (b) the first and in (d) the second half of cyclombandakamine A<sub>5</sub> (**55**) are shown below.

All other experimental outcomes and the ROESY interactions within and across the portions remained identical to those of **54**. Also typical were the deshielded <sup>1</sup>H and <sup>13</sup>C chemical shifts at C-1''' ( $\delta_{H,C}$  5.03, 71.4) and C-3''' ( $\delta_{H,C}$  4.40, 63.0), which should be considered from now on as characteristic of *cis*-configured and *N*-methylated (*N*-Me) tetrahydroisoquinoline located in the southeastern part of (cyclo)mbandakamines. The full stereochemical elements were ultimately determined to be 5*P*,1*S*,3*R*,1''*R*,2''*S*,8''*P*,1'''*S*,3'''*R*. The new alkaloid was named

cyclombandakamine A<sub>5</sub> (**55**). Its uniqueness arises from the fact that this dimer is the first unsymmetric naphthylisoquinoline alkaloid featuring two linked, *N*-H and *N*-Me, tetrahydroisoquinolines units, both being *cis*-configured.

Eluting on a Symmetry<sup>®</sup> column after the fraction mainly containing cyclombandakamine A<sub>5</sub> (**55**), another peak was better resolved from the series and still displayed the same UV and ECD spectra. Its HRESIMS profile exhibited a protonated molecular ion [M+H]<sup>+</sup> at *m/z* 781.34886, corresponding to a new calculated molecular formula C<sub>48</sub>H<sub>48</sub>N<sub>2</sub>O<sub>8</sub> with an index of hydrogen deficiency (IHD) of 26. Combined with the presence of only three doublets – with *J* ≈ 6.5 Hz – in the <sup>1</sup>H NMR high-field region, the molecular formula strongly suggested a dihydroisoquinoline derivative of cyclombandakamine A (**51**). Its shared structural features with those of **51** were evidenced by the presence of seven aromatic <sup>1</sup>H NMR signals, the two diastereotopic doublets at C-3" ( $\delta_{\text{H}}$  3.11 and 3.02,  $\delta_{\text{C}}$  52.2 ppm), as well as the carbon signals corresponding to C-1" ( $\delta_{\text{C}}$  85.3 ppm), C-2" ( $\delta_{\text{C}}$  92.5 ppm), and C-4" ( $\delta_{\text{C}}$  196.2 ppm).

The assignment of the dihydroisoquinoline moiety was proven by the lack of a proton in position 1 and the deshielded chemical shift of C-1 ( $\delta_{\text{C}}$  175.2 ppm), and the appearance of CH<sub>3</sub>-1 ( $\delta_{\text{H,C}}$  2.71, 24.9 ppm) in <sup>1</sup>H NMR as a singlet (Figure 38). Despite some chemical shift changes, the rest of this molecular half remained identical to the related one in **51**, and the absolute configurations at all C-3 positions were determined by oxidation to be also *R*.



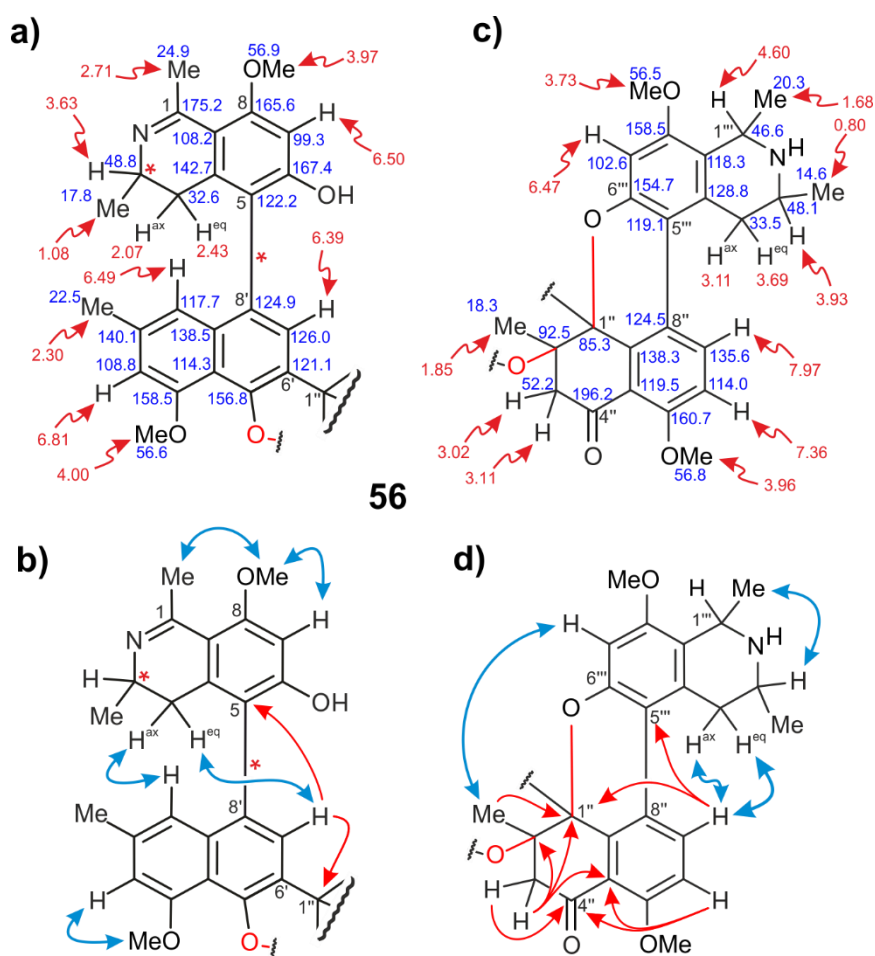


Figure 38. Chemical shifts (in ppm) of (a) the northwestern and (c) the southeastern halves of cyclombandakamine A<sub>6</sub> (**56**). Selected ROESY (double blue arrows) and HMBC (single red arrows) interactions in (b) the first and in (d) the second half of **56** are shown below.

The full assignment of the second half did not reveal any further dissimilarity to cyclombandakamine A (**51**), even with respect to the ROESY correlations across the molecular halves. Hence, the complete stereostructure of compound **56** was established as *5P,3R,1''R,2''S,8''P,1'''R,3'''R*, and it was named cyclombandakamine A<sub>6</sub> (**56**).

The last alkaloid fully characterized in this series required several cycles of purification at the semi-preparative HPLC with Chromolith<sup>®</sup> and using methanol instead of acetonitrile. The UV and ECD spectra were similar to those of the cyclic-mbandakamine alkaloids. The molecular formula was determined to be C<sub>49</sub>H<sub>50</sub>N<sub>2</sub>O<sub>8</sub> (794.93174) from a peak at *m/z* 811.35652 [M+H+O]<sup>+</sup> by HRESIMS (calcd for C<sub>49</sub>H<sub>51</sub>N<sub>2</sub>O<sub>9</sub>, 811.35946), with an IHD of 26. This oxygenated<sup>[185]</sup> molecular species suggested the presence of an additionally methylated dihydroisoquinoline derivative of cyclombandakamine A. The full set of NMR data confirmed

the mentioned hints at the compound class, but revealed, some peculiarities in both halves of the dimer compared to the hit structure, cyclombandakamine A (**51**).

The assignment of the northwestern molecular part led to the identification of a 5,8'-coupled naphthylisoquinoline like in **51** but consisting of a dihydroisoquinoline subunit similar to the one found in **56**. This was demonstrated by the presence of the typical signal corresponding to C-1 ( $\delta_C$  175.4 ppm) in the  $^{13}\text{C}$  spectra, the presence of three methyl doublets in the high-field region of the  $^1\text{H}$  spectrum, and the methyl singlet at the resonance of 2.73 ppm corresponding to  $\text{CH}_3$ -1. With respect to all relevant experimental data, this first portion was found to be identical to the corresponding one in **56**.

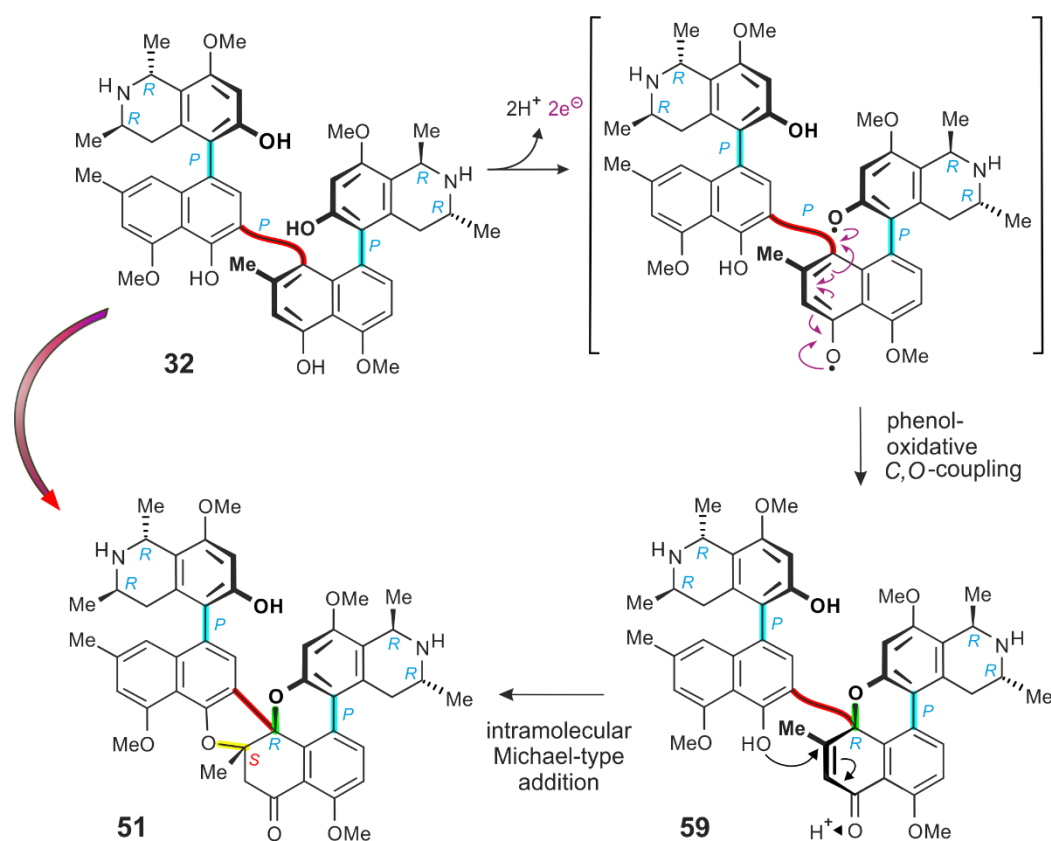
Compared to cyclombandakamine A (**51**), the southeastern portion of the new dimer displayed an additional *N*-methyl group in the isoquinoline moiety, appearing at the resonance of  $\delta_{\text{H,C}}$  3.04 and 49.5 ppm ( $\text{MeN-2}''$ ). Moreover, the characteristic  $^1\text{H}$ - and  $^{13}\text{C}$  NMR resonances corresponding to  $\text{H-1}'''$  ( $\delta_{\text{H,C}}$  5.01 and 71.3 ppm) and  $\text{H-3}'''$  ( $\delta_{\text{H,C}}$  4.39 and 63.3 ppm) enabled unequivocally to recognize the presence of an *N*-methylated tetrahydroisoquinoline subunit with a relative *cis*-configuration. These assumptions were confirmed by ROESY interactions, and by the presence of the *N*-methyl also found in the degradation experiments, which established *3R,3'''R*-configurations. The second molecular portion of this new compound was found to be identical to the corresponding one in **54** and **55**. Therefore, the new alkaloid was fully assigned as *5P,3R,1''R,2''S,8''P,1'''S,3'''R*, and was named cyclombandakamine A<sub>7</sub> (**57**).

Before the isolation of this thrilling series of compounds, a trace of such an alkaloid had been detected and fully characterized. The compound corresponded to  $2'''$ -*N*-methyl derivative of cyclombandakamine A,<sup>[178]</sup> and its natural occurrence was severely doubted because it had never been isolated again from scratch. All efforts aiming at the detection of further candidates or the hit structure cyclombandakamine A (**51**) had been unsuccessful until this discovery in *A. ealaensis*,<sup>[179]</sup> which confirmed independently the molecular array.

Since the occurrence of such structures had already raised questions, their biosynthetic origin (artifacts or natural products?), their probable precursors, and their stability and reactivity needed to be addressed. Like the mbandakamine-type dimers, cyclombandakamine A showed two 5,8'-coupled molecular halves with a central bond between C-6' and C-1'', even though in this case the 6',1''-C,C-linkage was no longer a chiral axis. Therefore, the possibility should not be excluded that **32** or **47** are the precursors to the cyclic **51** and **52**, respectively. Such products may result from oxidation generating two phenoxy radicals, which can undergo phenol-

oxidative coupling and intramolecular Michael-type addition reactions leading ultimately to the novel dimer cyclombandakamine A (Scheme 3, inspired from literature data).<sup>[178]</sup> Given the unprecedented *peri-peri* coupling of the two molecular halves, which exhibits the highest-known steric hindrance at the central axis, such cyclization processes involving a loss of conjugation in the naphthalene could be possible. The driving force for the oxidation of **32** might be the proximity of all chromophores involved and the gain of stability by the reduction of the steric load at the central axis.

Besides, the orientations of the HO-5' and HO-6''' functions on opposite sides of the plane formed by the C-1''-substituted naphthalene unit in mbandakamine A (**32**) are favorable for substitutions, which would lead to *trans*-configured 5''-methoxy-2''-methyl-tetralone, and specifically to the desired 1''*R*,2''*S*,8''*P* diastereomer only. This means also that its atropo-diastereomer, *i.e.* mbandakamine B, with its 6'*M*,8''*P* biaryl axes should lead to the *cis*-configured cyclic diastereomer, *viz.* to 1''*R*,2''*R*,8''*P* exclusively.

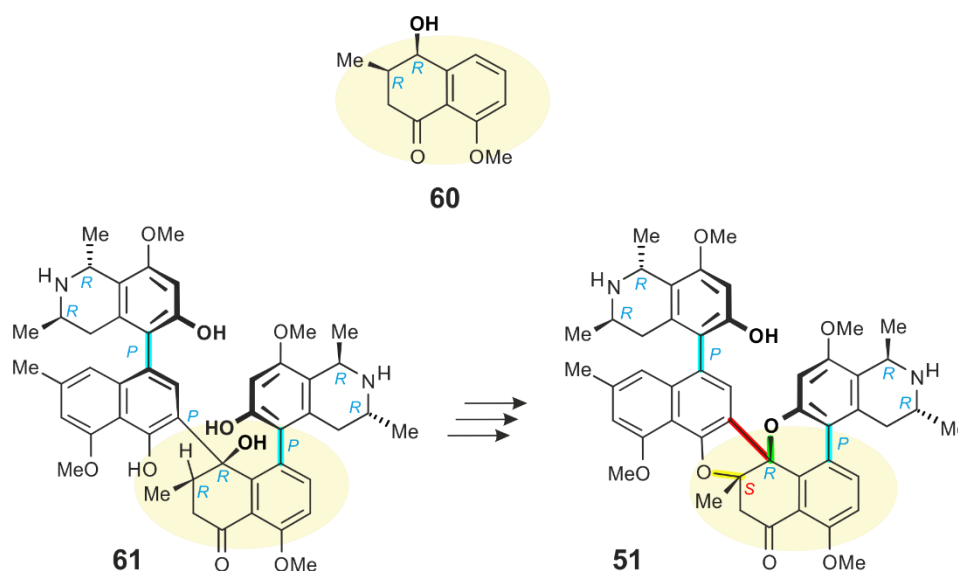


Scheme 3. Probable biosynthetic pathway of cyclombandakamine A (**51**) from mbandakamine A (**32**), inspired and adapted from published data.<sup>[178]</sup>

Another hypothesis may suggest on the other hand, that cyclombandakamine A may well share the similar biosynthetic pathway with mbandakamine A, based on the proven convergent biosynthesis of the building blocks,<sup>[184]</sup> but that a different enzyme may at a given stage be specific to a *cis*-isoshinanolone-like unit instead of a common naphthalene, which by further oxidative reactions might undergo cyclization to form a central 6',1"-linkage. *cis*-Isoshinanolone (**60**) is a widely spread naturally occurring tetralone, which has been also known from Dioncophyllaceae and Ancistrocladaceae species.<sup>[64, 184]</sup> In contrast to the *trans* diastereomer,<sup>[186]</sup> only the *cis*-stereoisomer has been known from *Ancistrocladus* species, particularly found in the Congolese *A. likoko* and *A. ileboensis*.<sup>[181-183]</sup>

The most intriguing fact is that the structure of *cis*-isoshinanolone, in which the HO-4 and CH<sub>3</sub>-3 – corresponding to C-1" and C-2" in cyclombandakamine A (**51**), respectively – are spatially oriented in the same plane. Once part of a mbandakamine-like dimer, the *cis*-arrangement in this cyclohexanone would be favorable to the cyclization, leading ultimately to the formation of the right stereoisomer of **51**. However, the comprehensive mechanism for such a biosynthetic process, as depicted in Scheme 4, remains unclear at this stage and might be just hypothetical. Such a probable dimer – reminiscent of the unnatural jozimine A<sub>4</sub> (structure not shown) – featuring a chiral sp<sup>3</sup>-sp<sup>2</sup> axis,<sup>[187]</sup> which has not been yet found in nature, might be the biosynthetic precursor – or its derivative – to cyclombandakamine A as shown in Scheme 4. It was named 'isoshinakamine A' (**61**). The co-occurrence of cyclombandakamine A with its open-chain form, under mild extraction conditions, and the exclusive 1"R,2"R,8"P-configuration observed in the whole series, plead for the co-existence of two pathways. However, further studies are needed to validate this hypothesis.

An additional strong indication of the natural occurrence of the cyclic mbandakamines is the fact that several related Congolese species may produce mbandakamine-type dimers, but only *A. ealaensis* has proven so far to be the main source of both dimeric types, thus, hinting at a broader enzymatic potential. The probably new liana, phylogenetically related to *A. ealaensis*, which has remained not fully botanically identified,<sup>[45]</sup> was found to be an intensive producer of mbandakamine A. Besides the single *N*-methylated cyclic mbandakamine A derivative found in an old fraction, compound **58**, all efforts for the detection of further such compounds by LC-DAD-MS were unsuccessful. These additional facts plead for the existence of one or several independent steps involved in the biosynthesis processes of mbandakamines and cyclombandakamines.



Scheme 4. Structures of *cis*-isoshinanolone (**60**) and a probable natural product of the type 'isoshinakamine A' (**61**). A compound like **61** may be an alternative biosynthetic precursor to cyclombandakamine A (**51**), by a mechanism which seems to be not clear at this stage.

The sensitivity of *cis*-configured *N*-protonated (*N*-H) naphthylisoquinolines to oxidation had been known for long in this field<sup>[165]</sup> so that their successful isolation has always been a sign of mild workup procedures. Since cyclombandakamines might be oxidation products from open-chain mbandakamine-like alkaloids, the discovery of such dimers with intact *N*-H *cis*-relative configurations is remarkable and of high significance. It may hint at strictly-regulated enzymatic processes involved in their biosynthesis, which would mean that the compounds were true natural scaffolds and no artificial follow-up products from the mbandakamines.

The similarity of the ECD spectra, despite different variations in the isoquinoline moieties further confirmed the aforementioned dominance of the twisted dihydrofuran-tetralone-pyran chromophore to other present elements of chirality. It shall be noticed that the combination of bridged and non-bridged biaryl axes have not been found in any class of dimeric naphthylisoquinoline alkaloids.

The isolation of this series of novel compounds indicates once more the impressive and unique biosynthetic potential of the tropical liana, *A. ealaensis*.

## Biological activities of cyclombandakamines

Depending on the availability of material, biological evaluations on the main representatives were performed in triplicates. In addition, for hits of series like cyclombandakamine A (**51**), the experiments were repeated, always simultaneously with a sample of mbandakamine A (**32**) for a reliable comparison of their biological profiles.

In general, the cyclombandakamines exhibited *in vitro* activities, but in the low micromolar range, against the chloroquine sensitive strain (NF54), and the resistant strain (K1) of *P. falciparum*, the latter being the agent of the most severe form of malaria. Cyclombandakamine A (**51**), 1-*epi*-cyclombandakamine A (**52**), cyclombandakamine A<sub>5</sub> (**55**), and cyclombandakamine A<sub>6</sub> (**56**) showed IC<sub>50</sub> values of 0.664 (NF54) and 0.268 μM (K1), 0.300 (NF54) and 0.148 μM (K1), – (NF54) and 0.350 μM (K1), and 0.666 (NF54) and 0.266 μM (K1), respectively. The calculated selectivity indices were found to be around 100 (Table 4). The tested alkaloids were representative of the most important structural variations observed within this class of compounds. From the profiles of these model substances, it could be noticed that the activities against the resistant strain of *P. falciparum* (K1) were at least two times better than the ones on the sensitive strain NF54. The lower activity of *N*-methylated derivatives was also predictable because of the reduced basicity of the nitrogen.<sup>[93]</sup> As observed in the previous cases, the *cis*-diastereomers were in each case more active than the *trans*-configured ones. Compared to the corresponding open-chain alkaloids, the reduced biological activities of **51** and **52** could be related to the formation of the rigid cage-like polycyclic system, which most likely may reduce the specific binding to the target on *P. falciparum*. The outstanding antimalarial potential of ealapasamine C (**44**) suggested that a certain degree of flexibility in the structure is favorable for efficient interaction and, thus, increases the chances for an excellent biological profile.

These results are in disagreement with the published values for cyclombandakamine A<sub>1</sub> (**58**), which had surprisingly shown an IC<sub>50</sub> value in the same range as that of **32**.<sup>[178]</sup> In conclusion, even though highly thrilling from the structural and biosynthetic point of views, the cyclized mbandakamines are less attractive for their antiprotozoal activities as compared to the related open-chain alkaloids.

If these secondary metabolites are produced, they should be certainly targeting other groups of diseases.<sup>[11]</sup> Therefore, further biological model systems were explored in order to learn more about the potential of this novel series of products. The hit compound cyclombandakamine A

was found to be the most active among three tested representatives on the human T-lymphoblastic leukemia cells CCRF-CEM with an  $IC_{50} = 3.113 \mu\text{M}$ , while **52** and **56** showed values of 4.200 and 12.261  $\mu\text{M}$ , respectively. Moreover, on the human pancreatic cancer PANC-1 and HeLa cells, cyclombandakamine A showed antiproliferative inhibition of 4.311 (PANC-1) and 9.414  $\mu\text{M}$  (HeLa), indicating the broad spectrum of the anticancer potential of the hit structure of cyclic mbandakamines. Further biological evaluations are still ongoing.

Table 4. Biological evaluations of **51**, **52**, **55**, and **56** against *Plasmodium falciparum* (strains: NF54 and K1), *Trypanosoma brucei rhodesiense*, *T. cruzi*, *Leishmania donovani*, and biotests on two human cancer cell lines, CCRF-CEM and PANC-1, were performed. The cytotoxicities against rat skeletal myoblasts (L6 cells) enabled the determination of the selectivity indices.

	<i>T. brucei rhod.</i>	<i>T. cruzi</i>	<i>L. donovani</i> ax. am.	<i>P. falciparum</i> NF54/K1	Selectivity index to NF54/K1	CCR-CEM	PANC-1	HeLa
	0.007 <sup>[1]</sup>	3.56 <sup>[2]</sup>	0.43 <sup>[3]</sup>	0.01 <sup>[4]</sup> : NF54 /0.272 <sup>[4]</sup> : K1	n.d.	0.017 <sup>[5]</sup>	n.d.	13.9 <sup>[6]</sup>
<b>51</b>	12.38	63.80	39.55	0.664/ <b>0.268</b>	<b>67 /166</b>	<b>3.113</b>	27.81/ <b>4.311</b>	9.414
<b>52</b>	6.36	58.31	>127.73	0.300/ <b>0.148</b>	- / <b>117</b>	<b>4.200</b>	-	-
<b>55</b>	-	-	-	- / 0.350	- / 52	-	-	-
<b>56</b>	50.22	95.79	>127.73	0.666/ <b>0.266</b>	138/ <b>346</b>	<b>12.261</b>	-	-

[1] Melarsoprol. [2] Benznidazole. [3] Miltefosine. [4] Chloroquine. [5] Doxorubicin. [6] 5-fluorouracil. All  $IC_{50}$  values given in  $\mu\text{M}$ . n.d.: not determined. Selectivity index determined for *P. falciparum*.

### Biomimetic synthesis of cyclombandakamine A from mbandakamine A

Since about 10 mg of isolated mbandakamine A (**47**) were available, a biomimetic synthesis of cyclombandakamine A (**51**) was envisaged to verify the first hypothesis. This latter suggested the generation of two phenoxy radicals from **47**, which by phenol-oxidation coupling and intramolecular Michael addition could lead to cyclombandakamine A (**51**).

This work was performed in cooperation with William Shamburger from our group, who was responsible for optimizing the oxidation reaction conditions with  $\text{Pb}(\text{OAc})_4$  (lead tetraacetate) and  $\text{BF}_3(\text{OEt}_2)$  (boron trifluoride ethyl etherate) in anhydrous dichloromethane and investigating further possible oxidation agents.

A particular emphasis was devoted to the oxidation with lead(IV) tetraacetate [Pb(OAc)<sub>4</sub>]. The choice was motivated by the fact that the reaction is usually fast (ca. 10 min) and the work-up relatively easy.<sup>[188]</sup> Another alternative would have been Ag<sub>2</sub>O, inspired from the synthesis of jozimine A<sub>3</sub>, in which the side product jozimine A<sub>4</sub> was also formed.<sup>[187]</sup> The structure of the unnatural jozimine A<sub>4</sub> features a *peri-peri* coupling at the central axis with one molecular half possessing a tetralone instead of naphthalene, suggesting that Ag<sub>2</sub>O oxidation conditions can lead to the formation of such tetralone derivatives. However, the preference to use Pb(OAc)<sub>4</sub> was motivated by the fact that no protective groups were necessary,<sup>[189]</sup> in contrast to the case of Ag<sub>2</sub>O.<sup>[187]</sup>

Two milligrams of mbandakamine A (**32**) were dissolved in anhydrous dichloromethane and cooled to 0 °C in an ice bath. After addition of 2.2 equivalents of a diluted solution of BF<sub>3</sub>(OEt<sub>2</sub>), the mixture turned light violet and was then stirred for 5 min at 0 °C. Subsequently, a 1.1 equivalent solution of Pb(OAc)<sub>4</sub> was added to the mixture, which turned dark, and the resulting reaction mixture was left stirring at room temperature for 45 min. Methanol was then added to the suspension and the whole mixture was filtered through a celite column, with methanol as the eluent. The homogeneous solution was evaporated to dryness and yielded approximately 60% of cyclombandakamine A (**51**).

The compound was analyzed by HPLC, identified by its retention time, its characteristic UV spectrum, its HRESIMS profile, and by a coelution experiment with an authentic sample of **51**. These biomimetic experiments proved the chemical plausibility of the first biosynthetic hypothesis (Scheme 3).



## II.4. Ealamines A-H, Enthralling Naphthylisoquinoline Alkaloids with Promising Bioactivities from *Ancistrocladus ealaensis*

So far the occurrence of dimeric NIQs in *A. ealaensis* was described. In this chapter, a series of ten 7,8'-coupled monomeric naphthylisoquinoline alkaloids will be reported, among which eight are new (Figure 39). The discovered compounds were named – after the plant species and the botanical garden 'Eala' located in the Northwestern Congo – ealamines A-H (**P-62** and **M-62**, **63-68**), along with the known yaoundamine A (**17**) and 6-*O*-demethylancistrobrevine A (**69**). Their relative and absolute configurations were assigned by means of spectroscopic techniques (like NMR), oxidative degradation, and comparison of experimental ECD spectra with quantum-chemically calculated ones. For the first-time, a single-crystal analysis of a 7,8'-coupled NIQ was performed for compound **P-62**, confirming the constitution and relative configuration.

Remarkably, this series of compounds consists of seven new tetrahydroisoquinoline representatives belonging to the sub-class of hybrid-type alkaloids, *i.e.* exhibiting a 7,8'-linkage bearing an oxygen function at C-6 and an *R*-configuration at C-3. From this peculiarity, *A. ealaensis* can be listed among the species violating the so-called Ancistrocladaceae/Dioncophyllaceae rule,<sup>[190]</sup> by displaying mixed features generally conserved within either family. Besides, 7,8'-coupled monomeric NIQs are quite unusual since very few had been reported.<sup>[83-84, 102, 191]</sup> Only yaoundamine A with its heteroside has been known to be of the hybrid type (6-OR, 3*R*), but it features a dihydroisoquinoline instead of a tetrahydroisoquinoline, as found in the new ealamines.<sup>[192]</sup> It is well-known that the structural elucidation of compounds with a 7,8'-coupling type is demanding.<sup>[116]</sup> In this case, a very unusual and unexpected conformational behavior has been observed and will be discussed.

The alkaloids displayed moderate to good antiprotozoal activities against selected pathogens and very good antiproliferative activities towards two human cancer cell lines. Ealamine C (**63**) was the most active alkaloid against *P. falciparum in vitro*, with an IC<sub>50</sub> value of 0.84 μM. Compound **P-62**, **M-62**, **63**, and **69** exhibited very promising antiproliferative potential on two human cancer cell lines, including a multi-drug resistance strain.

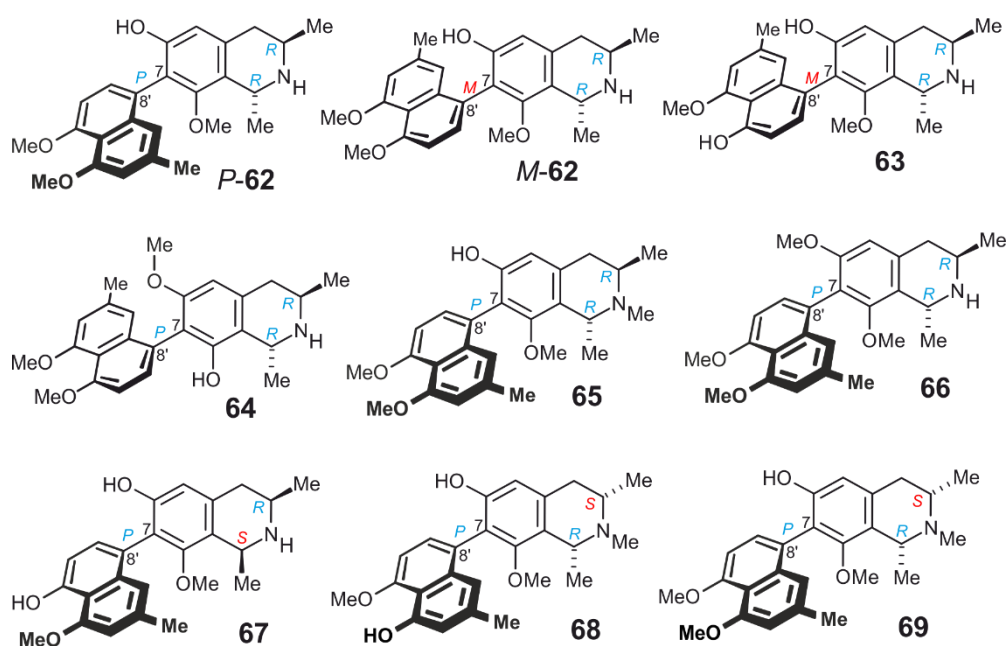


Figure 39. Ealamines A-H (**P-62**, **M-62**, **63-68**), seven new monomeric naphthylisoquinoline alkaloids from leaves and twigs of *Ancistrocladus ealaensis*, along with the known 6-*O*-demethylancistrobrevine A (**69**). The structure of yaoundamine A can be seen in Figures 2 and 4.

### Structural-elucidation details

A systematic fractionation procedure on air-dried leaves of *A. ealaensis*, as described in the experimental section, led to the isolation of six new 7,8'-coupled naphthylisoquinoline alkaloids. Further investigations on twigs material additionally led to the discovery of three metabolites of the same coupling type.

The main alkaloid, ealamine A (**P-62**) was obtained as an optically active brownish powder. From the detection of the fragment  $[M+H]^+$  at  $m/z$  408.21570 (calcd for  $C_{25}H_{30}NO_4$ , 408.21693), by HRESIMS the molecular formula was determined to be  $C_{25}H_{29}NO_4$ , with an IHD of 12. Analysis of the  $^{13}C$  NMR and the DEPT-135 spectra detected 25 non-equivalent carbon atoms, among which 16 were aromatic. Comprehensive analysis of the full NMR data led to the identification of a substituted naphthalene spin system, with four aromatic methines at  $\delta_H$  (in ppm) 7.21 (H-7'), 6.94 (H-6'), 6.85 (H-1'), 6.78 (H-3'), two methoxy groups at  $\delta_H$  3.96 ( $CH_3O$ -5') and 3.93 ( $CH_3O$ -4'), and one aromatic methyl group at  $\delta_H$  2.31 ( $CH_3$ -2'). Another spin system corresponding to a tetrahydroisoquinoline was evidenced by a shielded aromatic proton singlet at  $\delta_H$  (ppm) 6.56 (H-5), two unshielded aliphatic methine at the resonances of 4.72 (H-1) and 3.87 (H-3), two diastereotopic protons at 3.15 (4- $H_{eq}$ ) and 2.88 (4- $H_{ax}$ ), one shielded aromatic methoxy group at the resonance of 3.07 ( $CH_3O$ -8), and two methyl groups

at  $\delta_{\text{H}}$  1.65 (CH<sub>3</sub>-1) and 1.51 (CH<sub>3</sub>-3). All the assignments were in agreement with the <sup>1</sup>H, <sup>13</sup>C-HSQC, <sup>1</sup>H, <sup>13</sup>C-HMBC, <sup>1</sup>H, <sup>1</sup>H-COSY, and <sup>1</sup>H, <sup>1</sup>H-NOESY data. In particular, the HMBC interaction from CH<sub>3</sub>O-5' and H-7' to C-5' ( $\delta_{\text{C}}$  158.7 ppm), and the NOESY correlations between H-3' and CH<sub>3</sub>O-4', as well as of H-3' and H-1' with CH<sub>3</sub>-2', confirmed the identification of the naphthalene portion. The HMBC interaction of H-5 with only one oxygenated carbon (C-6,  $\delta_{\text{C}}$  157.7) and with C-4 ( $\delta_{\text{C}}$  34.6) proved the protonated position C-5, leaving C-7 as the coupling position in the tetrahydroisoquinoline moiety (Table 5). The coupling biaryl axis were determined to be located at C-7 and C-8' by the HMBC interactions from H-7' and H-5 to C-7 ( $\delta_{\text{C}}$  121.7), the observed <sup>4</sup>J HMBC interaction between H-5 and the signal at 124.6 ppm (C-8'), the NOEs from H-7', H-1', and H-1 with the shielded CH<sub>3</sub>O-8 (Figure 40).

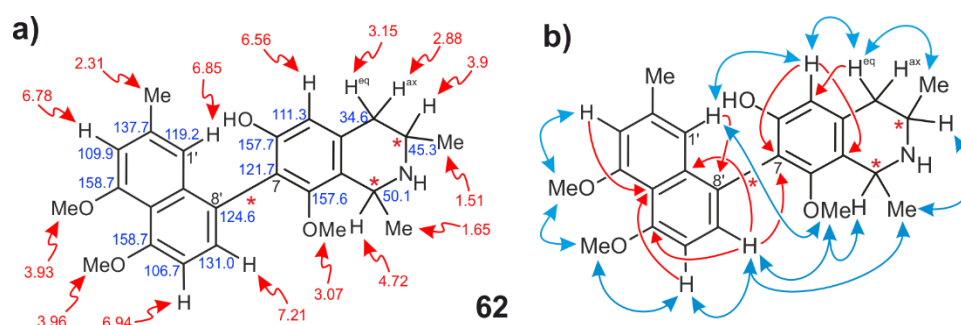


Figure 40. a) Constitution of ealamine A (*P*-62) (<sup>1</sup>H and <sup>13</sup>C chemical shifts in ppm). b) HMBC in red and NOESY interactions in blue for *P*-62.

Table 5. <sup>1</sup>H (600 MHz) and <sup>13</sup>C (151 MHz) Data of *P-62* and *M-62* in methanol-*d*<sub>4</sub> ( $\delta$  in ppm, *J* in Hz).

no.	ealamine A ( <i>P-62</i> )		ealamine B ( <i>M-62</i> )	
	$\delta_{\text{H}}$ ( <i>J</i> in Hz)	$\delta_{\text{C}}$ , type	$\delta_{\text{H}}$ ( <i>J</i> in Hz)	$\delta_{\text{C}}$ , type
1	4.72, q (6.8)	50.1, CH	4.73, q (6.8)	50.0, CH
3	3.87, m	45.3, CH	3.88, m	45.3, CH
4	3.15, dd (17.5, 4.8)	34.6, CH <sub>eq</sub>	3.20, dd (17.9, 4.9)	34.6, CH <sub>eq</sub>
	2.88, dd (17.5, 11.9)	34.6, CH <sub>ax</sub>	2.88, dd (17.9, 11.7)	34.6, CH <sub>ax</sub>
5	6.56, s	111.3, CH	6.56, s	111.3, CH
6		157.7, C		157.8, C
7		121.7, C		121.7, C
8		157.6, C		157.6, C
9		118.7, C		118.6, C
10		133.0, C		133.0, C
1'	6.85, d (1.1)	119.2, CH	6.84, d (1.1)	119.2, CH
2'		137.7, C		137.7, C
3'	6.78, d (1.4)	109.9, CH	6.78, d (1.2)	109.9, CH
4'		158.7, C		158.7, C
5'		158.7, C		158.7, C
6'	6.94, d (8.1)	106.7, CH	6.95, d (8.1)	106.7, CH
7'	7.21, d (8.0)	130.9, CH	7.21, d (8.1)	131.0, CH
8'		124.6, C		124.5, C
9'		137.7, C		137.7, C
10'		117.5, C		117.5, C
CH <sub>3</sub> -1	1.65, d (6.8)	19.6, CH <sub>3</sub>	1.65, d (6.8)	19.6, CH <sub>3</sub>
CH <sub>3</sub> -3	1.51, d (6.3)	19.4, CH <sub>3</sub>	1.51, d (6.4)	19.5, CH <sub>3</sub>
CH <sub>3</sub> -2'	2.31, s	22.2, CH <sub>3</sub>	2.31, s	22.2, CH <sub>3</sub>
CH <sub>3</sub> O-6	-	-	-	-
CH <sub>3</sub> O-8	3.07, s	60.8, CH <sub>3</sub>	3.07, s	60.8, CH <sub>3</sub>
CH <sub>3</sub> O-4'	3.93, s	57.1, CH <sub>3</sub>	3.93, s	57.1, CH <sub>3</sub>
CH <sub>3</sub> O-5'	3.96, s	56.9, CH <sub>3</sub>	3.96, s	56.9, CH <sub>3</sub>

The relative configuration at the two stereogenic centers was found to be 1,3-*trans*, as indicated by the NOESY correlation between the bi-axial H-3 and CH<sub>3</sub>-1. The absolute configurations at C-1 and C-3 were assigned by Ru(VIII)-mediated oxidative degradation.<sup>[113]</sup> The detection of *R*-configured  $\alpha$ -aminobutyric acid and alanine unambiguously indicated the 1*R*,3*R* absolute configuration, suggested by the NMR data. The elucidation of the axial configuration turned out to be not straightforward, and it was solved by a combination of techniques. First, it was deduced from the analysis of NOESY experiments (Figure 41). The observed long-range NOESY correlations between H-7' and CH<sub>3</sub>-1, and from H-1' to H-1 implied a *P*-configured axis, considering the results from the oxidative degradation. According to these data, the full structure of ealamine A is 7*P*,1*R*,3*R*. Further structural proofs will be addressed in depth together with the ones for compound *M-62*.

From the same sub-fraction, a second compound, yet occurring in distinctly lower amount and eluting faster on RP<sub>18</sub> material, was isolated and characterized. The new compound *M-62* was obtained as an optically active yellowish powder. The molecular formula was determined to be C<sub>25</sub>H<sub>29</sub>NO<sub>4</sub>, based on the fragment [M+H]<sup>+</sup> at *m/z* 408.21610, (calcd for C<sub>25</sub>H<sub>30</sub>NO<sub>4</sub>, 408.21693) like for *P-62*. Surprisingly, the constitution, the relative configuration at C-1 *versus* C-3, and the results of the oxidative degradation were identical to those of *P-62*, implying that *M-62* must be an isomer of *P-62*. However, no difference could be seen at this stage from all the analyzed data.

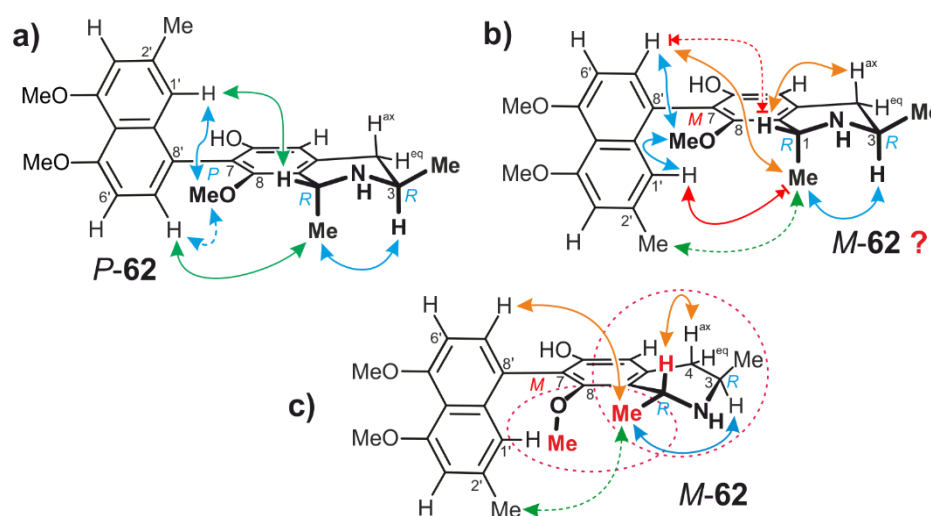


Figure 41. NOESY interactions: decisive ones in green, expected ones in blue, unexpected ones in orange, missing ones in red, and decisive ones for *M*-configuration in green for (a) in *P-62*, and (b) and (c) in *M-62*. (b) Represents a low-populated conformer of *M-62* in contrast to the most stable one in (c).

The possibility of enantiomers was not convincing because the ECD spectra were not mirror-imaged, and even in an exceptional case, the two compounds were well resolvable on an achiral RP<sub>18</sub> column excluding *de facto* this eventuality. Besides, the hypothesis of diastereomers was not fully undoubted either, because of the unexpected long-range NOE correlation observed between CH<sub>3</sub>-1 and H-7', and no cross peaks between CH<sub>3</sub>-1 to H-1', from which only the *P*-configuration could be also inferred for *M-62*.<sup>[102]</sup>

The first difference came out from the analysis of the ECD curves, which displayed a mismatch in the specific region around 225 nm. Since no comparable compound is known to discriminate them, quantum chemical calculations of the ECD spectra were inevitable to learn more about *P-62* and *M-62*.<sup>[187, 193]</sup> The experiments were performed by Dr. T. Bruhn at the TDCAM-B3LYP/def2-TZVP level. In Figure 42, the outcome of the calculations is shown, indicating

unambiguously that *P*-62 and *M*-62 are two *P*- and *M*-configured atropo-diastereomers. It is remarkable to notice the strong negative Cotton effect at 230 nm for the *M*-atropo-diastereomer in contrast to the weak positive one induced by the *P*-axial configuration.

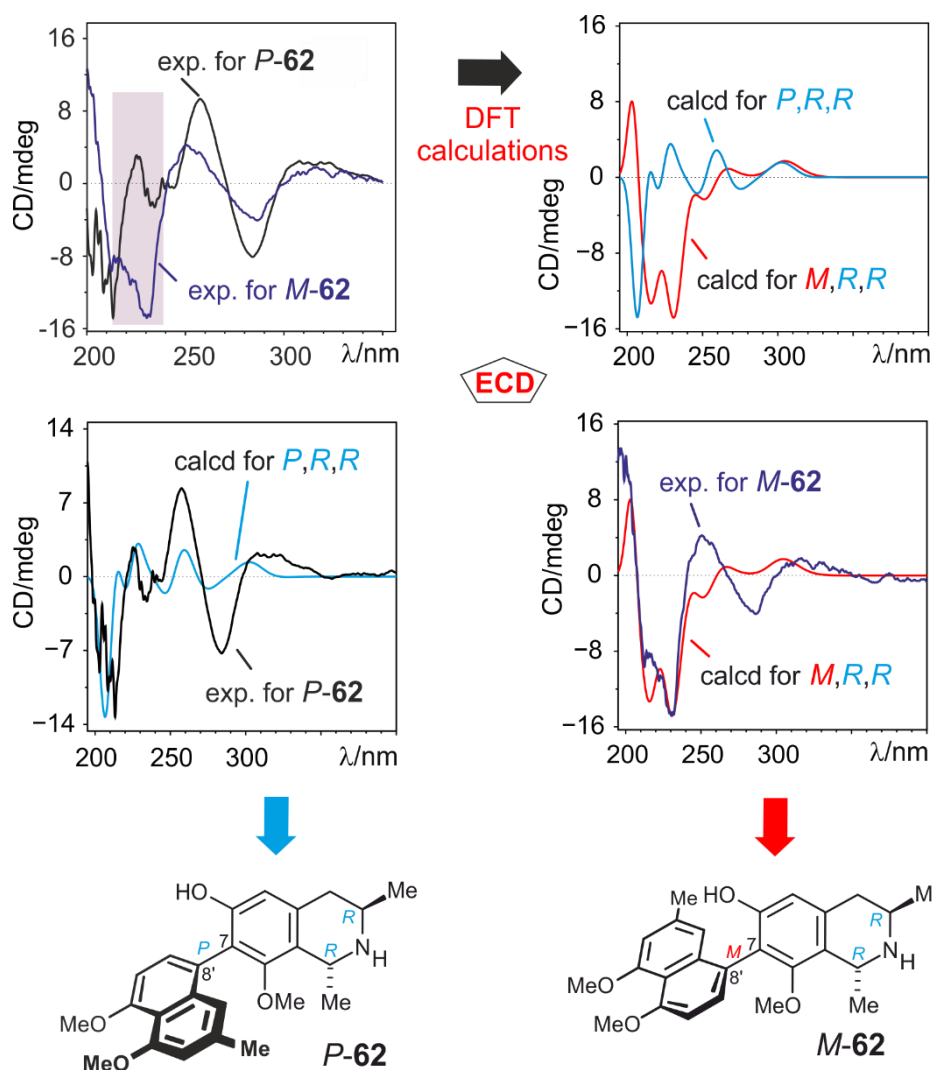


Figure 42. Experimental and quantum-chemical calculated ECD spectra of *P*-62 and *M*-62, and assignment of their absolute configuration. The ECD calculations were achieved at the TDCAM-B3LYP/def2-TZVP level.

Once the identity clarified, the mystery remained from the 'strange' NOE correlation observed between CH<sub>3</sub>-1 and H-7', and the lack of cross peaks between CH<sub>3</sub>-1 and H-1' were not predictable for the *M*-atropo-diastereomer considering the three-dimensional arrangement so far known for all 1,3-dimethyl-tetrahydroisoquinolines (Figure 43a,c). A comprehensive answer to this critical concern came from the computational analyses by the calculations of the minimum structures. Indeed, the DFT-calculated conformational analyses<sup>[187]</sup> and the most populated conformer with the *M* axial configuration revealed an unusual arrangement in the

hybrid-type tetrahydroisoquinoline moiety. It was observed that the CH<sub>3</sub>O-8 was pointing, unpredictably, towards H-1', hence pushing the CH<sub>3</sub>-1 to adopt a pseudo-equatorial position, while the H-1 becomes pseudo-axial and opposite to CH<sub>3</sub>O-8 (Figure 43b). This spatial orientation of CH<sub>3</sub>O-8 right between CH<sub>3</sub>-1 and H-1', hiding this latter, explains why the classically predicted NOEs between them were not detected. Moreover, the new equatorial conformation of the CH<sub>3</sub>-1 brought it to a spatially close distance to H-7' (4.704 Å), so that they can now display a long-range NOE. The spatial arrangement of H-1 is further corroborated by its NOE interaction to H<sub>ax</sub>-4, both being axial with a relatively short distance of 2.331 Å. These unprecedented conformational peculiarities have never been observed – or at least been described – within the class of naphthylisoquinoline alkaloids.

Since the H-1' is completely covered by CH<sub>3</sub>O-8, based on the NOESY experiments, we have found out that one can distinguish between them by looking at the long-range interaction between CH<sub>3</sub>-1 and CH<sub>3</sub>-2', which becomes in this case decisive to state for the *M*-axial configuration. However, for this, an optimal mixing time during the NOESY experiments and a firm confirmation by the ECD spectrum are required. Thence, the compound *M*-62 was elucidated to be 7*M*,1*R*,3*R*-configured and named ealamine B.

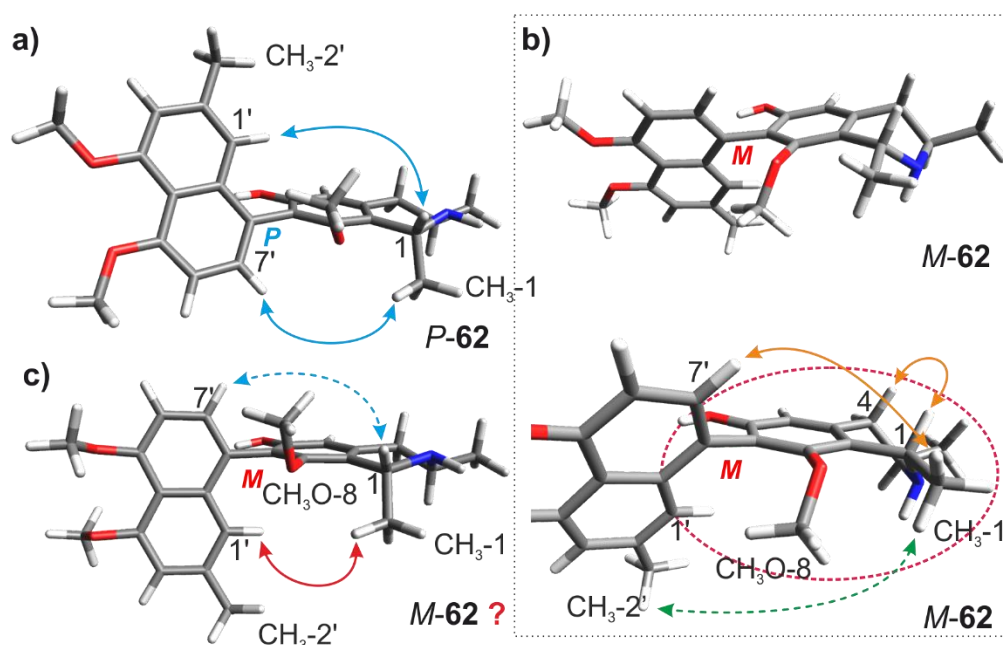


Figure 43. DFT calculated molecular minimum structures of (a) *P*-62 (*P*) and (b) *M*-62 (*M*), respectively. NOESY interactions depicted by arrows, expected ones in blue, unexpected ones in orange, missing ones in red, and decisive ones in green for the *M*-configuration. (c) Low-populated

conformer of *M*-**62**, wrongly expected initially to be the most stable. The calculated single-point energy difference between the conformations (c) and (b) was big ( $\Delta E = 14.1566 \text{ Kcal mol}^{-1}$ ).

Moreover, the constitution and the relative configuration of ealamine A (*P*-**62**) was confirmed by a single-crystal X-ray diffraction measurement, as depicted in Figure 44. Naphthylisoquinolines hardly crystallize without chemical derivatization, and even in the few cases, the quality of the crystals is usually not good enough.<sup>[89, 97, 194-197]</sup>

During our experiments, we were successful to obtain crystals of high quality, without any chemical derivatization of the natural product (Figure 44). However, the absence of a heavy atom in the single crystals, like a bromine, prevented an unambiguous assignment of the absolute configuration from this experiments, as denoted by the slightly high flack parameter = 0.053 (13). From the results of the crystallography, two species are possible, *7P,1R,3R* or *7M,1S,3S*. Since the absolute configurations at both stereogenic centers were reliably determined by the robust method of Ru(VIII)-mediated oxidative degradation, the full configuration of ealamine A (*P*-**62**) was firmly confirmed to be *7P,1R,3R*, as in perfect agreement with the ECD comparison of experimental and calculated spectra, and the observed decisive NOEs (as shown in green in Figures 41 and 43). Therefore, the full absolute structures of compounds *P*-**62** and *M*-**62** were unambiguously established.

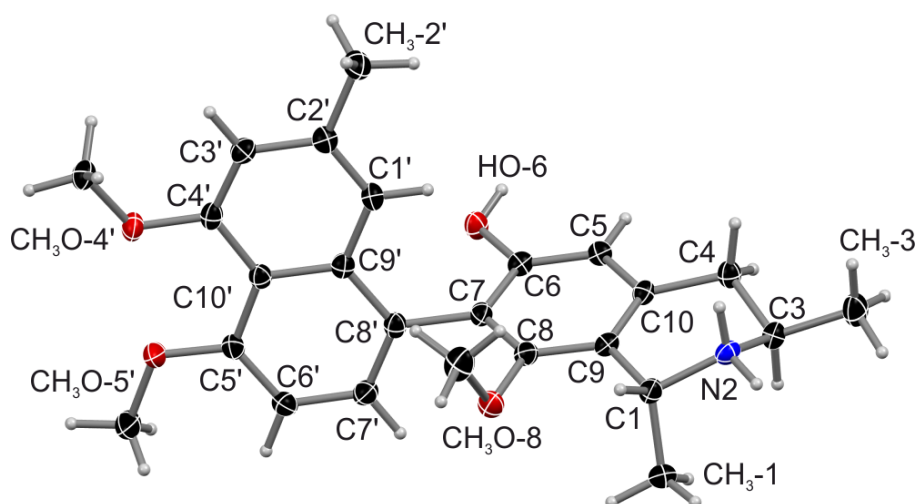


Figure 44. ORTEP display of the crystallographic structure of *P*-**62**.

Compound **63** was the first compound discovered from this series, along with the mbandakamines **47** and **32**. The substance was obtained as an optically active brownish powder. The molecular formula of  $\text{C}_{24}\text{H}_{27}\text{NO}_4$  was determined by HRESIMS from the



fragment  $[M+H]^+$  detected at  $m/z$  394.20194 (calcd for  $C_{24}H_{28}NO_4$ , 394.20128), with an unsaturation degree of 12 as well. Comprehensive NMR data analysis of **63** led to the constitution of a 5'-*O*-demethylated derivative of ealamine A (*P-1*). This point of difference was proven by the  $J^3$ -HMBC interaction from H-7' to C-5' ( $\delta_C = 156.12$  ppm) and the lack of NOESY interactions from H-6' and CH<sub>3</sub>O-4' to an *O*-methyl in position C-5'.

The relative configuration in the tetrahydroisoquinoline part was found to be *trans*, as determined by the NOESY experiment, like in the case of *P-62*. Ru-mediated oxidative degradation showed the same results as for *P-62*. The determination of the absolute configuration of **63** was also carefully carried out by the analysis of the NOESY and ECD spectra, based on the 1*R*,3*R*-configuration firmly established by oxidative degradation. In analogy to *M-62*, the unusual NOESY interaction between CH<sub>3</sub>-1 and H-7' was observed, and the decisive correlation from CH<sub>3</sub>-1 to CH<sub>3</sub>-2' was also monitored, indicating the *M*-axial configuration. A solid confirmation of this *M* configuration was provided by the comparison of the ECD spectra of **63** with the one of with *M-62*, which were nearly identical (Figure 45). This means that for all hybrid-type tetrahydroisoquinolines with a 7,8'-coupled biaryl axis, the *M*-atropo-diastereomers will show the same scarce conformational behavior as described for *M-62*, and the ECD comparison and the oxidative degradation remain reliable tools to assign the absolute axial configuration. The configuration was further confirmed by DFT-calculations of the minimum structure.<sup>[171]</sup> Therefore, compound **63** was 7*M*,1*R*,3*R*-configured and was named ealamine C.

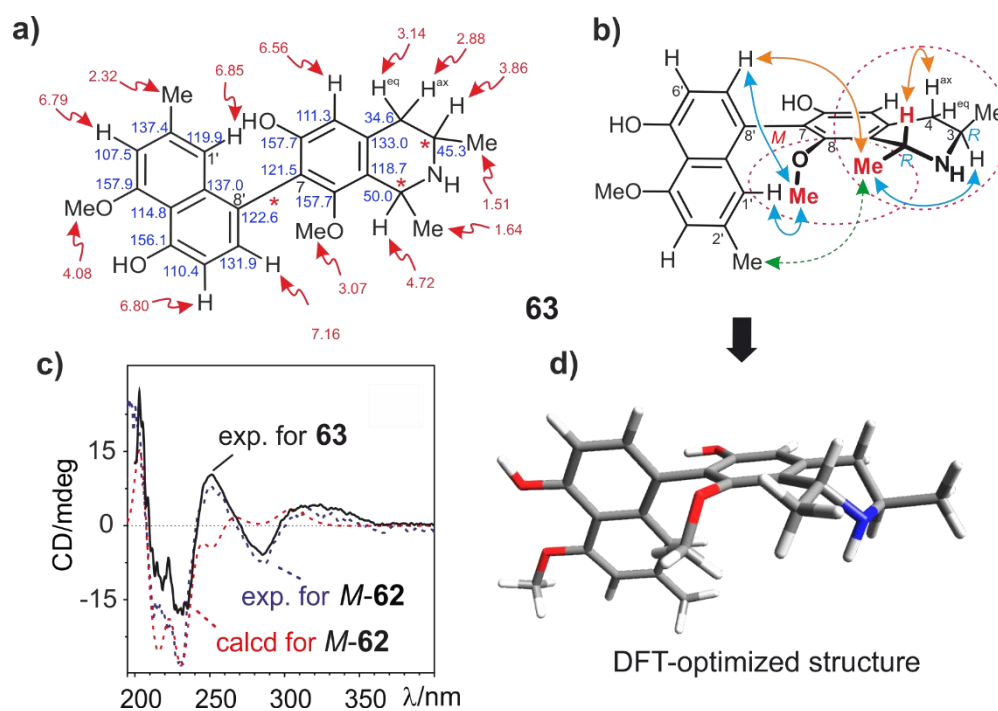


Figure 45. Chemical shifts ( $^1\text{H}$  in red and  $^{13}\text{C}$  in blue), NOESY interactions (decisive ones in green, expected ones in blue, unexpected ones in orange), the comparison of the experimental and calculated ECD spectra of *M*-**62** with the experimental one of ealamine C (**63**, in methanol), and the DFT-optimized minimum structure of **63** obtained with B3LYP-D3/def2-SVP.

Along with **63**, another trace alkaloid was also isolated and fully characterized. It was obtained as an optically active yellowish powder. From the found fragment at  $m/z$  408.21610  $[\text{M}+\text{H}]^+$  a molecular formula of  $\text{C}_{25}\text{H}_{30}\text{NO}_4$  was calculated, corresponding to a degree of unsaturation of 12. Comprehensive NMR data analysis led to a constitution nearly identical to *P*-**62**. In contrast to the isoquinoline portion in *P*-**62**, the new compound presented an *O*-methyl group in C-6 with a free C-8 position, inverting the order of priority around the axis. The *O*-methyl rest in position C-6 ( $\delta_{\text{C}} = 157.7$ ) was proven by the NOESY correlation between  $\text{CH}_3\text{O}$ -6 ( $\delta_{\text{H}} = 3.15$ , s, 3H) with H-5, H-7', and H-1', also by the observed HMBC interactions from H-5 and  $\text{CH}_3\text{O}$ -6 to C-6, and the lack of NOEs between H-1 and  $\text{CH}_3$ -1 to a methoxy group.

For this compound, the relative configuration at C-1 *versus* C-3 was found to be *trans*, as determined by NOESY experiments. Ru-mediated oxidative degradation revealed again that the stereogenic centers were *1R,3R*-configured, as for the previous cases. The elucidation of the axial configuration was pursued based on the determined configuration at the stereocenters. The observed NOESY interactions from  $\text{CH}_3$ -1 to H-1' and  $\text{CH}_3$ -2' indicated a *P*-axial configuration. Noticeably in this NIQ,  $\text{CH}_3$ -1 can now interact in NOESY with H-1' since a

hydroxy group in C-8 is less bulky than a methoxy. Moreover, the decisive long-range interaction from the axial CH<sub>3</sub>-1 to CH<sub>3</sub>-2' was also detected. However, the presence of the methoxy group at C-6 leads to an inversion of the axial chirality assignment due to the new priorities around the axis.

A further confirmation of this *P*-configuration was provided by comparison of its ECD spectrum with the one of *M*-62. Indeed, their ECD spectra were similar, but due to the inverted order of priority among the substituents around the axis, this compound **64** is *P*-configured (Figure 46). It could have been assumed that the *O*-methyl group in C-8 was the driving force for the above-described unusual conformational behavior observed in *M*-62 and **63**, but the DFT-calculated global minimum structure of **64** showed the same arrangement for the most lower-energy conformers. Thus, this must be linked to the axial relative configuration, where H-1' is on the same side as the axial CH<sub>3</sub>-1 and H-3. Therefore, compound **64** was assigned as *7P,1R,3R*-configured and named ealamine D.

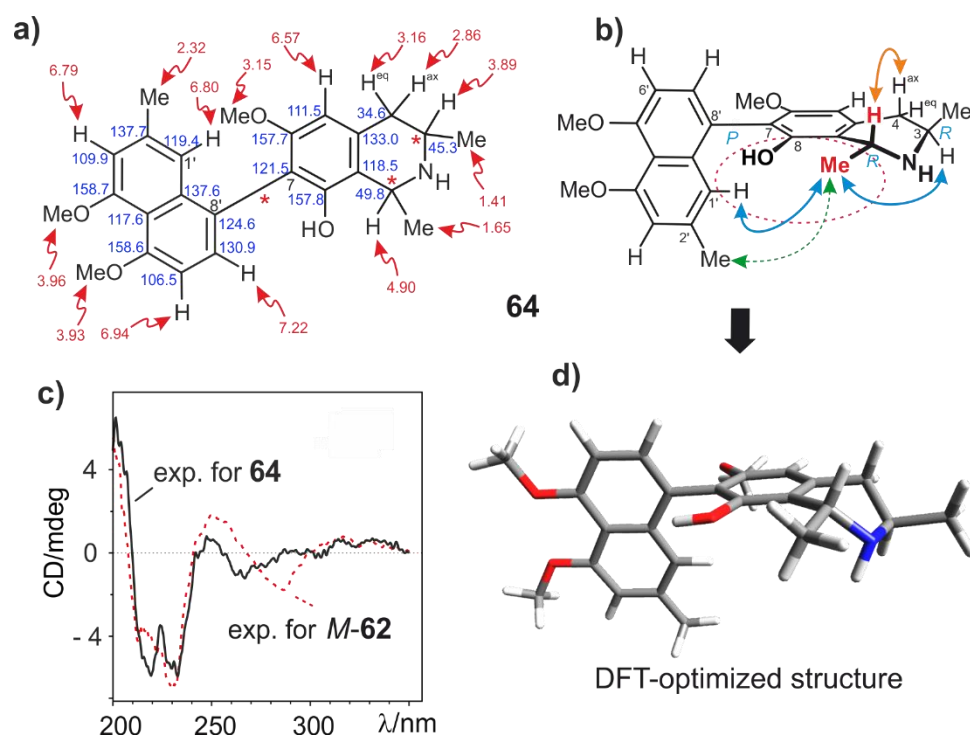


Figure 46. Chemical shifts (<sup>1</sup>H in red and <sup>13</sup>C in blue), NOESY interactions (decisive ones in green, expected ones in blue, unexpected ones in orange), the ECD spectra (in methanol), and the DFT-optimized structure of compound **64** obtained with B3LYP-D3/def2-SVP.

A further trace alkaloid was isolated and obtained as a yellowish powder. The molecular formula of C<sub>26</sub>H<sub>31</sub>NO<sub>4</sub> was deduced by HRESIMS with a degree of unsaturation of 12, as in

the previous cases. NMR data analysis of compound **65** indicated a constitution closed to the one of ealamine A (*P*-**62**). The point of difference came from the presence of an *N*-methylated tetrahydroisoquinoline. This was evidenced by the presence of an unshielded methyl group at the resonance of  $\delta_{\text{H}} = 2.87$  ppm (N-CH<sub>3</sub>), which interacted in NOESY with CH<sub>3</sub>-3 and H-1.

The relative configuration at C-1 *versus* C-3 was assigned to be *trans* by NOESY. Additionally, the strong NOEs from *N*-Me with CH<sub>3</sub>-3 and H-1 indicate that the favorable orientation of the methyl attached to the nitrogen is opposite to CH<sub>3</sub>-1 and H-3, confirming also the relative 1,3-*trans*-relative configuration.

The oxidative degradation showed an *R*-configured  $\alpha$ -aminobutyric acid. In combination with the relative *trans*-configuration at the stereogenic centers, the absolute configurations at C-1 and C-3 were unambiguously established to be 1*R*,3*R*. The absolute axial configuration was carefully investigated by NOESY and electronic circular dichroism, as in the previous cases. Since the compound was obtained in a trace amount, the long-range NOEs could not be unambiguously detected. However, it was remarkable that the NOESY interaction between CH<sub>3</sub>O-8 was much stronger with H-1' than with H-7'. It was likewise noticed that CH<sub>3</sub>O-8 had a stronger NOE interaction with H-1 and virtually none with CH<sub>3</sub>-1. Considering the absolute configuration at C-1 and C-3, firmly established by oxidative degradation, the axial absolute configuration could only be *P* based on the two facts from NOESY. This statement was confirmed by the measurement of its ECD spectrum and comparison with the one of *P*-**62**. In contrast to compounds *M*-**62**, **63**, and **64**, a weak positive Cotton effect was observed around 220 nm in the ECD spectrum of **65**, indicating a *P*-axial configuration (Figure 47). Therefore, the full configuration of compound **65** was 7*P*,1*R*,3*R*, and it was named ealamine E.

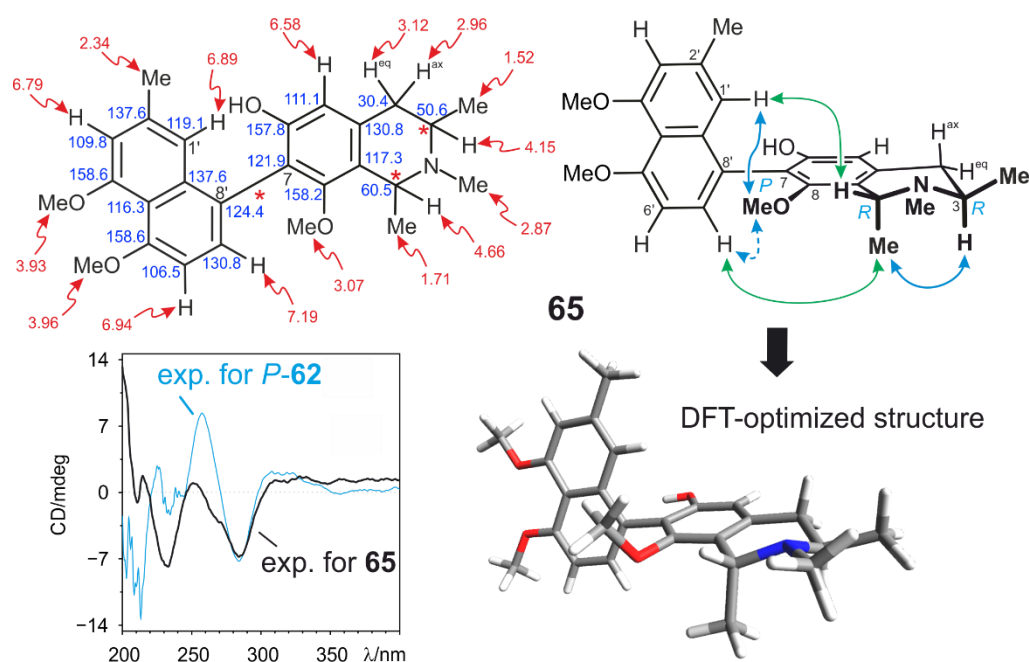


Figure 47. Chemical shifts (<sup>1</sup>H in red and <sup>13</sup>C in blue), NOESY interactions, the ECD spectra, and the DFT-optimized structure of **65** obtained at the B3LYP-D3/def2-SVP level.

The last trace new alkaloid isolated in the leaves was obtained as a yellow powder. A molecular formula of C<sub>26</sub>H<sub>31</sub>NO<sub>4</sub> was deduced from HRESIMS measurements as for **65**. The analysis of the NMR data of **66** indicated a constitution closed to the one of ealamine A (**P-62**). The difference here was due to the CH<sub>3</sub>O-6 group, leading to a new constitution without a free hydroxy group. This was evidenced by the presence of an additional singlet at the resonance of δ<sub>H</sub> 3.64 ppm, which showed cross peaks in NOESY with H-5, H-1', and H-7'. As described for **P-62**, the proposed constitution was likewise in agreement with all the spectroscopic data (Table 6).

The relative *trans*-configuration at C-1 vs C-3 was found by NOESY experiments. The oxidative degradation determined that the absolute configurations at these stereogenic centers were 1*R* and 3*R*, respectively. Once again, the axial configuration was deduced from NOESY experiments and electronic circular dichroism spectra, again taking the results of the degradation into account. Since only traces of the compound were available, the long-range NOEs were not taken for granted. Yet, it was noticed that the NOESY interaction between CH<sub>3</sub>O-8 was much stronger with H-1' than with H-7'. Moreover, CH<sub>3</sub>O-8 showed a strong NOE interaction with H-1, and virtually none with CH<sub>3</sub>-1. Knowing the absolute configuration at C-1 and C-3, the axial absolute configuration could only be *P*, based on the two facts from NOESY experiments (Figure 48). This assumption was confirmed by the comparison of the

ECD spectrum of **66** with *P*-**62**. As for compound *P*-**62**, the positive but characteristic weak Cotton effect observed around 220 nm in the ECD spectrum of **66** confirmed that its axial absolute configuration was *P*. Therefore, the full configuration of compound **66** is *7P,1R,3R*, and it was named ealamine F.

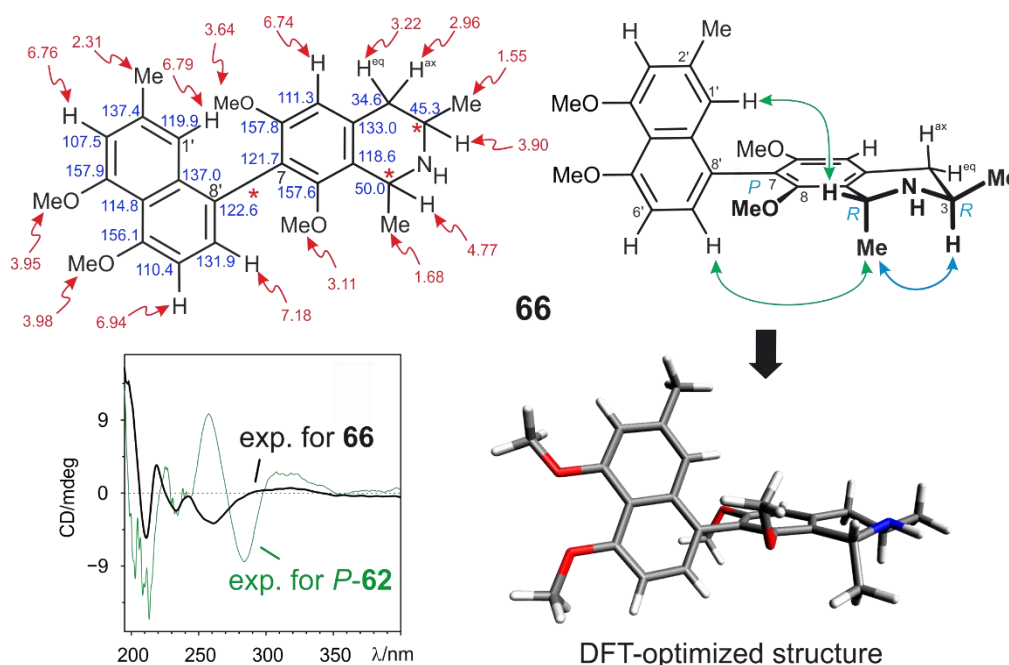


Figure 48. Chemical shifts (<sup>1</sup>H in red and <sup>13</sup>C in blue), NOESY interactions (decisive ones in green, expected ones in blue), the ECD spectra (in methanol), and the DFT-optimized structure of ealamine F (**66**) obtained with B3LYP-D3/def2-SVP.

From a different leaf fraction, yet another compound was detected. It was obtained as an optically active brownish powder. HRESIMS, ECD, NMR, and the oxidative degradation analyses led to the unambiguous identification of the known alkaloid yaoundamine A (**17**), which had been previously isolated together with its heteroside form, yaoundamine B.<sup>[192]</sup> The data obtained in this work were in agreement with the literature.<sup>[192]</sup>

Table 6.  $^1\text{H}$  (600 MHz) and  $^{13}\text{C}$  (151 MHz) data of **63-66** in methanol- $d_4$  ( $\delta$  in ppm,  $J$  in Hz).

no.	ealamine C ( <b>63</b> )		ealamine D ( <b>64</b> )		ealamine E ( <b>65</b> )		ealamine F ( <b>66</b> )	
	$\delta_{\text{H}}$ ( $J$ in Hz)	$\delta_{\text{C}}$ , type	$\delta_{\text{H}}$ ( $J$ in Hz)	$\delta_{\text{C}}$ , type	$\delta_{\text{H}}$ ( $J$ in Hz)	$\delta_{\text{C}}$ , type	$\delta_{\text{H}}$ ( $J$ in Hz)	$\delta_{\text{C}}$ , type
1	4.72, q (6.7)	50.0, CH	4.90, q (6.9)	49.8, CH	4.66, q (6.8)	60.5, CH	4.77, q (6.9)	50.0, CH
3	3.86, m	45.3, CH	3.89, m	45.3, CH	4.15, m	50.6, CH	3.90, m	45.3, CH
4	3.14, dd (17.8, 4.8)	34.6, CH <sub>eq</sub>	3.16, dd (17.4, 5.6)	34.6, CH <sub>eq</sub>	3.12, dd (18.8, 5.0)	30.4, CH <sub>eq</sub>	3.22, dd (16.7, 4.5)	34.6, CH <sub>eq</sub>
	2.88, dd (17.6, 11.7)	34.6, CH <sub>ax</sub>	2.86, dd (18.3, 11.7)	34.6, CH <sub>ax</sub>	2.96, dd (18.8, 12.0)	30.4, CH <sub>ax</sub>	2.96, dd (18.1, 11.7)	34.6, CH <sub>ax</sub>
5	6.56, s	111.3, CH	6.57, s	111.5, CH	6.58, s	111.1, CH	6.74, s	111.3, CH
6		157.8, C		157.7, C		157.8, C		157.8, C
7		121.7, C		121.5, C		121.9, C		121.7, C
8		157.6, C		157.8, C		158.2, C		157.6, C
9		118.6, C		118.5, C		117.3, C		118.6, C
10		133.0, C		133.0, C		130.8, C		133.0, C
1'	6.85, br s	119.9, CH	6.80, br s	119.4, CH	6.89, s	119.1, CH	6.79, br s	119.9, CH
2'		137.4, C		137.7, C		137.6, C		137.4, C
3'	6.79, d (1.2)	107.5, CH	6.79, s	109.9, CH	6.79, s	109.8, CH	6.76, d (1.2)	107.5, CH
4'		157.9, C		158.7, C		158.6, C		157.9, C
5'		156.1, C		158.6, C		158.6, C		156.1, C
6'	6.80, d (7.9)	110.4, CH	6.94, d (8.0)	106.5, CH	6.94, d (8.3)	106.5, CH	6.94, d (8.1)	110.4, CH
7'	7.16, d (7.9)	131.9, CH	7.22, d (8.0)	130.9, CH	7.19, d (8.0)	130.8, CH	7.18, d (7.9)	131.9, CH
8'		122.6, C		124.6, C		124.4, C		122.6, C
9'		137.0, C		137.6, C		137.6, C		137.0, C
10'		114.8, C		117.6, C		116.3, C		114.8, C
CH <sub>3</sub> -1	1.64, d (6.8)	19.6, CH <sub>3</sub>	1.65, d (6.8)	19.6, CH <sub>3</sub>	1.65, d (6.8)	20.2, CH <sub>3</sub>	1.68, d (6.9)	19.6, CH <sub>3</sub>
CH <sub>3</sub> -3	1.51, d (6.4)	19.4, CH <sub>3</sub>	1.51, d (6.5)	19.4, CH <sub>3</sub>	1.51, d (6.3)	16.8, CH <sub>3</sub>	1.55, d (6.5)	19.4, CH <sub>3</sub>
CH <sub>3</sub> -2'	2.32, br s	22.4, CH <sub>3</sub>	2.31, s	22.2, CH <sub>3</sub>	2.31, s	22.1, CH <sub>3</sub>	2.31, br s	22.4, CH <sub>3</sub>
CH <sub>3</sub> O-6	-	-	3.15, s	61.1, CH <sub>3</sub>	-	-	3.64, s	56.9, CH <sub>3</sub>
CH <sub>3</sub> O-8	3.07, s	60.7, CH <sub>3</sub>	-	-	3.07, s	60.7, CH <sub>3</sub>	3.11, s	60.7, CH <sub>3</sub>
CH <sub>3</sub> O-4'	4.08, s	56.9, CH <sub>3</sub>	3.96, s	56.9, CH <sub>3</sub>	3.93, s	56.9, CH <sub>3</sub>	3.95, s	56.9, CH <sub>3</sub>
CH <sub>3</sub> O-5'	-	-	3.93, s	57.1, CH <sub>3</sub>	3.96, s	56.7, CH <sub>3</sub>	3.98, s	56.9, CH <sub>3</sub>
CH <sub>3</sub> -N	-	-	-	-	2.87, s	34.2, CH <sub>3</sub>	-	-

Phytochemical investigations on the methanolic twig extract of *A. ealaensis* revealed the presence of ealamine A (*P*-**62**), already found in the leaves, which eluted first before an additional series of similar alkaloids. Among them, two additional new related alkaloids were found, leading to a total of eight new monomers from the leaves and the twigs fractions (Table 7).

Along with *P*-**62**, compound **67** was isolated and fully characterized by applying the classical procedure. This alkaloid was purified to yield an optically active yellowish powder displaying a molecular formula of  $C_{24}H_{27}NO_4$  by HRESIMS as for **63**. Comprehensive analysis of all spectroscopic data of **67** inferred to an identical constitution as ealamine C (**63**). However, its relative configuration at the two stereogenic centers was found to be *cis*-oriented, thus only four diastereomers were possible considering the chiral axis, *viz.*, *7P,1R,3S*, *7P,1S,3R*, *7M,1R,3S*, or *7M,1S,3R*. The absolute configuration at C-3 was firmly determined by oxidative degradation to be *R*, leaving out all diastereomers with *3S*. The axial configuration was assigned to be *P* based on the favorable NOESY interaction between H-1' and the equatorial CH<sub>3</sub>-1 (Figure 49). This assignment was further proven by the almost identical ECD spectra of **67** and *P*-**62**, and different to the spectrum of **63**. Hence, the new alkaloid **67** was elucidated to possess the following stereochemical features: *7P,1S,3R*, and was named ealamine G.

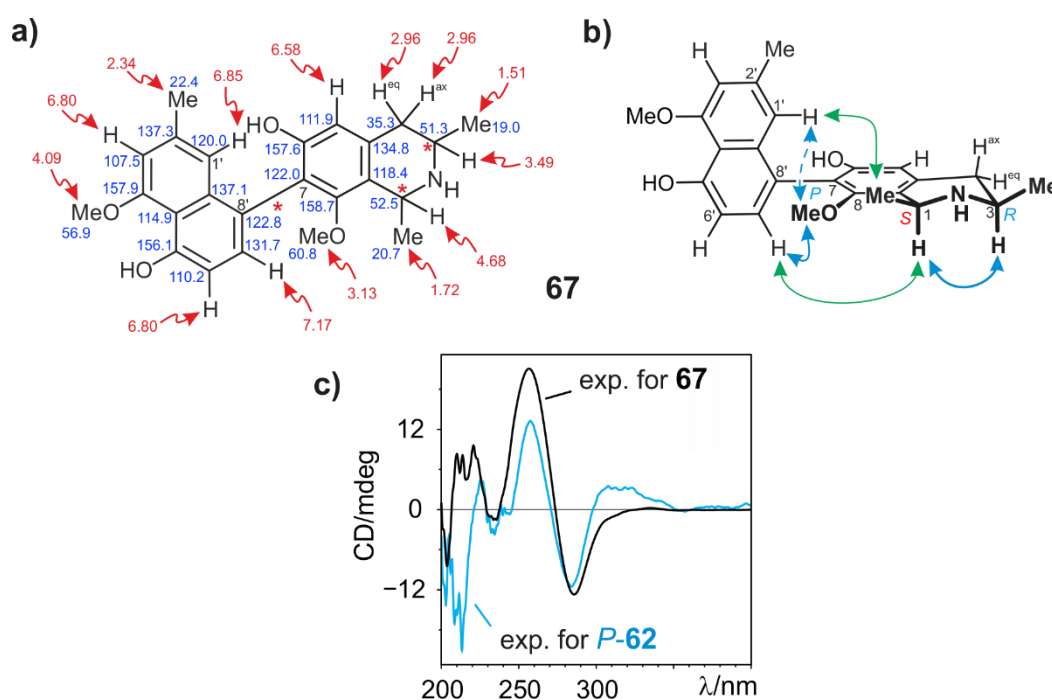


Figure 49. (a) Chemical shifts (<sup>1</sup>H in red and <sup>13</sup>C in blue), (b) NOESY interactions of ealamine G (**67**) shown as double blue double arrows (the green double arrows are decisive ones for the axial configuration), and (c) ECD spectrum of **67** compared to that of ealamine A.



From the same twig extract, yet more slowly eluting than ealamine G, was isolated and subsequently analyzed another new metabolite. Obtained also as a yellowish powder, the compound **68** displayed a molecular formula of  $C_{25}H_{29}NO_4$  by HRESIMS, identical to *P-62*. Comprehensive analysis of spectroscopic data led to the identification of a constitution corresponding to a 4'-*O*-demethylated derivative of ealamine E (**65**), so far undescribed in this thesis. The deshielded chemical shifts of C-1 and C-3 beyond 60 ppm clearly indicated an *N*-methylated 1,3-*cis*-configured tetrahydroisoquinoline, which was further confirmed by the NOEs experiments (Figure 50b).

As in the previous cases, the absolute configurations at the two chiral centers were enabled by determination of the configuration at C-3 by oxidative degradation. Since all seven compounds isolated so far have shown an *R* configuration at C-3, it could be likewise assumed for **68**, isolated from the same fraction, the configurations should be identical to the previous cases. To our biggest surprise, the oxidation of **68** delivered *S*-configured aminobutyric acid and methyl-aminobutyric acid, indicating for the first time that the configuration at C-3 was *S*. Based on the relative *cis*-orientation at the two stereogenic protons, and the NOEs across the axis the absolute configuration of the molecule should be 7*P*,1*R*,3*S* (Figure 50). This assignment was validated by the almost identical ECD spectrum of **68** with the one of *P-62*. Hence, the alkaloid was new and named ealamine H (**68**).

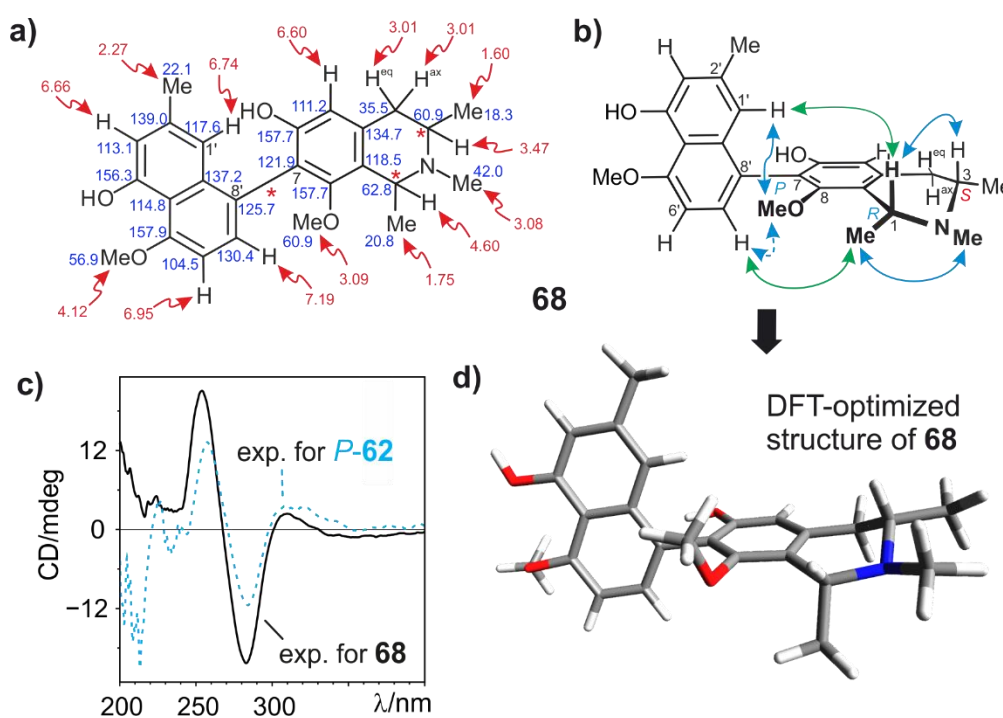


Figure 50. (a) Chemical shifts ( $^1\text{H}$  in red and  $^{13}\text{C}$  in blue), (b) NOESY interactions of ealamine H (**68**) shown as double blue arrows (the green arrows are decisive ones for the axial configuration), and (c) ECD spectrum of **68** compared to that of ealamine A (*P-62*). (d) DFT-optimized structure of **68** obtained at the B3LYP-D3/def2-SVP level.

Another compound eluting faster on an RP<sub>18</sub> HPLC column than ealamine G (**67**) was also isolated and characterized. The yellowish powder of compound **68** showed a protonated molecular ion by HRESIMS corresponding to C<sub>26</sub>H<sub>31</sub>NO<sub>4</sub>, as for ealamine F. Expecting an analog of this one, its extensive data analysis revealed an identical constitution to ealamine E (**65**). In contrast to **65**, the relative configuration at the stereocenters C-1 *versus* C-3 was found to be *cis* by NOESY experiments. The *N*-methylated tetrahydroisoquinoline with *cis*-configuration should have been anticipated by the typical chemical shifts of C-1 and C-3 around 60 ppm as mentioned earlier. The configuration at C-3 was chemically determined by oxidative degradation delivering *S*-aminobutyric acid, which implied that the configuration at C-1 to be *S* due to the diaxial orientation of both stereogenic protons (Figure 51). The axial configuration was also assigned by NOESY and ECD spectra comparison with the one of *P*-**62**, and the axial-*S*- (or *P*-) configuration was deduced. Therefore, the compound **69** (*7P,1R,3S*) was the known 6-*O*-demethylancistrobrevine A (**69**). In contrast to the new monomeric ealamine A-G (**62-67**), ealamine H (**68**) and 6-*O*-demethylancistrobrevine A (**69**) belong to the classical Ancistrocladaceae-type naphthylisoquinoline alkaloids.

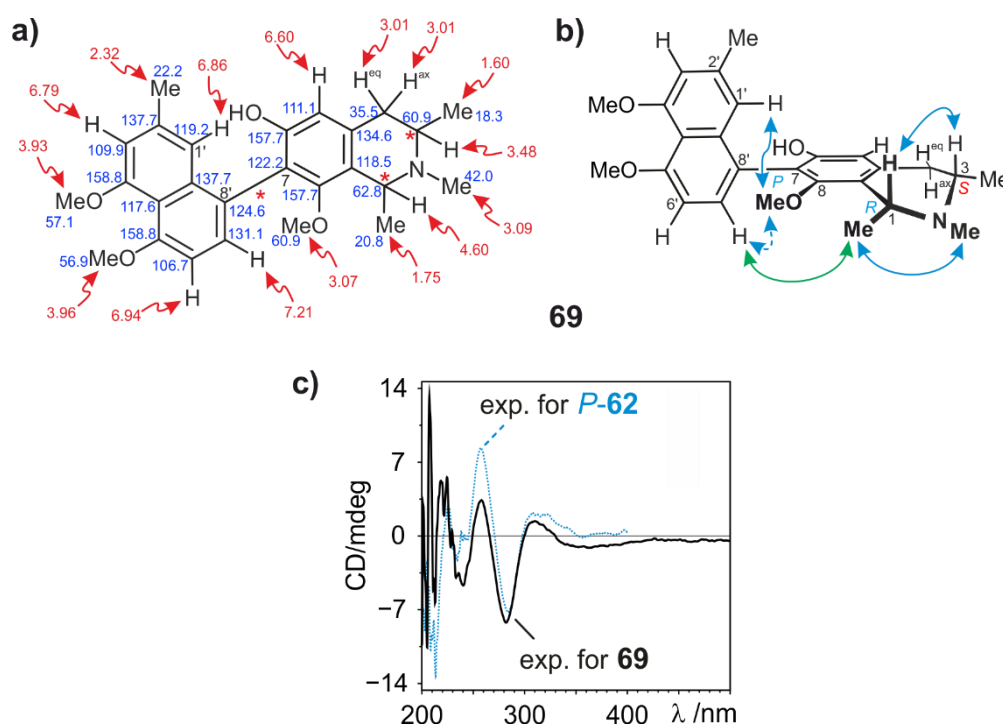


Figure 51. (a) Chemical shifts (<sup>1</sup>H in red and <sup>13</sup>C in blue), (b) decisive NOESY interactions, and (c) ECD spectrum of 6-*O*-demethylancistrobrevine A (**69**) compared to the one of ealamine A (*P*-**62**).

Table 7. <sup>1</sup>H (600 MHz) and <sup>13</sup>C (151 MHz) data of ealamines G (**67**) and H (**68**), and 6-O-demethylancistrobreve A (**69**) in methanol-*d*<sub>4</sub> ( $\delta$  in ppm, *J* in Hz).

no.	ealamine G ( <b>67</b> )		ealamine H ( <b>68</b> )		6- <i>O</i> -demethylancistrobreve A ( <b>69</b> )	
	$\delta_{\text{H}}$ ( <i>J</i> in Hz)	$\delta_{\text{C}}$ , type	$\delta_{\text{H}}$ ( <i>J</i> in Hz)	$\delta_{\text{C}}$ , type	$\delta_{\text{H}}$ ( <i>J</i> in Hz)	$\delta_{\text{C}}$ , type
1	4.68, q (6.5)	52.5, CH	4.60, q (6.9)	62.8, CH	4.60, q (6.6)	62.8, CH
3	3.49, m	51.3, CH	3.47, m	60.9, CH	3.48, m	60.9, CH
4	2.96, d (7.5)	35.3, CH <sub>eq</sub>	3.01, d (7.05)	35.5, CH <sub>eq</sub>	3.01, m	35.5, CH <sub>eq</sub>
	2.96, d (7.5)	35.3, CH <sub>ax</sub>	3.01, d (7.05)	35.5, CH <sub>ax</sub>	3.01, m	35.5, CH <sub>ax</sub>
5	6.58, s	111.9, CH	6.60, s	111.2, CH	6.60, s	111.1, CH
6		157.6, C		157.7, C		157.7, C
7		122.0, C		121.9, C		122.2, C
8		158.7, C		157.7, C		157.7, C
9		118.9, C		118.5, C		118.5, C
10		134.8, C		134.7, C		134.6, C
1'	6.85, br s	120.0, CH	6.74, br s	117.6, CH	6.86, br s	119.2, CH
2'		137.3, C		139.0, C		137.7, C
3'	6.80, d (1.1)	107.5, CH	6.66, d (1.3)	113.1, CH	6.79, d (1.3)	109.9, CH
4'		157.9, C		156.3, C		158.8, C
5'		156.1, C		157.9, C		158.8, C
6'	6.80, d (7.9)	110.2, CH	6.95, d (8.1)	104.5, CH	6.94, d (8.1)	106.7, CH
7'	7.17, d (7.9)	131.7, CH	7.19, d (8.0)	130.4, CH	7.21, d (8.0)	131.1, CH
8'		122.8, C		125.7, C		124.6, C
9'		137.1, C		137.2, C		137.7, C
10'		114.9, C		114.8, C		117.6, C
CH <sub>3</sub> -1	1.72, d (6.6)	20.7, CH <sub>3</sub>	1.75, d (6.7)	20.8, CH <sub>3</sub>	1.75, d (6.7)	20.8, CH <sub>3</sub>
CH <sub>3</sub> -3	1.51, d (6.5)	19.0, CH <sub>3</sub>	1.60, d (6.5)	18.3, CH <sub>3</sub>	1.60, d (6.5)	18.3, CH <sub>3</sub>
CH <sub>3</sub> -2'	2.34, br s	22.4, CH <sub>3</sub>	2.27, br s	22.1, CH <sub>3</sub>	2.32, br s	22.2, CH <sub>3</sub>
CH <sub>3</sub> O-6	-	-	-	-	-	-
CH <sub>3</sub> O-8	3.13, s	60.8, CH <sub>3</sub>	3.09, s	60.9, CH <sub>3</sub>	3.07, s	60.9, CH <sub>3</sub>
CH <sub>3</sub> O-4'	4.09, s	56.9, CH <sub>3</sub>	-	-	3.93, s	57.1, CH <sub>3</sub>
CH <sub>3</sub> O-5'	-	-	4.12, s	56.9, CH <sub>3</sub>	3.96, s	56.9, CH <sub>3</sub>
CH <sub>3</sub> -N	-	-	3.08, s	42.0, CH <sub>3</sub>	3.09, s	42.0, CH <sub>3</sub>

The assignment of the absolute configuration of these hybrid-type 7,8'-linked NIQs were quite delicate and needed to be performed with a lot of care, combining time-demanding techniques for solid confirmation. The distances between the decisive protons in each molecular building blocks were found to be not always in favor of displaying the decisive long-range NOEs from CH<sub>3</sub>-1 to CH<sub>3</sub>-2', an optimal mixing time is usually required. We have noticed that the *M*-configured atropo-diastereomers with an *O*-methyl group at C-8 adopt an unpredictably stable conformation, which further complicates the interpretation of the NOESY interactions. This unknown conformational behavior has led us to draw the tetrahydroisoquinoline part in compounds *M*-**62**, **63**, and **64** in a completely new manner, based on the results obtained by DFT geometric structural optimization. To be remarked is also the weak ECD effect of alkaloids with a 7,8'-linked biaryl axis, compared to that of the corresponding 5,8'-coupled, in particular, the *P*-atropisomers, which show a very poor positive Cotton effect around 223 nm. This poor ECD effect justifies why in the case of mixed-dimers like the ealapasamines A-C, the overall ECD spectra are dominated by the strong effects of the korupensamine-like (5,8'-coupled) moieties, thus, constituting a drawback for computational investigations of overall ECD spectra for ealapasamines.<sup>[168]</sup> The crystal structure of ealamine A (*P*-**62**) is especially noteworthy since it is one of the rare examples of an NIQ crystal structure, and the very first of a 7,8'-linked naphthylisoquinoline alkaloid.

The discovery of this compound series, featuring an untypical coupling type, further explains the ability of *A. ealaensis* to synthesize dimers, like ealapasamines A-C, possessing such molecular portions. Additionally, these findings may suggest that all the ealamines should be part of a mixed dimer like **43**, but that they have not yet been revealed. It may also indicate that only a few synthesized ealamine monomers are enzymatically coupled to form a heterodimer of the type ealapasamine. The last option seems to be the most plausible since not all metabolites produced by plants are used for further biosynthetic pathways,<sup>[11]</sup> which demonstrates the specificity in the broad biosynthetic potential of *A. ealaensis*.

## Biological evaluations

**Antiprotozoal activities:** Three model systems were used for the evaluation of the biological activities of the main isolated new alkaloids. Compounds *P-62*, *M-62*, **63** and **64** were tested *in vitro* for their antiprotozoal activities on several pathogens responsible for severe forms of tropical diseases: *Plasmodium falciparum* (NF54 and K1 strains), *Trypanosoma cruzi* (amastigotes of Tulahuen C4 strain), *Trypanosoma brucei rhodesiense* (trypomastigotes of STIB 900 strain), and *Leishmania donovani* (amastigotes of MHOM-ET-67/L82 strain), and the cytotoxicity on mammalian host cells (rat skeletal myoblast L6 cells). The results are summarized in Table 8. The compounds *P-62*, *M-62*, **63**, and **64** displayed all individually moderate to very good antiprotozoal activities. In particular, ealamine C (**63**) was active against on *P. falciparum* NF54 with an IC<sub>50</sub> value of 0.84 μM and a selectivity index (cytotoxicity/IC<sub>50</sub>) of 57, which presented the best antimalarial profile among the tested candidates. Interestingly, *P-62* and *M-62* showed differentiated antiplasmodial profiles on the chloroquine-sensitive (NF54) and chloroquine-resistant (K1) strains, demonstrating once again the influence of atropisomerism on the expression of the biological activity. Indeed, the *M*-configured compound *M-62* was not only more active on K1 (1.39 μM) than on NF54 (4.86 μM), but also performed better than the main atropo-diastereomer *P-62*, the latter showing IC<sub>50</sub> values of 1.61 μM (K1) and 6.28 μM (NF54). Besides, the bioactivities exhibited by *M-62* against *L. donovani* (IC<sub>50</sub> 53.38 μM) and *T. brucei rhodesiense* (IC<sub>50</sub> 7.79 μM) were significantly better than those for *P-62* with IC<sub>50</sub> values of 170.60 μM (for *L. donovani*) and 9.78 μM (for *T. brucei rhodesiense*). However, compound *P-62* displayed an IC<sub>50</sub> value of 73.42 μM on *T. cruzi*, much better than *M-62* (IC<sub>50</sub> 122.83 μM).

**Antileukemic activities:** Investigations on two anticancer cell lines were undertaken since the antiprotozoal activities were not impressive. The alkaloids **62-63**, **67** and **69** were tested on the human CCRF-CEM leukemia cells. Ealamine C (**63**) was found to be the most active, with an IC<sub>50</sub> of 7.41 μM. With an IC<sub>50</sub> of 8.04 μM, ealamine A (*P-62*) was more potent than its atropo-diastereomer *M-62* (IC<sub>50</sub> 11.75 μM). The least methylated compound **67** (IC<sub>50</sub> 14.63 μM) was also found to be more active than the **69** (IC<sub>50</sub> 28.58 μM), insinuating an unfavorable implication of the *N*-methylation on the activity on CCRF-CEM. Moreover, *P-62*, **63**, and **67** exhibited better profiles against the multidrug resistant strain CEM/ADR5000 than the reference drug doxorubicin (IC<sub>50</sub> = 30.1 μM) with IC<sub>50</sub> values of 20.90, 21.31, and 19.84 μM, respectively. Preliminary studies on human cervical cancer cells HeLa indicated promising inhibition potential for compounds *P-62* and **63** with IC<sub>50</sub> values of 6.68 and 21.34 μM,

respectively. These results indicated that this group of alkaloids could be a new source of promising antitumoral drug candidates, and that further investigations are highly required especially since the anticancer activities of NIQs have been poorly investigated in the literature, and it can be seen here that there is a promising potential.

Table 8. Antiprotozoal activities, and antiproliferative effects on human T-lymphoblastic leukemia cells CCRF-CEM and on cervical cancer cells HeLa for compounds **62-64**, **67** and **69** (IC<sub>50</sub> in μM).

Compounds	<i>T. br. rhod</i>	<i>T. cruzi</i>	<i>L. don. am</i>	<i>P. falc. NF54</i>	<i>P. falc. K1</i>	Cytotox L6	CCRF-CEM	CEM/ADR 5000	HeLa cells
Standard	0.007 <sup>[1]</sup>	3.56 <sup>[2]</sup>	0.43 <sup>[3]</sup>	0.008 <sup>[4]</sup>	0.364 <sup>[4]</sup>	0.041 <sup>[5]</sup>	0.017 <sup>[6]</sup>	30.1 <sup>[6]</sup>	13.9 <sup>[7]</sup>
<i>P-62</i>	9.78	73.42	170.60	6.28	1.61	9.07	8.04	20.90	6.68
<i>M-62</i>	7.79	122.83	53.38	4.86	1.39	20.85	11.75	n.d.	n.d.
<b>63</b>	9.35	102.67	>254.14	0.84	-	47.73	7.41	21.31	21.34
<b>64</b>	106.05	225.47	>245.40	22.18	8.19	>245.40	-	n.d.	n.d.
<b>65</b>	-	-	-	-	-	-	n.d.	-	n.d.
<b>66</b>	-	-	-	-	-	-	n.d.	-	n.d.
<b>67</b>	-	-	-	-	-	-	14.63	19.84	-
<b>69</b>	-	-	-	-	-	-	28.58	-	-

[1] Melarsoprol. [2] Benznidazole. [3] Miltefosine. [4] Chloroquine. [5] Podophyllotoxin.

[6] Doxorubicin. [7] 5-fluorouracil (5-FU). n.d.: not determined.

In conclusion, the discovery of such a vast series of hybrid-type 7,8'-linked NIQs proves that *Ancistrocladus ealaensis* is capable of producing Ancistrocladaceae- and the mixed Ancistrocladaceae/Dioncophyllaceae-type naphthylisoquinolines. This liana mainly produces coupling products with the biaryl axis at position C-8' of the naphthalene portion. The detection of ealamine C (**64**) in large quantities indicates that only its *P*-configured atropo-diastereomer is specifically (enzymatically) uptaken in the biosynthesis of the new hetero-dimers ealapasamines. The detection of ealamine G (**67**) is outstanding because exactly this monomer was observed in the second molecular half of the most active NIQ on K1, *viz.* ealapasamine C (**44**). The co-occurrence of yaoundamine A (**17**) with the new series of tetrahydro-related compounds implies that korundamine A might also be among the minor dimeric fractions. All this reveals the unique synthetic potential of this central African liana. Until now, this class of compounds was under-represented within the NIQ metabolites group.

## II.5. Synthesis of Ealajoziminone A and Ealajoziminone B

The abundant occurrence of the monomeric naphthylisoquinolines of the ealamine-type in *A. ealaensis* suggested the possible presence of dimeric alkaloids exclusively made of such basic units. The C<sub>2</sub>-symmetric ancistrogriffithine A (**30**) – known from *A. griffithii*<sup>[102]</sup> – featuring two 7,8'-linked building blocks, has remained the only dimer with this peculiarity.

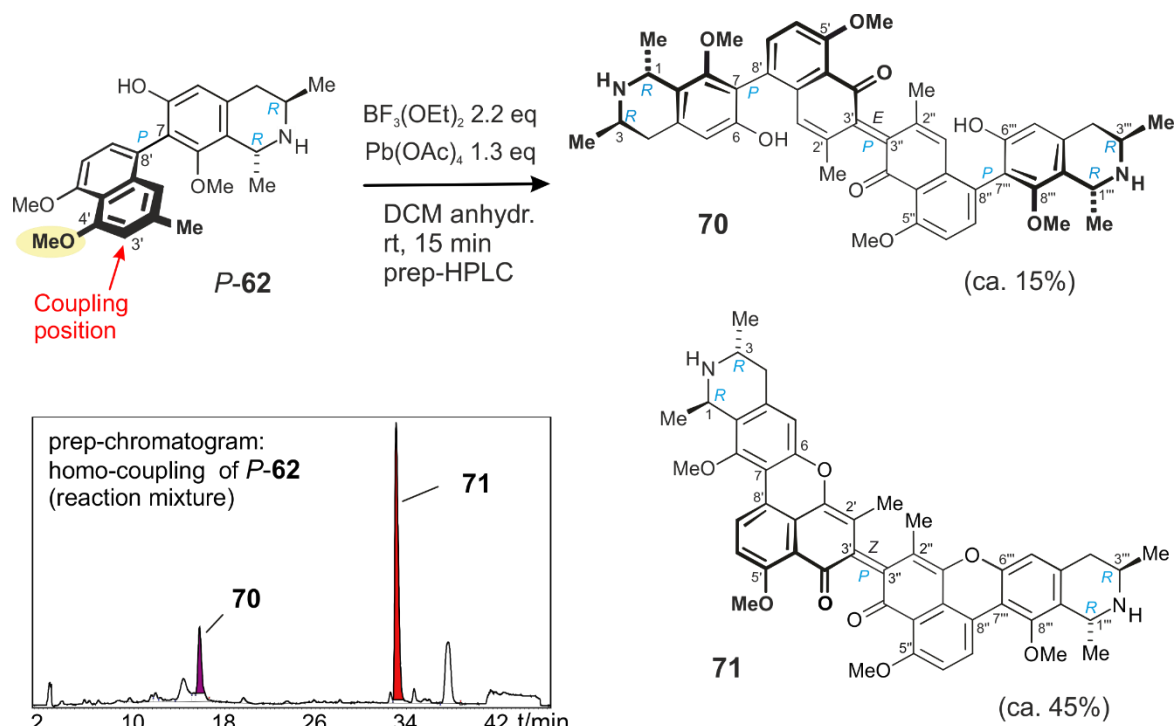
It was therefore decided to first aim at the synthesis of such dimers and then check their occurrence in the plant extract. Such strategy can serve for the discovery of minor natural products that might have been overlooked during the fractionation process.

For this reason, the semi-synthesis of such dimers, by one-step oxidative coupling reactions was chosen and optimized using Pb(OAc)<sub>4</sub> and BF<sub>3</sub>.OEt<sub>2</sub> – without protective groups – for the new alkaloids ealamine A (*P*-**62**) and ealamine C (**63**). The choice was motivated by the quantities of the isolated material and was aiming at the evaluation of their difference in terms of reactivity. The case of ealamine A (*P*-**62**) was even more interesting because of the *O*-*O*-dimethyl groups in the naphthalene unit, from which a weak reactivity and most probably a preference for a coupling at C-6' position should be expected, like in the case of jozimine B (structure not shown).<sup>[198]</sup> Based on the fact that no dimerization of dioncophylline A (**20**) with Pb(OAc)<sub>4</sub>/BF<sub>3</sub>.OEt<sub>2</sub> had been observed,<sup>[187]</sup> variations of the oxidation condition parameters were, in these cases (for *P*-**62** and **63**), undertaken in order to achieve this new synthetic goal.

Performing the reaction at room temperature, instead of 0 °C, as performed so far,<sup>[188, 198]</sup> now led to the detection of stable over-oxidized dimeric compounds, in both cases, for *P*-**62** and **63** by LC-MS and LC-DAD. However, the isolation and the structural elucidation was achieved only in the case of *P*-**62** due to time constraints. With a little excess of Pb(OAc)<sub>4</sub>, the oxidative coupling of ealamine A led to the formation of stable dimeric diphenoquinones. The two main compounds – promising based on their LC-MS profiles – were isolated by preparative HPLC and structurally characterized.

A solution of anhydrous dichloromethane (CH<sub>2</sub>Cl<sub>2</sub>) containing 10 mg of ealamine A (*P*-**62**) was cooled to 0 °C for 5 min. To this solution were added 2.2 equivalents of BF<sub>3</sub>.OEt<sub>2</sub>, prepared in anhydrous CH<sub>2</sub>Cl<sub>2</sub> and the mixture was stirred for 5 min at room temperature. Then, 1.3 equivalents of a freshly prepared solution of Pb(OAc)<sub>4</sub> were added to the mixture, which was then further stirred at room temperature for 15 min. The resulting reaction mixture was directly filtered through a Celite column, using HPLC-grade MeOH. The purification on preparative

HPLC, using a Symmetry<sup>®</sup> RP<sub>18</sub> column, afforded two dimeric compounds (Scheme 5), *i.e.* ealajoziminone A (**70**) and ealajoziminone B (**71**), which were novel structures.



Scheme 5. One-step synthesis of ealajoziminones A (**70**) and B (**71**) by oxidation of ealamine A (**P-62**) using an excess of  $\text{Pb}(\text{OAc})_4$  in presence of  $\text{BF}_3(\text{OEt})_2$ . One selected chromatogram of the reaction mixture at the preparative HPLC scale.

The faster eluting dimer **70** was obtained as a violet solid, corresponding to a molecular formula of  $\text{C}_{48}\text{H}_{50}\text{N}_2\text{O}_8$  as deduced from HRESIMS. In the NMR spectra, one set of signals was observed – 13 signals on the  $^1\text{H}$  and 24 on the  $^{13}\text{C}$  – suggested the presence of a  $\text{C}_2$ -symmetric dimer. Compared to ealamine A (**P-62**), the new compound showed only four aromatic and two methoxy signals in the  $^1\text{H}$  spectrum. The detection of two *ortho*-coupled doublets, corresponding to H-6' ( $\delta_{\text{H}} = 7.42$  ppm, d,  $J = 9.18$  Hz,  $\delta_{\text{C}} = 115.53$  ppm) and H-7' ( $\delta_{\text{H}} = 8.68$ , d,  $J = 9.08$  Hz,  $\delta_{\text{C}} = 133.50$ ), and one singlet at H-5 ( $\delta_{\text{H}} = 6.90$ , s,  $\delta_{\text{C}} = 114.92$ ) supported that the central coupling axis had to be located at C-1' ( $\delta_{\text{C}} = 132.0$  ppm) or at C-3' ( $\delta_{\text{C}} = 95.60$  ppm). The TOCSY interaction from H-7' to a proton singlet at the resonance of 6.39 ppm (H-1',  $\delta_{\text{C}} = 132.0$  ppm) confirmed the coupling to be located at the two C-3' positions. Moreover, a carbonyl function was identified at C-4' ( $\delta_{\text{C}} = 185.16$  ppm), as evidenced by the  $^4J$ -HMBC interactions from H-6' and  $\text{CH}_3$ -2' ( $\delta_{\text{H}} = 2.24$ , s,  $\delta_{\text{C}} = 16.68$ ) to C-4'. Considering its location and the low-field shielded chemical shift of the neighboring C-3', a diphenoquinone moiety was identified. The chemical shifts of the other positions remained unchanged compared to



ealamine A (*P*-**62**). The relative and absolute configurations of *P*-**62** should have remained the same at the stereocenters and the two outer axes in **70**. The weak ROESY interactions between CH<sub>3</sub>-2' and CH<sub>3</sub>O-5'' ( $\delta_{\text{H}} = 4.00$ , s,  $\delta_{\text{C}} = 56.83$ ) suggested an *E*-configuration at the central double bond (Figure 52a). The compound was given the trivial name ealajoziminone A (**70**).

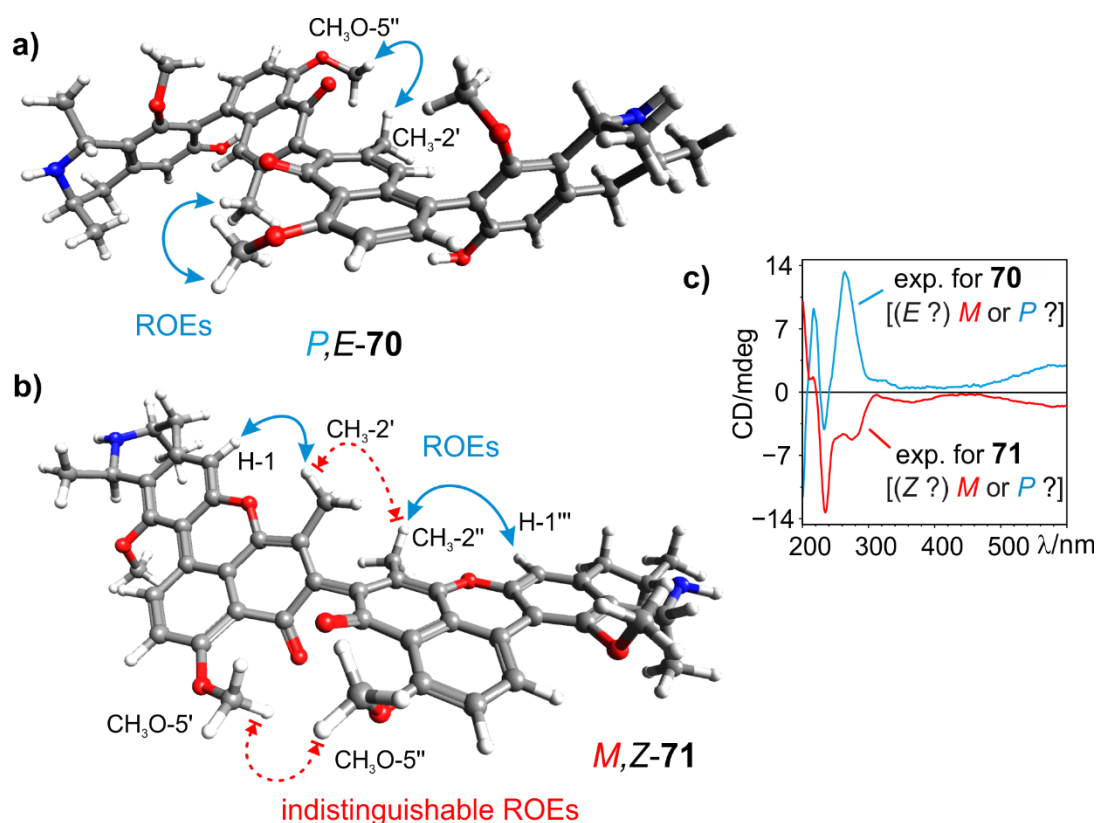


Figure 52. Geometries calculated for one diastereomer of (a) ealajoziminone A (**70**) and (b) ealajoziminone B (**71**), performed at the DFT-B3LYP/def2-SVP level. Observed (blue double arrows) and indistinguishable (red dotted arrows) ROESY interactions hinting at an *E*- and *Z*-configuration for **70** and **71**, respectively. (c) Overlaid offline experimental ECD spectra of **70** and **71** recorded in methanol.

The second, and main, compound of the oxidation reaction was isolated as a red crystalline material, possessing another UV and molecular weight as compared to **70**. By HRESIMS, the molecular formula was deduced as C<sub>48</sub>H<sub>46</sub>N<sub>2</sub>O<sub>8</sub>, four protons fewer and two IHD units higher than that of **70**. The <sup>1</sup>H and <sup>13</sup>C NMR spectra revealed the presence of another symmetric dimer, but this time with three aromatic proton signals only, as the main difference. Two deshielded aromatic doublets signal of H-6' ( $\delta_{\text{H}} = 7.61$  ppm, d,  $J = 9.59$  Hz,  $\delta_{\text{C}} = 119.88$  ppm) and H-7' ( $\delta_{\text{H}} = 8.96$ , d,  $J = 9.54$  Hz,  $\delta_{\text{C}} = 136.65$ ), and an upfield shifted singlet at H-5 ( $\delta_{\text{H}} = 7.12$ , s,  $\delta_{\text{C}} = 114.33$ ) were seen. These assignments were indicative, on the one hand, of the loss of a

hydrogen at C-1' ( $\delta_{\text{C}} = 160.48$  ppm), and on the other hand, of the formation of a pyran ring between the oxygen function at C-6 and the carbon C-1', most likely after an intramolecular Michael addition. The new ROEs between H-5 and CH<sub>3</sub>-2' ( $\delta_{\text{H}} = 2.08$ , s,  $\delta_{\text{C}} = 8.15$ ) – bringing them in a much closer spatial proximity – and the drastic upfield shift of C-1' unambiguously supported the formation of an oxygen bridge between O-6 and C-1'. All the remaining structural features were identical to those of ealajoziminone A (**70**), except for the lack of the ROESY interactions between CH<sub>3</sub>-2' and CH<sub>3</sub>O-5", hinting at a *Z*-configured central bond (Figure 52b). The compound was named ealajoziminone B (**71**). It is the first representative of such diphenoquinones featuring two pyran rings and lacking axial chirality in the outer axes.

For ealajoziminones A (**70**) and B (**71**), no generation of enantiomers was imaginable, and since the diastereomers should be easily resolved on HPLC, their stereochemical purity was for sure. However, the question about the rotational stability at the central axis, and the absolute configuration remained undefined at this stage. The full absolute assignments were addressed by means of ECD analysis and quantum-chemical calculations.<sup>[119]</sup>

The Minimum structures of the four possible diastereomers, in each case, were calculated by the DFT-B3LYP-D3/def2-TZVP method (Figures 53 and 54). This task was the most demanding one, compared to that of all of the compounds herein described. Our group has recently documented the challenges related to the conformational analysis of similar chiral systems, in simple tetralones already, which required coupled-cluster methods.<sup>[187]</sup> The accurate theoretical prediction of the properties of these two compounds, **70** and **71**, is extremely difficult. The calculations of the ECD spectra of the four respective stereoisomers for each dimer were performed by time-dependent DFT at three levels: by CAM-B3LYP/def2-TZVP, B3LYP/def2-TZVP, and wB97-D3/def2-TZVP. The calculations were performed by Dr. T. Bruhn. Fortunately, very good results were achieved with the first two TDDFT methods, enabling the firm elucidation of the full absolute configuration of **70** as *P,E* (see Figure 53) and **71** as *P,E* (see Figure 54).

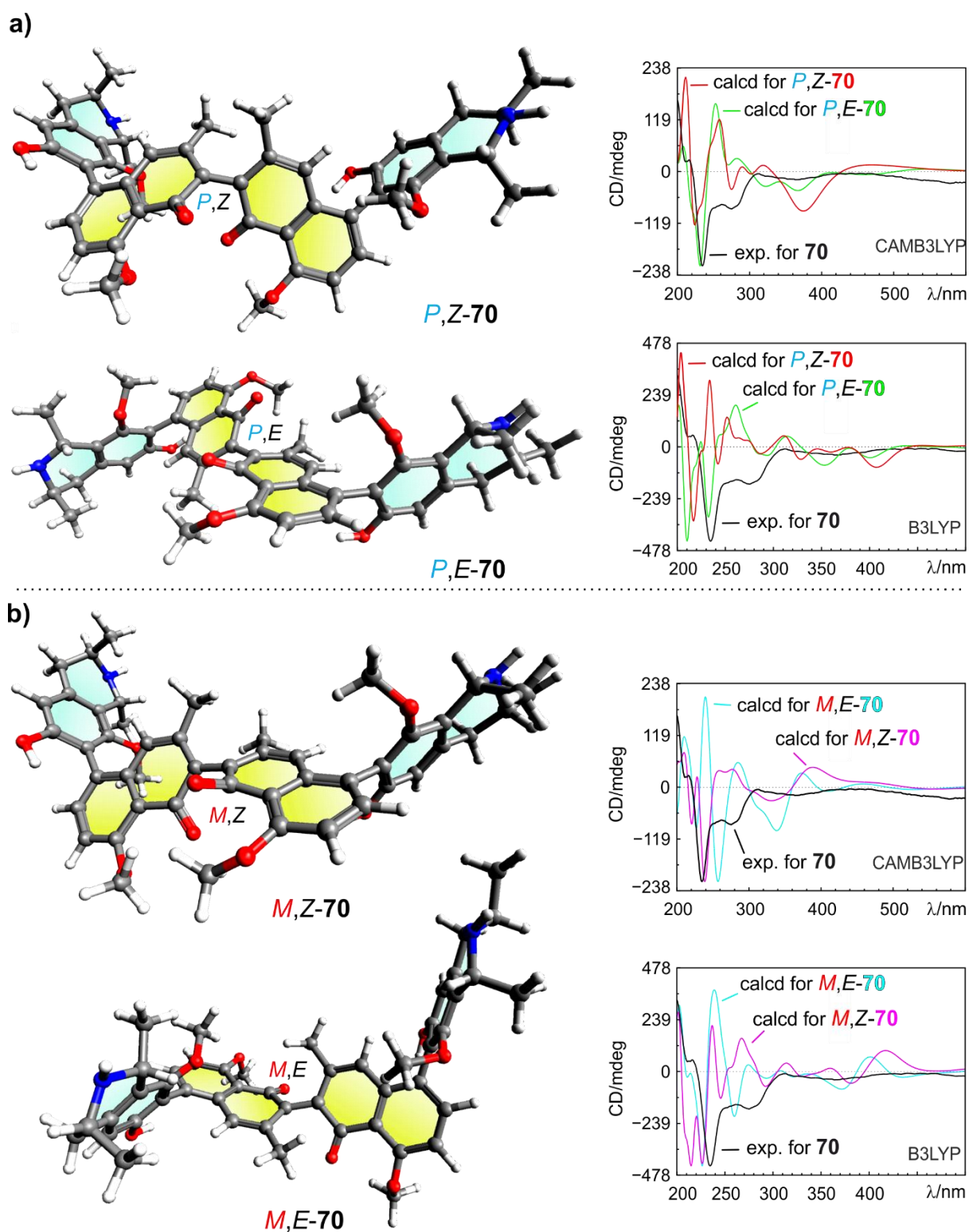


Figure 53. Minimum structures of the possible (a) two *P*-configured stereoisomers and (b) two *M*-diastereomers of ealajoziminone A (**70**) calculated at the DFT-B3LYP-D3/def2-TZVP level and the respective ECD spectra, calculated by TDCAM-B3LYP/def2-TZVP and TDB3LYP/def2-TZVP, compared with the experimental curve of **70**.<sup>[178-179]</sup>

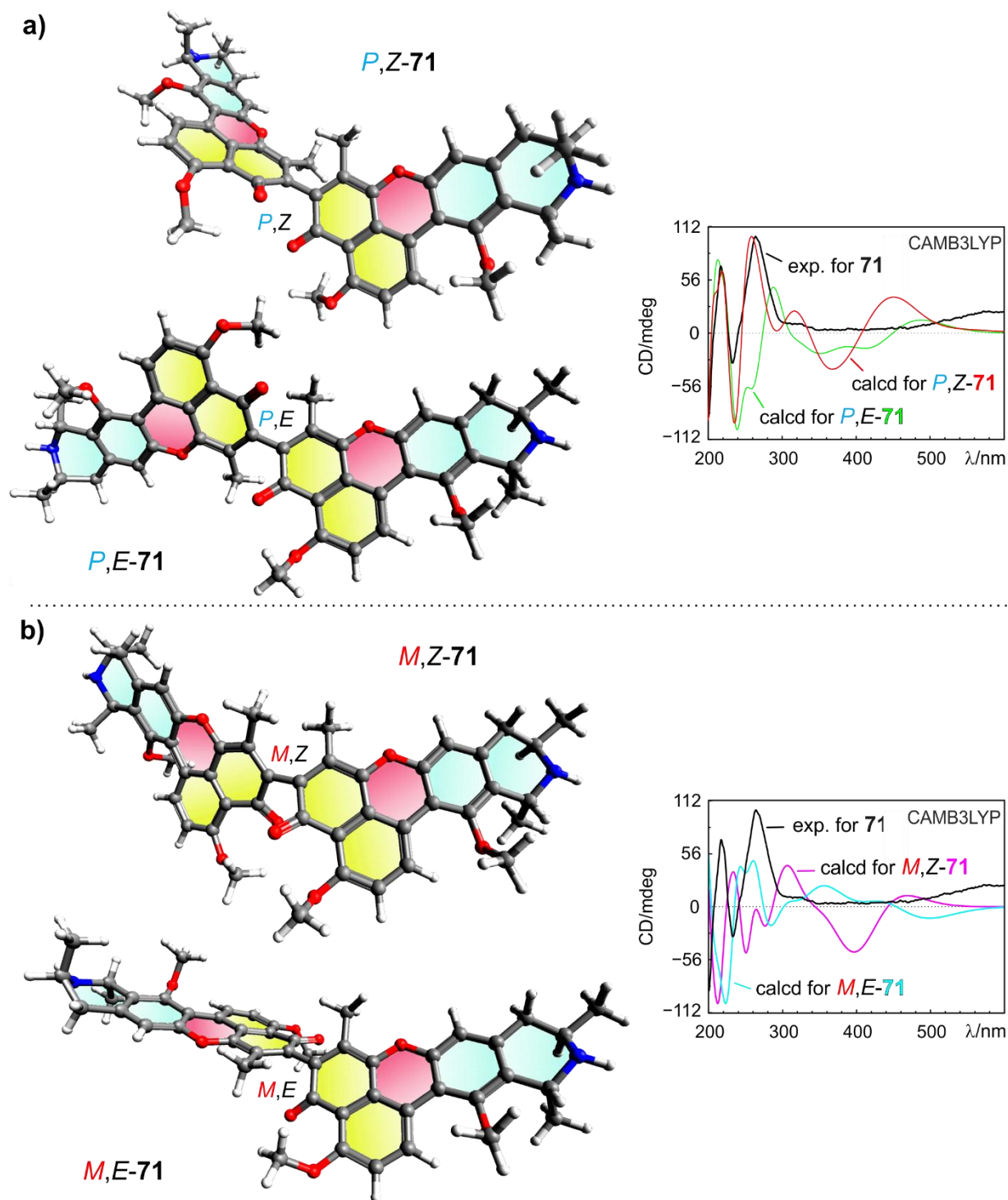


Figure 54. Minimum structures of the possible (a) two *P*-configured stereoisomers and (b) two *M*-diastereomers of ealajoziminone B (**71**) calculated at the DFT-B3LYP-D3/def2-TZVP level and the respective ECD spectra, calculated by TDCAM-B3LYP/def2-TZVP, compared to the experimental curve of **71**.<sup>[178-179]</sup>

Thus, the absolute structure of ealajoziminone A (**70**) was assigned to be *P*- and *E*-configured at the central double bond as depicted in Figure 55. Ealajoziminone B (**71**) was found to be *P*- and *Z*-configured (Figure 55).

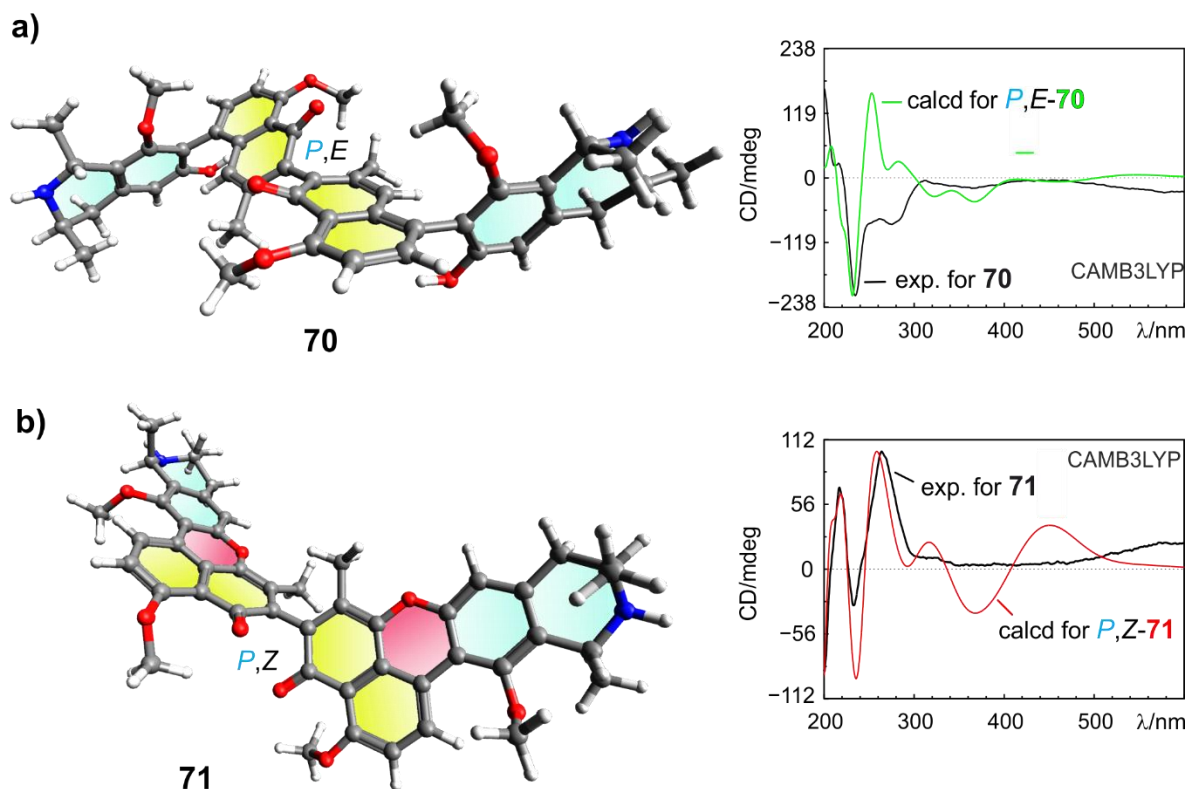


Figure 55. (a) The central double bond of ealajoziminone A (**70**) assigned as *P*- and *E*-configured, based on the satisfactory agreement between the experimental and the calculated ECD spectra. (b) The central double bond of ealajoziminone B (**71**) assigned as *P*- and *Z*-configured, based on the good agreement between the experimental and the calculated ECD spectra. The ECD calculations were successfully achieved at the TDCAM-B3LYP/def2-TZVP level.<sup>[178-179]</sup>

The presence or the lack of ROESY interactions between CH<sub>3</sub>-2' and CH<sub>3</sub>O-5'', which permitted assignment of the configuration at the central double bond in the two dimers, were therefore evidenced by the results from the DFT quantum-chemical calculations.

The formation of the pyran heterocycles in **71** force the newly linked naphthalene and isoquinoline building blocks to become coplanar, which, thus, leads to a loss of the axial chirality in the two outer axes. This phenomenon was unprecedented in the synthesis of this alkaloid class. The planarity in the molecule coupled to an extended conjugated system explained the observed intense red color.

In another case, the oxidation of dioncophylline A (**20**) using  $\text{Pb}(\text{OAc})_4$  and  $\text{BF}_3 \cdot \text{OEt}_2$  – under the standard conditions – had not led to dimerization, but rather to the formation of two tetralones, *viz.* dioncotetralones A and B (structures not shown).<sup>[187]</sup> Now, the dimerization of ealamine A (*P*-**62**) was successful only with a slight increase of lead(IV) tetraacetate and performing the reaction at room temperature instead of 0 °C. A striking fact about this reaction was the unexpected coupling selectivity at C-3', while C-6' remained free, which suggested that the *O*-demethylation at C-4' of ealamine A might precede the homo-coupling step.

Now that the structural elucidation was firmly achieved, the outcome of this oxidation remained unexplained in terms of the mechanism, the over-stoichiometric oxidation of the dimers, the diastereo-differentiation in the formation of **70** and **71**, and the regioselectivity in the coupling at C-3'.

This regioselectivity suggested that the reaction may proceed first by an *O*-demethylation at C-4' and, thus, an activation at C-3' instead of C-6', enabling the observed discrimination in the coupled products.

Unexpected was also the stability of these oxidized compounds in methanolic solution, while related diphenoquinones had been known<sup>[188, 199-200]</sup> – as intermediates in the phenol-oxidative dimerization of monomeric NIQs – to be easily reducible even by MeOH and column filtration.<sup>[188-189, 201]</sup>

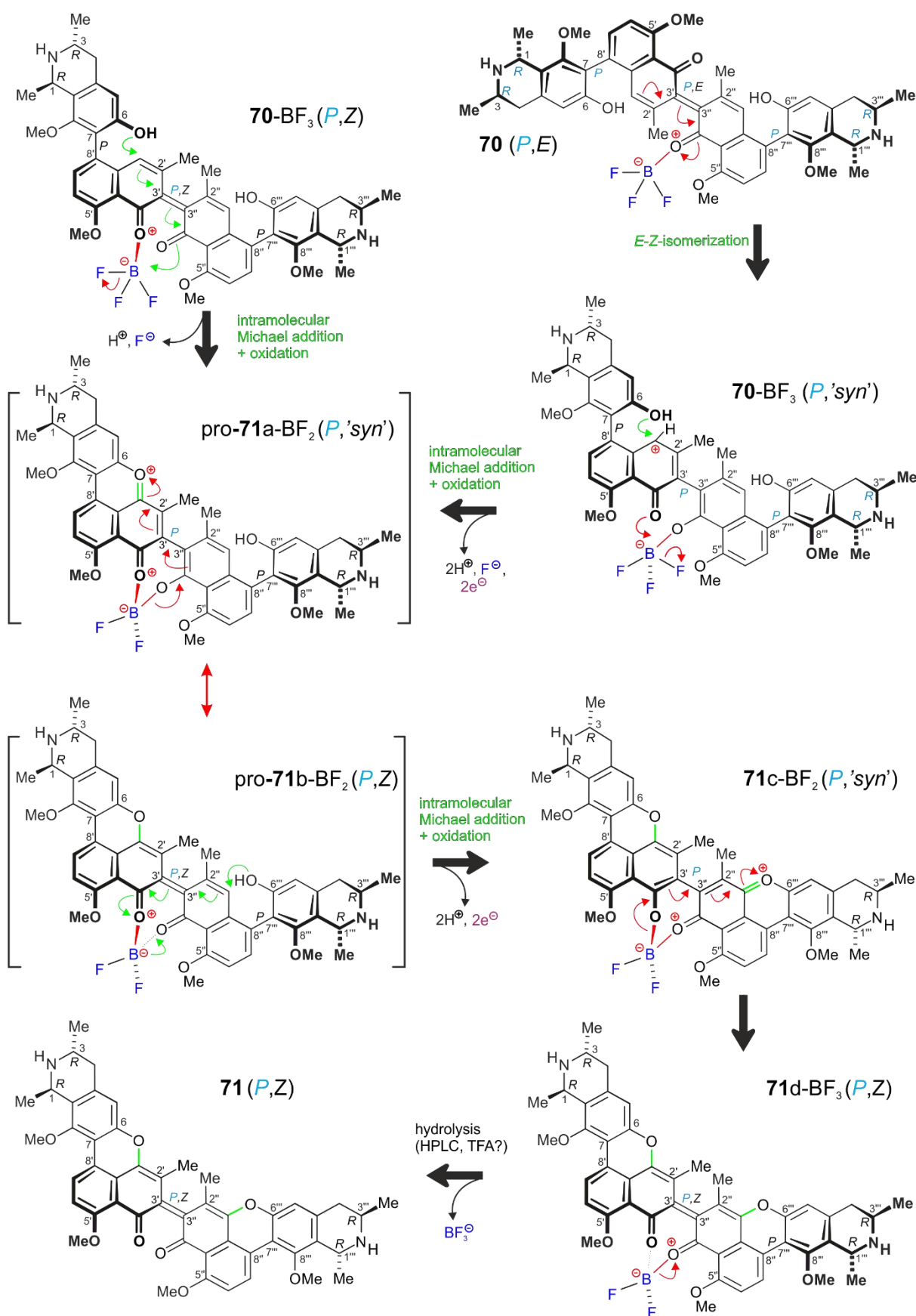
Another important concern is the preponderance of the *Z*-configured form (**71**), electronically unfavorable due to the expected dipole-dipole repulsions of the two carboxy functions at C-4'.

From the monitoring of the reaction by HPLC, the formation of the *Z*-configured **71** occurs very fast while the starting material, ealamine A (*P*-**62**) is being consumed and transformed into another monomeric intermediate (based on the LC-MS-DAD data). This suggests an unusual selectivity for the unfavorable *Z*-orientation in the *P*-configured **71**.

The measured torsion angles between the oxygen functions at C-3' and C-3'' in **71** and the calculated *P,Z*-**70** were found to be 65.4° and 47.1°, respectively. Thus, a difference of 18.3° (65 mÅ, in terms of distance) in favor of the main product **71**, hinting at a gain in stability – due to the reduced dipole-dipole repulsions – by the two additional heterocycles. Moreover, the calculated distances between O-6 and H-1' in **70** (*P,E*) and its stereoisomer *P,Z*-**70** were determined as 3.88 and 3.04 Å, respectively. This difference of 834 mÅ suggested that the *Z*-configuration was unfavorable for a constitution like that of **70**, thus, further explaining its easy

conversion to a more stable form like that of **71**. These facts and the geometries agreed with the observed *E,Z*-selectivities, and were in favor of an intramolecular tandem Michael addition, followed by an oxidation stereoselectively leading to **71**, as postulated in Scheme 6.





Scheme 6. Postulated convergent formation of ealajoziminone B (**71**) from two diastereomers of ealajoziminone A (**70**), *i.e.* the *P,Z*- and *P,E*-configured, via a boron difluoride complex from  $\text{BF}_3 \cdot \text{OEt}_2$ .



It could be assumed that the two diastereomers of **70**, viz. *P,E* and *P,Z*, may have been formed diastereoselectively first. The aforementioned stereoisomer *P,Z-70*, being more reactive, could be further stabilized by the formation of a complex with a Lewis acid in the medium, *i.e.* boron trifluoride, thus enhancing the electrophilic character of C-1' and C-1". These two carbon atoms become ideal targets for a Michael addition, followed by an oxidation leading to the pyran rings (see Scheme 6). The possible formation of boron difluoride complexes may lower the thermodynamic barrier for *E/Z*-isomerization, thus, providing enough rotation freedom for the conversion of **70** (*P,E*) to the reactive form *P,Z-70*, which would ultimately lead to a decrease in **70** and a preponderance of **71** (*P,Z*).

The formation of the boron difluoride complexes further explains the stability of these diphenoquinones, in particular the unfavorable *Z*-configured **71**. The intramolecular Michael addition and oxidation at C-1' and C-1" may require only the atmospheric oxygen in the flask, thus, explaining this over-stoichiometric reaction observed. However, further experiments should be performed to prove this assumption. This oxygen contribution could be evaluated by performing the reaction under an inert gas, like argon or nitrogen.

The formation of a boron difluoride complex and the possible conversion of *P,Z-70* and **70** could be proven by reacting the isolated **70** with  $\text{BF}_3 \cdot \text{OEt}_2$ , in the absence or presence of  $\text{Pb}(\text{OAc})_4$ . These two experiments will picture better the contribution of each reactant, including atmospheric oxygen, to the formation of the complex and/or ealajoziminone B (**71**).

Performing the reaction at room temperature, after the addition of  $\text{BF}_3 \cdot \text{OEt}_2$  seemed to bring the drastic change, which led to these unprecedented results. Therefore, an exhaustive understanding and elucidation of the reaction mechanism is required.

Considering the stability of the diphenoquinone **70** in MeOH, hydrogenation in the presence of Pd/C, as previously described,<sup>[188-189]</sup> could successfully reduce it into a most probable natural product form. This reaction was, however, not performed due to the lack of time.

The biological evaluations of these compounds against cancer cell lines are scheduled.

## II.6. Ealaines A-D, Naphthalene-Devoid Alkaloids

So far in this thesis, an emphasis has been put on the classical naphthylisoquinoline alkaloids, made of two building blocks linked by a biaryl axis. As above-mentioned, the plethora of structurally diverse such alkaloids is build up from a small number of basic units. Despite the reduced number of naphthalene and tetrahydroisoquinoline fragments recognizable in the NIQs, their detection and isolation had remained unsatisfactory in terms of representatives, especially for the tetrahydroisoquinoline portions. Several derivatives of the naphthalene part had been found in Dioncophyllaceae plant species and few in Ancistrocladaceae ones.<sup>[167, 202-205]</sup>

From *A. ealaensis*, ancistroealaines A and B had been reported with three structurally related naphthoic acids derivatives,<sup>[98]</sup> and no isoquinoline moiety had been found in the investigated plant materials.

During our investigations on the twigs and the leaves of *A. ealaensis*, several naphthalene-devoided isoquinoline alkaloids were detected and only four have been fully characterized (Figure 56). The metabolites were named ealaines A-D (**72-75**) to continue the series of the two related representatives known from *A. korupensis*.

Their structural elucidation and biological activities are described and discussed in the next section. To the best of our knowledge, such compounds had never been investigated for their biological activities against protozoa parasites or one of the cancer cell lines used in our biotesting systems. For the first-time, their biological activity and the correlation to the monomeric naphthylisoquinoline alkaloids were established.

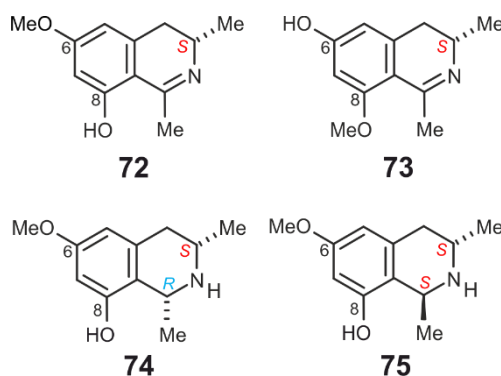


Figure 56. Ealaines A-D (**72-75**) isolated from the twigs and leaves of *A. ealaensis*.

## Structural elucidation and discussion

The first alkaloid was isolated as a colorless powder, showing a molecular formula of  $C_{11}H_{12}NO_2$  deduced by HRESIMS. The number of carbon atoms matched the signals observable on the  $^{13}C$  NMR spectrum. The proton spectrum revealed the presence of two meta-coupled aromatic multiplets, *i.e.* one doublet of triplets and a doublet, one methoxy function at the resonance of 3.88 ppm, which had cross peaks with both aromatic protons in the NOESY spectrum. Moreover, one proton multiplet at 3.92 ppm, two diastereotopic protons (at 3.06 and 2.82 ppm) and two methyls were detected in the spectrum. The multiplet at 3.92 ppm (H-3) and the methyl  $CH_3$ -1 at 2.78 ppm showed an HMBC correlation to a signal at the  $^{13}C$ -resonance of 176.0 ppm (C-1), indicative of the presence of a dihydroisoquinoline moiety, and further explaining the lack of the usually observed quartet at C-1. All the data were indicative of a typical dihydroisoquinoline moiety, which was unsubstituted at C-5 and C-7, showing an *O*-methyl group at C-6.

The alkaloid showed one element of chirality, and its absolute configuration was determined by oxidative degradation. The presence of an *S*-configured aminobutyric acid enabled to assign the full absolute stereostructure of compound **72**. Due to the structural similarities with known related alkaloids, the new alkaloid was named ealaine A.

A further metabolite was found with a closely related structure. The compound **73** seemed to be an isomer of ealaine A because it possessed the same molecular formula. Comprehensive NMR data analysis revealed that the plane structure of this compound differed from ealaine A (**72**) by an *O*-methyl group now in position C-8, instead of C-6.

The oxidative degradation enabled also the determination of the absolute configuration to be *S*, as for ealaine A. Therefore, the new alkaloid was named ealaine B.

From the same fraction as ealaine B, another peak with a longer retention on the reversed phase column was isolated. Compound **74** showed another exact mass, corresponding to a molecular formula of  $C_{11}H_{14}NO_2$  as determined by HRESIMS. The analysis of the spectroscopic data of **74** revealed the presence of a reduced derivative of ealaine A, leading to a tetrahydroisoquinoline alkaloid possessing a methoxy function at C-6.

The chemical shifts of C-3 ( $\delta_C$  51.3 ppm) and H-1 ( $\delta_H$  4.58 ppm) were already indicative of the 1,3-diaxial orientation of the two protons of the two stereogenic centers. This was also confirmed by the NOESY interactions between their respective NMR signals. Noticeably, the

diastereotopic protons, in this case, were not clearly separated on the proton spectrum, which may be indicative of a pseudo-equatorial orientation of both. This was similarly observed in the cases of *cis*-configured 7,8'-coupled ealamines (e.g. **67**) and in ealapasamines B (**43**) and C (**44**).

The absolute configuration at C-3 was assigned by degradation to be *S*, from which C-1 was deduced to be *R*-configured based on the relative configuration between the two stereocenters. This new alkaloid was named ealaine C (**74**).

Right next to ealaine C (**74**), another peak was detected, albeit in small quantities, possessing almost similar NMR data (Table 9) and the same molecular formula. The compound **75** was found to have a relative *trans*-configuration by NOESY experiments, which was corroborated by the chemical shifts of C-3 ( $\delta_{\text{H}} 45.6$  ppm) and H-1 ( $\delta_{\text{H}} 4.67$  ppm).

The Ru-mediated oxidative degradation of compound **75** delivered the *S*-configured aminobutyric acid indicative of the same configuration at C-3 position. From the relative *trans*-configuration, the full absolute structure at both stereogenic centers was established to be 1*R*3*R*. Following the pattern, the new alkaloid was given the named of ealaine D (**75**).

Table 9. <sup>1</sup>H (600 MHz) and <sup>13</sup>C (151 MHz) data of **72-75** in methanol-*d*<sub>4</sub> ( $\delta$  in ppm, *J* in Hz).

Position	ealaine A ( <b>72</b> )		ealaine B ( <b>73</b> )		ealaine C ( <b>74</b> )		ealaine D ( <b>75</b> )	
	$\delta_{\text{H}}$	$\delta_{\text{C}}$ ,	$\delta_{\text{H}}$	$\delta_{\text{C}}$ , type	$\delta_{\text{H}}$	$\delta_{\text{C}}$ , type	$\delta_{\text{H}}$	$\delta_{\text{C}}$ , type
1	-	176.0,	-	174.4, C	4.58, q	52.4, CH	4.67, q	52.0, CH
3	3.92, m	49.7, CH	3.86, m	49.6, CH	3.39, m	51.3, CH	3.79, dt (11.7, 5.7)	45.6, CH
4	3.06, dd (16.4, 5.2)	35.3, CHeq	3.01, dd (16.4, 5.3)	35.6, CHeq	2.86, m	35.6, CHeq	3.07, dd (17.6, 4.6)	33.1, CHeq
	2.82, dd (16.6, 11.8)	35.3, CHax	2.78, dd (16.4, 11.9)	35.6, CHax	2.86, m	35.6, CHax	2.79, dd (18.0, 10.6)	33.1, CHax
5	6.49, dt (2.3, 1.1)	108.9, CH	6.39, s	111.1, CH	6.28, s	105.7, CH	6.27, s	105.7, CH
6		169.7,		163.1, C		161.6, C		156.9, C
7	6.42, d (2.4)	101.2, CH	6.42, s	100.0, CH	6.31, s	101.7, CH	6.30, s	99.3, CH
8		165.9,		166.8, C		157.3, C		158.3, C
9		108.1,		107.5, C		113.7, C		114.5, C
10		142.7,		143.8, C		135.8, C		135.9, C
Me-1	2.78, d (1.5)	24.5, Me	2.04, s	23.7, Me	1.72, d (6.6)	19.7, Me	1.61, d (6.8)	20.3, Me
Me-3	1.43, d (6.7)	18.3, Me	1.42, d (6.7)	18.3, Me	1.46, d (6.5)	18.9, Me	1.46, d (6.4)	18.8, Me
6-OMe	3.88, s	56.7, Me	-	-	3.73, s	55.8, Me	3.73, s	56.0, Me
8-OMe	-	-	3.93, s	56.4, Me	-	-	-	-

It is remarkable to notice that the occurrence of such alkaloids might have been characteristic of a liana with a limited availability of coupling enzymes. On the other hand, after the plant material collection, the ongoing metabolism processes should end at a certain time point in time, offering, therefore, the possibility to find representatives of each stage of development within the biosynthetic pathway of the construction of bigger molecules. Their detection is a further proof that the biosynthesis of naphthylisoquinoline alkaloids proceeds by the formation of naphthoic acids and isoquinoline moieties before phenol-oxidative coupling enzymes intervene to build the classical NIQ alkaloids. This confirms further the role of compounds like **72-75** as intermediates in the biosynthesis of naphthylisoquinoline alkaloids.

It shall be pointed out that all the 6,8-dioxygenated 1,3-dimethyl-1,2,3,4-tetrahydroisoquinoline alkaloids have been synthesized and reported in this frame in the literature, including their dihydroisoquinoline forms.<sup>[165]</sup> In that synthetic report, the *cis* and *trans* diastereomers had been obtained by reduction of the dihydroisoquinoline form. A reduction by sodium hydroborate (NaBH<sub>4</sub>) led to the *cis*-configured tetrahydroisoquinolines,

with very good diastereoselectivities (d.r. 93:7, for both *cis versus trans*).<sup>[165]</sup> And when the reduction of the dihydroisoquinoline was performed with  $\text{AlMe}_3/\text{LiAlH}_4$ , the *trans*-diastereomers were formed by hydride transfer from the opposite sides.<sup>[165]</sup> Besides, it had been reported that the synthetic free base of ealaine C (**74**) rapidly oxidized back to the dihydro form by atmospheric oxygen, suggesting a cautious handling of these alkaloids. However, the natural occurrence of most such alkaloids had not been evidenced by isolation from the investigated lianas, leaving a gap to fill.

The co-occurrence of the *cis*-configured ealaine C (**74**) and the related dihydroisoquinoline, ealaine A (**72**), shows that both species can be part of the natural product. This statement is of high significance when bearing in mind that dihydroisoquinoline moieties have been for long considered as oxidation products from *cis*-configured tetrahydroisoquinolines, which are known to be prone to oxidation already by atm.  $\text{O}_2$ . Their joint discovery under the mild extraction conditions used in this work has suggested that some dihydroisoquinoline alkaloids are most likely formed directly from dihydroisoquinoline precursors and not necessarily from oxidized *cis*-moieties.

As already mentioned, these compounds had not been addressed in the literature for their antiprotozoal or cytotoxic activities. It was interesting to see that these basic building blocks did not show any anti-infective or cytotoxic activities in our testing systems. These results indicated that the pronounced activities of naphthylisoquinoline alkaloids originate from the specific combination of these building blocks.

## II.7. Further New and Known Monomeric Alkaloids from *A. ealaensis*

From the twigs and the leaf plant materials of *Ancistrocladus ealaensis*, further alkaloids were isolated and fully characterized. In this chapter, the isolation and structural elucidation of naturally occurring 5,8'-coupled naphthylisoquinoline alkaloids, and a few *N,C*-coupled monomers found in this tropical liana, will be described briefly. It shall be noticed that the 5,8'-linked naphthylisoquinolines represent the main type of alkaloids from Central African lianas. The probability to find new compounds with this coupling type is rather low due to the numerous representatives known in the literature.<sup>[70, 167, 181, 206-208]</sup>

Herein is reported the occurrence of nine monomeric naphthylisoquinoline alkaloids from twigs and leaves of *A. ealaensis* (Figure 57), among which only four are genuinely new compounds (**76**, **77**, **79**, and **81**), while five (**25**, **78**, **80**, **82**, and **26**) are already known from other plants. Additionally, the two monomeric alkaloids reported from this liana, *i.e.* ancistrocalines A (**34**) and B (**35**),<sup>[98]</sup> were also identified, attesting the reliability of the previous report. Most striking were the occurrence of compounds typical to Ancistrocladaceae type, *viz.* exhibiting an oxygenated C-6 and 3*S*, and Ancistrocladaceae/Dioncophyllaceae hybrid types featuring an *R*-configuration at C-3 instead of *S*.

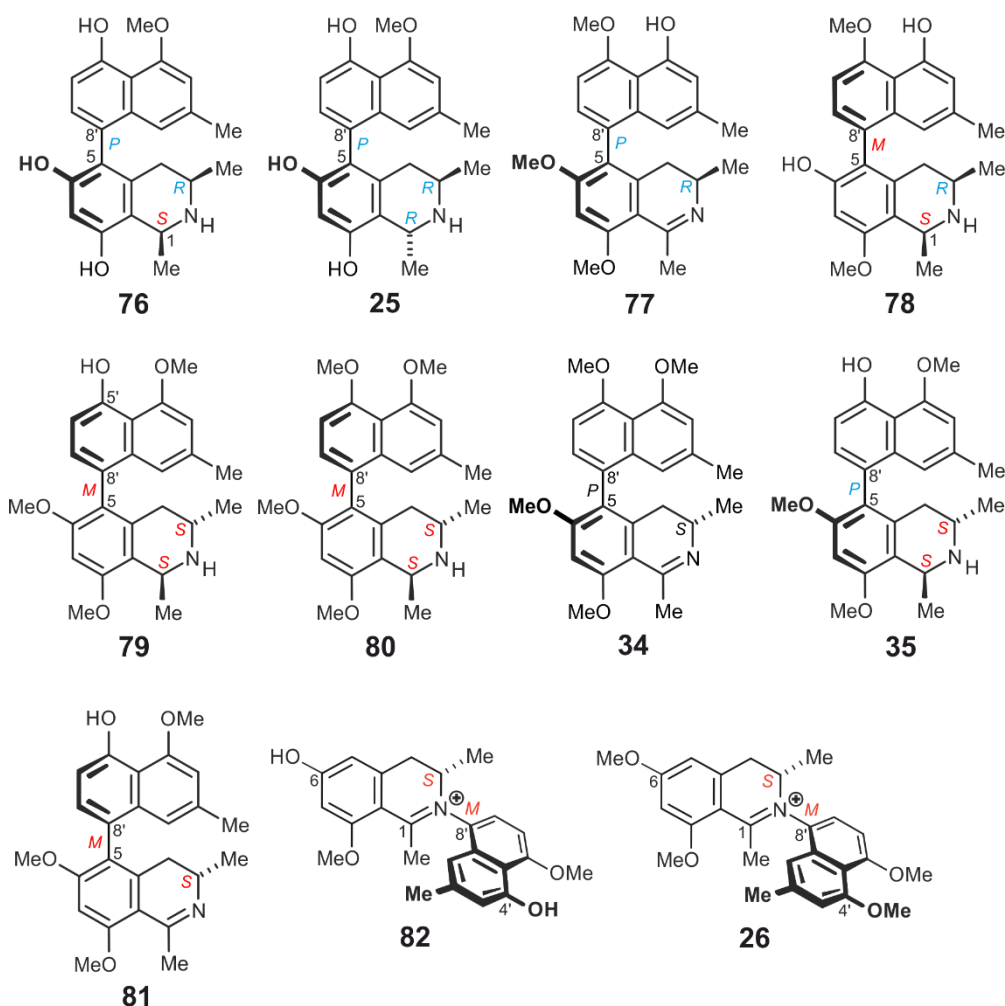


Figure 57. 1-*epi*-Korupensamine A (**76**), ancistroealaine C (**77**), 5-*epi*-ancistroealaine B (**79**), and ancistroealaine D (**81**), four new 5,8'-coupled naphthylisoquinoline alkaloids isolated from leaves and twigs of *A. ealaensis*, along with five known C,C-linked (**34**, **35**, **25**, **78**, and **80**) and two N,C-type (**82** and **26**) monomeric naphthylisoquinoline alkaloids.

### Structural elucidation

Found in the earliest fraction of the methanolic twig extract, the first compound **76** was isolated as a white powder, which showed a protonated molecular ion at  $m/z$  380.18537  $[M+H]^+$  by HRESIMS, corresponding to the molecular formula of  $C_{23}H_{25}NO_4$ . The number of signals in the  $^{13}C$  spectrum matched with the exact mass. Five aromatic protons were detected in the  $^1H$  spectrum. This latter additionally showed a pattern of two *ortho*-coupled doublets, two *meta*-coupled pseudo-singlets, one singlet, three methyl groups, two diastereotopic protons as doublets of doublets, one methoxy group, one quartet, and a multiplet.



The analysis of the NMR data revealed the presence of a C-8'-substituted 4'-*O*-methylated naphthalene moiety, confirmed by the NOESY interactions between H-3' ( $\delta_{\text{H}}$  6.81 ppm) and CH<sub>3</sub>O-4' ( $\delta_{\text{H,C}}$  4.09 and 56.8 ppm). A 6,8-*O*-didemethylated tetrahydroisoquinoline possessing two stereogenic centers at C-1 and C-3 was identified. The HMBC interaction of H-5 ( $\delta_{\text{H,C}}$  6.47 and 102.8 ppm) with C-5, C-6, C-8, and C-1 indicated that the coupling position in the isoquinoline portion must be at C-5. This was confirmed by the HMBC joint interactions of 4-H<sub>eq</sub> ( $\delta_{\text{H}}$  2.42 ppm) and H-7' with C-5.

The relative configuration in the isoquinoline moiety was found to be *cis*-oriented based on the observed NOEs between H-1 ( $\delta_{\text{H,C}}$  4.63 and 52.3 ppm) and H-3 ( $\delta_{\text{H,C}}$  3.26 and 50.8 ppm). As already mentioned several times, the chemical shifts of these positions, *e.g.* through the characteristic chemical shift of C-3, can easily be used for the assignment of the relative configuration.

The absolute configuration at the stereocenter C-3 was elucidated by oxidative degradation to be *R*. Combined with the relative configuration, the configuration at C-1 can only be *S*.

Once the configuration at the stereocenters was defined, the absolute configuration at the biaryl axis was established from the NOEs. The NOESY interactions between 4-H<sub>ax</sub> and H-1' ( $\delta_{\text{H}}$  6.79 ppm) and from 4-H<sub>eq</sub> to H-7' ( $\delta_{\text{H}}$  7.08 ppm) clearly indicated that the biaryl axis should be *P*-configured (Figure 58a). An additional confirmation of this assignment was provided by the comparison of the experimental ECD spectrum of **76** with the one of the closely related, known compound of korupensamine A (**25**). Compound **76** showed a strong positive couplet around 230 nm, almost similar to the one of **25**. Because of the structural relationship to **25**, the new compound **76** was named 1-*epi*-korupensamine A.

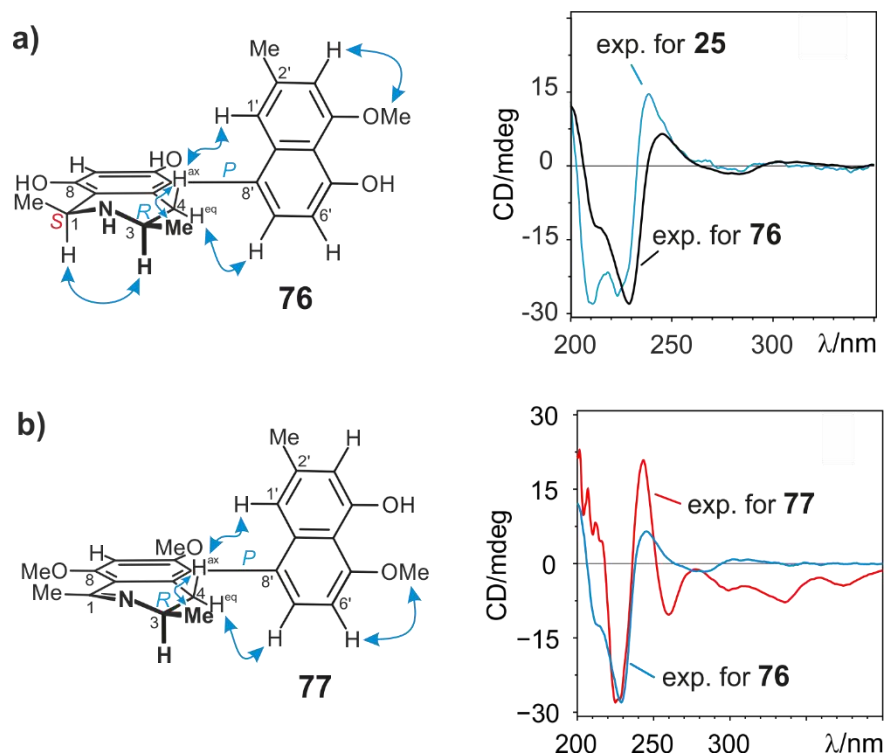


Figure 58. Decisive ROESY interactions and the compared ECD spectrum for (a) 1-*epi*-Korupensamine A (**76**) and (b) ancistroealaine C (**77**).

Resolved in the same sub-fraction, another peak was isolated and carefully submitted to characterization. This second compound displayed the same molecular formula, the same constitution, the same ECD spectrum, and HMBCs, and exhibited very similar NOEs as compared to 1-*epi*-korupensamine A (**76**). The difference was found in the relative configuration in the tetrahydroisoquinoline moiety, which was established to be *trans*-oriented, based on the NOESY spectrum and the chemical shifts at C-1 ( $\delta_{\text{H,C}}$  4.76 and 49.6 ppm) and C-3 ( $\delta_{\text{H,C}}$  3.66 and 45.2 ppm). Since the oxidative degradation indicated a 3*R*-configuration, the stereochemical elements in presence were 5*P*,1*R*,3*R*, which meant for this constitution that compound **25** was the known korupensamine A. All the data agreed with the published report of the natural product.<sup>[167]</sup> However, **25** was discovered for the first time in this liana. Common to the michellamine producers, *viz.* *A. korupensis* and *A. congolensis*,<sup>[104]</sup> korupensamine A, thus also occurs in *A. ealaensis*, which is of high chemotaxonomic significance.

From a slower eluting peak in the twigs extract, compound **77** was isolated – as a yellow powder – along with ealamines G-I. Its molecular formula was deduced from HRESIMS to be  $\text{C}_{25}\text{H}_{27}\text{NO}_4$ . The compound showed 14 and 25 signals on the  $^1\text{H}$  and  $^{13}\text{C}$  NMR spectra, respectively. Particularly, one methyl *doublet* was found in the high field with a coupling

constant of 6.72 Hz (CH<sub>3</sub>-3,  $\delta_{\text{H,C}}$  1.20 and 17.9 ppm), which, together with the lack of a quartet around 4.6 ppm, and combined with the presence of a signal at 176.0 ppm in the carbon spectrum, hinted at the presence of an imino function between C-1 and the nitrogen. Besides, three methoxy groups and five aromatic protons were detected.

Extensive data analysis led to the identification of a naphthalene part possessing two doublets in *meta*-coupling pattern, an *O*-methyl group in position C-5' right next to two *ortho*-coupled doublets, leaving thus C-8 as linkage point. Furthermore, a 6,8-*O*-dimethylated dihydroisoquinoline portion was also identified, with a proton in position C-7, leaving C-5 for the coupling with the naphthalene part. All the 2D NMR data agreed with these assignments.

The oxidative degradation experiments again delivered only (*R*)-3-aminobutyric acid, thus the absolute configuration at C-3 was ascribed to be *R*. The NOESY interactions from H-1' ( $\delta_{\text{H,C}}$  6.46 and 116.4 ppm) with the axial proton 4-H<sub>ax</sub> ( $\delta_{\text{H}}$  2.28 ppm,  $J = 17.0$  and 10.0 Hz), and from H-7' ( $\delta_{\text{H,C}}$  7.10 and 129.5 ppm) with the equatorial 4-H<sub>eq</sub> ( $\delta_{\text{H}}$  2.71 ppm,  $J = 17.0$  and 5.4 Hz) indicated that the 5,8'-coupled biaryl axis was *P*-configured. The ECD spectrum of compound **77**, which in this coupling-type is dominated by the biaryl axis, was compared with and found most identical to the one of **76**, confirming the *P*-configuration (Figure 58b). Compound **77** yet unknown and was named ancistroealaine C.

Along with the mbandakamines, another compound (**78**) was isolated from the leaf material and showed a molecular formula of C<sub>24</sub>H<sub>27</sub>NO<sub>4</sub>. The compound was constitutionally determined as a 5,8'-linked monomer, with *O*-methyl groups at C-8 and C-5'. The compound exhibited a 5*M*,1*S*,3*R*-configured structure. The assigned alkaloid **78** corresponded to 1-*epi*-korupensamine E, also known from leaves of the Congolese species *A. likoko* as ancistrolikokine B.<sup>[208]</sup> The experimental data agreed with those from the literature.

Thanks to the broad enzymatic potential of *A. ealaensis*, this plant species can incorporate these korupensamine-like building blocks to produce, additionally to michellamines and the mbandakamines, a wide range of cyclombandakamines and ealapasamines dimers, which is totally unprecedented in the genus and shows the uniqueness of this species.

First isolated from the twigs and later from the leaves, another peak was found to show a molecular formula of C<sub>25</sub>H<sub>29</sub>NO<sub>4</sub>. The constitution of **79** was most likely similar to the one of 1-*epi*-korupensamine A, except for a 6,8-*O*-dimethylated tetrahydroisoquinoline half. Like in the case of **25**, the compound displayed a relative 1,3-*trans*-relative configuration.

The oxidative degradation experiments performed on 0.5 mg of **79** revealed that the absolute configuration at C-3 was *S*, implying the configuration at C-1 to be also *Sinister* based on the *trans*-orientation of C-1 relative to C-3 (Figure 59a). Thus, the alkaloid displayed typical features of an Ancistrocladaceae-type alkaloid, *viz.* 6-OR and 3*S*. The axial configuration was deduced from the monitored NOEs between H-7' ( $\delta_{\text{H,C}}$  7.07 and 129.4 ppm) and the equatorial proton 4-H<sub>eq</sub> ( $\delta_{\text{H}}$  2.62 ppm,  $J = 18.2$  and 4.6 Hz), which indicated that the 5,8'-coupled axis was *M*-configured. Its ECD spectrum was opposite to the one of **76** by superimposition (see Figure 59a). Thus, the compound **79** was assigned to be a new natural product and was named based on its structural relationship to **35**, 5-*epi*-ancistroealaine B.

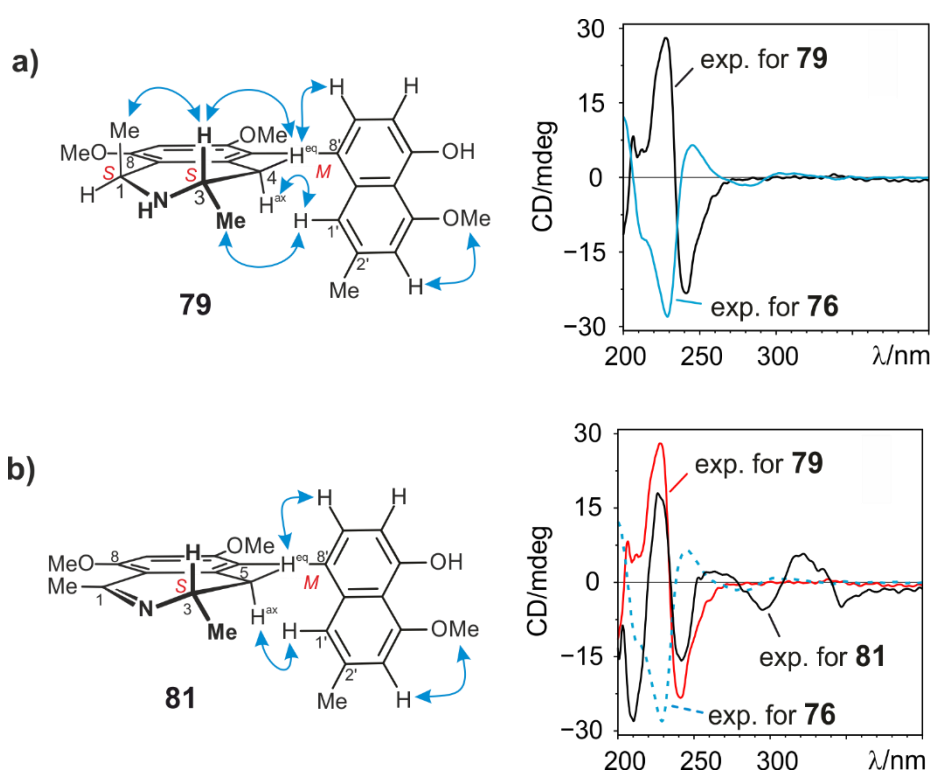


Figure 59. Decisive ROESY interactions and the compared ECD spectrum for (a) 5-*epi*-ancistroealaine B (**79**) and (b) ancistroealaine D (**81**).

Another main peak from the methanolic extract of the twigs was isolated and characterized. The analysis of the experimental data revealed only one difference with respect to the new 5-*epi*-ancistroealaine B, namely an additional 5'-*O*-methyl group. Consequently, this assignment meant that the compound was ancistroectoriline A (**80**), previously known from the Asian species *A. tectorius*<sup>[209]</sup> and the East-African *A. tanzaniensis*.<sup>[209-210]</sup> The recorded data set was in this case also in accordance with the published ones.

A further compound, isolated along with **80**, showed the same molecular formula as 5-*epi*-ancistroealaine B (**79**). Extensive data analysis revealed that not only the molecular formula was identical, but also the whole constitution, including the hydroxy-methoxy pattern and the relative *trans*-configuration in the tetrahydroisoquinoline part. The oxidative degradation indicated the same *S*-configuration at C-3. The difference was to be found in the NOESY experiments where the interactions across the axis were just opposite, hinting at a *P*-configured biaryl axis. The comparison of its ECD curve and the reported data enabled the structural determination of ancistroealaine B (**35**), previously known from this plant species.<sup>[98]</sup>

Right next to the ancistroealaine B in the chromatogram, Ancistroealaine A (**34**)<sup>[98]</sup> was also identified by applying the same rigor for the structural determination.

In the same fraction as the ancistroealaines A and B, a peak was found, which turned out to be a yet undescribed alkaloid (**81**). The compound was isolated as a yellow powder showing a molecular formula identical to the new ancistroealaine C. However, **81** displayed one free hydroxy group at C-5' ( $\delta_{\text{C}}$  154.9 ppm) – in the substituted naphthalene part –, three methoxy functions, and a dihydroisoquinoline moiety protonated at C-7. The HMBC interactions from H-7 ( $\delta_{\text{H,C}}$  6.50 and 94.2 ppm) to the two *O*-methylated carbon atoms, *viz.* C-6 ( $\delta_{\text{C}}$  166.9 ppm) and C-8 ( $\delta_{\text{C}}$  163.7 ppm), to C-5 ( $\delta_{\text{C}}$  122.5 ppm) and to C-1 ( $\delta_{\text{HC}}$  173.4 ppm) confirmed the assignment in the dihydroisoquinoline part. The NOESY interaction from one of the protons in *meta*-coupling pattern, namely H-3' ( $\delta_{\text{H,C}}$  6.68 and 106.7 ppm) with a methoxy group CH<sub>3</sub>O-4' ( $\delta_{\text{H,C}}$  4.11 and 56.2 ppm) proved the position of the *O*-methyl group in the naphthalene part.

Ruthenium-mediated oxidative degradation of half a milligram of **81** delivered *S*-configured aminobutyric acid, suggesting the configuration at C-3 to be *S*. As interpreted in the previous cases, the NOEs between H-1' ( $\delta_{\text{H}}$  6.55 ppm) and H-7' ( $\delta_{\text{H}}$  7.07 ppm) with the two diastereotopic protons at C-4 ( $\delta_{\text{H}}$  2.55 and 2.16 ppm) indicated an *M*-configuration at the biaryl axis (Figure 59b). The ECD spectrum was similar with the one of 5-*epi*-ancistroealaine B (Figure 59b). The new alkaloid **81** was given the trivial name of ancistroealaine D.

A slower eluting peak, right next to ancistroealaine D (**81**), a known *N,C*-coupled naphthylisoquinoline was likewise isolated and fully characterized. The compound showed six aromatic protons, among which two were attached to the 6-hydroxylated dihydroisoquinoline part. The coupling position in the naphthalene portion was identified to be at C-8' ( $\delta_{\text{C}}$  129.9 ppm). The lack of a quartet at C-1 ( $\delta_{\text{C}}$  173.9 ppm) and the deshielded signal of CH<sub>3</sub>-1 ( $\delta_{\text{H,C}}$

2.50 and 23.9 ppm) confirmed the presence of a dihydroisoquinoline moiety. The presence of two diastereotopic protons at C-4 ( $\delta_{H,C}$  3.0 and 3.6, 34.3 ppm), and a deshielded multiplet at C-3 ( $\delta_{H,C}$  4.10 and 57.6 ppm) suggested altogether the *N,C*-linkage of the two molecular portions. Based on the degradation results, the observed NOESY interactions, and the ECD spectra comparison, compound **82** was unambiguously identified as 6,4'-*O*-didemethyl-ancistrocladinium A, a known alkaloid occurring in the Asian *A. cochinchinensis*.<sup>[211]</sup>

In the twigs extract, a strongly retained peak on RP<sub>18</sub> column was observed, isolated and characterized. Comprehensive analysis of all structural data led to the identification of ancistrocladinium A (**26**).<sup>[35, 96]</sup>

It is worthy to emphasize the broad and striking structural diversity of the natural metabolites produced by the plant species *A. ealaensis*. Remarkably, all the isolated naphthylisoquinoline alkaloids displayed exclusively a coupling at the C-8' position of in the naphthalene parts, which seems to be a footprint of this plant species. This may suggest that one or only one type of enzymes is responsible for the coupling of the naphthalene part. Another notable fact is that in this series of monomeric 5,8'-linked biaryls none of the mentioned compounds were *N*-methylated. The tropical liana *A. ealaensis* produces alkaloids showing 3*R* or 3*S*-configuration, being *cis*- and *trans*-configured, possessing *P*- or *M*-configuration at the chiral axis, but all exclusively displaying oxygenation at C-6. Dioncophyllaceae-type alkaloids were not detected in this liana.

## Biological evaluation

The biological profiles of compounds **76**, **25**, **78-81** were evaluated on the classical series of tropical pathogens and cancer cell lines, as depicted in Table 10. The alkaloids **79** and **81** exhibited very pronounced activities on against *Trypanosoma cruzi*, *T. brucei rhodensis*, *T. cruzi*, and on *Leishmania donovani*, with a very good cytotoxicity profile on mammalian host cells (rat skeletal myoblast L6 cells). The compounds displayed in moderate antiplasmodial activities. However, compound **78**, **79**, and **81** showed much better profiles towards the resistant strain K1 of *P. falciparum*, with IC<sub>50</sub> values of 0.27, 0.76, and 1.06  $\mu$ M, respectively. The new alkaloid ancistroealaine C (**77**) showed very promising cytotoxic growth inhibition against the human T-lymphoblastic leukemia cells CCRF-CEM (IC<sub>50</sub> 11.69  $\mu$ M) and against its multi-drug resistant strain CEM/ADR5000 (IC<sub>50</sub> 19.94  $\mu$ M). Additionally, **77** shows a very weak cross-resistance (only 2-fold) compared to the reference drug doxorubicin (1771-fold),

suggesting ancistroealaine C as a good candidate for the treatment of the resistant form of this cell line.

Table 10. Antiprotozoal activities, and antiproliferative effects on human T-lymphoblastic leukemia cells CCRF-CEM and on cervical cancer cells HeLa for compounds **76**, **25**, **78-81** (IC<sub>50</sub> in  $\mu\text{M}$ ).

	<i>T. br. rhod</i>	<i>T. cruzi</i>	<i>L. don. am</i>	<i>P. falc. NF54</i>	<i>P. falc. K1</i>	Cytotox L6	CCRF-CEM	CEM/ADR 5000	HeLa cells
Standard	0.007 <sup>[1]</sup>	3.56 <sup>[2]</sup>	0.43 <sup>[3]</sup>	0.008 <sup>[4]</sup>	0.364 <sup>[4]</sup>	0.041 <sup>[5]</sup>	0.017 <sup>[6]</sup>	30.1 <sup>[6]</sup>	13.9 <sup>[7]</sup>
<b>76</b>	15.26	237.50	>26.35	9.94	12.86	79.06	-	-	<b>30.51</b>
<b>25</b>	15.31	234.15	>26.35	12.15	19.29	76.69	-	-	<b>48.30</b>
<b>77</b>	-	-	-	-	-	-	11.69	<b>19.94</b>	-
<b>78</b>	7.95	n.d.	>25.41	<b>1.14</b>	<b>0.27</b>	20.92	-	-	-
<b>79</b>	<b>3.85</b>	<b>32.51</b>	<b>37.91</b>	<b>1.74</b>	<b>0.76</b>	77.79	-	-	-
<b>80</b>	22.11	130.47	n.d.	5.41	n.d.	204.61	-	-	-
<b>81</b>	<b>1.46</b>	<b>43.40</b>	<b>13.37</b>	<b>2.69</b>	<b>1.06</b>	101.11	-	-	53.37

[1] Melarsoprol. [2] Benznidazole. [3] Miltefosine. [4] Chloroquine. [5] Podophyllotoxin.

[6] Doxorubicin. [7] 5-fluorouracil (5-FU). n.d.: not determined.

## II.8. Chemo-Taxonomic Position of *A. ealaensis* within the African Species

The aim of these investigations on *Ancistrocladus ealaensis* J. Léonard was to gain in-depth knowledge of the synthetic potential of this botanically well-described – but phytochemically less-investigated – Central African plant species. In other words, these investigations will enhance knowledge and will enable the establishment of a representative overview on the alkaloids occurring in this tropical liana. The herein reported metabolites were – at the same time – screened in order to find novel anti-infective and anticancer drug candidates. Once these goals reached, the obtained phytochemical profile of the liana can allow, on the one hand, the discrimination to some probably new – but phylogenetically close<sup>[45]</sup> – species and, on the other hand, permit the establishment of the chemotaxonomic relationships of *A. ealaensis* to the other African and Asian species.

The discovery of the dimeric mbandakamines A and B from a still undescribed Congolese species<sup>[103]</sup> had raised the question if these metabolites could be used as chemo-markers for the 'new' species, and thus the necessity to search for them in all related taxa. From our investigations, it became clear that mbandakamines were present in other related taxa occurring in the region of Mbandaka (DR Congo), thus, at least the name was specific to the habitat.

*Ancistrocladus ealaensis* J. Léonard showed an unprecedented and impressive synthetic potential. Additional to the two-known monomeric naphthylisoquinolines and four naphthoic acids, further phytochemical screening work led to the discovery of four naphthalene-devoid isoquinolines, 21 monomeric and 15 dimeric NIQs have been isolated from this tropical liana. The outcome of the work presented in this thesis now places this plant species among the best-investigated ones, next to the Cameroonian *A. korupensis*<sup>[99-100, 107, 167]</sup> and *A. tectorius* from Southeast Asia.<sup>[83]</sup>

Similarly to the Congolese species *A. likoko*<sup>[208]</sup> and *A. congolensis*,<sup>[104, 207]</sup> *A. ealaensis* predominantly synthesizes 5,8'-coupled naphthylisoquinoline alkaloids. So far, only three Congolese taxa show a metabolite profile dominated by NIQs with other coupling types. *A. ileboensis*<sup>[31]</sup> and a hitherto botanically undescribed *Ancistrocladus* spp<sup>[32]</sup>, predominately produce 7,1'- and 5,1'-linked alkaloids. From *A. letestui*,<sup>[212]</sup> only the 7,1'-linked dioncophylline A is known, thus, no clear statement can be made. However, the 5,8'-coupling type has been likewise observed – almost exclusively – in the Central African species *A. korupensis*<sup>[99-100, 106, 167]</sup> and *A. guineënsis*,<sup>[213]</sup> and in the East African taxon *A. tanzaniensis*<sup>[210]</sup>.



Remarkably, *A. ealaensis* produces alkaloids belonging to the subclasses of Ancistrocladaceae-type (6-OR, 3*S*) and the mixed-Ancistrocladaceae/Dioncophyllaceae-type compounds (6-OR, 3*R*). Despite some hints from the ESI-MS extract profiles, no compound showing characteristic features of Dioncophyllaceae-type NIQs (6-*R*, 3*R*) were isolated during these investigations. This plant also produces *C,C*- and *N,C*-linked naphthylisoquinolines. Compounds such as korupensamine A, have been found nearly in all of the 5,8'-producers and might be proposed as a chemotaxonomic marker for the Central African species.

Moreover, among the already known metabolites in the literature, compounds isolated for the first time in Asian species, *e.g.*, ancistrotectoriline A (**81**)<sup>[209]</sup> from *A. tectorius*, and 6,4',-*O*-didemethyl-ancistrocladinium A (**83**)<sup>[211]</sup> known from *A. cochinchinensis*, were also found in *A. ealaensis*. This suggests that this Congolese species has maintained – to some extent – mutual enzymatic abilities with other *Ancistrocladus* species around the world.

The occurrence of a scarce series of naphthalene-devoided isoquinoline alkaloids – ealaines A-D – indicates the similarities of the Congolese taxon *A. ealaensis* to the Cameroonian *A. korupensis*, from which two such compounds<sup>[167, 204]</sup> had been reported earlier. In contrast to the related species,<sup>[45]</sup> these two Central African lianas jointly produce yaoundamine A, a 7,8'-coupled alkaloid of the hybrid-type, *i.e.* with 6-OR pattern and 3*R*-configuration, featuring a dihydroisoquinoline subunit. Additionally, the more productive *A. ealaensis* exclusively synthesizes a series of nine 7,8'-linked monomers, the new ealamines A-H and the known 6-*O*-demethylancistrobrevine A, which is the largest known series of monomeric naphthylisoquinolines of this coupling type. Considering that such a series of compounds could not have been overlooked during the intense phytochemical screenings of *A. korupensis*,<sup>[99-100, 106, 167]</sup> and *A. congolensis*,<sup>[70, 104]</sup> the ealamines can be used in the future as chemo-markers for the Congolese *A. ealaensis* species.

Beyond the numerous metabolites fully characterized, the most remarkable asset of *A. ealaensis* is undeniably the unique structural diversity and complexity of occurring dimers. The biosynthetic potential of *A. ealaensis* is unprecedented. Compared to all known *Ancistrocladus* species phytochemically screened over the last four decades, it is the only species exclusively synthesizing unsymmetric NIQs dimers featuring extreme structural peculiarities. Four types of unsymmetric dimers were found to occur in this liana, namely the michellamines, the ealapasamines, the mbandakamines, and the cage-like cyclombandakamines.

The most outstanding facts are the structural divergence and the complexity of these dimers, which exhibit, on the one hand, three consecutive chiral biaryl axes, with the central one showing the highest steric hindrance ever observed in this class of alkaloids, *i.e.* the mbandakamines. On the other hand, another group of dimers comprises a configurationally unstable central axis, like in the case of michellamine-like dimers. Among the quateraryls possessing a freely rotating central axis, *A. ealaensis* jointly produces the classical michellamines – consisting of two related molecular halves, like michellamine F (**33**) – and the korundamine-A-like dimers exhibiting the most extreme unsymmetric coupling-type known so far with three divergent consecutive biaryl axes, *viz.* the ealapasamines. The achiral 6',6"-coupled central axis is characteristic for ealapasamines and michellamines. The same michellamines are even much closer to the mbandakamine-type dimers from the similarly linked molecular halves, featuring 5,8'-coupled monomers. Despite their impressive novel structural assets, cyclombandakamines seem to be a modified type of the open-chain mbandakamines, where the central axis has been suppressed by the formation of an unprecedented dihydrobenzofuran ring. Apparently, the enzymatic potential of *A. ealaensis* enables this species to use 5,8'- and 7,8'-linked monomeric halves to synthesize these four largely different types of hetero-quateraryls. This plant is the only one known so far, to produce exclusively unsymmetric dimers.

Another observed singularity is the occurrence of dimers – and monomers – build-up from *cis*-configured tetrahydroisoquinolines. Our studies demonstrated how the synthetic potential of *A. ealaensis* was specific, divergent, and unprecedented within the whole genus.

One of our specific objectives was to establish the chemotaxonomic position and relationship of *A. ealaensis* J. Léonard and the related *Ancistrocladus* taxa, particularly within the Central African lianas.

The metabolic profile of the Cameroonian species *A. korupensis* and the Congolese *A. congolensis* are dominated by the occurrence of michellamine-type dimers. Very recently, our group has identified some probable new *Ancistrocladus* species in the region of Mbandaka – phylogenetically related to *A. ealaensis* – one of them producing mbandakamines A and B.

After our studies, we are convinced that *A. ealaensis* is strongly related to the *Ancistrocladus* species mentioned above, representing a phylogenetic link species between *A. korupensis* and *A. congolensis*, the producers of michellamine-type alkaloids, and to the Congolese *Ancistrocladus* species around the town of Mbandaka, capable of synthesizing mbandakamine-

type alkaloids. Its connection to the lianas of this region is obvious from the wide variety of mbandakamines type dimers, predominantly formed within its metabolism. And its ascendancy is demonstrated by its ability to synthesize – additionally – a broad series of novel cyclombandakamine-type dimers.

Apart from that, *A. ealaensis* from the Northwestern DR Congo shows many similarities to the Cameroonian taxon *A. korupensis* as obvious from the occurrence of michellamine F<sub>2</sub> and ealapasamines A-C, which are structurally related to of its constituents, *i.e.* michellamine F and korundamine A. The common biosynthesis of yaoundamine A is an additional uniqueness of both taxa. Here also the demarcation is to be seen in the low abundance of michellamines and the additional *O*-methylation in dimeric compounds from the Eala species. An additional distinctiveness to *A. korupensis* is the occurrence of ealapasamines build-up from korupensamines and the exclusive ealamines monomers. So, *A. ealaensis* can presumably form korundamine-A-like dimers using a yaoundamine-A-like portion, and the related ealapasamines with the supply of the monomeric ealamines. The discovery of these two types of monomers further explained the production of these unique mixed-heterodimeric alkaloids.

A general trait inherent to all dimeric compounds isolated from *A. ealaensis* is the presence of four *O*-methyl functions. In contrast to the typical michellamines producing plants,<sup>[100, 104]</sup> the dimeric alkaloids of this liana – in a bigger extent including all related species from Mbandaka – show molecular masses around 784.9, instead of 756.9 as for *A. korupensis*, usually corresponding to two additional methoxy groups.

A genome analysis of *A. ealaensis* J. Léonard should reveal a rich enzymatic capacity, which would justify the observed unique and unprecedented alkaloid-production potential. Based on our achievements, this liana has become the largest reservoir of naphthylisoquinolines, all being exclusively unsymmetric quateraryls.

The biological activities shown by the monomeric and dimeric alkaloids from this peculiar tropical liana are interesting. Most of the monomers had exhibited very good antiprotozoal activities in the micromolar range, in particular some 5,8'-coupled metabolites, like ancistroalaines C and D, and some 7,8'-linked monomers like ealamine C. In particular, the monomers have shown significant activities against human cancer cell lines, like ealamine A against the multi-drug resistant strain CEM/ADR5000 of human T-lymphoblastic leukemia cells or the human cervical HeLa cancer cells.

The excellent antiprotozoal activities shown by ealapasamines A-C against the resistant strain of *P. falciparum* K1 are very promising, *e.g.* ealapasamine C is – not only the unique unsymmetric dimer consisted of two *N*-H *cis*-configured tetrahydroisoquinolines – but likewise the hitherto most active naphthylisoquinoline against K1 in the very low nanomolar range, far beyond the standard drugs. The biological profiles of mbandakamines on *P. falciparum* and selected cancer cell lines have proven that this plant is not only chemically exceptional but likewise a promising source for highly bioactive drug candidates.

## II.9. Gardenifolins A-H, Scalemic Neolignans from *Gardenia ternifolia*: Chiral Resolution of Eight Stereoisomers, Configurational Assignment, and Antiproliferative Activities

It was surprising to find that despite their biosynthetic origin, through free-radical processes,<sup>[124-125, 215]</sup> naturally occurring 2,3-dihydrobenzofurans (2,3-DBFs) have been rarely analyzed systematically for their enantiomeric purity in the literature. Given the wide-spread occurrence of these neolignans in the plant kingdom and their potential role as pharmaceutical lead compounds, it is of high value to develop analytical methods for the reliable assessment of the stereochemical purities of these compounds and their absolute configurations. The pertinence of performing such a test is due to the fact that a scalemic (*i.e.* non-equimolar) mixture of enantiomers will be isolated as a single chromatographic peak on the usual achiral phases, and that it will yield only one set of NMR signals.<sup>[152]</sup> Whether enantiomerically pure or 'only' a scalemic mixture, it will display an optical rotation and an ECD spectrum. Purification of enantiomers has thus been reported mostly for fully racemic mixtures, since in such cases there were no ECD spectrum and specific optical rotation ( $[\alpha]_D$ ) to be seen.<sup>[152, 154, 216-218]</sup> For scalemic mixtures, the measured ECD spectrum and/or  $[\alpha]_D$  value is dictated by the preponderance of one enantiomer.<sup>[219]</sup> In view of the sometimes drastically different bioactivities of enantiomers,<sup>[220]</sup> and the possible phylogenetic significance of stereoisomeric mixtures,<sup>[221]</sup> it is mandatory to resolve them and provide pure stereoisomers. This should be particularly considered for herbal medicines.

The tropical plant *Gardenia ternifolia* Schumach. & Thonn. (Rubiaceae) is an evergreen shrub widely used in the African traditional medicine against several infectious diseases.<sup>[159]</sup> As aforementioned, this taxon has virtually not been investigated to identify the occurring metabolites.<sup>[160-161]</sup>

In this chapter, eight stereoisomeric 2,3-dihydrobenzo[*b*]furan neolignans, named gardenifolins A-H (**83a-d** and **84a-d**), are described, which were isolated and fully structurally characterized (Figure 60). Reversed-phase chromatography of a stem bark extract afforded two peaks, *viz.* mixtures **I** and **II**, each of them consisting of two diastereomers and their respective enantiomers. They were afterward resolved and stereochemically analyzed by HPLC on a chiral phase coupled to electronic circular dichroism (ECD) spectroscopy, giving single ECD spectra of all eight possible stereoisomers of this chemical constitution. Most unusual was the fact that all pairs of enantiomers were detected in racemic form, but as scalemic mixtures, *i.e.*

not in 1:1 ratios. The double-bond geometries (*E* or *Z*) of the new gardenifolins A-H and their relative configurations (*cis* or *trans*) at the stereogenic centers C-7 and C-8 in the dihydrofuran ring system were assigned by 1D and 2D NMR methods, in particular using Nuclear Overhauser Effect difference (NOEDIFF) experiments, while the absolute configurations of the isolated enantiomers were established by ECD spectroscopy, applying the reversed helicity rule.<sup>[141, 154, 222]</sup>

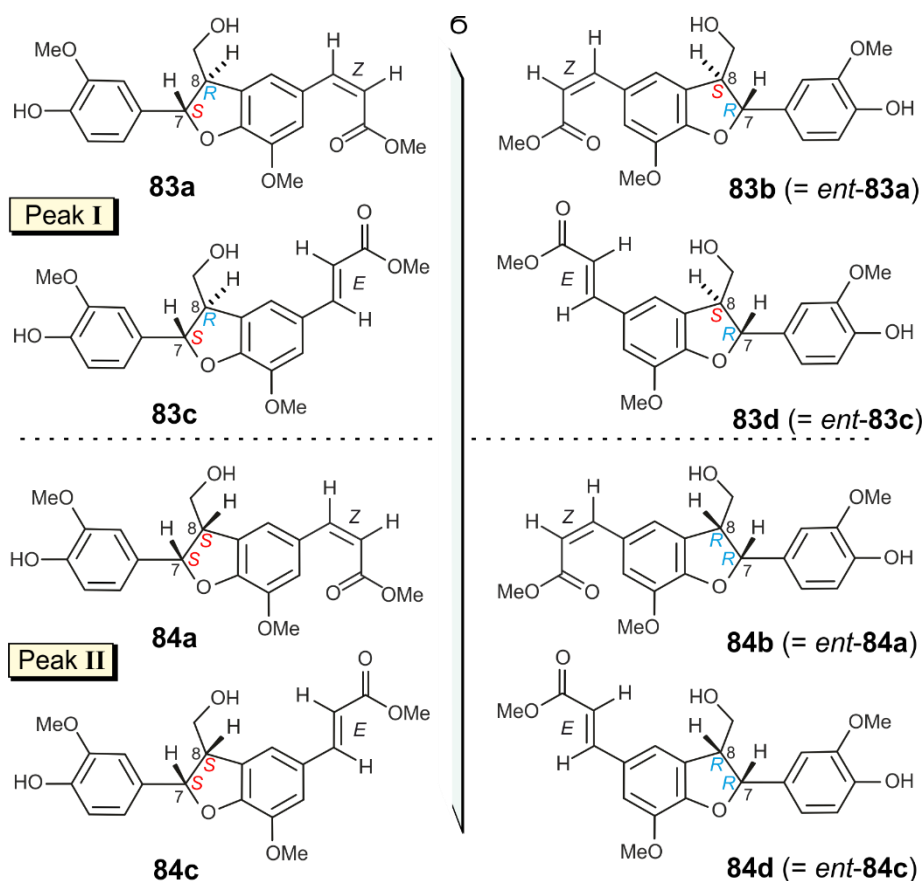


Figure 60. Structures of gardenifolins A-D (**83a-d**) and E-H (**84a-d**), stereoisomeric neolignans from the stem bark of *Gardenia ternifolia*, eluting as two peaks on an achiral reversed-phase column (see Figure 61). Mixtures **I** (consisting of **83a-d**) and **II** (containing **84a-d**), were and then further resolved by HPLC on a chiral phase (see Figure 64).

The results described in this chapter were published in *Journal of Natural Products*, and the text re-used, with modifications (upon permission from the journal).<sup>[214]</sup>

## Isolation and structural elucidation of neolignans

Resolution of the stem bark extract of *G. ternifolia* by preparative HPLC on a Symmetry® Prep-C<sub>18</sub> column led to the isolation of two peaks, denoted as **I** and **II** (Figure 61). All the components contained in peaks **I** and **II** corresponded to the same molecular formula of C<sub>21</sub>H<sub>22</sub>O<sub>7</sub>, as deduced by HRESIMS. The NMR data (Figure 62) of **I** and **II** were similar, too. The <sup>13</sup>C NMR spectrum exhibited 21 carbon signals, among them one ester carbonyl (C-9') and two methoxy-group carbons belonging to two different aromatic moieties. The DEPT-135 spectrum indicated one oxymethylene carbon (C-9), two vinylic carbons (C-7') and (C-8'), and five aromatic methine carbons (C-2, C-5', C-5, C-3', and C-6). The integration of the signals in the <sup>1</sup>H NMR spectrum indicated the presence of 20 protons, including five aromatic hydrogens belonging to two spin systems. The signals of two adjacent vinylic protons were detected as doublets, confirmed also by COSY interactions. Moreover, two geminal protons, H-9a,b, were recorded belonging to a methylene group attached to an sp<sup>3</sup> methine as established by TOCSY. Two sp<sup>3</sup> methine groups, H-8 and H-7, were deduced to be part of a dihydrofuran ring system. In addition, three methoxy groups were observed, one belonging to a methyl ester residue (CH<sub>3</sub>O-9'), while the other two, CH<sub>3</sub>O-3 and CH<sub>3</sub>O-6', were attached to an aromatic ring. A detailed analysis of the NMR data revealed the presence of a π-system consisting of an *O*-substituted *ortho*-methoxyphenol moiety. Taken together, the constitutions of **I** and **II** were assigned to be identical, representing stereoisomeric neolignans. The NMR spectra of **I** and **II** (Figure 62) additionally indicated that these two samples were, in fact, mixtures of *E*- and *Z*-diastereomeric 2,3-dihydrobenzo[*b*]furans.

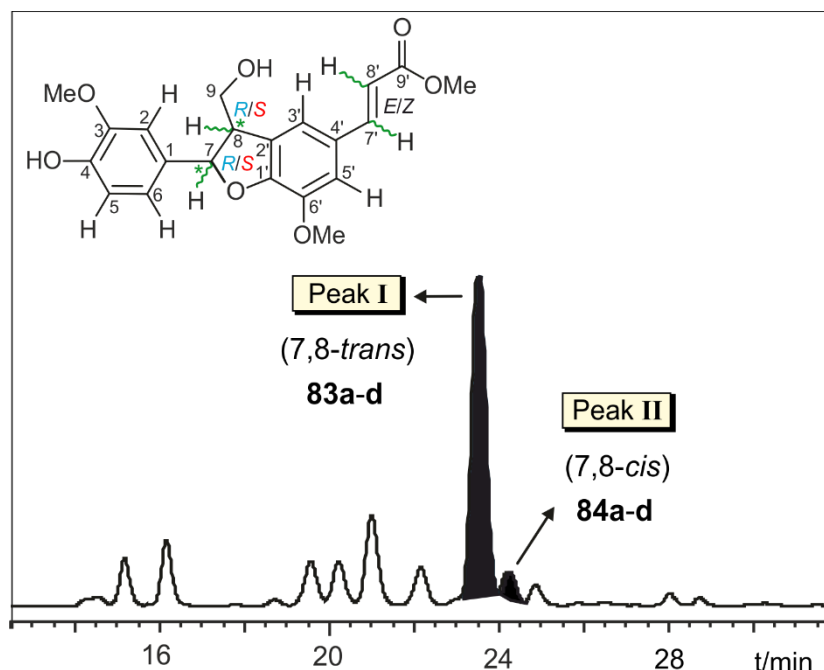


Figure 61. Reversed-phase chromatography of the extract of the stem bark of *Gardenia ternifolia* containing peak **I** (all 7,8-*trans*) and peak **II** (all 7,8-*cis*), consisting of two pairs of diastereomeric neolignans **83a**, **83c**, **84a**, and **84c** and their enantiomers **83b**, **83d**, **84b**, and **84d** (Figure 55), as non-racemic mixtures.

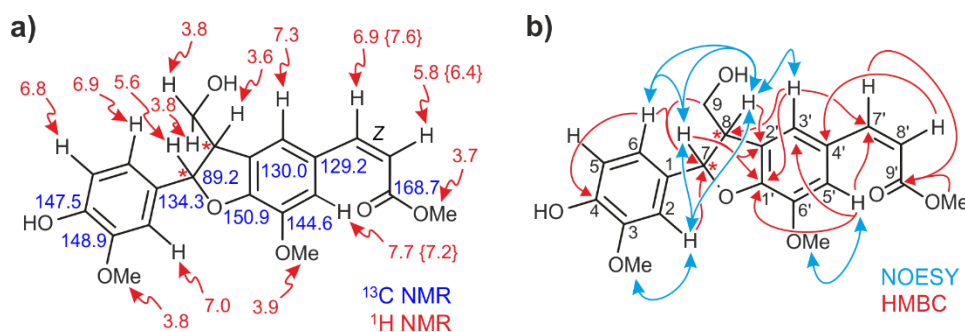


Figure 62. (a)  $^1\text{H}$  and  $^{13}\text{C}$  NMR spectroscopic data (in ppm) for the *Z*-isomeric forms contained in fractions **I** and **II**. Values of the *E*-isomers of **I** and **II**, as far as they are different from those of the corresponding *Z*-isomers, are denoted in curly brackets. (b) HMBC (red single arrows) and NOESY (blue double arrows) interactions evidencing the constitution of the neolignans of mixtures **I** and **II**.

Further resolution of **I** and **II** by repeated preparative HPLC on an achiral reversed-phase  $\text{C}_{18}$  column afforded four samples, each of which, gave the same molecular formula by HRESIMS as **I** and **II** in total, but the  $^1\text{H}$  NMR spectra suggested the presence of mixtures of *Z*- and *E*-isomers in **I** and **II** (Figure 62), as evidenced by the adjacent vinylic doublets signals of H-7' and H-8' ( $J_{7',8'} \approx 12.9$  Hz for *Z*) and ( $J_{7',8'} \approx 15.9$  Hz for *E*). The coupling constants  $J_{7,8}$  (6.65 versus 6.51 Hz) in  $^1\text{H}$  NMR of the isolated subfractions *Z*-**I** (6.65 Hz), *E*-**I** (6.51 Hz), *Z*-**II** (6.65



Hz), and *E*-**II** (6.51) were too similar to each other to permit to differentiate between the relative *cis*- and *trans*-orientations at C-7 versus C-8 in the dihydrofuran subunit in these four samples. NOESY measurements did not allow either to unambiguously assign the relative configurations of the two stereocenters for any of the *E*- or *Z*-isomers of **I** and **II**. The distinction finally succeeded by NOE difference (NOEDIFF) experiments<sup>[142]</sup> (Figure 63). Irradiation of H-7 led to a significant enhancement of the signals of H-9a,b in the NOEDIFF spectra of *E*-**I** and *Z*-**I**, indicating a relative *trans*-configuration of the two stereocenters at C-7 and C-8. By contrast, the H-8 signal was distinctly enhanced in the NOEDIFF spectra of *E*-**II** and *Z*-**II** when H-7 was irradiated, thus verifying a relative *cis*-configuration of the isomers of these two subfractions. Moreover, all four samples, *Z*-**I**, *E*-**I**, *Z*-**II**, and *E*-**II**, were found to be optically active.

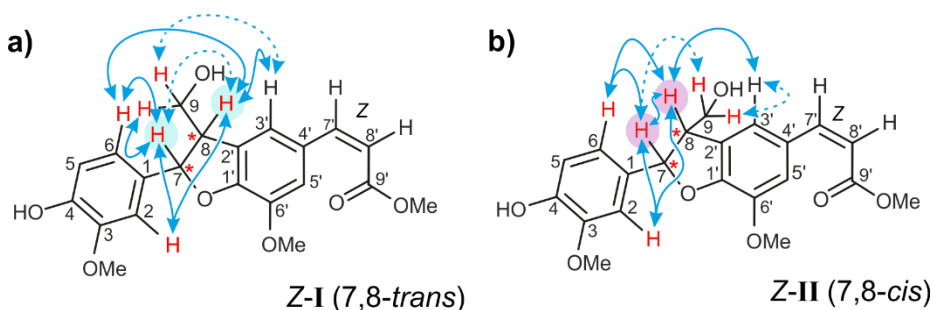


Figure 63. NOEDIFF enhancements upon irradiation (continuous blue double arrows), exemplarily illustrated (a) for *Z*-**I** (7,8-*trans*) and (b) for *Z*-**II** (7,8-*cis*). Similar results were also obtained for the samples *E*-**I** (7,8-*trans*) and *E*-**II** (7,8-*cis*). Weak interactions are depicted by dotted double arrows.

### Chiral resolution of the eight 2,3-DBF stereoisomers

Despite the optical and chiroptical activities of all four samples *Z*-**I**, *E*-**I**, *Z*-**II**, and *E*-**II**, chromatography on a chiral Lux Cellulose-1 phase, with acetonitrile and water as the mobile phase, afforded two peaks in each case, thus hinting at the presence of enantiomeric mixtures. This finding was further corroborated by the hyphenation of HPLC on that chiral phase with ECD spectroscopy, permitting the acquisition of two pairs of mirror-imaged ECD spectra, for each of the mixtures **I** and **II**, by HPLC-DAD-ECD hyphenation.<sup>[202]</sup> HPLC resolution on a preparative scale, directly starting from each of the mixtures **I** and **II**, finally even gave rise to four baseline-separated peaks each (Figure 64), thus corroborating that there were, in total, eight stereoisomers. In other words, the samples *Z*-**I**, *E*-**I**, *Z*-**II**, and *E*-**II** consisted each of scalemic mixtures of **83a** and **83b** (*Z*-**I**), **83c** and **83d** (*E*-**I**), **84a** and **84b** (*Z*-**II**), and **84c** and

**84d** (*E-II*), respectively. They were named gardenifolins A-H (**83a-d** and **84a-d**), due to their occurrence in *Gardenia ternifolia*.

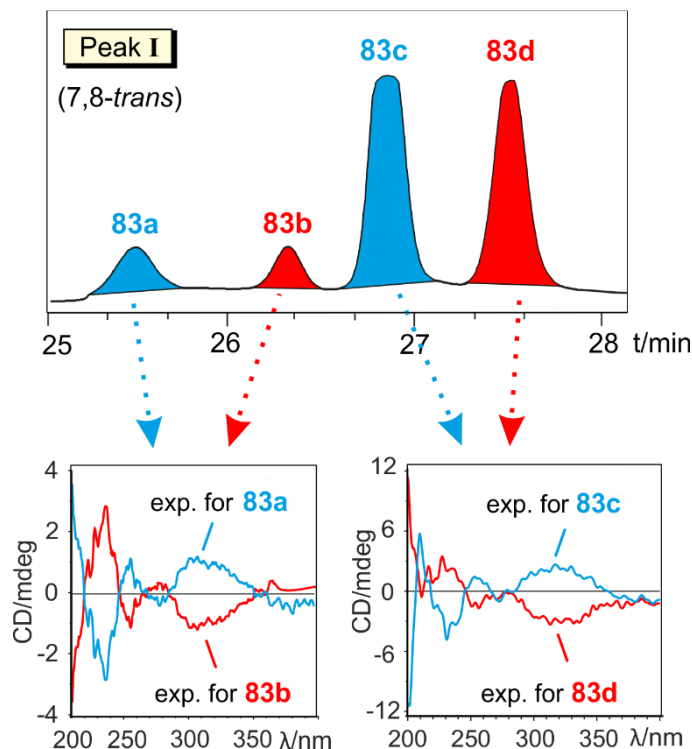


Figure 64. Online ECD spectra of four pure stereoisomers present in peak **I**, showing two similar pairs of mirror-imaged spectra. For the peak **II**, similar resolution and four ECD spectra were achieved.<sup>[214]</sup>

### Stereochemical assignment of stereoisomeric gardenifolins A-H

With the eight pure stereoisomers in hands, we focused on their reliable stereochemical attribution. For each isomer, the constitution was confirmed by NMR (Table 11), while the relative configurations were corroborated by NOEDIFF measurements (*vide supra*), as described above, for the scalemic mixtures.

Table 11.  $^1\text{H}$  (600 MHz) and  $^{13}\text{C}$  (151 MHz) data of gardenifolins A-H in acetone- $d_6$  ( $\delta$  in ppm,  $J$  in Hz).

no.	gardenifolins A ( <b>83a</b> ) and B ( <b>83b</b> )		gardenifolins C ( <b>83c</b> ) and D ( <b>83d</b> )		gardenifolins E ( <b>84a</b> ) and F ( <b>84b</b> )		gardenifolins G ( <b>84c</b> ) and F ( <b>84d</b> )	
	$\delta_{\text{H}}$ , mult. ( $J$ )	$\delta_{\text{C}}$ , type	$\delta_{\text{H}}$ , mult. ( $J$ )	$\delta_{\text{C}}$ , type	$\delta_{\text{H}}$ , mult. ( $J$ )	$\delta_{\text{C}}$ , type	$\delta_{\text{H}}$ , mult. ( $J$ )	$\delta_{\text{C}}$ , type
1		134.3, C		133.9, C		134.3, C		133.9, C
2	7.04, d (2.00)	110.6, CH	7.04, d (1.92)	110.6, CH	7.04, d (2.00)	110.6, CH	7.04, d (1.92)	110.6, CH
3		148.9, C		148.5, C		148.9, C		148.5, C
4		147.5, C		147.6, C		147.5, C		147.6, C
5	6.81, d (8.12)	116.2, CH	6.81, d (8.12)	115.8, CH	6.81, d (8.11)	116.2, CH	6.81, d (8.12)	115.8, CH
6	6.88, dd (1.79, 8.15)	119.7, CH	6.87, dd (1.99, 8.15)	119.7, CH	6.88, dd (1.79, 8.15)	119.7, CH	6.88, dd (1.95, 8.10)	119.7, CH
7	5.63, d (6.66)	89.2, CHOC	5.63, d (6.66)	89.3, CHOC	5.62, d (6.51)	89.2, CHOC	5.61, d (6.52)	89.3, CHOC
8	3.58, pq (6.36)	54.5, CH	3.58, pq (6.36)	54.4, CH	3.58, pq (6.20)	54.5, CH	3.59, pq (6.31)	54.4, CH
9a	3.88, m	64.6, CH <sub>2</sub> OH	3.89, m	64.4, CH <sub>2</sub> OH	3.88, m	64.6, CH <sub>2</sub> OH	3.89, m	64.4, CH <sub>2</sub> OH
9b	3.84, m	64.6, CH <sub>2</sub> O	3.84, m	64.4, CH <sub>2</sub> O	3.84, m	64.6, CH <sub>2</sub> O	3.85, m	64.4, CH <sub>2</sub> O
1'		150.9, C		150.6, C		150.9, C		150.6, C
2'		131.0, C		131.0, C		130.0, C		131.0, C
3'	7.34, br s	121.9, CH	7.25, br s	118.9, CH	7.34, br s	121.9, CH	7.25, br s	118.9, CH
4'		129.2, C		129.0, C		129.2, C		129.0, C
5'	7.72, d (1.50)	115.8, C	7.24, br s	113.3, C	7.72, d (1.50)	115.8, C	7.24, br s	113.3, C
6'		144.6, C		145.6, C		144.6, C		145.6, C
7'	6.90, d (12.93)	144.7, CH	7.60, d (15.90)	146.0, CH	6.90, d (12.93)	144.7, CH	7.60, d (15.90)	146.0, CH
8'	5.80, d (12.93)	116.5, CH	6.40, d (15.90)	115.6, CH	5.80, d (12.93)	116.5, CH	6.40, d (15.90)	115.6, CH
9'		167.5, CO <sub>2</sub> CH <sub>3</sub>		168.0, CO <sub>2</sub> CH <sub>3</sub>		167.5, CO <sub>2</sub> CH <sub>3</sub>		168.0, CO <sub>2</sub> CH <sub>3</sub>
3-OCH <sub>3</sub>	3.82, s	56.3, CH <sub>3</sub>	3.81, s	56.5, CH <sub>3</sub>	3.82, s	56.3, CH <sub>3</sub>	3.82, s	56.3, CH <sub>3</sub>
6'- OCH <sub>3</sub>	3.86, s	56.4, CH <sub>3</sub>	3.90, s	56.3, CH <sub>3</sub>	3.86, s	56.4, CH <sub>3</sub>	3.91, s	56.5, CH <sub>3</sub>
9'- OCH <sub>3</sub>	3.69, s	51.6, CH <sub>3</sub>	3.71, s	51.6, CH <sub>3</sub>	3.70, s	51.6, CH <sub>3</sub>	3.72, s	51.6, CH <sub>3</sub>

For the assignment of the absolute configurations, the online ECD spectra of the pure enantiomers were examined. Each pair of compounds displayed opposite ECD spectra, hinting at enantiomeric mixtures. All the four diastereomers *E-I*, *Z-I*, *E-II*, and *Z-II* were, in fact, pairs of enantiomers in unequal amounts, and were, thus, not racemic but scalemic, which was totally unprecedented in this sub-group of natural products. This explained why each of those four enantiomeric mixtures (like, *e.g.* *E-I*) had been optically active and had displayed clear ECD spectra.

Based on the reversed helicity rule for the  $^1L_b$  band ECD for 7-methoxy-2,3-dihydrobenzo[*b*]furan chromophores – already introduced in this thesis –, [141, 222] the positive  $^1L_b$  Cotton effect (CE) of **83a** observed around 308 nm ( $\Delta\epsilon + 1.4$ ) evidenced *P*-helicity and, consequently, *S*-configuration at C-7. The negative CE of **83b** around 309 nm ( $\Delta\epsilon - 1.2$ ) in turn, indicated 7*R*-configuration for this enantiomer. (+)-Gardenifolin A (**83a**) was thus assigned as 7*S*,8*R*,7'*Z*-configured and (–)-gardenifolin B (**83b** = *ent*-**83a**) as 7*R*,8*S*,7'*Z*. As presented in Figure 64, the neolignans **83c** and **83d** similarly exhibited mirror-image-like ECD curves. The CD spectrum of **83c** showed a positive CE around 317 nm ( $\Delta\epsilon + 3.0$ ) and, thus, *P*-helicity, while *M*-helicity was deduced for **83d** according to a negative CE around 314 nm ( $\Delta\epsilon - 3.5$ ), as depicted in Figure 65. Therefore, the absolute configurations of these two enantiomers were established as 7*S*,8*R*,7'*E* for (+)-gardenifolin C (**83c**) and 7*R*,8*S*,7'*E* for (–)-gardenifolin D (**83d** = *ent*-**83c**) (Figure 60).

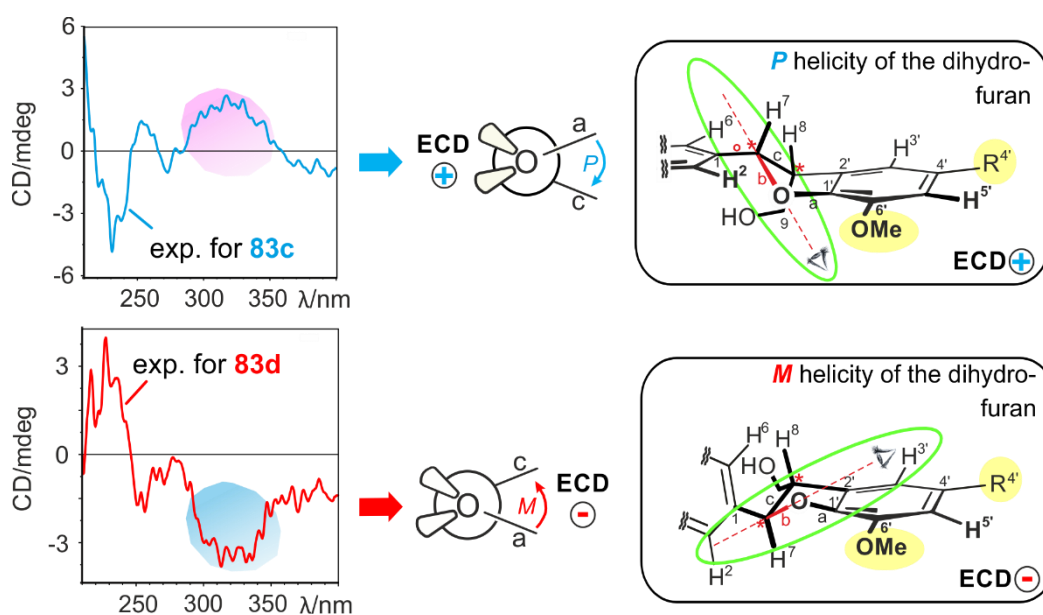


Figure 65. Online ECD spectra and assignments for of gardenifolins C (**83c**) and D (**83d**), applying the reversed helicity rule of dihydrobenzofuran neolignans.

In a similar way, the resolution of the stereoisomers of mixture **II** by HPLC on a chiral Lux Cellulose-1 phase provided two pairs of enantiomers, **84a/84b** and **84c/84d** (Figure 66). The gardenifolins **E** (**84a**) and **G** (**84c**) displayed positive CEs and, thus, *P*-helicity (and hence *S*-configuration at C-7), while *M*-helicities (and thus *7R*-configuration) were assigned for their corresponding enantiomers, gardenifolins **F** (**84b**) and **H** (**84d**). Based on the optical, chiroptical, and spectroscopic results obtained, the absolute configurations of these four stereoisomers were attributed as follows: (+)-*7S,8S,7'Z* for gardenifolin **E** (**84a**), (–)-*7R,8R,7'Z* for gardenifolin **F** (**84b** = *ent*-**84a**), (+)-*7S,8S,7'E* for gardenifolin **G** (**84c**), and (–)-*7R,8R,7'E* for gardenifolin **H** (**84d** = *ent*-**84c**). Thus, all eight possible stereoisomers for the 2D structure of gardenifolins were discovered in *G. ternifolia* as depicted in Figure 60.

Resolution of the *E*- and *Z*-diastereomers in both mixtures **I** and **II** by HPLC on a chiral phase provided the corresponding four pairs of enantiomers in ratios distinctly differing from 1:1 (Figure 66). All these – hence non-racemic – pairs of neolignan enantiomers were found to be mixtures occurring in ratios of about 1.5:1 (for **83a** and **83b**), 1.4:1 (for **83c** and **83d**), 1.9:1 (for **84a** and **84b**), and 2:1 (for **84c** and **84d**). The scalemic nature of the diastereomers in mixtures **I** and **II** in *G. ternifolia* may hint at a lack of stereocontrol and, thus, at a weak enzymatic assistance – by dirigent proteins<sup>[223-224]</sup> – in the biosynthesis of these compounds.

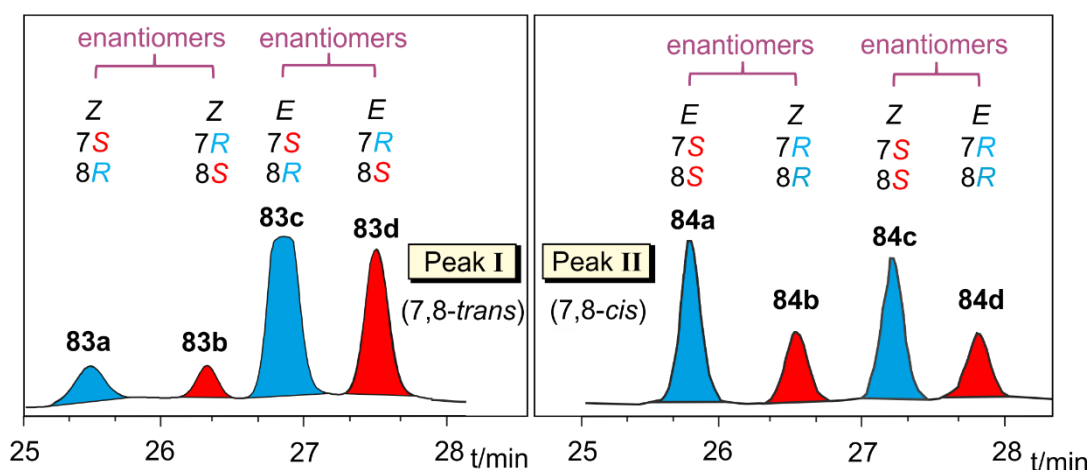


Figure 66. Chromatograms of the mixtures **I** (**83a-d**) and **II** (**84a-d**) resolved by preparative HPLC on a chiral Lux Cellulose-1 phase, and stereochemical assignment of the peaks (as achieved by ECD). The blue and the red colors referring to the *P*- and the *M*-helicities, respectively.

This is the first report on the discovery and successful resolution of two 2,3-dihydrobenzo[*b*]furan neolignan mixtures consisting of *all* possible stereoisomers, *i.e.*, four diastereomers and their four enantiomers, and their configurational assignment. As described

above, this separation was accomplished by two HPLC runs, first on an achiral column for the isolation of the diastereomers, followed by resolution of the enantiomers on a chiral phase. To the best of our knowledge, only one similar literature example is known<sup>[152]</sup> regarding the separation and characterization of four pairs of enantiomeric sesquieolignans isolated from the Chinese shrub *Phyllanthus glaucus* (Euphorbiaceae).<sup>[152]</sup> These sesquieolignans consist of a 2-phenyl-2,3-dihydrobenzo[*b*]furanpropanol moiety and a 1-phenylpropan-1,3-diol unit possessing two stereogenic centers. Similar to the gardenifolins A-H, a series of eight sesquieolignan enantiomers had been isolated by HPLC on a chiral phase from two stereoisomeric mixtures, each of them consisting of four diastereomers and their corresponding enantiomers. But, different from the neolignans from *G. ternifolia* described here, only eight out of a total of 16 possible stereoisomers had been identified in the case of those sesquieolignans from *P. glaucus*.<sup>[152]</sup>

The discovery of the gardenifolins E-H (**84a-d**), comprising a complete series of *cis*-configured isomers, was remarkable, also in view of the fact that – apart from those sesquieolignans from *P. glaucus*<sup>[152]</sup> – no further reliable similar example of the natural occurrence of four *cis*-configured isomers was known from the literature.

Only few examples of naturally occurring pairs of neolignan enantiomers with a 2,3-dihydrobenzo[*b*]furan motif have so far been described in the literature,<sup>[124, 133, 138, 145, 152, 225-226]</sup> and, even less frequently, reports on investigations concerning the enantiomeric purity of naturally occurring 2,3-DBFs and related neolignans.<sup>[152, 225-227]</sup> Thus, only little is known about the presence of these compounds as scalemic mixtures in nature. Only recently, some lignan, norlignan, and neolignan enantiomers have been isolated from two traditional Chinese medicinal plants,<sup>[152, 225-227]</sup> some of which were – related to the neolignan enantiomers herein reported – scalemic mixtures, too. That such cases have been discovered only now, might hint at a more widespread presence of scalemic mixtures of neolignan enantiomers in plants, in general, since enantiomeric mixtures with variable compositions might have been erroneously considered as stereochemically homogenous due to their reduced, but existing optical and chiroptical activities.<sup>[225-226]</sup>

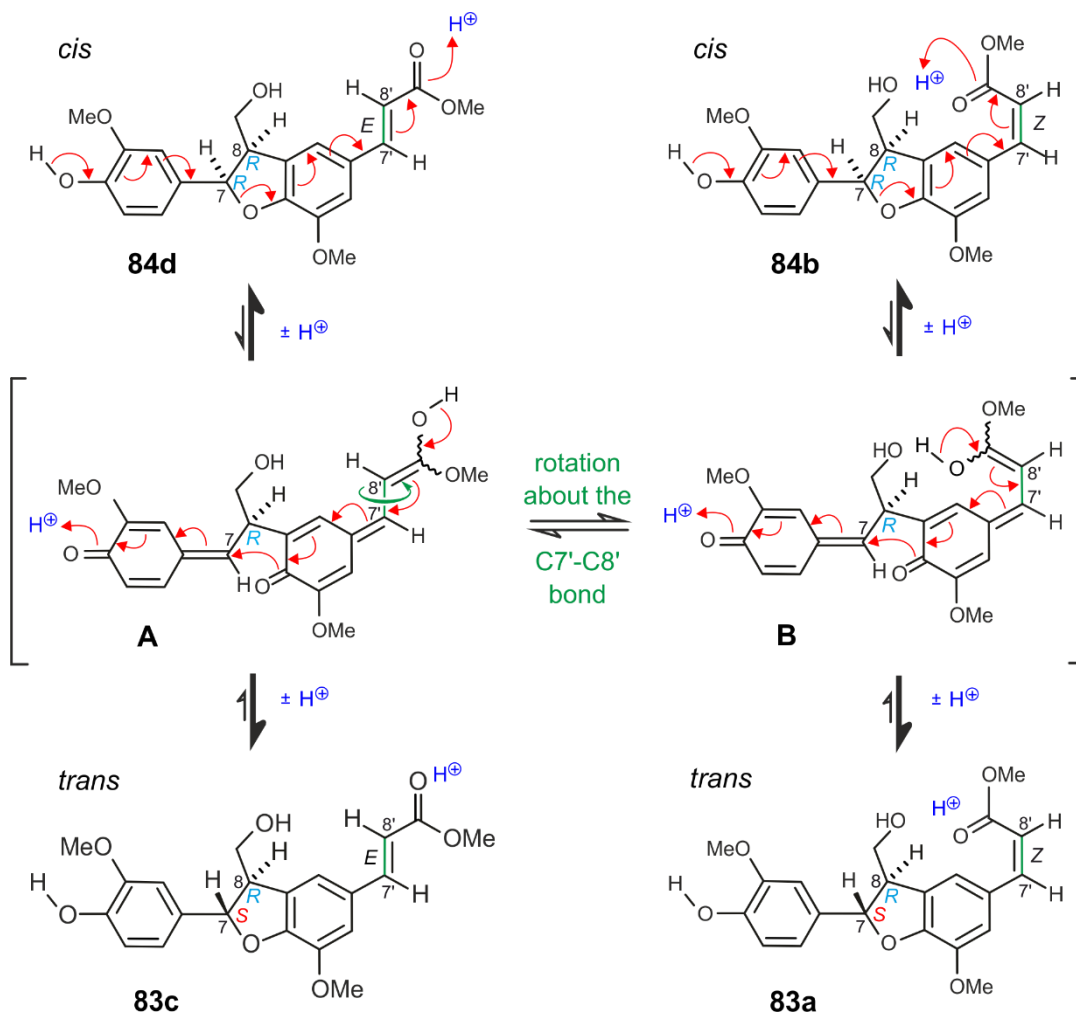
In the literature, one 2,3-dihydrobenzo[*b*]furan neolignan possessing the same constitution as the gardenifolins presented here, had been described as an endogenous prostacyclin (PGI<sub>2</sub>) inducer isolated from the leaves of *Zizyphus jujuba* (Rhamnaceae) in 1986.<sup>[136]</sup> Although like for **83c/d**, an *E*-configuration at the methyl acrylate unit and a relative *trans*-configuration

between the stereocenters at C-7 and C-8 in the dihydrofuran portion had been established for that neolignan, its absolute configuration has remained unknown. Moreover, neither a CD spectrum nor any optical rotation values had been reported for that compound, making it now impossible to assign the complete stereostructure of that plant metabolite based on the literature data.<sup>[136]</sup> Already in 1998, Yuen *et al.*<sup>[143]</sup> had to face the same dilemma: The group had synthesized the two respective enantiomers, but due to the insufficient information published on the absolute configuration and the enantiomeric purity of that natural PGI<sub>2</sub> inducer, a stereochemical assignment of the natural product from *Z. jujuba* was not possible. Thus, our phytochemical work on *G. ternifolia* is the first report on the reliable occurrence of **83c** and **83d** in nature.

In 1995, Wahl *et al.*<sup>[153]</sup> reported the isolation of a neolignan named xylobuxin from the stem bark of *Xylopia buxifolia* (Annonaceae), yet without mentioning that PGI<sub>2</sub> inducer isolated earlier from *Zizyphus jujuba*.<sup>[136]</sup> The compound was described to have the same constitution and was attributed the novelty of a relative *cis*-configuration in the furan ring based on the coupling constant of  $J = 6$  Hz, which was erroneously expected to have a value of  $J = 10.5$  Hz for a *trans*-configured 2,3-DBF neolignan.<sup>[153]</sup> Virtually nearly the same coupling constant ( $J = 6.7$  Hz), however, had already been reported for that *trans*-configured PGI<sub>2</sub> inducer.<sup>[136]</sup> As discussed above for *Z-I* (7,8-*trans*) and *Z-II* (7,8-*cis*), and also demonstrated for related neolignans, coupling constants for *cis*- and *trans*-configured 2,3-DBFs are too similar to each other,<sup>[142, 146, 228]</sup> so that a reliable attribution of the relative configuration of the 2,3-dihydrobenzofuran ring system can only be achieved by comprehensive 2D NMR measurements, in combination with NOEDIFF experiments.<sup>[129-130, 133, 142, 225-226]</sup>

The co-occurrence of *E*- and *Z*-isomers of the cinnamoyl residues in the gardenifolins A-H (**83a-d** and **84a-d**), as found in this study, is well documented for many other natural products in the literature.<sup>[229-230]</sup> It is also known that these moieties are prone to *E/Z* interconversion upon light exposure, even in the NMR tube.<sup>[231-235]</sup> This isomerization – even in combination with a *cis/trans* interconversion by epimerization at C-7 – might, however, also occur by acid (or base) catalyzed ring opening reaction as depicted in Scheme 7. From previous studies,<sup>[150, 236-242]</sup> it is well known that thermodynamically less stable *cis*-7-(4-hydroxyphenyl)-7,8-dihydrobenzofurans can undergo an epimerization reaction at C-7 to give the respective more stable *trans*-isomers by treatment with acid (*e.g.*, TFA in CH<sub>2</sub>Cl<sub>2</sub>)<sup>[150, 238-242]</sup> or base (*e.g.*, Na<sub>2</sub>CO<sub>3</sub> in MeOH).<sup>[236-237]</sup> Such *cis/trans* isomerization processes may possibly interconvert

any *cis*-gardenifolins into the respective *trans*-isomers, yet always within the same enantiomeric series, since the configuration at C-8 should remain unaffected.<sup>[150, 236-242]</sup>



Scheme 7. Possible chemically induced predominant formation of *trans*-configured gardenifolins, here exemplarily illustrated for the interconversion of the *cis*-configured gardenifolins F (**84b**) and H (**84d**) into the *trans*-isomers gardenifolins A (**83a**) and C (**83c**) (\* configurationally stable stereogenic center).

As illustrated in Scheme 7 exemplarily for the *cis*-configured gardenifolin **84d** (7*R*,8*R*,7'*E*), ring opening will give intermediate **A**, which will ring close preferentially to the thermodynamically more stable *trans*-isomer **83c** (7*S*,8*R*,7'*E*). Alternatively, **A** may cyclize back to **84d**. As a third possibility, **A** may also be transformed into intermediate **B** by rotation about the C7'-C8' bond. Renewed cyclization of **B** will then again mainly lead to the *trans*-isomer **83a** (7*S*,8*R*,7'*Z*), *i.e.*, to an overall *E/Z* isomerization in combination with epimerization at C-7, or (to a smaller degree) to the *cis*-compound **84b** (7*R*,8*R*,7'*Z*).



The 2,3-dihydrobenzo[*b*]furan neolignans (Figure 60) described in this thesis, however, were unexpectedly stable in the presence of acid – if light exposure was excluded. We also noticed that the *E/Z* isomerization of the gardenifolins A-H was significantly minimized when methanol was replaced by the aprotic solvent acetone, and the entire isolation process was performed under light-reduced conditions, *e.g.*, when using brown flasks, and acetone-*d*<sub>6</sub> for NMR. This might also be the reason why we, to our own surprise, succeeded to isolate the complete series of all possible *cis*-configured gardenifolin isomers E-H (**84a-d**) from *G. ternifolia*, although, for thermodynamic reasons, the formation of the *trans*-isomers A-D (**83a-d**) should be favored. The configurational stability of the gardenifolins A-H under the mild isolation conditions applied evidences that all eight stereoisomers are truly natural products.

### Biological evaluations: cytotoxic activities of gardenifolins A-H

Many lignans and neolignans are constituents of traditional herbal medicines and are, thus, in the focus of biological evaluations regarding their cytotoxic potential towards various cancer cell lines,<sup>[124-127]</sup> showing that some of them exhibited promising antiproliferative effects.<sup>[124-125, 217-218, 243]</sup> The availability of all the eight possible gardenifolin isomers A-H (**83a-d** and **84a-d**) in a stereochemically pure form from the African medicinal plant *G. ternifolia* now permitted measurement of their individual cytotoxic activities, here tested against the human cervical HeLa cell line. As shown in Table 12, all the gardenifolins reduced the growth of the tumor cells. While most isomers displayed only weak to moderate effects with IC<sub>50</sub> values of 78.8 – 105.0 μM, two of these neolignans, gardenifolin D (**83d**) and gardenifolin E (**84a**), strongly inhibited HeLa cell proliferation in a concentration range similar to that of 5-fluorouracil (5-FU) used as the positive reference. Dose-response curves (Figure 67) revealed compounds **83d** and **84a** to exhibit cytotoxicity towards the HeLa cell line with IC<sub>50</sub> values of 21.0 μM (for **83d**) and 32.5 μM (for **84a**).

The IC<sub>50</sub> values of the gardenifolins **83a** (IC<sub>50</sub> = 78.8 μM) and **84c** (IC<sub>50</sub> = 105.0 μM) were found to be nearly the same as those of their enantiomers **83b** (IC<sub>50</sub> = 87.3 μM) and **84d** (IC<sub>50</sub> = 96.1 μM), whereas for the other two pairs of gardenifolin enantiomers, the individual IC<sub>50</sub> values varied significantly. Compound **84a** (IC<sub>50</sub> = 32.5 μM) was far more active against HeLa cells (by a factor of 3.2) than its enantiomer **84b** (IC<sub>50</sub> = 103.0 μM), and **83d** (IC<sub>50</sub> = 21.0 μM) was more active than **83c** (IC<sub>50</sub> = 90 μM) even by a factor of 4.1. These findings underline the strong impact of chirality on the bioactivities of the new neolignans herein described.

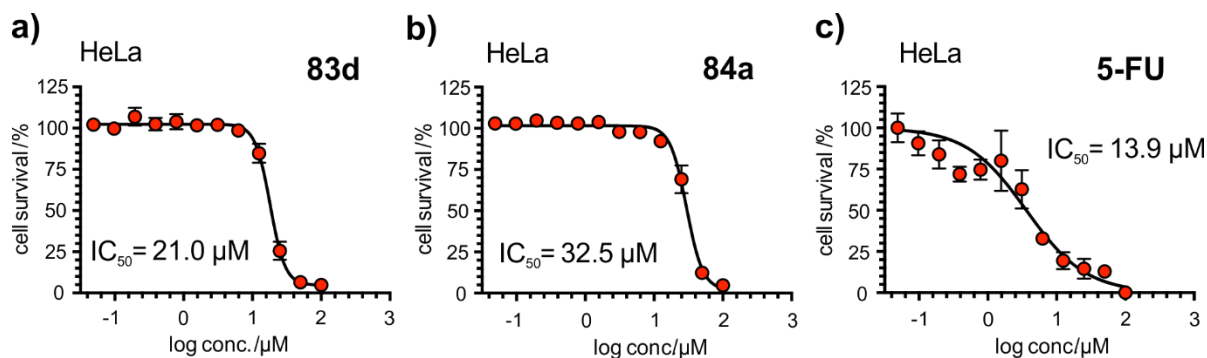


Figure 67. Inhibition of HeLa cells induced by the two most active of the new neolignans, (a) gardenifolin D (**83d**) and (b) gardenifolin E (**84a**), and by (c) 5-fluorouracil (5-FU) as the positive reference.

Table 12. Activities (IC<sub>50</sub> Values in μM) of the Gardenifolins A-D (**83a-d**) and E-H (**84a-d**), and 5-Fluorouracil Against Human Cervical HeLa Cancer Cells.

compound	HeLa cells	stereochemical features
5-fluorouracil	13.9	
<b>83a</b>	78.8	(+)-7 <i>S</i> ,8 <i>R</i> ,7' <i>Z</i>
<b>83b</b>	87.3	(-)-7 <i>R</i> ,8 <i>S</i> ,7' <i>Z</i>
<b>83c</b>	90.0	(+)-7 <i>S</i> ,8 <i>R</i> ,7' <i>Z</i>
<b>83d</b>	21.0	(-)-7 <i>R</i> ,8 <i>S</i> ,7' <i>Z</i>
<b>84a</b>	32.5	(+)-7 <i>S</i> ,8 <i>S</i> ,7' <i>E</i>
<b>84b</b>	103.2	(-)-7 <i>R</i> ,8 <i>R</i> ,7' <i>E</i>
<b>84c</b>	105.0	(+)-7 <i>S</i> ,8 <i>S</i> ,7' <i>E</i>
<b>84d</b>	96.1	(-)-7 <i>R</i> ,8 <i>R</i> ,7' <i>E</i>

<sup>a</sup>Used as a reference compound.

Gardenifolin D (**83d**), as the most potent isomer within this series of 2,3-dihydrobenzo[*b*]furan neolignans, was further studied for its effects on cell morphology and apoptosis using an acridine orange (AO) and Hoechst 33342 double staining assay (AO/Hoechst 33342) (Figure 68).<sup>[214]</sup> Untreated HeLa cells showed intact cell morphology with bright green AO fluorescence, counterstained with flattened blue nuclei (Figure 68, pictures A-D). Treatment of the tumor cells with 25 μM of **83d** (Figure 68, pictures E-H) induced apoptosis as indicated by the dramatic alteration of the morphology of the HeLa cells (Figure 68E, black arrows) and by fragmented nuclei (Figure 68G, white arrows).

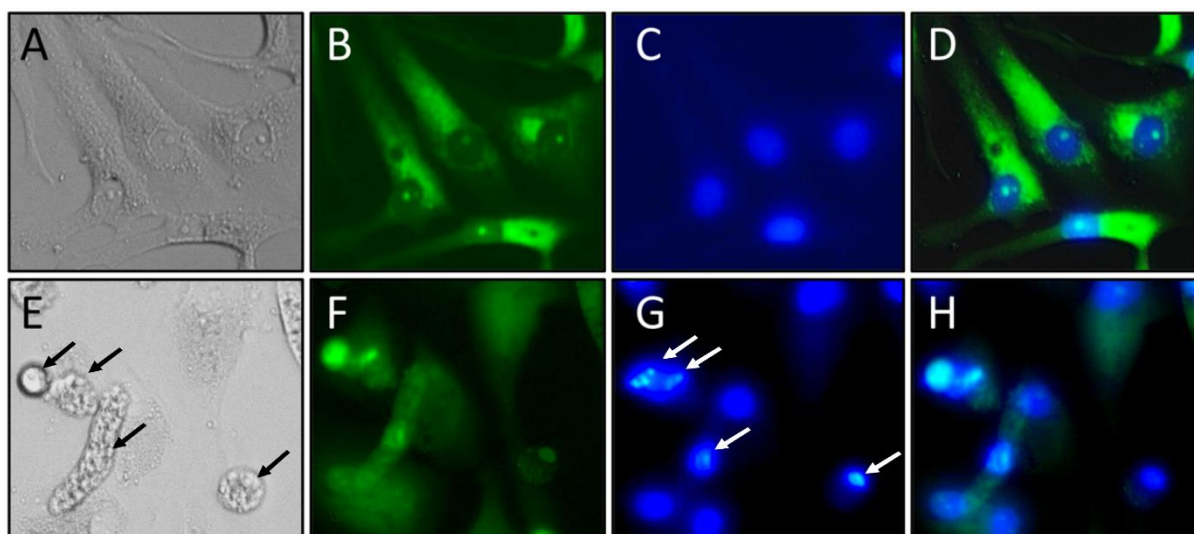


Figure 68. Morphological changes of HeLa cells induced by gardenifolin D (**83d**) (E-H) in comparison to untreated cells (A-D): HeLa cells ( $2 \times 10^4$ /well/500  $\mu$ L media) were treated with 25  $\mu$ M of **83d** in a 24-well plate and incubated for 72 h. Cells were then stained with acridine orange (AO) and Hoechst 33342, and further incubated for 10 min. The cells were then photographed under fluorescence and phase-contrast modes using an EVOS FL digital inverted microscope. (A and E) Phase contrast. (B and F) Cells stained with AO (green). (C and G) Nuclei stained with Hoechst 33342 (blue). (D and H) Merged images. (E-H) Cells treated with **83d** showed morphological alterations (black arrows) and nuclear fragmentation (white arrows) indicating apoptosis.

In the past decade, numerous new neolignans<sup>[124-125]</sup> including compounds with unusual carbon skeletons<sup>[152, 218, 225-227]</sup> were isolated from diverse plant sources, but the discovery of a complete series of all possible stereoisomers of such chiral plant metabolites, as presented here for the first time for the 2,3-dihydrobenzo[*b*]furan neolignans gardenifolins A-H (**83a-d** and **84a-d**), is unprecedented. All eight stereoisomers were isolated and fully characterized, with the four diastereomers occurring in the African medicinal plant *Gardenia ternifolia* as non-racemic mixtures. Likewise unusual was the identification of a complete series of all four possible *cis*-isomers. So far, *cis*-2-(4-hydroxyphenyl)-2,3-dihydrobenzo[*b*]furan neolignans<sup>[138, 152, 244]</sup> such as the gardenifolins E-H (**84a-d**) have less frequently been discovered in nature, because they may epimerize under acidic or basic conditions, to give, thermodynamically driven, the corresponding *trans*-compounds. The resolution of **83a-d** and **84a-d** was achieved on a chiral HPLC column, followed by stereochemical assignment, which succeeded by a combination of NOEDIFF measurements for the relative configurations and ECD spectroscopy, with the application of the reversed helicity rule, for the absolute

stereostructures. The work described in this chapter will be of particular value for the future structural characterization of other natural 2,3-DBF neolignans.

Along with the gardenifolins, the two known diastereomers: methyl *Z*-ferulate (**85**)<sup>[245-246]</sup> and methyl *E*-ferulate (**86**)<sup>[245, 247]</sup> were isolated and characterized from the same source (Figure 69), but no biological evaluations were performed.

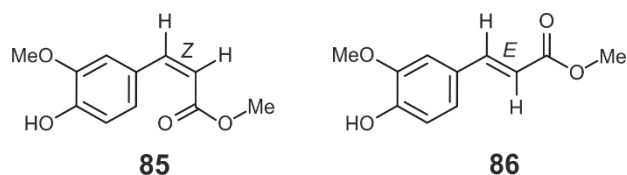


Figure 69. Methyl *Z*-ferulate (**85**) and methyl *E*-ferulate (**86**), further natural products isolated from *G. ternifolia* Schumach. & Thonn.

## II.10. Phytochemical and Qualitative Analysis of KILMA and N'Sansiphos

### II.10.1. Introduction to Congolese Herbal Medicinal Products

Herbal medicines are the most globally used type of medical drugs.<sup>[248-249]</sup> The World Health Organization (WHO) had reported that more than 60% of people in endemic areas rely on herbal products to heal severe diseases, like malaria tropica,<sup>[250]</sup> while many classical therapeutic schemes have been facing – for several reasons – failures.<sup>[40, 87-88, 250]</sup> This situation highlights the urgent need for new anti-infective agents to address – at least – the over-increasing drug resistance phenomenon.<sup>[38, 43]</sup>

Herbal preparations have been used for centuries, and many of them have been now approved as essential drugs in several countries, like in the DR Congo.<sup>[251]</sup> Their high cultural acceptance is due to the experienced safety and efficiency.<sup>[249-250]</sup> However, most of these African folk medicine products are virtually not phytochemically investigated and their constituents have been determined. The observed poor-quality management of this type of medicines exposes the patients to intentional and/or unconscious abuses by the producers.

Within this framework, basic issues related to less-investigated herbal medicines were addressed exemplarily for two Congolese medical drugs. A rational quality assessment procedure for less-inspected herbal medicines was established, and the methodology was applied to mainly two authorized Congolese herbal products, *i.e.* SIROP KILMA<sup>®</sup> and N'Sansiphos<sup>®</sup>.

For SIROP KILMA<sup>®</sup>,<sup>[252]</sup> which consists of ethanolic extract mixtures of *Lantana camara* L., *Gardenia ternifolia* Schumach. & Thonn., and *Crossopteryx febrifuga* Benth., selected markers from the main plant were chosen, isolated, structurally characterized, and used as internal standard for the development and validation of the analytical method. The method validation was based on the prime-marker acteoside, which was commercially available. The validated method was applied for the quantification of three batches of SIROP KILMA<sup>®</sup>.

On the herbal drug N'Sansiphos<sup>®</sup>, which is declared to be made of extracts from Clusiaceae, the methodology developed could not be rigorously applied due to the lack of cooperation from the phytoproducer. Therefore, the aim in this case was to identify, first of all, the Clusiaceae plant used for the syrup. In this case, the discovery of a massive usage of parabens preservatives – without any statement from the producer – was most alarming, since the concentrations were

far beyond the common limits. These compounds were quantified and some natural compounds were also identified.

## II.10.2. Rational Quality Assessment Procedure for Less-Investigated Herbal Drug: Case of SIROP KILMA®

Based on the preliminary fingerprinting of several Congolese herbal drugs,<sup>[158]</sup> an interdisciplinary approach for a rational quality assessment of herbal drugs, in general, was developed, using KILMA as a model case. The methodology combined an authentication step of the herbal remedy prior to any fingerprinting, the isolation of the major constituents, the development and validation of an HPLC-DAD analytical method with internal markers, and the application of the method to several batches of the herbal medicine (here for KILMA), thus, permitting the establishment of a quantitative fingerprint. From the constitutive plants of KILMA, acteoside (**87**),<sup>[253]</sup> isoacteoside (**88**),<sup>[254]</sup> stachannin A (**89**),<sup>[255-256]</sup> and pectolarigenin-7-*O*-glucoside (**90**)<sup>[257-258]</sup> were isolated (Figure 70). Acteoside was used as the prime marker for the validation of an analytical method.<sup>[259]</sup>

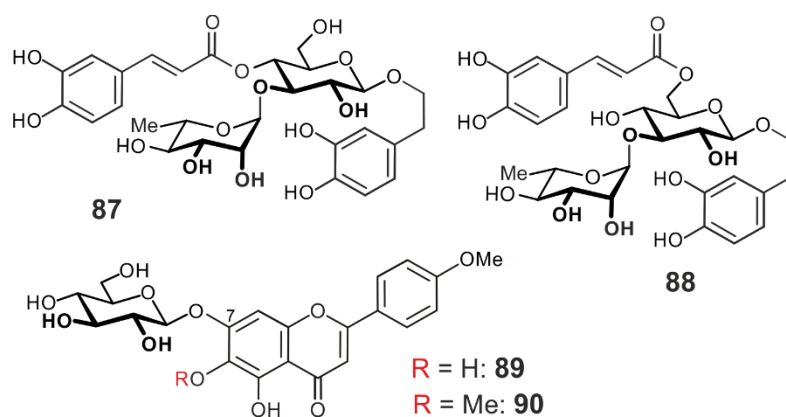


Figure 70. Marker compounds isolated and characterized from the herbal drug KILMA, originating from *Lantana camara* L.

The achievements accomplished in this study are very nicely and exhaustively described in the published paper in *Fitoterapia*<sup>[259]</sup> so that only a summary of the key aspects will be shown in this thesis, namely the chemical assignment of three markers **87**, **89** and **90** (Figure 71), the accuracy profile of the method (Figure 72), and the quantitative fingerprint obtained from the quantification of three batches of KILMA (Figure 73).

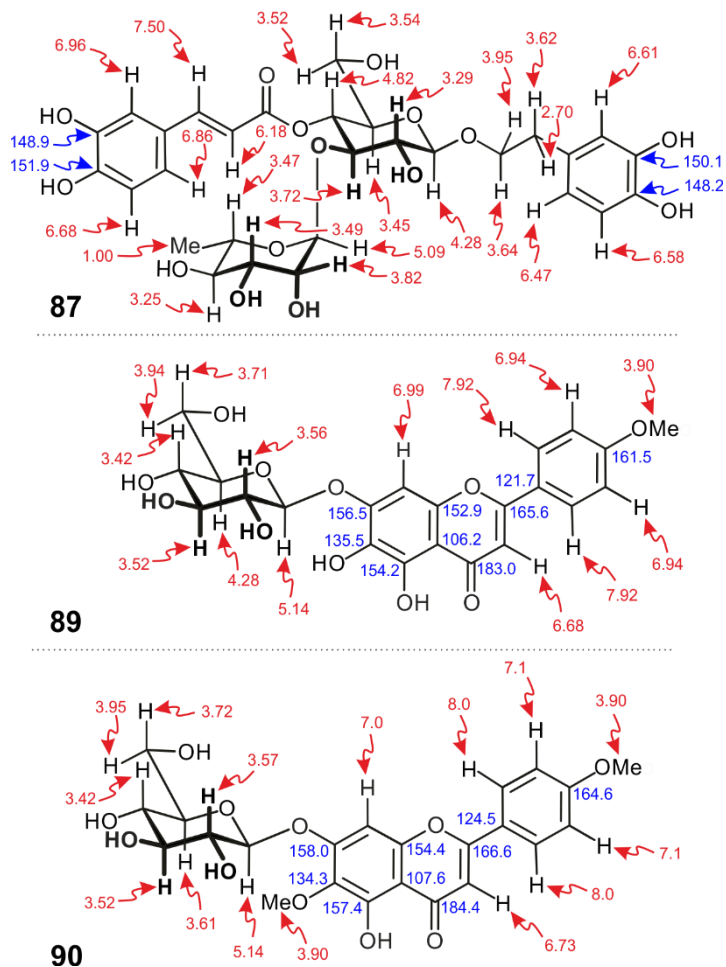


Figure 71. Chemical shifts ( $\delta$ ) in ppm of acteoside (**87**), stachannin A (**89**), and pectolarigenin-7-*O*-glucoside (**90**) ( $^1\text{H}$  in red, and  $^{13}\text{C}$  in blue). Isoacteoside (**88**) is not displayed.<sup>[259]</sup>

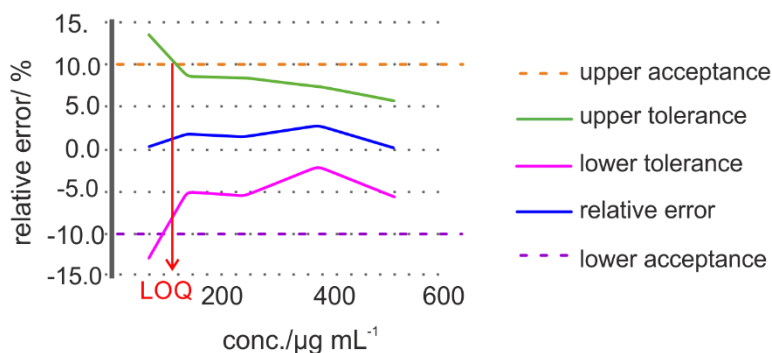


Figure 72. Accuracy profile obtained after the validation of the method and displaying the reliable quantification area for acteoside (**87**, in  $\mu\text{g mL}^{-1}$ ). The limit of quantification (LOQ) of acteoside in KILMA using the validated method is also shown.<sup>[259]</sup>

The accuracy profile defines a range of concentration (area), in which the quantification of acteoside (**87**) can be performed within the accepted relative error limits (see Figure 72).<sup>[259]</sup>



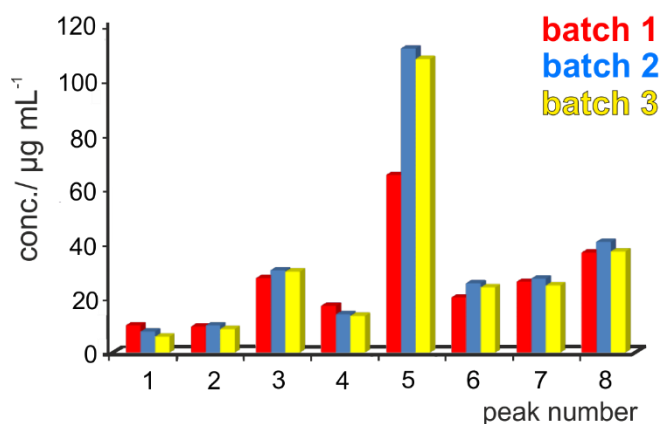


Figure 73. Content of three batches of KILMA: a quantitative fingerprint. Peak number 5 corresponds to **87**.<sup>[259]</sup>

The quantitative fingerprint, depicted in Figure 73, illustrates the content variation of eight compounds in the chromatographic fingerprint of SIROP KILMA. From this figure, the content in **87** seemed to be the most decisive parameter to consider for the standardization process of KILMA.<sup>[259]</sup>

All the four markers selected in this study were from *L. camara* L. Further phytochemical investigations on the constitutive *C. febrifuga* Benth. did not provide substantial hints to continue the screening analyses.

### II.10.3. Quality Analysis of Three Batches of N'Sansiphos®

Initial biological evaluations of the syrup N'Sansiphos® indicated a promising IC<sub>50</sub> value (0.8 µg mL<sup>-1</sup>) against *P. falciparum*, qualifying this herbal drug for further phytochemical analysis.

Surprisingly, the isolation and structural elucidation on this syrup led to the identification of three synthetic parahydroxybenzoates ('parabens'), namely methyl-paraben (**91**), ethyl-paraben (**92**), propyl-paraben (**93**), along with the natural product garcinoic acid (**94**).<sup>[260-261]</sup> The detection of garcinoic acid provided strong indication that the seeds of *Garcinia kola* – also known as 'bitter kola' – should be the 'secret' plant material involved in N'Sansiphos. This presumption was later phytochemically confirmed on authentic *G. kola* seeds, obtained in Kinshasa.

The authentication of the constituents of N'Sansiphos with *Garcinia kola*, indicated that the preservatives were not of natural origin, thus they had been deliberately added – in excessive amount – to prolong the conservation of the syrup. This was clearly a case of fraud and a criminal act. Most alarming fact is the undue quantity of the undeclared supplements that may be already in the toxic range.<sup>[262-264]</sup> Considering the well-known toxicity of parabens – e.g. propyl-paraben already at low concentrations – it was mandatory to perform quantitative analysis on several batches of this syrup.

The quantitative analyses were performed on HPLC-DAD, at 255 nm, using water and acetonitrile as mobile phases – like in the case of KILMA – on a Symmetry® RP<sub>18</sub> column. As shown in Table 13, the phytoproducer had used without any mention toxic amounts of harmful preservatives in a syrup, which is unjustifiable. The concentration of propyl-paraben incorporated in the formulation of this herbal product (72 µg mL<sup>-1</sup>), which is the only one used for pregnant women, demands for rapid measures to stop this criminal practice. Only regulatory authorities can act consequently in this specific case to stop these criminal practices. This bad and disquieting situation emphasizes once more the necessity to enable quality control of such preparations for the sake of the whole community.

Table 13. Quantitative determination of ethylparaben (**92**) and propylparaben (**93**) in three batches of N'Sansiphos syrup.

	batch 1	batch 2	batch 3	Mean
	conc. in mg L <sup>-1</sup>	conc. in mg L <sup>-1</sup>	conc. in mg L <sup>-1</sup>	conc. in mg L <sup>-1</sup>
<b>92</b>	1.75	3.8	2.95	2.83
<b>93</b>	72.55	74.20	69.25	72.00

Along with garcinoic acid, two known biflavonoids – GB1 (**95**)<sup>[265-266]</sup> and GB1a (**96**)<sup>[267]</sup> – were also isolated and structurally determined from the seeds of *Garcinia kola* (Figure 74). GB-1 and GB-2 have been known for their antiplasmodial activities,<sup>[268]</sup> so that their presence in the N'Sansiphos explains the initially observed *in vitro* activity. Interestingly, compound **94** exhibited – for the first time – an excellent and specific antileishmanial activity (IC<sub>50</sub> = 1.78 μM) with a very good selectivity index towards *Leishmania donovani*.

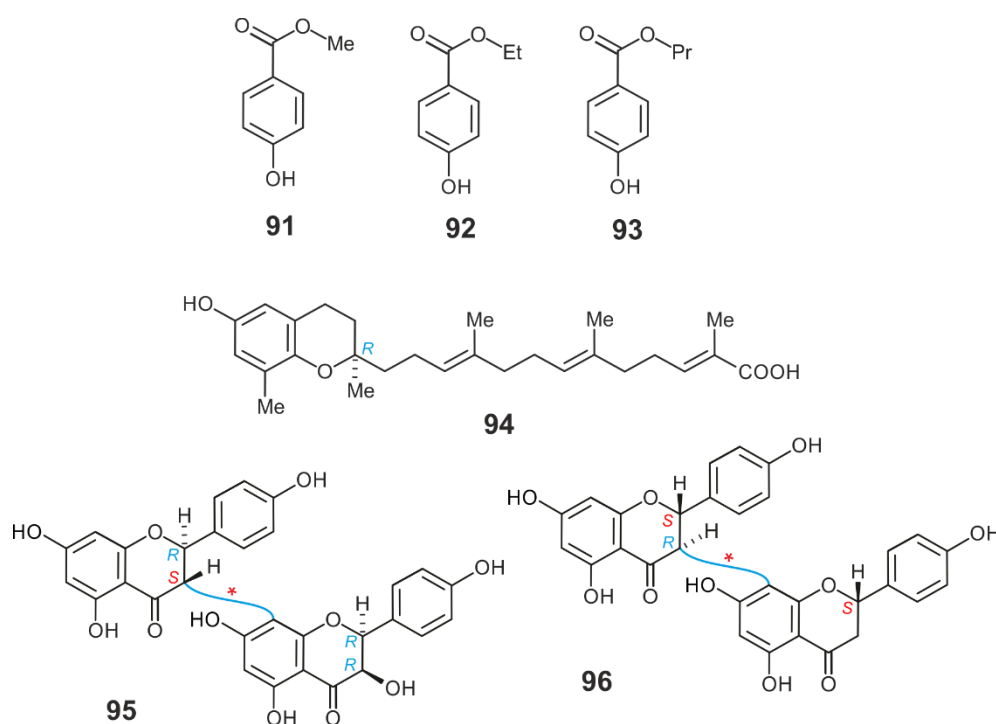


Figure 74. Compounds isolated from N'Sansiphos®: methyl-paraben (**91**), ethyl-paraben (**92**), propyl-paraben (**93**), and garcinoic acid (**94**). The biflavonoids GB1 (**95**) and GB1a (**96**) and the tocopherol derivative **94** were also isolated and characterized from *Garcinia kola*.

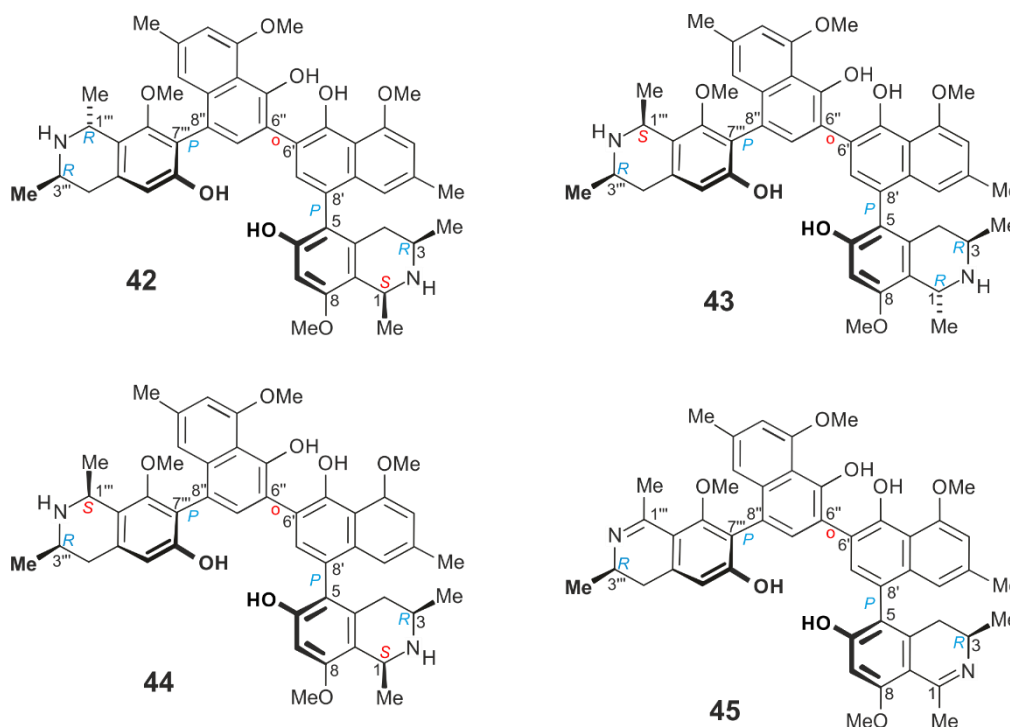
### III. Summary/Zusammenfassung

#### III.1. Summary

This thesis provides a glimpse on the structural variety and the therapeutic potential of plant-derived secondary metabolites. In this section, the main key aspects of the described results are summarized.

##### A) *Ealapasamines A-C, the first fully characterized 'mixed' heterodimers*

Three unusual heterodimeric naphthylisoquinoline alkaloids were isolated from the leaves of the tropical plant *Ancistrocladus ealaensis* J. Léonard, namely ealapasamine A (**42**), ealapasamine B (**43**), and ealapasamine C (**44**). These 'mixed', constitutionally unsymmetric dimers are the first stereochemically fully assigned cross-coupling products of 5,8'- and 7,8'-coupled naphthylisoquinoline compounds linked *via* C-6' of their naphthalene portions. This is the highest degree of coupling unsymmetry known so far within this class of alkaloids. The merely synthetic compound, ealapasamine C<sub>2</sub> (**45**) was obtained by oxidation of **44**.

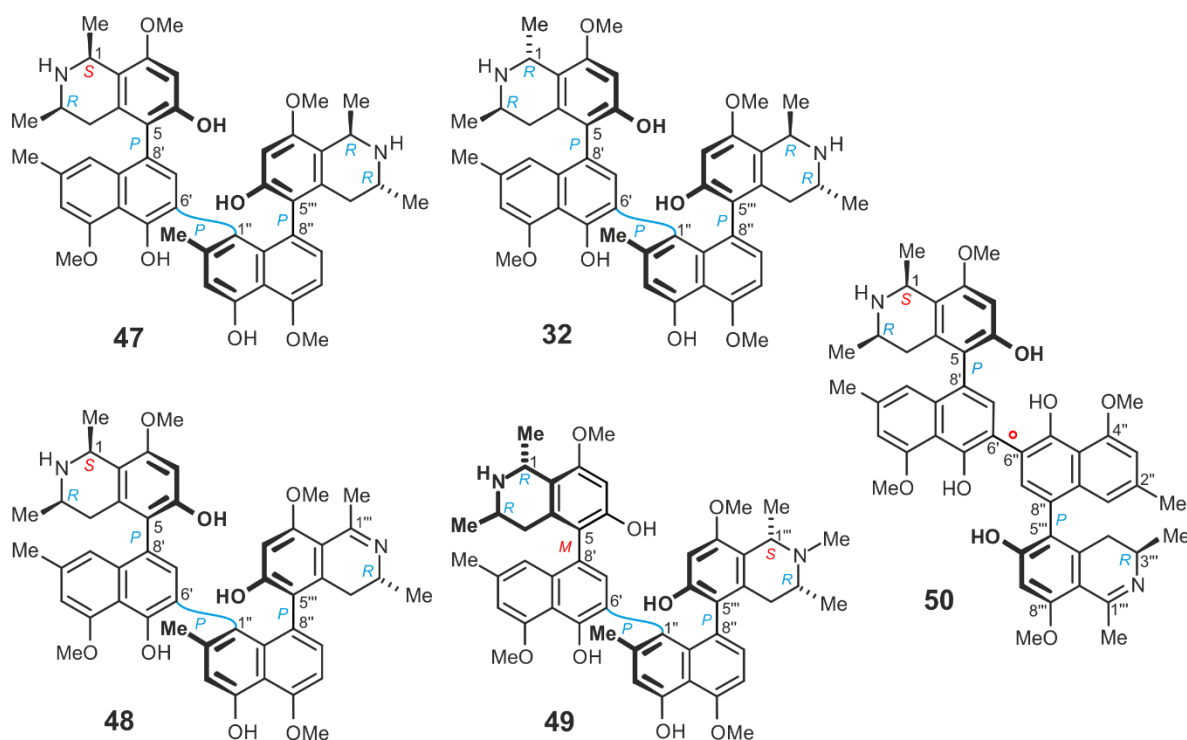


The new dimers **42-44** contain six elements of chirality, four stereogenic centers and the two outer, configurationally stable axes, while the central biaryl axis is configurationally unstable. The dimer ealapasamine C (**44**) is the first unsymmetric naphthylisoquinoline possessing two scarcely *cis*-configured halves. Besides their unique molecular architecture, the ealapasamines

A-C displayed high antiplasmodial activities with excellent half-maximum inhibition concentration values in the low nanomolar range. For example, ealapasamine C exhibited an  $IC_{50}$  value of 6 nm against K1 strain of *P. falciparum*, the latter being resistant to the standard drugs chloroquine and pyrimethamine, which makes **44** the most active naphthylisoquinoline alkaloid against this strain.

**B) *A. ealaensis* as a rich source of dimeric naphthylisoquinolines related to mbandakamine A and michellamine F**

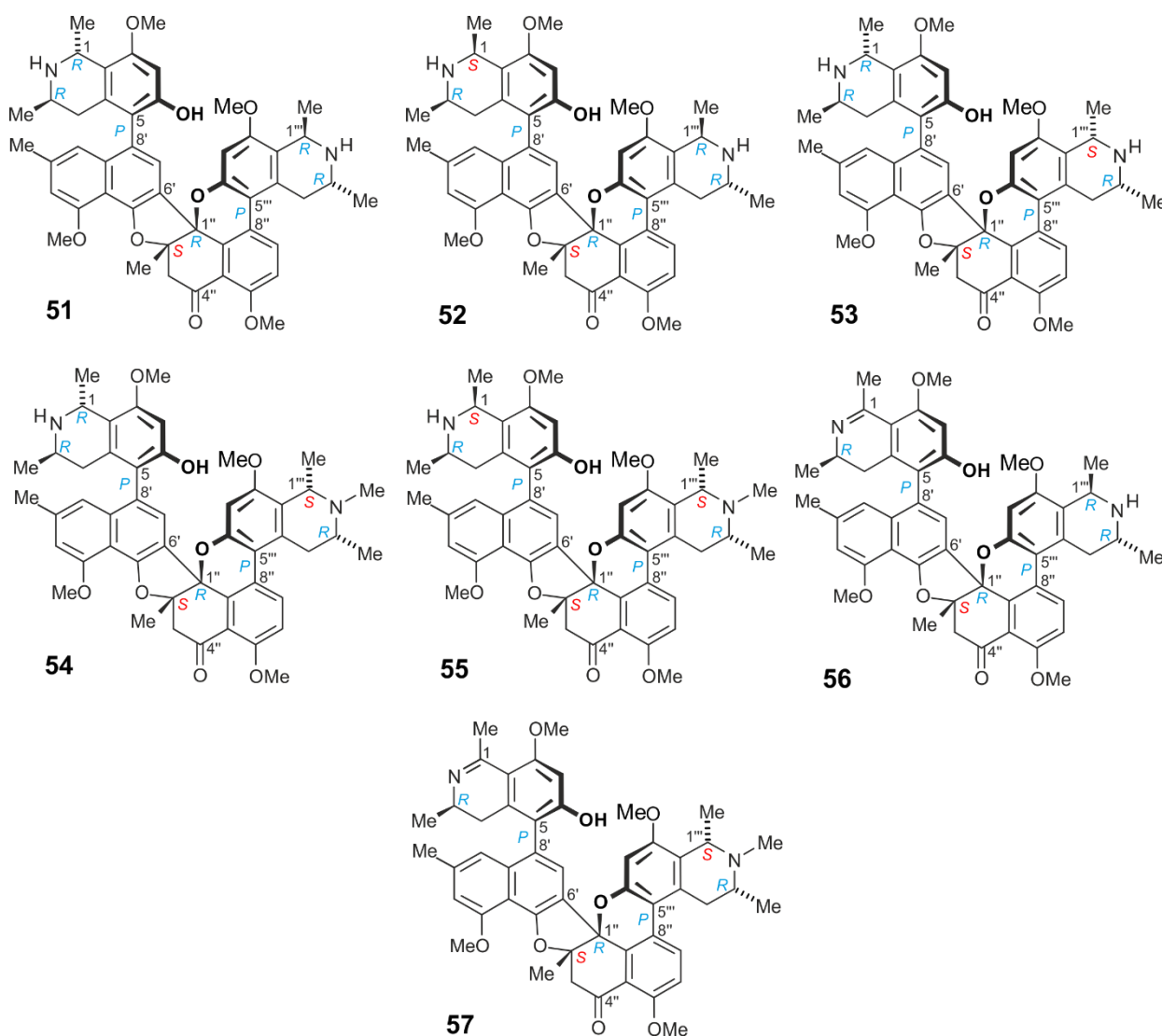
The known mbandakamine A (**32**) and three new dimeric mbandakamine-like compounds were isolated from leaf plant material of *A. ealaensis*, namely 1-*epi*-mbandakamine A (**47**), mbandakamine C (**48**), and mbandakamine D (**49**). Most unexpected was the discovery of michellamine F<sub>2</sub> (**50**), an unsymmetric derivative of the known michellamine F, suggesting that this tropical liana was a rich source of a broad variety of dimeric alkaloids.



These dimeric compounds showed excellent antiplasmodial activities, also against the resistant strain of K1. Especially interesting was the antiproliferative potential of **32**, **47**, and **48** on the multi-drug resistant strain CEM/ADR5000 of the human T-lymphoblastic leukemia cells. Considering, in addition, their very low degrees of resistance, these plant metabolites can be considered as promising lead compounds.

### C) Cyclombandakamines, a thrilling series of novel dimeric alkaloids from *A. ealaensis*

A thrilling series of seven novel dimeric alkaloids was discovered in leaf material of *A. ealaensis*. Their structural elucidation revealed an unprecedented structural array consisting of a twisted dihydrofuran-cyclohexenone-isochromene (pyrene) system. The compounds were named cyclombandakamine A (**51**), 1-*epi*-cyclombandakamine A (**52**), cyclombandakamine A<sub>3</sub> (**53**), cyclombandakamine A<sub>4</sub> (**54**), cyclombandakamine A<sub>5</sub> (**55**), cyclombandakamine A<sub>6</sub> (**56**), and cyclombandakamine A<sub>7</sub> (**57**). Their condensed cage-like polycyclic 'backbone' drastically reduced the degree of freedom in the molecule and stabilized the dimeric structures.

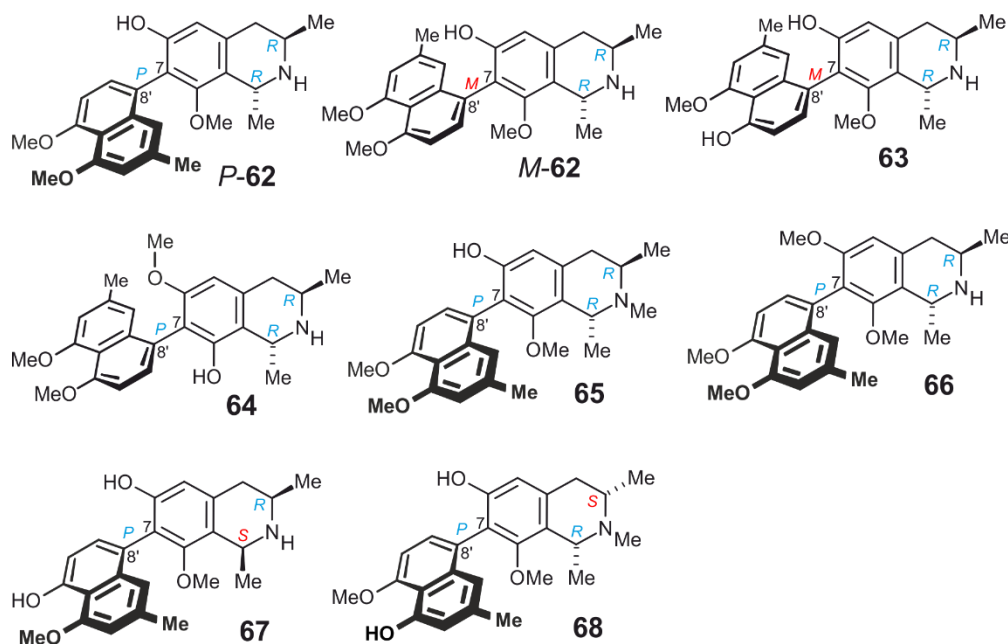


Apart from their unprecedented structural features, full of exclusivities within this class of natural products, the bioactivity indices against *P. falciparum* were lower as compared to the excellent ones for the open-chain mbandakamines. However, excellent antiproliferative activities were monitored emphasizing their attractiveness.

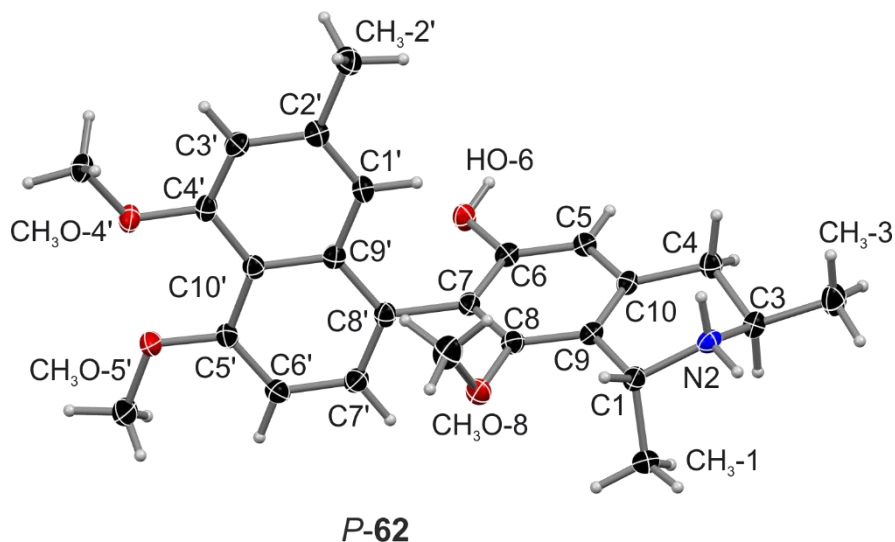
Furthermore, their probable biosynthetic origin from open-chain mbandakamine (*e.g.* **47**) was corroborated by biomimetic synthesis.

**D) Ealamines A-H, enthralling naphthylisoquinoline alkaloids with promising bioactivities from *A. ealaensis***

A series of eight new 7,8'-coupled naphthylisoquinoline alkaloids was discovered from the twigs and the leaves of the liana *A. ealaensis*, along with the known yaoundamine A and 6-*O*-demethylancistrobrevine A. They were named ealamine A (*P*-**62**), ealamine B (*M*-**62**), ealamine C (**63**), ealamine D (**64**), ealamine E (**65**), ealamine F (**66**), ealamine G (**67**), and ealamine H (**68**). This series consists of seven new natural products being the first representatives of this coupling type and displaying a so-called mixed Ancistrocladaceae- and Dioncophyllaceae-type tetrahydroisoquinoline scaffold, with an oxygen function at C-6 and *R* configuration at C-3.



An uncommon conformational behavior was noticed for these compounds and was closely investigated. Their relative and absolute structures were assigned by spectroscopic analyses (like NMR), oxidative degradation, and comparison with quantum-chemical calculations of the electronic circular dichroism (ECD) spectra. A single crystal analysis of ealamine A (*P*-**62**) confirmed all the conclusions drawn from NMR, ECD, quantum-chemical calculations and oxidative degradation.

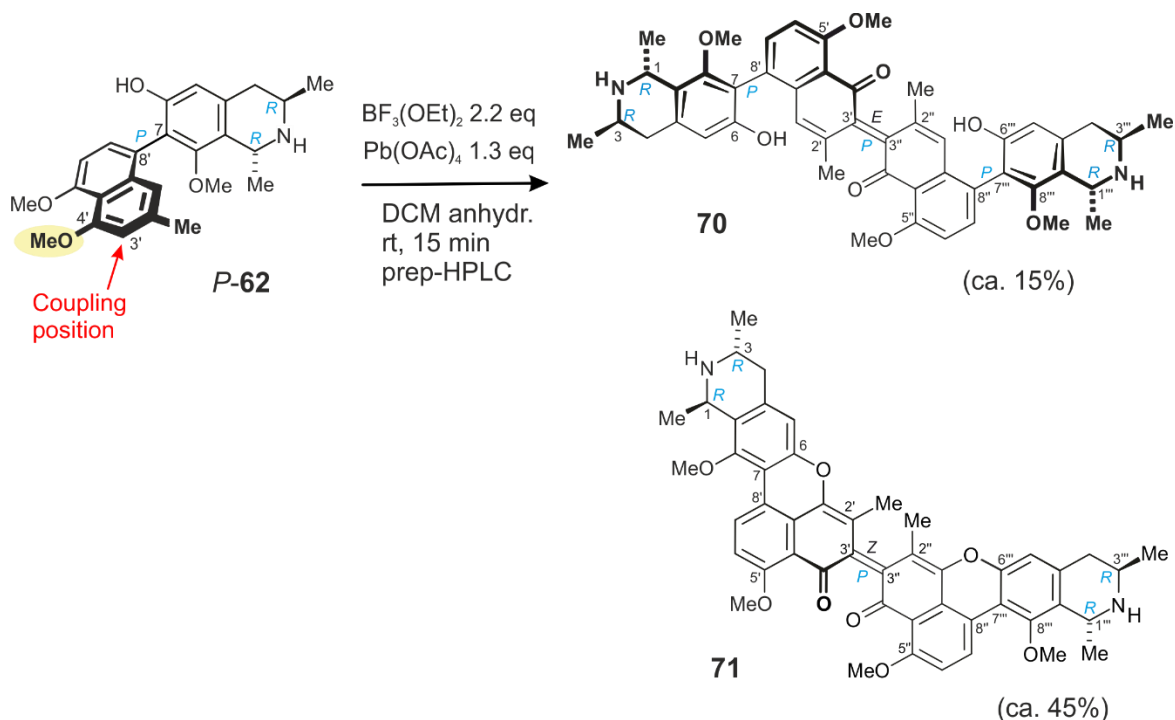


Moreover, the ealamines displayed moderate to good antiprotozoal activities against selected pathogens, and very good antiproliferative activities towards two human cancer cell lines. Ealamine C (**63**) proved to be the most active of these alkaloids against *P. falciparum in vitro*, with an  $IC_{50}$  value of  $0.84 \mu\text{M}$ . Compound **P-62** exhibited a very good antiproliferative potential on the human cervical HeLa cell line ( $IC_{50} = 6.68 \mu\text{M}$ ) and the T-lymphoblastic leukemia cells CCRF-CEM ( $IC_{50} = 8.04 \mu\text{M}$ ). These compounds might, therefore, be considered suited drug candidates.

#### ***E) Synthesis of ealajoziminone A and ealajoziminone B from the new ealamine A***

The synthesis of ealajoziminone A (**70**) and ealajoziminone B (**71**) was performed by phenol-oxidative coupling of ealamine A, using  $\text{Pb}(\text{OAc})_4$  and  $\text{BF}_3 \cdot \text{OEt}_2$  in  $\text{CH}_2\text{Cl}_2$ . They are the first diphenoquinones of the naphthylisoquinoline type possessing a chiral element at the central double bond, and surprisingly revealing high stability after column filtration and long storage in MeOH.



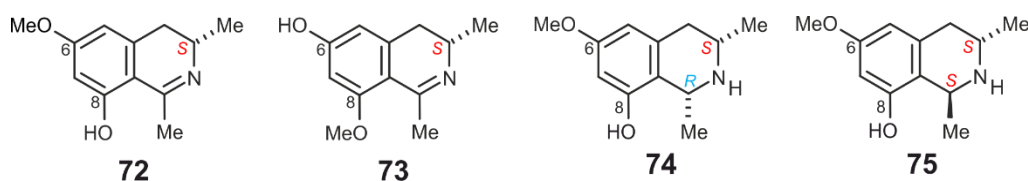


From their scaffold, these compounds may be good candidates for anticancer evaluations.

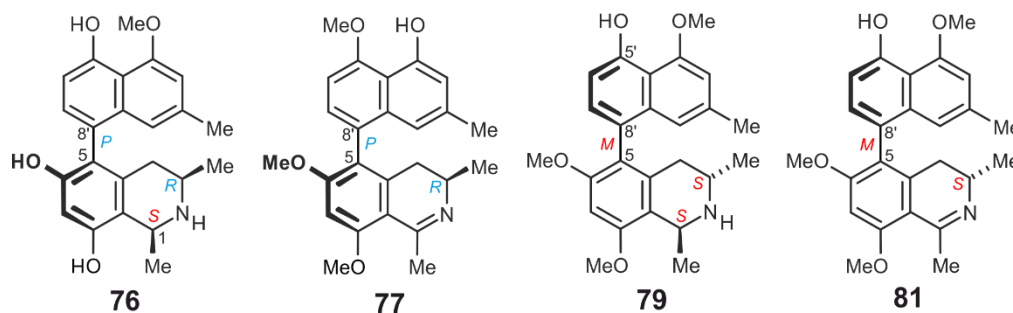
The research on these structures is ongoing.

#### F) *Ealaines A-D* and further monomeric naphthylisoquinoline alkaloids from *A. ealaensis*

From the twigs and the leaves of *A. ealaensis* four naphthalene-devoid isoquinoline alkaloids, namely ealaine A (**72**), ealaine B (**73**), ealaine C (**74**), and ealaine D (**75**) were isolated. After the first report on the occurrence of the naphthoic acid derivatives in the same plant species, the discovery of this type of compounds is of high biosynthetic significance and corroborates the unique biosynthesis of naphthylisoquinoline alkaloids.<sup>[184]</sup>



Additionally, a series of four new 5,8'-coupled monomeric naphthylisoquinolines were discovered from the same source as the ealaines, namely 1-*epi*-korupensamine A (**76**), ancistroealaine C (**77**), 5-*epi*-ancistroealaine B (**79**), ancistroealaine D (**81**). Their molecular features further explain the broad variety observed in the occurring dimers.



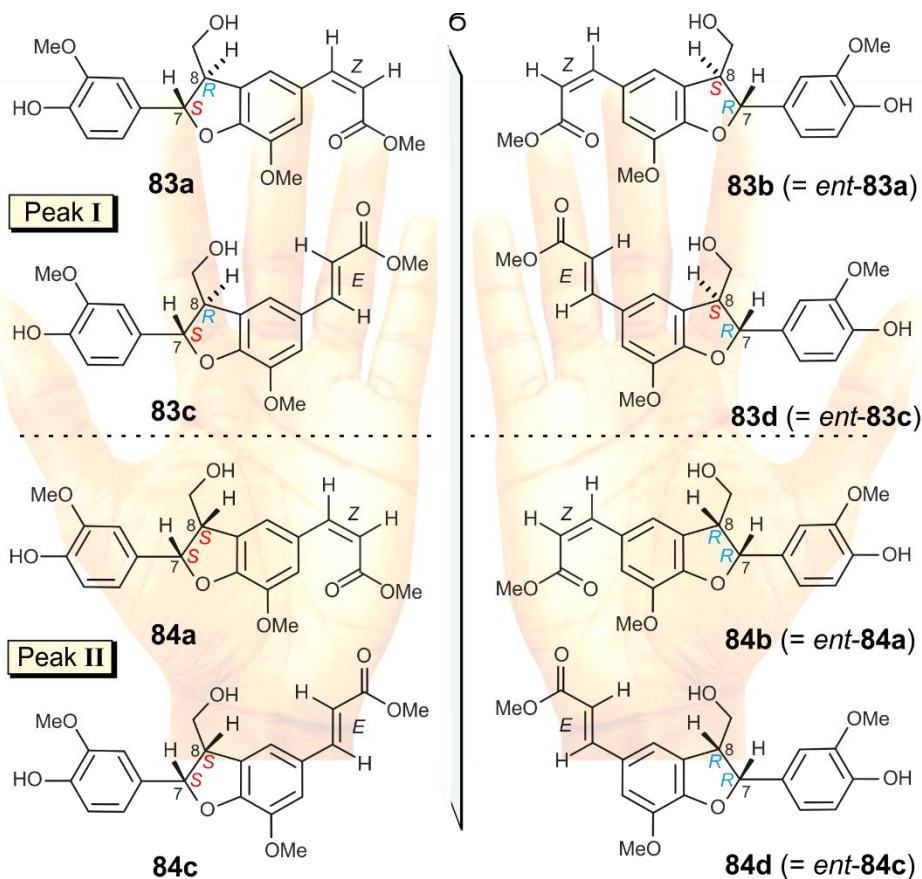
The biological evaluations of the alkaloids indicated no antiprotozoal and anticancer activities.

The monomeric naphthylisoquinoline alkaloids displayed good to moderate antiprotozoal activities. Compounds **79** and **81** exhibited pronounced activities against the two strains of *Trypanosoma brucei rhodesiense* and *T. cruzi*. They could therefore constitute promising therapeutic lead structures.

**G) Gardenifolins A-H, scalemic neolignans from *Gardenia ternifolia*: chiral resolution of all eight stereoisomers, configurational assignment, and antiproliferative potential**

From the tropical plant *Gardenia ternifolia* Schumacher and Thonn. (Rubiaceae), eight stereoisomeric 2,3-dihydrobenzo[b]furan neolignans, named gardenifolins A-H (**83a-d** and **84a-d**), were isolated and fully structurally characterized. Reversed-phase chromatography of a stem-bark extract afforded two peaks, *viz.* mixtures **I** and **II**, each one consisting of two diastereomers and their respective enantiomers. The metabolites were resolved and stereochemically analyzed by HPLC on a chiral phase in combination with electronic circular dichroism (ECD) spectroscopy, yielding single ECD spectra of all eight stereoisomers. The double-bond geometries (*E* or *Z*) of the gardenifolins A-H and their relative configurations at the stereogenic centers C-7 and C-8 in the dihydrofuran ring system (*cis* or *trans*) were assigned by 1D and 2D NMR methods, in particular, using NOE difference experiments, while the absolute configurations of the isolated enantiomers were established using ECD spectroscopy by applying the reversed helicity rule.

The individual pure gardenifolin isomers A–H showed most different cytotoxic effects against the human cancer HeLa cell line, with **83d** and **84a** displaying the highest activities, with IC<sub>50</sub> values of 21.0 and 32.5 μM, respectively.



Morphological experiments indicated that gardenifolin D (**83d**) induces apoptosis of HeLa cells at 25  $\mu\text{M}$ .

### H) Phytochemical and qualitative analysis of KILMA and N'Sansiphos®

A rational methodology was developed for qualitative assessment of less-investigated herbal medicinal products. A case study on the medical drug SIROP KILMA® was successfully conducted and demonstrates the applicability of the procedure.

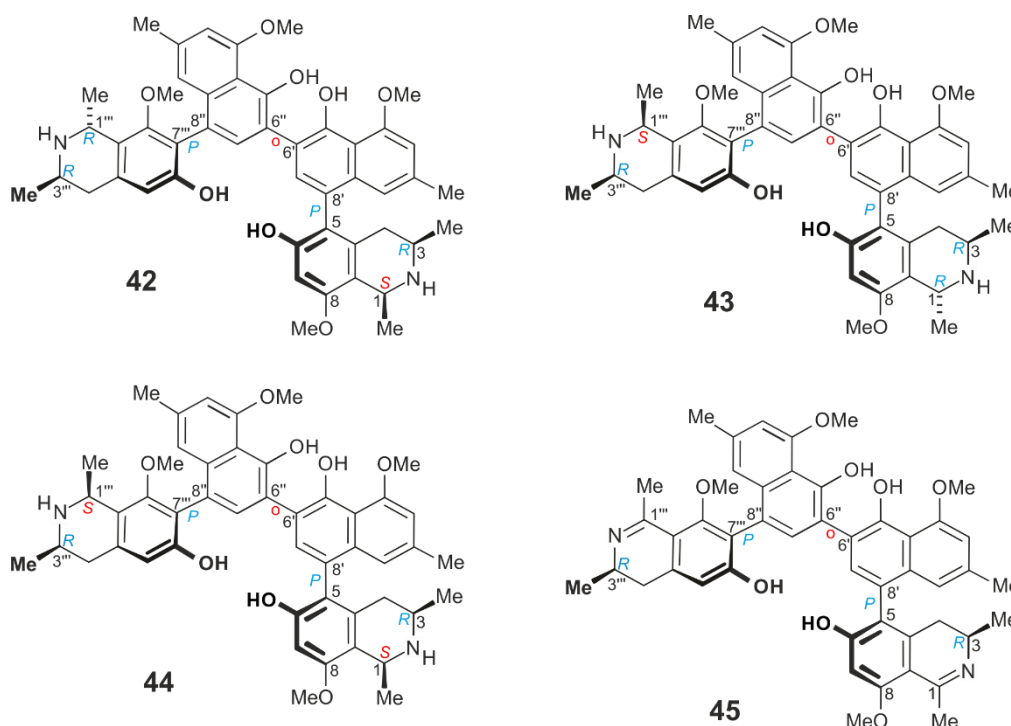
A most alarming discovery was made in the drug N'Sansiphos®, where abusive amounts of toxic preservatives were identified. The HPLC-DAD quantification of ethyl paraben and propyl paraben in the preparation revealed this worrying, which should impose immediate correction by the producer. Moreover, this bad product quality should also serve as a warning for the regulatory authorities and should emphasize the necessity to enable the quality assessment of all marketed herbal medicines.

### III.2. Zusammenfassung

Im Rahmen dieser Dissertation werden Einblicke in die strukturelle Vielfalt und das therapeutische Potenzial von pflanzlichen Sekundärmetaboliten gewährt. Die wichtigsten Aspekte der beschriebenen Ergebnisse sind hier zusammengefasst.

#### A) *Ealapasamine A-C, die ersten voll charakterisierten "gemischten" Heterodimere*

Drei ungewöhnliche heterodimere Naphthylisochinolin-Alkaloide, namentlich Ealapasamin A (**42**), Ealapasamin B (**43**) und Ealapasamin C (**44**), wurden aus den Blättern der tropischen Pflanze *Ancistrocladus ealaensis* J. Léonard isoliert. Diese "gemischten", konstitutionell unsymmetrischen Dimere sind die ersten stereochemisch vollständig aufgeklärten Kreuzkupplungsprodukte eines 5,8'- und eines 7,8'-gekuppelten Naphthylisochinolins, welche miteinander jeweils über die C-6'-Position des Naphthalin-Teils miteinander verknüpft sind. Dieser Kupplungstyp weist den höchsten bekannten Asymmetriegrad innerhalb dieser Alkaloid-Klasse auf. Die rein-synthetisch gewonnene Verbindung, Ealapasamin C<sub>2</sub> (**45**) wurde durch Oxidation von **44** erhalten.

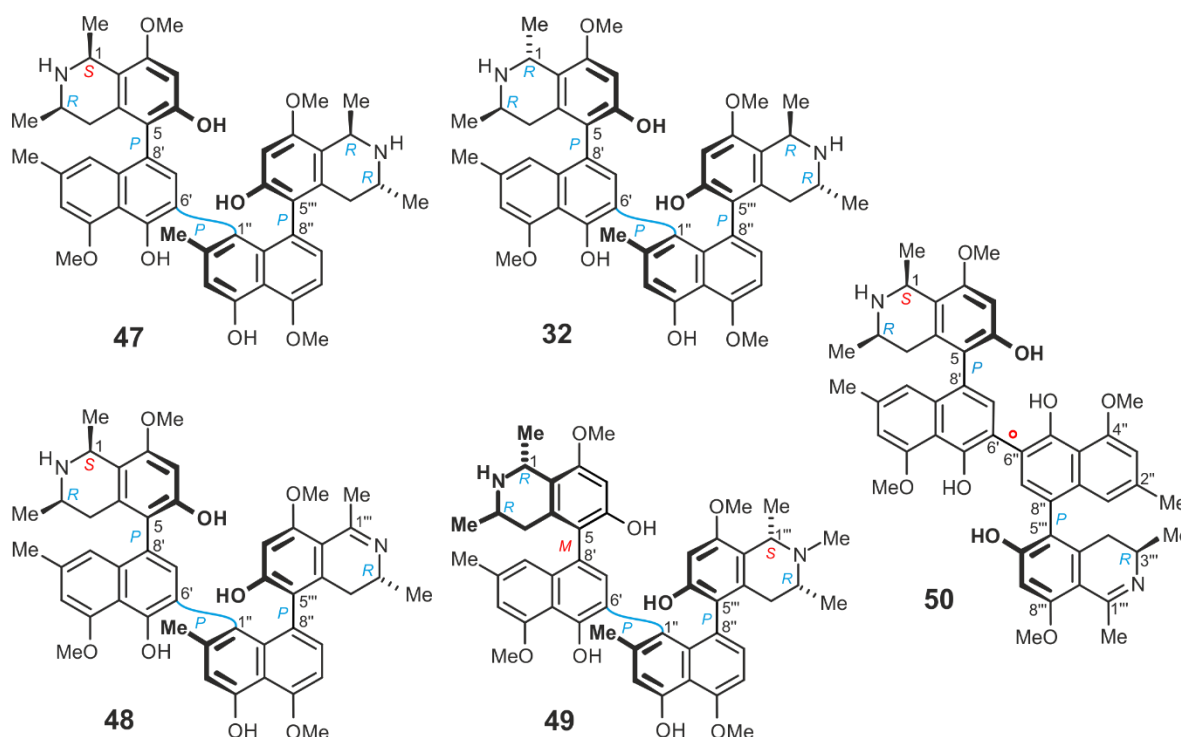


Die neuen Dimere **42-44** enthalten sechs Chiralitätselemente, vier stereogene Zentren sowie die zwei äußeren konfigurativen stabilen Biarylachsen, wohingegen die zentrale Biarylachse konfigurativen instabil ist. Das Dimer Ealapasamin C (**44**) ist das erste unsymmetrische

Naphthylisochinolin mit zwei beinahe *cis*-konfigurierten Hälften. Abgesehen von der einzigartigen molekularen Architektur zeigen die Ealapasamine A-C hohe antiplasmodische Aktivitäten mit exzellenten halbmaximalen Hemmkonzentrationswerten im niedrigen nanomolaren Bereich. Beispielsweise weist Ealapasamin C einen  $IC_{50}$  von 6 nm gegen den K1-Stamm von *P. falciparum* auf, welcher gegenüber den Standard-Arzneimitteln Chloroquin und Pyrimethamin resistent ist, wodurch **44** das aktivste Naphthylisochinolin-Alkaloid gegen diesen Stamm wird.

**B) *A. ealaensis* als zuverlässige Quelle von dimeren Naphthylisochinolin im Zusammenhang mit Mbandakamin A und Michellamine F**

Das bekannte Mbandakamin A (**32**) und die drei neuen dimeren Mbandakamin-ähnlichen Verbindungen 1-*epi*-mbandakamin A (**47**), Mbandakamin C (**48**), Mbandakamin D (**49**) wurden aus den Blättern von *A. ealaensis* isoliert. Besonders unerwartet war dabei die Entdeckung von Michellamin F<sub>2</sub> (**50**), einem unsymmetrischen Derivat des bekannten Michellamins F (**33**), was darauf hindeutet, dass diese tropische Liane eine reiche Quelle für eine breite Vielfalt von dimeren Alkaloiden ist.

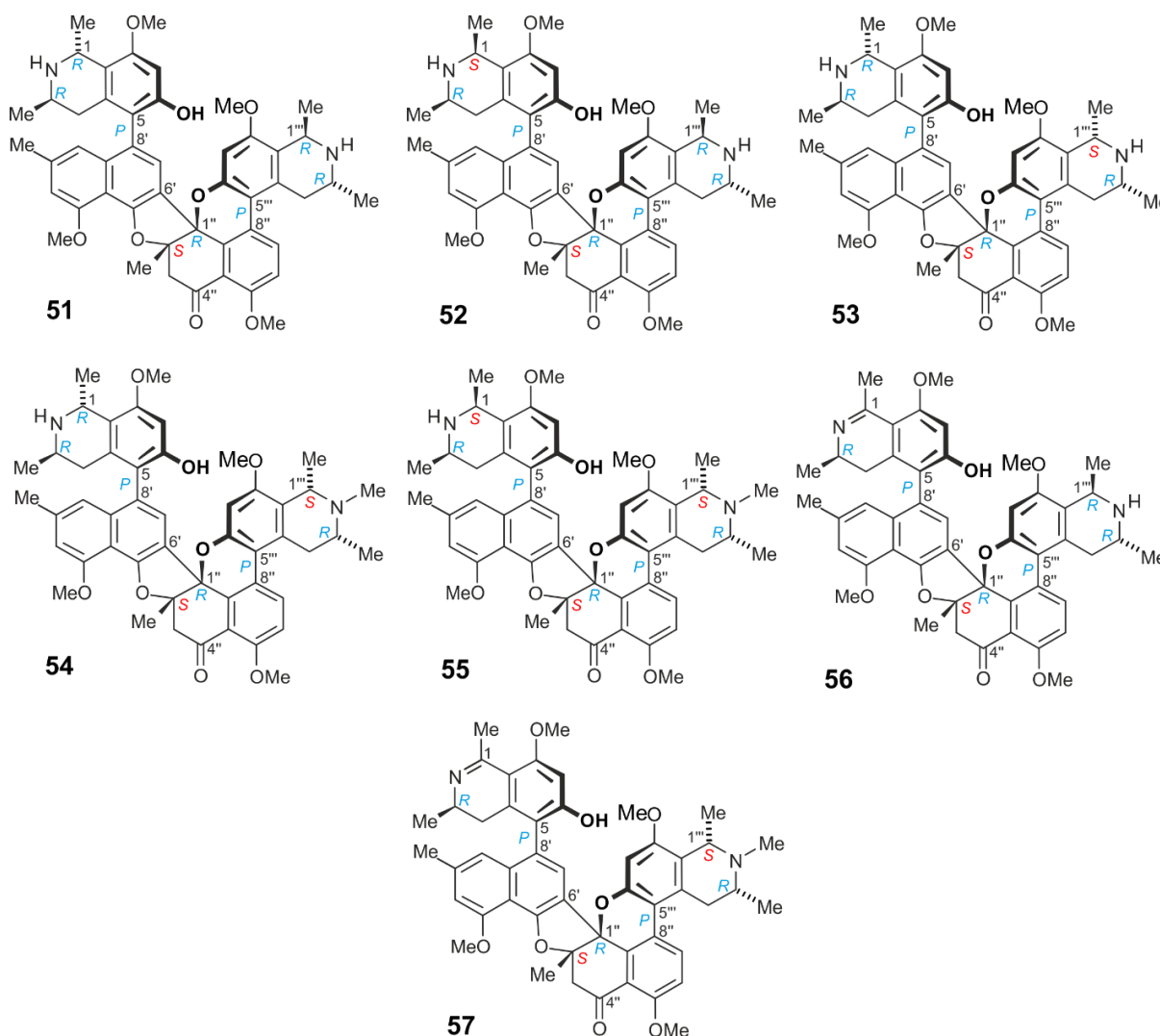


Diese dimeren Verbindungen zeigten eine ausgezeichnete antiplasmodische Aktivität, auch gegen den resistenten Stamm von K1. Besonders interessant war auch das antiproliferative Potential von **32**, **47** und **48** bezogen auf den multi-drug resistenten Stamm CEM/ADR5000

der humanen T-lymphoblastischen Leukämiezellen. Unter Berücksichtigung der ebenfalls sehr geringen Widerstandsgrade (degrees of resistance) können diese Pflanzenmetaboliten als vielversprechende Leitstrukturen betrachtet werden.

*C) Cyclombandakamine, eine spannende Reihe neuartiger dimerer Alkaloide aus A. ealaensis*

Eine spannende Serie von sieben neuartigen dimeren Alkaloiden wurde im Blattmaterial von *A. ealaensis* entdeckt. Die strukturelle Aufklärung lieferte ein beispielloses molekulares Gerüst, das aus einem verdrillten Dihydrofuran-Cyclohexenon-Isochromen-(pyren) -System bestand. Die Verbindungen wurden Cyclombandakamine A (**51**), 1-*epi*-Cyclombandakamine A (**52**), Cyclombandakamine A<sub>3</sub> (**53**), Cyclombandakamin A<sub>4</sub> (**54**), Cyclombandakamin A<sub>5</sub> (**55**), Cyclombandakamin A<sub>6</sub> (**56**) und Cyclombandakamin A<sub>7</sub> (**57**) getauft. Ihr kondensiertes käfigartiges polycyclisches "Rückgrat" reduziert den Freiheitsgrad im Molekül drastisch und stabilisiert die gesamte Dimerstruktur.



Abgesehen von ihren einmaligen strukturellen Merkmalen, gespickt mit Exklusivitäten innerhalb dieser Klasse von Naturprodukten, waren die Bioaktivitätsindizes gegen *P. falciparum* im Vergleich zu den ausgezeichneten Bioaktivitäten der offenkettigen Mbandakamine jedoch niedriger. Dafür wurden aber ausgezeichnete antiproliferative Aktivitäten beobachtet, welche wiederum die Attraktivität dieser Verbindungen unterstreichen.

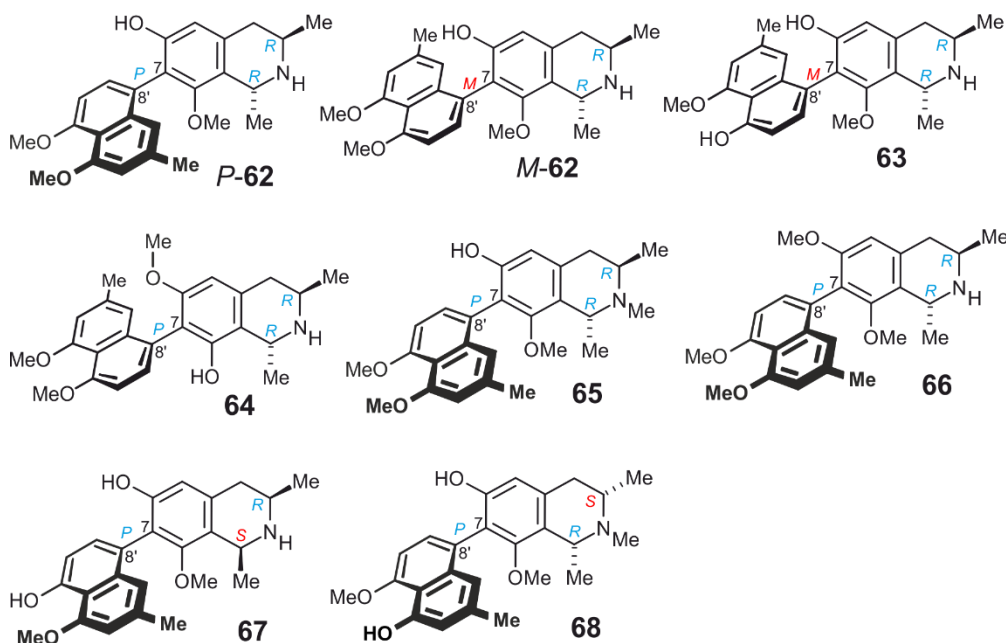
Darüber hinaus wurde ihr möglicher biosynthetischer Ursprung ausgehend vom offenkettigen Mbandakamin (z. B. **47**) durch biomimetische Synthese aufgezeigt.

#### ***D) Ealamine A-H, spannende Naphthylisochinolin-Alkaloide mit vielversprechenden Bioaktivitäten aus *A. ealaensis****

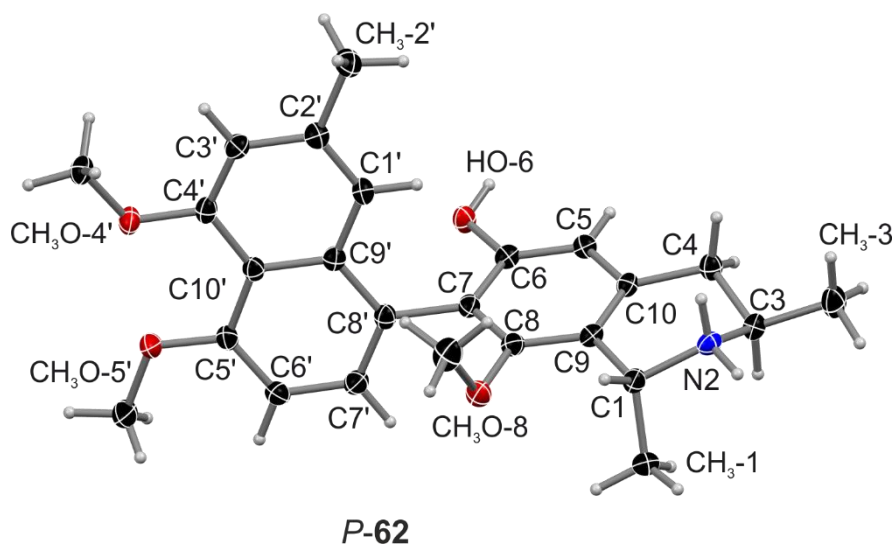
Eine Reihe von acht neuen 7,8'-gekuppelten Naphthylisochinolin-Alkaloiden wurde zusammen mit den bekannten Yaoundamin A (**17**) und 6-*O*-demethylancistrobrevin A (**69**) aus den Zweigen und den Blättern der Liane *A. ealaensis* isoliert. Die Verbindungen wurden Ealamin



A (*P*-62), Ealamin B (*M*-62), Ealamin C (63), Ealamin D (64), Ealamin E (65), Ealamin F (66), Ealamin G (67), und Ealamin H (68) genannt. Diese neuen Naturprodukte sind die ersten Vertreter dieses Kupplungstyps, und besitzen ein sogenanntes gemischtes Tetrahydrohydroisochinolin-Gerüst vom Ancistrocladaceae- und Dioncophyllaceae-Typ sowie eine Sauerstofffunktion an C-6 und die *R*-Konfiguration an C-3.



Die Verbindungen wiesen ein ungewöhnliches Konformationsverhalten auf, welches näher untersucht wurde. Ihre relativen und absoluten Konfigurationen wurden durch spektroskopische Analysen (wie NMR), oxidativen Abbau und den Vergleich mit quantenchemischen Berechnungen der ECD-Spektren (Elektronischer Circular dichroismus) zugeordnet. Eine Kristallanalyse von Ealamin A (*P*-62) bestätigte alle mittels NMR, ECD, quantenchemischer Berechnungen und oxidativem Abbau bestimmten Zuordnungen.

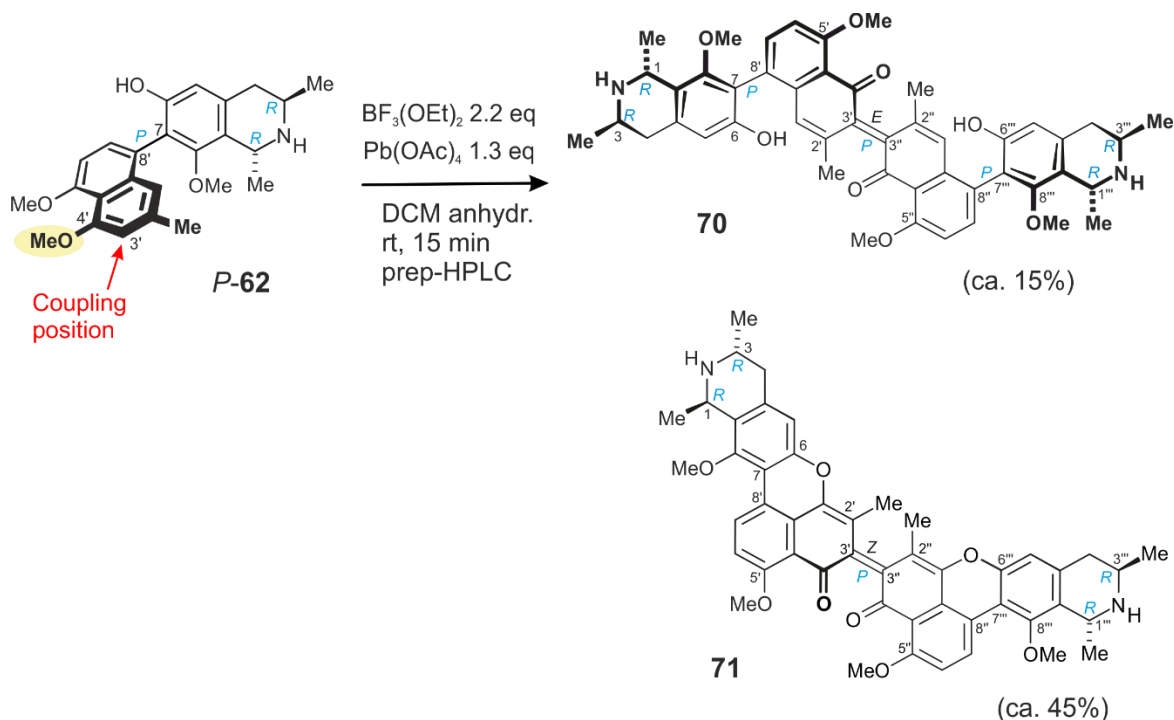




Darüber hinaus zeigten die Ealamine gute bis moderate antiprotozoale Aktivitäten gegen ausgewählte Pathogene und sehr gute antiproliferative Aktivitäten gegenüber zwei menschlichen Krebszelllinien. Ealamin C war das aktivste Alkaloid gegen *P. falciparum in vitro* mit einem  $IC_{50}$  von  $0,84 \mu\text{M}$ . Die Verbindung *P-62* zeigte ein sehr gutes antiproliferatives Potential auf der menschlichen zervikalen HeLa-Zelllinie ( $IC_{50} = 6,68 \mu\text{M}$ ) und den T-lymphoblastischen Leukämiezellen CCRF-CEM ( $IC_{50} = 8,04 \mu\text{M}$ ). Die Ealamine können daher auch als Arzneimittelkandidaten betrachtet werden.

### E) Synthese von Ealajoziminon A und Ealajoziminon B aus dem neuen Ealamin A

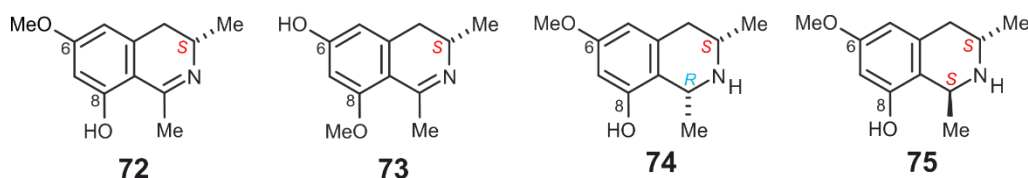
Die Synthese von Ealajoziminon A (**70**) und Ealajoziminon B (**71**) wurde durch Phenoloxidative Kupplung von Ealamin A unter Verwendung von  $\text{Pb}(\text{OAc})_4$  und  $\text{BF}_3 \cdot \text{OEt}_2$  in  $\text{CH}_2\text{Cl}_2$  durchgeführt. Die Verbindungen stellen die ersten Diphenochinone des Naphthylisochinolintyp dar. Sie besitzen ein chirales Element an der zentralen Doppelbindung und weisen eine überraschend hohe Stabilität nach Säulenfiltration und langer Lagerung in MeOH auf.



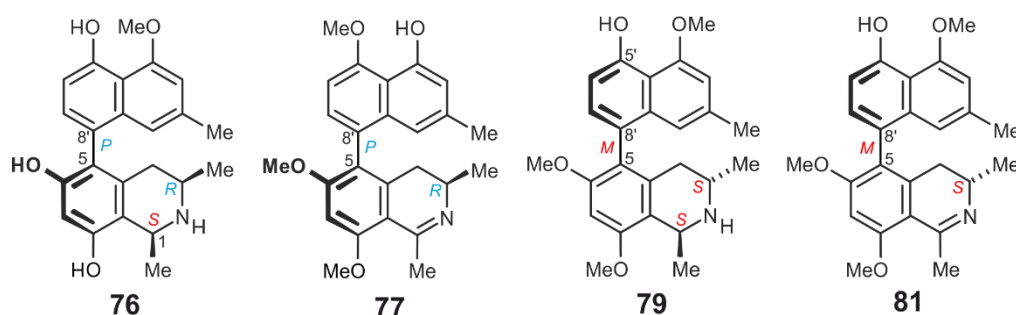
Aufgrund ihrer Molekülstruktur könnten diese Verbindungen gute Kandidaten für Antikrebsbewertungen werden. Diese Untersuchungen sind noch nicht abgeschlossen.

### F) Ealaine A-D und weitere monomere Naphthylisochinolin-Alkaloide aus *A. ealaensis*

Von den Zweigen und den Blättern von *A. ealaensis* wurden vier Naphthalin-freie Isochinolin-Alkaloide isoliert: Ealain A (**72**), Ealain B (**73**), Ealain C (**74**) und Ealain D (**75**). Die Entdeckung dieser Art von Verbindungen ist nach dem ersten Bericht über das Auftreten der Naphthoesäurederivaten in der selben Pflanzenart von hoher biosynthetischer Bedeutung und untermauert die einzigartige Biosynthese von Naphthylisochinolin-Alkaloiden.



Zusätzlich wurde aus der gleichen Quelle wie die Ealaine eine Reihe von vier neuen 5,8'-gekoppelten monomeren Naphthylisochinolin erhalten, welche 1-*epi*-korupensamin A (**76**), Ancistroealain C (**77**), 5-*epi*-Ancistroealain B (**79**) und Ancistroealaine D (**81**) sind. Ihre strukturellen Merkmale liefern eine weitere Erklärung für die breite Vielfalt, die bei den auftretenden Dimeren beobachtet wurde.



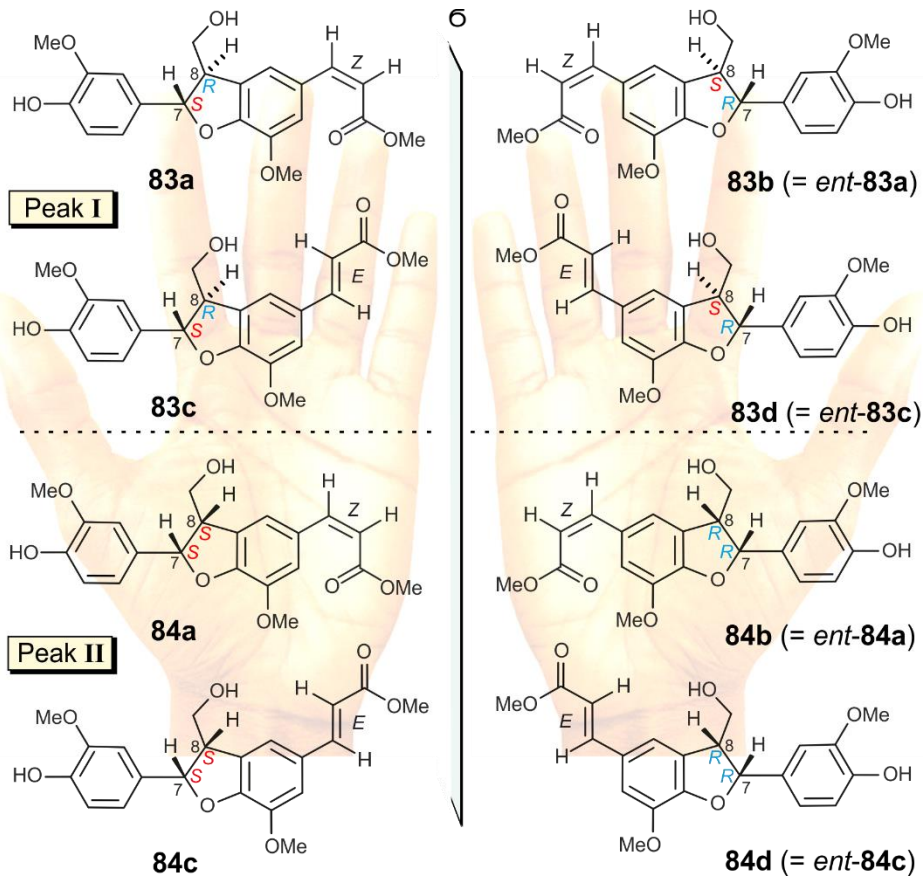
Die biologischen Auswertungen der Ealaine zeigten keine Antiprotozoen- und Antikrebsaktivitäten.

Die monomeren Naphthylisochinolin-Alkaloide zeigten gute bis moderierte antiprotozoale Aktivitäten. Die Verbindungen **79** und **81** zeigten ausgeprägte Aktivitäten gegen die beiden Stämme *Trypanosoma brucei rhodesiense* und *T. cruzi*, sie können daher vielversprechende therapeutische Leitstrukturen darstellen.

***G) Gardenifoline A-H, scalemische Neolignane aus *Gardenia ternifolia*: chirale Auflösung aller acht Stereoisomere, Konfigurationszuordnung und antiproliferatives Potential***

Aus der tropischen Pflanze *Gardenia ternifolia* Schumach. und Thonn. (Rubiaceae) wurden die Gardenifoline A-H (**83a-d** und **84a-d**) als Verbindungen von acht stereoisomeren 2,3-Dihydrobenzo[b]furan-Neolignanen isoliert und vollständig strukturell charakterisiert. Die *Reversed-phase*-Chromatographie eines Stammrindenextrakts ergab zwei Peaks **I** und **II**, welche Mischungen aus jeweils zwei Diastereomeren und ihren zugehörigen Enantiomeren darstellten. Diese Mischungen wurden getrennt und stereochemisch durch HPLC auf einer chiralen Phase analysiert, welche mit einem elektronischen Circular-Dichroismus-Spektrometer (ECD) gekoppelt war. Für alle acht Stereoisomere wurden dabei ECD-Spektren erhalten. Die Doppelbindungsgeometrien (*E* oder *Z*) der Gardenifoline A-H und ihre relativen Konfigurationen an den stereogenen Zentren C-7 und C-8 im Dihydrofuranringsystem (*cis* oder *trans*) wurden insbesondere durch 1D- und 2D-NMR-Verfahren unter Verwendung von NOE-Differenzversuchen bestimmt, während die absoluten Konfigurationen der isolierten Enantiomere durch ECD-Spektroskopie und Anwendung der umgekehrten Helicitätsregel ermittelt wurden.

Die einzelnen reinen Gardenifolin-Isomere A-H zeigten die unterschiedlichsten zytotoxischen Effekte gegen die menschliche Krebs-HeLa-Zelllinie, wobei **83d** und **84a** die höchsten Aktivitäten mit IC<sub>50</sub> von 21,0 bzw. 32,5 µM zeigten.



Morphologische Experimente zeigten, dass Gardenifolin D (**83d**) die Apoptose von HeLa-Zellen bei 25  $\mu\text{M}$  induziert.

### H) Phytochemische und Qualitative Analyse von KILMA und N'Sansiphos

Für die Qualitätsbewertung von weniger untersuchten pflanzlichen Arzneimitteln wurde eine einfache, rationale Methodik entwickelt. Am Fallbeispiel des Medikaments SIROP KILMA<sup>®</sup> wurde die Anwendbarkeit des Verfahrens erfolgreich demonstriert.

Die alarmierendsten Entdeckungen wurden bei dem Produkt N'Sansiphos<sup>®</sup> gemacht, in welchem sehr hohe Mengen an toxischen Konservierungsmitteln nachgewiesen wurden. Die Quantifizierung von Ethylparaben und Propylparaben in N'Sansiphos<sup>®</sup> ist besorgniserregend, und müsste eine sofortige Korrektur durch den Hersteller als Konsequenz haben. Darüber hinaus sollte diese schlechte Produktqualität auch die Regulierungsbehörden auf die Notwendigkeit aufmerksam machen, die Qualitätsbewertung aller vermarkteten pflanzlichen Arzneimittel zu ermöglichen.

*“Look deep into nature, and then you will understand everything better”<sup>[273]</sup>*

**Albert Einstein**

## **IV. Experimental Section**

## IV.1. General Experimental Aspects

### IV.1.1. Analytical Instruments

#### *High performance liquid chromatography (HPLC):*

The analytical and semi-preparative HPLC-DAD separations were performed on a Jasco<sup>®</sup> LC-2000Plus Series System (Gross-Umstadt, Germany). Comprising a DG-1580 degasser, an LG-1580 mixer, a PU-1580 pump, an AS-1555 autosampler (100- $\mu$ L loop for the analytical scale), a manual injector with a 1-mL loop (for isolation purposes), a CO-1560 column thermostat, and an MD-1510 or MD-2010 Plus diode-array detector (DAD). The chromatograms were acquired in the range from 200 to 680 nm. The data acquisition and processing were monitored with the Chrompass software (Jasco<sup>®</sup>).

#### *Liquid chromatography hyphenated to electrospray ionization mass spectrometry (LC-ESIMS):*

The LC-MS analyses were performed on an Agilent<sup>®</sup> 1100 Series System, equipped with a binary high-pressure mixing pumps with a degasser module, an autosampler with a Gilson 819 injection module (50- $\mu$ L loop), a Gilson 215 liquid handler, and an 1100 series photodiode array (PDA) detector (Agilent Technology, Germany). This LC system was linked to an Agilent 6300 Ion-Trap mass spectrometer with an electrospray ionization interface (Agilent Technology, Germany). The ion trap detector was equipped with an ESI source operating under the following parameters: capillary temperature at 350 °C, 3500 V as the ESI voltage, and N<sub>2</sub> as the heating gas.

#### *Gas chromatography coupled to a mass spectrometry detector (GC-MS):*

GC-MSD analyses of the products of oxidative degradation were carried out on a GCMS-QP2010 Systems (Shimadzu, Germany). These experiments were performed based on an established protocol.<sup>[113]</sup>

#### *High resolution electrospray mass spectrometry (HRESIMS):*

High resolution electrospray mass spectrometry (HRESIMS) measurements were performed on a Bruker Daltonics micrOTOF-focus mass instrument. A Bruker Daltonics micrOTOF focus was used for the high-resolution electrospray mass spectroscopy.

***Nuclear magnetic resonance spectroscopy (NMR):***

1D and 2D NMR analyses were acquired on an AMX 400 and DMX 600 Bruker spectrometers. Deuterated solvents were used, *e.g.* methanol- $d_4$  ( $\delta_H$  3.31 and 4.78, and  $\delta_C$  49.15 ppm) for most alkaloids. The chemical shifts ( $\delta$ ) and the coupling constants ( $J$ ) were expressed in parts per million (ppm) and in Hertz (Hz), respectively. NMR signal multiplicities are provided as singlet (s), pseudo-singlet (ps), doublet (d), doublet of doublets (dd), quartet (q), or multiplet (m). The NMR spectra were acquired with TopSpin 3.2 (Bruker Daltonics, Germany). The spectra were mainly processed with TopSpin 3.2 (Bruker, Germany) and ACD/NMR Processor 12.1 (Academic Edition).

***Electronic circular dichroism (ECD) and electronic optical rotary dispersion (ORD-E):***

The ECD and the ORD-E spectra were acquired on a Jasco<sup>®</sup> J-715 spectropolarimeter. The samples were measured – under nitrogen atmosphere – offline in different cells (mostly of 1 mm size) dissolved in UV grade solvents. For online ECD measurements, the hyphenation with HPLC-DAD was necessary. In this case, a baseline correction was performed by subtraction of the spectra of the eluent with proportions corresponding to the retention time of each peak analyzed. The data were visualized by the freely available SpecDis, version 164.<sup>[269]</sup>

***Ultra-violet spectroscopy (UV):***

A Shimadzu<sup>®</sup> UV-1800 spectrophotometer was used to perform in triplicate offline UV measurements. The solvents used were of UV grade. The spectral data was visualized by SpecDis, version 164.<sup>[269]</sup>

***Optical rotation (symbolized by  $[\alpha]_d$ ):***

The optical rotation values ( $[\alpha]_d$ ) were determined on a Jasco<sup>®</sup> P-1020-polarimeter operating with sodium-D-line light source ( $\lambda = 589$  nm). The values were means of twenty triplicates for each compound. 1,1'-Bi-2-naphthol enantiomers were used as references.

***Mill:***

A Retsch<sup>®</sup> SM1 (Haan, Germany) was used for grinding plant material.

***Mechanical shaker for maceration overnights:***

For maceration purposes, a Bottmingen<sup>®</sup> CH-4103 mechanical shaker was used, operating at the frequency of 160 rpm (rotation per minutes).



***Rotary evaporator:***

A BÜCHI® Rotavapor R-3 was used for solvent evaporation under vacuum.

***HPLC quality water source:***

Ultrapure water was obtained from an Elga® Purelab Classic system.

***Scales:***

The analytical scale was a Sartorius® Research R160 P (Goettingen, Germany).

**IV.1.2. Standardized Experiments*****Preparative Liquid Chromatography (PLC):***

Prior to fractionation on silicagel or RP<sub>18</sub> columns, TLC was performed. Silica gel 60 F<sub>254</sub> plates were purchased from Merck®. The pre-coated TLC-sheets ALUGRAM® RE-18W/UV<sub>254</sub> were used for reversed phase TLC (0.15 mm of layer thickness). TLC plates were visualized using Draggendorff reagent and/or 5% sulphuric acid in MeOH, or an UV-lamp at 254 and 365 nm. A hair dryer was used gently on the plates.

Sephadex LH-20 (Sigma-Aldrich®) was used for gel chromatography of some fractions.

***Ruthenium(VIII)-mediated oxidative degradation experiments for NIQs:***

Periodate degradation catalyzed by Ruthenium(VIII) was performed on ca. 0.5 mg of a monomer and 1.0 mg of each dimer, leading to amino acids which, after treatment with MeOH/HCl and *R*- $\alpha$ -methoxy- $\alpha$ -trifluoromethylacetyl chloride (*R*-MTPA-Cl, prepared from *S*-MTPA) for derivatization by a solution of Mosher's chloride in dichloromethane and triethylamine, then analyzed by GC-MSD as described by our group earlier.<sup>[113]</sup>

***Computational analysis:***

The quantum chemical calculations of the ECD spectra and some conformational analyses were performed by Dr. Torsten Bruhn, using ORCA and Gaussian09.<sup>[119, 171, 187]</sup> TDDFT was used for the simulation of the UV and the ECD properties,<sup>[119]</sup> and the calculated spectra were compared to the experimental ones using SpecDis.<sup>[269]</sup> Further DFT-based investigations were achieved with the B3LYP-D3/def2-SVP, B3LYP-D3/def2-TZVP or B97-D3/def2-TZVP methods using ORCA.<sup>[171, 187]</sup>

All the graphics were processed and harmonized using CorelDraw® version X8.

***Antiprotozoal biological evaluations:***

The *in vitro* antiprotozoal activities of the compounds were evaluated against the pathogens *Plasmodium falciparum* (NF54 and K1 strains), *Trypanosoma cruzi* (amastigotes of Tulahuen C4 strain), *Trypanosoma brucei rhodesiense* (trypomastigotes of STIB 900 strain), and *Leishmania donovani* (amastigotes of MHOM-ET-67/L82 strain), and the cytotoxicity on mammalian host cells (rat skeletal myoblast L6 cells), according to a well-established established protocol.<sup>[162]</sup> These tests were performed independently by our cooperation partners from the Swiss Tropical and Public Health Institute, based in Basel (Switzerland) ensuring the reliability of the results.

***Antiproliferative evaluations:***

These biological tests were performed using the human leukemia cell line CCRF-CEM (T-lymphoblasts) according to the reported protocol.<sup>[270]</sup>

Another anticancer test system was used against the human cervical HeLa adenocarcinoma.<sup>[271]</sup> A Cell Counting Kit-8 (Dojindo Molecular Technologies, Inc., USA) was applied to determine the viability of cells in the presence or absence of tested compounds. The HeLa cells were maintained in standard DMEM with 10% FBS supplement, 0.1% NaHCO<sub>3</sub>, and 1% of an antibiotic-antimycotic solution. For cytotoxicity evaluation, exponentially growing cells were harvested and distributed in 96-well plates ( $2 \times 10^3$ /well) in DMEM at 37 °C under an atmosphere of humidified 5% CO<sub>2</sub> and 95% air for 24 h. After washing the cells with PBS, the medium was changed to serially diluted test samples in DMEM, with the control and blank in each plate. After 72 h of incubation, the cells were washed twice with PBS and 100 µL of a DMEM solution containing 10% WST-8 cell counting solution was added to each well. After incubation for 3 h, the absorbance at 450 nm was measured (PerkinElmer EnSpire multilabel reader). Cell viability (in %) was calculated from the mean values from three wells using the given equation:

$$\text{Cell viability (\%)} = [(\text{Abs}_{(\text{test sample})} - \text{Abs}_{(\text{blank})}) / (\text{Abs}_{(\text{control})} - \text{Abs}_{(\text{blank})})] \times 100\%$$

***Solvents quality and source:***

All organic solvents used, during our own experiments without specific indication, were of analytical grade and purchased indistinctively from Merck® and Sigma-Aldrich®.

**IV.1.3. Samples: Source and Identification*****Plant material:***

Plant materials of *Ancistrocladus ealaensis* J. Léonard (Ancistrocladaceae) were collected in the Botanical Garden of Eala (Mbandaka, Democratic Republic of the Congo), in August 2008, and identified by Dr. J. Schlauer, University of Würzburg. Some leaf material was additionally collected in August 2015 by Mr. B.K. Lombe (GPS coordinates 00°03.605N, 018°18.886E). The material of 2015 was authenticated additionally by LC-DAD-MS to contain the same metabolites as the one of 2008. Voucher specimens are available at the Herbarium Bringmann at the Institute of Organic Chemistry, University of Würzburg (no. 43 and 57).

Stem barks of *Gardenia ternifolia* Schumach. & Thonn. (Rubiaceae) were harvested in February 2012 in the area of Kimwenza near Kinshasa (Democratic Republic of the Congo). The plant material was identified by Mr. N. Lukebakio of the *Institut National pour l'Etude et la Recherche Agronomiques (INERA)*, of the University of Kinshasa, where a voucher specimen was deposited under the number 843.

As for *G. ternifolia*, stem barks of *Crossopteryx febrifuga* Benth. (Rubiaceae) and the leaf material of *Lantana camara* L. (Verbenaceae) were also collected, at the same place, identified by Mr. N. Lukebakio, and kept under the voucher numbers 175 and 3653, respectively.

*Garcinia kola* Heckel seeds (the so-called bitter kola) were bought on the marketplace in Kinshasa, in 2014. The same botanist performed the identification of the species.

***Herbal preparations:***

Three batches of SIROP KILMA® (syrup) were purchased in February 2012 from the phytoproducer.<sup>[259]</sup>

Three batches of N'Sansiphos® (syrup) were purchased in 2015 at the phytoproducer.

## IV.2. Ealapasamines, the First Fully Characterized 'Mixed' Heterodimers Naphthylisoquinoline Alkaloids from *A. ealaensis*

### IV.2.1. Extractions, Isolation, and HPLC conditions

#### IV.2.1.1. Extraction and fractionation

The air-dried powder of the leaves (600 g) was macerated in methanol, under mechanical shaking (160 RPM) for 24 hours, after filtration the marc was further macerated until exhaustion. The 24h-macerates were mixed after filtration, and evaporated to a viscous solution. The methanolic extract was dissolved in water to permit the precipitation of the water-insoluble chlorophyll. The aqueous layer was partitioned first with *n*-hexane until the upper phase was cleared of residual chlorophyll, and then exhaustively extracted with dichloromethane. The organic layer was evaporated to dryness to obtain the metabolites-rich fraction A. The fraction A was subsequently submitted to preparative liquid chromatography using C<sub>18</sub>-reversed phase. The mobile phase consisted of acetonitrile (MeCN) and ultrapure water containing 0.05% TFA (trifluoroacetic acid). Elution was performed using a gradient from 0 to 50% H<sub>2</sub>O in MeCN and resulted in 100 fractions. Further fractionation of A<sub>77</sub> to A<sub>88</sub> was performed on five C<sub>18</sub>-SPE cartridges in series (Sep-Pak C<sub>18</sub> Plus Light Cartridge, 130 mg, 55-105 μm) using the same elution conditions. This led to several sub-fractions enriched with dimeric-alkaloids which were submitted to semi-preparative HPLC to isolate the dimers.

#### IV.2.1.2. Isolation and semi-preparative HPLC conditions

The isolation from alkaloid-enriched fractions was performed on a Symmetry<sup>®</sup> Prep-C<sub>18</sub> column (Waters, 300 × 19 mm, 7 μm) with the mobile phase consisting of A (H<sub>2</sub>O, 0.05% TFA), B (MeCN, 0.05% TFA), at a flow rate of 10 mL min<sup>-1</sup>. Further purification on a Chromolith<sup>®</sup> SemiPrep RP-18e column (100 x 10 mm) afforded the pure dimeric alkaloids, using a gradient elution and a mobile system as described above for the Symmetry<sup>®</sup> Prep column, but with MeCN (B) replaced by MeOH (C), at the same flow rate.

The fractionation on reversed phase silica gel was guided by LC-MS searching for masses hinting at the presence of dimeric alkaloids. The compounds of interest were distributed unequally between the fractions A<sub>77</sub> to A<sub>88</sub>. For the isolation of **42-44**, the fractions of interest were submitted to semi-preparative HPLC on a Symmetry<sup>®</sup> Prep-C<sub>18</sub> column using a linear gradient at a flow rate of 10 mL min<sup>-1</sup>: 0-13 min: 10-20% of B, 37 min: 45% of B, 39 min: 50%

of B, 42 min: 100% of B, 45 min: 100% of B. Some of the collected peaks (still impure, but containing **42-44**) required additional purification steps, which were performed by HPLC on a Chromolith® SemiPrep RP-18e column (100 x 10 mm) using a gradient solvent system consisting of A (H<sub>2</sub>O, 0.05% TFA) and C (MeOH, 0.05% TFA) at a flow rate of 10 mL min<sup>-1</sup>: 0-2 min: 10% of C, 8 min: 30% of C, 11 min: 30% of C, 11.2 min: 35% of C, 16 min: 35% of C, 20 min: 40% of C, 25 min: 45% of C, 27 min: 100% of C, 30 min: 100%, to yield 5 mg of ealapasamine A (**42**), 1.5 mg of ealapasamine B (**43**), and 3.5 mg of ealapasamine C (**44**).

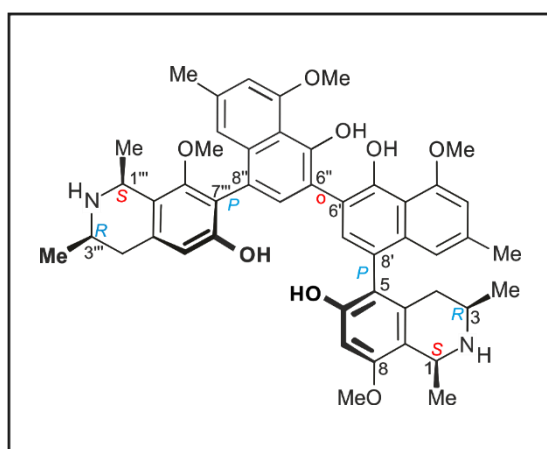
### IV.2.1.3. Isolated ealapasamines

#### *Ealapasamine A (42)*

White amorphous powder (10.1 mg).

$[\alpha]_D^{23} = -21$  ( $c = 0.09$ , MeOH).

UV (MeOH):  $\lambda_{\max}$  ( $\log \epsilon$ ) = 205 (1.32), 217 (0.91), 230 (1.09), 257 (0.54), 262 (0.54), 297 (0.24), 315 (0.28), 322 (0.28), 329 (0.29), 338 (0.28), 344 (0.29) nm.



ECD (MeOH,  $c$  0.02):  $\lambda_{\max}$  ( $\log \epsilon$  in cm<sup>2</sup> mol<sup>-1</sup>) = 195 (+10.1), 200 (+2.83), 210 (-7.81), 221 (-1.71), 227 (-3.51), 234 (-3.34), 240 (-3.32), 250 (+1.36), 267 (-11.01), 290 (-0.09), 303 (-2.96), 351 (+1.1), 395 (-0.6) nm.

ORD (MeOH,  $c$  0.02):  $\lambda_{\max}$  ( $\log \epsilon$  in cm<sup>2</sup> mol<sup>-1</sup>) = 200 (+5.3), 204 (+9.0), 207 (+7.7), 219 (-0.4), 226 (+1.8), 238 (+0.6), 244 (-1.4), 259 (+6.7), 279 (-6.6), 298 (-1.4), 317 (-4.7), 348 (-1.2), 363.8 (0.0), 380 (-0.5), 404 (-1.0) nm.

HRESIMS  $m/z$  785.37804 [M+H]<sup>+</sup> (calcd for C<sub>48</sub>H<sub>53</sub>N<sub>2</sub>O<sub>8</sub>, 785.37964).

<sup>1</sup>H NMR (CD<sub>3</sub>OD, 600 MHz):  $\delta_H$  (ppm) = 7.39 (s, 1H, H-7''), 7.28 (s, 1H, H-7'), 6.88 (d,  $J = 1.18$  Hz, 1H, H-1''), 6.87 (d,  $J = 1.22$  Hz, 1H, H-3'), 6.86 (d,  $J = 1.16$  Hz, 1H, H-3''), 6.80 (d,  $J = 1.18$  Hz, 1H, H-1'), 6.62 (s, 1H, H-7), 6.57 (s, 1H, H-5'''), 4.74 (q,  $J = 6.77$  Hz, 1H, H-1'''), 4.65 (q,  $J = 6.63$  Hz, 1H, H-1), 4.11<sup>a</sup> (s, 3H, 4'-OCH<sub>3</sub>), 4.11<sup>b</sup> (s, 3H, 4''-OCH<sub>3</sub>), 3.90 (s, 3H, 8-OCH<sub>3</sub>), 3.86 (m, 1H, H-3'''), 3.28 (m, 1H, H-3), 3.19 (s, 3H, 8'''-OCH<sub>3</sub>), 3.15 (dd,  $J = 4.81$ ,

17.58 Hz, 1H, 4'''-H<sub>eq</sub>), 2.88 (dd,  $J = 11.72, 17.78$  Hz, 1H, 4'''-H<sub>ax</sub>), 2.64 (dd,  $J = 3.35, 17.78$  Hz, 1H, 4-H<sub>eq</sub>), 2.36 (s, 1H, 2'-CH<sub>3</sub>), 2.35 (s, 1H, 2''-CH<sub>3</sub>), 2.27 (dd,  $J = 12.14, 17.37$  Hz, 1H, 4-H<sub>ax</sub>), 1.76 (d,  $J = 6.70$  Hz, 3H, 1-CH<sub>3</sub>), 1.63 (d,  $J = 6.90$  Hz, 3H, 1'''-CH<sub>3</sub>), 1.51 (d,  $J = 6.87$  Hz, 3H, 3'''-CH<sub>3</sub>), 1.24 (d,  $J = 6.52$  Hz, 3H, 3-CH<sub>3</sub>).

<sup>13</sup>C NMR (CD<sub>3</sub>OD, 150.9 MHz):  $\delta_C$  (ppm) = 158.5 (C-8), 158.2 (C-4'), 157.9 (C-4''), 157.6 (C-6'''), 157.5 (C-8'''), 157.1 (C-6), 152.6 (C-5'), 152.5 (C-5''), 137.6 (C-2'), 137.3 (C-2''), 136.9 (C-9'), 136.4 (C-9''), 135.3 (C-10), 135.2 (C-7'''), 134.7 (C-7'), 132.9 (C-10'''), 123.7 (C-8'), 122.0 (C-8''), 121.0 (C-7'''), 120.3 (C-6''), 120.2 (C-6'), 119.9 (C-5), 119.8 (C-1''), 119.1 (C-1'), 118.5 (C-9'''), 115.3 (C-10'), 114.9 (C-10''), 114.1 (C-9), 111.2 (C-2'''), 108.0 (C-3'), 107.9 (C-3''), 99.3 (C-7), 60.9 (8'''-OCH<sub>3</sub>), 57.0 (4'-OCH<sub>3</sub>), 57.0 (4''-OCH<sub>3</sub>), 55.9 (8-OCH<sub>3</sub>), 52.0 (C-1), 50.7 (C-3), 49.9 (C-1'''), 45.1 (C-3'''), 34.5 (C-4'''), 33.11 (C-4), 22.2 (2'-CH<sub>3</sub>), 22.1 (2''-CH<sub>3</sub>), 20.2 (1-CH<sub>3</sub>), 19.5 (1'''-CH<sub>3</sub>), 19.3 (3'''-CH<sub>3</sub>), 18.7 (3-CH<sub>3</sub>).

Table 14. Detailed 2D NMR data of ealapasamine A (**42**) in methanol-*d*<sub>4</sub> ( $\delta$  in ppm, *J* in Hz).

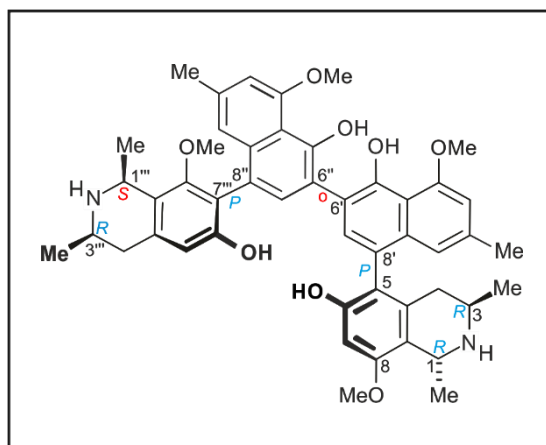
Position	$\delta_{\text{H}}$ ( <i>J</i> in Hz)	ealapasamine A ( <b>42</b> )		
		HMBC	COSY	ROESY
1	4.65, q (6.6)	8, 9, 10, 1-Me	1-Me	3, 8-OMe
3	3.28, m	4, 3-Me	4eq, 3-Me	1
4	2.64, dd	5, 9, 10	3, 4ax	7', 3-Me
	2.27, dd	3, 9, 10, 3-Me	3, 4eq	1', 3-Me
5				
6				
7	6.62, s	1, 5, 6, 8, 9, 8'		8-OMe
8				
9				
10				
1'	6.80, d (1.2)	2', 3', 10', 8', 9'		4ax, 1-Me, 2'-Me
2'				
3'	6.87, d (1.2)	1', 2', 4', 10'		2'-Me, 4'-OMe
4'				
5'				
6'				
7'	7.28, s	5, 5', 9', 10', 6''		4eq, 7, 7''
8'				
9'				
10'				
Me-1	1.76, d (6.7)	1, 9	1	8-OMe
Me-3	1.24, d (6.5)	3, 4	3	4eq, 4ax
Me-2'	2.36, s	1', 2', 3'		1', 3'
8-OMe	3.90, s	8		7, 1-Me
4'-OMe	4.11, s	4'		3'
1'''	4.74, q (6.8)	3''', 8''', 9''', 10''', 1'''-Me	1'''-Me	1'', 8'''-OMe
3'''	3.86, m	4''', 3'''-Me	4'''eq, 3'''-Me	1'''-Me
4'''	3.15, dd	5''', 9''', 10'''	4ax, 3'''	5''', 3'''-Me
	2.88, dd	3, 9, 10, 3'''-Me	4eq, 3'''	3'''-Me
5'''	6.57, s	4''', 6''', 7''', 9'''		4eq, 1''
6'''				
7'''				
8'''				
9'''				
10'''				
1''	6.88, d (1.2)	2'', 3'', 10'', 8'', 9''		2''-Me, 1''', 5''', 8'''-OMe
2''				
3''	6.86, d (1.2)	1'', 2'', 4'', 10''		2''-Me, 4''-OMe
4''				
5''				
6''				
7''	7.39, s	6', 5'', 9'', 10'', 7'''		7', 1'''-Me, 8'''-OMe
8''				
9''				
10''				
Me-1'''	1.63, d (6.9)	1''', 9'''	1'''	7'', 3''', 8'''-OMe
Me-3'''	1.51, d (6.9)	3''', 4'''	3'''	4'''eq, 4'''ax
Me-2''	2.35, s	1'', 2'', 3''		1'', 3''
8'''-	3.19, s	8'''		1'', 7'', 1'''
4''-OMe	4.11, s	4''		3''

*Ealapasamine B (43)*

White amorphous powder (3.0 mg).

$[\alpha]_D^{23} = -10$  ( $c$  0.04, MeOH).

UV (MeOH):  $\lambda_{\max}$  ( $\log \epsilon$ ) = 205 (1.2), 219 (0.81), 228 (0.85), 257 (0.42), 267 (0.45), 305 (0.16), 312 (0.17), 323 (0.16), 330 (0.16), 338 (0.16), 344 (0.16) nm.



ECD (MeOH,  $c$  0.005):  $\lambda_{\max}$  ( $\log \epsilon$  in  $\text{cm}^2 \text{mol}^{-1}$ ) = 195 (+1.3), 200 (-1.26), 207 (-7.68), 236 (+3.57), 240 (+2.43), 267 (-3.5), 290 (+0.7), 304 (-0.94), 334 (-0.23), 386 (+0.17) nm.

ORD (MeOH,  $c$  0.005):  $\lambda_{\max}$  ( $\log \epsilon$  in  $\text{cm}^2 \text{mol}^{-1}$ ) = 200 (+4.1), 202 (+5.0), 212 (-4.4), 221 (-2.8), 228 (-3.3), 242 (+1.8), 246 (+1.4), 258 (+2.6), 280 (-2.6), 297 (+0.1), 315 (-1.3), 355 (-0.6), 365 (-0.7), 400 (-0.3) nm.

HRESIMS  $m/z$  785.38042  $[\text{M}+\text{H}]^+$  (calcd for  $\text{C}_{48}\text{H}_{53}\text{N}_2\text{O}_8$ , 785.37964).

$^1\text{H}$  NMR ( $\text{CD}_3\text{OD}$ , 600 MHz):  $\delta_{\text{H}}$  (ppm) = 7.39 (s, 1H, H-7''), 7.30 (s, 1H, H-7'), 6.88 (d,  $J = 1.07$  Hz, 1H, H-1''), 6.86 (br s, 1H, H-3'), 6.86 (br s, 1H, H-3''), 6.70 (br s, 1H, H-1'), 6.60 (s, 1H, H-5'''), 6.59 (s, 1H, H-7), 4.78 (q,  $J = 6.80$  Hz, 1H, H-1), 4.69 (q,  $J = 6.70$  Hz, 1H, H-1'''), 4.11 (s, 1H, 4''-OCH<sub>3</sub>), 4.10 (s, 1H, 4'-OCH<sub>3</sub>), 3.92 (s, 1H, 8-OCH<sub>3</sub>), 3.70 (m, 1H, H-3), 3.47 (m, 1H, H-3'''), 3.27 (s, 1H, 8'''-OCH<sub>3</sub>), 2.97 (m d,  $J = 7.92$  Hz, 1H, 4'''-H<sub>eq</sub>), 2.97 (m d,  $J = 7.92$  Hz, 1H, 4'''-H<sub>ax</sub>), 2.83 (dd,  $J = 18.14, 4.63$  Hz, 1H, 4-H<sub>eq</sub>), 2.37 (s, 1H, H-2''), 2.34 (s, 1H, H-2'), 2.15 (dd,  $J = 18.14, 11.21$  Hz, 1H, 4-H<sub>ax</sub>), 1.73 (d,  $J = 6.58$  Hz, 1H, 1'''-CH<sub>3</sub>), 1.61 (d,  $J = 6.72$  Hz, 1H, 1-CH<sub>3</sub>), 1.51 (d,  $J = 6.45$  Hz, 1H, 3'''-CH<sub>3</sub>), 1.23 (d,  $J = 6.45$  Hz, 1H, 3-CH<sub>3</sub>).

$^{13}\text{C}$  NMR ( $\text{CD}_3\text{OD}$ , 151 MHz):  $\delta_{\text{C}}$  (ppm) = 158.7 (C-8'''), 158.4 (C-4''), 158.0 (C-4'), 157.8 (C-8), 157.6 (C-6'''), 157.5 (C-6), 152.8 (C-5'), 152.6 (C-5''), 137.8 (C-2'), 137.3 (C-2''), 136.7 (C-9'), 136.6 (C-9''), 135.1 (C-7''), 134.9 (C-10'''), 134.8 (C-7'), 133.5 (C-10), 123.8 (C-8'), 122.3 (C-8''), 121.9 (C-7'''), 120.5 (C-6'), 120.3 (C-6''), 120.1 (C-1''), 120.0 (C-5), 119.1 (C-1'), 118.5



(C-9'''), 115.4 (C-10'), 115.1 (C-10''), 114.2 (C-9), 111.9 (C-5'''), 108.2 (C-3'), 108.0 (C-3''), 98.8 (C-7), 61.0 (C-8'''), 57.1 (4'-OCH<sub>3</sub>), 57.1 (4''-OCH<sub>3</sub>), 56.22 (8-OCH<sub>3</sub>), 52.6 (C-1), 51.3 (C-1'''), 49.4 (C-3'''), 45.2 (C-3), 35.3 (C-4'''), 33.2 (C-4), 22.4 (2'-CH<sub>3</sub>), 22.3 (2''-CH<sub>3</sub>), 20.7 (1'''-CH<sub>3</sub>), 19.4 (1-CH<sub>3</sub>), 19.0 (3-CH<sub>3</sub>), 18.7 (3'''-CH<sub>3</sub>).

Table 15. Detailed 2D NMR data of ealapasamine B (**43**) in CD<sub>3</sub>OD ( $\delta$  in ppm, *J* in Hz).

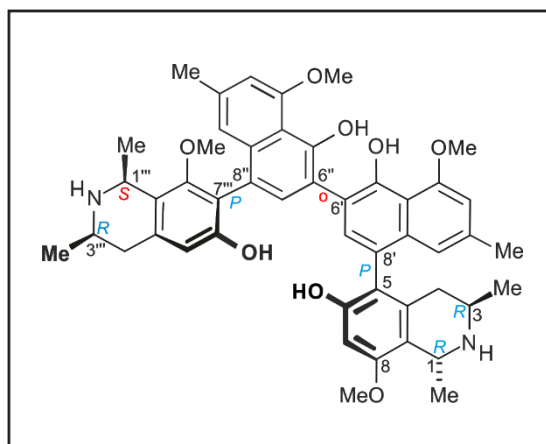
ealapasamine B ( <b>43</b> )				
Position	$\delta_{\text{H}}$ ( <i>J</i> in Hz)	HMBC	COSY	ROESY
1	4.78, q (6.8)	8, 9, 10, 1-Me	1-Me	8-OMe
3	3.70, m	4, 3-Me	4 <sub>eq</sub> , 3-Me	1-Me
4	2.83, dd	5, 9, 10	3, 4 <sub>ax</sub>	7', 3-Me
	2.15, dd	3, 9, 10, 3-Me	3, 4 <sub>eq</sub>	1', 3-Me
5				
6				
7	6.59, s	1, 5, 6, 8, 9, 8'		8-OMe
8				
9				
10				
1'	6.70, br s	2', 3', 10', 8', 9'		4 <sub>ax</sub> , 2'-Me
2'				
3'	6.86, br s	1', 2', 4', 10'		2'-Me, 4'-OMe
4'				
5'				
6'				
7'	7.30, s	5, 5', 9', 10', 6''		4 <sub>eq</sub> , 7, 7''
8'				
9'				
10'				
Me-1	1.61, d (6.7)	1, 9	1	8-OMe
Me-3	1.23, d (6.5)	3, 4	3	4 <sub>eq</sub> , 4 <sub>ax</sub>
Me-2'	2.34, s	1', 2', 3'		1', 3'
8-OMe	3.92, s	8		7, 1-Me
4'-OMe	4.10, s	4'		3'
1'''	4.69, q (6.7)	3''', 8''', 9''', 10''', 1'''-Me	1'''-Me	3''', 8'''-OMe
3'''	3.47, m	4''', 3'''-Me	4''' <sub>eq</sub> , 3'''-Me	1'''
	2.97, m	5''', 9''', 10'''	4 <sub>ax</sub> , 3'''	5''', 3'''-Me
4'''	2.97, m	3''', 9''', 10''', 3'''-Me	4 <sub>eq</sub> , 3'''	5''', 3'''-Me
	6.60, s	4''', 6''', 7''', 9'''		4 <sub>eq</sub> , 1''
6'''				
7'''				
8'''				
9'''				
10'''				
1''	6.88, d (1.2)	2'', 3'', 10'', 8'', 9''		2''-Me, 5''', 1'''-Me, 8'''-OMe
2''				
3''	6.86, br s	1'', 2'', 4'', 10''		2''-Me, 4''-OMe
4''				
5''				
6''				
7''	7.39, s	6', 5'', 9'', 10'', 7'''		7', 8'''-OMe
8''				
9''				
10''				
Me-1'''	1.74, d (6.9)	1''', 9'''	1'''	1'', 8'''-OMe
Me-3'''	1.51, d (6.5)	3''', 4'''	3'''	4''' <sub>eq</sub> , 4''' <sub>ax</sub>
Me-2''	2.37, s	1'', 2'', 3''		1'', 3''
8'''-	3.27, s	8'''		1'', 7'', 1'''
4''-OMe	4.11, s	4''		3''

*Ealapasamine C (44)*

White amorphous powder (6.3 mg).

$[\alpha]_D^{23} = -26$  ( $c$  0.1, MeOH).

UV (MeOH):  $\lambda_{\max}$  ( $\log \epsilon$ ) = 217 (0.83), 229 (0.93), 257 (0.37), 263 (0.4), 300 (0.14), 315 (0.16), 322 (0.15), 330 (0.16), 338 (0.16), 344 (0.17) nm.



ECD (MeOH,  $c$  0.01):  $\lambda_{\max}$  ( $\log \epsilon$  in  $\text{cm}^2 \text{mol}^{-1}$ ) = 195 (+7.34), 200 (-1.66), 202 (+5.2), 212 (-11.1), 224 (-6.23), 249 (+1.95), 267 (-13.66), 292 (+0.65), 305 (-1.89), 325 (+1.1), 349 (-0.56), 385 (-0.17) nm.

ORD (MeOH,  $c$  0.01):  $\lambda_{\max}$  ( $\log \epsilon$  in  $\text{cm}^2 \text{mol}^{-1}$ ) = 200 (-0.9), 206 (+13.2), 218 (-2.6), 222 (+0.1), 231 (-4.4), 242 (+0.0), 259 (+8.4), 280 (-8.5), 299 (-2.3), 315 (-4.2), 343 (-1.0), 354 (-1.7), 400 (-1.1) nm.

HRESIMS  $m/z$  785.37932  $[\text{M}+\text{H}]^+$  (calcd for  $\text{C}_{48}\text{H}_{53}\text{N}_2\text{O}_8$ , 785.37964).

$^1\text{H}$  NMR ( $\text{CD}_3\text{OD}$ , 600 MHz):  $\delta_{\text{H}}$  (ppm) = 7.38 (s, 1H, H-7''), 7.27 (s, 1H, H-7'), 6.88 (d,  $J = 1.01$  Hz, 1H, H-1''), 6.87 (d,  $J = 1.28$  Hz, 1H, H-3'), 6.86 (d,  $J = 1.16$  Hz, 1H, H-3''), 6.80 (s, 1H, H-1'), 6.62 (s, 1H, H-7), 6.60 (s, 1H, H-5'''), 4.68 (q,  $J = 6.55$  Hz, 1H, H-1'''), 4.65 (q,  $J = 6.55$  Hz, 1H, 1-H), 4.11 (s, 3H, 4'-OCH<sub>3</sub>), 4.11 (s, 3H, 4''-OCH<sub>3</sub>), 3.90 (s, 3H, 8-OCH<sub>3</sub>), 3.47 (m, 1H, 3'''-H), 3.25 (m, 1H, 3-H), 3.27 (s, 3H, 8'''-OCH<sub>3</sub>), 2.62 (dd,  $J = 3.40, 17.23$  Hz, 1H, 4'''-H<sub>eq</sub>), 2.97 (m, 2H, 4'''-H<sub>eq-ax</sub>), 2.36 (s, 1H, 2'-CH<sub>3</sub>), 2.36 (s, 1H, 2''-CH<sub>3</sub>), 2.28 (dd,  $J = 12.01, 17.81$  Hz, 1H, 4-H<sub>ax</sub>), 1.76 (d,  $J = 6.56$  Hz, 3H, 1-CH<sub>3</sub>), 1.73 (d,  $J = 6.61$  Hz, 3H, 1'''-CH<sub>3</sub>), 1.51 (d,  $J = 6.46$  Hz, 3H, 3'''-CH<sub>3</sub>), 1.24 (d,  $J = 6.51$  Hz, 3H, 3-CH<sub>3</sub>).

$^{13}\text{C}$  NMR ( $\text{CD}_3\text{OD}$ , 151 MHz):  $\delta_{\text{C}}$  (ppm) = 158.7 (C-8'''), 158.6 (C-8), 158.3 (C-4'), 158.0 (C-4''), 157.5 (C-6'''), 157.2 (C-6), 152.7 (C-5'), 152.5 (C-5''), 137.8 (C-2''), 137.4 (C-2'), 137.1 (C-9'), 136.6 (C-9''), 135.5 (C-10), 135.1 (C-7''), 134.9 (C-10'''), 134.9 (C-7'), 123.8 (C-8'), 122.3 (C-8''), 121.9 (C-7'''), 120.3 (C-6'), 120.2 (C-6''), 120.1 (C-1''), 120.0 (C-5), 119.3 (C-1'), 118.5 (C-9'''), 115.4 (C-10'), 115.1 (C-10''), 114.3 (C-9), 112.0 (C-5'''), 108.2 (C-3'), 108.1 (C-3''), 99.5 (C-7), 61.0 (8'''-OCH<sub>3</sub>), 57.2 (4'-OCH<sub>3</sub>), 57.2 (4''-OCH<sub>3</sub>), 56.1 (8-OCH<sub>3</sub>), 52.5 (1'''-C),

52.1 (1-C), 51.3 (3<sup>'''</sup>-C), 50.9 (3-C), 35.3 (4<sup>'''</sup>-C), 33.2 (4-C), 22.4 (2<sup>''</sup>-CH<sub>3</sub>), 22.3 (2<sup>'</sup>-CH<sub>3</sub>), 20.7 (1<sup>'''</sup>-CH<sub>3</sub>), 20.4 (1-CH<sub>3</sub>), 18.9 (3<sup>'''</sup>-CH<sub>3</sub>), 18.8 (3-CH<sub>3</sub>).

Table 16. Detailed NMR data of ealapasamine C (**44**) in methanol-*d*<sub>4</sub> ( $\delta$  in ppm, *J* in Hz).

Position	$\delta_{\text{H}}$ ( <i>J</i> in Hz)	ealapasamine C ( <b>44</b> )		
		HMBC	COSY	ROESY
1	4.65, q (6.6)	8, 9, 10, 1-Me	1-Me	3, 8-OMe
3	3.25, m	4, 3-Me	4eq, 3-Me	1
4	2.62, dd	5, 9, 10	3, 4ax	7', 3-Me
	2.28, dd	3, 9, 10, 3-Me	3, 4eq	1', 3-Me
5				
6				
7	6.62, s	1, 5, 6, 8, 9, 8'		8-OMe
8				
9				
10				
1'	6.80, s	2', 3', 10', 8', 9'		4ax, 1-Me, 2'-Me
2'				
3'	6.87, d (1.3)	1', 2', 4', 10'		2'-Me, 4'-OMe
4'				
5'				
6'				
7'	7.27, s	5, 5', 9', 10', 6''		4eq, 7, 7''
8'				
9'				
10'				
Me-1	1.76, d (6.6)	1, 9	1	8-OMe
Me-3	1.24, d (6.5)	3, 4	3	4eq, 4ax
Me-2'	2.36, s	1', 2', 3'		1', 3'
8-OMe	3.90, s	8		7, 1-Me
4'-OMe	4.11, s	4'		3'
1'''	4.68, q (6.6)	3''', 8''', 9''', 10''', 1'''-Me	1'''-Me	3''', 8'''-OMe
3'''	3.47, m	4''', 3'''-Me	4'''eq, 3'''-Me	1'''
4'''	2.97, m	5''', 9''', 10'''	4ax, 3'''	5''', 3'''-Me
	2.97, m	3, 9, 10, 3'''-Me	4eq, 3'''	5''', 3'''-Me
5'''	6.60, s	4''', 6''', 7''', 9'''		4eq, 1''
6'''				
7'''				
8'''				
9'''				
10'''				
1''	6.88, d (1.2)	2'', 3'', 10'', 8'', 9''		2''-Me, 5''', 1'''-Me, 8'''-OMe
2''				
3''	6.86, br s	1'', 2'', 4'', 10''		2''-Me, 4''-OMe
4''				
5''				
6''				
7''	7.39, s	6', 5'', 9'', 10'', 7'''		7', 8'''-OMe
8''				
9''				
10''				
Me-1'''	1.73, d (6.9)	1''', 9'''	1'''	1'', 8'''-OMe
Me-3'''	1.51, d (6.5)	3''', 4'''	3'''	4'''eq, 4'''ax
Me-2''	2.37, s	1'', 2'', 3''		1'', 3''
8'''-	3.27, s	8'''		1'', 7'', 1'''
4''-OMe	4.11, s	4''		3''

Table 17. <sup>1</sup>H and <sup>13</sup>C NMR Data of ealapasamines A-C in methanol-*d*<sub>4</sub> ( $\delta$  in ppm, *J* in Hz).

Position	ealapasamine A (1)		ealapasamine B (2)		ealapasamine C (3)	
	$\delta_{\text{H}}$ ( <i>J</i> in Hz)	$\delta_{\text{C}}$ , type	$\delta_{\text{H}}$ ( <i>J</i> in Hz)	$\delta_{\text{C}}$ , type	$\delta_{\text{H}}$ ( <i>J</i> in Hz)	$\delta_{\text{C}}$ , type
1	4.65, q (6.6)	52.0, CH	4.78, q (6.8)	49.4, CH	4.65, q (6.6)	52.1, CH
3	3.28, m	50.7, CH	3.70, m	45.1, CH	3.25, m	50.9, CH
4	2.64, dd (17.8, 2.27, dd (17.4,	33.1, 33.1,	2.83, dd (18.1, 2.15, dd (18.1,	33.2, 33.2,	2.62, dd (17.2, 2.28, dd (17.8,	33.2, 33.2,
5		119.9, C		120.0, C		120.0, C
6		157.1, C		157.5, C		157.2, C
7	6.62, s	99.3, CH	6.59, s	98.8, CH	6.62, s	99.5, CH
8		158.5, C		157.8, C		158.6, C
9		114.1, C		114.2, C		114.3, C
10		135.3, C		133.5, C		135.5, C
1'	6.80, d (1.2)	119.1,	6.70, br s	119.1,	6.80, s	119.3,
2'		137.6, C		137.8, C		137.4, C
3'	6.87, d (1.2)	108.0,	6.86, br s	108.2,	6.87, d (1.3)	108.2,
4'		158.2, C		158.0, C		158.3, C
5'		152.6, C		154.8, C		152.7, C
6'		120.2, C		120.5, C		120.3, C
7'	7.28, s	134.7,	7.30, s	134.8,	7.27, s	134.9,
8'		123.7, C		123.8, C		123.8, C
9'		136.9, C		136.7, C		137.1, C
10'		115.3, C		115.4, C		115.4, C
Me-1	1.76, d (6.7)	20.2, Me	1.61, d (6.7)	18.7, Me	1.76, d (6.6)	20.4, Me
Me-3	1.24, d (6.5)	18.7, Me	1.23, d (6.5)	19.4, Me	1.24, d (6.5)	18.8, Me
Me-2'	2.36, s	22.2, Me	2.34, s	22.3, Me	2.36, s	22.3, Me
8-OMe	3.90, s	55.9, Me	3.92, s	56.2, Me	3.90, s	56.1, Me
4'-OMe	4.11, s	57.0, Me	4.10, s	57.1, Me	4.11, s	57.2, Me
1'''	4.74, q (6.8)	49.9, CH	4.69, q (6.7)	52.6, CH	4.68, q (6.6)	52.5, CH
3'''	3.86, m	45.1, CH	3.47, m	51.3, CH	3.47, m	51.3, CH
4'''	3.15, dd (17.6, 2.88, dd (17.8,	34.5, 34.5,	2.97, m 2.97, m	35.3, 35.3,	2.97, m 2.97, m	35.3, 35.3,
5'''	6.57, s	111.2,	6.60, s	111.9,	6.60, s	112.0,
6'''		157.6, C		157.6, C		157.5, C
7'''		121.0, C		121.9, C		121.9, C
8'''		157.5, C		158.7, C		158.7, C
9'''		118.5, C		118.5, C		118.5, C
10'''		132.9, C		134.9, C		134.9, C
1''	6.88, d (1.2)	119.8,	6.88, d (1.2)	120.1,	6.88, d (1.2)	120.1,
2''		137.3, C		137.3, C		137.8, C
3''	6.86, d (1.2)	107.9,	6.86, br s	108.0,	6.86, br s	108.1,
4''		157.9, C		158.4, C		158.0, C
5''		152.5, C		152.6, C		152.5, C
6''		120.3, C		120.3, C		120.2, C
7''	7.39, s	135.2,	7.39, s	135.1,	7.39, s	135.1,
8''		122.0, C		122.3, C		122.3 C
9''		136.4, C		136.6, C		136.6, C
10''		114.9, C		115.1, C		115.1, C
Me-1'''	1.63, d (6.9)	19.5, Me	1.74, d (6.9)	20.7, Me	1.73, d (6.9)	20.7, Me
Me-3'''	1.51, d (6.9)	19.3, Me	1.51, d (6.5)	19.0, Me	1.51, d (6.5)	18.9, Me
Me-2''	2.35, s	22.1, Me	2.37, s	22.6, Me	2.37, s	22.4, Me
8'''-	3.19, s	60.9, Me	3.27, s	61.0, Me	3.27, s	61.0, Me
4''-OMe	4.11, s	57.0, Me	4.11, s	57.1, Me	4.11, s	57.2, Me

### **IV.3. *A. ealaensis* as a Reliable Source of Dimeric Naphthylisoquinolines Related to Mbandakamine A and Michellamine F**

#### **IV.3.1. Extractions, Isolation, and HPLC conditions**

##### **IV.3.1.1. Extraction and fractionation**

The macerate of the air-dried powder of the leaf material (600 g) was generated using the same procedure as described previously for the ealapasamines A-C. However, in this case, the compounds of interests, which contains the first group of dimers, were distributed between fractions A<sub>68</sub>-A<sub>76</sub>. After further fractionation on C<sub>18</sub>-SPE cartridges, the dimeric alkaloid enriched sub-fractions were sequentially submitted to semi-preparative HPLC for isolation of the dimers.

##### **IV.3.1.2. Isolation and semi-preparative HPLC conditions**

The isolation was performed also on a Symmetry<sup>®</sup> Prep-C<sub>18</sub> column (Waters, 300 × 19 mm, 7 μm) with the mobile phase consisting of A (H<sub>2</sub>O, 0.05% TFA) and B (MeCN, 0.05% TFA), at a flow rate of 10 mL min<sup>-1</sup>. A further purification on a Chromolith<sup>®</sup> SemiPrep RP-18e column (100 × 10 mm) was necessary to isolate the pure dimeric alkaloids, using a gradient elution mode with a flow rate of 10 mL min<sup>-1</sup>, and a mobile phase listed for the Symmetry<sup>®</sup> Prep column, but with MeOH (C) instead of MeCN (B). Furthermore, another purification method, using the mixture of A and C was developed to obtain more dimeric material.

The LC-MS-guided fractionation hinted at the presence of dimeric compounds in fractions A<sub>68</sub> to A<sub>76</sub>, which were further separated on SPE cartridges. For the isolation of **32**, **47-50**, the sub-fractions of interest were submitted to semi-preparative HPLC on a Symmetry<sup>®</sup> Prep-C<sub>18</sub> column using a gradient elution at a flow rate of 10 mL min<sup>-1</sup>: 0-13 min: 10-20% of B, 37 min: 45% of B, 39 min: 50% of B, 42 min: 100% of B, 45 min: 100% of B. Since the collected peaks showed impurities on analytical HPLC and NMR, they had required additional HPLC purification steps, which were achieved on a Chromolith<sup>®</sup> SemiPrep RP-18e column (100 × 10 mm) using a gradient solvent system consisting of A (H<sub>2</sub>O, 0.05% TFA) and C (MeOH, 0.05% TFA) at a flow rate of 10 mL min<sup>-1</sup>: 0-2 min: 5% of C, 8 min: 30% of C, 13 min: 40% of C, 19.0 min: 55% of C, 20 min: 100% of C, 22 min: 100% of C, to yield 15 mg of mbandakamine A (**32**) and 13.1 mg of 1-*epi*-mbandakamine A (**47**). The application of the same method on

Chromolith<sup>®</sup> SemiPrep RP-18e column as for **42-44**, yielded in this case 11.0 mg of mbandakamine C (**48**), 1.1 mg of mbandakamine D (**49**), and 2.2 mg of michellamine F<sub>2</sub> (**50**).

For further purification from advanced sub-fractions of these dimers, another method was developed on Symmetry<sup>®</sup> Prep-C<sub>18</sub> with A and C as mobile phase. The flow rate was set at 14.2 mL min<sup>-1</sup>, using the following gradient: 0-13 min: 20-40% of C, 58 min: 54% of C, 60 min: 100% of C.

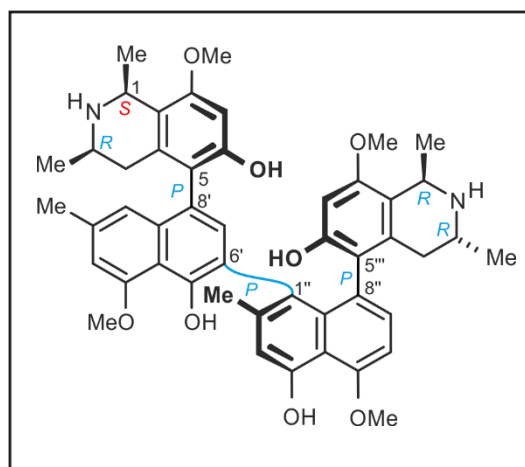
### IV.3.1.3. Isolated mbandakamines and michellamine F<sub>2</sub>

#### *1-epi-Mbandakamine A (47)*

White, amorphous powder (13.1 mg).

$[\alpha]_D^{23} = -17^\circ$  (*c* 0.05, MeOH).

UV (MeOH):  $\lambda_{\max}$  (log  $\epsilon$ ) = 203 (1.11), 218 (0.82), 230 (0.77), 283 (0.2), 317 (0.17), 322 (0.17), 331 (0.16), 340 (0.14), 345 (0.14) nm.



ECD (MeOH, *c* 0.3):  $\lambda_{\max}$  (log  $\epsilon$  in cm<sup>2</sup> mol<sup>-1</sup>) = 195 (+22.56), 200 (+68.29), 228.3 (-75.73), 248.8 (+14.84), 286.4 (-8.29), 319.4 (+11.0), 381.5 (+0.47), 396.2 (+0.42), 653.5 (0.00) nm.

HRESIMS *m/z* 785.38042 [M+H]<sup>+</sup> (calcd for C<sub>48</sub>H<sub>53</sub>N<sub>2</sub>O<sub>8</sub>, 785.37964).

<sup>1</sup>H NMR (CD<sub>3</sub>OD, 600 MHz):  $\delta_H$  (ppm) = 7.05 (d, *J* = 7.90 Hz, 1H, H-7''), 6.99 (d, *J* = 7.97 Hz, 1H, H-6''), 6.87 (d, *J* = 1.20 Hz, 1H, H-3'), 6.79 (s, 1H, H-3''), 6.75 (s, 1H, H-3'), 6.74 (d, *J* = 0.96 Hz, 1H, H-1'), 6.48 (s, 1H, H-7), 6.44 (s, 1H, H-7'), 5.32 (s, 1H, H-7'''), 4.65 (q, *J* = 6.66 Hz, 1H, H-1), 4.64 (q, *J* = 6.66 Hz, 1H, H-1'''), 4.15 (s, 3H, 5''-OCH<sub>3</sub>), 4.09 (s, 3H, 4'-OCH<sub>3</sub>), 3.83 (s, 3H, 8-OCH<sub>3</sub>), 3.68 (dd, *J* = 17.06, 3.13 Hz, 1H, 4-H<sub>eq</sub>), 3.50 (m, 1H, H-3'''), 3.27 (m, 1H, H-3), 3.05 (s, 3H, 8'''-OCH<sub>3</sub>), 2.55 (dd, *J* = 16.85, 11.66 Hz, 1H, 4-H<sub>ax</sub>), 2.42 (dd, *J* = 17.36, 12.36 Hz, 1H, 4'''-H<sub>ax</sub>), 2.37 (s, 1H, 2'-CH<sub>3</sub>), 1.95 (dd, *J* = 17.48, 4.21 Hz, 1H, 4'''-H<sub>eq</sub>), 1.91 (s, 1H, 2''-CH<sub>3</sub>), 1.76 (d, *J* = 6.56 Hz, 1H, 1-CH<sub>3</sub>), 1.53 (d, *J* = 6.71 Hz, 3H, 1'''-CH<sub>3</sub>), 1.50 (d, *J* = 6.51 Hz, 3H, 3-CH<sub>3</sub>), 1.25 (d, *J* = 6.41 Hz, 3H, 3'''-CH<sub>3</sub>).



$^{13}\text{C}$  NMR ( $\text{CD}_3\text{OD}$ , 151 MHz):  $\delta_{\text{C}}$  (ppm) = 158.48 (C-5"), 158.12 (C-8), 157.60 (C-4'), 157.47 (C-6), 156.66 (C-8'''), 155.40 (C-4''), 154.50 (C-6'''), 151.22 (C-5'), 141.04 (C-2''), 138.26 (C-9''), 136.56 (C-2'), 136.30 (C-9'), 135.97 (C-10), 134.92 (C-7'), 133.67 (C-10'''), 132.41 (C-7''), 128.04 (C-1''), 126.45 (C-8''), 124.30 (C-8'), 124.16 (C-6'), 122.84 (C-5'''), 120.81 (C-5), 118.91 (C-1'), 116.27 (C-10''), 114.56 (C-3''), 114.55 (C-10'), 113.52 (C-9), 113.48 (C-9'''), 106.94 (C-3'), 104.71 (C-6''), 99.24 (C-7), 97.00 (C-7'''), 57.01 (5''-OCH<sub>3</sub>), 56.85 (4'-OCH<sub>3</sub>), 55.97 (8-OCH<sub>3</sub>), 55.41 (8'''-OCH<sub>3</sub>), 52.07 (C-1), 51.69 (C-3), 49.72 (C-1'''), 46.18 (C-3'''), 33.21 (C-4'''), 33.12 (C-4), 22.30 (2'-CH<sub>3</sub>), 21.50 (2''-CH<sub>3</sub>), 20.58 (1-CH<sub>3</sub>), 19.01 (1'''-CH<sub>3</sub>), 18.90 (3'''-CH<sub>3</sub>), 18.85 (3-CH<sub>3</sub>).

Table 18. Detailed 2D NMR data of 1-*epi*-mbandakamine A (**47**) in MeOD ( $\delta$  in ppm, *J* in Hz).

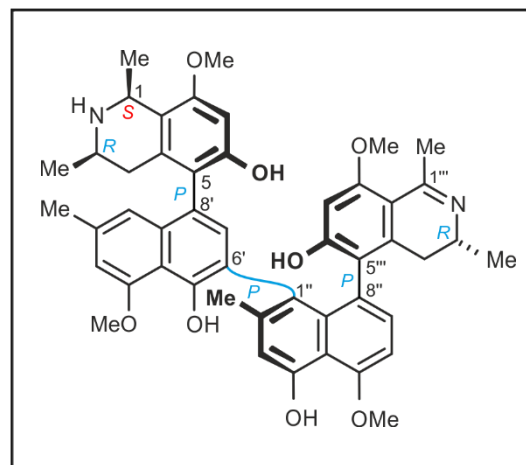
1- <i>epi</i> -mbandakamine A ( <b>47</b> )					
Position	$\delta_H$	$\delta_C$ , DEPT	HMBC	COSY	ROESY
1	4.65, q	52.1, CH	8, 9, 10, 1-Me	1-Me	3, 8-OMe
3	3.27, m	51.7, CH	4, 3-Me	4 <sub>eq</sub> , 3-Me	<b>1</b>
4	3.68, dd	33.1, CH <sub>eq</sub>	5, 9, 10	3, 4 <sub>ax</sub>	3-Me, 7', 7'''
	2.55, dd	33.1, CH <sub>ax</sub>	3, 9, 10, 3-Me	3, 4 <sub>eq</sub>	3-Me, 1', 7''', <b>8'''-OMe</b>
5		120.8, C			
6		157.5, C			
7	6.48, s	99.2, CH	1, 5, 6, 8, 9, 8'		8-OMe
8		158.1, C			
9		113.5, C			
10		136.0, C			
1'	6.74, d	118.9, CH	2', 3', 8', 9', 10', 2'-Me	3'	4 <sub>ax</sub> , 2'-Me, <b>8'''-OMe</b>
2'		136.6, C			
3'	6.87, d	106.9, CH	1', 2', 4', 10', 2'-Me		2'-Me, 4'-OMe
4'		157.6, C			
5'		151.2, C			
6'		124.2, C			
7'	6.44, s	134.9, CH	5, 5', 9', 10', <b>1''</b>		4 <sub>eq</sub> , 2''-Me
8'		124.3, C			
9'		136.3, C			
10'		114.6, C			
1-Me	1.76, d	20.6, Me	1, 9	1	8-OMe
3-Me	1.50, d	18.9, Me	3, 4	3	4 <sub>eq</sub> , 4 <sub>ax</sub> , 7''', 8'''-OMe
2'-Me	2.37, s	22.3, Me	1', 2', 3'		1', 3', 8'''-OMe
8-OMe	3.83, s	56.0, Me	8		7, 1-Me
4'-OMe	4.09, s	56.9, Me	4'		3', 1''', 8'''-OMe
1'''	4.64, q	50.0, CH	3''', 8''', 9''', 10''', 1'''-Me	1'''-Me	4'-OMe, 8'''-OMe
3'''	3.50, m	46.2, CH	4''', 3'''-Me	4''' <sub>eq</sub> , 3'''-Me	4''' <sub>eq</sub> , 1'''-Me, 3'''-Me
4'''	1.95, dd	33.2, CH <sub>eq</sub>	5''', 9''', 10'''	4 <sub>ax</sub> , 3'''	7'', 3'', 4''' <sub>ax</sub> , 3'''-Me
	2.42, dd	33.2, CH <sub>ax</sub>	3''', 9''', 10''', 3'''-Me	4 <sub>eq</sub> , 3'''	3''', 4''' <sub>eq</sub> , 3'''-Me
5'''		122.8, C			
6'''		154.5, C			
7'''	5.32, s	97.0, CH	1''', 5''', 6''', 8''', 9''', 8''		4 <sub>ax</sub> , 3-Me, 8'''-OMe
8'''		156.7, C			
9'''		113.5, C			
10'''		133.7, C			
1''		128.0, C			
2''		141.0, C			
3''	6.79, s	114.6, CH	1'', 2'', 4'', 10'', 2''-Me		2''-Me, 4'-OMe
4''		155.4, C			
5''		158.5, C			
6''	6.99, d	104.7, CH	5'', 8'', 10''	7''	5''-OMe
7''	7.05, d	132.4, CH	1'', 5'', 9'', 5'''	6''	4''' <sub>eq</sub>
8''		126.5, C			
9''		138.3, C			
10''		116.3, C			
1'''-Me	1.53, d	19.0, Me	1''', 9'''	1	1''', 3''', 8'''-OMe
3'''-Me	1.25, d	18.9, Me	3''', 4'''	3	3''', 4 <sub>ax</sub> ''', 4 <sub>eq</sub> '''
2''-Me	1.91, s	21.5, Me	1'', 2'', 3''		7', 3''
8'''-OMe	3.05, s	55.4, Me	8'''		4 <sub>ax</sub> , 1', 3', 1''', 7''', 3-Me, 2'-Me, 4'-OMe, 1'''-Me
5''-OMe	4.15, s	57.0, Me	5''		6''

### Mbandakamine C (48)

Yellow, amorphous powder (11.1 mg).

$[\alpha]_D^{23} = -21^\circ$  ( $c$  0.08, MeOH).

UV (MeOH):  $\lambda_{\max}$  ( $\log \epsilon$ ) = 205 (0.76), 218 (0.65),  
233 (0.73), 283 (0.09), 315 (0.17),  
321 (0.17), 332 (0.18), 340 (0.17),  
344 (0.17), 367 (0.06), 391 (0.12)  
nm.



ECD (MeOH,  $c$  0.1):  $\lambda_{\max}$  ( $\log \epsilon$  in  $\text{cm}^2 \text{mol}^{-1}$ ) = 199 (+30.5), 229 (-33.6), 246 (+8.8), 270  
(+2.7), 286 (+0.7), 316 (+6.1), 339 (+5.7), 389 (-8.0) nm.

HRESIMS  $m/z$  783.36203  $[\text{M}+\text{H}]^+$  (calcd for  $\text{C}_{48}\text{H}_{51}\text{N}_2\text{O}_8$ , 783.36399).

$^1\text{H}$  NMR ( $\text{CD}_3\text{OD}$ , 600 MHz):  $\delta_{\text{H}}$  (ppm) = 7.07 (d,  $J$  = 7.93 Hz, 1H, H-7''), 7.02 (d,  $J$  = 8.06 Hz, 1H, H-6''), 6.83 (s, 1H, H-3''), 6.82 (br s, 1H, H-3'), 6.77 (d,  $J$  = 1.07 Hz, 1H, H-1'), 6.51 (s, 1H, H-7'), 6.48 (s, 1H, H-7), 5.56 (s, 1H, H-7'''), 4.68 (q,  $J$  = 6.38 Hz, 1H, H-1), 4.16 (s, 3H, 5''-OCH<sub>3</sub>), 4.05 (s, 3H, 4'-OCH<sub>3</sub>), 3.83 (s, 3H, 8-OCH<sub>3</sub>), 3.58 (dd,  $J$  = 16.72, 3.02 Hz, 1H, 4-H<sub>eq</sub>), 3.50 (m, 1H, H-3'''), 3.35 (m, 1H, H-3), 3.28 (s, 3H, 8'''-OCH<sub>3</sub>), 2.85 (m,  $J$  = 16.79 Hz, 1H, 4'''-H<sub>ax</sub>), 2.71 (dd,  $J$  = 17.89, 12.29 Hz, 1H, 4-H<sub>ax</sub>), 2.65 (d,  $J$  = 1.81 Hz, 3H, 1'''-CH<sub>3</sub>), 2.38 (s, 1H, 2'-CH<sub>3</sub>), 2.00 (dd,  $J$  = 17.13, 4.90 Hz, 1H, 4'''-H<sub>eq</sub>), 1.90 (s, 1H, 2''-CH<sub>3</sub>), 1.78 (d,  $J$  = 6.58 Hz, 3 H, 1-CH<sub>3</sub>), 1.54 (d,  $J$  = 6.51 Hz, 3 H, 3-CH<sub>3</sub>), 1.28 (d,  $J$  = 6.72 Hz, 3H, 3'''-CH<sub>3</sub>).

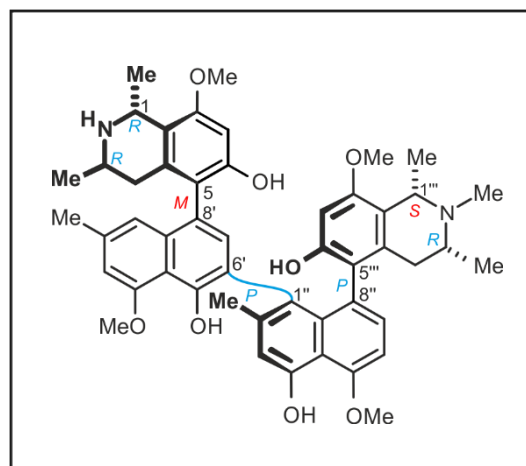
$^{13}\text{C}$  NMR ( $\text{CD}_3\text{OD}$ , 151 MHz):  $\delta_{\text{C}}$  (ppm) = 175.8 (C-1'''), 165.1 (C-8'''), 164.8 (C-6'''), 159.1 (C-5''), 158.3 (C-8), 157.7 (C-6), 157.5 (C-4'), 155.6 (C-4''), 152.4 (C-5'), 143.8 (C-10'''), 141.4 (C-2''), 138.0 (C-9''), 137.2 (C-2'), 136.8 (C-9'), 135.4 (C-7'), 135.4 (C-10), 132.1 (C-7''), 127.5 (C-1''), 125.4 (C-5'''), 124.8 (C-8''), 124.7 (C-8'), 123.6 (C-6'), 120.6 (C-5), 119.3 (C-1'), 116.2 (C-10''), 115.0 (C-3''), 114.2 (C-10'), 113.5 (C-9), 108.8 (C-9'''), 107.7 (C-3'), 104.7 (C-6''), 99.3 (C-7), 98.2 (C-7'''), 57.3 (4'-OCH<sub>3</sub>), 57.1 (5''-OCH<sub>3</sub>), 56.21 (8'''-OCH<sub>3</sub>), 56.0 (8-OCH<sub>3</sub>), 52.1 (C-1), 51.6 (C-3), 50.2 (3'''-C), 33.8 (4'''-C), 33.3 (4-C), 24.8 (1'''-CH<sub>3</sub>), 22.3 (2'-CH<sub>3</sub>), 21.5 (2''-CH<sub>3</sub>), 20.5 (1-CH<sub>3</sub>), 19.0 (3-CH<sub>3</sub>), 18.8 (3'''-CH<sub>3</sub>).

### Mbandakamine D (49)

White, amorphous powder (1.1 mg).

$[\alpha]_D^{23} = -14$  ( $c$  0.04, MeOH).

UV (MeOH):  $\lambda_{\max}$  ( $\log \epsilon$ ) = 202 (1.02), 217 (0.78),  
230 (0.77), 285 (0.2), 317 (0.17),  
322 (0.17), 331 (0.16), 340 (0.14),  
345 (0.14) nm.



ECD (MeOH,  $c$  0.1):  $\lambda_{\max}$  ( $\log \epsilon$  in  $\text{cm}^2 \text{mol}^{-1}$ ) = 200 (+42.29), 227.1 (-40.71), 251.1 (+5.84),  
286.4 (-4.21), 319.4 (+6.6), 380 (+0.12) nm.

HRESIMS  $m/z$  815.39085  $[\text{M}+\text{H}+\text{O}]^+$  (calcd for  $\text{C}_{49}\text{H}_{55}\text{N}_2\text{O}_9$ , which requires 815.39076). The molecular formula is  $\text{C}_{49}\text{H}_{54}\text{N}_2\text{O}_8$ .

$^1\text{H}$  NMR ( $\text{CD}_3\text{OD}$ , 600 MHz):  $\delta_{\text{H}}$  (ppm) = 7.02 (d,  $J$  = 8.02 Hz, 1H, H-6''), 6.98 (d,  $J$  = 8.02 Hz, 1H, H-7''), 6.88 (s, 1H, H-3''), 6.82 (br s, 1H, H-3'), 6.82 (s, 1H, H-7'), 6.69 (s, 1H, H-7), 6.55 (br s, 1H, H-1'), 5.61 (s, 1H, H-7'''), 4.95 (q,  $J$  = 6.8 Hz, 1H, H-1'''), 4.72 (q,  $J$  = 6.9 Hz, 1H, H-1), 4.16 (s, 3H, 4''-OCH<sub>3</sub>), 4.05 (s, 3H, 4'-OCH<sub>3</sub>), 3.96 (m, 1H, H-3'''), 3.94 (s, 3H, 8-OCH<sub>3</sub>), 3.66 (m, 1H, H-3), 3.43 (s, 3H, 8'''-OCH<sub>3</sub>), 3.32 (dd,  $J$  = 18.9, 11.7 Hz, 1H, 4'''-H<sub>ax</sub>), 3.01 (s, 3H, 2'''-NCH<sub>3</sub>), 2.89 (dd,  $J$  = 17.7, 4.9 Hz, 1H, 4-H<sub>eq</sub>), 2.29 (s, 3H, 2'-CH<sub>3</sub>), 2.08 (dd,  $J$  = 16.5, 5.4 Hz, 1H, 4'''-H<sub>eq</sub>), 2.07 (s, 1H, 2''-CH<sub>3</sub>), 1.76 (dd,  $J$  = 18.09, 11.5 Hz, 1H, 4-H<sub>ax</sub>), 1.57 (d,  $J$  = 6.7 Hz, 1H, 1-CH<sub>3</sub>), 1.48 (d,  $J$  = 6.6 Hz, 3H, 1'''-CH<sub>3</sub>), 1.18 (d,  $J$  = 6.7 Hz, 1H, 3'''-CH<sub>3</sub>), 1.16 (d,  $J$  = 6.2 Hz, 2H, 3-CH<sub>3</sub>).

$^{13}\text{C}$  NMR ( $\text{CD}_3\text{OD}$ , 151 MHz):  $\delta_{\text{C}}$  (ppm) = 158.5 (C-4''), 158.2 (C-4'), 158.0 (C-8), 157.6 (C-6''), 156.9 (C-6), 156.6 (C-8'''), 152.6 (C-5''), 151.2 (C-5'), 139.8 (C-2''), 137.1 (C-2'), 136.9 (C-9''), 136.3 (C-9'), 135.9 (C-10), 132.7 (C-7''), 132.2 (C-7'), 129.3 (C-10'''), 128.3 (C-1''), 126.5 (C-8''), 124.3 (C-8'), 122.8 (C-5'''), 121.5 (C-6'), 119.7 (C-5), 119.1 (C-9'''), 118.7 (C-1'), 116.3 (C-10'), 114.6 (C-3''), 114.5 (C-10''), 113.5 (C-9), 107.6 (C-3'), 104.7 (C-6''), 98.3 (C-7''), 97.9 (C-7), 71.9 (C-1'''), 62.3 (C-3'''), 56.9 (4'-OCH<sub>3</sub>), 56.8 (4''-OCH<sub>3</sub>), 56.1 (8-OCH<sub>3</sub>), 55.7 (8'''-OCH<sub>3</sub>), 49.0 (C-1), 44.6 (C-3), 34.1 (C-4'''), 33.1 (C-4), 22.2 (2'''-NCH<sub>3</sub>), 22.0 (2'-CH<sub>3</sub>), 21.6 (2''-CH<sub>3</sub>), 20.3 (1'''-CH<sub>3</sub>), 18.8 (3-CH<sub>3</sub>), 18.4 (1-CH<sub>3</sub>), 13.6 (3'''-CH<sub>3</sub>).

Table 19. Detailed 1D NMR data of **47-49** in MeOD ( $\delta$  in ppm,  $J$  in Hz).

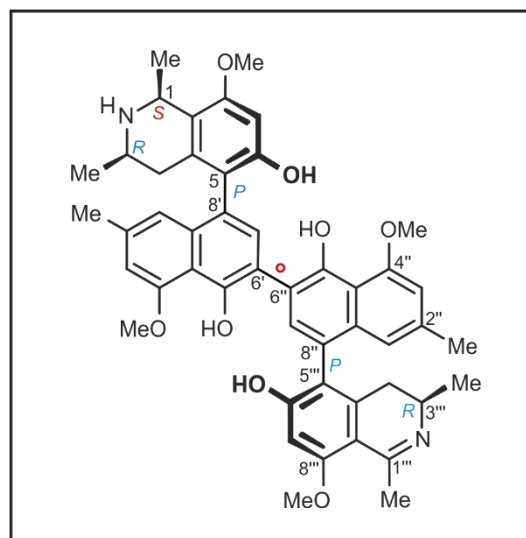
Position	1- <i>epi</i> -mbandakamine A ( <b>47</b> )		mbandakamine C ( <b>48</b> )		mbandakamine D ( <b>49</b> )	
	$\delta_{\text{H}}$	$\delta_{\text{C}}$ , type	$\delta_{\text{H}}$	$\delta_{\text{C}}$ , type	$\delta_{\text{H}}$	$\delta_{\text{C}}$ , type
1	4.65, q	52.1, CH	4.68, q	52.1, CH	4.72, q	49.0, CH
3	3.27, m	51.7, CH	3.35, m	51.7, CH	3.66, m	44.6, CH
4	3.68, dd	33.1, CH <sub>eq</sub>	3.58, dd	33.3, CH <sub>eq</sub>	2.89, dd	33.1, CH <sub>eq</sub>
	2.55, dd	33.1, CH <sub>ax</sub>	2.71, dd	33.3, CH <sub>ax</sub>	1.76, dd	33.1, CH <sub>ax</sub>
5		120.8, C		120.6, C		119.7, C
6		157.5, C		157.7, C		156.9, C
7	6.48, s	99.2, CH	6.48, s	99.3, CH	6.69, s	97.9, CH
8		158.1, C		158.3, C		158.0, C
9		113.5, C		113.5, C		113.5, C
10		136.0, C		135.4, C		135.9, C
1'	6.74, d	118.9, CH	6.77, d	119.3, CH	6.55, br s	118.7, CH
2'		136.6, C		137.2, C		137.2, C
3'	6.87, d	106.9, CH	6.82, br s	107.7, CH	6.82, br s	107.6, CH
4'		157.6, C		157.5, C		158.2, C
5'		151.2, C		152.4, C		152.6, C
6'		124.2, C		123.6, C		121.5, C
7'	6.44, s	134.9, CH	6.51, s	135.4, CH	6.82, s	132.2, CH
8'		124.3, C		124.7, C		124.3, C
9'		136.3, C		136.8, C		136.3, C
10'		114.6, C		114.2, C		116.3, C
Me-1	1.76, d	20.6, Me	1.78, d	20.5, Me	1.57, d	18.4, Me
Me-3	1.50, d	18.9, Me	1.54, d	19.0, Me	1.16, d	18.8, Me
Me-2'	2.37, s	22.3, Me	2.38, s	22.3, Me	2.29, s	22.0, Me
8-OMe	3.83, s	56.0, Me	3.83, s	56.0, Me	3.94, s	56.1, Me
4'-OMe	4.09, s	56.9, Me	4.05, s	57.5, Me	4.05, s	56.9, Me
1'''	4.64, q	50.0, CH		175.8, CN	4.95, q	71.9, CH
3'''	3.50, m	46.2, CH	3.52, m	50.2, CH	3.96, m	62.3, CH
	1.95, dd	33.2, CH <sub>eq</sub>	2.00, dd	33.8, CH <sub>eq</sub>	2.08, dd	34.1, CH <sub>eq</sub>
4'''	2.42, dd	33.2, CH <sub>ax</sub>	2.85, m	33.8, CH <sub>ax</sub>	3.32, dd	34.1, CH <sub>ax</sub>
		122.8, C		125.4, C		122.8, C
6'''		154.5, C		164.8, C		157.6, C
7'''	5.32, s	97.0, CH	5.56, s	98.2, CH	5.61, s	98.3, CH
8'''		156.7, C		165.1, C		158.3, C
9'''		113.5, C		108.8, C		119.1, C
10'''		133.7, C		143.8, C		129.3, C
1''		128.0, C		127.5, C		128.3, C
2''		141.0, C		141.4, C		137.2, C
3''	6.79, s	114.6, CH	6.83, s	115.0, CH	6.88, s	114.64, CH
4''		155.4, C		155.6, C		158.5, C
5''		158.5, C		159.1, C		151.2, C
6''	6.99, d	104.7, CH	7.02, d	104.7, CH	7.02, d	104.7, CH
7''	7.05, d	132.4, CH	7.07, d	132.3, CH	6.98, d	132.7, CH
8''		126.5, C		124.8, C		126.5, C
9''		138.3, C		138.0, C		136.9, C
10''		116.3, C		116.3, C		114.5, C
Me-1'''	1.53, d	19.0, Me	2.65, d	24.8, Me	1.48, d	16.5, Me
Me-3'''	1.25, d	18.9, Me	1.28, d	18.8, Me	1.18, d	13.6, Me
Me-2''	1.91, s	21.5, Me	1.90, s	21.5, Me	2.07, s	22.6, Me
8'''-OMe	3.05, s	55.4, Me	3.28, s	56.2, Me	3.43, s	55.7, Me
5''-OMe	4.15, s	57.0, Me	4.16, s	57.1, Me	4.16, s	56.8, Me
2'''-MeN					3.01, s	48.20, Me-N

### Michellamine $F_2$ (50)

White, amorphous powder (2.2 mg).

$[\alpha]_D^{23} = -12$  ( $c$  0.03, MeOH)

UV (CH<sub>3</sub>OH):  $\lambda_{\max}$  ( $\log \epsilon$ ) = 204 (1.30), 231 (1.01), 256 (0.45), 263 (0.54), 295 (0.17), 313 (0.30), 323 (0.25), 331 (0.24), 349 (0.12) nm.



ECD (MeOH,  $c$  0.1):  $\lambda_{\max}$  ( $\log \epsilon$  in  $\text{cm}^2 \text{mol}^{-1}$ ) 200

(+20.1), 229 (-19.5), 250 (+4.2), 265 (-1.0), 287 (+3.8), 311 (+0.8), 362 (-2.2) nm.

HRESIMS  $m/z$  783.36203  $[\text{M}+\text{H}]^+$  (calcd for C<sub>48</sub>H<sub>51</sub>N<sub>2</sub>O<sub>8</sub>, 783.36399).

<sup>1</sup>H NMR (CD<sub>3</sub>OD, 600 MHz):  $\delta_{\text{H}}$  (ppm) = 7.01 (s, 1H, H-7''), 7.01 (s, 1H, H-3''), 6.85 (s, 1H, H-1''), 6.82 (d,  $J = 1.11$  Hz, 1H, H-3'), 6.75 (s, 1H, H-7), 6.67 (ps,  $J = 1.07$  Hz, 1H, H-1'), 6.57 (s, 1H, H-7'), 6.28 (s, 1H, H-7'''), 4.59 (q,  $J = 6.56$  Hz, 1H, H-1), 4.16 (s, 3H, 4''-OCH<sub>3</sub>), 4.15 (s, 3H, 4'-OCH<sub>3</sub>), 3.90 (s, 3H, 8-OCH<sub>3</sub>), 3.67 (s, 3H, 8'''-OCH<sub>3</sub>), 3.45 (m, 1H, H-3'''), 3.16 (m, 1H, H-3), 2.75 (dd,  $J = 17.48, 11.72$  Hz, 1H, 4'''-H<sub>ax</sub>), 2.48 (dd,  $J = 17.78, 3.35$  Hz, 1H, 4'''-H<sub>eq</sub>), 2.33 (s, 1H, 2'-CH<sub>3</sub>), 2.18 (s, 3H, 1'''-CH<sub>3</sub>), 2.16 (dd,  $J = 17.78, 3.35$  Hz, 1H, 4-H<sub>eq</sub>), 1.93 (s, 1H, 2''-CH<sub>3</sub>), 1.86 (dd,  $J = 17.37, 10.48$  Hz, 1H, 4-H<sub>ax</sub>), 1.68 (d,  $J = 6.56$  Hz, 3H, 1-CH<sub>3</sub>), 1.31 (d,  $J = 7.06$  Hz, 3H, 1'''-CH<sub>3</sub>), 1.11 (d,  $J = 6.46$  Hz, 3H, 3-CH<sub>3</sub>).

<sup>13</sup>C NMR (CD<sub>3</sub>OD, 151 MHz):  $\delta_{\text{C}}$  (ppm) = 175.7 (C-1'''), 166.8 (C-6'''), 163.6 (C-8'''), 158.4 (4''-C), 158.3 (C-8), 157.8 (C-4'), 156.9 (C-6), 155.7 (C-5''), 152.6 (C-5'), 141.7 (C-10'''), 139.7 (C-2''), 137.2 (C-2'), 137.1 (C-9''), 136.9 (C-9'), 135.9 (C-10), 133.8 (C-7'), 132.1 (C-7''), 127.0 (C-8''), 126.8 (C-6'), 125.8 (C-5'''), 125.1 (C-8'), 120.9 (C-6''), 119.7 (C-5), 119.5 (C-1'), 116.5 (C-10''), 114.8 (C-1''), 114.6 (C-10'), 114.5 (C-9), 108.2 (C-9'''), 107.6 (C-3'), 104.8 (C-3''), 99.3 (C-7), 98.7 (C-7'''), 57.1 (4''-OCH<sub>3</sub>), 57.1 (4'-OCH<sub>3</sub>), 56.6 (8'''-OCH<sub>3</sub>), 56.0 (8-OCH<sub>3</sub>), 52.0 (C-1), 50.6 (C-3), 49.8 (C-3'''), 33.8 (C-4'''), 33.1 (C-4), 24.4 (1'''-CH<sub>3</sub>), 22.4 (2'-CH<sub>3</sub>), 22.2 (2''-CH<sub>3</sub>), 20.4 (1-CH<sub>3</sub>), 18.8 (3-CH<sub>3</sub>), 18.4 (3'''-CH<sub>3</sub>).

Table 20. Detailed 2D NMR data of michellamine F<sub>2</sub> (**50**) in methanol-*d*<sub>4</sub> ( $\delta$  in ppm, *J* in Hz).

Position	$\delta_H$	$\delta_C$	michellamine F <sub>2</sub> ( <b>50</b> )		
			HMBC	COSY	ROESY
1	4.59, q	52.0, CH	8, 9, 10, 1-Me	1-Me	3, 8-OMe
3	3.16, m	50.6, CH	4, 3-Me	4 <sub>eq</sub> , 3-Me	1
4	2.16, dd	33.1, CH <sub>eq</sub>	5, 9, 10	3, 4 <sub>ax</sub>	7', 3-Me
	1.86, dd	33.1, CH <sub>ax</sub>	3, 9, 10, 3-Me	3, 4 <sub>eq</sub>	1', 3-Me
5		119.7, C			
6		156.9, C			
7	6.75, s	99.3, CH	1, 5, 6, 8, 9, 8'		8-OMe
8		158.3, C			
9		114.5, C			
10		135.9, C			
1'	6.67, br	119.5, CH	2', 3', 10', 8', 9'		4 <sub>ax</sub> , 1-Me, 2'-Me
2'		137.2, C			
3'	6.82, d	107.6, CH	1', 2', 4', 10'		2'-Me, 4'-OMe
4'		158.8, C			
5'		152.6, C			
6'		126.8, C			
7'	6.57, s	133.8, CH	5, 5', 9', 10', 6''		4 <sub>eq</sub> , 6''
8'		125.1, C			
9'		136.9, C			
10'		114.6, C			
Me-1	1.68, d	20.3, Me	1, 9	1	8-OMe
Me-3	1.11, d	18.8, Me	3, 4	3	4 <sub>eq</sub> , 4 <sub>ax</sub>
Me-2'	2.33, s	22.2, Me	1', 2', 3'		1', 3'
8-OMe	3.90, s	56.0, Me	8		7, 1-Me
4'-OMe	4.15, s	57.1, Me	4'		3'
1'''		175.7, CN			
3'''	3.45, m	49.8, CH	4''', 3'''-Me	4''', 3'''-Me	
4'''	2.48, dd	33.8, CH <sub>eq</sub>	5''', 9''', 10'''	3''', 4'' <sub>ax</sub>	7'', 3'''-Me
	2.75, dd	33.8, CH <sub>ax</sub>	3''', 9''', 10''', 3'''-Me	3''', 4'' <sub>eq</sub>	1'', 3'''-Me
5'''		125.8, C			
6'''		166.8, C			
7'''	6.28, s	98.7, CH	1''', 5''', 6''', 8''', 9''', 8''		8'''-OMe
8'''		163.6, C			
9'''		108.2, C			
10'''		141.7, C			
1''	6.85, br	114.8, CH	2'', 3'', 10'', 8'', 9''	3''	4'' <sub>ax</sub> , 2''-Me
2''		139.7, C			
3''	7.01, s	104.8, CH	1'', 2'', 4'', 10''	1''	2''-Me, 4''-OMe
4''		158.4, C			
5''		155.7, C			
6''		123.3, C			
7''	7.01, s	132.1, CH	6'', 5'', 9'', 10'', 5'''		4'' <sub>eq</sub>
8''		127.0, C			
9''		137.1, C			
10''		116.5, C			
Me-1'''	2.18, d	24.4, Me	1''', 9'''		8'''-OMe
Me-3'''	1.31, d	18.4, Me	3''', 4'''	3'''	4'' <sub>eq</sub> , 4'' <sub>ax</sub>
Me-2''	1.93, s	22.2, Me	1'', 2'', 3''		1'', 3''
8'''-OMe	3.67, s	56.0, Me	8'''		7''', 1'''-Me
4''-OMe	4.16, s	57.1, Me	4''		3''

## IV.4. Cyclombandakamines, a Thrilling Series of Novel Dimeric Alkaloids

### IV.4.1. Extractions, Isolation, and HPLC conditions

#### IV.4.1.1. Extraction and fractionation

The procedure is the same as described for the ealapasamines (see IV.2.1.1) until the obtention of fraction A, by a partition with CH<sub>2</sub>Cl<sub>2</sub>, and the remaining aqueous phase. The aforementioned fraction A, which was a dichloromethane phase collected under neutral conditions (pH 7), likewise submitted reversed-phase chromatography led to the slower eluting subfractions A<sub>83</sub>-A<sub>96</sub>. The latter were enriched in cyclombandakamines, but still with the other of dimers present. The isolation by semi-preparative HPLC from these subfractions permitted the obtainment of these alkaloids in a pure form.

In this case, a second procedure was developed in parallel to increase the extraction yield. The abovementioned aqueous mother liquor, after extraction of the neutral fraction A, was further alkalized with two drops of diluted ammonia – to set free the alkaloids from their salts – at a pH 8.5 (not higher). This solution was further exhaustively partitioned with dichloromethane to afford fraction B, which was exclusively enriched in all dimeric alkaloids (Figure 75). Fraction B was as well fractionated on an RP<sub>18</sub> classical column providing 15 subfractions, B<sub>1</sub>-B<sub>15</sub>. Once submitted to semi-preparative HPLC, all groups of dimeric alkaloids were found in these sub-fractions, but the cyclombandakamines were distributed between B<sub>8</sub>-B<sub>12</sub>.

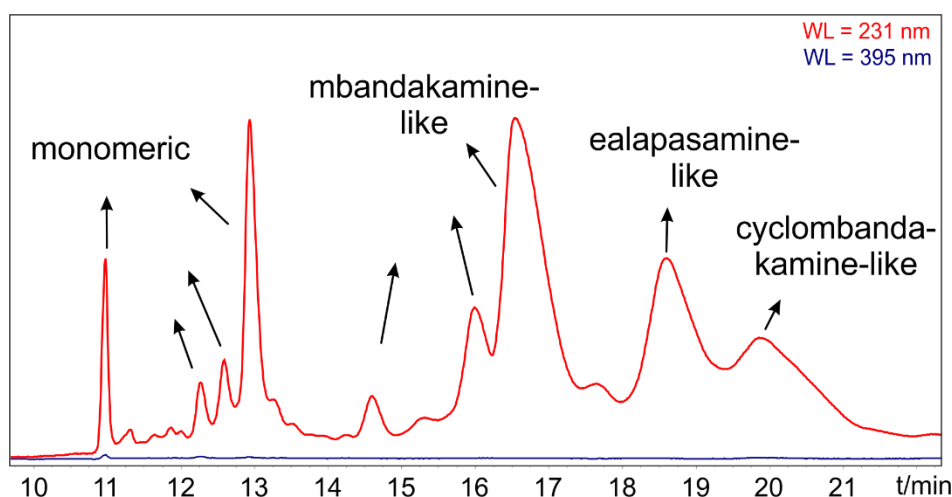


Figure 75. Chromatogram of a mixed subfraction (from subfraction B<sub>8</sub>) showing the elution on monomeric, mbandakamine-like, ealapasamine-like, and cyclombandakamine-like naphthylisoquinoline alkaloids. Chromatogram acquired at the wavelength of 231 nm, on Chromolith®



SemiPrep RP-18e column (100 x 10 mm), and a mobile phase made of A (H<sub>2</sub>O, 0.05% TFA) and C (MeOH, 0.05% TFA), at the flow rate of 14.2 mL min<sup>-1</sup>.

#### IV.4.1.2. Isolation and semi-preparative HPLC conditions

Four gradient elution conditions were used in this case:

- System 1: isolation performed on a Symmetry<sup>®</sup> Prep-C<sub>18</sub> column (Waters, 300 × 19 mm, 7 μm), using A (H<sub>2</sub>O, 0.05% TFA) and B (MeCN, 0.05% TFA), with a flow rate of 10 mL min<sup>-1</sup>. The gradient details were as described for the isolation of **42**.
- System 2: purification performed on a Discovery<sup>®</sup> HS F5-10 column (Supelco<sup>®</sup>, 250 × 21.2 mm, 10 μm), using A (H<sub>2</sub>O, 0.05% TFA) and B (MeCN, 0.05% TFA), with a flow rate of 13 mL min<sup>-1</sup>. The stationary phase was pentafluorophenyl bonded high-speed silica, which offers different separations processes from C<sub>18</sub>, characterized by stronger retention of alkaloids. The gradient used in this case was: 0-20 min: 35-55% of B, 25 min: 60% of B, 33 min: 70% of B, 48 min: 75% of B, 50 min: 100% of B, yielding 12.3 mg of cyclombandakamine A (**51**) and 6.1 mg of 1-*epi*-cyclombandakamine A (**52**), eluting faster than **32** and **47**.
- System 3: further purification using a Chromolith<sup>®</sup> SemiPrep RP-18e column (100 x 10 mm), and a mobile phase made of A and C (MeOH, 0.05% TFA), at the flow rate of 14.2 mL min<sup>-1</sup>. The gradient used was: 0-6 min: 5% of C, 11-15 min: 30% of C, 15.1-25 min: 33% of C, 26 min: 40% of C, 27 min: 45% of C, 28 min: 100% of C, to yield 5.5 mg of **55**, 11.3 mg of **56**, 2.5 mg of **57**, along with other related compounds, which were not fully characterized.
- System 4: further purification from system 1 was performed with Chromolith<sup>®</sup> SemiPrep RP-18e column and A and C (MeOH, 0.05% TFA), at the flow rate of 10 mL min<sup>-1</sup>. The gradient used was as: 0-2 min: 5% of C, 13-28 min: 30-50% of C, 29 min: 100% of C, yielding 1.5 mg of **53**, 4.6 mg of **54**, along with **55**.

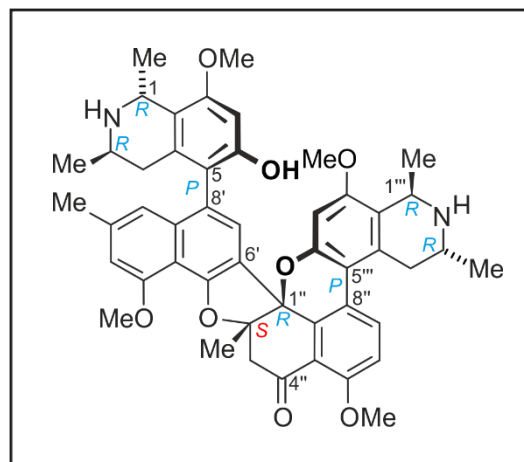
### IV.4.1.3. Isolated and fully characterized cyclombandakamine dimers

#### *Cyclombandakamine A (51)*

White amorphous powder (10.1 mg).

$[\alpha]_D^{23} = -22$  ( $c = 0.1$ , MeOH).

UV (MeOH):  $\lambda_{\max}$  ( $\log \epsilon$ ) = 201 (1.88), 216 (1.30), 233 (1.52), 257 (0.50), 277 (0.28), 288 (0.28), 295 (0.28), 315 (0.34), 330 (0.24), 340 (0.19), 385 (0.03) nm.



ECD (MeOH,  $c$  0.3):  $\lambda_{\max}$  ( $\log \epsilon$  in  $\text{cm}^2 \text{mol}^{-1}$ ) = 200 (+8.48), 207 (-5.19), 216 (+7.68), 219 (+6.55), 233 (+32.09), 247 (-21.84), 287 (+3.07), 304 (-10.12), 325 (+4.15), 347 (-0.26), 360 (+1.82), 400 (+0.04) nm.

ORD (MeOH,  $c$  0.3):  $\lambda_{\max}$  ( $\log \epsilon$  in  $\text{cm}^2 \text{mol}^{-1}$ ) = 201 (+6.27), 211 (-9.54), 217 (-4.22), 224 (-8.70), 239 (+40.49), 269 (-7.00), 295 (+6.09), 315 (-9.28), 340 (+0.07), 353 (-1.91), 386 (+0.65), 430 (+0.22) nm.

HRESIMS  $m/z$  783.36399  $[\text{M}+\text{H}]^+$  (calcd for  $\text{C}_{48}\text{H}_{51}\text{N}_2\text{O}_8$ , 783.36451).

$^1\text{H}$  NMR ( $\text{CD}_3\text{OD}$ , 600 MHz):  $\delta_{\text{H}}$  (ppm) = 7.96 ( $d$ ,  $J = 8.9$  Hz, 1H, H-7''), 7.35 ( $d$ ,  $J = 9.0$  Hz, 1H, H-6''), 6.79 ( $d$ ,  $J = 0.9$  Hz, 1H, H-3'), 6.52 ( $s$ , 1H, H-1'), 6.45 ( $s$ , 1H, H-7'''), 6.39 ( $s$ , 1H, H-7), 6.35 ( $s$ , 1H, H-7'), 4.68 ( $q$ ,  $J = 6.74$  Hz, 1H, H-1), 4.56 ( $q$ ,  $J = 6.91$  Hz, 1H, H-1'''), 4.00 ( $s$ , 3H, 4'-OCH<sub>3</sub>), 3.96 ( $s$ , 3H, 5''-OCH<sub>3</sub>), 3.91 ( $m$ , 1H, H-3'''), 3.85 ( $s$ , 3H, 8-OCH<sub>3</sub>), 3.72 ( $s$ , 3H, 8'''-OCH<sub>3</sub>), 3.68 ( $dd$ ,  $J = 16.53, 3.86$  Hz, 1H, 4'''-H<sub>ax</sub>), 3.52 ( $m$ , 1H, H-3), 3.13 ( $d$ ,  $J = 14.89$  Hz, 1H, 3''-H<sub>eq</sub>), 3.05 ( $dd$ ,  $J = 16.73, 8.1$  Hz, 1H, 4'''-H<sub>eq</sub>), 3.03 ( $d$ ,  $J = 14.53$  Hz, 1H, 3''-H<sub>eq</sub>), 2.35 ( $dd$ ,  $J = 17.84, 4.82$  Hz, 1H, 4-H<sub>eq</sub>), 2.28 ( $s$ , 3H, 2'-CH<sub>3</sub>), 1.94 ( $dd$ ,  $J = 17.51, 11.91$  Hz, 1H, 4-H<sub>ax</sub>), 1.84 ( $s$ , 3H, 2''-CH<sub>3</sub>), 1.67 ( $d$ ,  $J = 6.61$  Hz, 3H, 1'''-CH<sub>3</sub>), 1.50 ( $d$ ,  $J = 6.71$  Hz, 3H, 1-CH<sub>3</sub>), 1.08 ( $d$ ,  $J = 6.36$  Hz, 3H, 3-CH<sub>3</sub>), 0.72 ( $d$ ,  $J = 6.86$  Hz, 3H, 3'''-CH<sub>3</sub>).

$^{13}\text{C}$  NMR ( $\text{CD}_3\text{OD}$ , 151 MHz):  $\delta_{\text{H}}$  (ppm) = 196.3 (C-4'''), 160.7 (C-5'''), 158.6 (C-8'''), 158.5 (C-4'), 157.5 (C-8), 157.5 (C-6), 156.4 (C-5'), 154.7 (C-6'''), 139.6 (C-2'), 138.7 (C-9'), 138.5

(C-9"), 135.6 (C-7"), 133.0 (C-10), 128.7 (C-10"), 126.6 (C-8'), 126.0 (C-7'), 124.5 (C-8"), 121.1 (C-6'), 119.7 (C-5), 119.5 (C-10"), 119.2 (C-5""), 118.2 (C-9""), 118.0 (C-1'), 114.3 (C-10'), 113.9 (C-9), 108.7 (C-3'), 102.7 (C-7""), 98.6 (C-7), 92.4 (C-2"), 85.5 (C-1"), 56.8 (5"-OCH<sub>3</sub>), 56.6 (4'-OCH<sub>3</sub>), 56.5 (8""-OCH<sub>3</sub>), 56.2 (8-OCH<sub>3</sub>), 52.2 (C-3"), 49.7 (C-1), 48.1 (C-3""), 46.6 (C-1""), 44.9 (C-3), 33.5 (C-4""), 32.7 (C-4), 22.5 (2'-CH<sub>3</sub>), 20.2 (1""-CH<sub>3</sub>), 19.2 (3-CH<sub>3</sub>), 18.8 (1-CH<sub>3</sub>), 18.4 (C-2"), 14.9 (3""-CH<sub>3</sub>).

Table 21. Detailed NMR data of cyclombandakamine A (**51**) in methanol-*d*<sub>4</sub> ( $\delta$  in ppm, *J* in Hz).

Cyclombandakamine A ( <b>51</b> )					
Position	$\delta_{\text{H}}$ ( <i>J</i> in Hz)	HSQC	HMBC	COSY	ROESY
1	4.68, q (6.7)	49.7, CH	8, 9, 10, 1-Me	1-Me	8-OMe
3	3.52, m	44.9, CH	4, 3-Me	4 <sub>eq</sub> , 3-Me	1-Me, 4''' <sub>ax</sub>
4	2.35, dd(17.8, 4.8)	32.7, CH <sub>eq</sub>	5, 9, 10	3, 4 <sub>ax</sub>	7', 3-Me
	1.94, dd(17.5, 11.9)	32.7, CH <sub>ax</sub>	3, 9, 10, 3-Me	3, 4 <sub>eq</sub>	1', 3-Me
5		119.7, C			
6		157.5, C			
7	6.39, s	98.6, CH	1, 5, 6, 8, 9		8-OMe, 4''' <sub>ax</sub> , 1''', 3'''-Me
8		157.5, C			
9		113.9, C			
10		133.0, C			
1'	6.52, s	118.0, CH	3', 10', 8', 9'		4 <sub>ax</sub> , 2'-Me
2'		139.6, C			
3'	6.79, d (0.9)	108.7, CH	1', 2', 4', 10'		2'-Me, 4'-OMe
4'		158.5, C			
5'		156.4, C			
6'		121.1, C			
7'	6.35, s	126.0, CH	5, 5', 9', 10', 1''		4 <sub>eq</sub> , 3'''-Me
8'		126.6, C			
9'		138.7, C			
10'		114.3, C			
1-Me	1.50, d (6.7)	18.8, Me	1, 9	1	3, 8-OMe
3-Me	1.08, d (6.4)	19.2, Me	3, 4	3	4 <sub>eq</sub> , 4 <sub>ax</sub>
2'-Me	2.28, s	22.5, Me	1', 2', 3'		1', 3'
8-OMe	3.85, s	56.2, Me	8		1, 7, 1-Me
4'-OMe	4.00, s	56.6, Me	4'		3', 2''-Me
1''		85.5, C			
2''		92.4, C			
3''	3.03, d (14.5)	52.2, CH <sub>eq</sub>	1'', 2'', 4'', 10'', 2''-Me	3'' <sub>ax</sub>	2''-Me
	3.13, d (14.9)	52.2, CH <sub>ax</sub>	1'', 2'', 4'', 2''-Me	3'' <sub>eq</sub>	2''-Me
4''		196.3, C=O			
5''		160.7, C			
6''	7.35, d (9.0)	113.9, CH	4'', 5'', 8'', 10''	7''	5''-OMe
7''	7.96, d (8.9)	135.6, CH	1'', 5'', 9'', 5'''	6''	4''' <sub>eq</sub> , 4''' <sub>ax</sub>
8''		124.5, C			
9''		138.5, C			
10''		119.5, C			

Continuation of Table 21, see the next page.

Continuation of Table 21.

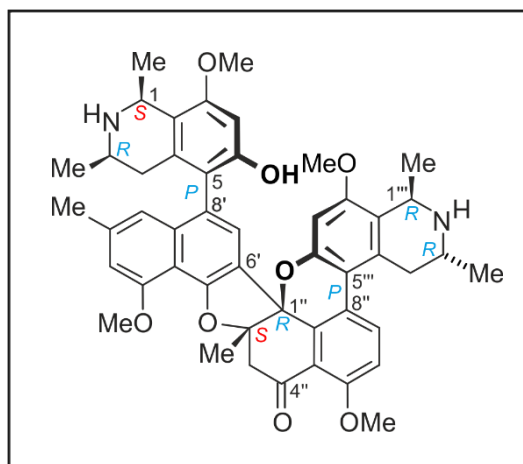
1'''	4.56, q (6.9)	46.6, CH	8'''',9'''',10'''',1'''-	1'''-Me	7, 8'''-OMe
3'''	3.91, m	48.1, CH	4'''', 3'''-Me	4'''eq,3'''-Me	1'''-Me
4'''	3.68, dd (16.5, 3.9)	33.5, CH <sub>eq</sub>	5'''', 9'''', 10'''	3'''', 4'''ax	7'', 3'''-Me
	3.05, <i>dd</i> (16.7, 8.1)	32.7, CH <sub>ax</sub>	3'''',9'''',10'''',3'''- Me	3'''', 4'''eq	3,7,7'',3'''-Me
5'''		119.2, C			
6'''		154.7, C			
7'''	6.45, <i>s</i>	102.7, CH	1'''', 5'''', 6'''', 8'''',		<b>2''-Me, 8'''-OMe</b>
8'''		158.6, C			
9'''		118.2, C			
10'''		128.7, C			
1'''-Me	1.67, <i>d</i> (6.6)	20.2, Me	1'''', 9'''	1'''	3'''', 8'''-OMe
3'''-Me	0.72, <i>d</i> (6.9)	14.9, Me	3'''', 4'''	3'''	7,7',4'''eq,4'''ax, 8- OMe
2''-Me	1.85, <i>s</i>	18.4, Me	1'', 2'', 3''		<b>3''eq, 3''ax, 4''-</b>
8'''-	3.72, <i>s</i>	56.5, Me	8'''		7'''', 1'''', 1'''-Me
5''-OMe	3.96, <i>s</i>	56.8, Me	5''		5''

*1-epi-Cyclombandakamine A (52)*

White amorphous powder (5.0 mg).

$[\alpha]_D^{23} = -21$  ( $c = 0.1$ , MeOH).

UV (MeOH):  $\lambda_{\max}$  ( $\log \epsilon$ ) = 201 (1.88), 216 (1.32),  
233 (1.49), 257 (0.50), 277 (0.28),  
288 (0.28), 295 (0.28), 315 (0.34),  
330 (0.24), 340 (0.19), 385 (0.03) nm.



ECD (MeOH,  $c$  0.3):  $\lambda_{\max}$  ( $\log \epsilon$  in  $\text{cm}^2 \text{mol}^{-1}$ ) = 200 (+8.48), 206 (−5.20), 216 (+7.68),  
218 (+6.54), 233 (+32.10), 247 (−21.80), 287 (+3.09), 304 (−11.10),  
325 (+4.15), 347 (−0.26), 360 (+1.82), 400 (+0.01) nm.

ORD (MeOH,  $c$  0.3):  $\lambda_{\max}$  ( $\log \epsilon$  in  $\text{cm}^2 \text{mol}^{-1}$ ) = 201 (+6.30), 211 (−9.50), 218 (−4.22), 224 (−  
8.70), 239 (+39.49), 269 (−7.05), 295 (+6.09), 315 (−9.28), 340 (+0.08),  
353 (−1.91), 386 (+0.65), 400 (+0.30) nm.

HRESIMS  $m/z$  783.36389  $[\text{M}+\text{H}]^+$  (calcd for  $\text{C}_{48}\text{H}_{51}\text{N}_2\text{O}_8$ , 783.36451).

$^1\text{H}$  NMR ( $\text{CD}_3\text{OD}$ , 600 MHz):  $\delta_{\text{H}}$  (ppm) = 7.97 (d,  $J = 8.9$  Hz, 1H, H-7''), 7.35 (d,  $J = 9.1$  Hz, 1H, H-6''), 6.80 (s, 1H, H-3'), 6.60 (s, 1H, H-1'), 6.47 (s, 1H, H-7'''), 6.40 (s, 1H, H-7), 6.38 (s, 1H, H-7'), 4.62 (q,  $J = 6.6$  Hz, 1H, H-1'''), 4.52 (q,  $J = 6.5$  Hz, 1H, H-1), 4.00 (s, 3H, 4'- $\text{OCH}_3$ ), 3.96 (s, 3H, 5''- $\text{OCH}_3$ ), 3.94 (m, 1H, H-3'''), 3.84 (s, 3H, 8- $\text{OCH}_3$ ), 3.73 (s, 3H, 8'''- $\text{OCH}_3$ ), 3.71 (dd,  $J = 16.1, 5.0$  Hz, 1H, 4'''- $\text{H}_{\text{ax}}$ ), 3.12 (d,  $J = 14.8$  Hz, 1H,  $\text{H}_{\text{ax}}-3''$ ), 3.09 (m, 1H, H-3), 3.06 (dd,  $J = 18.5, 11.6$  Hz, 1H, 4'''- $\text{H}_{\text{eq}}$ ), 3.02 (d,  $J = 14.8$  Hz, 1H, H-3''), 2.30 (s, 3H, 2'- $\text{CH}_3$ ), 2.17 (dd,  $J = 17.4, 3.4$  Hz, 1H, 4- $\text{H}_{\text{eq}}$ ), 2.05 (dd,  $J = 18.4, 11.8$  Hz, 1H, 4- $\text{H}_{\text{ax}}$ ), 1.83 (s, 3H, 2''- $\text{CH}_3$ ), 1.69 (d,  $J = 6.9$  Hz, 3H, 1'''- $\text{CH}_3$ ), 1.68 (d,  $J = 6.5$  Hz, 3H, 1- $\text{CH}_3$ ), 1.09 (d,  $J = 6.2$  Hz, 3H, 3- $\text{CH}_3$ ), 0.89 (d,  $J = 6.5$  Hz, 3H, 3'''- $\text{CH}_3$ ).

$^{13}\text{C}$  NMR ( $\text{CD}_3\text{OD}$ , 151 MHz):  $\delta_{\text{H}}$  (ppm) = 196.3 (C-4'''), 160.7 (C-5'''), 158.6 (C-8'''), 158.5 (C-4'), 158.5 (C-8), 157.0 (C-6), 156.5 (C-5'), 154.7 (C-6'''), 139.6 (C-2'), 139.0 (C-9'), 138.3 (C-9''), 135.5 (C-7'''), 135.1 (C-10), 128.7 (C-10'''), 126.3 (C-8'), 126.3 (C-7'), 124.5 (C-8''), 121.2 (C-6'), 119.9 (C-5), 119.6 (C-10''), 118.9 (C-5'''), 118.3 (C-9'''), 118.1 (C-1'), 114.4 (C-10'), 113.9 (C-9), 108.7 (C-3'), 102.6 (C-7'''), 99.6 (C-7), 92.4 (C-2''), 85.4 (C-1''), 56.8 (5''-

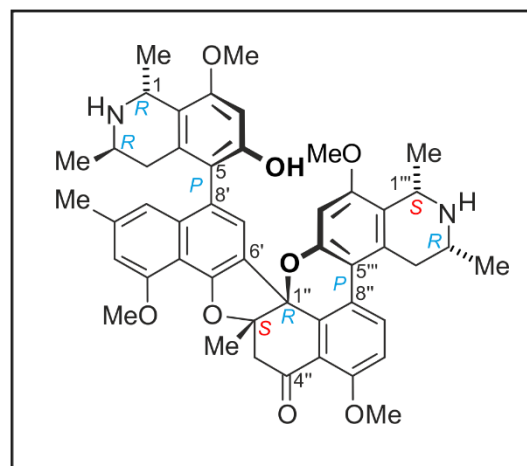
OCH<sub>3</sub>), 56.6 (4'-OCH<sub>3</sub>), 56.5 (8'''-OCH<sub>3</sub>), 56.0 (8-OCH<sub>3</sub>), 52.2 (C-3''), 52.0 (C-1), 50.6 (C-3), 48.1 (C-3'''), 46.7 (C-1'''), 33.6 (C-4'''), 32.9 (C-4), 22.6 (2'-CH<sub>3</sub>), 20.2 (1'''-CH<sub>3</sub>), 20.2 (1-CH<sub>3</sub>), 18.6 (3-CH<sub>3</sub>), 18.4 (C-2''), 14.9 (3'''-CH<sub>3</sub>).

*Cyclombandakamine A<sub>3</sub>* (**53**)

White amorphous powder (1.3 mg).

$[\alpha]_D^{23} = -13$  ( $c = 0.04$ , MeOH).

UV (MeOH):  $\lambda_{\max}$  ( $\log \epsilon$ ) = 201 (1.88), 216 (1.30),  
233 (1.52), 257 (0.50), 277 (0.28),  
288 (0.285), 295 (0.28), 315 (0.34),  
330 (0.24), 340 (0.19), 390 (0.02) nm.



ECD (MeOH,  $c$  0.1):  $\lambda_{\max}$  ( $\log \epsilon$  in  $\text{cm}^2 \text{mol}^{-1}$ ) = 200 (+2.23), 210 (+0.41), 212 (+0.49), 220 (–0.44), 234 (+4.66), 251 (–2.99), 286 (+0.29), 304 (–1.57), 328 (+0.43), 347 (–0.03), 354 (+0.20), 365 (+0.27), 400 (–0.01) nm.

ORD (MeOH,  $c$  0.1):  $\lambda_{\max}$  ( $\log \epsilon$  in  $\text{cm}^2 \text{mol}^{-1}$ ) = 201 (+3.13), 211 (–4.94), 217 (–2.12), 224 (–4.44), 240 (+19.23), 269 (–3.45), 294 (+3.05), 314 (–5.00), 340 (+0.02), 355 (–0.89), 388 (+0.35), 430 (+0.10) nm.

HRESIMS  $m/z$  783.36203  $[\text{M}+\text{H}]^+$  (calcd for  $\text{C}_{48}\text{H}_{51}\text{N}_2\text{O}_8$ , 783.36399).

$^1\text{H}$  NMR ( $\text{CD}_3\text{OD}$ , 600 MHz):  $\delta_{\text{H}}$  (ppm) = 7.97 (d,  $J = 9.21$  Hz, 1H, H-7''), 7.35 (d,  $J = 8.98$  Hz, 1H, H-6''), 6.79 (s, 1H, H-3'), 6.53 (s, 1H, H-1'), 6.43 (s, 1H, H-7'''), 6.39 (s, 1H, H-7), 6.36 (s, 1H, H-7'), 4.67 (q,  $J = 7.26$  Hz, 1H, H-1), 4.49 (br q, 1H, H-1'''), 4.00 (s, 3H, 4'-OCH<sub>3</sub>), 3.96 (s, 3H, 5''-OCH<sub>3</sub>), 3.86 (s, 3H, 8-OCH<sub>3</sub>), 3.81 (m, 1H, H-3'''), 3.72 (s, 3H, 8'''-OCH<sub>3</sub>), 3.64 (br dd, 1H, 4'''-H<sub>eq</sub>), 3.50 (m, 1H, H-3), 3.12 (d,  $J = 14.31$  Hz, 1H, 3''-H<sub>ax</sub>), 3.03 (d,  $J = 14.61$  Hz, 1H, 3''-H<sub>eq</sub>), 2.99 (br dd, 1H, 4'''-H<sub>ax</sub>), 2.33 (br dd, 1H, 4-H<sub>eq</sub>), 2.28 (s, 3H, 2'-CH<sub>3</sub>), 1.94 (br dd, 1H, 4-H<sub>ax</sub>), 1.85 (s, 3H, 2''-CH<sub>3</sub>), 1.63 (d,  $J = 6.40$  Hz, 3H, 1'''-CH<sub>3</sub>), 1.50 (d,  $J = 6.66$  Hz, 3H, 1-CH<sub>3</sub>), 1.07 (d,  $J = 6.31$  Hz, 3H, 3-CH<sub>3</sub>), 0.71 (d,  $J = 6.90$  Hz, 3H, 3'''-CH<sub>3</sub>).

$^{13}\text{C}$  NMR ( $\text{CD}_3\text{OD}$ , 151 MHz):  $\delta_{\text{C}}$  (ppm) = 196.3 (C-4''), 160.67 (C-5''), 158.6 (C-8'''), 158.5 (C-4'), 157.6 (C-6), 157.5 (C-8), 156.4 (C-5'), 154.7 (C-6'''), 139.6 (C-2'), 138.7 (C-9'), 138.7 (C-9''), 135.6 (C-7'''), 133.12 (C-10), 131.0 (C-10'''), 126.5 (C-8'), 126.1 (C-7'), 125.2 (C-8''), 121.2 (C-6'), 119.8 (C-5), 119.3 (C-5'''), 118.9 (C-9'''), 118.0 (C-1'), 114.3 (C-10'), 114.2 (C-9), 108.7 (C-3'), 102.4 (C-7'''), 98.6 (C-7), 92.4 (C-2''), 85.3 (C-1''), 56.8 (5''-OCH<sub>3</sub>), 56.6 (4'-OCH<sub>3</sub>), 56.4 (8'''-OCH<sub>3</sub>), 56.2 (8-OCH<sub>3</sub>), 52.9 (C-1'''), 52.3 (C-3''), 50.2 (C-3'''), 49.0 (C-1),



---

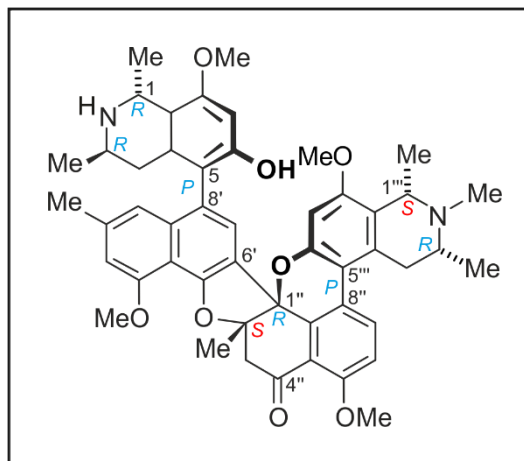
44.8 (C-3), 33.2 (C-4'''), 32.8 (C-4), 22.5 (2'-CH<sub>3</sub>), 20.4 (1'''-CH<sub>3</sub>), 19.3 (3-CH<sub>3</sub>), 18.8 (1-CH<sub>3</sub>), 18.4 (2''-CH<sub>3</sub>), 14.6 (3'''-CH<sub>3</sub>).

*Cyclombandakamine A<sub>4</sub>* (**54**)

White powder amorphous powder (2.9 mg).

$[\alpha]_D^{23} = -14$  ( $c = 0.04$ , MeOH).

UV (MeOH):  $\lambda_{\max}$  ( $\log \epsilon$ ) = 205 (1.11), 217 (0.70),  
230 (1.01), 257 (0.24), 262 (0.25),  
297 (0.14), 315 (0.15), 322 (0.21),  
329 (0.19), 338 (0.25), 344 (0.29)  
nm.



ECD (MeOH,  $c$  0.1):  $\lambda_{\max}$  ( $\log \epsilon$  in  $\text{cm}^2 \text{mol}^{-1}$ ) = 200 (+2.25), 205 (+0.72), 213 (-2.74),  
220 (+2.16), 232 (+7.16), 248 (-5.94), 287 (+0.05), 304 (-3.18),  
325 (+0.68), 347 (-0.59), 360 (+0.34), 385 (-0.12), 400 (-0.31) nm.

ORD (MeOH,  $c$  0.1):  $\lambda_{\max}$  ( $\log \epsilon$  in  $\text{cm}^2 \text{mol}^{-1}$ ) = 202 (-0.35), 209 (-1.79), 217 (-0.13), 224 (-0.92),  
240 (+10.15), 269 (-1.31), 295 (+1.59), 316 (-2.57), 341 (-0.13),  
353 (-0.94), 382 (+0.09), 393 (+0.14), 460 (-0.23) nm.

HRESIMS  $m/z$  813.37506  $[\text{M}+\text{H}+\text{O}]^+$  (calcd for  $\text{C}_{49}\text{H}_{53}\text{N}_2\text{O}_9$ , 813.37511). The molecular formula is  $\text{C}_{49}\text{H}_{52}\text{N}_2\text{O}_8$ .

$^1\text{H}$  NMR ( $\text{CD}_3\text{OD}$ , 600 MHz):  $\delta_{\text{H}}$  (ppm) = 8.29 (d,  $J = 9.1$  Hz, 1H, H-7''), 7.35 (d,  $J = 9.2$  Hz, 1H, H-6''), 6.80 (s, 1H, H-3'), 6.48 (s, 1H, H-1'), 6.47 (s, 1H, H-7'''), 6.39 (s, 1H, H-7), 6.34 (s, 1H, H-7'), 5.04 (q,  $J = 6.9$  Hz, 1H, H-1'''), 4.70 (q,  $J = 6.8$  Hz, 1H, H-1), 4.46 (m, 1H, H-3'''), 4.43 (dd,  $J = 18.1, 6.5$  Hz, 1H,  $\text{H}_{\text{eq}}\text{-4}''$ ), 4.00 (s, 3H, 4'- $\text{OCH}_3$ ), 3.97 (s, 3H, 5''- $\text{OCH}_3$ ), 3.88 (s, 3H, 8- $\text{OCH}_3$ ), 3.73 (s, 3H, 8'''- $\text{OCH}_3$ ), 3.50 (m, 1H, H-3), 3.11 (d,  $J = 14.9$  Hz, 1H, 3''- $\text{H}_{\text{ax}}$ ), 3.04 (d,  $J = 14.9$  Hz, 1H, 3''- $\text{H}_{\text{eq}}$ ), 3.03 (br. s., 3H, 2'''- $\text{NCH}_3$ ), 2.91 (dd,  $J = 18.1, 11.2$  Hz, 1H, 4'''- $\text{H}_{\text{ax}}$ ), 2.34 (dd,  $J = 18.2, 4.9$  Hz, 1H, 4- $\text{H}_{\text{eq}}$ ), 2.28 (s, 3H, 2'- $\text{CH}_3$ ), 1.95 (dd,  $J = 18.2, 11.6$  Hz, 1H, 4- $\text{H}_{\text{ax}}$ ), 1.84 (s, 3H, 2''- $\text{CH}_3$ ), 1.78 (d,  $J = 6.6$  Hz, 3H, 1'''- $\text{CH}_3$ ), 1.53 (d,  $J = 6.8$  Hz, 1H, 1- $\text{CH}_3$ ), 1.46 (d,  $J = 6.3$  Hz, 3H, 3'''- $\text{CH}_3$ ), 1.09 (d,  $J = 6.4$  Hz, 3H, 3- $\text{CH}_3$ ).

$^{13}\text{C}$  NMR ( $\text{CD}_3\text{OD}$ , 151 MHz):  $\delta_{\text{C}}$  (ppm) = 196.2 (C-4''), 160.8 (C-5''), 158.5 (C-4'), 158.0 (C-8'''), 157.7 (C-8), 157.7 (C-6), 156.6 (C-5'), 155.5 (C-6'''), 139.8 (C-2'), 138.8 (C-9''), 138.7 (C-9'), 135.1 (C-7''), 133.6 (C-10), 127.9 (C-10'''), 126.6 (C-8'), 126.0 (C-7'), 124.6 (C-8''), 121.0

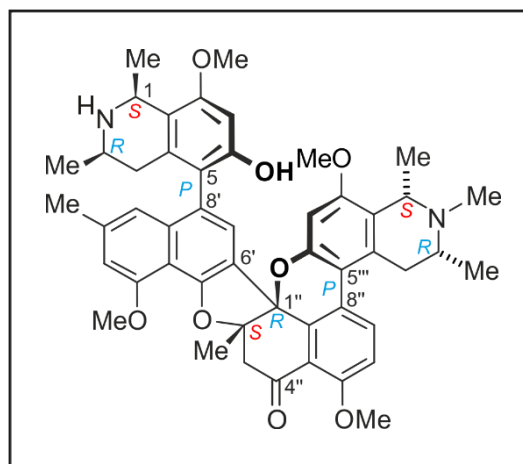
(C-6'), 120.0 (C-5), 119.4 (C-10''), 119.2 (C-9'''), 117.9 (C-1'), 117.7 (C-5'''), 114.4 (C-10'), 114.3 (C-9), 114.0 (C-6''), 108.8 (C-3'), 102.7 (C-7'''), 98.4 (C-7), 92.5 (C-2''), 85.4 (C-1''), 71.3 (C-1'''), 63.3 (C-3'''), 56.8 (5''-OCH<sub>3</sub>), 56.7 (8''-OCH<sub>3</sub>), 56.6 (4'-CH<sub>3</sub>), 56.3 (8-OCH<sub>3</sub>), 52.0 (C-3''), 49.3 (2''-NCH<sub>3</sub>), 49.1 (C-1), 44.9 (C-3), 33.5 (C-4'''), 32.8 (C-4), 22.5 (2'-CH<sub>3</sub>), 19.1 (3-CH<sub>3</sub>), 18.8 (1-CH<sub>3</sub>), 18.3 (2''-CH<sub>3</sub>), 16.5 (1'''-CH<sub>3</sub>), 14.8 (3'''-CH<sub>3</sub>).

*Cyclombandakamine A<sub>5</sub> (55)*

White powder amorphous powder (3.5 mg).

$[\alpha]_D^{23} = +18$  ( $c = 0.09$ , MeOH).

UV (MeOH):  $\lambda_{\max}$  ( $\log \epsilon$ ) = 201 (1.88), 216 (1.32), 233 (1.49), 257 (0.50), 277 (0.28), 288 (0.28), 295 (0.28), 315 (0.34), 330 (0.24), 340 (0.19), 385 (0.03) nm.



ECD (MeOH,  $c$  0.2):  $\lambda_{\max}$  ( $\log \epsilon$  in  $\text{cm}^2 \text{mol}^{-1}$ ) = 202 (+7.25), 215 (+11.11), 219 (+10.24), 231 (+20.50), 247 (-19.08), 287 (+0.97), 304 (-10.16), 325 (+4.11), 333 (+2.13), 347 (-0.75), 361 (+2.25), 400 (+0.05) nm.

ORD (MeOH,  $c$  0.2):  $\lambda_{\max}$  ( $\log \epsilon$  in  $\text{cm}^2 \text{mol}^{-1}$ ) = 198 (-5.03), 208 (-3.00), 218 (+2.01), 223 (+1.46), 239 (+31.68), 269 (-4.94), 295 (+5.11), 315 (-9.53), 341 (-0.16), 353 (-2.86), 373 (+0.22), 387 (+0.56), 437 (-0.46) nm.

HRESIMS  $m/z$  813.37280  $[\text{M}+\text{H}+\text{O}]^+$  (calcd for  $\text{C}_{49}\text{H}_{53}\text{N}_2\text{O}_9$ , 813.37511). The molecular formula is  $\text{C}_{49}\text{H}_{52}\text{N}_2\text{O}_8$ .

$^1\text{H}$  NMR ( $\text{CD}_3\text{OD}$ , 600 MHz):  $\delta_{\text{H}}$  (ppm) = 8.32 (d,  $J = 9.2$  Hz, 1H, H-7''), 7.34 (d,  $J = 9.2$  Hz, 1H, H-6''), 6.81 (s, 1H, H-3'), 6.55 (s, 1H, H-1'), 6.46 (s, 1H, H-7'''), 6.39 (s, 1H, H-7), 6.37 (s, 1H, H-7'), 5.03 (q,  $J = 6.5$  Hz, 1H, H-1'''), 4.53 (q,  $J = 6.5$  Hz, 1H, H-1), 4.42 (dd,  $J = 18.2, 6.2$  Hz, 1H, 4'''-H<sub>eq</sub>), 4.40 (m, 1H, H-3'''), 4.00 (s, 3H, 4'-OCH<sub>3</sub>), 3.96 (s, 3H, 4''-OCH<sub>3</sub>), 3.86 (s, 3H, 8-OCH<sub>3</sub>), 3.73 (s, 3H, 8'''-OCH<sub>3</sub>), 3.11 (d,  $J = 14.8$  Hz, 1H, 3''-H<sub>ax</sub>), 3.11 (br. s., 3H, 2'''-NCH<sub>3</sub>), 3.09 (m, 1H, H-3), 3.02 (d,  $J = 14.8$  Hz, 1H, 3''-H<sub>eq</sub>), 2.90 (dd,  $J = 18.5, 11.6$  Hz, 1H, 4'''-H<sub>ax</sub>), 2.30 (s, 3H, 2'-CH<sub>3</sub>), 2.17 (dd,  $J = 17.4, 3.4$  Hz, 1H, 4-H<sub>eq</sub>), 2.05 (dd,  $J = 18.4, 11.8$  Hz, 1H, 4-H<sub>ax</sub>), 1.83 (s, 3H, 2''-CH<sub>3</sub>), 1.78 (d,  $J = 6.9$  Hz, 3H, 1'''-CH<sub>3</sub>), 1.69 (d,  $J = 6.5$  Hz, 1H, 1-CH<sub>3</sub>), 1.50 (d,  $J = 6.2$  Hz, 3H, 3'''-CH<sub>3</sub>), 1.09 (d,  $J = 6.5$  Hz, 3H, 3-CH<sub>3</sub>).

$^{13}\text{C}$  NMR ( $\text{CD}_3\text{OD}$ , 151 MHz):  $\delta_{\text{C}}$  (ppm) = 196.2 (C-4''), 160.8 (C-5''), 158.6 (C-8), 158.5 (C-4'), 158.0 (C-8'''), 157.0 (C-6), 156.6 (C-5'), 155.5 (C-6'''), 139.8 (C-2'), 139.0 (C-9'), 138.8 (C-9''), 135.1 (C-7''), 133.6 (C-10), 128.1 (C-10'''), 126.2 (C-7'), 126.1 (C-8'), 124.6 (C-8''), 121.0 (C-6'), 120.0 (C-5), 119.8 (C-9'''), 119.5 (C-10''), 118.1 (C-1'), 117.4 (C-5'''), 114.5 (C-10'),

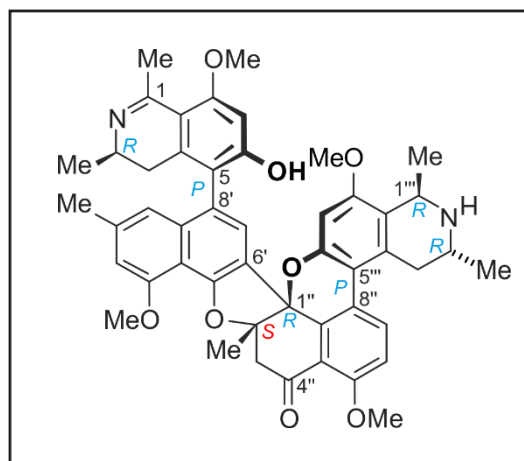
114.2 (C-9), 114.0 (C-6"), 108.7 (C-3'), 102.7 (C-7""), 99.1 (C-7), 92.4 (C-2"), 85.4 (C-1"), 71.4 (C-1""), 63.0 (C-3""), 56.8 (5"-OCH<sub>3</sub>), 56.7 (8""-OCH<sub>3</sub>), 56.6 (4'-OCH<sub>3</sub>), 56.2 (8-OCH<sub>3</sub>), 52.0 (C-1), 52.0 (C-3"), 50.6 (C-3), 49.7 (2""-NCH<sub>3</sub>), 34.9 (C-4""), 33.0 (C-4), 22.6 (2'-CH<sub>3</sub>), 20.2 (1-CH<sub>3</sub>), 18.6 (3""-CH<sub>3</sub>), 18.3 (2"-CH<sub>3</sub>), 16.6 (1""-CH<sub>3</sub>), 14.8 (3-CH<sub>3</sub>).

Cyclombandakamine A<sub>6</sub> (**56**)

Yellowish amorphous powder (6.5 mg).

$[\alpha]_D^{23} = -20$  ( $c = 0.09$ , MeOH).

UV (MeOH):  $\lambda_{\max}$  ( $\log \epsilon$ ) = 201 (1.12), 224 (0.72),  
232 (0.73), 263 (0.24), 296 (0.15),  
315 (0.19), 329 (0.16), 340 (0.15),  
350 (0.17), 361 (0.14), 380 (0.16),  
400 (0.06), 420 (0.01) nm.



ECD (MeOH,  $c$  0.09):  $\lambda_{\max}$  ( $\log \epsilon$  in  $\text{cm}^2 \text{mol}^{-1}$ ) = 200 (+5.60), 208 (+2.19), 212 (+2.98),  
220 (+1.58), 231 (+5.60), 245 (-4.76), 280 (-0.90), 290 (+0.28),  
304 (-1.65), 326 (+1.64), 355 (-1.49), 389 (+0.09), 400 (-0.09) nm.

ORD (MeOH,  $c$  0.09):  $\lambda_{\max}$  ( $\log \epsilon$  in  $\text{cm}^2 \text{mol}^{-1}$ ) = 200 (-1.96), 204 (-0.15), 209 (-0.89), 218  
(+0.73), 225 (-0.61), 238 (+7.76), 254 (-0.09), 272 (-0.35), 283 (-  
0.90), 296 (+0.69), 315 (-1.84), 342 (1.55), 371 (-0.69), 397 (-0.09),  
443 (-0.03) nm.

HRESIMS  $m/z$  781.34886  $[\text{M}+\text{H}]^+$  (calcd for  $\text{C}_{48}\text{H}_{49}\text{N}_2\text{O}_8$ , 781.348892).

$^1\text{H}$  NMR ( $\text{CD}_3\text{OD}$ , 600 MHz):  $\delta_{\text{H}}$  (ppm) = 7.97 (d,  $J = 9.0$  Hz, 1H, H-7''), 7.36 (d,  $J = 9.0$  Hz,  
1H, H-6''), 6.81 (s, 1H, H-3'), 6.50 (s, 1H, H-7), 6.49 (s, 1H, H-1'), 6.47 (s, 1H, H-7'''), 6.39 (s,  
1H, H-7'), 4.60 (q,  $J = 6.7$  Hz, 1H, H-1'''), 4.00 (s, 3H, 4'-OCH<sub>3</sub>), 3.93 (m, 1H, H-3'''), 3.97 (s,  
3H, 8-OCH<sub>3</sub>), 3.96 (s, 3H, 5''-OCH<sub>3</sub>), 3.73 (s, 3H, 8'''-OCH<sub>3</sub>), 3.69 (dd,  $J = 18.1, 5.0$  Hz, 1H,  
4'''-H<sub>eq</sub>), 3.63 (m, 1H, H-3), 3.11 (dd,  $J = 18.1, 9.0$  Hz, 1H, 4'''-H<sub>ax</sub>), 3.11 (d,  $J = 14.1$  Hz, 1H,  
3''-H<sub>ax</sub>), 3.02 (d,  $J = 14.6$  Hz, 1H, 3''-H<sub>eq</sub>), 2.71 (s, 3H, 1-CH<sub>3</sub>), 2.43 (dd,  $J = 17.2, 5.8$  Hz, 1H,  
4-H<sub>eq</sub>), 2.30 (s, 3H, 2'-CH<sub>3</sub>), 2.07 (dd,  $J = 17.3, 9.9$  Hz, 1H, 4-H<sub>ax</sub>), 1.85 (s, 3H, 2''-CH<sub>3</sub>), 1.68  
(d,  $J = 6.6$  Hz, 3H, 1'''-CH<sub>3</sub>), 1.08 (d,  $J = 6.7$  Hz, 3H, 3-CH<sub>3</sub>), 0.80 (d,  $J = 6.8$  Hz, 3H, 3'''-  
CH<sub>3</sub>).

$^{13}\text{C}$  NMR ( $\text{CD}_3\text{OD}$ , 151 MHz):  $\delta_{\text{H}}$  (ppm) = 196.2 (C-4''), 175.2 (C-1), 167.4 (C-6), 165.6 (C-  
8), 160.7 (C-5''), 158.5 (C-4'), 158.5 (C-8'''), 156.8 (C-5'), 154.7 (C-6'''), 142.7 (C-10), 140.1  
(C-2'), 138.5 (C-9'), 138.3 (C-9''), 135.6 (C-7''), 128.8 (C-10'''), 126.0 (C-7'), 124.9 (C-8'), 124.5

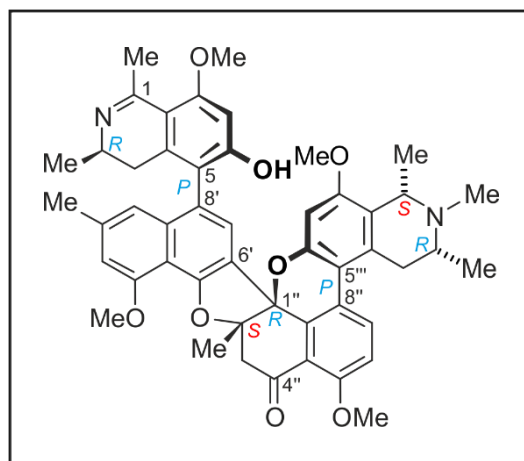
(C-8"), 122.2 (C-5), 121.1 (C-6'), 119.5 (C-10"), 119.1 (C-5'''), 118.3 (C-9'''), 117.7 (C-1'), 114.3 (C-10'), 114.0 (C-6''), 108.8 (C-3'), 108.2 (C-9), 102.6 (C-7'''), 99.3 (C-7), 92.5 (C-2''), 85.3 (C-1''), 56.9 (8-OCH<sub>3</sub>), 56.8 (5''-OCH<sub>3</sub>), 56.6 (4'-OCH<sub>3</sub>), 56.5 (8'''-OCH<sub>3</sub>), 52.2 (C-3''), 48.8 (C-3), 48.1 (C-3'''), 46.6 (C-1'''), 33.5 (C-4'''), 32.6 (C-4), 24.9 (1-CH<sub>3</sub>), 22.5 (2'-CH<sub>3</sub>), 20.3 (1'''-CH<sub>3</sub>), 18.3 (2''-CH<sub>3</sub>), 17.8 (3-CH<sub>3</sub>), 14.6 (3'''-CH<sub>3</sub>).

Cyclombandakamine A<sub>7</sub> (**57**)

Yellowish amorphous powder (2.5 mg).

$[\alpha]_D^{23} = -19$  ( $c = 0.08$ , MeOH).

UV (MeOH):  $\lambda_{\max}$  ( $\log \epsilon$ ) = 201 (1.12), 224 (0.72),  
232 (0.73), 263 (0.24), 296 (0.15),  
315 (0.19), 329 (0.16), 340 (0.15),  
350 (0.17), 361 (0.14), 380 (0.16),  
400 (0.06), 420 (0.01) nm.



ECD (MeOH,  $c$  0.06):  $\lambda_{\max}$  ( $\log \epsilon$  in  $\text{cm}^2 \text{mol}^{-1}$ ) = 201 (+3.55), 208 (+1.70), 213 (+1.67), 220  
(+0.88), 231 (+3.33), 244 (-2.56), 280 (-0.52), 290 (+0.15), 305  
(-1.00), 326 (+0.98), 355 (-0.87), 400 (-0.02) nm.

ORD (MeOH,  $c$  0.06):  $\lambda_{\max}$  ( $\log \epsilon$  in  $\text{cm}^2 \text{mol}^{-1}$ ) = 200 (-1.36), 205 (-0.11), 209 (-0.71), 217  
(+0.61), 225 (-0.61), 238 (+4.89), 254 (-0.04), 272 (-0.25), 283  
(-0.68), 296 (+0.51), 315 (-1.14), 342 (1.15), 371 (-0.52), 397 (-0.10),  
440 (-0.02) nm.

HRESIMS  $m/z$  811.35652  $[\text{M}+\text{H}+\text{O}]^+$  (calcd for  $\text{C}_{49}\text{H}_{51}\text{N}_2\text{O}_9$ , 811.35891). The molecular  
formula  $[\text{M}]$  is  $\text{C}_{49}\text{H}_{50}\text{N}_2\text{O}_8$ .

$^1\text{H}$  NMR ( $\text{CD}_3\text{OD}$ , 600 MHz):  $\delta_{\text{H}}$  (ppm) = 8.31 (d,  $J = 9.08$  Hz, 1H, H-7''), 7.36 (d,  $J = 9.13$   
Hz, 1H, H-6''), 6.81 (s, 1H, H-3'), 6.52 (s, 1H, H-7), 6.46 (s, 1H, H-7'''), 6.45 (s, 1H, H-1'), 6.37  
(s, 1H, H-7'), 5.01 (q,  $J = 6.93$  Hz, 1H, H-1'''), 4.42 (dd, 1H, 4'''-H<sub>eq</sub>), 4.39 (m, 1H, H-3'''), 4.01  
(s, 3H, 8-OCH<sub>3</sub>), 4.00 (s, 3H, 4'-OCH<sub>3</sub>), 3.97 (s, 3H, 5''-OCH<sub>3</sub>), 3.73 (s, 3H, 8'''-OCH<sub>3</sub>), 3.64  
(m, 1H, H-3), 3.09 (d,  $J = 14.88$  Hz, 1H, 3''-H<sub>ax</sub>), 3.04 (br. s, 3H, 2'''-NCH<sub>3</sub>), 3.02 (d,  $J = 14.72$   
Hz, 1H, 3''-H<sub>eq</sub>), 2.96 (dd, 1H, 4'''-H<sub>ax</sub>), 2.73 (d,  $J = 1.16$  Hz, 3H, 1-CH<sub>3</sub>), 2.43 (dd,  $J = 16.90$ ,  
5.60 Hz, 1H, 4-H<sub>eq</sub>), 2.29 (s, 3H, 2'-CH<sub>3</sub>), 2.06 (dd,  $J = 16.93$ , 10.07 Hz, 1H, 4-H<sub>ax</sub>), 1.83 (s,  
3H, 2''-CH<sub>3</sub>), 1.78 (d,  $J = 6.66$  Hz, 3H, 1'''-CH<sub>3</sub>), 1.48 (d,  $J = 6.26$  Hz, 3H, 3'''-CH<sub>3</sub>), 1.09 (d,  $J$   
= 6.71 Hz, 3H, 3-CH<sub>3</sub>).

$^{13}\text{C}$  NMR ( $\text{CD}_3\text{OD}$ , 151 MHz):  $\delta_{\text{H}}$  (ppm) = 196.1 (C-4''), 175.4 (C-1), 167.4 (C-6), 165.7 (C-  
8), 160.8 (C-5''), 158.5 (C-4'), 158.0 (C-8'''), 157.0 (C-5'), 155.5 (C-6'''), 143.0 (C-10), 140.2



(C-2'), 138.8 (C-9''), 138.5 (C-9'), 135.2 (C-7''), 128.2 (C-10'''), 125.9 (C-7'), 124.7 (C-8'), 124.7 (C-8''), 122.2 (C-5), 121.0 (C-6'), 119.8 (C-9'''), 119.4 (C-10''), 117.6 (C-1'), 117.6 (C-5'''), 114.3 (C-10'), 114.0 (C-6''), 108.9 (C-3'), 108.5 (C-9), 102.7 (C-7'''), 99.0 (C-7), 92.5 (C-2''), 85.4 (C-1''), 71.3 (C-1'''), 63.3 (C-3'''), 57.0 (8-OCH<sub>3</sub>), 56.8 (5''-OCH<sub>3</sub>), 56.8 (8'''-OCH<sub>3</sub>), 56.6 (4'-OCH<sub>3</sub>), 51.9 (C-3''), 49.52 (2'''-NCH<sub>3</sub>), 48.8 (C-3), 34.7 (C-4'''), 32.6 (C-4), 25.0 (1-CH<sub>3</sub>), 22.5 (2'-CH<sub>3</sub>), 18.3 (2''-CH<sub>3</sub>), 17.8 (3-CH<sub>3</sub>), 16.5 (1'''-CH<sub>3</sub>), 14.8 (3'''-CH<sub>3</sub>).

## **IV.5. Ealamines A-H, Enthralling Naphthylisoquinoline Alkaloids with Promising Bioactivities from *Ancistrocladus ealaensis***

### **IV.5.1. Extractions, Isolation, and HPLC conditions**

#### **IV.5.1.1. Extraction and fractionation**

The air-dried powder of leave materials (600 g) was macerated in methanol, with a mechanical shaker (160-170 RPM) for 24 hours. After filtration, the marc was further macerated until exhaustiveness. The 24h-macerates were mixed after filtration and evaporated to a viscous solution. Water was added to the solution to allow precipitation of chlorophyll and other side components. The solution was further partitioned with *n*-hexane to clear the upper phase of residual chlorophyll. The aqueous phase was partitioned until exhaustion with CH<sub>2</sub>Cl<sub>2</sub>. The lower CH<sub>2</sub>Cl<sub>2</sub> phase was evaporated to obtain the alkaloid-rich fraction A. This fraction, was subsequently submitted to preparative liquid chromatography using C<sub>18</sub>-reversed phase. Further fractionation of sub-fractions A<sub>12</sub> to A<sub>35</sub> was carried out on a series of five C<sub>18</sub>-SPE cartridges (Sep-Pak C<sub>18</sub> Plus Light Cartridge, 130 mg, 55-105 μm) and led to several alkaloids enriched fractions. The mobile system contained 0.05% TFA (trifluoroacetic acid) in ultrapure water (H<sub>2</sub>O) and acetonitrile (CH<sub>3</sub>CN), using a gradient elution from 0 to 50% in CH<sub>3</sub>CN. The enriched sub-fractions were submitted to preparative HPLC for isolation.

The isolation was performed on a Symmetry<sup>®</sup> Prep-C<sub>18</sub> column (Waters, 300 × 19 mm, 7 μm) with the mobile phase consisting of A (H<sub>2</sub>O, 0.05% TFA) and B (CH<sub>3</sub>CN, 0.05% TFA). Further purification steps with a Chromolith<sup>®</sup> SemiPrep RP-18e column (100 x 10 mm) were necessary to afford the compounds of interest, using the previously described elution system for the Symmetry<sup>®</sup> column, where B was replaced by C (MeOH, 0.05% TFA), at the same flow rate.

Further phytochemical investigations on the methanolic twig extract of *A. ealaensis*, revealed the presence of ealamine A, already found in the leaves and eluting first before an additional series of similar alkaloids. Among them, three additional new ealamines alkaloids were characterized, leading to a total of eight new monomers from leaves and twigs fractions.

#### IV.5.1.2. Isolation and HPLC conditions

For the isolation of *P-62*, *M-62*, **63-66**, the following gradient system was used on the Symmetry<sup>®</sup> Prep-C<sub>18</sub> column with a flow rate of 10 mL min<sup>-1</sup> using solvent A (H<sub>2</sub>O, 0.05% TFA) and B (MeCN, 0.05% TFA): 0-12 min: 10-20% of B, 35 min: 45% of B, 37 min: 50% of B, 40 min: 100% of B, 44 min: 100% of B. Several peaks (fractions) were generated and required additional purification steps. Therefore, fractions (containing **62-66**) were further purified progressively by chromatography on a Chromolith<sup>®</sup> SemiPrep RP-18e column (100 x 10 mm) using a gradient solvent system consisting of A (H<sub>2</sub>O, 0.05% TFA) and C (MeOH, 0.05% TFA) with a flow rate of 10 mL min<sup>-1</sup>: 0-2 min: 10% of C, 8 min: 30% of C, 11 min: 30% of C, 11.2 min: 35% of C, 16 min: 35% of C, 20 min: 40% of C, 25 min: 45% of C, 27 min: 100% of C, 30 min: 100%, to yield 18.5 mg of ealamine A (*P-62*), 10.3 mg of ealamine B (*M-62*), 11.1 mg of ealamine C (**63**), 4.0 mg of ealamine D (**64**), 0.9 mg of ealamine E (**65**). Alkaloids **66** and **17** were found in two different fractions, the separation was carried out on a Symmetry<sup>®</sup> Prep-C<sub>18</sub> column with another gradient using the same flow and solvents A and B: 0-5 min: 15% of B, 6 min: 20% of B, 20 min: 25% of B, 30 min: 30% of B, 37 min: 55% of B, 40 min: 100% of B, 44 min: 100% of B. Oriented by their LC-MS profiles, the two selected peaks were further purified independently on Chromolith<sup>®</sup> SemiPrep RP-18e column (100 x 10 mm) using the same flow rate and solvents systems (A and C) but a different gradient: 0-8 min: 10-30% of C, 13 min: 40% of C, 19 min: 55% of C, 20 min: 100% of C, 23 min: 100% of C, to yield ealamine F (**66**, 0.7 mg) and yaoundamine A (**17**, 1.2 mg).

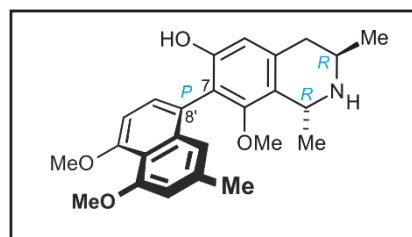
Along with *P-62* and **17**, compounds **67-69** were found in the twigs extract in a common subfraction. The isolation was carried out at the preparative HPLC on a Symmetry<sup>®</sup> Prep-C<sub>18</sub> column eluting with solvents A (H<sub>2</sub>O, 0.05% TFA) and B (MeCN, 0.05% TFA) and a flow rate of 20 mL min<sup>-1</sup>: 0-10 min: 18% of B, 13-25 min: 20% of B, 45 min: 50% of B, 48 min: 100% of B, to afford 5.3 mg of **67**, 3.1 mg of **68**, 3.4 mg of **69**, along with yaoundamine A and ealamine A.

### IV.5.1.3. Isolated ealamines

#### *Ealamine A (P-62)*

Brownish amorphous powder (18.5 mg).

$[\alpha]_D^{23} = -15^\circ$  ( $c$  0.05, MeOH).



UV (MeOH):  $\lambda_{\max}$  (log  $\epsilon$ ) 200 (5.9), 203 (6.9), 219 (4.6), 231 (5.6), 265 (0.5), 307 (1.2), 321 (1.0), 350 (0.2) nm.

ECD (MeOH,  $c$  0.1):  $\lambda_{\max}$  (log  $\epsilon$ ) 213 (-13.3), 225 (+2.8), 236 (-1.5), 240 (+0.1), 244 (-0.4), 257 (+8.4), 284 (-7.3), 318 (+2.1), 322 (+2.1) nm.

HRESIMS  $m/z$  408.21570  $[M+H]^+$  (calcd for  $C_{25}H_{30}NO_4$ , 408.21693).

$^1H$  NMR ( $CD_3OD$ , 600 MHz):  $\delta_H$  (ppm) = 7.21 (d,  $J$  = 8.08 Hz, 1H, H-7'), 6.94 (d,  $J$  = 8.08 Hz, 1H, H-6'), 6.85 (d,  $J$  = 1.10 Hz, 1H, H-1'), 6.78 (d,  $J$  = 1.42 Hz, 1H, H-3'), 6.56 (s, 1H, H-5), 4.72 (q,  $J$  = 6.83 Hz, 1H, H-1), 3.96 (s, 3H, 5'-OCH<sub>3</sub>), 3.93 (s, 3H, 4'-OCH<sub>3</sub>), 3.87 (m, 1H, H-3), 3.15 (dd,  $J$  = 17.54, 4.77 Hz, 1H, 4-H<sub>eq</sub>), 3.07 (s, 3H, 8-OCH<sub>3</sub>), 2.88 (dd,  $J$  = 17.54, 11.86 Hz, 1H, 4-H<sub>ax</sub>), 2.31 (s, 3H, 2'-CH<sub>3</sub>), 1.65 (d,  $J$  = 6.83 Hz, 3H, 1-CH<sub>3</sub>), 1.51 (d,  $J$  = 6.32 Hz, 3H, 3-CH<sub>3</sub>).

$^{13}C$  NMR ( $CD_3OD$ , 151 MHz):  $\delta_C$  (ppm) = 158.7 (C-4'), 158.7 (C-5'), 157.7 (C-6), 157.6 (C-8), 137.7 (C-9'), 137.7 (C-2'), 133.0 (C-10), 130.9 (C-7'), 124.6 (C-8'), 121.6 (C-7), 119.2 (C-1'), 118.7 (C-9), 117.5 (C-10'), 111.3 (C-5), 109.9 (C-3'), 106.7 (C-6'), 60.8 (8-OCH<sub>3</sub>), 57.1 (4'-OCH<sub>3</sub>), 56.9 (5'-OCH<sub>3</sub>), 50.1 (C-1), 45.3 (C-3), 34.6 (C-4), 22.2 (2'-CH<sub>3</sub>), 19.6 (1-CH<sub>3</sub>), 19.4 (3-CH<sub>3</sub>).

#### *X-ray Crystallographic Analysis of Ealamine A (P-62)*

Single crystals of ealamine A (*P-62*) were obtained by gentle diffusion of *n*-hexane into an acetone solution. Single crystal X-ray diffraction data for ealamine A (*P-62*) were collected at 100 K on a Bruker D8 Quest Kappa Diffractometer with a Photon100 CMOS detector and multi-layered mirror monochromated  $CuK\alpha$  radiation. The structure was solved using direct methods, expanded with Fourier techniques and refined with the Shelx software package.<sup>[272]</sup> All non-hydrogen atoms were refined anisotropically. Hydrogen atoms were included in the

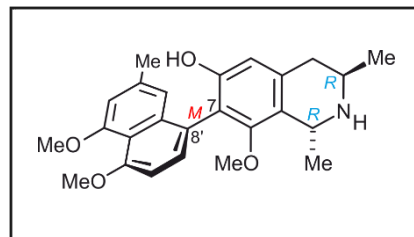
structure factor calculation on geometrically idealized positions. Crystallographic data will be soon deposited with the Cambridge Crystallographic Data Centre as supplementary publication (**P-62**).

*Crystal data for ealamine A (P-62)* ( $2 \text{ C}_{27}\text{H}_{30}\text{NO}_6\text{F}_3 \cdot \text{C}_3\text{H}_6\text{O}$ ):  $M_r = 1101.12$ ,  $0.463 \times 0.424 \times 0.285 \text{ mm}^3$ , triclinic space group P1,  $a = 8.9167(7) \text{ \AA}$ ,  $\alpha = 68.987(6)^\circ$ ,  $b = 11.8688(12) \text{ \AA}$ ,  $\beta = 73.430(7)^\circ$ ,  $c = 14.7500(15) \text{ \AA}$ ,  $\gamma = 77.232(7)^\circ$ ,  $V = 1384.3(2) \text{ \AA}^3$ ,  $Z = 1$ ,  $\rho(\text{calcd}) = 1.321 \text{ g.cm}^{-3}$ ,  $\mu = 0.900 \text{ mm}^{-1}$ ,  $F_{(000)} = 580$ ,  $\text{Goof}(F^2) = 1.051$ ,  $R_I = 0.0277$ ,  $wR^2 = 0.0744$  for  $I > 2\sigma(I)$ ,  $R_1 = 0.0278$ ,  $wR^2 = 0.0745$  for all data, 10743 unique reflections [ $\theta \leq 74.538^\circ$ ] with a completeness of 99.9 % and 725 parameters, 3 restraints.

### *Ealamine B* (M-62)

Yellowish amorphous powder (10.3 mg).

$[\alpha]_D^{23} = -15$  ( $c$  0.04, MeOH).



UV (MeOH):  $\lambda_{\max}$  ( $\log \epsilon$ ) 200 (4.1), 206 (4.6), 218 (3.6), 231 (4.7), 265 (0.4), 307 (1.1), 321 (0.9), 350 (0.01) nm.

ECD (MeOH,  $c$  0.1):  $\lambda_{\max}$  ( $\log \epsilon$ ) 200 (+10.4), 214 (-8.6), 218 (-11.3), 225 (+11.5), 241 (+0), 251 (+3.8), 284 (-3.5), 311 (+1.7), 349 (-0.7), 360 (+0.1) nm.

HRESIMS  $m/z$  408.21610  $[M+H]^+$  (calcd for  $C_{25}H_{30}NO_4$ , 408.21693).

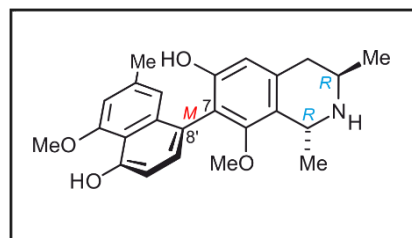
$^1H$  NMR ( $CD_3OD$ , 600 MHz):  $\delta_H$  (ppm) = 7.21 (d,  $J = 8.08$  Hz, 1H, H-7'), 6.95 (d,  $J = 8.08$  Hz, 1H, H-6'), 6.84 (d,  $J = 1.10$  Hz, 1H, H-1'), 6.78 (d,  $J = 1.17$  Hz, 1H, H-3'), 6.56 (s, 1H, H-5), 4.73 (q,  $J = 6.79$  Hz, 1H, H-1), 3.96 (s, 3H, 5'-OCH<sub>3</sub>), 3.93 (s, 3H, 4'-OCH<sub>3</sub>), 3.88 (m, 1H, H-3), 3.20 (dd,  $J = 17.91, 4.92$  Hz, 1H, 4-H<sub>eq</sub>), 3.07 (s, 3H, 8-OCH<sub>3</sub>), 2.88 (dd,  $J = 17.91, 11.71$  Hz, 1H, 4-H<sub>ax</sub>), 2.31 (s, 3H, 2'-CH<sub>3</sub>), 1.65 (d,  $J = 6.79$  Hz, 3H, 1-CH<sub>3</sub>), 1.51 (d,  $J = 6.44$  Hz, 3H, 3-CH<sub>3</sub>).

$^{13}C$  NMR ( $CD_3OD$ , 151 MHz):  $\delta_C$  (ppm) = 158.7 (C-4'), 158.7 (C-5'), 157.8 (C-6), 157.6 (C-8), 137.7 (C-9), 137.7 (C-2'), 133.0 (C-10), 131.0 (C-7), 124.5 (C-8'), 121.7 (C-7), 119.2 (C-1'), 118.6 (C-9), 117.5 (C-10'), 111.3 (C-5), 109.9 (C-3'), 106.7 (C-6'), 60.8 (8-OCH<sub>3</sub>), 57.1 (4'-OCH<sub>3</sub>), 56.9 (5'-OCH<sub>3</sub>), 50.0 (C-1), 45.3 (C-3), 34.6 (C-4), 22.2 (2'-CH<sub>3</sub>), 19.6 (1-CH<sub>3</sub>), 19.5 (3-CH<sub>3</sub>).

### *Ealamine C* (**63**)

Brownish amorphous powder (11.1 mg).

$[\alpha]_D^{23} = -24$  ( $c$  0.07, MeOH).



UV (MeOH):  $\lambda_{\max}$  ( $\log \epsilon$ ) 200 (5.4), 205 (6.9), 218 (5.3), 231 (7.1), 260 (0.5), 307 (1.3), 321 (1.2), 333 (0.8), 350 (0.01) nm.

ECD (MeOH,  $c$  0.2):  $\lambda_{\max}$  ( $\log \epsilon$ ) 200 (-25.6), 203 (-59.4), 215 (+7.6), 217 (-25.1), 222 (+1.7), 227 (-79.9), 232 (+8.1), 252 (+15.4), 285 (-9.3), 315 (+6.1), 360 (+0.5) nm.

HRESIMS  $m/z$  394.20194  $[M+H]^+$  (calcd for  $C_{24}H_{28}NO_4$ , 394.20128).

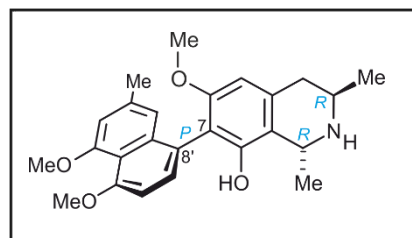
$^1H$  NMR ( $CD_3OD$ , 600 MHz):  $\delta_H$  (ppm) = 7.16 (d,  $J = 7.87$  Hz, 1H, H-7'), 6.85 (br s, 1H, H-1'), 6.80 (d,  $J = 7.87$  Hz, 1H, H-6'), 6.79 (d,  $J = 1.16$  Hz, 1H, H-3'), 6.56 (s, 1H, H-5), 4.72 (q,  $J = 6.74$  Hz, 1H, H-1), 4.08 (s, 3 H, 4'-OCH<sub>3</sub>), 3.86 (m, 1H, H-3), 3.14 (dd,  $J = 17.81, 4.84$  Hz, 1H, 4-H<sub>eq</sub>), 3.07 (s, 3H, 8-OCH<sub>3</sub>), 2.88 (dd,  $J = 17.58, 11.73$  Hz, 1H, 4-H<sub>ax</sub>), 2.32 (br s, 3H, 2'-CH<sub>3</sub>), 1.64 (d,  $J = 6.76$  Hz, 3H, 1-CH<sub>3</sub>), 1.51 (d,  $J = 6.36$  Hz, 3H, 3-CH<sub>3</sub>).

$^{13}C$  NMR ( $CD_3OD$ , 151 MHz):  $\delta_C$  (ppm) = 157.9 (C-4'), 157.7 (C-6), 157.7 (C-8), 156.1 (C-5'), 137.4 (C-2'), 137.0 (C-9'), 133.0 (C-10), 131.9 (C-7'), 122.6 (C-8'), 121.5 (C-7), 119.9 (C-1'), 118.7 (C-9), 114.8 (C-10'), 111.3 (C-5), 110.4 (C-6'), 107.5 (C-3'), 60.7 (8-OCH<sub>3</sub>), 56.9 (4'-OCH<sub>3</sub>), 50.0 (C-1), 45.3 (C-3), 34.6 (C-4), 22.4 (2'-CH<sub>3</sub>), 19.6 (1-CH<sub>3</sub>), 19.4 (3-CH<sub>3</sub>).

### *Ealamine D (64)*

Yellowish amorphous powder (4.0 mg).

$[\alpha]_D^{23} = -17$  ( $c$  0.06, MeOH).



UV (MeOH):  $\lambda_{\max}$  ( $\log \epsilon$ ) 200 (6.0), 205 (6.4), 218 (5.0), 227 (4.8), 271 (1.3), 288 (1.1), 307 (1.1), 350 (0.4) nm.

ECD (MeOH,  $c$  0.03):  $\lambda_{\max}$  ( $\log \epsilon$ ) 200 (+4.9), 215 (-5.1), 219 (-5.9), 224 (-3.5), 232 (-5.9), 242 (+0.03), 247 (+0.8), 267 (-1.2), 287 (+0.2), 303 (-0.2), 314 (+0.7), 323 (+0.3), 332 (+0.7), 360 (-0.2) nm.

HRESIMS  $m/z$  408.21610  $[M+H]^+$  (calcd for  $C_{25}H_{30}NO_4$ , 408.21693).

$^1H$  NMR ( $CD_3OD$ , 600 MHz):  $\delta_H$  (ppm) = 7.22 (d,  $J = 7.87$  Hz, 1H, H-7'), 6.94 (d,  $J = 7.97$  Hz, 1H, H-6'), 6.80 (br s, 1H, H-1'), 6.79 (s, 1H, H-3'), 6.57 (s, 1H, H-5), 4.90 (q,  $J = 6.91$  Hz, 1H, H-1), 3.96 (s, 3H, 4'-OCH<sub>3</sub>), 3.93 (s, 3H, 5'-OCH<sub>3</sub>), 3.89 (m, 1H, H-3), 3.16 (dd,  $J = 17.41$ , 5.63 Hz, 1H, 4-H<sub>eq</sub>), 3.15 (s, 3H, 6-OCH<sub>3</sub>), 2.86 (dd,  $J = 17.36$ , 11.40 Hz, 1H, 4-H<sub>ax</sub>), 2.31 (d,  $J = 0.61$  Hz, 3H, 2'-CH<sub>3</sub>), 1.65 (d,  $J = 6.76$  Hz, 3H, 1-CH<sub>3</sub>), 1.51 (d,  $J = 6.46$  Hz, 3H, 3-CH<sub>3</sub>).

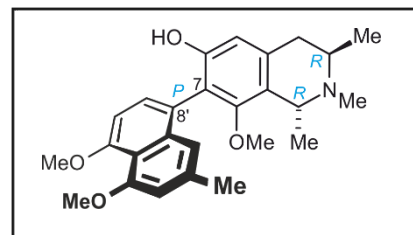
$^{13}C$  NMR ( $CD_3OD$ , 151 MHz):  $\delta_C$  (ppm) = 158.7 (C-4'), 158.6 (C-5'), 157.8 (C-8), 157.6 (C-6), 137.7 (C-2'), 137.6 (C-9'), 133.0 (C-10), 130.9 (C-7'), 124.6 (C-8'), 121.5 (C-7), 119.4 (C-1'), 118.5 (C-9), 117.6 (C-10'), 111.5 (C-5), 109.9 (C-3'), 106.5 (C-6'), 61.2 (8-OCH<sub>3</sub>), 57.1 (s, 5'-OCH<sub>3</sub>), 56.9 (5'-OCH<sub>3</sub>), 49.8 (C-1), 45.3 (C-3), 34.6 (C-4), 22.2 (2'-CH<sub>3</sub>), 19.6 (1-CH<sub>3</sub>), 19.4 (3-CH<sub>3</sub>).



### *Ealamine E* (**65**)

Yellowish amorphous powder (0.9 mg).

$[\alpha]_D^{23} = -13$  ( $c$  0.02, MeOH).



UV (MeOH):  $\lambda_{\max}$  ( $\log \epsilon$ ) 200 (4.2), 205 (5.9), 218 (5.1), 231 (6.3), 260 (0.1), 307 (1.2), 321 (1.0), 333 (0.3) nm.

ECD (MeOH,  $c$  0.02):  $\lambda_{\max}$  ( $\log \epsilon$ ) 200 (+2.5), 211 (-0.2), 215 (+0.3), 233 (-1.5), 251 (+0.2), 284 (-1.3), 311 (+0.3), 323 (+0.3), 348 (+0.2) nm.

HRESIMS  $m/z$  422.23295  $[M+H]^+$  (calcd for  $C_{26}H_{32}NO_4$ , 422.23303).

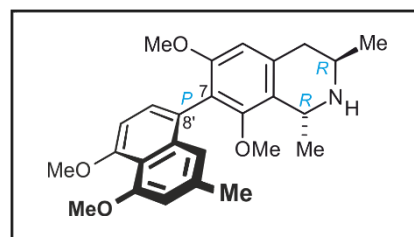
$^1H$  NMR ( $CD_3OD$ , 600 MHz):  $\delta_H$  (ppm) = 7.19 (d,  $J = 7.97$  Hz, 1H, H-7'), 6.94 (d,  $J = 8.28$  Hz, 1H, H-6'), 6.89 (s, 1H, H-1'), 6.79 (s, 1H, H-3'), 6.58 (s, 1H, H-5), 4.66 (q,  $J = 6.76$  Hz, 1H, H-1), 4.15 (m, 1H, H-3), 3.96 (s, 3H, 5'-OCH<sub>3</sub>), 3.93 (s, 3H, 4'-OCH<sub>3</sub>), 3.12 (dd,  $J = 18.79, 5.01$  Hz, 1H, 4-H<sub>eq</sub>), 3.07 (s, 3H, 8-OCH<sub>3</sub>), 2.96 (dd,  $J = 18.79, 12.02$  Hz, 1H, 4-H<sub>ax</sub>), 2.87 (s, 3H, 2-NCH<sub>3</sub>), 2.34 (s, 3H, 2'-CH<sub>3</sub>), 1.71 (d,  $J = 6.66$  Hz, 3H, 1-CH<sub>3</sub>), 1.52 (d,  $J = 6.46$  Hz, 3H, 3-CH<sub>3</sub>).

$^{13}C$  NMR ( $CD_3OD$ , 151 MHz):  $\delta_C$  (ppm) = 158.6 (C-4'), 158.6 (C-5'), 158.2 (C-8), 157.8 (C-6), 137.6 (C-2'), 137.6 (C-9'), 130.8 (C-10), 130.8 (C-7'), 124.4 (C-8'), 121.9 (C-7), 119.1 (C-1'), 117.3 (C-9), 116.3 (C-10'), 111.1 (C-5), 109.8 (C-3'), 106.5 (C-6'), 60.7 (8-OCH<sub>3</sub>), 60.5 (C-1), 56.9 (4'-OCH<sub>3</sub>), 56.7 (5'-OCH<sub>3</sub>), 50.6 (C-3), 34.2 (2-NCH<sub>3</sub>), 30.4 (C-4), 22.1 (2'-CH<sub>3</sub>), 20.2 (1-CH<sub>3</sub>), 16.8 (3-CH<sub>3</sub>).

### *Ealamine F* (**66**)

Yellow amorphous powder (0.7 mg).

$[\alpha]_D^{23} = -15$  ( $c$  0.04, MeOH).



UV (MeOH):  $\lambda_{\max}$  ( $\log \epsilon$ ) 200 (4.1), 206 (5.9), 217 (4.8),

230 (5.8), 261 (0.2), 307 (1.1), 321 (1.0), 333 (0.2) nm.

ECD (MeOH,  $c$  0.06):  $\lambda_{\max}$  ( $\log \epsilon$ ) 200 (+9.8), 211 (-4.7), 219 (+2.9), 233 (-1.8), 242 (-0.3),

261 (-3.1), 310 (+0.4), 318 (+0.5), 352 (-0.3), 365 (-0.3) nm.

HRESIMS  $m/z$  422.23356  $[M+H]^+$  (calcd for  $C_{26}H_{32}NO_4$ , 422.23303).

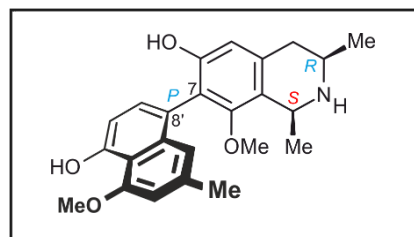
$^1\text{H}$  NMR ( $\text{CD}_3\text{OD}$ , 400 MHz):  $\delta_{\text{H}}$  (ppm) = 7.18 (d,  $J$  = 7.93 Hz, 1H, H-7'), 6.94 (d,  $J$  = 8.06 Hz, 1H, H-6'), 6.79 (s, 1H, H-1'), 6.76 (s, 1H, H-3'), 6.74 (s, 1H, H-5), 4.77 (q,  $J$  = 6.85 Hz, 1H, H-1), 3.98 (s, 3H, 5'-OCH<sub>3</sub>), 3.95 (s, 3H, 4'-OCH<sub>3</sub>), 3.90 (m, 1H, H-3), 3.64 (s, 3H, 6-OCH<sub>3</sub>), 3.22 (dd,  $J$  = 16.65, 4.52, 1H, 4-H<sub>eq</sub>), 3.11 (s, 3H, 8-OCH<sub>3</sub>), 2.96 (dd,  $J$  = 18.13, 11.69 Hz, 1H, 4-H<sub>ax</sub>), 2.31 (d,  $J$  = 0.54 Hz, 3H, 2'-CH<sub>3</sub>), 1.68 (d,  $J$  = 6.85 Hz, 3H, 1-CH<sub>3</sub>), 1.55 (d,  $J$  = 6.45 Hz, 3H, 3-CH<sub>3</sub>).

$^{13}\text{C}$  NMR ( $\text{CD}_3\text{OD}$ , 101 MHz):  $\delta_{\text{C}}$  (ppm) = 157.9 (C-4'), 157.8 (C-6), 157.6 (C-8), 156.1 (C-5'), 137.4 (C-2'), 137.0 (C-9'), 133.0 (C-10), 131.9 (C-7'), 122.6 (C-8'), 121.7 (C-7), 119.9 (C-1'), 118.6 (C-9), 114.8 (C-10'), 111.3 (C-5), 107.5 (C-3'), 110.4 (C-6'), 50.0 (C-1), 45.3 (C-3), 60.7 (8-OCH<sub>3</sub>), 56.9 (4'-OCH<sub>3</sub>), 56.9 (5'-OCH<sub>3</sub>), 34.6 (C-4), 22.4 (2'-CH<sub>3</sub>), 19.6 (1-CH<sub>3</sub>), 19.4 (3-CH<sub>3</sub>).

### *Ealamine G* (67)

Yellowish amorphous powder (5.3 mg).

$[\alpha]_D^{23} = -20$  ( $c$  0.08, MeOH).



UV (MeOH):  $\lambda_{\max}$  ( $\log \epsilon$ ) 200 (3.4), 205 (6.9), 218 (5.3),

231 (7.1), 260 (0.5), 307 (1.3), 321 (1.2), 333 (0.8), 350 (0.01) nm.

ECD (MeOH,  $c$  0.09):  $\lambda_{\max}$  ( $\log \epsilon$ ) 200 (+1.07), 204 (-8.46), 210 (+8.32), 212 (+5.51), 213 (+8.15), 216 (+4.45), 221 (+9.58), 234 (-1.55), 257 (+21.07), 286 (-12.70), 335 (+0.24), 400 (0.00) nm.

HRESIMS  $m/z$  394.2018  $[M+H]^+$  (calcd for  $C_{24}H_{28}NO_4$ , 394.2013).

$^1H$  NMR ( $CD_3OD$ , 400 MHz):  $\delta_H$  (ppm) = 7.17 (d,  $J = 7.86$  Hz, 1H, H-7'), 6.85 (br s, 1H, H-1'), 6.80 (d,  $J = 7.92$  Hz, 1H, H-6'), 6.80 (d,  $J = 1.05$  Hz, H-3'), 6.58 (s, 1H, H-5), 4.68 (q,  $J = 6.54$  Hz, 1H, H-1), 4.09 (s, 3H, , 4'-OCH<sub>3</sub>), 3.49 (m, 1H, H-3), 3.13 (s, 3H, 8-OCH<sub>3</sub>), 2.96 (pd,  $J = 7.45$  Hz, 2H, 4-H<sub>eq/ax</sub>), 2.34 (d,  $J = 0.60$  Hz, 3H, 2'-CH<sub>3</sub>), 1.72 (d,  $J = 6.58$  Hz, 3H, 1-CH<sub>3</sub>), 1.51 (d,  $J = 6.45$  Hz, 3H, 3-CH<sub>3</sub>).

$^{13}C$  NMR ( $CD_3OD$ , 101 MHz):  $\delta_C$  (ppm) = 158.7 (C-8), 157.9 (C-4'), 157.6 (C-6), 156.1 (C-5'), 137.3 (C-2'), 137.1 (C-9'), 134.8 (C-10), 131.7 (C-7'), 122.8 (C-8'), 122.0 (C-7), 120.0 (C-1'), 118.4 (C-9), 114.9 (C-10'), 111.9 (C-5), 110.2 (C-6'), 107.5 (C-3'), 60.8 (8-OCH<sub>3</sub>), 56.9 (4'-OCH<sub>3</sub>), 52.5 (C-1), 51.3 (C-3), 35.3 (C-4), 22.4 (2'-CH<sub>3</sub>), 20.7 (1-CH<sub>3</sub>), 19.0 (3-CH<sub>3</sub>).

### *Ealamine H (68)*

Yellowish amorphous powder (3.1 mg).

$[\alpha]_D^{23} = -14$  ( $c$  0.02, MeOH).

UV (MeOH):  $\lambda_{\max}$  ( $\log \epsilon$ ) 200 (2.3), 205 (5.3), 218 (5.2),

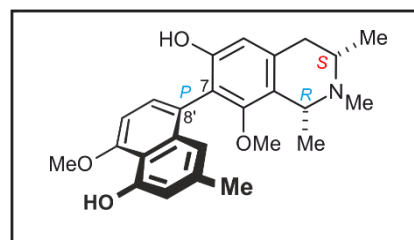
231 (8.1), 260 (0.3), 307 (1.3), 321 (1.2), 333 (0.8), 350 (0.01) nm.

ECD (MeOH,  $c$  0.02):  $\lambda_{\max}$  ( $\log \epsilon$ ) 200 (+3.59), 207 (+2.57), 216 (+0.53), 224 (1.41), 228 (+0.82), 235 (+0.75), 254 (+5.84), 283 (-5.63), 310 (+0.66), 337 (-0.24), 381 (-0.20) nm.

HRESIMS  $m/z$  408.2164  $[M+H]^+$  (calcd for  $C_{25}H_{30}NO_4$ , 408.2169).

$^1H$  NMR ( $CD_3OD$ , 400 MHz):  $\delta_H$  (ppm) = 7.19 (d,  $J = 7.99$  Hz, 1H, H-7'), 6.95 (d,  $J = 8.06$  Hz, 1H, H-6'), 6.74 (ps, 1H, H-1'), 6.66 (ps, 1H, H-3'), 6.60 (s, 1H, H-5), 4.60 (q,  $J = 6.85$  Hz, 1H, H-1), 4.12 (s, 3H, 5'-OCH<sub>3</sub>), 3.47 (m, 1H, H-3), 3.09 (s, 3H, 8-OCH<sub>3</sub>), 3.08 (s, 3H, 2-NCH<sub>3</sub>), 3.01 (pd,  $J = 7.05$  Hz, 1H, 4-H<sub>eq</sub>), 3.01 (pd,  $J = 7.05$  Hz, 1H, 4-H<sub>ax</sub>), 2.27 (s, 3H, 2'-CH<sub>3</sub>), 1.65 (d,  $J = 6.79$  Hz, 3H, 1-CH<sub>3</sub>), 1.51 (d,  $J = 6.44$  Hz, 3H, 3-CH<sub>3</sub>).

$^{13}C$  NMR ( $CD_3OD$ , 101 MHz):  $\delta_C$  (ppm) = 157.9 (s, C-5'), 157.7 (C-6), 157.7 (s, C-8), 156.3 (C-4'), 139.0 (C-2'), 137.2 (C-9'), 134.7 (C-10), 130.4 (C-7'), 125.7 (C-8'), 121.7 (C-7), 118.5 (s, C-9), 117.6 (C-1'), 114.8 (C-10'), 113.1 (C-3'), 111.2 (C-5), 104.5 (C-6'), 60.9 (8-OCH<sub>3</sub>), 60.9 (C-3), 62.8 (C-1), 56.9 (5'-OCH<sub>3</sub>), 42.0 (2-NCH<sub>3</sub>), 35.5 (C-4), 22.1 (2'-CH<sub>3</sub>), 20.8 (1-CH<sub>3</sub>), 18.3 (3-CH<sub>3</sub>).



## IV.6. Synthesis of Ealajoziminone A and Ealajoziminone B

### IV.6.1. Isolation and HPLC conditions

After celite-column filtration, the reaction mixture was evaporated in vacuum and applied to a preparative HPLC-UV for the isolation of the two compounds. The purification method was developed on a Symmetry<sup>®</sup> Prep-C<sub>18</sub> column with a flow rate of 16 mL min<sup>-1</sup> using solvents A (H<sub>2</sub>O, 0.05% TFA) and B (MeCN, 0.05% TFA), with the following gradient elution: 0-5 min: 18% of B, 15-21 min: 25% of B, 22-33 min: 30-40% of B, 55 min: 50% of B, 58 min: 100% of B, to yield ealajoziminone A (**70**, 2.2 mg) and the main ealajoziminone A (**71**, 5.3 mg).

#### *Ealajoziminone A (70)*

Purple powder (2.2 mg).

$[\alpha]_D^{23} = -32$  (*c* 0.4, MeOH).

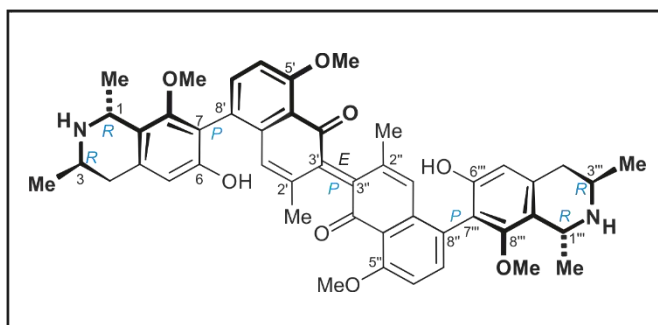
UV (MeOH):  $\lambda_{\max}$  (log  $\epsilon$ ) 200 (7.3), 212 (5.7), 223 (6.6), 254 (2.1), 273 (3.3), 285 (3.8), 312 (1.3), 324 (0.2), 373 (0.5), 416 (0.0), 600 (0.0) nm.

ECD (MeOH, *c* 0.1):  $\lambda_{\max}$  (log  $\epsilon$ ) 200 (+7.9), 211 (+1.1), 234 (-10.4), 245 (-4.6), 261 (-3.61), 275 (-4.1), 313 (-0.2), 322 (-0.5), 340 (-0.7), 364 (-0.9), 441 (-0.2), 578 (-1.3), 600 (-1.2) nm.

HRESIMS *m/z* 408.17971 [M+2H+2O]<sup>2+</sup> (calcd for C<sub>48</sub>H<sub>52</sub>N<sub>2</sub>O<sub>10</sub>, which requires 408.18110). The molecular formula is C<sub>48</sub>H<sub>50</sub>N<sub>2</sub>O<sub>8</sub>.

<sup>1</sup>H NMR (CD<sub>3</sub>OD, 600 MHz):  $\delta_{\text{H}}$  (ppm) = 8.68 (d, *J* = 9.08 Hz, 2H, H-7' and H-7''), 7.42 (d, *J* = 9.18 Hz, 2H, H-6' and H-6''), 6.90 (s, 2H, H-5 and H-5'''), 6.39 (d, *J* = 1.51 Hz, 2H, H-3' and H-3''), 4.83 (q, *J* = 6.90 Hz, 2H, H-1 and H-1'''), 4.00 (s, 6H, 5'-OCH<sub>3</sub> and 5''-OCH<sub>3</sub>), 3.88 (m, 2H, H-3 and H-3'''), 3.79 (s, 6H, 8-OCH<sub>3</sub> and 8'''-OCH<sub>3</sub>), 3.22 (dd, *J* = 17.99, 4.57 Hz, 2H, 4-H<sub>eq</sub> and 4'''-H<sub>eq</sub>), 2.89 (dd, *J* = 18.01, 12.01 Hz, 2H, 4-H<sub>ax</sub> and 4'''-H<sub>ax</sub>), 2.24 (s, 6H, 2'-CH<sub>3</sub> and 2'''-CH<sub>3</sub>), 1.74 (d, *J* = 6.81 Hz, 6H, 1-CH<sub>3</sub> and 1'''-CH<sub>3</sub>), 1.51 (d, *J* = 6.36 Hz, 6H, 3-CH<sub>3</sub> and 3'''-CH<sub>3</sub>).

<sup>13</sup>C NMR (CD<sub>3</sub>OD, 151 MHz):  $\delta_{\text{C}}$  (ppm) = 185.2 (C-4'/4'''), 161.0 (C-5'/5'''), 155.7 (C-8/8'''),



151.9 (C-6/6'''), 151.6 (C-2'/2''), 134.6 (C-9'/9''), 134.1 (C-10/10'''), 133.5 (C-7'/7''), 132.0 (C-1'/1'''), 122.9 (C-9/9'''), 120.9 (C-8/8''), 119.3 (C-10'/10''), 115.5 (C-7/7'''), 115.5 (C-6/6''), 114.9 (C-5/5'''), 95.6 (C-3'/3''), 61.7 (8-OCH<sub>3</sub>/8'''-OCH<sub>3</sub>), 56.8 (5'-OCH<sub>3</sub>/5''-OCH<sub>3</sub>), 49.9 (C-1/1'''), 45.2 (C-3/3'''), 34.4 (C-4/4'''), 19.7 (1-CH<sub>3</sub>/1'''-CH<sub>3</sub>), 19.3 (3-CH<sub>3</sub>/3'''-CH<sub>3</sub>), 16.7 (2'-CH<sub>3</sub>/2''-CH<sub>3</sub>).

Table 22. Detailed 2D NMR data of ealajoziminone A (**70**) in MeOD ( $\delta$  in ppm,  $J$  in Hz).

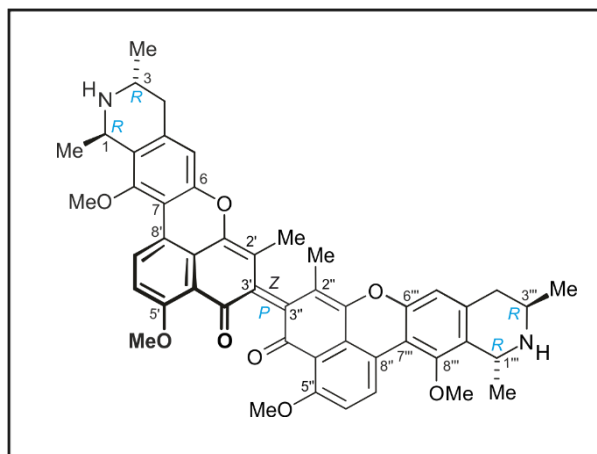
ealajoziminone A ( <b>70</b> )					
Position	$\delta_{\text{H}}$	$\delta_{\text{C}}$ , DEPT	HMBC	TOCSY	ROESY
1	4.83, q	49.9, CH	3, 8, 9, 10, 1-Me	3, 5, 1-Me, 3-Me, 8-OMe	8-OMe
3	3.88, m	45.2, CH	1, 4, 3-Me	4 <sub>eq</sub> , 4 <sub>ax</sub> , 5, 1-Me, 3-Me	<b>1-Me</b>
4	3.22, dd	34.4, CH <sub>eq</sub>	5, 9, 10, 3-Me	3, 5, 3-Me	3-Me
	2.89, dd	34.4, CH <sub>ax</sub>	3, <b>5</b> , 9, 10, 3-Me	3, 5, 3-Me	5, 3-Me
5	6.90, s	114.9, CH	4, 6, 7, 8, 8'	1, 3, 4 <sub>ax</sub> , 1-Me, 3-Me	4 <sub>ax</sub> , 8-OMe, 2'-Me
6		151.9, C			
7		115.5, C			
8		155.7, C			
9		122.9, C			
10		134.1, C			
1'	6.39, s	132.0, CH	3', 8', 9', 10', 2'-	<b>7'</b> , 2'-Me	2'-Me, <b>8-OMe</b>
2'		151.6, C			
3'		95.6, C			
4'		185.2, C			
5'		161.0, C			
6'	7.42, d	115.5, CH	<b>4'</b> ( <sup>4</sup> <i>J</i> ), 5', 8', 10'	7', 5'-OMe	5'-OMe
7'	8.68, d	133.5, CH	7, <b>1'</b> ( <sup>4</sup> <i>J</i> ), 5', 9', 10'	<b>1'</b> , 6', 5'-OMe	8-OMe
8'		120.9, C			
9'		134.6, C			
10'		119.3, C			
1-Me	1.74, d	19.7, Me	1, 9	1, 3	<b>3</b> , 8-OMe
3-Me	1.51, d	19.3, Me	3, 4	3, 4 <sub>eq</sub> , 4 <sub>ax</sub>	4 <sub>eq</sub> , 4 <sub>ax</sub> , 5
2'-Me	2.24, s	16.7, Me	1', 2', 3', <b>4'</b> ( <sup>4</sup> <i>J</i> )	1'	5, 1', <b>5'-OMe</b> (weak)
8-OMe	3.79, s	61.7, Me	8	1, 6', 7', 1-Me	1, 1', 7', 1-Me
5'-OMe	4.00, s	56.8, Me	5'	6', 7'	<b>6'</b> , <b>2'-Me</b> (weak)

*Ealajoziminone B (71)*

Red crystalline powder (5.2 mg).

$[\alpha]_D^{23} = -23$  ( $c$  0.3, MeOH).

UV (MeOH):  $\lambda_{\max}$  ( $\log \epsilon$ ) 200 (4.8), 206 (4.2), 215 (3.9), 227 (4.4), 244 (3.3), 259 (5.4), 307 (0.8), 328 (1.4), 336 (1.2), 343 (1.2), 351 (0.4), 404 (0.1), 502 (1.0), 600 (0.0) nm.



ECD (MeOH,  $c$  0.1):  $\lambda_{\max}$  ( $\log \epsilon$ ) 200 (-5.79), 217 (+4.63), 233 (-2.06), 264 (+6.67), 402 (+0.25), 470 (+0.29), 600 (1.49) nm.

HRESIMS  $m/z$  428.14575  $[M+Na+2O]^{2+}$ , 833.30419  $[M+Na+2O]^+$  (calcd for  $C_{48}H_{46}N_2O_{10}$ , which requires 428.14740). The molecular formula is  $C_{48}H_{46}N_2O_8$ .

$^1H$  NMR ( $CD_3OD$ , 600 MHz):  $\delta_H$  (ppm) = 8.96 (d,  $J = 9.54$  Hz, 2H, H-7' and H-7''), 7.61 (d,  $J = 9.59$  Hz, 2H, H-6' and H-6''), 7.12 (s, 2H, H-5 and H-5'''), 4.90 (q,  $J = 7.02$  Hz, 2H, H-1 and H-1'''), 4.09 (s, 6H, 5'-OCH<sub>3</sub> and 5''-OCH<sub>3</sub>), 3.92 (dt,  $J = 11.79, 5.94$  Hz, 2H, H-3 and H-3'''), 3.80 (s, 6H, 8-OCH<sub>3</sub> and 8''-OCH<sub>3</sub>), 3.28 (dd,  $J = 17.52, 4.87$  Hz, 2H, 4-H<sub>eq</sub> and 4'''-H<sub>eq</sub>), 2.93 (dd,  $J = 18.14, 11.48$  Hz, 2H, 4-H<sub>ax</sub> and 4'''-H<sub>ax</sub>), 2.08 (s, 6H, 2'-CH<sub>3</sub> and 2''-CH<sub>3</sub>), 1.76 (d,  $J = 6.91$  Hz, 6H, 1-CH<sub>3</sub> and 1'''-CH<sub>3</sub>), 1.54 (d,  $J = 6.41$  Hz, 6H, 3-CH<sub>3</sub> and 3'''-CH<sub>3</sub>).

$^{13}C$  NMR ( $CD_3OD$ , 151 MHz):  $\delta_C$  (ppm) = 180.1 (C-2'/2''), 179.5 (C-4'/4''), 164.7 (C-5'/5''), 160.5 (C-1'/1'''), 156.1 (C-8/8'''), 152.0 (C-6/6'''), 136.7 (C-7/7'''), 135.8 (C-10/10'''), 125.9 (C-9/9''), 125.7 (C-9/9'''), 121.1 (C-8'/8'''), 119.9 (C-6'/6'''), 116.7 (C-10'/10'''), 115.7 (C-3'/3'''), 114.3 (C-5/5'''), 111.6 (C-7/7'''), 62.0 (8-OCH<sub>3</sub>/8''-OCH<sub>3</sub>), 57.4 (5'-OCH<sub>3</sub>/5''-OCH<sub>3</sub>), 49.7 (C-1/1'''), 45.1 (C-3/3'''), 34.3 (C-4/4'''), 19.5 (1-CH<sub>3</sub>/1'''-CH<sub>3</sub>), 19.3 (3-CH<sub>3</sub>/3'''-CH<sub>3</sub>), 8.2 (2'-CH<sub>3</sub>/2''-CH<sub>3</sub>).

Table 23. Detailed 2D NMR data of ealajoziminone B (**71**) in MeOD ( $\delta$  in ppm,  $J$  in Hz).

ealajoziminone B ( <b>71</b> )					
Position	$\delta_{\text{H}}$	$\delta_{\text{C}}$ , DEPT	HMBC	TOCSY	ROESY
1	4.90, q	49.7, CH	3, 8, 9, 10, 1-Me	3, 5, 1-Me, 3-Me, 8-OMe	8-OMe
3	3.92, m	45.1, CH	1, 4, 3-Me	4 <sub>eq</sub> , 4 <sub>ax</sub> , 5, 3-Me	<b>1-Me</b>
4	3.28, dd	34.3, CH <sub>eq</sub>	5, 9, 10, 3-Me	3, 5, 3-Me	3-Me
	2.93, dd	34.3, CH <sub>ax</sub>	3, <b>5</b> , 9, 10, 3-Me	3, 5, 3-Me	5, 3-Me
5	7.12, s	114.3, CH	4, 6, 7, 8, 8'	1, 3, 4 <sub>ax</sub> , 1-Me, 3-Me, <b>2'-Me</b>	4 <sub>ax</sub> , <b>2'-Me</b>
6		152.0, C			
7		111.6, C			
8		156.1, C			
9		125.7, C			
10		135.8, C			
1'		160.5, C			
2'		180.1, C			
3'		115.7, C			
4'		179.5, C			
5'		164.7, C			
6'	7.61, d	119.9, CH	<b>4'(<sup>4</sup>J)</b> , 5', 8', 10'	7', 5'-OMe	5'-OMe
7'	8.96, d	136.7, CH	7, <b>1'(<sup>4</sup>J)</b> , 5', 9', 10'	<b>1'</b> , 6', 5'-OMe	8-OMe
8'		121.1, C			
9'		125.9, C			
10'		116.7, C			
1-Me	1.76, d	19.5, Me	1, 9	1, 3	<b>3</b> , 8-OMe
3-Me	1.54, d	19.3, Me	3, 4	3, 4 <sub>eq</sub> , 4 <sub>ax</sub>	4 <sub>eq</sub> , 4 <sub>ax</sub> , 5
2'-Me	2.08, s	8.2, Me	1', 2', 3', 10'	<b>5</b> , 7'	5, <b>5'-OMe</b> (weak)
8-OMe	3.80, s	62.0, Me	8	1, 6', 7', 1-Me	1, 7', 1-Me
5'-OMe	4.09, s	57.4, Me	5'	6', 7'	6', <b>2'-Me</b> (weak)



## IV.7. Ealaines A-D, Naphthalene-Devoid Alkaloids

### IV.7.1. Extractions, Isolation, and HPLC conditions

#### IV.7.1.1. Extraction and fractionation

Four new naphthalene devoid isoquinoline alkaloids were isolated from leaf material of *A. ealaensis*, along with the new series of ealamines, in a more remote region of the chromatogram on the C<sub>18</sub> column. The extraction and fractionation procedures were the same as the one used for the dimers.

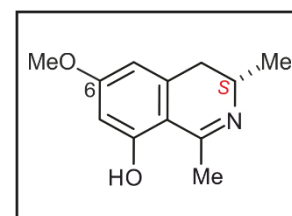
#### IV.7.1.2. Isolation and HPLC conditions

The same method applied for the isolation of ealamine G was used for the pre-separation of these compounds. The isolation and purification from these late subfractions were further possessed on a Symmetry<sup>®</sup> Prep-C<sub>18</sub> column, with a mobile phase of A (H<sub>2</sub>O, 0.05% TFA) and B (MeCN, 0.05% TFA), and a flow rate of 10 mL min<sup>-1</sup>: 0-10 min: 10-20% of B, 13-25 min: 20-45% of B, 30 min: 60% of B, 32 min: 100% of B, to afford 2.1 mg of **72**, 10.3 mg of **73**, 3.8 mg of **74**, 0.9 mg of **75**.

#### *Ealaine A (72)*

Colorless amorphous powder (2.1 mg).

$[\alpha]_D^{23} = -11$  (*c* 0.08, MeOH).



UV (MeOH):  $\lambda_{\max}$  (log  $\epsilon$ ) = 201 (1.3), 219 (0.8), 228 (0.5), 238 (0.4), 259 (0.04), 312 (0.8), 329 (0.8), 359 (0.1) nm.

ECD (MeOH, *c* 0.2):  $\lambda_{\max}$  (log  $\epsilon$  in cm<sup>2</sup> mol<sup>-1</sup>) = 200 (+20.70), 231 (-6.80), 250 (-0.30), 273 (-2.15), 335 (-13.51), 376 (-0.70), 400 (-0.42) nm.

HRESIMS *m/z* 206.1173 [M+H]<sup>+</sup> (calcd for C<sub>12</sub>H<sub>16</sub>NO<sub>2</sub>, 206.1176).

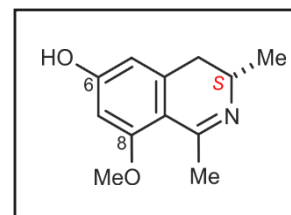
<sup>1</sup>H NMR (CD<sub>3</sub>OD, 400 MHz):  $\delta_H$  (ppm) = 6.49 (dt, *J* = 2.27, 1.05 Hz, 1H, H-5), 6.42 (d, *J* = 2.35 Hz, 1H, H-7), 3.92 (m, 1H, H-3), 3.88 (s, 3H, 8-OCH<sub>3</sub>), 3.06 (dd, *J* = 16.36, 5.22 Hz, 1H, 4-H<sub>eq</sub>), 2.82 (dd, *J* = 16.62, 11.79 Hz, 1H, 4-H<sub>ax</sub>), 2.78 (d, *J* = 1.48 Hz, 3H, 1-CH<sub>3</sub>), 1.43 (d, *J* = 6.72 Hz, 3H, 3-CH<sub>3</sub>).

$^{13}\text{C}$  NMR ( $\text{CD}_3\text{OD}$ , 151 MHz):  $\delta_{\text{C}}$  (ppm) = 176.0 (C-1), 169.7 (C-6), 165.9 (C-8), 142.7 (C-10), 108.9 (C-5), 108.1 (C-9), 101.2 (C-7), 56.7 (8-OCH<sub>3</sub>), 49.7 (C-3), 35.3 (C-4), 24.5 (1-CH<sub>3</sub>), 18.3 (3-CH<sub>3</sub>).

### *Ealaine B (73)*

Colorless amorphous powder (10.3 mg).

$[\alpha]_D^{23} = -22$  (*c* 0.1, MeOH).



UV (MeOH):  $\lambda_{\text{max}}$  ( $\log \epsilon$ ) = 201 (1.0), 218 (0.6), 229 (0.4), 237 (0.4), 257 (0.03), 311 (0.7), 330 (0.7), 370 (0.1) nm.

ECD (MeOH, *c* 0.2):  $\lambda_{\text{max}}$  ( $\log \epsilon$  in  $\text{cm}^2 \text{mol}^{-1}$ ) = 200 (+20.68), 230 (-6.62), 248 (-0.28), 270 (-2.11), 333 (-13.40), 375 (-0.70), 400 (-0.42) nm.

HRESIMS  $m/z$  206.1173  $[\text{M}+\text{H}]^+$  (calcd for  $\text{C}_{12}\text{H}_{16}\text{NO}_2$ , 206.1176).

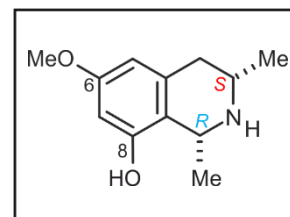
$^1\text{H}$  NMR ( $\text{CD}_3\text{OD}$ , 600 MHz):  $\delta_{\text{H}}$  (ppm) = 6.41 (d,  $J = 1.92$  Hz, 1H, H-7), 6.39 (d,  $J = 1.01$  Hz, 1H, H-5), 3.93 (s, 3H, 8-OCH<sub>3</sub>), 3.86 (m, 1H, H-3), 3.01 (dd,  $J = 16.36, 5.27$  Hz, 1H, 4-H<sub>eq</sub>), 2.78 (dd,  $J = 16.36, 11.92$  Hz, 1H, 4-H<sub>ax</sub>), 2.04 (s, 3H, 1-CH<sub>3</sub>), 1.42 (d,  $J = 6.71$  Hz, 3H, 3-CH<sub>3</sub>).

$^{13}\text{C}$  NMR ( $\text{CD}_3\text{OD}$ , 101 MHz):  $\delta_{\text{C}}$  (ppm) = 174.4 (C-1), 166.8 (C-8), 163.1 (C-6), 143.8 (C-10), 111.1 (C-5), 107.5 (C-9), 100.0 (C-7), 56.6 (8-OCH<sub>3</sub>), 49.6 (C-3), 35.6 (C-4), 23.7 (1-CH<sub>3</sub>), 18.3 (3-CH<sub>3</sub>).

*Ealaine C (74)*

Colorless amorphous powder (3.8 mg).

$[\alpha]_D^{23} = -13$  ( $c$  0.02, MeOH).



UV (MeOH):  $\lambda_{\max}$  ( $\log \epsilon$ ) = 200 (1.7), 208 (2.8), 219 (1.0), 231 (0.8), 255 (0.2), 275 (0.3), 283 (0.3), 295 (0.1), 330 (0.1), 350 (0.04) nm.

ECD (MeOH,  $c$  0.2):  $\lambda_{\max}$  ( $\log \epsilon$  in  $\text{cm}^2 \text{mol}^{-1}$ ) = 197 (-12.32), 203 (-33.16), 218 (-1.42), 235 (+3.75), 250 (+0.71), 277 (+3.36), 301 (-0.22), 350 (-0.06) nm.

HRESIMS  $m/z$  208.1333  $[\text{M}+\text{H}]^+$  (calcd for  $\text{C}_{12}\text{H}_{18}\text{NO}_2$ , 208.1332).

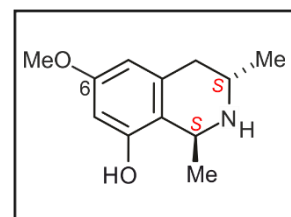
$^1\text{H}$  NMR ( $\text{CD}_3\text{OD}$ , 400 MHz):  $\delta_{\text{H}}$  (ppm) = 6.31 (d,  $J = 2.48$  Hz, 1H, H-7), 6.28 (d,  $J = 2.49$  Hz, 1H, H-5), 4.58 (q,  $J = 6.67$  Hz, 1H, H-1), 3.73 (s, 3H, 6-OCH<sub>3</sub>), 3.39 (m, 1H, H-3), 2.86 (m, 2H, 4-H<sub>eq/ax</sub>), 1.72 (d,  $J = 6.58$  Hz, 3H, 1-CH<sub>3</sub>), 1.46 (d,  $J = 6.51$  Hz, 3H, 3-CH<sub>3</sub>).

$^{13}\text{C}$  NMR ( $\text{CD}_3\text{OD}$ , 101 MHz):  $\delta_{\text{C}}$  (ppm) = 161.6 (C-6), 157.3 (C-8), 135.8 (C-10), 113.7 (C-9), 105.7 (C-5), 101.7 (C-7), 55.8 (8-OCH<sub>3</sub>), 52.4 (C-1), 51.3 (C-3), 35.5 (C-4), 19.7 (1-CH<sub>3</sub>), 18.9 (3-CH<sub>3</sub>).

*Ealaine D (75)*

Colorless amorphous powder (0.9 mg).

$[\alpha]_D^{23} = +15$  (*c* 0.05, MeOH).



UV (MeOH):  $\lambda_{\max}$  ( $\log \epsilon$ ) = 200 (1.0), 205 (1.1), 216 (0.6), 228 (0.4), 251 (0.2), 285 (0.1), 298 (0.1), 350 (0.04) nm.

ECD (MeOH, *c* 0.03):  $\lambda_{\max}$  ( $\log \epsilon$  in  $\text{cm}^2 \text{mol}^{-1}$ ) = 200 (+2.20), 203 (+1.34), 211 (+4.12), 239 (-1.63), 242 (-1.65), 257 (-0.51), 265 (-0.66), 283 (-1.45), 349 (-0.20), 450 (-0.40) nm.

HRESIMS  $m/z$  208.1331  $[\text{M}+\text{H}]^+$  (calcd for  $\text{C}_{12}\text{H}_{18}\text{NO}_2$ , 208.1332).

$^1\text{H}$  NMR ( $\text{CD}_3\text{OD}$ , 400 MHz):  $\delta_{\text{H}}$  (ppm) = 6.30 (d,  $J = 2.28$  Hz, 1H, H-7), 6.27 (d,  $J = 2.35$  Hz, 1H, H-5), 4.67 (q,  $J = 6.72$  Hz, 1H, H-1), 3.79 (m, 1H, H-3), 3.73 (s, 3H, 6-OCH<sub>3</sub>), 3.07 (dd, 17.60, 4.63 Hz, 1H, 4-H<sub>eq</sub>), 2.79 (dd, 18.00, 10.59 Hz, 1H, 4-H<sub>ax</sub>), 1.61 (d,  $J = 6.78$  Hz, 3H, 1-CH<sub>3</sub>), 1.46 (d,  $J = 6.38$  Hz, 3H, 3-CH<sub>3</sub>).

$^{13}\text{C}$  NMR ( $\text{CD}_3\text{OD}$ , 101 MHz):  $\delta_{\text{C}}$  (ppm) = 161.6 (C-6), 157.2 (C-8), 135.8 (C-10), 113.5 (C-9), 105.7 (C-5), 101.7 (C-7), 55.8 (8-OCH<sub>3</sub>), 51.1 (C-1), 45.1 (C-3), 35.5 (C-4), 19.7 (1-CH<sub>3</sub>), 18.9 (3-CH<sub>3</sub>).

## IV.8. Further New Monomeric Alkaloids from *A. ealaensis*

### IV.8.1. Extractions, Isolation, and HPLC conditions

#### IV.8.1.1. Extraction and fractionation

Additional monomeric 8'-coupled naphthylisoquinoline alkaloids were discovered within the twigs extracts and alongside with the occurring ealamines and the dimeric compounds. The extraction and fractionation procedures from leaf material were identical to the one used for the dimers. Air-dried twig material of *A. ealaensis* (300 g) was exhaustively macerated in the mixture MeOH/CH<sub>2</sub>Cl<sub>2</sub> (7:3), at room temperature. Followed by fractionation on a classical deactivated (with triethylamine) silica column with an increasing concentration of MeOH in CH<sub>2</sub>Cl<sub>2</sub>.

#### IV.8.1.2. Isolation and HPLC conditions

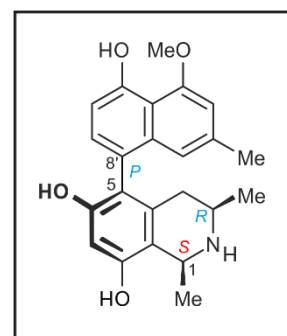
The isolation from the leaf subfractions was performed following the previously protocol using the Symmetry<sup>®</sup> Prep-C<sub>18</sub> column, and solvents A (H<sub>2</sub>O, 0.05% TFA) and B (MeCN, 0.05% TFA) and a flow rate of 20 mL min<sup>-1</sup>: 0-10 min: 18% of B, 13-25 min: 20% of B, 45 min: 50% of B, 48 min: 100% of B, to afford 4.3 mg of **79**, 4.0 mg of **81**, 5.1 mg of **77**, along with **34**, **35**, **80**. Further purification of the early fractions led to the isolation of 3.1 mg of **76**, together with its known epimer **25**.

#### *1-epi-Korupensamine A (76)*

White solid (3.1 mg).

$[\alpha]_D^{23} = -18$  (*c* 0.07, MeOH).

UV (MeOH):  $\lambda_{\max}$  (log  $\epsilon$ ) 200 (4.0), 206 (4.6), 218 (3.6), 230 (4.5),  
265 (0.3), 307 (1.3), 321 (0.9), 350 (0.01) nm.



ECD (MeOH, *c* 0.08):  $\lambda_{\max}$  (log  $\epsilon$  in cm<sup>2</sup> mol<sup>-1</sup>) = 200 (+6.92), 213 (-9.57), 228 (-19.01), 244 (+4.14), 286 (-1.84), 301 (-0.41), 376 (-0.40) nm.

HRESIMS *m/z* 380.18537 [M+H]<sup>+</sup> (calcd for C<sub>23</sub>H<sub>26</sub>NO<sub>4</sub>, 380.18563).

<sup>1</sup>H NMR (CD<sub>3</sub>OD, 600 MHz):  $\delta_H$  (ppm) = 7.08 (d, *J* = 7.86 Hz, 1H, H-7'), 6.81 (s, 1H, H-3'), 6.80 (d, *J* = 7.74 Hz, 1H, H-6'), 6.79 (s, 1H, H-1'), 6.47 (s, 1H, H-7), 4.63 (*q*, *J* = 6.65 Hz, 1H,

H-1), 4.09 (s, 3H, 4'-OCH<sub>3</sub>), 3.26 (m, 1H, H-3), 2.42 (dd,  $J = 17.35, 3.35$  Hz, 1H, 4-H<sub>eq</sub>), 2.19 (dd,  $J = 17.74, 11.93$  Hz, 1H, 4-H<sub>ax</sub>), 2.34 (s, 1H, 2'-CH<sub>3</sub>), 1.80 (d,  $J = 6.55$  Hz, 3H, 1-CH<sub>3</sub>), 1.21 (d,  $J = 6.48$  Hz, 3H, 3-CH<sub>3</sub>).

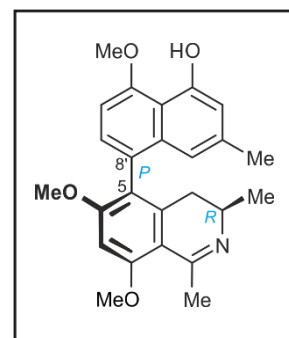
<sup>13</sup>C NMR (CD<sub>3</sub>OD, 151 MHz):  $\delta_c$  (ppm) = 158.0 (C-4'), 156.7 (C-6), 156.3 (C-8), 155.6 (C-5'), 137.6 (C-9'), 137.5 (C-2'), 135.0 (C-10), 131.4 (C-7'), 124.8 (C-8'), 119.4 (C-5), 119.1 (C-1'), 115.1 (C-10'), 113.0 (C-9), 110.4 (C-6'), 107.5 (C-3'), 102.8 (C-7), 56.8 (4'-OCH<sub>3</sub>), 52.3 (C-1), 50.8 (C-3), 33.2 (C-4), 22.2 (2'-CH<sub>3</sub>), 19.8 (1-CH<sub>3</sub>), 18.7 (3-CH<sub>3</sub>).

*Ancistroealaine C (77)*

Yellow amorphous solid (5.1 mg).

$[\alpha]_D^{23} = -17$  ( $c$  0.05, MeOH).

UV (MeOH):  $\lambda_{\max}$  ( $\log \epsilon$ ) = 203 (1.6), 224 (1.0), 233 (1.11), 276 (0.3), 280 (0.3), 309 (0.4), 332 (0.3), 336 (0.3), 352 (0.3), 370 (0.2) nm.



ECD (MeOH,  $c$  0.1):  $\lambda_{\max}$  ( $\log \epsilon$  in  $\text{cm}^2 \text{mol}^{-1}$ ) = 201 (+8.56), 215 (+1.68), 227 (-10.27), 243 (+7.80), 260 (-3.85), 277 (-0.43), 299 (-2.03), 308 (-1.70), 336 (-2.92), 359 (-1.06), 374 (-1.66), 400 (-0.50) nm.

HRESIMS  $m/z$  406.2014  $[\text{M}+\text{H}]^+$  (calcd for  $\text{C}_{25}\text{H}_{28}\text{NO}_4$ , 406.2013).

$^1\text{H}$  NMR ( $\text{CD}_3\text{OD}$ , 400 MHz):  $\delta_{\text{H}}$  (ppm) = 7.10 (d,  $J$  = 7.92 Hz, 1H, H-7'), 6.94 (d,  $J$  = 7.99 Hz, 1H, H-6'), 6.84 (s, 1H, H-7), 6.67 (d,  $J$  = 1.41 Hz, 1H, H-3'), 6.46 (br s, 1H, H-1'), 4.15 (s, 3H, 8-OCH<sub>3</sub>), 4.11 (s, 3H, 5'-OCH<sub>3</sub>), 3.85 (s, 3H, 6-OCH<sub>3</sub>), 3.80 (m, 1H, H-3), 2.82 (d,  $J$  = 1.14 Hz, 3H, 1-CH<sub>3</sub>), 2.71 (dd,  $J$  = 16.98, 5.40 Hz, 1H, 4-H<sub>eq</sub>), 2.28 (dd,  $J$  = 16.96, 9.97 Hz, 1H, 4-H<sub>ax</sub>), 2.24 (s, 3H, 2'-CH<sub>3</sub>), 1.20 (d,  $J$  = 6.72 Hz, 3H, 3-CH<sub>3</sub>).

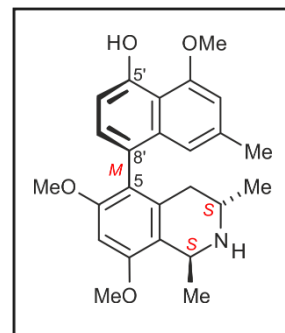
$^{13}\text{C}$  NMR ( $\text{CD}_3\text{OD}$ , 101 MHz):  $\delta_{\text{C}}$  (ppm) = 176.0 (C-1), 168.6 (C-6), 166.4 (C-8), 157.9 (C-5'), 156.3 (C-4'), 141.6 (C-10), 139.6 (C-2'), 137.1 (C-9'), 129.5 (C-7'), 126.3 (C-8'), 123.6 (C-5), 116.4 (C-1'), 114.8 (C-10'), 113.4 (C-3'), 109.0 (C-9), 104.4 (C-6'), 95.9 (C-7), 56.9 (5'-OCH<sub>3</sub>), 57.2 (8-OCH<sub>3</sub>), 57.1 (6-OCH<sub>3</sub>), 49.2 (C-3), 32.7 (C-4), 22.0 (2'-CH<sub>3</sub>), 25.1 (1-CH<sub>3</sub>), 17.9 (3-CH<sub>3</sub>).

**5-*epi*-Ancistroealaine B (79)**

Yellow amorphous solid (4.3 mg).

$[\alpha]_D^{23} = +17$  ( $c$  0.05, MeOH).

UV (MeOH):  $\lambda_{\max}$  ( $\log \epsilon$ ) 200 (4.1), 206 (4.5), 218 (3.7), 231 (4.6),  
265 (0.3), 307 (1.5), 321 (0.9), 339 (0.01) nm.



ECD (MeOH,  $c$  0.09):  $\lambda_{\max}$  ( $\log \epsilon$  in  $\text{cm}^2 \text{mol}^{-1}$ ) = 199 (−4.58), 207 (+3.06), 213 (+1.89), 227  
(+10.36), 241 (−8.62), 272 (−0.12), 312 (+0.10), 349 (+0.01) nm.

HRESIMS  $m/z$  408.21610  $[\text{M}+\text{H}]^+$  (calcd for  $\text{C}_{25}\text{H}_{30}\text{NO}_4$ , 408.21693).

$^1\text{H}$  NMR ( $\text{CDCl}_3$ , 400 MHz):  $\delta_{\text{H}}$  (ppm) = 7.07 (d,  $J = 7.79$  Hz, 1H, H-7'), 6.87 (d,  $J = 7.79$  Hz, 1H, H-6'), 6.65 (d,  $J = 1.34$  Hz, 1H, H-1'), 6.61 (ps, 1H, H-3'), 6.55 (d,  $J = 1.41$  Hz, 1H, H-7), 4.90 (q,  $J = 6.18$  Hz, 1H, H-1), 4.08 (s, 3H, 4'-OCH<sub>3</sub>), 3.96 (s, 3H, 8-OCH<sub>3</sub>), 3.67 (s, 3H, 6-OCH<sub>3</sub>), 3.50 (m, 1H, H-3), 2.62 (dd,  $J = 18.20, 4.63$  Hz, 1H, 4-H<sub>eq</sub>), 2.33 (d,  $J = 0.54$  Hz, 3H, 2'-CH<sub>3</sub>), 2.23 (dd,  $J = 18.40, 11.95$  Hz, 1H, 4-H<sub>ax</sub>), 1.68 (d,  $J = 6.72$  Hz, 3H, 1-CH<sub>3</sub>), 1.28 (d,  $J = 6.45$  Hz, 3H, 3-CH<sub>3</sub>).

$^{13}\text{C}$  NMR ( $\text{CD}_3\text{OD}$ , 101 MHz):  $\delta_{\text{C}}$  (ppm) = 158.5 (C-6), 156.1 (C-8), 156.1 (C-4'), 154.3 (C-5'), 136.7 (C-2'), 135.5 (C-9'), 131.8 (C-10), 129.4 (C-7'), 123.3 (C-8'), 121.0 (C-5), 118.0 (C-1'), 113.6 (C-10'), 113.4 (C-9), 109.4 (C-6'), 106.7 (C-3'), 94.2 (C-7), 56.2 (4'-OCH<sub>3</sub>), 56.1 (6-OCH<sub>3</sub>), 55.5 (8-OCH<sub>3</sub>), 48.2 (C-1), 44.7 (C-3), 31.9 (C-4), 21.9 (2'-CH<sub>3</sub>), 18.6 (1-CH<sub>3</sub>), 18.9 (3-CH<sub>3</sub>).

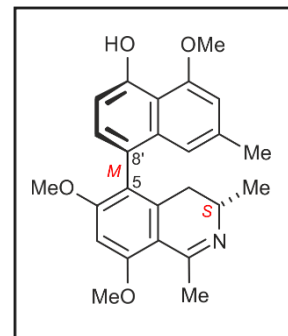


*Ancistroealaine D (81)*

Yellow amorphous solid (4.0 mg).

$[\alpha]_D^{23} = +17$  (*c* 0.08, MeOH).

UV (MeOH):  $\lambda_{\max}$  ( $\log \epsilon$ ) = 203 (1.1), 220 (1.1), 231 (0.9), 276 (0.3), 285 (0.2), 309 (0.5), 322 (0.2), 334 (0.2), 346 (0.1), 347 (0.2) nm.



ECD (MeOH, *c* 0.1):  $\lambda_{\max}$  ( $\log \epsilon$  in  $\text{cm}^2 \text{mol}^{-1}$ ) = 201 (-5.10), 203 (-2.91), 210 (-9.18), 226 (+5.90), 242 (-5.18), 253 (+0.31), 258 (+0.68), 295 (-1.82), 317 (+1.75), 332 (+0.75), 334 (+0.89), 347 (-1.63), 386 (-0.61) nm.

HRESIMS  $m/z$  406.2015  $[\text{M}+\text{H}]^+$  (calcd for  $\text{C}_{25}\text{H}_{28}\text{NO}_4$ , 406.2013).

$^1\text{H}$  NMR ( $\text{CDCl}_3$ , 400 MHz):  $\delta_{\text{H}}$  (ppm) = 7.07 (d,  $J = 7.93$  Hz, 1H, H-7'), 6.90 (d,  $J = 7.75$  Hz, 1H, H-6'), 6.68 (d,  $J = 1.44$  Hz, 1H, H-3'), 6.55 (ps, 1H, H-1'), 6.55 (d,  $J = 1.41$  Hz, 1H, H-7), 4.11 (s, 3H, 4'-OCH<sub>3</sub>), 4.10 (s, 3H, 8-OCH<sub>3</sub>), 3.82 (s, 3H, 6-OCH<sub>3</sub>), 3.81 (m, 1H, H-3), 2.89 (s, 3H, 1-CH<sub>3</sub>), 2.62 (dd,  $J = 16.60, 5.41$  Hz, 1H, 4-H<sub>eq</sub>), 2.36 (s, 3H, 2'-CH<sub>3</sub>), 2.25 (dd,  $J = 16.78, 9.47$  Hz, 1H, 4-H<sub>ax</sub>), 1.28 (d,  $J = 6.91$  Hz, 3H, 3-CH<sub>3</sub>).

$^{13}\text{C}$  NMR ( $\text{CD}_3\text{OD}$ , 101 MHz):  $\delta_{\text{C}}$  (ppm) = 173.4 (C-1), 166.9 (C-6), 163.7 (C-8), 156.6 (C-4'), 154.9 (C-5'), 136.6 (C-2'), 135.2 (C-9'), 132.7 (C-10), 129.9 (C-7'), 122.5 (C-5), 121.4 (C-8'), 117.4 (C-1'), 113.7 (C-10'), 109.5 (C-6'), 108.0 (C-9), 106.7 (C-3'), 93.9 (C-7), 56.2 (4'-OCH<sub>3</sub>), 56.2 (6-OCH<sub>3</sub>), 56.0 (8-OCH<sub>3</sub>), 47.7 (C-3), 31.6 (C-4), 22.2 (2'-CH<sub>3</sub>), 24.4 (1-CH<sub>3</sub>), 17.2 (3-CH<sub>3</sub>).

## IV.9. Gardenifolins A-H, Scalemic Neolignans from *Gardenia ternifolia*

### IV.9.1. Extractions, Isolation, and HPLC conditions

#### IV.9.1.1. Extraction and fractionation

The air-dried powder of stem barks of *Gardenia ternifolia* (650 g) was macerated in MeOH for 48 h under light-reduced conditions, assisted by mechanical shaking, followed by a filtration. The procedure was repeated several times for exhaustive extraction. The combined filtrates were evaporated to a small volume affording a viscous solution, which was then partitioned between water and *n*-hexane to remove traces of chlorophyll. The aqueous phase was repeatedly extracted with CH<sub>2</sub>Cl<sub>2</sub> until exhaustion. The organic phases were evaporated to dryness to yield 202 mg of extract A. The remaining aqueous phase was exhaustively extracted with EtOAc. The combined EtOAc fractions were evaporated to dryness to give 101 mg of extract B. Throughout the whole process, precautions were taken to minimize the light exposure of the samples. The extracts A and B were each dissolved in MeOH and separately applied to column chromatography on silica gel, and successively eluted with CH<sub>2</sub>Cl<sub>2</sub>/MeOH: 10:0, 10:1, 10:2, 8:3, 7:5, 5:5, 0:5 to afford ten fractions for each of the two extracts (fractions F<sub>1</sub>-F<sub>10</sub>).<sup>[214]</sup>

#### IV.9.1.2. Isolation and HPLC conditions

Fractions F<sub>3</sub> from the extracts A and B were combined and directly subjected to preparative HPLC on a Symmetry<sup>®</sup> Prep-C<sub>18</sub> column (Waters, 300 × 19 mm, 7 μm) at room temperature, with the mobile phase: (M<sub>1</sub>) H<sub>2</sub>O (0.05% TFA), (M<sub>2</sub>) CH<sub>3</sub>CN (0.05% TFA). The flow rate was of 8 mL min<sup>-1</sup>, using the following gradient: 0-4 min: 25-30% M<sub>2</sub>; 4-28 min: 30-60% M<sub>2</sub>; 28-30 min: 60-98% M<sub>2</sub>, resulting in two subfractions, Peak I and Peak II (Figure 61), which were further separated and purified by renewed chromatography under identical conditions as described above, to yield four samples (*Z*-I, *E*-I, *Z*-II, and *E*-II). The gardenifolins A-D (**83a-83d**) and E-H (**84a-84d**) were finally obtained in a stereochemically homogeneous form by preparative HPLC on a chiral Lux<sup>®</sup> PrepCellulose-1 column (Phenomenex, 250 × 21.2 mm, 5 μm); mobile phase: (M<sub>1</sub>) H<sub>2</sub>O (0.05% TFA), (M<sub>2</sub>) CH<sub>3</sub>CN (0.05% TFA). The flow rate was set to 10 mL min<sup>-1</sup>, using the following gradient: 0-7 min: 20-35% M<sub>2</sub>; 7-23 min: 35-55% M<sub>2</sub>; 23-28 min: 55-98% M<sub>2</sub>. From peak I, 1.5 mg of gardenifolin A (**83a**) (retention time 25.4 min), 1.4 mg of gardenifolin B (**83b**) (retention time 26.3 min), 3.5 mg of gardenifolin C (**83c**) (retention time 26.8 min), and 3.2 mg of gardenifolin D (**83d**) (retention time 27.6 min) were

obtained. Peak **II** provided 1.8 mg of gardenifolin E (**84a**) (retention time 25.6 min), 1.0 mg of gardenifolin F (**84b**) (retention time 26.6 min), 1.7 mg of gardenifolin G (**84c**) (retention time 27.2 min), and 0.9 mg of gardenifolin H (**84d**) (retention time 27.8 min).

#### IV.9.1.3. Stereochemical Analysis of the Gardenifolins A-H

The resolution of the compounds at the analytical scale was achieved on a Phenomenex Lux<sup>®</sup> Cellulose-1 column: cellulose tris(3,5-dimethylphenylcarbamate, 250 × 4.6 mm, 5 μm), using a dual mobile phase system consisting of 0.05% TFA in water (M<sub>1</sub>) and in acetonitrile (M<sub>2</sub>). At a flow rate of 1 mL min<sup>-1</sup>, the following gradient was used: 0-5 min: 10-40% M<sub>2</sub>; 5-25 min: 40-50% M<sub>2</sub>; 25-27 min: 50-98% M<sub>2</sub>. These conditions were likewise used for the online HPLC-DAD-ECD measurements in the stopped-flow mode. For these investigations, the system was equipped with a motor valve, thus, giving rise to the acquisition of the ECD spectra of the compounds directly after identifying their UV spectra using a diode array detector. The peaks were analyzed at their highest absorbances. The ECD spectra were subtracted by the blank recorded at a solvent ratio corresponding to their retention time.

#### IV.9.1.4. Biological and morphological evaluations conditions

The gardenifolins A-H (**83a-d** and **84a-d**) were tested for their individual cytotoxic activities in vitro using the human cervical HeLa cell line, based on the procedure abovedescribed.

Additionally, morphological effects of gardenifolin D on HeLa cancer cells were further monitored. HeLa cells were seeded in 24-well plates (1.0 × 10<sup>4</sup>/well) and incubated in fresh DMEM at 37 °C under an atmosphere of 5% CO<sub>2</sub> and 95% air for 24 h for the attachment. Cells were washed twice with PBS before the medium was changed with the test samples and incubated for 72 h. After incubation, acridine orange (AO, 30 μL, 100 mg mL<sup>-1</sup> concentration) and Hoechst 33342 (NucBlue live readyprobes reagent, one drop) were added to each test well and the sample was further incubated for 10 min. The cells were then photographed using EVOS<sup>®</sup>FL cell imaging system (40 × objective) under fluorescent and phase contrast mode.

### IV.9.1.5. Structural Details of gardenifolins A-H

#### *Gardenifolin A (83a)*

White, amorphous powder (1.5 mg).

$[\alpha]_D^{23} = +20$  (*c* 0.02, acetone).

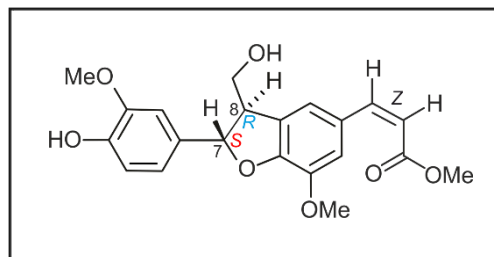
UV (acetone):  $\lambda_{\max}$  ( $\log \epsilon$ ) 207 (4.9), 226 (4.4), 288 (3.5), 321 (4.1) nm.

ECD (MeCN/H<sub>2</sub>O):  $\lambda_{\max}$  ( $\log \epsilon$ ) 210 (3.2), 236 (-2.5), 256 (+1.3), 275 (-0.5), 308 (+1.4), 352 (0.0) nm.

HRESIMS  $m/z$  409.12485 [M+Na]<sup>+</sup> (calcd for C<sub>21</sub>H<sub>22</sub>O<sub>7</sub>Na, 409.12632).

<sup>1</sup>H NMR (CD<sub>3</sub>COCD<sub>3</sub>, 600 MHz):  $\delta_H$  (ppm) = 7.72 (d, *J* = 1.50 Hz, 1H, H-5'), 7.34 (br s, 1H, H-3'), 7.04 (d, *J* = 2.00 Hz, 1H, H-2), 6.90 (d, *J* = 12.93 Hz, 1H, H-7'), 6.88 (dd, *J* = 1.79, 8.15 Hz, 1H, H-6), 6.81 (d, *J* = 8.12 Hz, 1H, H-5), 5.80 (d, *J* = 12.97 Hz, 1H, H-8'), 5.63 (d, *J* = 6.66 Hz, 1H, H-7), 3.88 (m, 1H, H-9<sup>a</sup>), 3.86 (s, 3H, 6'-OCH<sub>3</sub>), 3.84 (m, 1H, H-9<sup>b</sup>), 3.82 (3H, s, 3-OCH<sub>3</sub>), 3.69 (s, 3H, 9'-OCH<sub>3</sub>), 3.58 (pq, *J* = 6.36 Hz, 1H, H-8).

<sup>13</sup>C NMR (CD<sub>3</sub>COCD<sub>3</sub>, 151 MHz):  $\delta_C$  (ppm) = 168.7 (C-9', COOCH<sub>3</sub>), 150.9 (C-1', C), 148.9 (C-3, C-OCH<sub>3</sub>), 147.5 (C-4, C-OH), 144.7 (C-7', C), 144.6 (C-6', C-OCH<sub>3</sub>), 134.3 (C-1, C), 131.0 (C-2', C), 129.2 (C-4', C), 121.9 (C-3', C), 119.7 (C-6, C), 116.5 (C-8', C), 116.2 (C-5, C), 115.8 (C-5', C), 110.6 (C-2, C), 89.2 (C-7, CH-O), 64.6 (C-9, CH<sub>2</sub>OH), 56.4 (6'-OCH<sub>3</sub>, C-OCH<sub>3</sub>), 56.3 (3-OCH<sub>3</sub>, C-OCH<sub>3</sub>), 54.5 (C-8, CH), 51.6 (9'-OCH<sub>3</sub>, COOCH<sub>3</sub>).



**Gardenifolin B (83b)**

White, amorphous powder (1.4 mg).

$[\alpha]_D^{23} = -15$  (c 0.02, acetone).

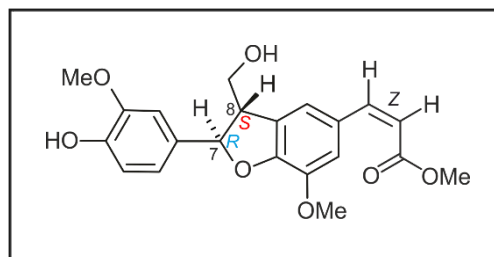
UV (acetone):  $\lambda_{\max}$  (log  $\epsilon$ ) 207 (5.1), 226 (4.2), 288 (1.9), 321 (5.2) nm.

ECD (MeCN/H<sub>2</sub>O):  $\lambda_{\max}$  (log  $\epsilon$ ) 209 (-1.9), 234 (+2.9), 255 (-1.2), 275 (+0.3), 309 (-1.2), 353 (0.0) nm.

HRESIMS  $m/z$  409.12485 [M+Na]<sup>+</sup> (calcd for C<sub>21</sub>H<sub>22</sub>O<sub>7</sub>Na, 409.12632).

<sup>1</sup>H NMR (CD<sub>3</sub>COCD<sub>3</sub>, 600 MHz):  $\delta_H$  (ppm) = 7.72 (d,  $J = 1.50$  Hz, 1H, H-5'), 7.34 (br s, 1H, H-3'), 7.04 (d,  $J = 2.00$  Hz, 1H, H-2), 6.90 (d,  $J = 12.93$  Hz, 1H, H-7'), 6.88 (dd,  $J = 1.79, 8.15$  Hz, 1H, H-6), 6.81 (d,  $J = 8.12$  Hz, 1H, H-5), 5.80 (d,  $J = 12.97$  Hz, 1H, H-8'), 5.63 (d,  $J = 6.66$  Hz, 1H, H-7), 3.88 (m, 1H, H-9<sup>a</sup>), 3.86 (s, 3H, 6'-OCH<sub>3</sub>), 3.84 (m, 1H, H-9<sup>b</sup>), 3.82 (3H, s, 3-OCH<sub>3</sub>), 3.69 (s, 3H, 9'-OCH<sub>3</sub>), 3.58 (pq,  $J = 6.36$  Hz, 1H, H-8).

<sup>13</sup>C NMR (CD<sub>3</sub>COCD<sub>3</sub>, 151 MHz):  $\delta_C$  (ppm) = 168.7 (C-9', COOCH<sub>3</sub>), 150.9 (C-1', C), 148.9 (C-3, C-OCH<sub>3</sub>), 147.5 (C-4, C-OH), 144.7 (C-7', C), 144.6 (C-6', C-OCH<sub>3</sub>), 134.3 (C-1, C), 131.0 (C-2', C), 129.2 (C-4', C), 121.9 (C-3', C), 119.7 (C-6, C), 116.5 (C-8', C), 116.2 (C-5, C), 115.8 (C-5', C), 110.6 (C-2, C), 89.2 (C-7, CH-O), 64.6 (C-9, CH<sub>2</sub>OH), 56.4 (6'-OCH<sub>3</sub>, C-OCH<sub>3</sub>), 56.3 (3-OCH<sub>3</sub>, C-OCH<sub>3</sub>), 54.5 (C-8, CH), 51.6 (9'-OCH<sub>3</sub>, COOCH<sub>3</sub>).

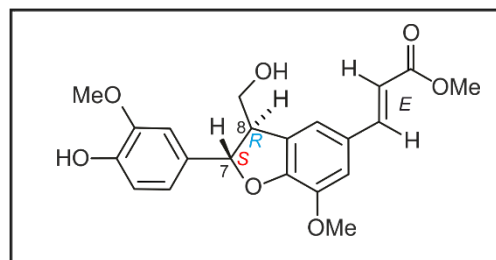


**Gardenifolin C (83c)**

White, amorphous powder (3.5 mg).

$[\alpha]_D^{23} = +21$  (*c* 0.04, acetone).

UV (acetone):  $\lambda_{\max}$  (log  $\epsilon$ ) 226 (4.3), 287 (1.9), 327 (5.2) nm.



ECD (MeCN/H<sub>2</sub>O):  $\lambda_{\max}$  (log  $\epsilon$ ) 234 (-5.0), 255 (+2.1), 317 (+3.0), 330 (+2.9), 353 (0.0) nm.

HRESIMS *m/z* 409.12486 [M+Na]<sup>+</sup> (calcd for C<sub>21</sub>H<sub>22</sub>O<sub>7</sub>Na, 409.12632).

<sup>1</sup>H NMR (CD<sub>3</sub>COCD<sub>3</sub>, 600 MHz):  $\delta_H$  (ppm) = 7.60 (d, *J* = 15.90 Hz, 1H, H-7'), 7.25 (br s, 1H, H-3'), 7.24 (br s, 1H, H-5'), 7.04 (d, *J* = 1.92 Hz, 1H, H-2), 6.87 (dd, *J* = 1.99, 8.15 Hz, 1H, H-6), 6.81 (d, *J* = 8.12 Hz, 1H, H-5), 6.40 (d, *J* = 15.95 Hz, 1H, H-8'), 5.63 (d, *J* = 6.66 Hz, 1H, H-7), 3.90 (s, 3H, 6'-OCH<sub>3</sub>), 3.89 (m, 1H, H-9<sup>a</sup>), 3.84 (m, 1H, H-9<sup>b</sup>), 3.81 (3H, s, 3-OCH<sub>3</sub>), 3.71 (s, 3H, 9'-OCH<sub>3</sub>), 3.58 (q, *J* = 6.36 Hz, 1H, H-8).

<sup>13</sup>C NMR (CD<sub>3</sub>COCD<sub>3</sub>, 151 MHz):  $\delta_C$  (ppm) = 168.0 (C-9', COOCH<sub>3</sub>), 150.6 (C-1', C), 148.5 (C-3, C-OCH<sub>3</sub>), 147.6 (C-4, C-OH), 146.0 (C-7', C), 145.6 (C-6', C-OCH<sub>3</sub>), 133.9 (C-1, C), 131.0 (C-2', C), 129.0 (C-4', C), 119.7 (C-6, C), 118.9 (C-3', C), 115.8 (C-5, C), 115.6 (C-8', C), 113.3 (C-5', C), 110.6 (C-2, C), 89.3 (C-7, CH-O), 64.4 (C-9, CH<sub>2</sub>OH), 56.5 (6'-OCH<sub>3</sub>, C-OCH<sub>3</sub>), 56.3 (3-OCH<sub>3</sub>, C-OCH<sub>3</sub>), 54.4 (C-8, CH), 51.6 (9'-OCH<sub>3</sub>, COOCH<sub>3</sub>).

***Gardenifolin D (83d)***

White, amorphous powder (3.2 mg).

$[\alpha]_D^{23} -21$  (*c* 0.03, acetone).

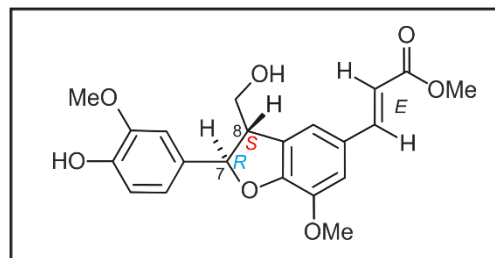
UV (acetone):  $\lambda_{\max}$  (log  $\epsilon$ ) 226 (2.3), 287 (1.7), 327 (4.3) nm.

ECD (MeCN/H<sub>2</sub>O):  $\lambda_{\max}$  (log  $\epsilon$ ) 227 (+3.3), 236 (+2.9), 256 (-2.0), 277 (-0.1), 314 (-3.5), 330 (-2.9), 358 (-0.5) nm.

HRESIMS *m/z* 409.12486 [M+Na]<sup>+</sup> (calcd for C<sub>21</sub>H<sub>22</sub>O<sub>7</sub>Na, 409.12632).

<sup>1</sup>H NMR (CD<sub>3</sub>COCD<sub>3</sub>, 600 MHz):  $\delta_H$  (ppm) = 7.60 (d, *J* = 15.90 Hz, 1H, H-7'), 7.25 (br s, 1H, H-3'), 7.24 (br s, 1H, H-5'), 7.04 (d, *J* = 1.92 Hz, 1H, H-2), 6.87 (dd, *J* = 1.99, 8.15 Hz, 1H, H-6), 6.81 (d, *J* = 8.12 Hz, 1H, H-5), 6.40 (d, *J* = 15.95 Hz, 1H, H-8'), 5.63 (d, *J* = 6.66 Hz, 1H, H-7), 3.90 (s, 3H, 6'-OCH<sub>3</sub>), 3.89 (m, 1H, H-9<sup>a</sup>), 3.84 (m, 1H, H-9<sup>b</sup>), 3.81 (3H, s, 3-OCH<sub>3</sub>), 3.71 (s, 3H, 9'-OCH<sub>3</sub>), 3.58 (q, *J* = 6.36 Hz, 1H, H-8).

<sup>13</sup>C NMR (CD<sub>3</sub>COCD<sub>3</sub>, 151 MHz):  $\delta_C$  (ppm) = 168.0 (C-9', COOCH<sub>3</sub>), 150.6 (C-1', C), 148.5 (C-3, C-OCH<sub>3</sub>), 147.6 (C-4, C-OH), 146.0 (C-7', C), 145.6 (C-6', C-OCH<sub>3</sub>), 133.9 (C-1, C), 131.0 (C-2', C), 129.0 (C-4', C), 119.7 (C-6, C), 118.9 (C-3', C), 115.8 (C-5, C), 115.6 (C-8', C), 113.3 (C-5', C), 110.6 (C-2, C), 89.3 (C-7, CH-O), 64.4 (C-9, CH<sub>2</sub>OH), 56.5 (6'-OCH<sub>3</sub>, C-OCH<sub>3</sub>), 56.3 (3-OCH<sub>3</sub>, C-OCH<sub>3</sub>), 54.4 (C-8, CH), 51.6 (9'-OCH<sub>3</sub>, COOCH<sub>3</sub>).



**Gardenifolin E (84a)**

White, amorphous powder (1.8 mg).

$[\alpha]_D^{23} = +27$  (*c* 0.03, acetone).

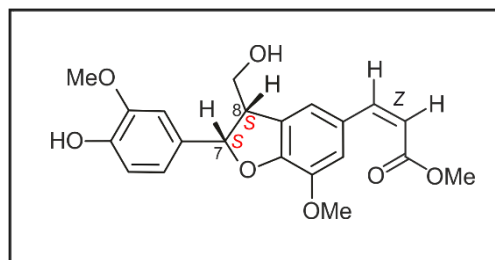
UV (acetone):  $\lambda_{\max}$  ( $\log \epsilon$ ) 207 (5.3), 226 (4.3), 288 (3.6), 321 (4.5) nm.

ECD (MeCN/H<sub>2</sub>O):  $\lambda_{\max}$  ( $\log \epsilon$ ) 210 (4.5), 234 (-2.7), 255 (+2.1), 275 (-0.7), 308 (+1.9), 355 (0.0) nm.

HRESIMS  $m/z$  409.12487 [M+Na]<sup>+</sup> (calcd for C<sub>21</sub>H<sub>22</sub>O<sub>7</sub>Na, 409.12632).

<sup>1</sup>H NMR (CD<sub>3</sub>COCD<sub>3</sub>, 600 MHz):  $\delta_H$  (ppm) = 7.72 (d, *J* = 1.50 Hz, 1H, H-5'), 7.34 (br s, 1H, H-3'), 7.04 (d, *J* = 2.00 Hz, 1H, H-2), 6.90 (d, *J* = 12.91 Hz, 1H, H-7'), 6.88 (dd, *J* = 1.79, 8.15 Hz, 1H, H-6), 6.81 (d, *J* = 8.12 Hz, 1H, H-5), 5.80 (d, *J* = 12.97 Hz, 1H, H-8'), 5.62 (d, *J* = 6.51 Hz, 1H, H-7), 3.88 (m, 1H, H-9<sup>a</sup>), 3.86 (s, 3H, 6'-OCH<sub>3</sub>), 3.84 (m, 1H, H-9<sup>b</sup>), 3.82 (3H, s, 3-OCH<sub>3</sub>), 3.69 (s, 3H, 9'-OCH<sub>3</sub>), 3.58 (pq, *J* = 6.36 Hz, 1H, H-8).

<sup>13</sup>C NMR (CD<sub>3</sub>COCD<sub>3</sub>, 151 MHz):  $\delta_C$  (ppm) = 168.7 (C-9', COOCH<sub>3</sub>), 150.9 (C-1', C), 148.9 (C-3, C-OCH<sub>3</sub>), 147.5 (C-4, C-OH), 144.7 (C-7', C), 144.6 (C-6', C-OCH<sub>3</sub>), 134.3 (C-1, C), 130.0 (C-2', C), 129.2 (C-4', C), 121.9 (C-3', C), 119.7 (C-6, C), 116.5 (C-8', C), 116.2 (C-5, C), 115.8 (C-5', C), 110.6 (C-2, C), 89.2 (C-7, CH-O), 64.6 (C-9, CH<sub>2</sub>OH), 56.4 (6'-OCH<sub>3</sub>, C-OCH<sub>3</sub>), 56.3 (3-OCH<sub>3</sub>, C-OCH<sub>3</sub>), 54.5 (C-8, CH), 51.6 (9'-OCH<sub>3</sub>, COOCH<sub>3</sub>).



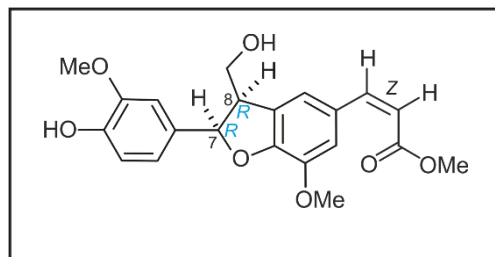


**Gardenifolin F (84b)**

White, amorphous powder (1.1 mg).

$[\alpha]_D^{23} = -23$  (*c* 0.03, acetone).

UV (acetone):  $\lambda_{\max}$  (log  $\epsilon$ ) 207 (3.1), 226 (4.2), 288 (1.7), 321 (5.2) nm.



ECD (MeCN/H<sub>2</sub>O):  $\lambda_{\max}$  (log  $\epsilon$ ) 209 (-1.9), 235 (+1.8), 254 (-1.1), 277 (+0.4), 310 (-1.4), 355 (0.0) nm.

HRESIMS  $m/z$  409.12485 [M+Na]<sup>+</sup> (calcd for C<sub>21</sub>H<sub>22</sub>O<sub>7</sub>Na, 409.12632).

<sup>1</sup>H NMR (CD<sub>3</sub>COCD<sub>3</sub>, 600 MHz):  $\delta_H$  (ppm) = 7.72 (d, *J* = 1.50 Hz, 1H, H-5'), 7.34 (br s, 1H, H-3'), 7.04 (d, *J* = 2.00 Hz, 1H, H-2), 6.90 (d, *J* = 12.91 Hz, 1H, H-7'), 6.88 (dd, *J* = 1.79, 8.15 Hz, 1H, H-6), 6.81 (d, *J* = 8.12 Hz, 1H, H-5), 5.80 (d, *J* = 12.97 Hz, 1H, H-8'), 5.62 (d, *J* = 6.51 Hz, 1H, H-7), 3.88 (m, 1H, H-9<sup>a</sup>), 3.86 (s, 3H, 6'-OCH<sub>3</sub>), 3.84 (m, 1H, H-9<sup>b</sup>), 3.82 (3H, s, 3-OCH<sub>3</sub>), 3.69 (s, 3H, 9'-OCH<sub>3</sub>), 3.58 (pq, *J* = 6.36 Hz, 1H, H-8).

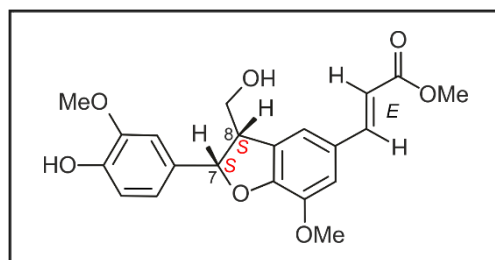
<sup>13</sup>C NMR (CD<sub>3</sub>COCD<sub>3</sub>, 151 MHz):  $\delta_C$  (ppm) = 168.7 (C-9', COOCH<sub>3</sub>), 150.9 (C-1', C), 148.9 (C-3, C-OCH<sub>3</sub>), 147.5 (C-4, C-OH), 144.7 (C-7', C), 144.6 (C-6', C-OCH<sub>3</sub>), 134.3 (C-1, C), 130.0 (C-2', C), 129.2 (C-4', C), 121.9 (C-3', C), 119.7 (C-6, C), 116.5 (C-8', C), 116.2 (C-5, C), 115.8 (C-5', C), 110.6 (C-2, C), 89.2 (C-7, CH-O), 64.6 (C-9, CH<sub>2</sub>OH), 56.4 (6'-OCH<sub>3</sub>, C-OCH<sub>3</sub>), 56.3 (3-OCH<sub>3</sub>, C-OCH<sub>3</sub>), 54.5 (C-8, CH), 51.6 (9'-OCH<sub>3</sub>, COOCH<sub>3</sub>).

**Gardenifolin G (84c)**

White, amorphous powder (1.7 mg).

$[\alpha]_D^{23} = +26$  ( $c$  0.05, acetone).

UV (acetone):  $\lambda_{\max}$  ( $\log \epsilon$ ) 226 (4.3), 287 (1.9), 327 (5.2) nm.



ECD (MeCN/H<sub>2</sub>O):  $\lambda_{\max}$  ( $\log \epsilon$ ) 234 (-5.2), 255 (+2.6), 318 (+3.0), 330 (+3.0), 354 (0.0) nm.

HRESIMS  $m/z$  409.12488 [ $M+Na$ ]<sup>+</sup> (calcd for C<sub>21</sub>H<sub>22</sub>O<sub>7</sub>Na, 409.12632).

<sup>1</sup>H NMR (CD<sub>3</sub>COCD<sub>3</sub>, 600 MHz):  $\delta_H$  (ppm) = 7.60 (d,  $J$  = 15.90 Hz, 1H, H-7'), 7.25 (br s, 1H, H-3'), 7.24 (br s, 1H, H-5'), 7.04 (d,  $J$  = 1.92 Hz, 1H, H-2), 6.88 (dd,  $J$  = 1.95, 8.10 Hz, 1H, H-6), 6.81 (d,  $J$  = 8.11 Hz, 1H, H-5), 6.40 (d,  $J$  = 15.95 Hz, 1H, H-8'), 5.61 (d,  $J$  = 6.52 Hz, 1H, H-7), 3.91 (s, 3H, 6'-OCH<sub>3</sub>), 3.89 (m, 1H, H-9<sup>a</sup>), 3.85 (m, 1H, H-9<sup>b</sup>), 3.82 (3H, s, 3-OCH<sub>3</sub>), 3.72 (s, 3H, 9'-OCH<sub>3</sub>), 3.59 (q,  $J$  = 6.31 Hz, 1H, H-8).

<sup>13</sup>C NMR (CD<sub>3</sub>COCD<sub>3</sub>, 151 MHz):  $\delta_C$  (ppm) = 168.0 (C-9', COOCH<sub>3</sub>), 150.6 (C-1', C), 148.5 (C-3, C-OCH<sub>3</sub>), 147.6 (C-4, C-OH), 146.0 (C-7', C), 145.6 (C-6', C-OCH<sub>3</sub>), 133.9 (C-1, C), 131.0 (C-2', C), 129.0 (C-4', C), 119.7 (C-6, C), 118.9 (C-3', C), 115.8 (C-5, C), 115.6 (C-8', C), 113.3 (C-5', C), 110.6 (C-2, C), 89.3 (C-7, CH-O), 64.4 (C-9, CH<sub>2</sub>OH), 56.5 (6'-OCH<sub>3</sub>, C-OCH<sub>3</sub>), 56.3 (3-OCH<sub>3</sub>, C-OCH<sub>3</sub>), 54.4 (C-8, CH), 51.6 (9'-OCH<sub>3</sub>, COOCH<sub>3</sub>).

***Gardenifolin H (84d)***

White, amorphous powder (0.9 mg).

$[\alpha]_D^{23} = -20$  (*c* 0.04, acetone).

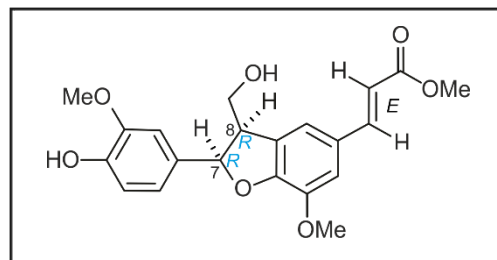
UV (acetone):  $\lambda_{\max}$  (log  $\epsilon$ ) 226 (2.3), 287 (1.7),  
327 (4.3) nm.

ECD (MeCN/H<sub>2</sub>O):  $\lambda_{\max}$  (log  $\epsilon$ ) 227 (+3.3), 236 (+2.9), 256 (-2.0), 277 (-0.1), 313 (-5.0), 329  
(-1.8), 355 (0.0) nm.

HRESIMS  $m/z$  409.12486 [M+Na]<sup>+</sup> (calcd for C<sub>21</sub>H<sub>22</sub>O<sub>7</sub>Na, 409.12632).

<sup>1</sup>H NMR (CD<sub>3</sub>COCD<sub>3</sub>, 600 MHz):  $\delta_H$  (ppm) = 7.60 (d, *J* = 15.90 Hz, 1H, H-7'), 7.25 (br s, 1H, H-3'), 7.24 (br s, 1H, H-5'), 7.04 (d, *J* = 1.92 Hz, 1H, H-2), 6.88 (dd, *J* = 1.95, 8.10 Hz, 1H, H-6), 6.81 (d, *J* = 8.11 Hz, 1H, H-5), 6.40 (d, *J* = 15.95 Hz, 1H, H-8'), 5.61 (d, *J* = 6.52 Hz, 1H, H-7), 3.91 (s, 3H, 6'-OCH<sub>3</sub>), 3.89 (m, 1H, H-9<sup>a</sup>), 3.85 (m, 1H, H-9<sup>b</sup>), 3.82 (3H, s, 3-OCH<sub>3</sub>), 3.72 (s, 3H, 9'-OCH<sub>3</sub>), 3.59 (q, *J* = 6.31 Hz, 1H, H-8).

<sup>13</sup>C NMR (CD<sub>3</sub>COCD<sub>3</sub>, 151 MHz):  $\delta_C$  (ppm) = 168.0 (C-9', COOCH<sub>3</sub>), 150.6 (C-1', C), 148.5 (C-3, C-OCH<sub>3</sub>), 147.6 (C-4, C-OH), 146.0 (C-7', C), 145.6 (C-6', C-OCH<sub>3</sub>), 133.9 (C-1, C), 131.0 (C-2', C), 129.0 (C-4', C), 119.7 (C-6, C), 118.9 (C-3', C), 115.8 (C-5, C), 115.6 (C-8', C), 113.3 (C-5', C), 110.6 (C-2, C), 89.3 (C-7, CH-O), 64.4 (C-9, CH<sub>2</sub>OH), 56.5 (6'-OCH<sub>3</sub>, C-OCH<sub>3</sub>), 56.3 (3-OCH<sub>3</sub>, C-OCH<sub>3</sub>), 54.4 (C-8, CH), 51.6 (9'-OCH<sub>3</sub>, COOCH<sub>3</sub>).



#### IV.10. Quality Analysis of Three Batches of N'Sansiphos

Three batches of the herbal product N'Sansiphos were subjected to HPLC-DAD analysis in order to determine the content in ethyl-paraben (**95**) and propylparaben (**96**). An HPLC-DAD method was developed on a Symmetry<sup>®</sup> RP<sub>18</sub> column (250 x 4.6 mm) with 0.05% of TFA in H<sub>2</sub>O (A) and MeCN (B) using the following gradient conditions: 0-5 min: 25% of B, 10 min: 35% of B, 20-26 min: 55-60% of B, and 29 min: 100% of B. The quantification of the compounds was performed at 255 nm.

The calibration curves parameters were determined by measuring five concentration levels of ethyl paraben and propyl paraben, purchased from Sigma-Aldrich, in MeOH. The results are summarized in Table 24.

Table 24. Calibration curves for the quantification of **95** and **96** in N'Sansiphos.

	ethylparaben ( <b>95</b> )		propylparaben ( <b>96</b> )	
	conc. [ $\mu\text{g mL}^{-1}$ ]	area mean	conc. [ $\mu\text{g mL}^{-1}$ ]	area mean
	10	6.00	8.91	4.95
	25	14.98	22.28	12.1
	40	22.77	35.65	18.65
	50	29.27	44.56	23.65
	65	36.71	57.93	29.65
Intercept		0.6603		0.6533
Slope		0.5601		0.5063
R <sup>2</sup>		0.998702		0.998989

Methanolic solutions of 25-mL were prepared from 5 mL of the syrup (N'Sansiphos), followed by filtration through a 0.22- $\mu\text{m}$ PET syringe filter. Using a developed method HPLC-DAD, five levels of concentrations were evaluated by adding known solutions of the two reference chemical substances (see Table 25). The determinations were performed in three consecutive days. The injection volume was fixed at 15  $\mu\text{L}$  and the peak areas were monitored at 255 nm.

Table 25. Quantitative determinations of ethylparaben (**95**) and propylparaben (**96**) in three batches of N'Sansiphos (matrix solution of the syrup in MeOH: 0.2  $\mu\text{l mL}^{-1}$ ).

	batch 1			batch 2			batch 3		
	conc. [ $\mu\text{g mL}^{-1}$ ]	area mean	conc. [ $\mu\text{g mL}^{-1}$ ]	conc. [ $\mu\text{g mL}^{-1}$ ]	area mean	conc. [ $\mu\text{g mL}^{-1}$ ]	conc. [ $\mu\text{g mL}^{-1}$ ]	area mean	conc. [ $\mu\text{g mL}^{-1}$ ]
<b>95</b>	0	0.46	0.35	0	0.23	0.76	0	0.33	0.59
	10.08	6.47	10.36	10.08	6.50	10.42	10.08	6.63	10.66
	25.2	15.55	26.58	25.2	15.32	26.17	25.2	15.52	26.53
	40.32	24.40	42.39	40.32	24.90	43.28	40.32	24.87	43.22
	50.4	30.27	52.87	50.4	30.87	53.93	50.4	29.94	52.28
	65.52	38.93	68.32	65.52	40.12	70.45	65.52	39.13	68.68
	Initial	<b>0.35 <math>\mu\text{g mL}^{-1}</math></b>		<b>0.76 <math>\mu\text{g mL}^{-1}</math></b>		<b>0.59 <math>\mu\text{g mL}^{-1}</math></b>			
<b>96</b>	0	8	14.51	0	8.17	14.84	0	7.67	13.85
	8.9	12.27	22.94	8.9	13.13	24.65	8.9	12.90	24.19
	22.3	19.23	36.70	22.3	20.17	38.54	22.3	19.57	37.36
	35.7	26.80	51.64	35.7	27.77	53.55	35.7	27.33	52.70
	44.6	31.07	60.07	44.6	32.57	63.03	44.6	30.93	59.81
	57.9	38.17	74.09	57.9	39.60	76.92	57.9	38.70	75.15
	Initial	<b>14.51 <math>\mu\text{g mL}^{-1}</math></b>		<b>14.84 <math>\mu\text{g mL}^{-1}</math></b>		<b>13.85 <math>\mu\text{g mL}^{-1}</math></b>			

## V. Literature

- [1] D. A. Dias, S. Urban, U. Roessner; A historical overview of natural products in drug discovery; *Metabolites* **2012**, *2*, 303.
- [2] P. M. Dewick, *Medicinal Natural Products: A Biosynthetic Approach, 3rd Edition*, John Wiley & Sons Ltd, Chichester, West Sussex, **2009**.
- [3] F. Bourgaud, A. Gravot, S. Milesi, E. Gontier; Production of plant secondary metabolites: a historical perspective; *Plant Sci.* **2001**, *161*, 839–851.
- [4] K. Liu, A. A. Abdullah, M. Huang, T. Nishioka, M. Altaf-Ul-Amin, S. Kanaya; Novel approach to classify plants based on metabolite-content similarity; *Biomed. Res. Int.* **2017**, *2017*, 5296729.
- [5] M. Wink; Evolution of secondary metabolites from an ecological and molecular phylogenetic perspective; *Phytochemistry* **2003**, *64*, 3–19.
- [6] R. Singh; Chemotaxonomy: a tool for plant classification; *J. Med. Plants Stud.* **2016**, *4*, 90–93.
- [7] M. P. Speed, A. Fenton, M. G. Jones, G. D. Ruxton, M. A. Brockhurst; Coevolution can explain defensive secondary metabolite diversity in plants; *New Phytol.* **2015**, *208*, 1251–1263.
- [8] J. Bero, M. Frederich, J. Quetin-Leclercq; Antimalarial compounds isolated from plants used in traditional medicine; *J. Pharm. Pharmacol.* **2009**, *61*, 1401–1433.
- [9] K. M. Witherup, S. A. Look, M. W. Stasko, T. J. Ghiorzi, G. M. Muschik, G. M. Cragg; *Taxus* spp. needles contain amounts of taxol comparable to the bark of *Taxus brevifolia*: analysis and isolation; *J. Nat. Prod.* **1990**, *53*, 1249–1255.
- [10] X. Wang, Y. Zhang, L. V. Ponomareva, Q. Qiu, R. Woodcock, S. I. Elshahawi, X. Chen, Z. Zhou, B. E. Hatcher, J. C. Hower, C.-G. Zhan, S. Parkin, M. K. Kharel, S. R. Voss, K. A. Shaaban, J. S. Thorson; Mccreamycins A–D, Geldanamycin-derived cyclopentenone macrolactams from an Eastern Kentucky abandoned coal mine microbe; *Angew. Chem. Int. Ed.* **2017**, *56*, 2994–2998.
- [11] R. D. Firn, C. G. Jones; Natural products—a simple model to explain chemical diversity; *Nat. Prod. Rep.* **2003**, *20*, 382–391.

- [12] D. J. Newman, G. M. Cragg, K. M. Snader; The influence of natural products upon drug discovery; *Nat. Prod. Rep.* **2000**, *17*, 215–234.
- [13] J. G. Mahdi, A. J. Mahdi, A. J. Mahdi, I. D. Bowen; The historical analysis of aspirin discovery, its relation to the willow tree and antiproliferative and anticancer potential; *Cell Prolif.* **2006**, *39*, 147–155.
- [14] K. A. El Sayed, M. Kelly, U. A. K. Kara, K. K. H. Ang, I. Katsuyama, D. C. Dunbar, A. A. Khan, M. T. Hamann; New manzamine alkaloids with potent activity against infectious diseases; *J. Am. Chem. Soc.* **2001**, *123*, 1804–1808.
- [15] T. Kubota, K. Nakamura, S. I. Kurimoto, K. Sakai, J. Fromont, T. Gonoï, J. Kobayashi; Zamamidine D, a manzamine alkaloid from an Okinawan *Amphimedon* sp. marine sponge; *J. Nat. Prod.* **2017**, *80*, 1196–1199.
- [16] H. Li, X. Wang, X. Lei; Total syntheses of Lycopodium alkaloids (+)-fawcettimine, (+)-fawcettidine, and (–)-8-deoxyserratinine; *Angew. Chem. Int. Ed.* **2012**, *51*, 491–495.
- [17] M. Kuramoto, N. Miyake, Y. Ishimaru, N. Ono, H. Uno; Cylindradines A and B: novel bromopyrrole alkaloids from the marine sponge *Axinella cylindratus*; *Org. Lett.* **2008**, *10*, 5465–5468.
- [18] H. Morita, J. i. Kobayashi; Calyciphyllines A and B, two novel hexacyclic alkaloids from *Daphniphyllum calycinum*; *Org. Lett.* **2003**, *5*, 2895–2898.
- [19] D. J. Abraham, N. R. Farnsworth; Structure elucidation and chemistry of *Catharanthus* alkaloids III: structure of leurosine, an active anticancer alkaloid; *J. Pharm. Sci.* **1969**, *58*, 694–698.
- [20] J. Bero, J. Quetin-Leclercq; Natural products published in 2009 from plants traditionally used to treat malaria; *Planta Med.* **2011**, *77*, 631–640.
- [21] G. Philippe, E. Prost, J.-M. Nuzillard, M. Zèches-Hanrot, M. Tits, L. Angenot, M. Frédérick; Strychnohexamine from *Strychnos icaia*, a naturally occurring trimeric indolomonoterpenic alkaloid; *Tetrahedron Lett.* **2002**, *43*, 3387–3390.
- [22] G. Ma, H. Wu, D. Chen, N. Zhu, Y. Zhu, Z. Sun, P. Li, J. Yang, J. Yuan, X. Xu; Antimalarial and antiproliferative cassane diterpenes of *Caesalpinia sappan*; *J. Nat. Prod.* **2015**, *78*, 2364–2371.

- [23] J. I. Seeman; The Woodward–Doering/Rabe–Kindler total synthesis of quinine: setting the record straight; *Angew. Chem. Int. Ed.* **2007**, *46*, 1378–1413.
- [24] P. Rabe, K. Kindler; Über die partielle Synthese des Chinins. Zur Kenntnis der Chinaalkaloide XIX; *Ber. Dtsch. Chem. Ges.* **1918**, *51*, 466–467.
- [25] Y.-X. Han, Y.-L. Jiang, Y. Li, H.-X. Yu, B.-Q. Tong, Z. Niu, S.-J. Zhou, S. Liu, Y. Lan, J.-H. Chen, Z. Yang; Biomimetically inspired asymmetric total synthesis of (+)-19-dehydroxyl arisandilactone A; *Nat. Commun.* **2017**, *8*, 14233.
- [26] H. Liu, Y. Jia; Ergot alkaloids: synthetic approaches to lysergic acid and clavine alkaloids; *Nat. Prod. Rep.* **2017**, *34*, 411–432.
- [27] F. Eiden; Ausflug in die Vergangenheit: Chinin und andere Chinaalkaloide. 1. Teil: Von der Isolierung der Chinaalkaloide bis zur Konstitutionsaufklärung; *Pharm. Unserer Zeit* **1998**, *27*, 15.
- [28] D. L. Klayman; Qinghaosu (artemisinin): an antimalarial drug from China; *Science* **1985**, *228*, 1049–1055.
- [29] Y. Y. Tu, M. Y. Ni, Y. R. Zhong, L. N. Li, S. L. Cui, M. Q. Zhang, X. Z. Wang, X. T. Liang; Studies on the constituents of *Artemisia annua* L.; *Yao xue xue bao = Acta pharmaceutica Sinica* **1981**, *16*, 366–370.
- [30] The 2015 Nobel Prize in Physiology or Medicine; Press Release, Nobel Media AB 2014. <[http://www.nobelprize.org/nobel\\_prizes/medicine/laureates/2015/press.html](http://www.nobelprize.org/nobel_prizes/medicine/laureates/2015/press.html)> Web. 3 Jul. 2017.
- [31] J. Li, R. Seupel, D. Feineis, V. Mudogo, M. Kaiser, R. Brun, D. Brännert, M. Chatterjee, E.-J. Seo, T. Efferth, G. Bringmann; Dioncophyllines C<sub>2</sub>, D<sub>2</sub>, and F and related naphthylisoquinoline alkaloids from the Congolese liana *Ancistrocladus ileboensis* with potent activities against *Plasmodium falciparum* and against multiple myeloma and leukemia cell lines; *J. Nat. Prod.* **2017**, *80*, 443–458.
- [32] G. Bringmann, G. Zhang, T. Buttner, G. Bauckmann, T. Kupfer, H. Braunschweig, R. Brun, V. Mudogo; Jozimine A<sub>2</sub>: the first dimeric Dioncophyllaceae-type naphthylisoquinoline alkaloid, with three chiral axes and high antiplasmodial activity; *Chem. Eur. J.* **2013**, *19*, 916–923.



- [33] G. Bringmann, M. Rübenacker, R. Weirich, L. A. Assi; Dioncophylline C from the roots of *Triphyophyllum peltatum*, the first 5,1'-coupled dioncophyllaceae alkaloid; *Phytochemistry* **1992**, *31*, 4019–4024.
- [34] S. R. Ibrahim, G. A. Mohamed; Naphthylisoquinoline alkaloids potential drug leads; *Fitoterapia* **2015**, *106*, 194–225.
- [35] G. Bringmann, I. Kajahn, M. Reichert, S. E. H. Pedersen, J. H. Faber, T. Gulder, R. Brun, S. B. Christensen, A. Ponte-Sucre, H. Moll, G. Heubl, V. Mudogo; Ancistrocladinium A and B, the first *N,C*-coupled naphthyldihydroisoquinoline alkaloids, from a Congolese *Ancistrocladus* species; *J. Org. Chem.* **2006**, *71*, 9348–9356.
- [36] A. S. Awaad, H. A. Al-Mudhayyif, M. R. Al-Othman, M. E. Zain, R. M. El-Meligy; Amhezole, a novel fungal secondary metabolite from *Aspergillus terreus* for treatment of microbial mouth Infection; *Phytother. Res.* **2017**, *31*, 395–402.
- [37] C. C. Presley, P. Krai, S. Dalal, Q. Su, M. Cassera, M. Goetz, D. G. I. Kingston; New potently bioactive alkaloids from *Crinum erubescens*; *Bioorg. Med. Chem.* **2016**, *24*, 5418–5422.
- [38] N. Nagasundaram, C. George Priya Doss, C. Chakraborty, V. Karthick, D. Thirumal Kumar, K. N. Balaji, R. Siva, A. Lu, Z. Ge, H. Zhu; Mechanism of artemisinin resistance for malaria PfATP6 L263 mutations and discovering potential antimalarials: an integrated computational approach; *Sci. Rep.* **2016**, *6*, 30106.
- [39] E. K. Karlsson, D. P. Kwiatkowski, P. C. Sabeti; Natural selection and infectious disease in human populations; *Nat. Rev. Genet.* **2014**, *15*, 379–393.
- [40] W. H. O. (WHO); World Malaria Report 2016; *Geneva, Switzerland* **2016**.
- [41] R. Carter, K. N. Mendis; Evolutionary and historical aspects of the burden of malaria; *Clin. Microbiol. Rev.* **2002**, *15*, 564–594.
- [42] M. J. Chan-Bacab, L. M. Pena-Rodriguez; Plant natural products with leishmanicidal activity; *Nat. Prod. Rep.* **2001**, *18*, 674–688.
- [43] S. Das, S. Sinha, B. Das, R. Jayabalan, M. Suar, A. Mishra, A. J. Tamhankar, C. Stalsby Lundborg, S. K. Tripathy; Disinfection of multidrug resistant *Escherichia coli* by solar-photocatalysis using Fe-doped ZnO nanoparticles; *Sci. Rep.* **2017**, *7*, 104.

- [44] D. Hughes, D. I. Andersson; Evolutionary consequences of drug resistance: shared principles across diverse targets and organisms; *Nat. Rev. Genet.* **2015**, *16*, 459–471.
- [45] F. G. Turini, C. Steinert, G. Heubl, G. Bringmann, B. K. Lombe, V. Mudogo, H. Meimberg; Microsatellites facilitate species delimitation in Congolese *Ancistrocladus* (Ancistrocladaceae), a genus with pharmacologically potent naphthylisoquinoline alkaloids; *Taxon* **2014**, *63*, 329–341.
- [46] C. M. Taylor, R. E. Gereau, G. M. Walters; Revision of *Ancistrocladus* Wall. (Ancistrocladaceae); *Ann. Missouri Bot. Gard.* **2005**, *92*, 360–399.
- [47] E. J. Lee, P. J. Facchini; Tyrosine aminotransferase contributes to benzyloquinoline alkaloid biosynthesis in opium poppy; *Plant Physiol.* **2011**, *157*, 1067–1078.
- [48] G. A. W. Beaudoin, P. J. Facchini; Benzyloquinoline alkaloid biosynthesis in opium poppy; *Planta* **2014**, *240*, 19–32.
- [49] Y. Huang, H. Tan, Z. Guo, X. Wu, Q. Zhang, L. Zhang, Y. Diao; The biosynthesis and genetic engineering of bioactive indole alkaloids in plants; *J. Plant Biol.* **2016**, *59*, 203–214.
- [50] G. Bringmann, C. Gunther, M. Ochse, O. Schupp, S. Tasler; Biaryls in nature: a multifaceted class of stereochemically, biosynthetically, and pharmacologically intriguing secondary metabolites; *Fortschr. Chem. Org. Naturst.* **2001**, *82*, 1–249.
- [51] M. Cheek; A synoptic revision of *Ancistrocladus* (Ancistrocladaceae) in Africa, with a new species from Western Cameroon; *Kew Bull.* **2000**, *55*, 871–882.
- [52] M. Cheek, M. Christian Frimodt, xf, ller, H. Vibeke, xf, rlyck; A new Submontane species of *Ancistrocladus* from Tanzania; *Kew Bull.* **2000**, *55*, 207–212.
- [53] H. Meimberg, H. Rischer, F. G. Turini, V. Chamchumroon, M. Dreyer, M. Sommaro, G. Bringmann, G. Heubl; Evidence for species differentiation within the *Ancistrocladus tectorius* complex (Ancistrocladaceae) in Southeast Asia: a molecular approach; *Plant Syst. Evol.* **2010**, *284*, 77–98.
- [54] H. Meimberg, P. Dittrich, G. Bringmann, J. Schlauer, G. Heubl; Molecular phylogeny of Caryophyllidae s.l. based on matK sequences with special emphasis on carnivorous taxa; *Plant Biol.* **2000**, *2*, 218–228.

- [55] Ancistrocladaceae in the *Germplasm Resources Information Network* (GRIN), USDA, ARS, National Genetic Resources Program. National Germplasm Resources Laboratory, Beltsville, Maryland. Web. 3 Jul. 2017.
- [56] Z. Y. U. Ibrahim, Adamu A.; Abechi, Stephen E.; Quantitative structure-activity relationship analysis of naphthylisoquinoline derivatives as antimalarial agents using multiple linear regression approach; *J. Chem. Biol. Phys. Sci.* **2016**, *6*, 19.
- [57] L. Mammino, M. K. Bilonda; Computational study of naphthylisoquinoline alkaloids with antimalarial activity from Dioncophyllaceae and Ancistrodaceae *in vacuo*; *Theor. Chem. Acc.* **2016**, *135*, 101.
- [58] G. Bringmann, S. K. Bischof, S. Müller, T. Gulder, C. Winter, A. Stich, H. Moll, M. Kaiser, R. Brun, J. Dreher, K. Baumann; QSAR guided synthesis of simplified antiplasmodial analogs of naphthylisoquinoline alkaloids; *Eur. J. Med. Chem.* **2010**, *45*, 5370–5383.
- [59] A. Ponte-Sucre, T. Gulder, A. Wegehaupt, C. Albert, C. Rikanovic, L. Schaefflein, A. Frank, M. Schultheis, M. Unger, U. Holzgrabe, G. Bringmann, H. Moll; Structure-activity relationship and studies on the molecular mechanism of leishmanicidal *N,C*-coupled arylisoquinolinium salts; *J. Med. Chem.* **2009**, *52*, 626–636.
- [60] G. Bringmann; Naphthylisoquinoline alkaloids in *The Alkaloids, Vol. 29* (Ed.: A. Brossi), Academic Press, New York, **1986**, pp. 141–184.
- [61] E. Kugelmann, C. R. Albert, G. Bringmann, U. Holzgrabe; Fenton's oxidation: a tool for the investigation of potential drug metabolites; *J. Pharm. Biomed. Anal.* **2011**, *54*, 1047–1058.
- [62] R. B. Herbert, in *The Chemistry and Biology of Isoquinoline Alkaloids* (Eds.: J. D. Phillipson, M. F. Roberts, M. H. Zenk), Springer Berlin Heidelberg, Berlin, Heidelberg, **1985**, pp. 213–228.
- [63] G. Bringmann, M. Wohlfarth, H. Rischer, M. Grune, J. Schlauer; A new biosynthetic pathway to alkaloids in plants: acetogenic isoquinolines; *Angew. Chem. Int. Ed.* **2000**, *39*, 1464–1466.
- [64] G. Bringmann, D. Feineis; Stress-related polyketide metabolism of Dioncophyllaceae and Ancistrocladaceae; *J. Exp. Bot.* **2001**, *52*, 2015–2022.

- [65] G. Bringmann, J. Mutanyatta-Comar, M. Greb, S. Rüdener, T. F. Noll, A. Irmer; Biosynthesis of naphthylisoquinoline alkaloids: synthesis and incorporation of an advanced  $^{13}\text{C}_2$ -labeled isoquinoline precursor; *Tetrahedron* **2007**, *63*, 1755–1761.
- [66] G. Bringmann, M. Rueckert, M. Wenzel, C. Guenther, K. Wolf, J. Holenz, J. Schlauer; Biological activities and biosynthetic origin of acetogenic isoquinoline alkaloids; *Pharm. Pharmacol. Lett.* **1998**, *8*, 5–7.
- [67] E. Leete; The biosynthesis of coniine from four acetate units; *J. Am. Chem. Soc.* **1963**, *85*, 3523–3524.
- [68] S. M. C. Dietrich, R. O. Martin; Biosynthesis of *Conium* alkaloids using carbon-14 dioxide. Interrelation of gamma-coniceine, coniine, and *N*-methylconiine; *J. Am. Chem. Soc.* **1968**, *90*, 1921–1923.
- [69] R. Binev, in *Natural Products: Phytochemistry, Botany and Metabolism of Alkaloids, Phenolics and Terpenes* (Eds.: K. G. Ramawat, J.-M. Mérillon), Springer Berlin Heidelberg, Berlin, Heidelberg, **2013**, pp. 883–907.
- [70] G. Bringmann, J. Spuziak, J. H. Faber, T. Gulder, I. Kajahn, M. Dreyer, G. Heubl, R. Brun, V. Mudogo; Six naphthylisoquinoline alkaloids and a related benzopyranone from a Congolese *Ancistrocladus* species related to *Ancistrocladus congolensis*; *Phytochemistry* **2008**, *69*, 1065–1075.
- [71] G. P. Moss; Basic terminology of stereochemistry; *Pure and Appl. Chem.* **1996**, *68*, 2193–2222.
- [72] A. Ciogli, S. Vivek Kumar, M. Mancinelli, A. Mazzanti, S. Perumal, C. Severi, C. Villani; Atropisomerism in 3-arylthiazolidine-2-thiones. A combined dynamic NMR and dynamic HPLC study; *Organic & Biomolecular Chemistry* **2016**, *14*, 11137–11147.
- [73] K. M. Peese; Selective atropisomer preparation in natural product synthesis (University of Illinois, Chemistry Faculty), **2002**. [http://www.chemistry.illinois.edu/research/organic/seminar\\_extracts/2002\\_2003/abstract\\_peese1.pdf](http://www.chemistry.illinois.edu/research/organic/seminar_extracts/2002_2003/abstract_peese1.pdf) Web. 3 Jul. 2017.
- [74] G. Bringmann, T. Gulder, T. A. M. Gulder, M. Breuning; Atroposelective total synthesis of axially chiral biaryl natural products; *Chem. Rev.* **2011**, *111*, 563–639.

- [75] X. Fu, M. B. Hossain, D. van der Helm, F. J. Schmitz; Longithorone A: unprecedented dimeric prenylated quinone from the tunicate *Aplydium longithorax*; *J. Am. Chem. Soc.* **1994**, *116*, 12125–12126.
- [76] X. Fu, M. B. Hossain, F. J. Schmitz, D. van der Helm; Longithorones, unique prenylated para- and metacyclophane type quinones from the Tunicate *Aplidium longithorax*; *J. Org. Chem.* **1997**, *62*, 3810–3819.
- [77] M. E. Layton, C. A. Morales, M. D. Shair; Biomimetic synthesis of (–)-longithorone A; *J. Am. Chem. Soc.* **2002**, *124*, 773–775.
- [78] T. Kato, K. Nagae, M. Hoshikawa; Synthesis of longithorone B, a sixteen-membered farnesylated *p*-benzoquinone; *Tetrahedron Lett.* **1999**, *40*, 1941–1944.
- [79] H. H. Sun, C. J. Barrow, D. M. Sedlock, A. M. Gillum, R. Cooper; Benzomalvins, new substance P inhibitors from a *Penicillium* sp; *J. Antibiot. (Tokyo)* **1994**, *47*, 515–522.
- [80] J. Clayden, W. J. Moran, P. J. Edwards, S. R. LaPlante; The challenge of atropisomerism in drug discovery; *Angew. Chem. Int. Ed.* **2009**, *48*, 6398–6401.
- [81] J. E. Smyth, N. M. Butler, P. A. Keller; A twist of nature-the significance of atropisomers in biological systems; *Nat. Prod. Rep.* **2015**, *32*, 1562–1583.
- [82] E. Kumarasamy, R. Raghunathan, M. P. Sibi, J. Sivaguru; Nonbiaryl and heterobiaryl atropisomers: molecular templates with promise for atropselective chemical transformations; *Chem. Rev.* **2015**, *115*, 11239–11300.
- [83] G. Bringmann, G. Zhang, T. Olschlager, A. Stich, J. Wu, M. Chatterjee, R. Brun; Highly selective antiplasmodial naphthylisoquinoline alkaloids from *Ancistrocladus tectorius*; *Phytochemistry* **2013**, *91*, 220–228.
- [84] G. Bringmann, F. Pokorny; The naphthylisoquinoline alkaloids in *The Alkaloids, Vol. 46* (Ed.: G. A. Cordell), Academic Press, New York, **1995**, pp. 127–271.
- [85] G. Bringmann, Modified graphic from a template of the research group Bringmann, University of Wuerzburg, **2013**.
- [86] L. Conteh, T. Engels, D. H. Molyneux; Socioeconomic aspects of neglected tropical diseases; *Lancet* **2010**, *375*, 239–247.

- [87] Z. A. Bhutta, J. Sommerfeld, Z. S. Lassi, R. A. Salam, J. K. Das; Global burden, distribution, and interventions for infectious diseases of poverty; *Infect. Dis. Poverty* **2014**, *3*, 21.
- [88] K. A. Murray, N. Preston, T. Allen, C. Zambrana-Torrel, P. R. Hosseini, P. Daszak; Global biogeography of human infectious diseases; *Proc. Natl. Acad. Sci. USA* **2015**, *112*, 12746–12751.
- [89] N. Ruangrunsi, V. Wongpanich, P. Tantivatana, H. J. Cowe, P. J. Cox, S. Funayama, G. A. Cordell; Traditional medicinal plants of Thailand, V. ancistrocladine, a new naphthalene-isoquinoline alkaloid from *Ancistrocladus tectorius*; *J. Nat. Prod.* **1985**, *48*, 529–535.
- [90] C. Wiart, S. Mogana, S. Khalifah, M. Mahan, S. Ismail, M. Buckle, A. K. Narayana, M. Sulaiman; Antimicrobial screening of plants used for traditional medicine in the state of Perak, Peninsular Malaysia; *Fitoterapia* **2004**, *75*, 68–73.
- [91] G. François, G. Bringmann, J. D. Phillipson, L. A. Assi, C. Dochez, M. Ruebenacker, C. Schneider, M. Wery, D. C. Warhurst, G. C. Kirby; Acetogenic isoquinoline alkaloids. Part 52. Activity of extracts and naphthylisoquinoline alkaloids from *Triphyophyllum peltatum*, *Ancistrocladus abbreviatus* and *A. barteri* against *Plasmodium falciparum* *in vitro*; *Phytochemistry* **1994**, *35*, 1461–1464.
- [92] A. Ponte-Sucre, T. Gulder, A. Wegehaupt, C. Albert, C. Rikanović, L. Schaefflein, A. Frank, M. Schultheis, M. Unger, U. Holzgrabe, G. Bringmann, H. Moll; Structure-activity relationship and studies on the molecular mechanism of leishmanicidal *N,C*-coupled arylisoquinolinium salts; *J. Med. Chem.* **2009**, *52*, 626–636.
- [93] G. François, G. Timperman, J. Holenz, L. Ake Assi, T. Geuder, L. Maes, J. Dubois, M. Hanocq, G. Bringmann; Naphthylisoquinoline alkaloids exhibit strong growth-inhibiting activities against *Plasmodium falciparum* and *P. berghei* *in vitro* structure-activity relationships of dioncophylline C; *Ann. Trop. Med. Parasitol.* **1996**, *90*, 115–123.
- [94] A. A. U. Zakari Y. Ibrahim, Stephen E. Abechi; Structure-toxicity relationships of naphthylisoquinoline derivatives as antimalarial agents using molecular descriptors; *Am. J. Trop. Med. Hyg.* **2016**, *11*, 16.

- [95] G. Bringmann, S. K. Bischof, S. Muller, T. Gulder, C. Winter, A. Stich, H. Moll, M. Kaiser, R. Brun, J. Dreher, K. Baumann; QSAR guided synthesis of simplified antiplasmodial analogs of naphthylisoquinoline alkaloids; *Eur. J. Med. Chem.* **2010**, *45*, 5370–5383.
- [96] G. Bringmann, T. Gulder, B. Hertlein, Y. Hemberger, F. Meyer; Total synthesis of the *N,C*-coupled naphthylisoquinoline alkaloids ancistrocladinium A and B and related analogues; *J. Am. Chem. Soc.* **2010**, *132*, 1151–1158.
- [97] G. Bringmann, R. Zagst, B. Schoner, H. Busse, M. Hemmerling, C. Burschka; Acetogenic isoquinoline alkaloids. XXIII. Structure of the naphthyl isoquinoline alkaloid dioncophylline A; *Acta Cryst. C* **1991**, *47*, 1703–1705.
- [98] G. Bringmann, A. Hamm, C. Guenther, M. Michel, R. Brun, V. Mudogo; Ancistroealaines A and B, two new bioactive naphthylisoquinolines, and related naphthoic acids from *Ancistrocladus ealaensis*; *J. Nat. Prod.* **2000**, *63*, 1465–1470.
- [99] M. R. Boyd, I. J. H. Cardellina II, K. P. Manfredi, J. W. Blunt, L. K. Pannell, J. B. McMahon, R. J. Gulakowski, G. M. Cragg, G. Bringmann, D. Thomas, J. Jato, *Michellamine antiviral agents, compositions, and treatment methods*, (United States Dept. of Health and Human Services, USA); United States Patent, **1995**.
- [100] Y. F. Hallock, K. P. Manfredi, J.-R. Dai, J. H. Cardellina II, R. J. Gulakowski, J. B. McMahon, M. Schaeffer, M. Stahl, K.-P. Gulden, G. Bringmann, G. François, M. R. Boyd; Michellamines D-F, new HIV-inhibitory dimeric naphthylisoquinoline alkaloids, and korupensamine E, a new antimalarial monomer, from *Ancistrocladus korupensis*; *J. Nat. Prod.* **1997**, *60*, 677–683.
- [101] M. Xu, T. Bruhn, B. Hertlein, R. Brun, A. Stich, J. Wu, G. Bringmann; Shuangancistroectorines A-E, dimeric naphthylisoquinoline alkaloids with three chiral biaryl axes from the Chinese plant *Ancistrocladus tectorius*; *Chem. Eur. J.* **2010**, *16*, 4206–4216.
- [102] G. Bringmann, M. Wohlfarth, H. Rischer, J. Schlauer, R. Brun; Extract screening by HPLC coupled to MS-MS, NMR, and CD: a dimeric and three monomeric naphthylisoquinoline alkaloids from *Ancistrocladus griffithii*; *Phytochemistry* **2002**, *61*, 195–204.

- [103] G. Bringmann, B. K. Lombe, C. Steinert, K. N. Ioset, R. Brun, F. Turini, G. Heubl, V. Mudogo; Mbandakamines A and B, unsymmetrically coupled dimeric naphthylisoquinoline alkaloids, from a Congolese *Ancistrocladus* species; *Org. Lett.* **2013**, *15*, 2590–2593.
- [104] G. Bringmann, C. Steinert, D. Feineis, V. Mudogo, J. Betzin, C. Scheller; HIV-inhibitory michellamine-type dimeric naphthylisoquinoline alkaloids from the Central African liana *Ancistrocladus congolensis*; *Phytochemistry* **2016**, *128*, 71–81.
- [105] M. R. Boyd, Y. F. Hallock, J. H. Cardellina II, K. P. Manfredi, J. W. Blunt, J. B. McMahon, R. W. Buckheit, Jr., G. Bringmann, M. Schaffer, G. M. Cragg, D. W. Thomas, J. G. Jato; Anti-HIV michellamines from *Ancistrocladus korupensis*; *J. Med. Chem.* **1994**, *37*, 1740–1745.
- [106] J. B. McMahon, M. J. Currens, R. J. Gulakowski, R. W. Buckheit, Jr., C. Lackman-Smith, Y. F. Hallock, M. R. Boyd; Michellamine B, a novel plant alkaloid, inhibits human immunodeficiency virus-induced cell killing by at least two distinct mechanisms; *Antimicrob. Agents Chemother.* **1995**, *39*, 484–488.
- [107] Y. F. Hallock, J. H. Cardellina II, M. Schaffer, G. Bringmann, G. François, M. R. Boyd; Korundamine A, a novel HIV-inhibitory and antimalarial "hybrid" naphthylisoquinoline alkaloid heterodimer from *Ancistrocladus korupensis*; *Bioorg. Med. Chem. Lett.* **1998**, *8*, 1729–1734.
- [108] G. Bringmann, M. Rübenacker, J. R. Jansen, D. Scheutzow, L. Aké Assi; On the structure of the dioncophyllaceae alkaloids dioncophylline a ("triphyophylline") and "O-methyl-triphyophylline"; *Tetrahedron Lett.* **1990**, *31*, 639–642.
- [109] J.-P. Foucher, J.-L. Pousset, A. Cavé, A. Cavé; L'ancistrocladonine et l'ancistroealaensine deux alcaloides nouveaux isolés de l'*Ancistrocladus ealaensis*; *Phytochemistry* **1974**, *13*, 1253–1256.
- [110] J. P. Foucher, J. L. Pousset, A. Cavé; Ancistrine, ancistine, ancistrocladeine trois alcaloides isolés de l'*Ancistrocladus ealaensis*; *Phytochemistry* **1975**, *14*, 2699–2702.
- [111] J. P. Foucher, J. L. Pousset, A. Cavé, A. Bouquet, R. Paris; Chimiotaxinomie des Ancistrocladacées : I. Sur les alcaloïdes de l'*Ancistrocladus ealaensis*; *Plant. Médic. Phytothér.* **1971**, *5*, 16–24.



- [112] G. Bringmann, T. A. Gulder, M. Reichert, T. Gulder; The online assignment of the absolute configuration of natural products: HPLC-CD in combination with quantum chemical CD calculations; *Chirality* **2008**, *20*, 628–642.
- [113] G. Bringmann, R. God, M. Schäffer; An improved degradation procedure for determination of the absolute configuration in chiral isoquinoline and  $\beta$ -carboline derivatives; *Phytochemistry* **1996**, *43*, 1393–1403.
- [114] E. Breitmaier, *Structure Elucidation by NMR in Organic Chemistry: A Practical Guide*, John Wiley & Sons Ltd, **1993**.
- [115] E. Breitmaier, *Structure elucidation by NMR in organic chemistry: a practical guide*, John Wiley & Sons Ltd, **2002**.
- [116] G. Bringmann, D. Koppler, D. Scheutzow, A. Porzel; Determination of configuration at the biaryl axes of naphthylisoquinoline alkaloids by long-range NOE effects; *Magn. Reson. Chem.* **1997**, *35*, 297–301.
- [117] G. Bringmann, D. Götz, T. Bruhn, in *Comprehensive Chiroptical Spectroscopy*, John Wiley & Sons Ltd, **2012**, pp. 355–386.
- [118] T. van Mourik, M. Bühl, M.-P. Gageot; Density functional theory across chemistry, physics and biology; *Philos. Trans. R. Soc.* **2014**, *372*, 20120488.
- [119] G. Pescitelli, T. Bruhn; Good computational practice in the assignment of absolute configurations by TDDFT calculations of ECD spectra; *Chirality* **2016**, *28*, 466–474.
- [120] D. A. Lightner, J. E. Gurst, *Organic conformational analysis and stereochemistry from circular dichroism spectroscopy*, John Wiley & Sons Ltd, **2000**.
- [121] N. Berova, P. L. Polavarapu, K. Nakanishi, R. W. Woody, *Comprehensive Chiroptical Spectroscopy, Applications in Stereochemical Analysis of Synthetic Compounds, Natural Products, and Biomolecules*, John Wiley & Sons Ltd, **2012**.
- [122] G. Batta, K. Kövér, C. Szántay, *Methods for structure elucidation by high-resolution NMR: Applications to organic molecules of moderate molecular weight*, Elsevier Science, **1997**.
- [123] F. Rouessac, A. Rouessac, *Analyse chimique : méthodes et techniques instrumentales modernes : cours et exercices corrigés*, Masson, Paris, **2009**.

- [124] R. B. Teponno, S. Kusari, M. Spiteller; Recent advances in research on lignans and neolignans; *Nat. Prod. Rep.* **2016**, *33*, 1044–1092.
- [125] J. Y. Pan, S. L. Chen, M. H. Yang, J. Wu, J. Sinkkonen, K. Zou; An update on lignans: natural products and synthesis; *Nat. Prod. Rep.* **2009**, *26*, 1251–1292.
- [126] S. Apers, A. Vlietinck, L. Pieters; Lignans and neolignans as lead compounds; *Phytochem. Rev.* **2003**, *2*, 201–217.
- [127] M. Saleem, H. J. Kim, M. S. Ali, Y. S. Lee; An update on bioactive plant lignans; *Nat. Prod. Rep.* **2005**, *22*, 696–716.
- [128] K. Sawasdee, T. Chaowasku, V. Lipipun, T.-H. Dufat, S. Michel, K. Likhitwitayawuid; Neolignans from leaves of *Milium mollis*; *Fitoterapia* **2013**, *85*, 49–56.
- [129] L. H. Rakotondraibe, P. R. Graupner, Q. Xiong, M. Olson, J. D. Wiley, P. Krai, P. J. Brodie, M. W. Callmander, E. Rakotobe, F. Ratovoson, V. E. Rasamison, M. B. Cassera, D. R. Hahn, D. G. I. Kingston, S. Fotso; Neolignans and other metabolites from *Ocotea cymosa* from the Madagascar rain forest and their biological activities; *J. Nat. Prod.* **2015**, *78*, 431–440.
- [130] L. G. de Castro Oliveira, L. M. Brito, M. M. de Moraes Alves, L. V. Amorim, E. P. Sobrinho-Junior, C. E. de Carvalho, K. A. da Franca Rodrigues, D. D. Arcanjo, A. M. das Gracias Lopes Cito, F. A. de Amorim Carvalho; *In vitro* effects of the neolignan 2,3-dihydrobenzofuran against *Leishmania amazonensis*; *Basic Clin. Pharmacol. Toxicol.* **2017**, *120*, 52–58.
- [131] C. W. Song, S. M. Wang, L. L. Zhou, F. F. Hou, K. J. Wang, Q. B. Han, N. Li, Y. X. Cheng; Isolation and identification of compounds responsible for antioxidant capacity of *Euryale ferox* seeds; *J. Agric. Food Chem.* **2011**, *59*, 1199–1204.
- [132] R.-Q. Mei, Y.-H. Wang, G.-H. Du, G.-M. Liu, L. Zhang, Y.-X. Cheng; Antioxidant lignans from the fruits of *Broussonetia papyrifera*; *J. Nat. Prod.* **2009**, *72*, 621–625.
- [133] X.-X. Huang, C.-C. Zhou, L.-Z. Li, Y. Peng, L.-L. Lou, S. Liu, D.-M. Li, T. Ikejima, S.-J. Song; Cytotoxic and antioxidant dihydrobenzofuran neolignans from the seeds of *Crataegus pinnatifida*; *Fitoterapia* **2013**, *91*, 217–223.

- [134] S. Baek, X. Xia, B. S. Min, C. Park, S. H. Shim; Trogopterins A–C: three new neolignans from feces of *Trogopterus xanthipes*; *Beilstein J. Org. Chem.* **2014**, *10*, 2955–2962.
- [135] W. S. Suh, K. H. Kim, H. K. Kim, S. U. Choi, K. R. Lee; Three new lignan derivatives from *Lindera glauca* (Siebold et Zucc.) Blume; *Helv. Chim. Acta* **2015**, *98*, 1087–1094.
- [136] Y. Fukuyama, K. Mizuta, K. Nakagawa, Q. Wenjuan, W. Xiue; A new neo-lignan, a prostaglandin I<sub>2</sub> inducer from the leaves of *Zizyphus jujuba*; *Planta Med.* **1986**, 501–502.
- [137] J.-X. Zhuo, Y.-H. Wang, X.-L. Su, R.-Q. Mei, J. Yang, Y. Kong, C.-L. Long; Neolignans from *Selaginella moellendorffii*; *Nat. Prod. Bioprospect.* **2016**, *6*, 161–166.
- [138] G.-H. Tang, Z.-W. Chen, T.-T. Lin, M. Tan, X.-Y. Gao, J.-M. Bao, Z.-B. Cheng, Z.-H. Sun, G. Huang, S. Yin; Neolignans from *Aristolochia fordiana* prevent oxidative stress-induced neuronal death through maintaining the Nrf2/HO-1 pathway in HT22 cells; *J. Nat. Prod.* **2015**, *78*, 1894–1903.
- [139] Y.-P. Li, L.-B. Dong, D.-Z. Chen, H.-M. Li, J.-D. Zhong, F. Li, X. Liu, B. Wang, R.-T. Li; Two new dihydrobenzofuran-type neolignans from *Breynia fruticosa*; *Phytochem. Lett.* **2013**, *6*, 281–285.
- [140] Y. Natori, H. Tsutsui, N. Sato, S. Nakamura, H. Nambu, M. Shiro, S. Hashimoto; Asymmetric synthesis of neolignans (–)-*epi*-conocarpan and (+)-conocarpan via Rh(II)-catalyzed C–H insertion process and revision of the absolute configuration of (–)-*epi*-conocarpan; *J. Org. Chem.* **2009**, *74*, 4418–4421.
- [141] S. Antus, T. Kurtan, L. Juhasz, L. Kiss, M. Hollosi, Z. Majer; Chiroptical properties of 2,3-dihydrobenzo[b]furan and chromane chromophores in naturally occurring *O*-heterocycles; *Chirality* **2001**, *13*, 493–506.
- [142] L. Xiong, C. Zhu, Y. Li, Y. Tian, S. Lin, S. Yuan, J. Hu, Q. Hou, N. Chen, Y. Yang, J. Shi; Lignans and neolignans from *Sinocalamus affinis* and their absolute configurations; *J. Nat. Prod.* **2011**, *74*, 1188–1200.
- [143] M. S. M. Yuen, F. Xue, T. C. W. Mak, H. N. C. Wong; On the absolute structure of optically active neolignans containing a dihydrobenzo[b]furan skeleton; *Tetrahedron* **1998**, *54*, 12429–12444.

- [144] I. R. Nascimento, L. M. X. Lopes, L. B. Davin, N. G. Lewis; Stereoselective Synthesis of 8,9-licarinediols; *Tetrahedron* **2000**, *56*, 9181–9193.
- [145] Y.-S. Shi, Y.-B. Liu, S.-G. Ma, Y. Li, J. Qu, L. Li, S.-P. Yuan, Q. Hou, Y.-H. Li, J.-D. Jiang, S.-S. Yu; Bioactive sesquiterpenes and lignans from the fruits of *Xanthium sibiricum*; *J. Nat. Prod.* **2015**, *78*, 1526–1535.
- [146] Y.-H. Wang, Q.-Y. Sun, F.-M. Yang, C.-L. Long, F.-W. Zhao, G.-H. Tang, H.-M. Niu, H. Wang, Q.-Q. Huang, J.-J. Xu, L.-J. Ma; Neolignans and caffeoyl derivatives from *Selaginella moellendorffii*; *Helv. Chim. Acta* **2010**, *93*, 2467–2477.
- [147] A. C. Pereira, L. G. Magalhães, A. H. Januário, P. M. Pauletti, W. R. Cunha, J. K. Bastos, D. N. P. Nanayakkara, M. L. A. e Silva; Enantiomeric resolution of ( $\pm$ )-licarin A by high-performance liquid-chromatography using a chiral stationary phase; *J. Chromatogr. A* **2011**, *1218*, 7051–7054.
- [148] S. M. Colegate, R. J. Molyneux, *Bioactive Natural Products Detection, Isolation, and Structural Determination*, Taylor & Francis, **1993**.
- [149] 1D NOE Difference, in *Avance User's Manual, Updated for XWinNMR 3.0*, Bruker AG, Fällanden, Switzerland, **2000**, pp. 141–148.
- [150] W. Kurosawa, T. Kan, T. Fukuyama; An efficient synthesis of optically active trans-2-Aryl-2,3-dihydrobenzofuran-3-carboxylic acid esters via C-H insertion reaction; *Synlett* **2003**, 1028–1030.
- [151] Q.-B. Liu, X.-X. Huang, X.-J. Yan, M. Bai, L.-H. Yu, C. Hu, T. Zhu, L.-Z. Li, S.-J. Song; Neolignans from the seeds of *Prunus tomentosa* (Rosaceae) and their chemotaxonomic interest; *Biochem. Syst. Ecol.* **2014**, *55*, 236–240.
- [152] Z. Wu, Y. Lai, L. Zhou, Y. Wu, H. Zhu, Z. Hu, J. Yang, J. Zhang, J. Wang, Z. Luo, Y. Xue, Y. Zhang; Enantiomeric lignans and neolignans from *Phyllanthus glaucus*: enantioseparation and their absolute configurations; *Sci. Rep.* **2016**, *6*, 24809.
- [153] A. Wahl, F. Roblot, A. Cavé; Isolation and structure elucidation of xylobuxin, a new neolignan from *Xylopiya buxifolia*; *J. Nat. Prod.* **1995**, *58*, 786–789.
- [154] T. Kurtán, S. Antus, G. Pescitelli, in *Comprehensive Chiroptical Spectroscopy*, John Wiley & Sons Ltd, **2012**, pp. 73–114.

- [155] G. Snatzke, P. C. Ho; Circular dichroism—XLVI: rules for benzene Cotton-effects; *Tetrahedron* **1971**, 27, 3645–3653.
- [156] S. Antus, G. Snatzke, I. Steinke; Circular dichroismus, LXXXI. Synthese und circular dichroismus von steroiden mit isochromanon-chromophor; *Liebigs Ann. Chem.* **1983**, 1983, 2247–2261.
- [157] S. Antus, E. Baitz-Gács, G. Snatzke, T. S. Tóth; Synthesis and circular dichroism of steroids with a 1,4-benzodioxane chromophore: on the absolute configuration of (–)-silandrin; *Liebigs Ann. Chem.* **1991**, 1991, 633–641.
- [158] D. T. Tshitenge, Authentication and quality control approach of two phytopharmaceuticals from DR Congo, Master thesis (written in French), University of Kinshasa (DR Congo), **2013**.
- [159] H. J. Von Maydell, *Trees and Shrubs of the Sahel: Their Characteristics and Uses*, Verlag Josef Margraf, Scientific Books, **1990**.
- [160] H. M. Farah, T. H. E. Amin, H. S. Khalid, S. M. Hassan, A. R. M. E. Hussein; *In vitro* activity of the aqueous extract of *Gardenia ternifolia* fruits against *Theileria lestoquardi*; *J. Med. Plants Res.* **2012**, 6, 5447–5451.
- [161] A. Asase, A. A. Oteng-Yeboah, G. T. Odamtten, M. S. Simmonds; Ethnobotanical study of some Ghanaian anti-malarial plants; *J. Ethnopharmacol.* **2005**, 99, 273–279.
- [162] I. Orhan, B. Sener, M. Kaiser, R. Brun, D. Tasdemir; Inhibitory activity of marine sponge-derived natural products against parasitic protozoa; *Marine drugs* **2010**, 8, 47–58.
- [163] D. T. Tshitenge, D. Feineis, V. Mudogo, M. Kaiser, R. Brun, G. Bringmann; Antiplasmodial ealapasamines A-C, 'mixed' naphthylisoquinoline dimers from the Central African liana *Ancistrocladus ealaensis*; *Sci. Rep.* **2017**. (in press by the submission of this thesis)
- [164] G. Bringmann, M. Wohlfarth, H. Rischer, M. Heubes, W. Saeb, S. Diem, M. Herderich, J. Schlauer; A photometric screening method for dimeric naphthylisoquinoline alkaloids and complete on-line structural elucidation of a dimer in crude plant extracts, by the LC-MS/LC-NMR/LC-CD triad; *Anal. Chem.* **2001**, 73, 2571–2577.

- [165] G. Bringmann, R. Weirich, H. Reuscher, J. R. Jansen, L. Kinzinger, T. Ortmann; The synthesis of all possible isomeric 6,8-dioxygenated 1,3-dimethyl-1,2,3,4-tetrahydroisoquinoline methyl ethers - useful chiral building blocks for naphthylisoquinoline alkaloids; *Liebigs Ann. Chem.* **1993**, 877–888.
- [166] G. Bringmann, K.-P. Gulden, Y. F. Hallock, K. P. Manfredi, J. H. Cardellina II, M. R. Boyd, B. Kramer, J. Fleischhauer; Acetogenic isoquinoline alkaloids. 63. Circular dichroism of michellamines: independent assignment of axial chirality by calculated and experimental CD spectra; *Tetrahedron* **1994**, *50*, 7807–7814.
- [167] Y. F. Hallock, K. P. Manfredi, J. W. Blunt, J. H. Cardellina II, M. Schaeffer, K.-P. Gulden, G. Bringmann, A. Y. Lee, J. Clardy, et al.; Korupensamines A-D, novel antimalarial alkaloids from *Ancistrocladus korupensis*; *J. Org. Chem.* **1994**, *59*, 6349–6355.
- [168] J. Muehlbacher, Molecular modeling and chirality: elucidation of the absolute configuration of natural and active substances with unusual circular dichroism; PhD thesis, University of Wuerzburg (Wuerzburg), **2003**.
- [169] X.-C. Li, D. Ferreira, Y. Ding; Determination of absolute configuration of natural products: theoretical calculation of electronic circular dichroism as a tool; *Curr. Org. Chem.* **2010**, *14*, 1678–1697.
- [170] C. L. Covington, V. P. Nicu, P. L. Polavarapu; Determination of the absolute configurations using exciton chirality method for vibrational circular dichroism: right answers for the wrong reasons?; *J. Phys. Chem. A* **2015**, *119*, 10589–10601.
- [171] F. Neese; The ORCA program system; *Wiley Interdiscip. Rev. Comput. Mol. Sci.* **2012**, *2*, 73–78.
- [172] V. Kuete, L. P. Sandjo, A. T. Mbaveng, J. A. Seukep, B. T. Ngadjui, T. Efferth; Cytotoxicity of selected Cameroonian medicinal plants and *Nauclea pobeguinii* towards multi-factorial drug-resistant cancer cells; *BMC Complement Altern. Med.* **2015**, *15*, 309.
- [173] V. Kuete, T. Efferth; African flora has the potential to fight multidrug resistance of cancer; *Biomed. Res. Int.* **2015**, *2015*, 914813.
- [174] D. A. Baker; Malaria gametocytogenesis; *Mol. Biochem. Parasitol.* **2010**, *172*, 57–65.

- [175] C. L. Peatey, T. P. Spicer, P. S. Hodder, K. R. Trenholme, D. L. Gardiner; A high-throughput assay for the identification of drugs against late-stage *Plasmodium falciparum* gametocytes; *Mol. Biochem. Parasitol.* **2011**, *180*, 127–131.
- [176] S. Duffy, S. Loganathan, J. P. Holleran, V. M. Avery; Large-scale production of *Plasmodium falciparum* gametocytes for malaria drug discovery; *Nat. Protocols* **2016**, *11*, 976–992.
- [177] J. Reader, M. Botha, A. Theron, S. B. Lauterbach, C. Rossouw, D. Engelbrecht, M. Wepener, A. Smit, D. Leroy, D. Mancama, T. L. Coetzer, L. M. Birkholtz; Nowhere to hide: interrogating different metabolic parameters of *Plasmodium falciparum* gametocytes in a transmission blocking drug discovery pipeline towards malaria elimination; *Malar. J.* **2015**, *14*, 213.
- [178] B. K. Lombe, T. Bruhn, D. Feineis, V. Mudogo, R. Brun, G. Bringmann; Cyclombandakamines A<sub>1</sub> and A<sub>2</sub>, oxygen-bridged naphthylisoquinoline dimers from a Congolese *Ancistrocladus liana*; *Org. Lett.* **2017**, *19*, 1342–1345.
- [179] D. T. Tshitenge, D. Feineis, B. K. Lombe, G. Bringmann, *Korundamines and mbandakamines, unsymmetric naphthylisoquinoline dimers from the congolese liana Ancistrocladus ealaensis*, Poster at the *Journées de Chimie Organique 2016*, Palaiseau-France, **2016**.
- [180] Sigma-Aldrich.com/Supelco, *Utility of pentafluorophenylpropyl stationary phases for RP-HPLC analyses: Biogenic amines on Discovery HS F5*, The Sigma-Aldrich Family, Pennsylvania, USA **2003**.
- [181] G. Bringmann, W. Saeb, M. Ruckert, J. Mies, M. Michel, V. Mudogo, R. Brun; Ancistrolilikokine D, a 5,8'-coupled naphthylisoquinoline alkaloid, and related natural products from *Ancistrocladus likoko*; *Phytochemistry* **2003**, *62*, 631–636.
- [182] M. Unger, M. Dreyer, S. Specker, S. Laug, M. Pelzing, C. Neusuess, U. Holzgrabe, G. Bringmann; Analytical characterisation of crude extracts from an African *Ancistrocladus* species using high-performance liquid chromatography and capillary electrophoresis coupled to ion trap mass spectrometry; *Phytochem. Anal.* **2004**, *15*, 21–26.

- [183] G. Heubl, F. Turini, V. Mudogo, I. Kajahn, G. Bringmann; *Ancistrocladus ileboensis* (D.R. Congo), a new liana with unique alkaloids; *Plant Ecol. Evol.* **2010**, *143*, 63–69.
- [184] G. Bringmann, A. Irmer, D. Feineis, T. A. Gulder, H. P. Fiedler; Convergence in the biosynthesis of acetogenic natural products from plants, fungi, and bacteria; *Phytochemistry* **2009**, *70*, 1776–1786.
- [185] Y. Hongo, T. Nakamura, S. Takahashi, T. Motoyama, T. Hayashi, H. Hirota, H. Osada, H. Koshino; Detection of oxygen addition peaks for terpendole E and related indole-diterpene alkaloids in a positive-mode ESI-MS; *J. Mass Spectrom.* **2014**, *49*, 537–542.
- [186] G. Bringmann, M. Münchbach, K. Messer, D. Koppler, M. Michel, O. Schupp, M. Wenzel, A. M. Louis; *cis*- and *trans*-Isoshinanolone from *Dioncophyllum thollonii*: absolute configuration of two 'known', wide-spread natural products; *Phytochemistry* **1999**, *51*, 693–699.
- [187] Y. Hemberger, G. Zhang, R. Brun, M. Kaiser, G. Bringmann; Highly antiplasmodial non-natural oxidative products of dioncophylline A: synthesis, absolute configuration, and conformational stability; *Chem. Eur. J.* **2015**, *21*, 14507–14518.
- [188] G. Bringmann, S. Tasler; Oxidative aryl coupling reactions: a biomimetic approach to configurationally unstable or axially chiral biaryl natural products and related bioactive compounds; *Tetrahedron* **2001**, *57*, 331–343.
- [189] G. Bringmann, W. Saeb, J. Mies, K. Messer, M. Wohlfarth, R. Brun; One-step oxidative dimerization of genuine, unprotected naphthylisoquinolines alkaloids to give michellamines and other bioactive quateraryls; *Synthesis* **2000**, *2000*, 1843–1847.
- [190] G. Bringmann, C. Günther, M. Ochse, O. Schupp, S. Tasler, in *Progress in the Chemistry of Organic Natural Products, Vol. 82* (Eds.: W. Herz, H. Falk, G. W. Kirby, R. E. Moore, C. Tamm), Wien, **2001**, pp. 1–293.
- [191] G. Bringmann, D. Koppler, B. Wiesen, G. François, A. S. S. Narayanan, M. R. Almeida, H. Schneider, U. Zimmermann; Ancistroheynine A, the first 7,8'-coupled naphthylisoquinoline alkaloid from *Ancistrocladus heyneanus*; *Phytochemistry* **1996**, *43*, 1405–1410.



- [192] Y. F. Hallock, J. H. Cardellina II, M. Schaeffer, M. Stahl, G. Bringmann, G. François; Yaoundamines A and B, new antimalarial naphthylisoquinoline alkaloids from *Ancistrocladus korupensis*; *Tetrahedron* **1997**, *53*, 8121–8128.
- [193] G. Bringmann, T. A. M. Gulder, M. Reichert, T. Gulder; The online assignment of the absolute configuration of natural products: HPLC-CD in combination with quantum chemical CD calculations; *Chirality* **2008**, *20*, 628–642.
- [194] G. Bringmann, G. Zhang, T. Büttner, G. Bauckmann, T. Kupfer, H. Braunschweig, R. Brun, V. Mudogo; Jozimine A<sub>2</sub>: the first dimeric Dioncophyllaceae-type naphthylisoquinoline alkaloid, with three chiral axes and high antiplasmodial activity; *Chem. Eur. J.* **2013**, *19*, 916–923.
- [195] G. Bringmann, M. Rübenacker, P. Vogt, H. Busse, L. A. Assi, K. Peters, H. G. von Schnering; Dioncopeltine A and dioncolactone A: alkaloids from *Triphyophyllum peltatum*; *Phytochemistry* **1991**, *30*, 1691–1696.
- [196] G. Bringmann, T. Ortmann, R. Zagst, B. Schöner, L. A. Assi, C. Burschka; (±)-dioncophyllacine A, A naphthylisoquinoline alkaloid with A 4-methoxy substituent from the leaves of *Triphyophyllum peltatum*; *Phytochemistry* **1992**, *31*, 4015–4018.
- [197] T. R. Govindachari, K. Nagarajan, P. C. Parthasarathy, T. G. Rajagopalan, H. K. Desai, G. Kartha, S.-m. L. Chen, K. Nakanishi; Absolute stereochemistry of ancistrocladine and ancistrocladinine; *J. Chem. Soc., Perkin Trans. 1* **1974**, 1413–1417.
- [198] G. Bringmann, W. Saeb, J. Kraus, R. Brun, G. François; Jozimine B, a constitutionally unsymmetric, antiplasmodial 'dimer' of the naphthylisoquinoline alkaloid ancistrocladine; *Tetrahedron* **2000**, *56*, 3523–3531.
- [199] G. Bringmann, R. Götz, G. François; Synthesis of pindikamine A, a michellamine-related dimer of a non-natural, 'skew' naphthylisoquinoline; *Tetrahedron* **1996**, *52*, 13419–13426.
- [200] G. Bringmann, S. Tasler; Oxidative aryl coupling reactions: a biomimetic approach to configurationally unstable or axially chiral biaryl natural products and related bioactive compounds; *Tetrahedron* **2001**, *57*, 331–343.
- [201] G. Bringmann, J. Holenz, R. Weirich, M. Rübenacker, C. Funke, M. R. Boyd, R. J. Gulakowski, G. François; First synthesis of the antimalarial naphthylisoquinoline

- alkaloid dioncophylline C, and its unnatural anti-HIV dimer, jozimine C; *Tetrahedron* **1998**, *54*, 497–512.
- [202] G. Bringmann, K. Messer, M. Wohlfarth, J. Kraus, K. Dumbuya, M. Rueckert; HPLC-CD on-line coupling in combination with HPLC-NMR and HPLC-MS/MS for the determination of the full absolute stereostructure of new metabolites in plant extracts; *Anal. Chem.* **1999**, *71*, 2678–2686.
- [203] G. Bringmann, C. Schneider, U. Moehler, R.-M. Pfeifer, R. Goetz, L. Ake Assi, E.-M. Peters, K. Peters; Two atropisomeric *N*-methyldioncophyllines A and *N*-methylphylline, their naphthalene-free heterocyclic moiety, from *Ancistrocladus barteri*; *Z. Naturforsch. B* **2003**, *58*, 577–584.
- [204] Y. F. Hallock, J. H. Cardellina II, T. Kornek, K.-P. Gulden, G. Bringmann, M. R. Boyd; Gentrymine B, the first quaternary isoquinoline alkaloid from *Ancistrocladus korupensis*; *Tetrahedron Lett.* **1995**, *36*, 4753–4756.
- [205] A. Montagnac, A. H. A. Hadi, F. Remy, M. Païs; Isoquinoline alkaloids from *Ancistrocladus tectorius*; *Phytochemistry* **1995**, *39*, 701–704.
- [206] G. Bringmann, R. Zagst, H. Reuscher, L. A. Assi; Ancistrobrevine B, the first naphthylisoquinoline alkaloid with a 5,8'-coupling site, and related compounds from *Ancistrocladus abbreviatus*; *Phytochemistry* **1992**, *31*, 4011–4014.
- [207] G. Bringmann, K. Messer, R. Brun, V. Mudogo; Ancistrocongolines A-D, new naphthylisoquinoline alkaloids from *Ancistrocladus congolensis*; *J. Nat. Prod.* **2002**, *65*, 1096–1101.
- [208] G. Bringmann, C. Gunther, W. Saeb, J. Mies, A. Wickramasinghe, V. Mudogo, R. Brun; Ancistrolkokines A-C: new 5,8'-coupled naphthylisoquinoline alkaloids from *Ancistrocladus likoko*; *J. Nat. Prod.* **2000**, *63*, 1333–1337.
- [209] C. P. Tang, Y. P. Yang, Y. Zhong, Q. X. Zhong, H. M. Wu, Y. Ye; Four new naphthylisoquinoline alkaloids from *Ancistrocladus tectorius*; *J. Nat. Prod.* **2000**, *63*, 1384–1387.
- [210] G. Bringmann, M. Dreyer, J. H. Faber, P. W. Dalsgaard, D. Strk, J. W. Jaroszewski, H. Ndangalasi, F. Mbago, R. Brun, M. Reichert, K. Maksimenka, S. B. Christensen; Ancistrotanzanine A, the first 5,3'-coupled naphthylisoquinoline alkaloid, and two

- further, 5,8'-linked related compounds from the newly described species *Ancistrocladus tanzaniensis*; *J. Nat. Prod.* **2003**, *66*, 1159–1165.
- [211] G. Bringmann, B. Hertlein-Amslinger, I. Kajahn, M. Dreyer, R. Brun, H. Moll, A. Stich, K. N. Ioset, W. Schmitz, L. H. Ngoc; Phenolic analogs of the *N,C*-coupled naphthylisoquinoline alkaloid ancistrocladinium A, from *Ancistrocladus cochinchinensis* (Ancistrocladaceae), with improved antiprotozoal activities; *Phytochemistry* **2011**, *72*, 89–93.
- [212] Y. F. Hallock, C. B. Hughes, J. H. Cardellina II, M. Schaffer, K.-P. Gulden, G. Bringmann, M. R. Boyd; Dioncophylline A, the principal cytotoxin from *Ancistrocladus letestui*; *Nat. Prod. Lett.* **1995**, *6*, 315–320.
- [213] G. Bringmann, C. Gunther, S. Busemann, M. Schaffer, J. D. Olowokudejo, B. I. Alo; Ancistroguineines A and B as well as ancistrosectorine-naphthylisoquinoline alkaloids from *Ancistrocladus guineensis*; *Phytochemistry* **1998**, *47*, 37–43.
- [214] D. T. Tshitenge, D. Feineis, S. Awale, G. Bringmann; Gardenifolins A–H, scalemic neolignans from *Gardenia ternifolia*: chiral resolution, configurational assignment, and cytotoxic activities against the HeLa cancer cell line; *J. Nat. Prod.* **2017**, *80*, 1604–1614.
- [215] S. Suzuki, T. Umezawa; Biosynthesis of lignans and norlignans; *J. Wood Sci.* **2007**, *53*, 273.
- [216] H. Li, S.-Y. Peng, D.-P. Yang, B. Bai, L.-P. Zhu, C.-Y. Mu, Y.-J. Tian, D.-M. Wang, Z.-M. Zhao; Enantiomeric neolignans and a sesquiterpene from *Solanum erianthum* and their absolute configuration assignment; *Chirality* **2016**, *28*, 259–263.
- [217] Y. Shi, Y. Liu, Y. Li, L. Li, J. Qu, S. Ma, S. Yu; Chiral resolution and absolute configuration of a pair of rare racemic spirodienone sesqueneolignans from *Xanthium sibiricum*; *Org. Lett.* **2014**, *16*, 5406–5409.
- [218] Z.-B. Cheng, X. Lu, J.-M. Bao, Q.-H. Han, Z. Dong, G.-H. Tang, L.-S. Gan, H.-B. Luo, S. Yin; (±)-Torreyunlignans A–D, rare 8–9' linked neolignan enantiomers as phosphodiesterase-9A inhibitors from *Torreya yunnanensis*; *J. Nat. Prod.* **2014**, *77*, 2651–2657.
- [219] D. F. Swinehart; The Beer-Lambert law; *J. Chem. Educ.* **1962**, *39*, 333.

- [220] I. Agranat, H. Caner, J. Caldwell; Putting chirality to work: the strategy of chiral switches; *Nat. Rev. Drug. Discov.* **2002**, *1*, 753–768.
- [221] W. Song, M. Staudt, I. Bourgeois, J. Williams; Laboratory and field measurements of enantiomeric monoterpene emissions as a function of chemotype, light and temperature; *Biogeosciences* **2014**, *11*, 1435–1447.
- [222] T. H. Kim, H. Ito, K. Hayashi, T. Hasegawa, T. Machiguchi, T. Yoshida; Aromatic constituents from the heartwood of *Santalum album* L.; *Chem. Pharm. Bull. (Tokyo)* **2005**, *53*, 641–644.
- [223] L. B. Davin, N. G. Lewis; Dirigent phenoxy radical coupling: advances and challenges; *Curr. Opin. Biotechnol.* **2005**, *16*, 398–406.
- [224] D. Fournand, B. Cathala, C. Lapiere; Initial steps of the peroxidase-catalyzed polymerization of coniferyl alcohol and/or sinapyl aldehyde: capillary zone electrophoresis study of pH effect; *Phytochemistry* **2003**, *62*, 139–146.
- [225] Y. Lu, Y. Xue, J. Liu, G. Yao, D. Li, B. Sun, J. Zhang, Y. Liu, C. Qi, M. Xiang, Z. Luo, G. Du, Y. Zhang; ( $\pm$ )-Acortatarinowins A–F, norlignan, neolignan, and lignan enantiomers from *Acorus tatarinowii*; *J. Nat. Prod.* **2015**, *78*, 2205–2214.
- [226] Y. Lu, Y. Xue, S. Chen, H. Zhu, J. Zhang, X.-N. Li, J. Wang, J. Liu, C. Qi, G. Du, Y. Zhang; Antioxidant lignans and neolignans from *Acorus tatarinowii*; *Sci. Rep.* **2016**, *6*, 22909.
- [227] Y. Lai, T. Liu, R. Sa, X. Wei, Y. Xue, Z. Wu, Z. Luo, M. Xiang, Y. Zhang, G. Yao; Neolignans with a rare 2-oxaspiro[4.5]deca-6,9-dien-8-one motif from the stem bark of *Cinnamomum subavenium*; *J. Nat. Prod.* **2015**, *78*, 1740–1744.
- [228] S. García-Muñoz, M. Álvarez-Corral, L. Jiménez-González, C. López-Sánchez, A. Rosales, M. Muñoz-Dorado, I. Rodríguez-García; Synthesis of dihydrodehydrodiconiferyl alcohol and derivatives through intramolecular C–H insertion; *Tetrahedron* **2006**, *62*, 12182–12190.
- [229] N. C. Veitch, R. J. Grayer; Flavonoids and their glycosides, including anthocyanins; *Nat. Prod. Rep.* **2011**, *28*, 1626–1695.
- [230] S. Bienz, P. Bisegger, A. Guggisberg, M. Hesse; Polyamine alkaloids; *Nat. Prod. Rep.* **2005**, *22*, 647–658.

- [231] B. F. Tawil, A. Guggisberg, M. Hesse; Preparation of two novel spermine alkaloids by *E/Z* isomerisation of the cinnamoyl chromophore; *J. Photochem. Photobiol. A Chem.* **1990**, *54*, 105–111.
- [232] K. Yoshida, R. Okuno, K. Kameda, M. Mori, T. Kondo; Influence of *E,Z*-isomerization and stability of acylated anthocyanins under the UV irradiation; *Biochem. Eng. J.* **2003**, *14*, 163–169.
- [233] K. Yoshida, R. Okuno, K. Kameda, T. Kondo; Prevention of UV-light induced *E,Z*-isomerization of caffeoyl residues in the diacylated anthocyanin, gentiodelphin, by intramolecular stacking; *Tetrahedron Lett.* **2002**, *43*, 6181–6184.
- [234] V. O. Silva, A. A. Freitas, A. L. Maçanita, F. H. Quina; Chemistry and photochemistry of natural plant pigments: the anthocyanins; *J. Phys. Org. Chem.* **2016**, *29*, 594–599.
- [235] O. Talhi, G. R. Lopes, S. M. Santos, D. C. G. A. Pinto, A. M. S. Silva; Visible light-induced diastereoselective *E/Z*-photoisomerization equilibrium of the C=C benzofuran-3-one-hydantoin dyad; *J. Phys. Org. Chem.* **2014**, *27*, 756–763.
- [236] H. Wada, T. Kido, N. Tanaka, T. Murakami, Y. Saiki, C.-M. Chen; Chemical and chemotaxonomical studies of ferns. LXXXI. Characteristic lignans of Blechnaceous ferns; *Chem. Pharm. Bull.* **1992**, *40*, 2099–2101.
- [237] C. López-Sánchez, M. Álvarez-Corral, L. Jiménez-González, M. Muñoz-Dorado, I. Rodríguez-García; Rh(II)-catalyzed enantioselective synthesis of acuminatin through a C–H insertion reaction of a non-stabilized carbenoid; *Tetrahedron* **2013**, *69*, 5511–5516.
- [238] Y. Matsuo, Y. Mimaki; Lignans from *Santalum album* and their cytotoxic activities; *Chem. Pharm. Bull.* **2010**, *58*, 587–590.
- [239] K. J. Chavez, X. Feng, J. A. Flanders, E. Rodriguez, F. C. Schroeder; Spirocyclic lignans from *Guaiacum* (Zygophyllaceae) induce apoptosis in human breast cancer cell lines; *J. Nat. Prod.* **2011**, *74*, 1293–1297.
- [240] X.-X. Huang, C.-C. Zhou, L.-Z. Li, F.-F. Li, L.-L. Lou, D.-M. Li, T. Ikejima, Y. Peng, S.-J. Song; The cytotoxicity of 8-*O*-4' neolignans from the seeds of *Crataegus pinnatifida*; *Bioorg. Med. Chem. Lett.* **2013**, *23*, 5599–5604.

- [241] X.-M. Gao, R.-R. Wang, D.-Y. Niu, C.-Y. Meng, L.-M. Yang, Y.-T. Zheng, G.-Y. Yang, Q.-F. Hu, H.-D. Sun, W.-L. Xiao; Bioactive dibenzocyclooctadiene lignans from the stems of *Schisandra neglecta*; *J. Nat. Prod.* **2013**, *76*, 1052–1057.
- [242] D.-T. Yang, S.-S. Lin, J.-H. Chen, S.-T. Yuan, J.-S. Shi, J.-S. Wang, A.-Q. Jia; (+)- and (–)-Liriodenol, a pair of novel enantiomeric lignans from *Liriodendron hybrid*; *Bioorg. Med. Chem. Lett.* **2015**, *25*, 1976–1978.
- [243] H.-G. Jin, A. R. Kim, H. J. Ko, S. K. Lee, E.-R. Woo; Three new lignan glycosides with IL-6 inhibitory activity from *Akebia quinata*; *Chem. Pharm. Bull.* **2014**, *62*, 288–293.
- [244] A. Setiawati; Celecoxib, a COX-2 selective inhibitor, induces cell cycle arrest at the G2/M phase in HeLa cervical cancer cells; *Asian Pac. J. Cancer Prev.* **2016**, *17*, 1655–1659.
- [245] P. L. Wu, T. S. Wu, C. X. He, C. H. Su, K. H. Lee; Constituents from the stems of *Hibiscus taiwanensis*; *Chem. Pharm. Bull. (Tokyo)* **2005**, *53*, 56–59.
- [246] T. Aoki, K. Takagi, T. Hirata, T. Suga; Two naturally occurring acyclic diterpene and norditerpene aldehydes from *Tetragonia tetragonoides*; *Phytochemistry* **1982**, *21*, 1361–1363.
- [247] Y.-L. Leu, Y.-Y. Chan, M.-Y. Hsu, I.-S. Chen, T.-S. Wu; The constituents of the stem and roots of *Aristolochia foveolata*; *J. Chin. Chem. Soc.* **1998**, *45*, 539–541.
- [248] W. H. Organization, *WHO Global Atlas of Traditional, Complementary and Alternative Medicine*, WHO Centre for Health Development, **2005**.
- [249] A. Singh, *Herbal Drugs as Therapeutic Agents*, CRC Press, **2014**.
- [250] A. Viljoen; Transforming ancient knowledge into phytomedicines – a South African perspective; *Planta Med.* **2013**, *79*, IL24.
- [251] Liste nationale des médicaments essentiels, Public Health Ministry of the DR Congo, Kinshasa, **2007**. <<http://apps.who.int/medicinedocs/documents/s18818fr/s18818fr.pdf>> Web. 3 Jul. 2017.
- [252] C. D. Kabala, V. N. Nzingula, N. Maluantesa, N. Basilua, A. P. Mbenza, J. N. Lami, U. Mbangu, R. B. Suami, P. N. Mambanzulua; Evaluation de l'activité antipaludique

- du SIROP KILMA®; *Annales de Pharmacie* **2005**, *3*, 103–106. (available also upon request per email)
- [253] C. Andary, R. Wylde, C. Laffite, G. Privat, F. Winternitz; Structures of verbascoside and orobanchoside, caffeic acid sugar esters from *Orobanche rapum-genistae*; *Phytochemistry* **1982**, *21*, 1123–1127.
- [254] Q. Xiong, S. Kadota, T. Tani, T. Namba; Antioxidative effects of phenylethanoids from *Cistanche deserticola*; *Biol. Pharm. Bull.* **1996**, *19*, 1580–1585.
- [255] I. P. Sheremet, N. F. Komissarenko; Flavonoid glycosides of *Stachys annuae*; *Chem. Pap. - Chem. Zvesti* **1971**, *7*, 563–566.
- [256] D. C. Albach, C. Held Gotfredsen, S. R. Jensen; Iridoid glucosides of *Paederota lutea* and the relationships between *Paederota* and *Veronica*; *Phytochemistry* **2004**, *65*, 2129–2134.
- [257] L. A. Refahy; Chemical investigation on constituents of *Lantana camara* plant; *Egypt. J. Chem.* **2003**, *46*, 537–543.
- [258] E. A. Aboutabl, F. A. Hashem, A. A. Sleem, A. A. Maamoon; Flavonoids, anti-inflammatory activity and cytotoxicity of *Macfadyena unguis-cati* L.; *Afr. J. Tradit. Complement. Altern. Med.* **2007**, *5*, 18–26.
- [259] D. T. Tshitenge, K. N. Ioset, J. N. Lami, J. Ndelo-di-Phanzu, J. P. Mufusama, G. Bringmann; Rational quality assessment procedure for less-investigated herbal medicines: case of a Congolese antimalarial drug with an analytical report; *Fitoterapia* **2016**, *110*, 189–195.
- [260] M. Birringer, D. Lington, S. Vertuani, S. Manfredini, D. Scharlau, M. Gleis, M. Ristow; Proapoptotic effects of long-chain vitamin E metabolites in HepG2 cells are mediated by oxidative stress; *Free Radic. Biol. Med.* **2010**, *49*, 1315–1322.
- [261] F. D. Monache, M. Marta, M. Mac-Quhae, M. Nicoletti; Two new tocotrienoloic acids from the fruits of *Clusia grandiflora* Splith; *Gazz. Chim. Ital.* **1984**, *114*, 135–137.
- [262] L. Jian, A. L. W. Po; Ciliotoxicity of methyl- and propyl-*p*-hydroxybenzoates: a dose-response and surface-response study; *J. Pharm. Pharmacol.* **1993**, *45*, 925–927.

- [263] J. Boberg, C. Taxvig, S. Christiansen, U. Hass; Possible endocrine disrupting effects of parabens and their metabolites; *Reprod. Toxicol.* **2010**, *30*, 301–312.
- [264] N. Aubert, T. Ameller, J.-J. Legrand; Systemic exposure to parabens: pharmacokinetics, tissue distribution, excretion balance and plasma metabolites of [<sup>14</sup>C]-methyl-, propyl- and butylparaben in rats after oral, topical or subcutaneous administration; *Food Chem. Toxicol.* **2012**, *50*, 445–454.
- [265] M. M. Iwu, O. A. Igboko, U. A. Onwuchekwa, C. O. Okunji; Evaluation of the antihepatotoxic activity of the biflavonoids of *Garcinia kola* seed; *J. Ethnopharmacol.* **1987**, *21*, 127–138.
- [266] Q.-B. Han, S.-F. Lee, C.-F. Qiao, Z.-D. He, J.-Z. Song, H.-D. Sun, H.-X. Xu; Complete NMR assignments of the antibacterial biflavonoid GB1 from *Garcinia kola*; *Chem. Pharm. Bull.* **2005**, *53*, 1034–1036.
- [267] C. Okunji, S. Komarnytsky, G. Fear, A. Poulev, D. M. Ribnicky, P. I. Awachie, Y. Ito, I. Raskin; Preparative isolation and identification of tyrosinase inhibitors from the seeds of *Garcinia kola* by high-speed counter-current chromatography; *J. Chromatogr. A* **2007**, *1151*, 45–50.
- [268] A. Oluwatosin, A. Tolulope, K. Ayokulehin, O. Patricia, K. Aderemi, F. Catherine, A. Olusegun; Antimalarial potential of kolaviron, a biflavonoid from *Garcinia kola* seeds, against *Plasmodium berghei* infection in Swiss albino mice; *Asian Pac. J. Trop. Med.* **2014**, *7*, 97–104.
- [269] T. Bruhn, A. Schaumlöffel, Y. Hemberger, G. Bringmann; SpecDis: quantifying the comparison of calculated and experimental electronic circular dichroism Spectra; *Chirality* **2013**, *25*, 243–249.
- [270] T. Efferth, M. Davey, A. Olbrich, G. Rucker, E. Gebhart, R. Davey; Activity of drugs from traditional Chinese medicine toward sensitive and MDR1- or MRP1-overexpressing multidrug-resistant human CCRF-CEM leukemia cells; *Blood Cells Mol. Dis.* **2002**, *28*, 160–168.
- [271] F. Li, S. Awale, Y. Tezuka, S. Kadota; Cytotoxic constituents of propolis from Myanmar and their structure-activity relationship; *Biol. Pharm. Bull.* **2009**, *32*, 2075–2078.



[272] G. M. Sheldrick; A short history of SHELX; *Acta Cryst. A* **2008**, *64*, 112–122.

[273] <http://www.goodreads.com/quotes/32930-look-deep-into-nature-and-then-you-will-understand-everything>. (The primary source was not found) Web. 5 Jul. 2017.

## VI. Acknowledgements

I want to use this unique chance to give credit to all the people who contributed and supported me for the successful completion of my Ph.D. thesis here in Würzburg.

“*À tout Seigneur, tout honneur*”, my deepest and sincere expression of gratitude goes first to my supervisor, Prof. Dr. Dr. h.c. mult. Gerhard Bringmann. He guided and mentored me with high competence, excellence, and patience. His trust and support to me deserve all superlatives. I owe him so much in the development and the success made within this wonderful years. For the rest of my life, nothing will ever change my endless gratitude and admiration towards him. I will never enough say thank you for everything you did to me and for me.

I am extremely grateful to Prof. Ulrike Holzgrabe, P.D. Heike Bruhn, and Prof. Dr. Karine Ndjoko-Ioset, honorable members of my Thesis Committee, who supported and accompanied me through this nice achievement. From our meetings, your brilliant ideas and advices had enabled me to step over my problems, I felt so lucky to have you.

The deepest expression of my gratitude is also devoted to Dr. Doris Feineis, for the wonderful time, extensive brainstorming, support and collaboration. My memory will never forget your high competence, creativity and your good heart. *Liebe Doris, danke so sehr!*

How to miss this opportunity to thank the Excellence Initiative at the Graduate School of Life Sciences at the University of Würzburg, from which I got my Ph.D. Fellowship. My special thanks are addressed to Dr. Gabrielle Blum-Oehler and Ms. Jennifer Heilig for the support and professionalism.

This work was supported by the Deutsche Forschungsgemeinschaft (SFB 630 "Recognition, Preparation, and Functional Analysis of Agents against Infectious Diseases"), from which funds were provided for the lab work.

My Gratitude is also devoted to the Excellence Scholarship Program BEBUC and the *Else-Kröner-Fresenius* Foundation, from which I have been supported since 2008 and got book money during my Ph.D. time.

I am very grateful to our partners who performed the biological evaluations with reliability:

- Prof. Dr. Reto Brun and Prof. Dr. Marcel Kaiser of the Swiss Tropical and Public Health Institute in Basel (Switzerland), for the antiprotozoal biotests;
- Prof. Dr. Suresh Awale of the Division of Natural Drug Discovery, Institute of Natural Medicine, University of Toyama (Japan), for the antiproliferative tests on HeLa and pancreatic cells lines;
- Prof. Dr. Thomas Efferth from the Institute of Pharmacy and Biochemistry, University of Mainz (Germany), for the anticancer tests on the T-lymphoblastic leukemia cells.

My gratitude to Prof. Dr. J. Ndelo-di-Phanzu, Prof. J. Lami Nzunzu, Prof. Dr. N. Ngombe Kabamba, and Prof. Dr. Kabala Dihuidi from the *Faculté des Sciences Pharmaceutiques* (University of Kinshasa, DR Congo) for their permanent support through this pathway.

All the TDDFT quantum-chemical calculations and most conformational analyses were performed by Dr. Torsten Bruhn. From him, I got a lot of advices and support professionally and personally. *Lieber Torsten, Vielen Dank!*

My bottomless gratitude to Ms. Manuela Michel, who performed the oxidative degradation experiments of all the isolated alkaloids reported in this thesis.

I would also like to thank warmly Dr. David Schmidt for the X-ray crystallography of ealamine A (**P-62**), William Shamburger for the cooperation in the join-biomimetic synthesis of cyclombandakamine A (**51**), Dr. Mathias Grüne for the setup of the 600 MHz NMR experiments, and Dr. Michael Büchner for his contribution in the high-resolution MS measurements.

I express my gratitude to Florian Behrendt and Erik Endres, who contributed, under my supervision, to the isolation by HPLC of more pure material of some compounds for further investigations. The synthesis of ealajoziminones A (**70**) and B (**71**) were also repeated by Florian, under my guidance.

Prof. Dr. Virima Mudogo deserves also my gratitude for the collection of *Ancistrocladus ealaensis*. Likewise, thanks to B. Kimbadi Lombe for the collection of fresh plant material for comparison in 2015, and all the members of the working group Bringmann for the nice working spirit.

I am infinitely thankful to Dr. Anu Schaumlöffel, Michael Pfletscher, Dr. Henrike Miess, Dr. Soura Challal, and an anonymous person for correcting and suggesting major improvements in my Ph.D. thesis. Their prompt enthusiasm and feedback to read me first have touched me so much.

I would have been not successful if you were not next to me, spent a thought or a smile with me, you know how much you mean to me, so I just say THANK YOU my dearest: Sylvia Pöhlmann, Judith Grieshaber, Wolfgang Grieshaber, Jean-Pierre Mufusama Koy Sita, Michael Pfletscher, Ann-Kathrin, and Family Tshitenge (papa Dieudo, maman Alphonsine, maman Pierrette, Julie, Berinia, Marina, Doris, Joie, Merveil, Beni, Marie-Michel).

Finally, to all of you who contributed by any mean to the achievement of this project.

## VII. Publications, Posters, Oral Presentations, and Workshops

### Original research papers (state of June 16<sup>th</sup>, 2017)

1. **D. T. Tshitenge**, K. Ndjoko Ioset, J. N. Lami, J. Ndelo-di-Phanzu, J.-P. Koy Sita Mufusama, G. Bringmann; Rational quality assessment procedure for less-investigated herbal medicines: case of a Congolese antimalarial drug with an analytical report, *Fitoterapia*, **2016**, *110*, 189-195
2. **D. T. Tshitenge**, D. Feineis, S. Awale, G. Bringmann; Gardenifolins A-H, scalemic neolignans from *Gardenia ternifolia*: Chiral resolution, configurational assignment, and cytotoxic activities against the HeLa cancer cell line, *Journal of Natural Products*, **2017**, *80*, 1604-1614
3. **D. T. Tshitenge**, D. Feineis, V. Mudogo, M. Kaiser, R. Brun., G. Bringmann; Antiplasmodial ealapasamines A-C, 'mixed' naphthylisoquinoline dimers from the Central African liana *Ancistrocladus ealaensis*, *Scientific Reports*, *2017*, (Accepted paper, in press)
4. **D. T. Tshitenge**, T. Bruhn, D. Schmidt, D. Feineis, V. Mudogo, T. Efferth, S. Awale, F. Würthner, G. Bringmann; Structural characterization and biological assessment of ealamines A-H, alkaloids from *Ancistrocladus ealaensis*. (Manuscript soon to be submitted to *Journal of Natural Products*, copy available upon request)
5. **D. T. Tshitenge**, D. Feineis, V. Mudogo, M. Kaiser, T. Efferth, R. Brun, G. Bringmann; Cyclombandakamines, a thrilling series of novel dimeric alkaloids from *Ancistrocladus ealaensis*. (Manuscript under preparation for *Scientific Reports*)
6. **D. T. Tshitenge**, D. Feineis, V. Mudogo, M. Kaiser, T. Efferth, R. Brun, G. Bringmann; *Ancistrocladus ealaensis* as a reliable source of bioactive monomeric and dimeric naphthylisoquinolines. (Manuscript under preparation for *Journal of Natural Products*, all data available)
7. **D. T. Tshitenge**, T. Bruhn, F. Behrendt, G. Bringmann; Ealajoziminones A and B, two synthetic diphenquinones with thrilling insights. (Manuscript under preparation)

### Selected talks

1. **D. T. Tshitenge**, Unsymmetric naphthylisoquinoline Dimers from *Ancistrocladus ealaensis*, at the 51<sup>th</sup> Natural Products Meeting in Bayreuth, **April 2016**.
2. **D. T. Tshitenge**, Neolignans as Potential Markers for KILMA, a Congolese Phytomedicine, at the Joint Symposium organized by the SFB 630 (Würzburg, main), SFB 766 (Tübingen), and FOR 854 (Bonn) DFG research networks, in Retzbach (Germany), **December 2014**. (With a Talk Prize).
3. **D. T. Tshitenge**, Analysis of Congolese Phytomedicines, at the 48<sup>th</sup> Natural Products Meeting in Leipzig, **October 2014**.

### Selected posters

1. **D. T. Tshitenge**, D. Feineis, B. K. Lombe, G. Highly Unsymmetric Dimeric Naphthylisoquinoline Alkaloids from *Ancistrocladus ealaensis*, at the 29<sup>th</sup> Irsee Natural Products Meeting, Kloster Irsee (Germany), **February 2017**.
2. **D. T. Tshitenge**, D. Feineis, B. K. Lombe, G. Bringmann. Korundamines and Mbandakamines, unsymmetric naphthylisoquinoline dimers from the Congolese liana *Ancistrocladus ealaensis*, at the "*Journées de Chimie Organique*" organized by the French Chemical Society, in Palaiseau (France), **September 2016**.  
  
(Poster Award at Chem-SyStM, by the *JungChemikerForum*, in Würzburg, December 2016)
3. **D. T. Tshitenge**, G. Bringmann, K. Ndjoko Ioset, U. Holzgrabe, J. Ndelo-di-Phanzu, J. N. Lami. Antimalarial Phytomedicines Widely Used in the Congo: Characterization of Markers, and Development and Validation of a Method for their Quality Control, at the Advanced School of Bioorganic Chemistry in São Paulo (Brazil), in **July 2013**.

**Workshops** (Transferable skills):

1. Poster Design (September 10<sup>th</sup>, 2013), by Valeska Russo, organized by the Graduate School of Life Sciences, Würzburg, Germany.
2. Intercultural Communication and Cooperation (March 9<sup>th</sup>, 2015), by Ernestine Schneider, organized by the Graduate School of Life Sciences, Würzburg, Germany.
3. Good Scientific Practice (March 15<sup>th</sup>, 2015), by Dr. Stephan Schroeder-Koehne, organized by the Graduate School of Life Sciences, Würzburg, Germany.
4. Time and Self Management (December 1<sup>st</sup> and 2<sup>nd</sup>, 2016), by Dr. Jan Stamm, organized by the Graduate School of Life Sciences, Würzburg, Germany.

## VIII. Resume

### Dieudonné Tshitenge Tshitenge

Born on June 3<sup>rd</sup>, 1987 in Kananga (Dem. Rep. Congo)  
Sartoriusstrasse 18, 97072 Wuerzburg, Germany  
Tel.: 0931 29 69 68 94/ 0176 72 82 52 95  
E-mail: dtshitenge2007@yahoo.com



### Education

- Since April 2013 **Ph.D. thesis** at the Institute of Organic Chemistry, Julius-Maximilians-Universität (JMU) Würzburg, with a scholarship from the Graduate School of Life Sciences. Under the supervision of Prof. Dr. Dr. h.c. mult. Gerhard Bringmann
- February 2012 - March 2013 **MSc.:** In the field of Quality Analysis and Isolation of Natural Products. A sandwich program between the University of Kinshasa (DR Congo) and the JMU Würzburg. Co-supervision of Prof. Dr. Dr. h.c. mult. G. Bringmann and Prof. Dr. J. Ndelo-di-Phanzu. Toppest grade, rank 1
- January 2006 - December 2011 **Pharmacist diploma** (12 semesters): at the University of Kinshasa, DR Congo. Completed with the best grade of the year at the Faculty

### Selected Awards

- December 2016, Poster Award at Chem-SyStM, by the *JungChemikerForum*, in Germany
- December 2014, Talk Award at the Symposium of the SFB 630 network, in Germany
- July 2013, selected for a Travel Grant to attend and hold a Poster at the Advanced School of Bioorganic Chemistry, in São Paulo (Brazil)
- April 2013, selected among several applicants for a Ph.D. Scholarship by the DFG-funded Excellence Initiative at the Graduate School of Life Sciences, in Germany
- March 2012, Master Scholarship by the Excellence Scholarship Program BEBUC
- From 2008 to 2011, Excellence Scholarship BEBUC and Guest Student at JMU Würzburg
- In 2005, National Award for the best pupils: **400 USD** granted by the Congolese State

### Selected commitments

- From May 2013 to February 2016, elected in the Directory Panel of the NGO *fUNIKIN*
- May 2014, co-organizer of the *1. Würzburger Kongo-Tagung*, at JMU Würzburg

Würzburg, June 16<sup>th</sup>, 2017,

Dieudonné T. Tshitenge



## Affidavit

I hereby declare that my thesis entitled: **“Isolation and Structural Elucidation of Novel Anti-infective Naphthylisoquinoline Alkaloids from *Ancistrocladus ealaensis*, and Phytochemical Analysis of Two Congolese Medicinal Plants”** is the result of my own work. I did not receive any help or support from commercial consultants. All sources and / or materials applied are listed and specified in the thesis.

Furthermore, I verify that this thesis has not yet been submitted as part of another examination process neither in identical nor in similar form.

Würzburg,

Date

Signature

Dieudonné Tshitenge Tshitenge